CHARLES UNIVERSITY PRAGUE

faculty of mathematics and physics

Construction of pseudoscalar meson amplitudes in chiral perturbation theory using a dispersive approach

Martin Zdráhal

Institute of Particle and Nuclear Physics

Doctoral thesis
Thesis advisor: RNDr. Jiří Novotný, CSc.
Study programme: Physics
Specialization: Subnuclear Physics
Prague 2011

Acknowledgements

I would like to thank all my collaborators with whom we have managed to bring this extensive subject into a successful finish, namely my thesis advisor J. Novotný for his enthusiasm, all his ideas and comments not only on this text but on the physics in general, as I have learned many interesting methods and subjects under his guidance; M. Knecht, who in spite of his enormous workload managed to find enough time for cooperating with me on this subject but also for reading a substantial part of this text; and finally K. Kampf, who always managed to moderate our highly academic discussions back down to earth and guided our work also towards its practical use and the comparison with experiment.

Many thanks belong to my more experienced office mates in Prague, M. Kladiva and M. Kolesár, and also to the Prague senior staff, among others J. Hořejší, J. Dolejší, J. Formánek, P. Cejnar for many stimulating discussions about physics but also about other subjects, which have helped to shape me into a real physicist.

The essential part of the presented work was carried out at University of Vienna, where I was supported by a Marie Curie Fellowship of the European Commission ("Flavianet" Research Training Network). I am very grateful to G. Ecker, H. Neufeld and W. Grimus for their hospitality in that time and for many discussions related to all subjects of life which have also enhanced my knowledge about physics and mainly about the life of a researcher.

I have benefited from many discussions on the presented subject with J. Bijnens, J. Gasser, B. Kubis, S. Lanz, G. Colangelo and E. Passemar.

However, the most important people without whom this work would never be finished are my friends and my family. Especially, I want to thank my parents and my sister for all their support. From the bottom of my hearth I thank my wife Jarmila and my daughter Nikoleta for their love, their patience, their understanding for my work, their full support and especially for making my life happier. I would like to dedicate this thesis to them, to Jarmila and Nikoletka.

I declare that I carried out this doctoral thesis independently, and only with the cited sources, literature and other professional sources.

I understand that my work relates to the rights and obligations under the Act No. 121/2000 Coll., the Copyright Act, as amended, in particular the fact that the Charles University in Prague has the right to conclude a license agreement on the use of this work as a school work pursuant to Section 60 paragraph 1 of the Copyright Act.

In Prague date ..... Signature

Název práce: Kostrukce pseudoskalárních mezonových amplitud v chirální poruchové teorii za použití disperzních metod

Autor: Martin Zdráhal

Katedra: Ústav částicové a jaderné fyziky, Matematicko-fyzikální fakulta, Univerzita Karlova v Praze

Vedoucí disertační práce: RNDr. Jiří Novotný, CSc.

Abstrakt:
Vyvinuli jsme metodu umožňující konstrukci dvousmyčkových $2 \to 2$ rozptylových amplitud pseudoskalárních mezonů založenou na disperzních relacích a relacích unitarity. Použití této metody jsme nejprve ilustrovali na příkladu konstrukce všech takovýchto amplitud zachovávajících isospin v chirální poruchové teorii za předpokladu pouze silných interakcí.

Poté jsme ji použili ke konstrukci amplitud popisujících $\pi\pi$ rozptyl a rozpady $K \to 3\pi$ a $\eta \to 3\pi$, kde jsme vzali v úvahu efekty narušující isospin způsobené různými hmotami částic příslušejících do stejného isomultipletu. Takto vzniklé parametrizace jsou připraveny k fenomenologickým studiím $\pi\pi$ rozptylových délek a efektů narušení isospinu, které nám mohou poskytnout důležité informace k pochopení kvantové chromodynamiky při nízkých energiích.

Nakonec jsme provedli analýzu rozpadu $\eta \to 3\pi$, z níž jsme získali hodnotu poměru kvarkových hmot $1/R = (m_d - m_u)/(m_s - \hat{m})$. Náš konzervativní odhad této veličiny je $R = 39.6^{+2.5}_{-5.1}$. Zkombinování této hodnoty s výsledky pro izospinové hmoty $\hat{m} = (m_u + m_d)/2$ a m_s plynoucími z jiných metod (sumační pravidla nebo lattice) vede k v současné době nejpřesnějšímu určení hmot u a d kvarku, jejichž hodnoty uvádíme v textu.

Klíčová slova: procesy pseudoscalárních mezonů, disperzní relace, chiralní poruchová teorie, narušení isospinu, určení kvarkových hmot

Title: Construction of pseudoscalar meson amplitudes in chiral perturbation theory using a dispersive approach

Author: Martin Zdráhal

Department: Institute of Particle and Nuclear Physics, Faculty of Mathematics and Physics, Charles University in Prague

Supervisor: RNDr. Jiří Novotný, CSc.

Abstract:
We have developed a method enabling a construction of two-loop $2 \to 2$ scattering amplitudes of pseudoscalar mesons based on the dispersion and the unitarity relations. This method is illustrated on the construction of the amplitudes of all such processes in chiral perturbation theory in isospin limit taking into account strong interactions only.

Then it was used for the construction of $\pi\pi$ scattering amplitudes and of $K \to 3\pi$ and $\eta \to 3\pi$ decay amplitudes including isospin breaking effects induced by different masses of the particles belonging to the same isomultiplet. These parametrizations are prepared for various phenomenological analyses of the $\pi\pi$ scattering lengths and of the isospin breaking effects, both of which could provide us important information for the understanding of quantum chromodynamics at low energies.

Finally, we have performed the phenomenological study of $\eta \to 3\pi$ decay and obtained a value of the quark mass ratio $1/R = (m_d - m_u)/(m_s - \hat{m})$. Our conservative estimate is $R = 39.6^{+2.5}_{-5.1}$. This value supplemented by the values of the isospin symmetric masses $\hat{m} = (m_u + m_d)/2$ and m_s from other methods (as sum-rules or lattice) enables us to obtain currently the most precise determination of the m_u and m_d quark masses, whose values are quoted in the text.

Keywords: pseudoscalar meson processes, dispersion relations, chiral perturbation theory, isospin breaking, quark masses determination

Contents

List of Tables

List of Figures

Preface

Whenever we want to describe some phenomenon occurring in the world around us and construct a relevant physical model that will give numerical predictions of further experiments related to it, at several places of its construction we are faced with choosing between various alternatives.

The first such choice occurs in formulation of the basic principles our model should possess. Without their right choice, the model we construct will not reproduce the results of the observations and of the experiments dealing with the phenomenon. It is believed that in the end there exists only one genuine choice corresponding to the world in which we live and that after a shorter or longer time we will identify it. Therefore, when some choice of the set of principles proves itself to be wrong, we completely forget this alternative and concentrate ourselves on the new one. The challenging aspect of it is, however, the fact that it can take much time before one finds some observation which contradicts the expectations of the model thereby indicating that his choice of the basic principles was in fact only approximate or even incorrect and it can take even longer until we really end up with the genuine correct choice. Nowadays, thanks to the long history of our endeavor to describe the world around us and to the belief that there exists only one general physics, we have gained some experience that can be used as a guiding line for the formulation of the principles. However, still each time we enter a new area (and era) of physics where the old ideas do not work or give improper/incorrect answers, we are once again faced with the questions which of the principles we already have should be abandoned or adjusted and whether we should add some new one.

There follows the second choice — the choice of the right mathematical framework that would possess the right properties compatible with the basic principles we have chosen. Also here the tradition can help substantially but can also be misleading. Whereas the basic principles are usually stated in simple words, in order to explore all the properties of the mathematical framework we need much more patient and careful studies.

Although these two steps on the quests for the physical models with the correct basic principles and with the correct mathematical framework are amusing and in the recent years in the form of the search for new physics beyond the Standard model very popular and topical, in this work we will deal with another appearances of alternatives in physics.

Even within the right framework with the correct basic principles we still have more alternative techniques how to compute some physical quantity. Here there comes into the game a new sort of alternatives. This time the different alternatives using the correct

assumptions usually lead to the same results and the criterion determining which of the techniques should be preferred is predominantly the simplicity with which the results are obtained. In this situation it is therefore important to keep in mind the existence of all such alternatives since in some other applications it can show up that some of them is more useful than the one originally chosen. Moreover, in the nowadays physics we usually do not know the way how to obtain the complete non-perturbative result, and thus we need to make some approximations leading to an approximate result with a required precision. In that case, in addition to the freedom of choice of the effects we neglect and to the approximations we can make, there could happen that the method we have originally chosen for the computation as the right one can cease to be compatible with these approximations or that some other alternative would be now more suitable.

In this work we discuss one such alternative method to the traditional approaches in the low-energy regime of strong interactions and demonstrate how it can be useful for gaining the insight into the results that can be obtained by both the traditional and the alternative methods, but also for obtaining the results that go beyond the traditional approach.

Chapter 1

Introduction

The basic principles of the theory of strong interactions are believed to be well-known — they are formulated in the full elegance in the mathematical model called quantum chromodynamics (QCD). Its quantum field origin offers us an ample amount of methods that can be used to solve problems within it. However, despite the success of the perturbative QCD exploiting the property of asymptotic freedom, at the low-energy region, where the confinement rules, the degrees of freedom are no longer quarks and gluons but rather hadrons and we feel the lack of complete non-perturbative methods that would operate in terms of these particles. We have, therefore, no other choice than adding some additional principles, even though the approximate ones, that enable the use of approximate non-perturbative methods. Probably the best known of them is the lattice QCD, which discretizes the space-time and using huge supercomputers computes path-integrals of QCD (nowadays there exists a vast amount of literature dealing with different topics of this subject; we recommend as a good starting point for the interested reader the recent attempt to provide a summary of many lattice results for non-lattice experts [46]).

The fact that in the hadron spectrum there appears a gap between the light pseudoscalar mesons, π, K, η, and the other hadrons, which start to appear at $\Lambda_H \sim 1\,\mathrm{GeV}$; together with the existence of a suitable approximate symmetric structure of the low-energy theory enabling us to understand these mesons as pseudo-Goldstone bosons of a specific chiral symmetry breaking are the basic ideas behind the chiral perturbation theory (χPT) [130, 73, 74, 26] as the further non-perturbative method. We recall here only few important properties of it, which will be important in the following chapters. For the introduction to the subject, one can use either author's diploma thesis [I] or some standard introduction [62, 121, 70, 26]. Texts [131, 106, 71] written by the founding fathers of χPT are as well recommended — they contain also some interesting historical remarks and foundational aspects of this framework. In addition, the last of these papers covers the more general subject of the history of $\pi\pi$ scattering, whose studies have been one of the most important motivations for our current work.

Chiral perturbation theory introduces the so-called chiral expansion containing two expansion parameters, the momenta of pseudo-Goldstone particle p/Λ and the measure

of the explicit breaking of the chiral symmetry by the non-zero lightest quark masses m_q/Λ, in both these parameters the quantity Λ is the scale of chiral symmetry breaking $\Lambda \sim 1\,\mathrm{GeV}$. Although this framework is non-renormalizable there exists a natural power-counting scheme that organizes the contribution of higher-order diagrams so that to a given order there contributes a finite number of diagrams and there appears a finite number of low-energy constants (LEC). The importance of a given diagram is determined by its chiral order $O(p^d)$. Besides the standard chiral power-counting of Weinberg [130] there appeared in 1991 also a less predictive generalized chiral power-counting [67, 125, 97] that included the possibility of a small chiral condensate $\langle 0|qq|0\rangle$, which was not studied before. This inspired Stern and collaborators [125] for developing an S-matrix method for construction of the $\pi\pi$ scattering amplitude, which was Lagrangian-free and thereby not depending on the particular power-counting scheme. Even though the recent experiments favor more the standard scenario[1], the analyses based on their S-matrix method, which is referred nowadays as the "reconstruction theorem", can still have a few interesting applications as is presented in this work. But for the next few lines let us return back to the chiral perturbation theory.

In the last quarter-century χPT has made a considerable progress, mainly in the mesonic sector. There the calculation of most of the processes of interest and of the corresponding observables have been done at the two-loop level (including two loops, in chiral counting of order $O(p^6)$) and very accurate predictions based on such calculations have been made (cf. [26]). The prominent examples of this sort are the S-wave $\pi\pi$ scattering lengths a_0 and a_2 [48, 49]. However, the non-renormalisibility of this approach causes the following limitations of the method when we want to include higher and higher orders. Raising the level of computation to two loops means a rapid increase of the number of effective LEC that have to be estimated before one can make reliable physical predictions. Such an estimate usually appears to be the weakest point of the two-loop numerics. On the other hand, since the physical amplitudes depend on a few specific combinations of LEC that can be shared by different amplitudes and observables, we can still use the two-loop results for finding some nontrivial combinations of observables independent on the unknown LEC. Nevertheless, because of the extreme length of the generic $O(p^6)$ results that provides no easy survey, this task might be very tricky. Similarly, the large extent of the $O(p^6)$ results make rather difficult to reveal the analytic structure of the result, which is in fact governed by unitarity. Last but not least, the $O(p^6)$ calculations based directly on the chiral Lagrangian represent themselves a very hard technical problem combining both advanced analytical as well as numerical methods.

Therefore, there is a place for some alternative and complementary approaches to the Lagrangian-based two-loop calculations that might prove to be useful. They can provide two distinct benefits. First, they can be helpful for a better organization and understanding of the complicated structure of the $O(p^6)$ results, namely by means of revealing the repetitious combinations of LEC and chiral logs and moreover, elucidating the analytic structure of the results through their connection to the unitarity. Secondly, they can pos-

[1] For more details about this vivid history of the size of the chiral condensate, we recommend again [71].

sibly serve as a tool enabling us to go at least partially beyond the standard χPT and beyond the $O(p^6)$ accuracy. The latter might be useful either for theoretical estimates of the uncertainties of the Lagrangian-based $O(p^6)$ results or, taking into account possible problems with the convergence of the standard chiral expansion (cf. for instance the studies of $\eta \to 3\pi$, discussed in Section 9.2), it can be used to improve the convergence in "dangerous" kinematic regions by virtue of matching both approaches at the points where the convergence is guaranteed from general considerations.

One sort of such approaches that are on the market are the Lagrangian-free S-matrix methods based on the dispersion relations and the unitarity, which are nowadays understood as an integral part of the analyses of many processes. Let us emphasize among others the $\pi\pi$ scattering [118, 13, 48, 125, 95, 94] (and many references thereof), πK scattering [11, 12], $K_{\ell 3}$ decays [25] and finally $\eta, K \to 3\pi$ decays [17, 90, 44, 50].

In the case we do not want to modify significantly the assumptions of χPT and we do not have any information about the high-energy asymptotics of the amplitudes, or when we want to reproduce exactly the standard χPT results, the most useful are the methods based on the "reconstruction theorem" referred above. The original paper [125] presented a Lagrangian-free S-matrix method for construction of the $\pi\pi$ scattering amplitude up to and including two loops in two flavor χPT, based on the most general principles of analyticity, unitarity and crossing combined with the assumption of chiral expansion (neglecting only the effects of order higher than the two-loop one). Employing this method iteratively with the help of two-particle unitarity in [95] allowed to parametrize the two-loop $\pi\pi$ amplitude in terms of six independent parameters prior to the standard Lagrangian-based $O(p^6)$ calculation [30, 31]. The latter fitted the general form from [95] and the six relevant parameters have been identified in terms of LEC and chiral logs.

Moreover, because of its generality, the parametrization is valid regardless of the particular scheme of the chiral power counting and therefore it can be understood as a way beyond the standard scheme or alternatively as a tool to resum partially the higher order unitarity corrections.

In this work we discuss the generic derivation of the reconstruction theorem, its important properties and its application for the construction of two-loop amplitudes in all generality. Then the illustration of this construction on the example of isospin symmetric $2 \to 2$ meson scattering amplitudes is presented. Thereafter, we concentrate on the isospin breaking $\pi\pi$ scattering amplitudes and their influence on the η and K decays into three pions. As is recalled in Section 6.2, where also a list of the recent theoretical studies of these two decays is presented, they are nowadays in the center of interest either as a tool for determination of the isospin breaking ratio of the quark masses $R = \frac{m_s - \hat{m}}{m_d - m_u}$ from $\eta \to 3\pi$, or as a clean method for extracting the $\pi\pi$ S-wave scattering lengths a_0 and a_2 from the cusp effect in the final $\pi^0\pi^0$ invariant spectrum of the $K^+ \to \pi^+\pi^0\pi^0$ decay. The reconstruction procedure used iteratively for the amplitudes of these processes can provide us with the most general parametrization of them including two-loop effects. Because we have a freedom in the exact choice of the parameters used there, we can use, among other choices, the S-wave scattering lengths, thereby already performing a partial resummation going beyond the strict Lagrangian-based $O(p^6)$ calculation. These parametrizations for

the amplitudes of interest are prepared for the phenomenological analyses. We explicitly perform such analyses in these work only for the $\eta \to 3\pi$ and from the experimental information on it we obtain the value of R. As is discussed in Section 9.1, in connection with the isospin symmetric studies on the lattice or by QCD sum-rule techniques this enables us to determine the m_u and m_d quark masses with a very high precision.

The main text of this thesis is divided into four parts. Part I concerns general discussion of the reconstruction theorem and its applications for the construction of the two-loop four-meson amplitudes. In Chapter 2 we derive the reconstruction theorem with a careful discussion of all of its assumptions. This topic was partially presented in author's diploma thesis [I] and paper [II], however, the discussion in the current text is more detailed, especially in discussions of the number of subtractions, of the freedom of choice of the subtraction scheme, and of the possible simplifications that can be used for the resulting form of the dispersion integrals. In Chapter 3 we describe the application of the theorem for the construction of the meson-meson scattering amplitudes. In addition to the material presented in [I, II], the discussion of the second iteration in Sections 3.4–3.5 is included. We have also added the section about the properties of the polynomial part of the amplitude in the chiral limit (Section 3.3) and the important discussion about the possible interpretations of the polynomial parameters of our representation (Section 3.6). In Chapter 4 we illustrate this method on the example of isospin symmetric $2 \to 2$ meson scattering amplitudes. We do not repeat the complete analysis of [I, II] but instead concentrate more on the connection of our parametrization to the χPT result.

Part II containing just the single Chapter 5 deals with the construction of the $\pi\pi$ scattering amplitudes, with the main emphasis on the isospin breaking ones. After the construction of the complete two-loop parametrization, we have included in Section 5.11 also the determination of the values of its parameters compatible with the χPT result and with the experimental information on the $\pi\pi$ phase shifts.

Part III uses all these results for construction of the $K \to 3\pi$ and $\eta \to 3\pi$ decay amplitudes. In Chapter 6 we summarize important properties of these decays and the state of art in analyses of them. In Chapters 7 and 8 we have elaborated separately the case of the amplitudes in the leading order in isospin breaking, which is important mainly for the $\eta \to 3\pi$ processes, and the case where all the isospin breaking effects induced by the different masses of the mesons belonging to the same iso-multiplets are taken into account. The results on this part and partially also those of Part II will be presented in our forthcoming publication [X]. Some topics were already presented in our proceedings [III, IV, V] and in paper [VI].

Finally, in Part IV we perform the phenomenological analysis of $\eta \to 3\pi$ decay based on our analytic dispersive representation that uses the information from the NNLO chiral result and the one from the measurement of the charged $\eta \to 3\pi$ decay by KLOE for the determination of the value of the quark mass ratio R. Part of this analysis was published in [VI]. Here, we do not repeat the analyses performed in [VI] but we analyze another distribution compatible with the KLOE results (note that the genuine KLOE data are unavailable) in order to study the dependence of the result on the particular form of the distribution and we discuss into more detail the possible sources of errors. In Section 9.10

we use the determined value of R together with the results of the other recent analyses presented in the literature for constraining the m_u and the m_d quark masses. This subject was discussed also in [VII, VIII, IX], however, in the current work the most recent numbers (including the complete error budget from the $\eta \to 3\pi$ analysis) are presented.

In Chapter 10 we summarize the important conclusions of the thesis and partially discuss also the outlook of the further applications of the presented methods.

Note that we use the appendices not only for the technical details and the extensive expressions but also for the important subjects that could be otherwise dissipated in the main text. Especially, the essential part of the material of Appendices A, E and J–K is therefore deferred there not because of its unimportance or in order to save the reader from a tedious reading of dense formulas but in opposite for sake of simpler referring to them.

Appendix A is part of our derivation of the reconstruction theorem[2] as it gives the general solution of the crossing relations for the polynomial parts of the amplitudes. Appendix B discusses a few important properties of Hilbert transform and lists some relations used for the determination of Hilbert transform of some function from the knowledge of the transform of a related function. In Appendix C we follow the procedure of [124] and find the kinematic regions where the validity of dispersion relations and further assumptions of the reconstruction theorem for the amplitudes from Chapters 4 and 5 can be proved directly from the axiomatic theory. In Appendix D we list the values of the polynomial parameters for the amplitudes of Chapter 4 that reproduce the standard $O(p^4)$ chiral amplitudes (from [78]) — they were also published in [II]. In Appendix E we derive the important relations between the scattering-length parameters and the derivatives of the amplitudes and then employ them for the unitarity corrections of these parameters in our representation — they define the restoring polynomials used in Chapter 5 for keeping the values of these parameters at their physical values. In Appendix F we list all kinematical functions appearing in our results. In Appendix G there are given the explicit forms of the polynomials of the NLO partial waves of the $\pi\pi$ amplitudes, these polynomials then occur also in the two-loop results of $\pi\pi$ scattering and of $K \to 3\pi$ and $\eta \to 3\pi$ decay amplitudes. Appendix H reviews the relations between the usual Dalitz plot parametrization of the $\eta \to 3\pi$ amplitude and its linear form and then gives also the relation between these parametrizations for the neutral and for the charged decays valid in the first order of isospin breaking. In Appendix I the isospin structure of $K \to 3\pi$ amplitudes is derived. In Appendix J we extent the analysis of [40, 86] deriving the analytic properties of $K\pi \to \pi\pi$ and $\eta\pi \to \pi\pi$ amplitudes also to the case of isospin breaking. We use the method of Landau equations for the determination of the analytic properties of the individual Feynman diagrams contributing to this processes. In Appendix K the resulting prescription for the correct analytic continuation in the mass of the decaying particle is used for the continuations of the partial waves of the $K\pi \to \pi\pi$ and $\eta\pi \to \pi\pi$ amplitudes, which are then used in Chapters 7 and 8 for computation of the correct result of the second iteration for these processes. The thesis is closed with Appendix L, where the polynomials appearing in NLO partial waves and in the NNLO amplitudes of $K \to 3\pi$ and $\eta \to 3\pi$ decays are listed.

[2]This appendix represents author's reformulation of the text of unpublished note of J. Novotný.

Part I

Reconstruction procedure in general

Chapter 2

Reconstruction theorem

In this chapter we formulate and prove the reconstruction theorem in the formulation written for any meson-meson scattering, which will be used in the following chapters for the construction of amplitudes of several particular processes. We state here all the assumptions essential for the theorem, which will simplify our further discussion of validity and limitations of the results computed for the individual processes, and also of the further applications of the theorem.

2.1 Notation

Kinematics

We consider a quasi-elastic scattering process of two particles of the type

$$A(p_A)B(p_B) \to C(p_C)D(p_D) \tag{2.1}$$

and define its amplitude according to

$${}_f\langle C(p_C)D(p_D)|A(p_A)B(p_B)\rangle_i = \delta_{if} + i\,(2\pi)^4\,\delta^{(4)}(p_C + p_D - p_A - p_B)A_{AB\to CD}(s,t,u). \tag{2.2}$$

It depends on two independent kinematic variables. It is convenient to choose them to be the total energy squared s and the angle θ between the momenta p_A and p_C in the center of mass system (CMS); or the Mandelstam variables

$$s = (p_A + p_B)^2 = (p_C + p_D)^2, \tag{2.3}$$
$$t = (p_A - p_C)^2 = (p_B - p_D)^2, \tag{2.4}$$
$$u = (p_A - p_D)^2 = (p_B - p_C)^2. \tag{2.5}$$

Only two of them are independent since

$$s + t + u = 3s_0, \tag{2.6}$$

where $3s_0$ is the sum of squared masses of all the particles appearing in the process,

$$3s_0 = m_A^2 + m_B^2 + m_C^2 + m_D^2, \tag{2.7}$$

and the point $s = t = u = s_0$ corresponds to the center of the Dalitz plot.

The transition between the scattering angle and the Mandelstam variables is possible using the relation

$$\cos\theta = \frac{s(t-u) + \Delta_{AB}\Delta_{CD}}{\lambda_{AB}^{1/2}(s)\lambda_{CD}^{1/2}(s)}, \tag{2.8}$$

where

$$\Delta_{xy} = m_x^2 - m_y^2 \tag{2.9}$$

and $\lambda_{xy}^{1/2}(s)$ is a square root of the Källen's quadratic form[1]

$$\lambda_{xy}(s) = \left(s - (m_x + m_y)^2\right)\left(s - (m_x - m_y)^2\right), \tag{2.10}$$

which reduces for the particles of the same masses to $\lambda_{xx}(s) = s^2\sigma_x^2(s)$ with

$$\sigma_x(s) = \sqrt{1 - \frac{4m_x^2}{s}}\,. \tag{2.11}$$

Crossed channels

Later on, we will employ the crossing property. We define the amplitudes of the crossed processes in the following way. The amplitude of the direct process is denoted by $\mathrm{S}(s,t,u)$, i.e. $A_{AB\to CD}(s,t,u) = \mathrm{S}(s,t,u)$. The amplitude of the T-crossed channel is

$$A_{A\overline{C}\to\overline{B}D}(s,t,u) = \epsilon_{\mathrm{T}}\mathrm{T}(s,t,u) \tag{2.12}$$

with the phase factor ϵ_{T} defined so that $\mathrm{T}(s,t,u)$ fulfills crossing relation

$$\mathrm{S}(s,t,u) = \mathrm{T}(t,s,u) \tag{2.13}$$

and similarly for the U-crossed channel.

[1] In some applications of the theorem it is necessary to continue analytically partial waves of amplitudes below their physical thresholds. It involves a continuation of $\cos\theta$, which is connected with a continuation of this square root and hence requires a careful study of its analytic properties. For such cases it will be given separately in the particular chapters. For now, we just stress that in the following relations we take this square root within the physical region to be the regular positive-valued square root of positive real numbers.

Partial wave decomposition

In the reconstruction theorem, we deal with the S and P partial-wave projections of the amplitude $A(s,t,u)$. Our notation for them is

$$A(s,t,u) = 16\pi N\,(f_0(s) + 3f_1(s)\cos\theta) + A_{\ell\geq 2}(s,t,u), \tag{2.14}$$

where $A_{\ell\geq 2}$ denotes the contribution of higher partial waves and θ is the CMS scattering angle connected with Mandelstam variables by (2.8). We have introduced the factor N here since our definition in different applications of the theorem changes in order to be consistent with those used in the literature — $N = 2$ in Chapter 4 whereas $N = 1$ in all the other chapters.

The lowest partial waves are extracted by integrations

$$f_0(s) = \frac{1}{32\pi N}\int_{-1}^{1} \mathrm{d}(\cos\theta)\, A(s,t,u), \tag{2.15}$$

$$f_1(s) = \frac{1}{32\pi N}\int_{-1}^{1} \mathrm{d}(\cos\theta)\, \cos\theta\, A(s,t,u). \tag{2.16}$$

As will be emphasized a few more times in this work, we do not require the existence of all partial waves or the convergence of the full partial wave decomposition. Our only requirement is the existence of the S and P partial waves given by these two integrals and the specific suppression of the $A_{\ell\geq 2}(s,t,u)$ remainder of amplitude as will be specified in the assumptions of the theorem.

We will construct the lowest partial waves iteratively and so it turns out to be useful to distinguish the contributions of different orders. We denote the $O(p^2)$ part of partial waves as ϕ, the $O(p^4)$ one as φ and finally their $O(p^6)$ part is denoted as ψ, so the complete partial waves read

$$f_\ell(s) = \phi_\ell(s) + \varphi_\ell(s) + \psi_\ell(s) + O(p^8). \tag{2.17}$$

Unitarity relation

In order to use the reconstruction theorem as a tool for constructing the amplitudes it is necessary to specify the input for the imaginary parts of the partial waves appearing there. These will be provided by the relation coming from the unitarity of S-matrix projected on the corresponding partial waves. In the next chapter we show that we will deal only with the processes for which the intermediate states appearing there are in the low-energy region and up to two loops restricted to pairs of light pseudoscalar mesons. The contribution of the other states should be then included by the polynomials and the higher orders. Assuming it and the T-invariance of the amplitudes together with their real analyticity, we can write

$$\mathrm{Im}\, f_\ell^{i\to f}(s) = \sum_k \frac{N}{S_k}\frac{\lambda_k^{1/2}(s)}{s}\, f_\ell^{i\to k}(s)\left(f_\ell^{f\to k}(s)\right)^\star \theta(s-\mathrm{thr}_k). \tag{2.18}$$

The sum goes over all the possible intermediate states k (those containing two mesons) that have the same (conserved) quantum numbers as the initial state i and the final state f of the process in question. S_k denote their symmetry factors — $S_k = 2$ for indistinguishable states and $S_k = 1$ otherwise. thr_k is the threshold at which the particular channel k opens and $\lambda_k(s)$ is the triangle function (2.10) corresponding to this two-particle state.

Further shorthand notation

Together with the notation already defined in this section, we will use also the following shortcuts that simplify the form of relations in this text. It will hopefully also add more clarity to the results that will be presented.

$$\Sigma_{xy} = m_x^2 + m_y^2, \tag{2.19}$$

$$\mu_{xy}^{\pm} = (m_x \pm m_y)^2 . \tag{2.20}$$

At the beginning of the chapters with the particular applications of the theorem, we introduce further notation useful for the individual processes under consideration.

2.2 Statement of the theorem

Suppose the following assumptions (which are discussed in more detail in the next section)

(i) existence of a threshold Λ up to which we can regard the theory under consideration to be complete;

(ii) existence of a well-behaved expansion of the considered amplitude in powers of p/Λ;

(iii) good behaved partial wave decomposition (2.14) and such suppression of the absorptive part of $A_{\ell\geq 2}(s,t,u)$ part of the amplitude that it starts at $O(p^8)$ order;

(iv) validity of three-times-subtracted u-fixed dispersion relation for amplitude $\mathrm{S}(s,t,u)$ in the form (2.27);

(v) analyticity of the amplitude considered as a function of a single Mandelstam variable in some unempty open region;

(vi) validity of the crossing relations $\mathrm{S}(s,t,u) = \mathrm{T}(t,s,u) = \mathrm{U}(u,t,s)$;

(vii) finiteness of the amplitude in the chiral limit with the external momenta fixed.

Then we can construct the amplitude $\mathrm{S}(s,t,u) \equiv A_{AB\to CD}(s,t,u)$ up to two loops in the form

$$\mathrm{S}(s,t,u) = R(s,t,u) + U(s,t,u) + O(p^8), \tag{2.21}$$

where $R(s,t,u)$ denotes a third order polynomial in the Mandelstam variables having the same s, t, u symmetries as the amplitude $\mathrm{S}(s,t,u)$; and $U(s,t,u)$ is the non-analytic unitarity part

$$\begin{aligned} U(s,t,u) = {} & W^0_{\mathrm{S}}(s) + (t-u)W^1_{\mathrm{S}}(s) + W^0_{\mathrm{T}}(t) + (s-u)W^1_{\mathrm{T}}(t) \\ & + W^0_{\mathrm{U}}(u) + (t-s)W^1_{\mathrm{U}}(u) \end{aligned} \tag{2.22}$$

given in terms of single variable dispersion integrals over the imaginary parts of S and P partial waves of all the crossed amplitudes,

$$\begin{aligned} W^0_{\mathrm{S}}(s) = {} & 16Ns^3 \int_{s_{\mathrm{thr}}}^{\Lambda^2} \frac{\mathrm{d}x}{x^3(x-s)} \operatorname{Im} f_0^S(x) \\ & + 48N\Delta_{AB}\Delta_{CD}\, s^3 \int_{s_{\mathrm{thr}}}^{\Lambda^2} \frac{\mathrm{d}x}{x^3(x-s)} \operatorname{Im} \frac{f_1^S(x)}{\lambda^{1/2}_{AB}(x)\lambda^{1/2}_{CD}(x)}\,, \end{aligned} \tag{2.23}$$

$$W^1_{\mathrm{S}}(s) = 48Ns^2 \int_{s_{\mathrm{thr}}}^{\Lambda^2} \frac{\mathrm{d}x}{x(x-s)} \operatorname{Im} \frac{f_1^S(x)}{\lambda^{1/2}_{AB}(x)\lambda^{1/2}_{CD}(x)}\,. \tag{2.24}$$

The lower limit of the integrations s_{thr} is the non-analyticity threshold in the S channel [cf. (2.28)]. Similar relations for the contributions of T and U crossed processes, $W^0_{\mathrm{T}}(t)$ and $W^1_{\mathrm{T}}(t)$ and $W^0_{\mathrm{U}}(u)$ and $W^1_{\mathrm{U}}(u)$ respectively, are easy to obtain from the obvious cyclic permutations.

2.3 Assumptions of the theorem

Here we specify the assumptions of the theorem more precisely. We are interested in the description of meson-meson scattering processes, where the framework of chiral perturbation theory can be used. This simplifies their discussion considerably already at the general level. Eventual additional comments and justifications of the assumptions are given for the particular applications in question in the appropriate chapters.

(i)+(ii) **Existence of a threshold Λ and a good-behaved expansion in powers of p/Λ**

There should exist a threshold Λ up to which we can regard the theory under consideration as complete and the amplitudes should have convergent expansions in powers of p/Λ below this Λ. This means, among others, that below this threshold there occurs no particle of a type other than those which are already explicitly included in the theory and all the influence of such extra particles is under the threshold negligible or already taken into account effectively. Naturally, there could be also other reasons for the introduction of the threshold Λ besides the one that we do not know the complete theory valid also above it. We can for example introduce it as a cut-off of numerical integrations. Nevertheless, for the validity of

the theorem it is still necessary that the expansion in p/Λ below such threshold is convergent.

In chiral perturbation theory the natural choice of Λ is the threshold of production of other particles than the psedo-Goldstone bosons in the particular process, $\Lambda \sim 1\,\mathrm{GeV}$. [Note that in the $SU(2)$ version of χPT such threshold has to prohibit in that region also the occurrence of kaons, as the first particles not included in the theory.] The expansion in powers of momenta required above then corresponds to the regular chiral expansion. For these assumptions the existence of any chiral expansion where $M_P^2 \sim p^2$, $P = \pi, K, \eta$, is therefore sufficient, it is not needed to be the standard Weinberg one [130], where in addition quark masses are counted as $m_q \sim p^2$.

As is common in χPT, instead of $O((p/\Lambda)^n)$ we write just $O(p^n)$ for short.

(iii) **Existence of S and P partial waves of the amplitude and suppression of the absorptive part of the rest to $O(p^8)$**

For the considered amplitude there should exist convergent integrals (2.15) and (2.16) defining S and P partial waves. Their behavior in the p/Λ expansion together with the one of the rest of the amplitude $A_{\ell\geq 2}(s,t,u)$ from (2.14) should be

$$\mathrm{Re}\, f_{\ell=0,1}(s) = O(p^2), \quad \mathrm{Im}\, f_{\ell=0,1} = O(p^4), \tag{2.25}$$

$$\mathrm{Re}\, A_{\ell\geq 2} = O(p^4), \quad \mathrm{Im}\, A_{\ell\geq 2} = O(p^8). \tag{2.26}$$

Thanks to this p/Λ behavior we can (up to $O(p^8)$ order) deal in the theorem just with the first two partial waves.

Within χPT the integrals (2.15) and (2.16) are guaranteed to exist and chiral behaviors (2.25) and (2.26) can be justified there from assumptions (vii), i.e. finiteness of the S-matrix in the chiral limit; (v), i.e. analyticity of the amplitudes; and from the Goldstone-boson character of the particles under consideration as follows. In χPT the amplitudes behave dominantly as $O(p^2)$ and do not contain any bound state poles. Unitarity relation (2.18) then implies that their imaginary parts behave as $O(p^4)$, which means that the amplitudes are dominantly real. According to analyticity of the amplitude, its leading $O(p^2)$ part should be a polynomial in Mandelstam variables. Moreover, it has to be a polynomial of first order; otherwise its coefficients would grow up as masses of the particles went to zero, which would contradict the finiteness of the S-matrix in the chiral limit with the external momenta fixed. However, since the first-order polynomial could not contribute to $\ell \geq 2$ partial waves, these partial waves should behave in chiral limit as $O(p^4)$. Using the unitarity relation once more, we see that imaginary parts of these partial waves are at least of $O(p^8)$ order.

Note that we require the existence only of the S and the P partial waves and the theorem is valid even if the higher partial waves do not exist. Nevertheless,

for some of the processes we can find a domain where the complete partial wave decomposition is convergent already from the axiomatic field theory.

(iv) **Validity of three-times subtracted dispersion relation**

The essential assumption of the proof is that we can write an n-times subtracted dispersion relation for the amplitude $\mathrm{S}(s,t;u)$ in the complex s-plane for a fixed value of u in the form (2.27). The legitimacy of this assumption has to be discussed separately for each process.

The connected important question is of the number of subtractions needed in the dispersion relations. Jin and Martin [85] have shown that thanks to the Froissart bound [66] it suffices to consider just two subtractions. However, the Froissart bound deals with the complete theory (in our case with the full QCD), whereas in the framework of an effective theory one does not know (or more exactly one does not deal with) what is above Λ, and so there can occur a situation that more than two subtractions are needed. In other words, Froissart tells us that two subtractions are sufficient if we supply the dispersion integral above Λ with the complete theory. Moreover, not only the incompleteness of the theory above Λ but also the fact that we take only S and P waves of the amplitudes calls for the higher number of subtractions — as is obvious from the proof, taking a smaller number of them can disrupt the suppression of contribution of $\ell \geq 2$ partial waves to the $O(p^8)$ order. This is the reason why we begin with $n \geq 2$ subtractions in the theorem and then show that in order to obtain the amplitude including all two-loop corrections [i.e. with a remainder of order $O(p^8)$] at least three subtraction are needed and the natural choice is $n = 3$.

(v) **Analyticity of the amplitude**

Assuming analyticity of the amplitude considered as a function of a single Mandelstam variable (with the other variable fixed at some appropriate value) in some unempty open region enables us to prove a simple and symmetric form of the polynomial $R(s,t,u)$. In our applications, chiral perturbation theory provides such an unempty region.

(vi) **Crossing property** $\mathrm{S}(s,t,u) = \mathrm{T}(t,s,u) = \mathrm{U}(u,t,s)$

The widely accepted assumption of the crossing property has been even proved for a general $2 \to 2$ process from the axiomatic theory by Bross, Epstein, and Glaser [42].

(vii) **Finiteness of the amplitude in the chiral limit with the external momenta fixed**

This is a basic assumption of the chiral perturbation theory requiring a smooth chiral limit of the amplitudes.

2.4 Proof of the theorem

We begin with n-times subtracted dispersion relation for the scattering amplitude with a fixed value of u (for now not specifying the number n) in the form

$$\mathrm{S}(s,t,u) = P_n(s,t,u) + \frac{s^n}{\pi}\int_{s_{\mathrm{thr}}}^{\infty}\frac{\mathrm{d}x}{x^n}\,\mathrm{Im}\,\frac{\mathrm{S}(x,3s_0-x-u,u)}{x-s} + \frac{t^n}{\pi}\int_{t_{\mathrm{thr}}}^{\infty}\frac{\mathrm{d}x}{x^n}\,\mathrm{Im}\,\frac{\mathrm{S}(3s_0-x-u,x,u)}{x-t}, \quad (2.27)$$

where $P_n(s,t,u)$ denotes a polynomial[2] of $(n-1)$-th order in s and t with u-dependent coefficients, and s_{thr} is the non-analyticity threshold in S-channel, i.e. the minimum of squared invariant masses of all possible intermediate states (α,β) in this channel (or rather the lowest mass of the state with the same quantum numbers as the *in* and *out* states)[3],

$$s_{\mathrm{thr}} = \min_{(\alpha,\beta)}(m_\alpha + m_\beta)^2, \quad (2.28)$$

and analogically t_{thr} for T channel (later on we will also need threshold u_{thr} in U channel).

Thanks to the crossing property we can replace the amplitude $\mathrm{S}(s,t;u)$ in the second integral with $\mathrm{T}(t,s;u)$. Furthermore, since we assume that we know the complete theory only up to some threshold Λ (up to which the chiral expansion of the amplitude is convergent), we have to split the dispersion integral into two parts — the low-energy ($x \le \Lambda^2$) and the high-energy ($x \ge \Lambda^2$) part.

The amplitude then depends on Λ, on pseudoscalar masses (in the following we write them generically as M), and on Mandelstam variables. Because it is dimensionless, we can write[4]

$$\mathrm{S}\big(s,t(s,u,M^2);u;M^2,\Lambda^2\big) = \mathcal{S}\left(\frac{s}{\Lambda^2};\frac{u}{\Lambda^2},\frac{M^2}{\Lambda^2}\right). \quad (2.29)$$

The high-energy part of the integrals can be expanded for $|s| < \Lambda^2$ (together with the substitution $x = y\Lambda^2$),

$$H_{\mathrm{S}}(s;u) = \frac{s^n}{\pi}\int_{\Lambda^2}^{\infty}\frac{\mathrm{d}x}{x^n}\frac{\mathrm{Im}\,\mathrm{S}(x,t(x;u);u)}{x-s} = \left(\frac{s}{\Lambda^2}\right)^n\int_1^{\infty}\frac{\mathrm{d}y}{\pi}\frac{\mathrm{Im}\,\mathcal{S}\left(y;\frac{u}{\Lambda^2},\frac{M^2}{\Lambda^2}\right)}{y^{n+1}}\sum_{k=0}^{\infty}\frac{1}{y^k}\left(\frac{s}{\Lambda^2}\right)^k. \quad (2.30)$$

[2]Due to relation (2.6) for the sum of Mandelstam variables, such polynomials can be written in the form $P_n(s,t;u) = \alpha(u) + \beta(u)(s-t) + \gamma(u)(s-t)^2 + \cdots + \omega(u)(s-t)^{n-1}$.

[3]In this relation we anticipate that in the cases that will be considered the only relevant intermediate states are just the two-particle ones.

[4]Note that all further quantities that can appear in amplitudes do not change the analysis that follows. For instance, the decay constant F_π translates in this relation into dimensionless constant $\frac{F_\pi^2}{\Lambda^2}$ that does not change the chiral behavior of the amplitude as it does not scale with λ in (2.33).

The existence of a smooth chiral limit of $\mathrm{S}(x,t(x;u);u)$ and its nonsingular behavior for $u\to 0$ imply that

$$H_{\mathrm{S}} = \left(s/\Lambda^2\right)^n K_{\mathrm{S}}(u) + O\left((p/\Lambda)^{2n+2}\right), \tag{2.31}$$

where $K_{\mathrm{S}}(u)$ is a u-dependent function. A similar situation occurs also for the high-energy part of the integration of $\mathrm{T}(s,t,u)$. Hence, up to an $O((p/\Lambda)^{2n+2})$ remainder we can replace the infinity in the upper bounds of integrations with Λ^2 provided we take in the theorem a polynomial P_{n+1} of n-th order[5]. After that, the dispersion relation is of the form

$$\begin{aligned}\mathrm{S}(s,t;u) = P_{n+1}(s,t;u) &+ \frac{s^n}{\pi}\int_{s_{\mathrm{thr}}}^{\Lambda^2}\frac{\mathrm{d}x}{x^n}\frac{\operatorname{Im}\mathrm{S}(x,3s_0-x-u;u)}{x-s}\\ &+ \frac{t^n}{\pi}\int_{t_{\mathrm{thr}}}^{\Lambda^2}\frac{\mathrm{d}x}{x^n}\frac{\operatorname{Im}\mathrm{T}(x,3s_0-x-u;u)}{x-t} + O(p^{2n+2}).\end{aligned} \tag{2.32}$$

Now, we introduce partial waves from decomposition (2.14) for the imaginary parts of the amplitudes. One of our assumptions tells $\operatorname{Im} f_{0,1} = O(p^4)$ and $\operatorname{Im} A_{\ell\geq 2} = O(p^8)$ and we could naively expect that the contribution of $\operatorname{Im} A_{\ell\geq 2}$ in the dispersion integrals is also suppressed as $O(p^8)$. However, we will see that depending on the particular number of subtractions n we take in the theorem, it can contribute also with a lower chiral order. We identify chiral order of each contribution after the formal rescaling

$$(s,t,u,s_{\mathrm{thr}},M^2,\Lambda^2)\to(\lambda s,\lambda t,\lambda u,\lambda s_{\mathrm{thr}},\lambda M^2,\Lambda^2) \tag{2.33}$$

as the leading behavior for $\lambda\to 0$.

Before performing the explicit determination of chiral orders of various contributions, we present a toy example illustrating its true dependence on n. If we assumed that the imaginary part of the higher-partial-wave remainder behaved simply as s^4, i.e. of order $O(p^8)$, the S-integration after this rescaling would give

$$\frac{\lambda^n s^n}{\pi}\int_{\lambda s_{\mathrm{thr}}}^{\Lambda^2}\frac{\mathrm{d}x}{x^n}\frac{x^4}{x-\lambda s} = \lambda^4\frac{s^n}{\pi}\int_{s_{\mathrm{thr}}}^{\Lambda^2/\lambda}\frac{\mathrm{d}y}{y^n}\frac{y^4}{y-s}\,.$$

This integral is easy to compute and we see that the λ-dependence of the upper limit of the last integration (which would not occur without the introduction of the cut-off Λ of this integration) is the actual origin of a possible change of the chiral order of its contribution. Indeed, for $n=2$, we obtain the leading-order behavior in λ as $\lambda^2\Lambda^4\frac{s^2}{2\pi}$, i.e. it would contribute with chiral order $O(p^4)$. Similarly, for $n=3$ we obtain $\lambda^3\Lambda^2\frac{s^3}{\pi}+O(\lambda^4)$, which means chiral order $O(p^6)$; and only when $n=4$, this integral equals $\lambda^4\frac{s^4}{\pi}$ times a logarithm and so the integral contributes with the order $O(p^8)$ that was naively expected.

[5] As a consequence, we can formally extend the validity of the effective theory even beyond threshold Λ and compute the dispersion integrals up to infinity, pretending that the effective theory is in fact complete — with the appropriate modification of the third-order polynomial. Naturally, provided such integrals converge.

Already from this toy example, we have seen the basic properties of this n-dependence: Such anomalies in chiral orders appear when the dispersion integral diverges for $\Lambda \to \infty$. Secondly, in order to have the contribution of $A_{\ell\geq 2}$ suppressed to $O(p^8)$ for any possible $A_{\ell\geq 2}$, we have to take at least four subtractions, whereas three subtractions induce a polynomial term of lower chiral order and the remainder of order $O(p^8)$.

After this illustration we return to the general case and determine chiral orders of individual contributions of f_ℓ and $A_{\ell\geq 2}$. Let us write for $x < \Lambda^2$ generic chiral expansions

$$\operatorname{Im} f_\ell^{\mathrm{S}}(x) = \sum_{k\geq 2} \mathcal{F}_\ell^{(2k)}\left(\frac{x}{\Lambda^2}, \frac{M^2}{\Lambda^2}\right), \quad \operatorname{Im} A_{\ell\geq 2}^{\mathrm{S}}(x) = \sum_{k\geq 4} \mathcal{S}_{\ell\geq 2}^{(2k)}\left(\frac{x}{\Lambda^2}, \frac{u}{\Lambda^2}, \frac{M^2}{\Lambda^2}\right), \tag{2.34}$$

where the quantities with an upper index $(2k)$ are of a given chiral order $O(p^{2k})$.

We start with the discussion of the contribution of $\mathcal{F}_\ell^{(2k)}$ for $\ell = 0, 1$. (Note that in the case when there exists a complete partial wave decomposition, the contribution of the complete amplitude can be written in the form of $\mathcal{F}_\ell^{(2k)}$ with $\ell \geq 0$.) After the rescaling (followed by the substitution $x = \lambda y$), we obtain

$$\begin{aligned} 16N\lambda^n s^n \int_{\lambda s_{\mathrm{thr}}}^{\Lambda^2} \frac{\mathrm{d}x}{x^n} \frac{\mathcal{F}_\ell^{(2k)}\left(\frac{x}{\Lambda^2}, \lambda\frac{M^2}{\Lambda^2}\right) \mathrm{P}_\ell(\cos\theta(x, \lambda u, \lambda M^2))}{x - \lambda s} \\ = 16N\lambda^k s^n \int_{s_{\mathrm{thr}}}^{\Lambda^2/\lambda} \frac{\mathrm{d}y}{y^n} \frac{\mathcal{F}_\ell^{(2k)}\left(\frac{y}{\Lambda^2}, \frac{M^2}{\Lambda^2}\right) \mathrm{P}_\ell(\cos\theta(y, u, M^2))}{y - s}, \end{aligned} \tag{2.35}$$

where $\mathrm{P}_\ell(x)$ is a Legendre polynomial coming from the PW decomposition. Here, we have used the fact that $\mathcal{F}_\ell^{(2k)}$ and $\cos\theta$ are homogeneous[6] functions of the rescaled variables of degree k and 0 respectively.

Let us study the last integral in the limit $\lambda \to 0$. We split the integration into two parts $\int_{s_{\mathrm{thr}}}^{\Lambda^2} + \int_{\Lambda^2}^{\Lambda^2/\lambda}$. The first one precisely respects the chiral order of $\mathcal{F}_\ell^{(2k)}$, whereas the chiral order of the second part can be affected by its behavior for large upper bound. In the case of finite or logarithmically divergent integral

$$16Ns^n \int_{\Lambda^2}^{\infty} \frac{\mathrm{d}y}{y^n} \frac{\mathcal{F}_\ell^{(2k)}\left(\frac{y}{\Lambda^2}, \frac{M^2}{\Lambda^2}\right) \mathrm{P}_\ell(\cos\theta(y, u, M^2))}{y - s} \tag{2.36}$$

also the second part respects the chiral order of $\mathcal{F}_\ell^{(2k)}$. However, in the case where this integral is at least linearly divergent, the λ dependence of the upper bound can influence the chiral order we want to determine and so we have to proceed more carefully.

From the finiteness of the amplitude in the chiral limit and also in the limit $u \to 0$, functions $\mathcal{F}_\ell^{(2k)}\left(\frac{y}{\Lambda^2}, \frac{M^2}{\Lambda^2}\right)$ have to behave with large y as $O(y^k)$ or lower, whereas $\cos\theta(y, u, M^2) =$

[6]The usual appearance of chiral logarithms in the amplitude violates such homogeneity. Nevertheless, we are interested in the asymptotic behavior of the functions, which remains the same even in the presence of the logarithms and thus for simplicity we can claim the functions formally homogeneous.

$O(y^0)$. Therefore, the degree of divergence of integral (2.36) is $D \leq k-n$. As a consequence, for $k > n$ (provided the maximal divergence of the integral realizes) the integral in (2.35) behaves at worst as $\lambda^k \left(\frac{1}{\lambda}\right)^{k-n}$ and the minimal order with which $\mathcal{F}_\ell^{(2k)}$ contributes is $O(p^{2n})$, independently on the original chiral order $2k$.

From this discussion it should be obvious that we come to the same conclusions also for the functions $\mathcal{S}_{\ell\geq 2}^{(2k)}\left(\frac{x}{\Lambda^2}, \frac{u}{\Lambda^2}, \frac{M^2}{\Lambda^2}\right)$ from chiral expansion (2.34) since they are homogeneous function of degree k in all rescaled variables and from the same arguments as were presented for f_ℓ, they have to behave for large y as $O(y^k)$. [Note that in relations (2.35) and (2.36) there appears instead of $F_\ell^{(2k)}\mathrm{P}_\ell(\cos\theta)$ just $\mathcal{S}_{\ell\geq 2}^{(2k)}$.]

In the usual formulation of the theorem (such as [125]) the $\ell \geq 2$ contributions [with $k \geq 4$] are claimed to be thrown away as a remainder of $O(p^8)$ order. It could seem, therefore, that one should begin with at least four subtractions. However, by the following simple trick we show that the lower order contribution [of $O(p^6)$ order] of the $\ell \geq 2$ PW dispersion integral is just a polynomial.

For any function $X(x)$ (provided all integrals on both sides exist) it is possible to write

$$s^3 \int_{s_{\mathrm{thr}}}^{\Lambda^2} \frac{\mathrm{d}x}{x^3}\frac{X(x)}{x-s} = s^3 \int_{s_{\mathrm{thr}}}^{\Lambda^2} \frac{\mathrm{d}x\, X(x)}{x^4} + s^4 \int_{s_{\mathrm{thr}}}^{\Lambda^2} \frac{\mathrm{d}x}{x^4}\frac{X(x)}{x-s}\,. \tag{2.37}$$

This relation implies that the thrice subtracted integral of the terms giving the $O(p^6)$ contribution can be divided into two parts — the first one is a polynomial term, which can be included into $P_4(s,t;u)$, and the second part leads according to the analysis from the previous paragraphs to a contribution of the lower order from either $O(p^8)$ or $O(p^{2k})$, with k being the chiral order of the function $X(x)$. From that it is obvious that it is sufficient to begin with three subtractions since both the $O(p^6)$ part of the contribution of remainder $A_{\ell\geq 2}$ and the $O(p^6)$ contribution stemming from the parts of S and P partial waves that are of chiral order $O(p^8)$ or higher can be absorbed into the subtraction polynomial of third order $P_4(s,t;u)$.

Note also that integral (2.36) corresponds in fact to the difference between having in the upper bound of integrations Λ^2 and having there infinity. Its possible divergence is therefore the reason, why we have to be careful if we want to change the upper bound in these integrals back to infinity in the final form of the theorem[7]. We have seen that its maximal order of divergence is $k-n$, so in order to guarantee this change in all possible dispersion integrals to the $O(p^8)$ order in general, it would be safer to begin with four subtractions. However, in the practical applications of the theorem, we can examine divergences of the integrals appearing there one by one and potentially apply the trick (2.37) for increasing the number of subtraction in the individual integrals, thereby making this change of the upper bound possible also for them. (In Section 2.5 we will see how this works for a specific sort of functions appearing in our particular applications of the theorem.)

But now, let us continue with the proof of the theorem. We have shown that it is natural to choose $n = 3$ and truncate the partial-wave expansion of imaginary parts taking

[7]The footnote 5 on page 19 is valid only for the complete amplitude $S(s,t,u)$. Its expansion into PWs could in principle disrupt this possibility.

into account just S and P waves (and we do not even need the existence of the further PWs). From the P-wave contribution we extract the following polynomial term with its coefficients depending on u (on the last line in the following relation), which can be included into $P_4(s,t;u)$,

$$48Ns^3\int_{s_{\rm thr}}^{\Lambda^2}\frac{{\rm d}x}{x^3}\frac{x(s+t-x-u)}{x-s}\,{\rm Im}\,\frac{f_1^{\rm S}(x)}{\lambda_{AB}^{1/2}(x)\lambda_{CD}^{1/2}(x)}$$
$$=48Ns^3(t-u)\int_{s_{\rm thr}}^{\Lambda^2}\frac{{\rm d}x}{x^2(x-s)}\,{\rm Im}\,\frac{f_1^{\rm S}(x)}{\lambda_{AB}^{1/2}(x)\lambda_{CD}^{1/2}(x)}$$
$$-48Ns^3\int_{s_{\rm thr}}^{\Lambda^2}\frac{{\rm d}x}{x^2}\,{\rm Im}\,\frac{f_1^{\rm S}(x)}{\lambda_{AB}^{1/2}(x)\lambda_{CD}^{1/2}(x)}\,. \quad (2.38)$$

In order to implement the $s\leftrightarrow u$ crossing into the dispersive part $U(s,t,u)$, we add and subtract the U-channel terms written as the following third order polynomial in s and t (with u-dependent coefficients)

$$16Nu^3\int_{u_{\rm thr}}^{\Lambda^2}\frac{{\rm d}x}{x^3}\,\frac{{\rm Im}\,f_0^{\rm U}(x)}{x-u}+48Nu^3(t-s)\int_{u_{\rm thr}}^{\Lambda^2}\frac{{\rm d}x}{x^2(x-u)}\,{\rm Im}\,\frac{f_1^{\rm U}(x)}{\lambda_{AD}^{1/2}(x)\lambda_{CB}^{1/2}(x)}$$
$$+48Nu^3\Delta_{AD}\Delta_{CB}\int_{u_{\rm thr}}^{\Lambda^2}\frac{{\rm d}x}{x^3(x-u)}\,{\rm Im}\,\frac{f_1^{\rm U}(x)}{\lambda_{AD}^{1/2}(x)\lambda_{CB}^{1/2}(x)}\,. \quad (2.39)$$

Until now, we have restricted in no way the u-dependence of the polynomial $P_4(s,t;u)$. However, we can write similar representations for the T- and the U-crossed amplitudes starting with fixed u and fixed t dispersion relations for ${\rm T}(s,t;u)$ and ${\rm U}(s;t,u)$, respectively, obtaining so the corresponding subtraction polynomials $P_4^{\rm T}(s,t;u)$ and $P_4^{\rm U}(s;t,u)$. Crossing property and the symmetric form of the dispersive part imply that these polynomials should obey relation

$$P_4^{\rm S}(s,t;u)=P_4^{\rm T}(t,s;u)=P_4^{\rm U}(u;t,s). \quad (2.40)$$

In Appendix A we show that under assumption (v) of the theorem, the analyticity of the amplitude, the subtraction function $P_4(s,t;u)$ that satisfies relations (2.40) has to be a sixth order polynomial in all Mandelstam variables $R(s,t,u)$. On top of that, in the following we discuss how to take care of the terms that are of higher than third polynomial order.

Discarding the terms that contribute only to the $O(p^8)$ remainder, the coefficients of the remaining above-mentioned higher-polynomial-order terms have to be singular in the chiral limit. However, as the complete amplitude should be finite in that limit, these divergences have to be canceled with the divergences of the dispersive part. We can use this fact for the determination of these coefficients. Therefore, they are completely fixed by the divergences of the dispersion integrals, which we obtain from the following correspondence

between the divergences in the chiral limit and the UV asymptotics of the integrals [cf. with the asymptotic conditions of [95]]. For every term $\Phi_i^{(2k)}$ of chiral order $O(p^{2k})$, there holds for $\lambda \to \infty$

$$\Phi_i^{(2k)}(\lambda s, \lambda t; \lambda u; M^2) = \lambda^k \Phi_i^{(2k)}(s, t; u; M^2/\lambda). \tag{2.41}$$

It means that $\Phi_i^{(2k)}$ behaves for $\lambda \to \infty$ as $O(\lambda^{k+d})$, where d is the degree of divergence of $\Phi_i^{(2k)}$ in the chiral limit. As a consequence, dispersion integrals with higher than logarithmic divergences in the chiral limit have to have UV asymptotics at least $O(\lambda^3)$ [since their chiral order is at least $O(p^4)$].

The UV asymptotic behavior of the individual integrals is

$$s^3 \int_{s_{\rm thr}}^{\Lambda^2} \frac{{\rm d}x}{x^3} \frac{{\rm Im}\, f_0^{\rm S}(x)}{x-s} \to -\lambda^2 s^2 \int_{s_{\rm thr}}^{\Lambda^2} \frac{{\rm d}x}{x^3}\, {\rm Im}\, f_0^{\rm S}(x), \tag{2.42}$$

$$\begin{aligned} &s^3 \Delta_{AB}\Delta_{CD} \int_{s_{\rm thr}}^{\Lambda^2} \frac{{\rm d}x}{x^3(x-s)}\, {\rm Im}\, \frac{f_1^{\rm S}(x)}{\lambda_{AB}^{1/2}(x)\lambda_{CD}^{1/2}(x)} \\ &\qquad \to -\lambda^2 s^2 \Delta_{AB}\Delta_{CD} \int_{s_{\rm thr}}^{\Lambda^2} \frac{{\rm d}x}{x^3}\, {\rm Im}\, \frac{f_1^{\rm S}(x)}{\lambda_{AB}^{1/2}(x)\lambda_{CD}^{1/2}(x)}\,, \end{aligned} \tag{2.43}$$

$$\begin{aligned} &s^3 (t-u) \int_{s_{\rm thr}}^{\Lambda^2} \frac{{\rm d}x}{x^2(x-s)}\, {\rm Im}\, \frac{f_1^{\rm S}(x)}{\lambda_{AB}^{1/2}(x)\lambda_{CD}^{1/2}(x)} \\ &\qquad \to -\lambda^3 s^2 (t-u) \int_{s_{\rm thr}}^{\Lambda^2} \frac{{\rm d}x}{x^2}\, {\rm Im}\, \frac{f_1^{\rm S}(x)}{\lambda_{AB}^{1/2}(x)\lambda_{CD}^{1/2}(x)}\,. \end{aligned} \tag{2.44}$$

Hence, the first two integrals possess in chiral limit maximally logarithmic divergence, whereas the last one diverges like $1/M^2$ and this divergence has to be canceled by the divergent part of the coefficients of the polynomial $R(s,t,u)$. Note also that the only divergent coefficient is the one accompanying the polynomial of third order, and so the terms of higher than third order contributes in fact at least as $O(p^8)$ and can be therefore included into the remainder.

Finally, we simplify further the reconstructed form of the amplitude by making use of relation (2.37). The linearly divergent part of the polynomial together with the divergent part of the dispersion integral combine into

$$\begin{aligned} &s^3 (t-u) \int_{s_{\rm thr}}^{\Lambda^2} \frac{{\rm d}x}{x^2(x-s)}\, {\rm Im}\, \frac{f_1^{\rm S}(x)}{\lambda_{AB}^{1/2}(x)\lambda_{CD}^{1/2}(x)} \\ &\qquad + s^2 (t-u) \int_{s_{\rm thr}}^{\Lambda^2} \frac{{\rm d}x}{x^2}\, {\rm Im}\, \frac{f_1^{\rm S}(x)}{\lambda_{AB}^{1/2}(x)\lambda_{CD}^{1/2}(x)} \\ &\qquad\qquad = s^2 (t-u) \int_{s_{\rm thr}}^{\Lambda^2} \frac{{\rm d}x}{x(x-s)}\, {\rm Im}\, \frac{f_1^{\rm S}(x)}{\lambda_{AB}^{1/2}(x)\lambda_{CD}^{1/2}(x)} \end{aligned} \tag{2.45}$$

and we end up with the final form of the theorem (2.21).

2.5 Possible further simplifications in the theorem

As is obvious from the proof of the theorem, one can work with the theorem also considering it as a search for functions $W^{\ell}_{S,T,U}(s)$ analytic in complex s-plane, with the exception of the right-hand cut on the real axis that is given by the discontinuities (imaginary parts)

$$\operatorname{Im} W^0_{\mathrm{S}}(s) = 16\pi N \left(\operatorname{Im} f^{\mathrm{S}}_0(s) + 3\Delta_{AB}\Delta_{CD} \operatorname{Im} \frac{f^{\mathrm{S}}_1(s)}{\lambda^{1/2}_{AB}(s)\lambda^{1/2}_{CD}(s)} \right) \theta(s - s_{\mathrm{thr}}), \tag{2.46}$$

$$\operatorname{Im} W^1_{\mathrm{S}}(s) = 48\pi N \operatorname{Im} \frac{f^{\mathrm{S}}_1(s)}{\lambda^{1/2}_{AB}(s)\lambda^{1/2}_{CD}(s)} \, \theta(s - s_{\mathrm{thr}}) \tag{2.47}$$

[and similarly for T and U channel functions]; that have maximally logarithmic divergence in the chiral limit. All such functions differ just in a polynomial which can be included into $R(s,t,u)$. The way how one finds them is therefore not that important and one can for instance try to assemble them from some functions of known analytic behavior without even calculating a single integral as was presented in [95]. However, many times we will not succeed in finding the functions $W^{\ell}_{S,T,U}(s)$ in such a closed form and the only representation we will have for them will be the integral one [from (2.23) and (2.24)]. Not only in that case the following discussion of further possible simplifications of these integrals will be useful.

The situation is simplified even more by the fact that in all applications in that we use the theorem the integrands factorize into Laurent polynomials[8] multiplying some dimensionless functions $F_i(x)$ of chiral order $O(p^0)$, so we are in fact computing integrals of the type

$$w_i(s) = s^3 \int_{s_{\mathrm{thr}}}^{\Lambda^2} \frac{\mathrm{d}x}{x^3} \frac{F_i(x)}{x - s} \sum_m a^{(i)}_m x^m \equiv \sum_m w^{(i)}_m(s). \tag{2.48}$$

In the following we discuss the conditions under which we can factor these polynomials out of the integral, thereby leaving in the dispersion integrals just the functions $F_i(x)$ with some given numbers of subtractions. Naturally after performing this we have to change appropriately the polynomial coefficients of the theorem.

For any meromorphic function $F_i(x)$ growing at infinity not faster than any polynomial, there exists an integer $n_{\min}$ such that n-times subtracted dispersion integral

$$G^n_i(s) = s^n \int_{s_{\mathrm{thr}}}^{\infty} \frac{\mathrm{d}x}{x^n} \frac{F_i(x)}{x - s} \tag{2.49}$$

converges for $n \geq n_{\min}$. For the further uses we denote also

$$g^n_i(s) = s^n \int_{s_{\mathrm{thr}}}^{\Lambda^2} \frac{\mathrm{d}x}{x^n} \frac{F_i(x)}{x - s} \,. \tag{2.50}$$

[8] Laurent polynomials are generalized polynomials containing also terms with negative powers of their variables.

We start by formal factoring of the polynomial term $a_m^{(i)} s^m$ out of integral (2.48),

$$w_m^{(i)}(s) = a_m^{(i)} s^m s^{3-m-n} s^n \int_{s_{\rm thr}}^{\Lambda^2} \frac{\mathrm{d}x}{x^n} \frac{F_i(x)}{x-s} x^{m+n-3}. \tag{2.51}$$

For various values of $m+n$ we use an analogue of (2.37) to obtain an expression where the polynomial multiplies precisely the dispersion integral $g_i^n(s)$:

- $m+n=3$. In this simple case, we directly have

$$w_m^{(i)}(s) = a_m^{(i)} s^m g_i^n(s). \tag{2.52}$$

- $m+n>3$. Here we use the identity

$$\frac{x^{m+n-3}}{x-s} = \frac{s^{m+n-3}}{x-s} + \sum_{j=0}^{m+n-4} s^j x^{m+n-4-j} \tag{2.53}$$

  to obtain

$$w_m^{(i)}(s) = a_m^{(i)} s^m g_i^n(s) + a_m^{(i)} \sum_{j=3-m}^{n-1} s^{m+j} \int_{s_{\rm thr}}^{\Lambda^2} \mathrm{d}x \frac{F_i(x)}{x^{j+1}}\,. \tag{2.54}$$

  Obviously the sum generates only a polynomial contribution.

- $m+n<3$. Using

$$\frac{1}{x-s}\frac{1}{x^{3-m-n}} = \frac{1}{x-s}\frac{1}{s^{3-m-n}} - \sum_{j=1}^{3-m-n} \frac{1}{s^j}\frac{1}{x^{4-m-n-j}} \tag{2.55}$$

  the integral can be rewritten into

$$w_m^{(i)}(s) = a_m^{(i)} s^m g_i^n(s) - a_m^{(i)} \sum_{j=n}^{2-m} s^{m+j} \int_{s_{\rm thr}}^{\Lambda^2} \mathrm{d}x \frac{F_i(x)}{x^{j+1}}. \tag{2.56}$$

  For $m+n \geq 0$ the sum generates again just a polynomial contribution.

In summary, for $n \geq \max(n_{\min}, -m)$ the difference induced by the discussed factorization is just a polynomial. Now, we shall determine its behavior in the chiral limit similarly as in the proof of the theorem. To that end we use again the correspondence between the UV asymptotics and the degree of divergence in the chiral limit (as in (2.41)). Since n was chosen so that $G_i^n(s)$ converges, the UV asymptotics ($\lambda \to \infty$) of $g_i^n(s)$ reads [we indicate here explicitly the dependence on the generic mass M and on the threshold Λ]

$$g_i^n(\lambda s, M^2, \Lambda^2) = O(\lambda^{n-1}) \tag{2.57}$$

and its chiral order is $O(p^0)$. This gives us its behavior in the chiral limit (for $\mu \to 0$) as

$$g_i^n\left(s, \mu M^2, \Lambda^2\right) = O\left(\mu^{1-n}\right). \tag{2.58}$$

Therefore, if the chiral order of $a_m^{(i)} s^m$ is $O(p^{2d})$, which means

$$a_m^{(i)}\left(\mu M^2, \Lambda^2\right) s^m = \mu^{-m} a_m^{(i)}\left(\mu M^2, \Lambda^2\right)(\mu s)^m = O\left(\mu^{d-m}\right), \tag{2.59}$$

the integral with the factorized polynomial behaves as

$$a_m^{(i)}(\mu M^2, \Lambda^2) s^m g_i^n(s, \mu M^2, \Lambda^2) = O(\mu^{d+1-m-n}). \tag{2.60}$$

Thus, this object is divergent in the chiral limit with the degree of divergence $m+n-d-1$ in the cases when this number is positive. Since the full amplitude is at worst logarithmic divergent, such divergence has to be canceled out by the divergence of the polynomial, which is by this condition fixed.

This leads us to the conclusion that if we take n from the interval

$$\max(n_{\min}, -m) \leq n \leq d + 1 - m, \tag{2.61}$$

the difference between the original integral and the factorized one is a polynomial, which is maximally logarithmic divergent in the chiral limit and can be included into the third order polynomial of the theorem with a remainder of $O(p^8)$ order.

Finally, we discuss the possibility of replacement of the upper bound in $g_i^n(s)$ from Λ^2 back to ∞, i.e. the replacement of $g_i^n(s)$ with the corresponding $G_i^n(s)$. The difference induced by this replacement is

$$\Delta g_i^n(s, M^2, \Lambda^2) = s^n \int_{\Lambda^2}^{\infty} \frac{\mathrm{d}x}{x^n} \frac{F_i(x)}{x - s}. \tag{2.62}$$

Before studying its properties we note that already from using the same methods as in the proof of the theorem [around relations (2.35) and (2.36)] we can determine its chiral order. Indeed, from the existence of a finite $G_i^{n_{\min}}$ it follows that the difference $\Delta g_i^n(\lambda s, \lambda M^2, \Lambda^2)$ behaves in the limit $\lambda \to 0$ at worst as $O\left((\frac{1}{\lambda})^{n_{\min}-n}\right)$ and its contribution is at least of chiral order $O\left(p^{2(d+n-n_{\min})}\right)$, where $O\left(p^{2d}\right)$ is chiral order of the polynomial $a_m^{(i)} s^m$. For $n > n_{\min}$ we can therefore include this difference into the $O\left(p^{2d+2}\right)$ remainder of the theorem. However, in order to enable such replacement in the case $n = n_{\min}$, one needs to impose additional requirements on the functions $F_i(s)$.

We start our analysis of (2.62) by increasing the number of subtraction [cf. with (2.37)]

$$\Delta g_i^n(s, M^2, \Lambda^2) = s^n \int_{\Lambda^2}^{\infty} \frac{\mathrm{d}x}{x^{n+1}} F_i(x) + s^{n+1} \int_{\Lambda^2}^{\infty} \frac{\mathrm{d}x}{x^{n+1}} \frac{F_i(x)}{x - s} \tag{2.63}$$

and the observation that the only potentially problematic term is $\gamma_i^{n_{\min}} s^{n_{\min}}$ with the coefficient

$$\gamma_i^n(M^2, \Lambda^2) = \int_{\Lambda^2}^{\infty} \frac{\mathrm{d}x}{x^{n+1}} F_i(x). \tag{2.64}$$

We make use of the dimensionlessness of the functions $F_i(s)$, i.e. of the possibility to write $F_i(s, M^2) = \mathcal{F}_i\left(\frac{s}{M^2}\right)$. Rescaling $M^2 \to \lambda M^2$ in the limit $\lambda \to 0$ then leads to

$$\gamma_i^n(\lambda M^2, \Lambda^2) = \int_{\Lambda^2}^{\infty} \frac{\mathrm{d}x}{x^{n+1}} \mathcal{F}_i\left(\frac{x}{\lambda M^2}\right) = \frac{1}{\lambda^n} \int_{\Lambda^2/\lambda}^{\infty} \frac{\mathrm{d}y}{y^{n+1}} \mathcal{F}_i\left(\frac{y}{M^2}\right) = \frac{1}{\lambda^n} \int_{\Lambda^2/\lambda}^{\infty} \frac{\mathrm{d}y}{y^{n+1}} F_i(y). \tag{2.65}$$

For $n > n_{\min}$ we first check the above-stated chiral behavior of this term. The existence of $G_i^{n_{\min}}(s)$ implies $\lim_{x\to\infty} \frac{F_i(x)}{x^{n_{\min}}} = 0$, which means that for any $\varepsilon > 0$

$$\left|\frac{F_i(x)}{x^{n_{\min}}}\right| \leq \frac{\varepsilon}{\Lambda^{2n_{\min}}} \tag{2.66}$$

for all $x > x_0$ and some suitable x_0. Then, for $n > n_{\min}$ and small enough λ

$$\left|\gamma_i^n(\lambda M^2, \Lambda^2)\right| \leq \frac{1}{\lambda^n} \frac{\varepsilon}{\Lambda^{2n_{\min}}} \int_{\Lambda^2/\lambda}^{\infty} \frac{\mathrm{d}y}{y^{n-n_{\min}+1}} = \frac{\varepsilon}{(n-n_{\min})\Lambda^{2n}} \frac{1}{\lambda^{n_{\min}}}, \tag{2.67}$$

and so the polynomial difference $a_m^{(i)} s^m \gamma_i^n s^n$ contributes indeed with chiral order at least $O\left(p^{2(d+n-n_{\min})}\right)$.

Also for $n = n_{\min}$ one could try to include this polynomial into polynomial $R(s,t,u)$ of the theorem. Nevertheless, by performing this we could introduce divergences to its coefficients since γ_i^n can diverge as bad as $\frac{1}{\lambda^{n_{\min}}}$.

Naturally, this was just a general reasoning and there exist sorts of functions for which the change of the upper bound back to infinity induces just a difference, which can be included into the remainder and eventually also to the polynomial of the theorem. One example of such functions are the functions behaving for $x \to \infty$ as $x^{n_{\min}-1}$, i.e. those for which there exist suitable K and x_0 such that

$$\left|\frac{F_i(x)}{x^{n_{\min}-1}}\right| \leq \frac{K}{\Lambda^{2(n_{\min}-1)}} \tag{2.68}$$

for all $x > x_0$. (Note that this condition implies (2.66).) Then the bounds on $\gamma_i^n(\lambda M^2, \Lambda^2)$ for $n > n_{\min} - 1$ read

$$\left|\gamma_i^n(\lambda M^2, \Lambda^2)\right| \leq \frac{1}{\lambda^n} \frac{K}{\Lambda^{2n_{\min}-2}} \int_{\Lambda^2/\lambda}^{\infty} \frac{\mathrm{d}y}{y^{n-n_{\min}+2}} = \frac{K}{(n-n_{\min}+1)\Lambda^{2n}} \frac{1}{\lambda^{n_{\min}-1}}. \tag{2.69}$$

The polynomial difference of such function therefore contributes with chiral order at least $O\left(p^{2(d+n-n_{\min}+1)}\right)$ and thus it can be included into the $O\left(p^{2(d+1)}\right)$ remainder of the theorem even for $n = n_{\min}$.

Looking carefully at the reasoning of this statement we can realize that even if we take a function behaving at infinity as $x^{n_{\min}-1}\log^j x$, with some integer j (i.e. if we add some logarithmic divergence), the conclusion will be the same. For λ small enough and $n > n_{\min} - 1$, we have

$$\left|\gamma_i^n(\lambda M^2, \Lambda^2)\right| \leq \frac{1}{\lambda^n} \frac{K}{\Lambda^{2n_{\min}-2}} \int_{\Lambda^2/\lambda}^{\infty} \frac{\log y\, \mathrm{d}y}{y^{n-n_{\min}+2}} = \frac{K}{\Lambda^{2n}} \frac{1}{\lambda^{n_{\min}-1}} \frac{\frac{1}{n-n_{\min}+1} + \log\Lambda^2 - \log\lambda}{(n-n_{\min}+1)}. \tag{2.70}$$

The logarithm $\log\lambda$ does not spoil the above-mentioned chiral power-counting and similarly also for any $j \geq 1$.

This partial discussion has the conclusion that in the reconstructed form of amplitudes we can replace the function $g_i^n(s)$ with $G_i^n(s)$ at least in the following three cases

$$\left.\begin{array}{ll} 1) & n > n_{\min}, \\ 2) & n \geq n_{\min} \text{ and } F_i(x) \sim x^{n_{\min}-1} \text{ for } x \to \infty, \\ 3) & n \geq n_{\min} \text{ and } F_i(x) \sim x^{n_{\min}-1} \log^j x \text{ for } x \to \infty. \end{array}\right\} \tag{2.71}$$

In these cases the difference induced by this replacement can be included into the remainder of chiral order $O(p^{2d+2})$. We will see that all the functions that appear in our applications belong to either one of these categories.

For the second integral of the reconstruction theorem,

$$v_i(s) = s^2 \int_{s_{\rm thr}}^{\Lambda^2} \frac{\mathrm{d}x}{x} \frac{F_i(x)}{x-s} \left(\frac{1}{x} \sum_m b_m^{(i)} x^m \right) \equiv \sum_m v_m^{(i)}(s), \tag{2.72}$$

we can repeat a similar procedure. To keep the analogy as close as possible, we have shifted the powers m of the polynomial by factoring $\frac{1}{x}$ out of it. By that the integrals looks like regular twice subtracted dispersion integral and the arguments of the case discussed above remain valid with the simple change of the number of subtractions from three into two. However, since we are not interested in the exact form of the difference obtained by the factorization of the polynomial (we include it into the polynomial of the theorem) and since the condition for n (2.61) does not depend on the number of subtractions we have started with, it remains unaltered. The only difference is connected with the chiral order of the corrections (2.62). They are multiplied by $(t-u)b_m^{(i)}s^m$ and thus they contribute with chiral order $O\left(p^{2(d+1+n+m)}\right)$.

Summary

Summarily, in the theorem we can write instead of integral

$$s^3 \int_{s_{\rm thr}}^{\Lambda^2} \frac{\mathrm{d}x}{x^3} \frac{F_i(x)}{x-s}\, a_m^{(i)} x^m \tag{2.73}$$

with a dimensionless function $F_i(s)$ and a polynomial term $a_m^{(i)}s^m$ of chiral order $O(p^{2d})$, its simplified form

$$a_m^{(i)} s^m G_i^n(s), \tag{2.74}$$

where $G_i^n(s)$ is n-times subtracted dispersion integral of the function $F_i(s)$

$$G_i^n(s) = s^n \int_{s_{\rm thr}}^{\infty} \frac{\mathrm{d}x}{x^n} \frac{F_i(x)}{x-s} \tag{2.75}$$

and this number of subtractions lies in the interval

$$\max(n_{\min}, -m) \leq n \leq d + 1 - m \tag{2.76}$$

with $n_{\min}$ being the minimal number of subtraction for which the dispersion integral (2.75) converges. The number n has to be connected with the function $F_i(x)$ also by fulfillment of one of the conditions (2.71). This change is connected with a redefinition of the polynomial parameters of the theorem.

Further, the integral

$$s^2 \int_{s_{\text{thr}}}^{\Lambda^2} \frac{\mathrm{d}x}{x} \frac{F_i(x)}{x - s} \frac{1}{x} b_m^{(i)} x^m \tag{2.77}$$

in the theorem with a polynomial term $b_m^{(i)} s^m$ of chiral order $O(p^{2d})$ can be simplified (together with a redefinition of the polynomial parameters) into

$$b_m^{(i)} s^m G_i^n(s), \tag{2.78}$$

where n satisfies inequality (2.76) and one of the conditions (2.71).

We conclude with the remark that since a constant is also a polynomial, this procedure can be used as well for lowering of the number of subtractions in the integral to any number satisfying (2.76).

Chapter 3

Application of the theorem for reconstruction of amplitudes in χPT

The reconstruction theorem enables us to construct a representation of an amplitude including two-loop corrections provided we know the discontinuities of the partial waves appearing in its formulation. For that end we can use the unitarity relation (2.18). For a successful construction of the amplitude we will therefore require to know all the intermediate amplitudes of the considered process. If they can be also constructed using the reconstruction theorem, we obtain a self-consistent system of amplitudes whose representations can be gained employing the two-step procedure depicted on Figure 1.

Its actual form varies for different processes but we will discuss here its general properties for any two-pseudoscalar-meson scattering process. For them we show in the next paragraph that in low-energy region up to and including two-loop order, it is sufficient to consider just the discontinuities connected with the intermediate states composed of two pseudoscalar mesons. Then the only inputs required for a successful application of the reconstruction procedure will be leading orders of all these amplitudes. Moreover, within the discussion of assumption (iii) of the theorem on page 16, we have shown that the LO amplitudes of the considered type have to be first order polynomials in Mandelstam variables.

We are concerned with processes up to (and excluding) $O(p^8)$ chiral order and (in accordance with the first assumption of the theorem) in the region below appearance of all non-Goldstone particles, we are thus away from the poles and the cuts of such intermediate states, and their effect is included just by the coefficient of polynomial part $R(s,t,u)$ of the reconstruction theorem (2.21) and by the higher orders. The intermediate states involving odd numbers of Goldstone bosons are forbidden by the chiral order of the odd-intrinsic-parity part of the effective Lagrangian — because the effect of the axial anomaly enters at the $O(p^4)$ order (Wess, Zumino and Witten [132,133]), such intermediate states induce the contribution of the order of at least $O(p^8)$. Furthermore, the contribution of the states with more than two Goldstone bosons is also suppressed to $O(p^8)$ since the n-Goldstone-boson invariant phase-space scales like p^{2n-4} and amplitudes with an arbitrary number of external

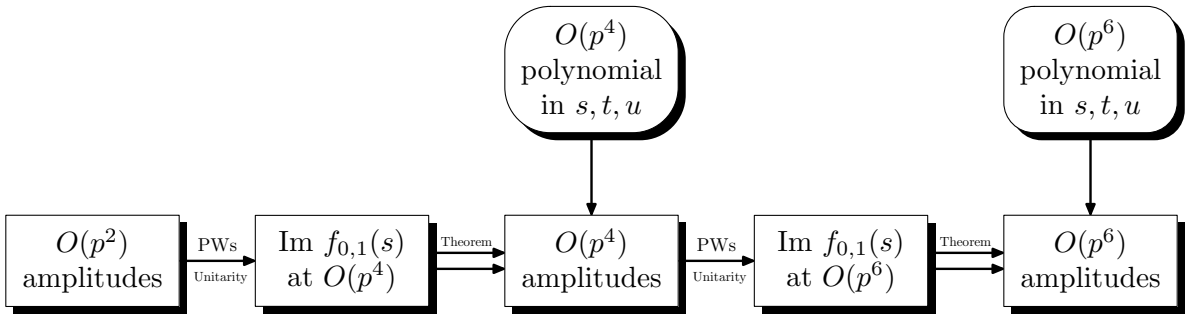

Figure 1: Schematic representation of the iterative two-step reconstruction procedure

Goldstone boson legs behave dominantly as $O(p^2)$. Consequently, the contribution of such $(n > 2)$ intermediate states to the imaginary part of the amplitude is according to the unitarity relation [cf. (2.18)] at least $O(p^8)$. Thus, we conclude that the only intermediate states that have to be taken into account are the two-Goldstone-boson ones.

3.1 First iteration

We show here how the first iteration generally works. In addition, we will be even able to present a general result of this iteration. But first, let us observe one simplification appearing here. Using similar arguments stemming from finiteness of the S-matrix in chiral limit as in the proof of the theorem, we observe that in order to obtain the amplitude valid up to $O(p^4)$, the required polynomial is just of the second order in Mandelstam variables.

Since the leading-order amplitudes are first order polynomials and the Mandelstam variables obey (2.6), we can decompose them according to

$$A = C\left(\alpha(s) + \beta(t-u)\right), \tag{3.1}$$

where $\alpha(s)$ is a first order polynomial in s. For further convenience we have introduced an overall normalization factor C. At this order, the amplitude therefore decomposes exactly into S and P waves only [using (2.15), (2.16) and (2.8)]

$$\phi_0(s) = \frac{C}{16\pi N}\left(\alpha(s) - \beta\frac{\Delta_{AB}\Delta_{CD}}{s}\right), \tag{3.2}$$

$$\phi_1(s) = \frac{C}{48\pi N}\,\beta\,\frac{\lambda_{AB}^{1/2}(s)\lambda_{CD}^{1/2}(s)}{s}\,. \tag{3.3}$$

By introducing them into unitarity relation (2.18) we obtain the following discontinuities

$$\begin{aligned}\operatorname{Im}\varphi_0(s) = \sum_k \frac{NC_{ik}C_{kf}}{S_k}\left[\left(\alpha_{ik}(s) - \beta_{ik}\frac{\Delta_{AB}\Delta_k}{s}\right)\left(\alpha_{kf}(s) - \beta_{kf}\frac{\Delta_k\Delta_{CD}}{s}\right)\right] \\ \times\left(\frac{1}{16\pi N}\right)^2\frac{\lambda_k^{1/2}(s)}{s}\,\theta(s-\mathrm{thr}_k),\end{aligned} \tag{3.4}$$

$$\begin{aligned}\operatorname{Im}\varphi_1(s) = \sum_k \frac{NC_{ik}C_{kf}}{S_k}\left[\beta_{ik}\,\frac{\lambda_{AB}^{1/2}(s)\lambda_k^{1/2}(s)}{s}\,\beta_{kf}\,\frac{\lambda_k^{1/2}(s)\lambda_{CD}^{1/2}(s)}{s}\right] \\ \times\left(\frac{1}{48\pi N}\right)^2\frac{\lambda_k^{1/2}(s)}{s}\,\theta(s-\mathrm{thr}_k),\end{aligned} \tag{3.5}$$

where the sums go over all the possible (two-meson) intermediate states k with the symmetry factor of such state S_k. All objects with lower index k are quantities related to this intermediate state. Similarly indices i and f refer to the initial and the final state, respectively. Finally, thr_k is the threshold of production of the intermediate state k.

Integrals (2.23)–(2.24) then read

$$\begin{aligned}W_{\mathrm{S}}^0(s) = \frac{1}{16\pi^2}\sum_k\frac{C_{ik}C_{kf}}{S_k}s^3\int_{\mathrm{thr}_k}^\infty\frac{\mathrm{d}x}{x^3(x-s)}\,\frac{\lambda_k^{1/2}(x)}{x}\Bigg(\alpha_{ik}(x)\alpha_{kf}(x) \\ -\left(\beta_{ik}\alpha_{kf}(x)\Delta_{AB}+\alpha_{ik}(x)\beta_{kf}\Delta_{CD}\right)\frac{\Delta_k}{x}+\beta_{ik}\beta_{kf}\Delta_{AB}\Delta_{CD}\frac{\Delta_k^2}{x^2} \\ +\frac{1}{3}\Delta_{AB}\Delta_{CD}\beta_{ik}\beta_{kf}\left(1-2\frac{\Sigma_k}{x}+\frac{\Delta_k^2}{x^2}\right)\Bigg),\end{aligned} \tag{3.6}$$

$$W_{\mathrm{S}}^1(s) = \frac{1}{48\pi^2}\sum_k\frac{C_{ik}C_{kf}}{S_k}\,\beta_{ik}\beta_{kf}\,s^2\int_{\mathrm{thr}_k}^\infty\frac{\mathrm{d}x}{x(x-s)}\,\frac{\lambda_k^{1/2}(x)}{x}\frac{1}{x}\left(x-2\Sigma_k+\frac{\Delta_k^2}{x}\right). \tag{3.7}$$

Now, we simplify them by using the methods discussed in Section 2.5. We see that in both cases we integrate the function $F(s)=\frac{\lambda_k^{1/2}(s)}{s}$ multiplied by some Laurent polynomial. Thanks to the behavior of the square root of triangle function $\lambda^{1/2}(s)\to s$ for $s\to\infty$, the dispersion integral of this function converges already for one subtraction, $n_{\min}=1$, and this function is of the type 2) from conditions (2.71). The first integral contains a polynomial of chiral order $O(p^4)$, i.e. $d=2$, and of polynomial order[1] $m=-2,\ldots,2$. The inequality (2.76) tells us that for $m=-2$ we have to take at least two subtractions, whereas for all the other polynomial terms it suffices just one of them (for $m=2$ it is at the same time their maximal number in order to obtain a difference that is at worst logarithmic divergent in the chiral limit). The polynomial[2] in the second integral has $d=1$ and its polynomial order takes values $m=-1,\ldots,1$. Hence, in this case the condition (2.76) restricts the number of subtraction to at least one (and for the terms with $m=-1$ and $m=0$ it is possible also to take more of them). For sake of simplicity we take always the minimal allowed number of subtractions. Using the once and the twice subtracted one-loop integrals, which are defined by

$$\bar{J}_{yz}(s) = \frac{s}{16\pi^2}\int_{(m_y+m_z)^2}^\infty\frac{\mathrm{d}x}{x(x-s)}\frac{\lambda_{yz}^{1/2}(x)}{x}, \tag{3.8}$$

[1] $\alpha(s)$ is a polynomial of maximally first order in s.

[2] Note that in this integral we have to identify the polynomial $b_m^{(i)}s^m$ without the $\frac{1}{x}$ that is extracted in front of the brackets in order to be in correspondence with the definitions of the quantities of Section 2.5.

$$\bar{\bar{J}}_{yz}(s) = \frac{s^2}{16\pi^2}\int_{(m_y+m_z)^2}^{\infty} \frac{\mathrm{d}x}{x^2(x-s)}\frac{\lambda_{yz}^{1/2}(x)}{x} \tag{3.9}$$

and discussed in the next section, we rewrite the functions of the theorem into the reduced form (with an appropriate change of the constants of polynomial $R(s,t,u)$)

$$W_{\mathrm{S}}^0(s) = \sum_k \frac{C_{ik}C_{kf}}{S_k}\Bigg(\left(\alpha_{ik}(s)\alpha_{kf}(s) - (\beta_{ik}\alpha_{kf}(s)\Delta_{AB} + \alpha_{ik}(s)\beta_{kf}\Delta_{CD})\,\frac{\Delta_k}{s}\right)\bar{J}_k(s) + \frac{4}{3}\beta_{ik}\beta_{kf}\Delta_{AB}\Delta_{CD}\frac{\Delta_k^2}{s^2}\bar{\bar{J}}_k(s) + \frac{1}{3}\beta_{ik}\beta_{kf}\Delta_{AB}\Delta_{CD}\left(1-\frac{2\Sigma_k}{s}\right)\bar{J}_k(s)\Bigg), \tag{3.10}$$

$$W_{\mathrm{S}}^1(s) = \frac{1}{3}\sum_k \frac{C_{ik}C_{kf}}{S_k}\,\beta_{ik}\beta_{kf}\,\left(s - 2\Sigma_k + \frac{\Delta_k^2}{s}\right)\bar{J}_k(s). \tag{3.11}$$

We obtain similar results also for the T- and the U-crossed parts. If we carry out the same extraction of polynomials also for the crossed parts, the symmetries of the polynomial of the theorem remain intact.

3.2 The one-loop integrals

In the results of first iteration, there appear integrals (3.8) and (3.9). For accomplishment of the second iteration we need to compute the S-wave and the P-wave projection of these results, i.e. we need to compute integrals of $\bar{J}(s)$ and $\bar{\bar{J}}(s)$. Moreover, for some processes it will be necessary to have an analytic continuation of the partial waves below the physical region[3] and thus also of the one-loop functions. Therefore, we make this small digression and discuss them here.

In accordance to the integral representation (3.8) and (3.9), we can write[4]

$$\bar{J}_{yy}(s) = \frac{1}{16\pi^2}\left(2 + \sigma_y(s)\log\frac{\sigma_y(s)-1}{\sigma_y(s)+1}\right), \tag{3.13}$$

$$\bar{J}_{yz}(s) = \frac{1}{16\pi^2}\left[1 + \left(\frac{\Delta_{yz}}{s} - \frac{\Sigma_{yz}}{\Delta_{yz}}\right)\log\frac{m_z}{m_y} + \frac{\lambda_{yz}^{1/2}(s)}{s}\log\frac{\lambda_{yz}^{1/2}(s) - \left(s-\mu_{yz}^-\right)}{\lambda_{yz}^{1/2}(s) + \left(s-\mu_{yz}^-\right)}\right], \tag{3.14}$$

$$\bar{\bar{J}}_{yz}(s) = \bar{J}_{yz}(s) - \frac{1}{16\pi^2}\left(\frac{\Sigma_{yz}}{2} + \frac{2m_y^2m_z^2}{\Delta_{yz}}\log\frac{m_z}{m_y}\right)\frac{s}{\Delta_{yz}^2}\,. \tag{3.15}$$

[3]The physical region is given by $s > (m_x + m_y)^2$.

[4]From relations (3.10) and (3.11) we observe that in the results there does not appear the double subtracted one-loop function for the states containing two particles of the same mass, $\bar{\bar{J}}_{yy}(s)$.

Note also that [cf. with (2.37)]

$$\bar{\bar{J}}_{yz}(s) = \bar{J}_{yz}(s) - \frac{s}{16\pi^2}\int_{(m_y+m_z)^2}^{\infty}\frac{\mathrm{d}x}{x^2}\frac{\lambda_{yz}^{1/2}(x)}{x} = \bar{J}_{yz}(s) - sJ'_{yz}(0). \tag{3.12}$$

In order to get a correct analytic continuation of these functions, we take the following choice of branch cuts and of the appropriate branches of the many-valued functions occurring there.

- the square root appearing in σ_y with the cut $(-\infty, 0)$ and the argument of its result belonging to the interval $(-\frac{\pi}{2}, \frac{\pi}{2}\rangle$; [Then within the physical region we have just the usual positive square root of positive real numbers.]
- all the logarithms with their cuts located on $(-\infty, 0)$ and $\operatorname{Im} \log z \in (-\pi, \pi\rangle$;
- square root of $\lambda_{yz}(s)$ with its cut on $\left(\mu_{yz}^-, \mu_{yz}^+\right)$ and the signs of the result according to

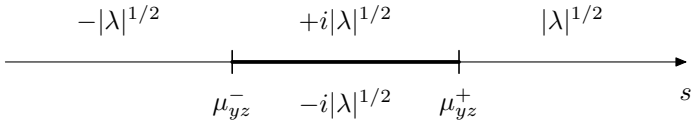

(3.16)

  i.e. it is positive within the physical scattering region. This choice is in accordance with the sign choice in the same mass limit $\lambda_{yz}^{1/2}(s) \underset{m_z \to m_y}{\to} s\sigma_y(s)$.

This is just one of a few possible choices resulting in the one-loop functions (3.13)–(3.15) being analytic in the complex plane with the physical cut $\left(\mu_{yz}^+, \infty\right)$. [The situation will be more complicated for the applications of the reconstruction procedure in the case of $K \to 3\pi$ and $\eta \to 3\pi$ as is discussed in Chapter 6.]

3.3 Obtaining the divergent parts of the chiral logarithms

Our arguments used in the proof of the theorem leading to the computation of divergences of dispersion integrals in the chiral limit can be used also for obtaining the divergent parts of chiral logarithms that appear in the amplitudes constructed using the theorem. We illustrate this on the result obtained by the first iteration. In all processes there appear just two dispersion integrals $\bar{J}_k(s)$ and $\bar{\bar{J}}_k(s)$, which are of chiral order $O(p^0)$. From the condition of finiteness of the complete amplitude in the chiral limit, we know that all their divergences have to be canceled by the divergences of coefficients of the polynomial which we are looking for. Using the correspondence (2.41) between these divergences and the UV asymptotics of the integrals ($\lambda \to \infty$)

$$16\pi^2 \bar{J}_{yz}(\lambda s) = -\int_{(m_y+m_z)^2}^{\Lambda^2} \frac{\mathrm{d}x}{x} \frac{\lambda_{yz}^{1/2}(x)}{x}\,, \tag{3.17}$$

$$16\pi^2 \bar{\bar{J}}_{yz}(\lambda s) = -\lambda s \int_{(m_y+m_z)^2}^{\Lambda^2} \frac{\mathrm{d}x}{x^2} \frac{\lambda_{yz}^{1/2}(x)}{x} - \int_{(m_y+m_z)^2}^{\Lambda^2} \frac{\mathrm{d}x}{x} \frac{\lambda_{yz}^{1/2}(x)}{x}\,, \tag{3.18}$$

we see that the first integral has only logarithmic divergence and the second also $1/M^2$. Indeed, after their integration (with the upper bound Λ^2), we obtain for the divergent parts

$(M^2 \to 0)$

$$\bar{J}_{yz}(s) \to \frac{1}{16\pi^2} \log \frac{M^2}{\Lambda^2}\,, \tag{3.19}$$

$$\bar{\bar{J}}_{yz}(s) \to -\frac{s\left(m_y^4 - m_z^4 + 2m_y^2 m_z^2 \log m_z^2/m_y^2\right)}{32\pi^2(m_y^2 - m_z^2)^3} + \frac{1}{16\pi^2} \log \frac{M^2}{\Lambda^2}\,. \tag{3.20}$$

The mass M^2 in the logarithms can be changed into any mass just by change of the finite part of the polynomial. Similarly, the scale Λ can be changed into any other scale, however, we have to introduce this scale also into the finite part of the coefficients in order to restore the independence on such scale of the complete result.

From relations (3.10) and (3.11), we gain the part of $U(s,t,u)$ that is divergent in the chiral limit,

$$W_{\mathrm{S}}^0(s) \to \frac{1}{16\pi^2} \sum_k \frac{C_{ik}C_{kf}}{S_k}\, \alpha_{ik}(s)\alpha_{kf}(s)\, \log \frac{M^2}{\Lambda^2}\,, \tag{3.21}$$

$$W_{\mathrm{S}}^1(s) \to \frac{1}{16\pi^2}\, \frac{s}{3} \sum_k \frac{C_{ik}C_{kf}}{S_k}\, \beta_{ik}\beta_{kf}\, \log \frac{M^2}{\Lambda^2}\,, \tag{3.22}$$

where in both $\alpha(s)$ we take only the parts which do not vanish for $M \to 0$ (as the rest is finite in the chiral limit), i.e. the terms of first order in s. The divergent part of the polynomial is determined by the requirement of canceling this divergence of the unitarity part.

3.4 Computation of the S and the P partial waves in NLO

The determination of the leading order partial waves was trivial since the amplitudes at that order were just polynomials. At the next-to-leading order the situation is different, we have to integrate some combinations of one-loop functions and the results will be more complicated since there could in principle appear six different masses in the expressions for partial waves. Naturally, this case would take place only provided in the application we are dealing with, there appeared so many masses and the process with all the masses different was kinematically possible. (In all the cases considered in this work there occur at most three different masses in the results.) Moreover, as we have already pointed out, in many particular cases we need to continue analytically the partial waves below the physical threshold and also to deform the integration contour of the PW integration, which is better to perform carefully for the individual processes. That are the reasons why we do not give the explicit results generally but instead we present the formulae leading to them, which are used thereafter for each particular application for obtaining the corresponding partial waves.

The unitarity part of the NLO results can be separated into three parts, each containing

the one-loop functions depending on one of the Mandelstam variables,

$$\begin{aligned} U(s,t,u) = &\left(P^a_{\rm S}(s,t)\bar{J}_a(s) + Q^a_{\rm S}\frac{\bar{\bar{J}}_a(s)}{s^2} \right) + \left(P^a_{\rm T}(t,s)\bar{J}_a(t) + Q^a_{\rm T}\frac{\bar{\bar{J}}_a(t)}{t^2} \right) \\ &+ \left(P^a_{\rm U}(u,s)\bar{J}_a(u) + Q^a_{\rm U}\frac{\bar{\bar{J}}_a(u)}{u^2} \right) = U_{\rm S}(s,t) + U_{\rm T}(t,s) + U_{\rm U}(u,s), \end{aligned} \tag{3.23}$$

where Q^a_I are constants and P^a_I Laurent polynomials containing terms with the power of Mandelstam variables varying from -1 to 2 [the remaining variable is eliminated from the polynomials by using relation (2.6)]. In this relation we sum over a being all the possible intermediate states.

To obtain the partial waves we perform integrations (2.15) and (2.16) of the amplitudes over cosine of the CMS scattering angle. The polynomial part of the amplitude, $R(s,t,u)$, and the S-part of the unitarity part, $U_{\rm S}(s,t,u)$, can be integrated trivially using inverted relations to (2.8),

$$t = \frac{3s_0 - s}{2} + \frac{\lambda^{1/2}_{AB}(s)\lambda^{1/2}_{CD}(s)\cos\theta - \Delta_{AB}\Delta_{CD}}{2s}, \tag{3.24}$$

$$u = \frac{3s_0 - s}{2} - \frac{\lambda^{1/2}_{AB}(s)\lambda^{1/2}_{CD}(s)\cos\theta - \Delta_{AB}\Delta_{CD}}{2s}. \tag{3.25}$$

For the integration of the T-part [depending only on t and s] and of the U-part [depending only on u and s], we perform the substitutions

$$\cos\theta = \frac{s(2t + s - 3s_0) + \Delta_{AB}\Delta_{CD}}{\lambda^{1/2}_{AB}(s)\lambda^{1/2}_{CD}(s)} = \frac{s(3s_0 - 2u - s) + \Delta_{AB}\Delta_{CD}}{\lambda^{1/2}_{AB}(s)\lambda^{1/2}_{CD}(s)}, \tag{3.26}$$

$$\mathrm{d}\cos\theta = \frac{2s}{\lambda^{1/2}_{AB}(s)\lambda^{1/2}_{CD}(s)}\,\mathrm{d}t = -\frac{2s}{\lambda^{1/2}_{AB}(s)\lambda^{1/2}_{CD}(s)}\,\mathrm{d}u \tag{3.27}$$

with the corresponding boundary values equal to

$$t_\pm(s) = \frac{3s_0 - s}{2} - \frac{\Delta_{AB}\Delta_{CD}}{2s} \pm \frac{\lambda^{1/2}_{AB}(s)\lambda^{1/2}_{CD}(s)}{2s}, \tag{3.28}$$

$$u_\pm(s) = \frac{3s_0 - s}{2} + \frac{\Delta_{AB}\Delta_{CD}}{2s} \mp \frac{\lambda^{1/2}_{AB}(s)\lambda^{1/2}_{CD}(s)}{2s}. \tag{3.29}$$

It means, we have

$$\varphi_0(s) = \frac{s}{16\pi N\lambda^{1/2}_{AB}(s)\lambda^{1/2}_{CD}(s)} \int_{\mathcal{C}(t_-(s),t_+(s))} \mathrm{d}t\, U_{\rm T}(t,s), \tag{3.30}$$

$$\varphi_1(s) = \frac{s^2}{16\pi N\lambda_{AB}\lambda_{CD}} \int_{\mathcal{C}(t_-(s),t_+(s))} \mathrm{d}t\, (2t - t_+ - t_-)U_{\rm T}(t,s) \tag{3.31}$$

and similarly for the integration over u of the U-part. The contour $\mathcal{C}\left(t_-(s), t_+(s)\right)$ connecting t_+ and t_- has to be deformed so that it avoids cuts of $U_{\mathrm{T}}(s,t)$, i.e. the T-channel cuts of the amplitude.

If the contour $\mathcal{C}\left(t_-(s), t_+(s)\right)$ has in addition the property that there exists an open neighborhood of every point on the contour where the integrands are continuous [i.e. if the contour not only avoids the cuts of $U_{\mathrm{T}}(s,t)$, but if its open neighborhood also does], the complex analysis (cf. e.g. [119]) tells us that the contour integral is equal to the difference between the values of the primitive function of integrand evaluated in the two endpoints t_+ and t_- (in the cases when such primitive function exists).

Since the integrands in (3.30) and (3.31) are linear combinations of $t^n \bar{J}_{yz}(t)$ and $t^{\bar{n}} \bar{\bar{J}}_{yz}(t)$ with $n = -1, \ldots, 3$ and $\bar{n} = -2, -1$, in that case it should be enough to find the following primitive functions

$$I_n^{yz}(t) = 16\pi^2 \int \mathrm{d}t\, t^n \bar{J}_{yz}(t), \quad \text{for } n = -1, \ldots, 3; \tag{3.32}$$

$$I_{-2}^{yz}(t) = 16\pi^2 \int \mathrm{d}t\, \frac{\bar{\bar{J}}_{yz}(t)}{t^2}\,, \tag{3.33}$$

and also

$$16\pi^2 \int \mathrm{d}t\, \frac{\bar{\bar{J}}_{yz}(t)}{t} = I_{-1}^{yz}(t) - \left(\frac{\Sigma_{yz}}{2} + \frac{2m_y^2 m_z^2}{\Delta_{yz}} \log\frac{m_z}{m_y}\right) \frac{t}{\Delta_{yz}^2}\,; \tag{3.34}$$

and evaluate them in the endpoints $t_\pm$. Naturally, the same chain of reasoning can be followed also for the U-part integration.

3.4.1 Primitive functions

From formulae (3.13)–(3.15) for the one-loop functions, we find the primitive functions introduced in the previous section. First, we deal with the case of different masses, where for sake of simple notation we denote the ratio of these masses q,

$$q = \frac{m_z}{m_y}\,. \tag{3.35}$$

The same-mass case will be obtained afterwards just by limiting $q \to 1$.

The following transformation of variables will prove to be useful [Remember our choice of the analytic continuation of $\lambda^{1/2}(t)$ in (3.16).]

$$\tau_{yz} = \frac{\lambda_{yz}^{1/2}(t) - (t - \mu_{yz}^-)}{\lambda_{yz}^{1/2}(t) + (t - \mu_{yz}^-)} = -\frac{t - \Sigma_{yz} - \lambda_{yz}^{1/2}(t)}{2m_y m_z}\,, \tag{3.36}$$

which simplifies in the equal-mass case to

$$\tau_y = \frac{\sigma_y(t) - 1}{\sigma_y(t) + 1}\,. \tag{3.37}$$

This transformation maps the complex plane with the cut (μ_{yz}^-, μ_{yz}^+) onto the unit disc. As denoted on Figure 2 the points slightly above the cut $(t + i\epsilon)$ are mapped slightly below the upper semi-circle while the points slightly below this cut $(t - i\epsilon)$ slightly above the lower semi-circle. (The points lying exactly on the upper and on the lower semi-circle have to be identified.) Ray $(\mu_{yz}^+ + i\epsilon, \infty + i\epsilon)$, where the branch cut of the one-loop function is located, is mapped onto line segment $(-1 + i\epsilon, 0 + i\epsilon)$. The inverse transformation

$$t(\tau_{yz}) = \Sigma_{yz} - m_y m_z \left(\tau_{yz} + \frac{1}{\tau_{yz}}\right), \tag{3.38}$$

$$\lambda_{yz}^{1/2}(t(\tau_{yz})) = m_y m_z \left(\tau_{yz} - \frac{1}{\tau_{yz}}\right), \tag{3.39}$$

$$\mathrm{d}t = -\frac{m_y m_z}{\tau_{yz}^2}\left(\tau_{yz}^2 - 1\right)\mathrm{d}\tau_{yz} \tag{3.40}$$

can be continued to the whole complex τ_{yz}-plane and satisfies

$$t(\tau_{yz}) = t(1/\tau_{yz}). \tag{3.41}$$

This means that the points τ and $1/\tau$ should be identified, which implies also the identification of τ and $\tau^\star = 1/\tau$ on the unit disc boundary of Figure 2.

In the same mass case $(q = 1)$ the inversion reduces to

$$t(\tau_y) = -\frac{m_y^2}{\tau_y}\left(\tau_y - 1\right)^2, \tag{3.42}$$

$$\sigma(\tau_y) = \frac{\tau_y + 1}{1 - \tau_y}, \tag{3.43}$$

$$\mathrm{d}t = -\frac{m_y^2}{\tau_y^2}\left(\tau_y^2 - 1\right)\mathrm{d}\tau_y\,. \tag{3.44}$$

The transformed one-loop functions read[5]

$$16\pi^2 \bar{J}_q(\tau_{yz}) = 1 - \frac{\Sigma_{yz}}{\Delta_{yz}}\log q - \frac{\tau_{yz}(1-q^2)}{(\tau_{yz}-q)(\tau_{yz}q-1)}\log q + \frac{q(1-\tau_{yz}^2)}{(\tau_{yz}-q)(\tau_{yz}q-1)}\log\tau_{yz}, \tag{3.46}$$

$$16\pi^2 \bar{J}_1(\tau_{yz}) = 2 + \frac{1+\tau_{yz}}{1-\tau_{yz}}\log\tau_{yz}. \tag{3.47}$$

Their analyticity in the unit disc with the segment $\langle -1, 0\rangle$ removed and the symmetry $\bar{J}(\tau) = \bar{J}(1/\tau)$ are in these relations manifest.

[5]We note the following relation enabling the computation of the one-loop function $q \neq 1$ from the knowledge of the equal-mass one

$$\bar{J}_q(\tau_{yz}) = \frac{1}{2}\left(\bar{J}_1(q\tau_{yz}) + \bar{J}_1\left(\frac{\tau_{yz}}{q}\right) - \bar{J}_1\left(q^2\right)\right). \tag{3.45}$$

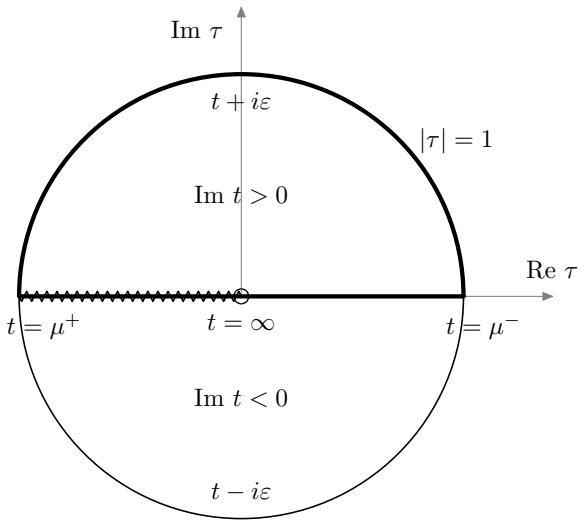

Figure 2: Conformal transformation (3.36) mapping complex t-plane onto unit disc in τ-plane. The points on upper and on the lower semi-circle are identified. In the transformed plane the one-loop functions to which the transformation corresponds have their branch cut located on the line segment $\tau \in (-1 + i\epsilon, 0 + i\epsilon)$.

From the mixed form of the integral

$$16\pi^2 \bar{J}_q(t) = 1 + \left(\frac{\Delta_{yz}}{t} - \frac{\Sigma_{yz}}{\Delta_{yz}}\right)\log q + \frac{m_y m_z}{t}\frac{\tau_{yz}^2 - 1}{\tau_{yz}}\log \tau_{yz}, \tag{3.48}$$

one obtain the following simple form of the derivative

$$16\pi^2 \frac{\mathrm{d}}{\mathrm{d}t}\left(t\bar{J}_q(t)\right) = \frac{1 + \tau_{yz}^2}{1 - \tau_{yz}^2}\log \tau_{yz} - \frac{1 + q^2}{1 - q^2}\log q, \tag{3.49}$$

which makes it easy to check the primitive functions given here.

Finally, we introduce the following function appearing in the results of integration

$$\mathcal{J}(\tau_{yz}) = \log q \log \tau_{yz} + \mathrm{Li}_2(1 - q\tau_{yz}) - \mathrm{Li}_2\left(1 - \frac{\tau_{yz}}{q}\right). \tag{3.50}$$

Having prepared all the necessary ingredients, we present here a list of all primitive functions that will be needed for computation of S and P partial waves.

$$I_1^{yz}(t) = 8\pi^2 \bar{J}_q(t) t(t - \Sigma_{yz}) + \frac{t^2}{4} - 2m_y^2 m_z^2 t \frac{\log q}{\Delta_{yz}} + m_y^2 m_z^2 \log^2 \tau_{yz}, \tag{3.51}$$

$$\begin{aligned} I_2^{yz}(t) = {} & \frac{8\pi^2}{3}\bar{J}_q(t) t\left(2t^2 - \Sigma_{yz} t - (\Sigma_{yz}^2 + 8m_y^2 m_z^2)\right) + \frac{t^3}{9} + \frac{\Sigma t^2}{12} \\ & - 2m_y^2 m_z^2 t\left(\frac{t}{3} + \Sigma_{yz}\right)\frac{\log q}{\Delta_{yz}} + m_y^2 m_z^2 \Sigma_{yz} \log^2 \tau_{yz}, \end{aligned} \tag{3.52}$$

$$
\begin{aligned}
I_3^{yz}(t) &= \frac{t^4}{16} + \Sigma_{yz}\frac{t^3}{18} + \frac{t^2}{24}(\Sigma_{yz}^2 + 6m_y^2m_z^2) + m_y^2m_z^2(\Sigma_{yz}^2 + m_y^2m_z^2)\log^2\tau_{yz} \\
&\quad - m_y^2m_z^2t\left(\frac{t^2}{3} + \frac{5\Sigma_{yz}t}{6} + 2(\Sigma_{yz}^2 + m_y^2m_z^2)\right)\frac{\log q}{\Delta_{yz}} \\
&\quad + \frac{4\pi^2}{3}\bar{J}_q(t)t\big(3t^3 - \Sigma_{yz}t^2 - (\Sigma_{yz}^2 + 6m_y^2m_z^2)t - \Sigma_{yz}(\Sigma_{yz}^2 + 26m_y^2m_z^2)\big),
\end{aligned} \tag{3.53}
$$

$$
I_0^{yz}(t) = 16\pi^2\bar{J}_q(t)t + t + \frac{\Sigma_{yz}}{2}\log^2\tau_{yz} - \Delta_{yz}\,\mathcal{J}(\tau_{yz}), \tag{3.54}
$$

$$
I_{-1}^{yz}(t) = -16\pi^2\bar{J}_q(t) - \frac{1}{2}\log^2\tau_{yz} + \frac{\Sigma_{yz}}{\Delta_{yz}}\,\mathcal{J}(\tau_{yz}), \tag{3.55}
$$

$$
I_{-2}^{yz}(t) = 8\pi^2\bar{J}_q(t)\left(\frac{\Sigma_{yz}}{\Delta_{yz}^2} - \frac{1}{t}\right) + \frac{2m_y^2m_z^2}{\Delta_{yz}^3}\,\mathcal{J}(\tau_{yz}). \tag{3.56}
$$

All of them have a smooth limit for the ratio of pion masses q going to one with the exception of $I_{-2}^{yz}(t)$, where we need to add a constant with the appropriate divergence. We have chosen to add $-\frac{\Sigma_{yz}}{\Delta_{yz}^2} + \frac{13}{36m_ym_z}$, which has the advantage that then $I_{-2}^{y}(t)$ goes to zero for $t = 0$. [However, as we have already noted, in the equal mass case there appears no $I_{-2}^{y}(t)$ in the result.] From the same reason we have added -2 to the function $I_{-1}^{y}(t)$. The primitive functions of integrations of $t^n\bar{J}_{PP}(t)$, which in addition vanish for $t = 0$, are therefore

$$
\begin{aligned}
I_1^{y}(t) &= 8\pi^2\bar{J}_1(t)t(t - 2m_y^2) + \frac{t^2}{4} + tm_y^2 + m_y^4\log^2\tau_y \\
&= \frac{m_y^4}{4\tau_y^2}\Big((\tau_y - 1)^2(5 - 6\tau_y + 5\tau_y^2) - 2(\tau_y^4 - 1)\log\tau_y\Big) + m_y^4\log^2\tau_y,
\end{aligned} \tag{3.57}
$$

$$
\begin{aligned}
I_2^{y}(t) &= \frac{16\pi^2}{3}\bar{J}_1(t)t\left(t^2 - tm_y^2 - 6m_y^4\right) + \frac{t^3}{9} + \frac{t^2}{2}m_y^2 + 2tm_y^4 + 2m_y^6\log^2\tau_y \\
&= \frac{m_y^6}{18\tau_y^3}\Big(-(\tau_y - 1)^2(2 - 7\tau_y + 2\tau_y^2)(7 - 2\tau_y + 7\tau_y^2) \\
&\quad + 6(\tau_y^2 - 1)(1 + \tau_y + \tau_y^2)(1 - 4\tau_y + \tau_y^2)\log\tau_y\Big) + 2m_y^6\log^2\tau_y,
\end{aligned} \tag{3.58}
$$

$$
\begin{aligned}
I_3^{y}(t) &= \frac{4\pi^2}{3}\bar{J}_1(t)t\left(3t^3 - 2t^2m_y^2 - 10tm_y^4 - 60m_y^6\right) + \frac{t^4}{16} + \frac{5t^3m_y^2}{18} + \frac{5t^2m_y^4}{4} \\
&\quad + 5tm_y^6 + 5m_y^8\log^2\tau_y \\
&= \frac{m_y^8}{144\tau_y^3}\Big((\tau_y - 1)^2\big(81 - 478\tau_y + 1123\tau_y^2 - 732\tau_y^3 + 1123\tau_y^4 - 478\tau_y^5 + 81\tau_y^6\big) \\
&\quad - 12(\tau_y^2 - 1)\big(3 - 16\tau_y + 27\tau_y^2 + 32\tau_y^3 + 27\tau_y^4 - 16\tau_y^5 + 3\tau_y^6\big)\log\tau_y\Big) + 5m_y^8\log^2\tau_y,
\end{aligned} \tag{3.59}
$$

$$
I_0^{y}(t) = 16\pi^2\bar{J}_1(t)t + t + m_y^2\log^2\tau_y = \frac{m_y^2}{\tau}\big((\tau_y^2 - 1)\log\tau_y - 3(\tau_y - 1)^2\big) + m_y^2\log^2\tau_y, \tag{3.60}
$$

$$I^y_{-1}(t) = -32\pi^2 \bar{J}_1(t) - \frac{1}{2}\log^2\tau = -4 + 2\,\frac{\tau_y+1}{\tau_y-1}\log\tau_y - \frac{1}{2}\log^2\tau_y, \tag{3.61}$$

$$\begin{aligned} I^y_{-2}(t) &= \left(1 - \frac{4m_y^2}{t}\right)\frac{8\pi^2}{3m_y^2}\bar{J}_1(t) + \frac{1}{9m_y^2} \\ &= \frac{1}{18m_y^2(\tau_y-1)^3}\left(8(\tau_y^3-1) - 3(1+\tau_y)^3\log(\tau_y)\right). \end{aligned} \tag{3.62}$$

3.4.2 Integration in the same mass channel

To perform the explicit calculation we should plug in the endpoints (3.28) and (3.29) into the particular primitive functions (provided there exists a trajectory connecting the endpoints fulfilling the condition for possibility of use of the primitive functions). That gives in general complicated expressions. However, in particular cases the situation simplifies — one of them, which we discuss already on this general level, is the same mass case.

Denoting

$$T_\pm = \frac{4m_y^2 - t_\pm(s)}{2m_y^2} \tag{3.63}$$

and

$$\sigma_{T_\pm} := \frac{1}{\sigma_y(t_\pm(s))} = \frac{1}{\sqrt{1-\frac{4m_y^2}{t_\pm(s)}}} = \sqrt{\frac{T_\pm - 2}{T_\pm}}, \tag{3.64}$$

where σ_y is the square root function corresponding to $\bar{J}_y$, we obtain the argument of logarithm equal to

$$\tau(t_\pm(s)) = T_\pm - 1 - T_\pm\sigma_{T_\pm}, \tag{3.65}$$

its reciprocal value

$$\frac{1}{\tau(t_\pm(s))} = T_\pm - 1 + T_\pm\sigma_{T_\pm}, \tag{3.66}$$

and the logarithm simplified to

$$L_{T_\pm} = \log\tau(t_\pm(s)) = \log\left(\frac{1-\sigma_{T_\pm}}{1+\sigma_{T_\pm}}\right). \tag{3.67}$$

Inserting these relations into primitive functions (3.57)–(3.62) (and using the simplification $T_\pm\sigma^2_{T_\pm} = T_\pm - 2$), we arrive at

$$16\pi^2\bar{J}_{yy}(t_\pm) = 2 + \frac{L_{T_\pm}}{\sigma_{T_\pm}}, \tag{3.68}$$

$$16\pi^2\bar{\bar{J}}_{yy}(t_\pm) = 2 + \frac{L_{T_\pm}}{\sigma_{T_\pm}} - \frac{t_\pm}{6m_y^2}, \tag{3.69}$$

$$I^y_1(t_\pm) = m_y^4\big((T_\pm-2)(5T_\pm-8) + 2T_\pm(T_\pm-1)\sigma_{T_\pm}L_{T_\pm} + L^2_{T_\pm}\big), \tag{3.70}$$

$$I_2^y(t_\pm) = \frac{m_y^6}{9}\big(2(T_\pm-2)(7T_\pm-8)(11-4T_\pm) - 12T_\pm(T_\pm-3)(2T_\pm-1)\sigma_{T_\pm}L_{T_\pm} + 18L_{T_\pm}^2\big), \tag{3.71}$$

$$I_3^y(t_\pm) = \frac{m_y^8}{9}\big((T_\pm-2)(81{T_\pm}^3 - 482{T_\pm}^2 + 941T_\pm - 512) + 6T_\pm(6{T_\pm}^3 - 34{T_\pm}^2 + 59T_\pm - 15)\sigma_{T_\pm}L_{T_\pm} + 45L_{T_\pm}^2\big), \tag{3.72}$$

$$I_0^y(t_\pm) = m_y^2\big(6(2-T_\pm) - 2T_\pm\sigma_{T_\pm}L_{T_\pm} + L_{T_\pm}^2\big), \tag{3.73}$$

$$I_{-1}^y(t_\pm) = -4 - \frac{2T_\pm}{T_\pm-2}\,\sigma_{T_\pm}L_{T_\pm} - \frac{1}{2}L_{T_\pm}^2, \tag{3.74}$$

$$I_{-2}^y(t_\pm) = \frac{1}{18m_y^2}\left(\frac{4(2T_\pm-1)}{T_\pm-2} + \frac{3{T_\pm}^2}{(T_\pm-2)^2}\sigma_{T_\pm}L_{T_\pm}\right). \tag{3.75}$$

3.5 Second iteration

After employing the expressions of the previous section, we obtain the NLO partial waves of the amplitudes. They are in the form

$$\varphi_0(s) = \frac{1}{(16\pi)^2\pi}\frac{C}{N}\sum_j \mathcal{M}_j(s)p_j^0(s), \tag{3.76}$$

$$\varphi_1(s) = \frac{1}{(48\pi)^2\pi}\frac{C}{N}\sum_j \mathcal{M}_j(s)\left(\lambda_i^{1/2}(s)\lambda_f^{1/2}(s)p_j^1(s) + \frac{1}{\lambda_i^{1/2}(s)\lambda_f^{1/2}(s)}p_j^{1,(\lambda)}(s)\right), \tag{3.77}$$

where $p_j^\ell(x)$ and $p_j^{1,(\lambda)}(x)$ are Laurent polynomials depending on the parameters of amplitudes; $\mathcal{M}_j(x)$ are some kinematic functions that are independent of those parameters; and finally $\lambda_i(s)$ and $\lambda_f(s)$ are triangle functions corresponding to the initial and to the final states respectively.

For the second iteration we need NNLO discontinuities of partial waves of all crossed processes as inputs to the reconstruction theorem. They can be obtained from unitarity relation (2.18),

$$\operatorname{Im}\psi_\ell^{i\to f}(s) = \sum_k \frac{N}{S_k}\frac{\lambda_k^{1/2}(s)}{s}\left(\phi_\ell^{i\to k}(s)\left(\varphi_\ell^{f\to k}(s)\right)^\star + \varphi_\ell^{i\to k}(s)\left(\phi_\ell^{f\to k}(s)\right)^\star\right)\theta(s-\mathrm{thr}_k), \tag{3.78}$$

where there appear products of $O(p^2)$ partial waves $\phi_\ell(s)$ and of $O(p^4)$ ones $\varphi_\ell(s)$.

Since one can separate the polynomials depending on the parameters of amplitudes from the kinematic functions also for the $O(p^2)$ partial waves [as is obvious from (3.2) and (3.3), in that case the only non-polynomial kinematic functions are some combinations of square roots of triangle functions], the NNLO discontinuities can be reparametrized into

$$\operatorname{Im}\psi_0(s) = \frac{1}{(16\pi)^3\pi}\sum_k \frac{C_{ik}C_{kf}}{NS_k}\sum_j \mathcal{K}_j(s)\mathcal{P}_j^{k;0}(s), \tag{3.79}$$

$$\mathrm{Im}\,\frac{\psi_1(s)}{\lambda_i^{1/2}(s)\lambda_f^{1/2}(s)} = \frac{1}{s}\frac{1}{(48\pi)^3\pi} \times \sum_k \frac{C_{ik}C_{kf}}{NS_k}\sum_j \mathcal{K}_j(s)\left(\mathcal{P}_j^{k;1}(s) + \frac{sM^2}{\lambda_i(s)}\mathcal{P}_{j;(\lambda_i)}^{k;1}(s) + \frac{sM^2}{\lambda_f(s)}\mathcal{P}_{j;(\lambda_f)}^{k;1}(s)\right), \tag{3.80}$$

with $\mathcal{P}_j^{k;\ell}(s)$ and $\mathcal{P}_{j;(\lambda)}^{k;\ell}(s)$ being parameter-dependent Laurent polynomials obtained as combinations of polynomials $p_j^\ell(s)$ and the polynomials of the $O(p^2)$ partial waves; and $\mathcal{K}_j(s)$ are dimensionless kinematic functions arising as products of functions $\mathcal{M}_i(s)$ with square roots of triangle functions. We have extracted factor sM^2, where M denotes a generic mass, from the polynomials $\mathcal{P}_{j;(\lambda)}^{k;1}(s)$ in order to have the functions that multiplies them again dimensionless. As usual, the quantities with indices i, f, k are in turn connected with the initial, the final and the intermediate states.

After this reparametrization, the integrands appearing in relations (2.23)–(2.24) for functions $W^\ell(s)$ are in the form of (2.73) or (2.77) and we can factor the polynomials out of the integrals using the methods of Section 2.5. Thus, we arrive at

$$\begin{aligned} W^0(s) = \frac{1}{(16\pi)^2\pi^2}\sum_k \frac{C_{ik}C_{kf}}{S_k}\Bigg(\sum_j \mathcal{H}_j(s)\mathcal{P}_j^{k;0}(s) \\ + \frac{\Delta_i\Delta_f}{9}\sum_j \frac{1}{s}\left(\mathcal{H}_j(s)\mathcal{P}_j^{k;1}(s) + \mathcal{H}_{j;(\lambda_i)}(s)\mathcal{P}_{j;(\lambda_i)}^{k;1}(s) + \mathcal{H}_{j;(\lambda_f)}(s)\mathcal{P}_{j;(\lambda_f)}^{k;1}(s)\right)\Bigg), \end{aligned} \tag{3.81}$$

$$W^1(s) = \frac{1}{(48\pi)^2\pi^2}\left(\mathcal{H}_j(s)\mathcal{P}_j^{k;1}(s) + \mathcal{H}_{j;(\lambda_i)}(s)\mathcal{P}_{j;(\lambda_i)}^{k;1}(s) + \mathcal{H}_{j;(\lambda_f)}(s)\mathcal{P}_{j;(\lambda_f)}^{k;1}(s)\right). \tag{3.82}$$

With $\mathcal{H}_j(s)$ we formally denote Hilbert transforms (dispersion integrals) of functions $\mathcal{K}_j(s)$,

$$\mathcal{H}_j^n(s) = s^n\int_{s_{\mathrm{thr}}}^\infty \frac{\mathrm{d}x}{x^n}\frac{\mathcal{K}_j(x)}{x-s}. \tag{3.83}$$

with number of subtractions n varying for different orders of the polynomial term multiplying the particular function.

More precisely, instead of the formal symbol $\mathcal{H}_j(s)\mathcal{P}_j^{k;\ell}(s)$, we should write for a given polynomial

$$\mathcal{P}_j^{k;\ell}(s) = \sum_m a_m s^m \tag{3.84}$$

the expression

$$\mathcal{H}_j(s)\mathcal{P}_j^{k;\ell}(s) \mapsto \sum_m a_m s^m \mathcal{H}_j^{n_m}(s), \tag{3.85}$$

where n_m depends on m, on the chiral order[6] of polynomial $\mathcal{P}_j^{k;\ell}(s)$ and also on the asymptotic behavior of function $\mathcal{K}_j(s)$ [on the convergence of integrals (3.83)] such that it satisfies

[6]Note that in the terms with $\Delta_i\Delta_f$ in (3.81), the determining chiral orders are the one of $\frac{1}{s}\mathcal{P}_j^{k;1}(s)$ and the one of $\frac{1}{s}\mathcal{P}_{j;(\lambda)}^{k;1}(s)$. Note also that we have factored out of polynomials $\mathcal{P}_{j;(\lambda)}^{k;1}(s)$ some powers of s and masses that are written in (3.80) symbolically as sM^2.

inequality (2.76) and one of the conditions (2.71). For some of the terms there still remains ambiguity in the final choice of n from all the values satisfying both of these conditions. In that case, we will choose the number that gives the simplest results, videlicet the minimum of the absolute value of such n with the preference of non-negative values.

In equations (3.80)–(3.82), we have indicated the appearance of functions $\frac{sM^2}{\lambda}\mathcal{K}_j(s)$. We could naturally introduce them as new functions $\mathcal{K}_j(s)$ thereby simplifying the schematic form of these equations. Nevertheless, in Appendix B we show that a computation of Hilbert transform $\mathcal{H}_{j;(\lambda)}(s)$ of a function $\frac{sM^2}{\lambda}\mathcal{K}_j(s)$ is easy provided we already know the transform $\mathcal{H}_j(s)$ of the function $\mathcal{K}_j(s)$.

We have seen that the only non-trivial task in performing the second iteration is finding of Hilbert transforms of the functions appearing in the expressions for discontinuities. We discuss some properties of Hilbert transform useful in this regard in Appendix B.

3.6 Interpretation of the polynomial parameters

In the results of reconstruction procedure there appear polynomials which are determined just by their polynomial order (by the powers of Mandelstam variables appearing there), by the symmetries they have to obey, and naturally also by the condition of chiral convergence of this expansion. Their choice is otherwise unrestricted and we can choose in each application in principle any parametrization we like. However, together with the ambiguity of parametrization of the leading order amplitudes their choice can affect the convergence rate in chiral expansion of the parametrization and it has influence on the stability of an eventual fit to experimental data.

In most cases we use the parametrization having the subthreshold parameters, viz. values of the amplitudes, of their slopes, etc. in the center of Dalitz plot, as the polynomial parameters. This has been used also in all the previous analyses inspired by the reconstruction theorem [125, 95, 11, 12] and should be an appropriate choice for discussion of the quantities whose expansion in light quark masses converges rapidly.

On the other hand, for studies of the processes where we cannot rely on such rapid convergence, there could exist more suitable choices. For instance, in studies of experimental data on $\pi\pi$ scattering (what is one of the main tasks of this work), there seems to be more appropriate to use the partial-wave parametrization with scattering lengths, effective ranges, and further shape characteristics as the polynomial parameters of amplitudes. As will be discussed in Chapter 5, working in such parametrization, however, brings one additional complication. Since the unitarity corrections affect at each order all the partial waves and thereby also the scattering lengths and the further partial-wave parameters, we have to reorganize the parametrization at each order by adding to the unitarity part some "restoring polynomials" that retain physical interpretations of the parameters also after including such corrections. With more of these parameters fixed at their correct physical values at higher orders there appears a necessity of more complicated restoring polynomials. (Nevertheless, one should bear in mind that there are still just polynomials.)

We will deal also with the processes where although the sufficient rate of chiral conver-

gence is questioned in any point, up to now there exists no reasonably better expansion of them and so we stay with the subthreshold expansion in the center of Dalitz plot. To this class of processes there belong $K\pi \to \pi\pi$ and $\eta\pi \to \pi\pi$ processes of Chapters 6–8, where the kinematic constraint (2.6) implies that there is always one crossed channel whose center of mass energy exceeds many times the threshold energy of production of the final states (therefore, the center of Dalitz plot is in a way indeed a point of minimum).

Independently on the parametrization and on the form of polynomials we choose for some process, there is still one issue connected with the interpretation of the polynomial parameters we should also discuss. From Figure 1 it is obvious that starting with some parameter of the polynomial part of an $O(p^d)$ amplitude, the same parameter appears in the higher order $O(p^{d+2})$ parametrization on two different places with two different orders. The parameter appearing in the polynomial part obtains some higher order corrections, thereby changing its value, whereas the same parameter in the unitarity part of $O(p^d)$ parametrization exactly coincides with that lower-order one. Roughly speaking, the parameters in the unitarity part are therefore one step behind the parameters of the polynomial part. With this appearance of parameters in a parametrization of a given order in such double orders we can deal in two ways:

- order-by-order approach — We can exactly respect chiral orders of each part and thus distinguish contributions of every order. This approach is therefore more suitable in the cases when the convergence of the chiral expansion is expected. Its benefit emerges especially when one wants to make a comparison with the results of χPT.

  Moreover, when performing a fit of our parameters to data or to some theory, there suggests itself the following simplification of the fitting process. We start with comparing (fitting) the lowest order formulae and then at each higher order we use those lower order values for computation of the unitarity part and afterward fit the contributions of the higher orders only to the polynomial part. By that we fit at each order just a polynomial, while the more complicated unitarity part is already fixed by the lower order fit.

- resummed approach — We can include into results also a part of the neglected orders by replacing all the parameters by their highest order values. By that we reorganize the chiral expansion of the amplitude (from which there follows the adjective "resummed"). It is possible, albeit not guaranteed, that this resummation can lead to the results that will be closer to the final non-perturbative physical values of the amplitudes than the strict respecting the chiral orders. Nevertheless, the contrary can also happen to be true. It seams to be more natural to use this interpretation in the cases when we want to keep a physical meaning (values) of the parameters (this will be of use for instance for scattering lengths in $\pi\pi$ data).

  This interpretation is an intermediate step in the way to the complete dispersive approaches that try to include unitarity contributions of some specific intermediate states to an infinite order ignoring the actual counting of the chiral orders.

Chapter 4

Pseudoscalar meson-meson scattering in isospin conserving strong chiral perturbation theory

As the first application of the procedure outlined in the previous chapter and for the illustration how the procedure works, we construct the $2 \to 2$ scattering amplitudes for all pseudoscalar mesons K, η and π in pure strong chiral perturbation theory with isospin conservation.

In this simple case, if we in addition neglect the appearance of all the other particles (vector resonances, etc. — see the discussion in Section 4.6), also the assumptions (iii), (iv), and (v) of the theorem, viz. existence of the dispersion relation, analyticity and the complete partial wave decomposition of the amplitude, can be justified from the first principles of the axiomatic quantum field theory — at least in some domains in kinematic region. This justification is discussed in Appendix C with these domains plotted on Figure 25. By that, all of the assumptions of the theorem are justified without the need of the existence of the Lagrangian of χPT. Therefore, if we take the leading order amplitudes entering the procedure in a model-independent form, by that we construct a parametrization of the amplitudes in more general form than the result of χPT, for instance independent on the particular power-counting scheme in use. In this aspect the results of this chapter can be understood as an extension of the work of Osborn [114] constructing the general form of the amplitudes of the considered type to the higher orders.

Note, however, that for the construction of the amplitudes using the theorem we do not need the fulfillment of such general assumptions — the complete (non-perturbative) amplitude does not need to fulfill these conditions. For the construction it is enough that the perturbative amplitudes that would be constructed by all of the possible Lagrangians by the Feynman diagram methods possess these analytic properties.

The meson-meson scattering amplitudes in strong, isospin symmetric chiral perturbation theory form a closed set with respect to the reconstruction theorem and the unitarity relations. Therefore, we can use the reconstruction procedure from the previous chapter and construct general forms of these amplitudes to two-loop order. Nevertheless, we perform here only the first iteration since in the context of our present work the main reason

of this chapter is just to give a specific example of amplitudes which can be constructed by the reconstruction procedure and can be compared afterwards to the result of one-loop calculation of chiral perturbation theory, obtaining so the particular values of the general parameters that correspond to these chiral perturbation theory results. To that end, we have used the work of Nicola and Pelaez [78], which lists the one-loop results in the unitarised form that is suitable for such comparison.

With these tasks we have dealt already in author's diploma thesis [I] and in article [II]. Therefore, for reasons of space, we do not go here into detail of their construction and present here only a part of the results and refer the interested reader to [I] and [II].

4.1 Notation

In addition to the general notation introduced in the previous chapters, we need to specify our definition of the (signs of) meson fields. They are collected in the matrix

$$\phi(x) = \lambda_a \phi_a(x) = \begin{pmatrix} \pi^0 + \frac{1}{\sqrt{3}}\eta & -\sqrt{2}\pi^+ & -\sqrt{2}K^+ \\ \sqrt{2}\pi^- & -\pi^0 + \frac{1}{\sqrt{3}}\eta & -\sqrt{2}K^0 \\ \sqrt{2}K^- & -\sqrt{2}\overline{K^0} & -\frac{2}{\sqrt{3}}\eta \end{pmatrix}. \tag{4.1}$$

Our choice of the phase convention corresponds to the Condon and Shortley convention and brings to a matrix element of mesons one minus sign for each charged particle in the final state.

4.2 Symmetry properties of the considered amplitudes

We work here in the strong isospin conservation limit. In [I] and [II] we have shown that then Ward identities[1] imply just 7 independent meson-meson scattering processes, in the notation which follows $A_{\eta\eta}, A_{\eta\pi}, A_{\pi\pi}, A_{K\eta}, A_{K\eta\pi}, A_{K\pi}, B_{K\pi}$ and A_{KK}. From them the amplitudes of all the possible physical processes can be determined using the crossing property and the following relations. We list here also the s, t, u symmetries of the independent amplitudes which stem from their crossing and Bose symmetry.

1. $\eta\eta \to \eta\eta$

$$A(\eta\eta \to \eta\eta) = A_{\eta\eta}(s,t,u) = A_{\eta\eta}(t,s,u) = A_{\eta\eta}(u,t,s). \tag{4.2}$$

2. $\eta\pi \to \eta\pi$

$$A(\eta\pi^\pm \to \eta\pi^\pm) = A(\eta\pi^0 \to \eta\pi^0) = A_{\eta\pi}(s,t,u), \tag{4.3}$$

$$A_{\eta\pi}(s,t,u) = A_{\eta\pi}(u,t,s). \tag{4.4}$$

[1] Note also the existence of the alternative method that is used in Appendix I for the construction of the independent $K \to 3\pi$ amplitudes.

3. $\pi\pi \to \pi\pi$

$$A(\pi^+\pi^- \to \pi^0\pi^0) = -A_{\pi\pi}(s,t,u), \tag{4.5}$$
$$A(\pi^+\pi^- \to \pi^+\pi^-) = A_{\pi\pi}(s,t,u) + A_{\pi\pi}(t,s,u), \tag{4.6}$$
$$A(\pi^0\pi^0 \to \pi^0\pi^0) = A_{\pi\pi}(s,t,u) + A_{\pi\pi}(t,s,u) + A_{\pi\pi}(u,t,s); \tag{4.7}$$
$$A_{\pi\pi}(s,t,u) = A_{\pi\pi}(s,u,t). \tag{4.8}$$

4. $KK \to \eta\eta$

$$A(\overline{K^0}K^0 \to \eta\eta) = -A(K^-K^+ \to \eta\eta) = A_{K\eta}(s,t,u) = A_{K\eta}(s,u,t). \tag{4.9}$$

5. $KK \to \eta\pi$

$$A(K^-K^+ \to \eta\pi^0) = A(\overline{K^0}K^0 \to \eta\pi^0) = -A_{K\eta\pi}(s,t,u), \tag{4.10}$$
$$A(K^-K^0 \to \eta\pi^-) = A(\overline{K^0}K^+ \to \eta\pi^+) = -\sqrt{2}A_{K\eta\pi}(s,t,u), \tag{4.11}$$
$$A_{K\eta\pi}(s,t,u) = A_{K\eta\pi}(s,u,t). \tag{4.12}$$

6. $KK \to \pi\pi$

$$A(\overline{K^0}K^0 \to \pi^0\pi^0) = -A(K^-K^+ \to \pi^0\pi^0) = A_{K\pi}(s,t,u), \tag{4.13}$$
$$A(K^-K^0 \to \pi^-\pi^0) = -A(\overline{K^0}K^+ \to \pi^+\pi^0) = \sqrt{2}B_{K\pi}(s,t,u), \tag{4.14}$$
$$A(K^-K^+ \to \pi^-\pi^+) = A_{K\pi}(s,t,u) + B_{K\pi}(s,t,u), \tag{4.15}$$
$$A(\overline{K^0}K^0 \to \pi^-\pi^+) = -A_{K\pi}(s,t,u) + B_{K\pi}(s,t,u). \tag{4.16}$$

For the determination of all $KK \to \pi\pi$ amplitudes it could seem that one needs two basic amplitudes — the symmetric

$$A_{K\pi}(s,t,u) = A_{K\pi}(s,u,t), \tag{4.17}$$

and the antisymmetric one

$$B_{K\pi}(s,t,u) = -B_{K\pi}(s,u,t). \tag{4.18}$$

However, in fact, we can consider the only independent amplitude to be (4.15) since the amplitudes $A_{K\pi}$ and $B_{K\pi}$ can be extracted from it as its symmetric and its antisymmetric part, respectively, under the exchange of t and u variables.

7. $KK \to KK$

$$A(K^-K^+ \to \overline{K^0}K^0) = -A_{KK}(s,t,u), \tag{4.19}$$
$$A(K^-K^+ \to K^-K^+) = A(\overline{K^0}K^0 \to \overline{K^0}K^0) = A_{KK}(s,t,u) + A_{KK}(t,s,u). \tag{4.20}$$

We want to point out that the isospin symmetry leaves only two independent $KK \to KK$ amplitudes, which are, however, constraint by crossing. Thus, we end up with only one independent amplitude $K^-K^+ \to \overline{K^0}K^0$, knowledge of which enables us the determination of all the other $KK \to KK$ amplitudes.

4.3 Leading order parametrization of the amplitudes

To preserve the model-independence of the construction of the amplitudes, we write also the leading-order amplitudes entering the first iteration as the most general amplitudes coming from our assumptions with no dependence on any particular power-counting scheme. We have already discussed that they should be first order polynomials in Mandelstam variables. Since they should satisfy the crossing, Bose and isospin symmetries from the previous section, we can write them in the form:

$$A_{\eta\eta} = -\frac{m_\pi^2}{3F_\pi^2}\alpha_{\eta\eta}\left(1-\frac{4m_\eta^2}{m_\pi^2}\right), \tag{4.21}$$

$$A_{\eta\pi} = \frac{1}{3F_\pi^2}\left(\beta_{\eta\pi}(3t-2m_\eta^2-2m_\pi^2)+\alpha_{\eta\pi}m_\pi^2\right), \tag{4.22}$$

$$A_{\pi\pi} = \frac{1}{3F_\pi^2}\left(\beta_{\pi\pi}\left(3s-4m_\pi^2\right)+\alpha_{\pi\pi}m_\pi^2\right), \tag{4.23}$$

$$A_{K\eta} = \frac{1}{4F_\pi^2}\left[\beta_{K\eta}(3s-2m_K^2-2m_\eta^2)+\alpha_{K\eta}\left(2m_\eta^2-\frac{2}{3}m_K^2\right)\right], \tag{4.24}$$

$$A_{K\eta\pi} = \frac{1}{4\sqrt{3}F_\pi^2}\left[\beta_{K\eta\pi}\left(3s-2m_K^2-m_\eta^2-m_\pi^2\right)-\left(2m_K^2-m_\eta^2-m_\pi^2+\alpha_{K\eta\pi}m_\pi^2\right)\right], \tag{4.25}$$

$$A_{K\pi} = \frac{1}{12F_\pi^2}\left[\beta_{K\pi}\left(3s-2m_K^2-2m_\pi^2\right)+2(m_K-m_\pi)^2+4\alpha_{K\pi}m_Km_\pi\right], \tag{4.26}$$

$$B_{K\pi} = \frac{1}{4F_\pi^2}\gamma_{K\pi}(t-u), \tag{4.27}$$

$$A_{KK} = \frac{1}{6F_\pi^2}\left(\beta_{KK}\left(4m_K^2-3u\right)+3\gamma_{KK}(s-t)+2\alpha_{KK}m_K^2\right). \tag{4.28}$$

Imposing chiral symmetry (cf. also with PCAC argumentation of [114]), one can show that the leading order amplitude $A_{\eta\pi}$ has to be a constant independent on the Mandelstam variables, i.e. $\beta_{\eta\pi}^{\mathrm{LO}} = 0$ independently on the particular power-counting scheme in use. Similar arguments lead to $\gamma_{KK} = 0$ in the leading order in all power-counting schemes.

Different choices of these (13+2) parameters in our parametrization reproduce results of the particular models (with the particular power-countings). For instance, the standard leading order χPT results [74] are obtained by the choice:

$$\alpha_{\eta\eta}^{\mathrm{std}} = \alpha_{\eta\pi}^{\mathrm{std}} = \alpha_{\pi\pi}^{\mathrm{std}} = \alpha_{K\eta}^{\mathrm{std}} = \alpha_{K\pi}^{\mathrm{std}} = \alpha_{KK}^{\mathrm{std}} = 1, \tag{4.29}$$

$$\beta_{\pi\pi}^{\mathrm{std}} = \beta_{K\eta}^{\mathrm{std}} = \beta_{K\eta\pi}^{\mathrm{std}} = \beta_{K\pi}^{\mathrm{std}} = \gamma_{K\pi}^{\mathrm{std}} = \beta_{KK}^{\mathrm{std}} = 1, \tag{4.30}$$

$$\alpha_{K\eta\pi}^{\mathrm{std}} = 0, \tag{4.31}$$

$$\beta_{\eta\pi}^{\mathrm{std}} = \gamma_{KK}^{\mathrm{std}} = 0. \tag{4.32}$$

4.4 Results of first iteration

Performing first iteration means merely a straightforward use of relations (3.10) and (3.11) for the leading order parametrization of the amplitudes from the previous section.

Since the results are rather involved, we do not put here the complete expressions for the polynomials denoted by $Z_{ij}^k, Y_{ij}^k, X_{ij}^k, W_{ij}^k$ depending on Mandelstam variables, pseudoscalar masses and the leading order parameters from the previous section. Interested reader can find them in [II] or [I]. Nevertheless, for illustration and also for the possibility of comparison with the results of Chapter 5, we present here the full form of the polynomials for the $\pi\pi$ scattering process.

- $\pi^+\pi^- \to \pi^0\pi^0$

  Note that the amplitude of the process $\pi^+\pi^- \to \pi^0\pi^0$ is equal to $-A_{\pi\pi}$.

$$\begin{aligned}
-A_{\pi\pi} &= \frac{1}{3F_\pi^2}\left(\beta_{\pi\pi}\left(3s-4m_\pi^2\right)+\alpha_{\pi\pi}m_\pi^2\right)+\frac{1}{F_\pi^4}\delta_{\pi\pi}(s-2m_\pi^2)^2\\
&+\frac{1}{F_\pi^4}\varepsilon_{\pi\pi}\left((t-2m_\pi^2)^2+(u-2m_\pi^2)^2\right)\\
&+\frac{1}{72F_\pi^4}\left(Z_{\pi\pi}^{\pi\pi}(s)\overline{J}_{\pi\pi}(s)+Z_{\pi\pi}^{KK}(s)\overline{J}_{KK}(s)+Z_{\pi\pi}^{\eta\eta}\overline{J}_{\eta\eta}(s)\right)\\
&+\left[\frac{1}{72F_\pi^4}\left(Y_{\pi\pi}^{\pi\pi}(t,u)\overline{J}_{\pi\pi}(t)+Y_{\pi\pi}^{KK}(t,u)\overline{J}_{KK}(t)\right)\right]+[t\leftrightarrow u]+O(p^6).
\end{aligned} \tag{4.33}$$

$$Z_{\pi\pi}^{\pi\pi}(s) = 4\left(3\beta_{\pi\pi}s+(7\alpha_{\pi\pi}-4\beta_{\pi\pi})m_\pi^2\right)\left(3\beta_{\pi\pi}s+(\alpha_{\pi\pi}-4\beta_{\pi\pi})m_\pi^2\right), \tag{4.34}$$

$$Z_{\pi\pi}^{KK}(s) = \left(3\beta_{K\pi}s+2(1-\beta_{K\pi})(m_K^2+m_\pi^2)+4(\alpha_{K\pi}-1)m_Km_\pi\right)^2, \tag{4.35}$$

$$Z_{\pi\pi}^{\eta\eta} = 4\alpha_{\pi\eta}^2m_\pi^4, \tag{4.36}$$

$$Y_{\pi\pi}^{\pi\pi}(t,u) = 4\left(3\beta_{\pi\pi}^2t(t-u)+6\beta_{\pi\pi}(2\beta_{\pi\pi}u-\alpha_{\pi\pi}t)m_\pi^2+2(\alpha_{\pi\pi}^2+4\beta_{\pi\pi}(\alpha_{\pi\pi}-2\beta_{\pi\pi}))m_\pi^4\right), \tag{4.37}$$

$$Y_{\pi\pi}^{KK}(t,u) = 3\gamma_{\pi K}^2(t-4m_K^2)(4m_\pi^2-t-2u). \tag{4.38}$$

- $\eta\pi^0 \to \eta\pi^0$

$$\begin{aligned}
A_{\eta\pi} &= \frac{1}{3F_\pi^2}\Big(\beta_{\eta\pi}(3t-2m_\eta^2-2m_\pi^2)+m_\pi^2\alpha_{\eta\pi}\Big)\\
&+\frac{1}{3F_\pi^4}\left(\delta_{\eta\pi}\left((s-\Sigma_{\eta\pi})^2+(u-\Sigma_{\eta\pi})^2\right)+\varepsilon_{\eta\pi}(t-2m_\pi^2)(t-2m_\eta^2)\right)\\
&+\frac{1}{72F_\pi^4}\Big(Z_{\eta\pi}^{KK}(t)\overline{J}_{KK}(t)+Z_{\eta\pi}^{\eta\eta}\overline{J}_{\eta\eta}(t)+Z_{\eta\pi}^{\pi\pi}(t)\overline{J}_{\pi\pi}(t)\Big)\\
&+\left[\frac{1}{9F_\pi^4}\left(Y_{\eta\pi}^{\eta\pi}\overline{J}_{\eta\pi}(s)+Y_{\eta\pi}^{KK}(s)\overline{J}_{KK}(s)\right)\right]+[s\leftrightarrow u]+O(p^6).
\end{aligned} \tag{4.39}$$

- $\eta\eta \to \eta\eta$

$$\begin{aligned}A_{\eta\eta} &= \frac{1}{3F_\pi^2}\alpha_{\eta\eta}\left(4m_\eta^2 - m_\pi^2\right) + \frac{1}{3F_\pi^4}\delta_{\eta\eta}(s^2+t^2+u^2-4m_\eta^4) \\ &\quad + \left[\frac{1}{6F_\pi^4}\left(Z_{\eta\eta}^{\eta\eta}\overline{J}_{\eta\eta}(s) + Z_{\eta\eta}^{KK}(s)\overline{J}_{KK}(s) + Z_{\eta\eta}^{\pi\pi}\overline{J}_{\pi\pi}(s)\right)\right] + [s\leftrightarrow t] + [s\leftrightarrow u] + O(p^6).\end{aligned} \tag{4.40}$$

- $\overline{K^0}K^0 \to \pi^0\eta$

$$\begin{aligned}A_{K\eta\pi} &= \frac{1}{4\sqrt{3}F_\pi^2}V_{K\eta\pi}(s) + \frac{1}{4\sqrt{3}F_\pi^4}\delta_{K\eta\pi}(s-2m_K^2)(s-\Sigma_{\eta\pi}) \\ &\quad + \frac{1}{4\sqrt{3}F_\pi^4}\varepsilon_{K\eta\pi}\left((t-\Sigma_{K\eta})(t-\Sigma_{K\pi}) + (u-\Sigma_{K\eta})(u-\Sigma_{K\pi})\right) \\ &\quad + \frac{1}{24\sqrt{3}F_\pi^4}\left(Z_{K\eta\pi}^{KK}(s)\overline{J}_{KK}(s) + Z_{K\eta\pi}^{\eta\pi}\overline{J}_{\eta\pi}(s)\right)V_{K\eta\pi}(s) \\ &\quad + \Big[-\frac{1}{96\sqrt{3}F_\pi^4}\left(Y_{K\eta\pi}^{K\eta}(t,u)\overline{J}_{K\eta}(t) + Y_{K\eta\pi}^{K\pi}(t,u)\overline{J}_{K\pi}(t)\right) \\ &\qquad - \frac{1}{32\sqrt{3}F_\pi^4}\frac{1}{t}\left(X_{K\eta\pi}^{K\eta}(u)\overline{J}_{K\eta}(t) + X_{K\eta\pi}^{K\pi}(u)\overline{J}_{K\pi}(t)\right) \\ &\qquad\quad + \frac{1}{16\sqrt{3}F_\pi^4}\frac{\Delta_{K\eta}\Delta_{K\pi}}{t^2}\beta_{K\eta\pi}\left(W_{K\eta\pi}^{K\eta}\overline{\overline{J}}_{K\eta}(t) + W_{K\eta\pi}^{K\pi}\overline{\overline{J}}_{K\pi}(t)\right)\Big] + [t\leftrightarrow u] + O(p^6).\end{aligned} \tag{4.41}$$

In this amplitude we have used the shorthand notation

$$V_{K\eta\pi}(s) = \beta_{K\eta\pi}\left(3s - 2m_K^2 - m_\eta^2 - m_\pi^2\right) - \left(2m_K^2 - m_\eta^2 - m_\pi^2 + \alpha_{K\eta\pi}m_\pi^2\right). \tag{4.42}$$

- $\overline{K^0}K^0 \to \pi^0\pi^0$

$$\begin{aligned}A_{K\pi} &= \frac{1}{12F_\pi^2}\left(\beta_{K\pi}\left(3s-2m_K^2-2m_\pi^2\right) + 2(m_K-m_\pi)^2 + 4\alpha_{K\pi}m_Km_\pi\right) \\ &\quad + \frac{1}{12F_\pi^4}\left(\delta_{K\pi}(s-2m_\pi^2)(s-2m_K^2) + \varepsilon_{K\pi}\left((t-\Sigma_{K\pi})^2 + (u-\Sigma_{K\pi})^2\right)\right) \\ &\quad + \frac{1}{72F_\pi^4}\Big(Z_{K\pi}^{KK}(s)\overline{J}_{KK}(s) + Z_{K\pi}^{\eta\eta}(s)\overline{J}_{\eta\eta}(s) + Z_{K\pi}^{\pi\pi}(s)\overline{J}_{\pi\pi}(s)\Big) \\ &\quad + \Big[\frac{1}{96F_\pi^4}\left(Y_{K\pi}^{K\pi}(t,u)\overline{J}_{K\pi}(t) + Y_{K\pi}^{K\eta}(t,u)\overline{J}_{K\eta}(t)\right) \\ &\qquad + \frac{1}{32F_\pi^4}\frac{1}{t}\left(X_{K\pi}^{K\pi}(u)\overline{J}_{K\pi}(t) + X_{K\pi}^{K\eta}(u)\overline{J}_{K\eta}(t)\right) \\ &\qquad\quad + \frac{1}{16F_\pi^4}\frac{1}{t^2}\Delta_{K\pi}^2\left(W_{K\pi}^{K\pi}\overline{\overline{J}}_{K\pi}(t) + W_{K\pi}^{K\eta}\overline{\overline{J}}_{K\eta}(t)\right)\Big] + [t\leftrightarrow u] + O(p^6).\end{aligned} \tag{4.43}$$

- $K^-K^0 \to \pi^-\pi^0$

$$\begin{aligned}
B_{K\pi} &= \frac{1}{4F_\pi^2}\gamma_{K\pi}(t-u) + \frac{1}{4F_\pi^4}\varphi_{K\pi}s(t-u) \\
&+ \frac{1}{48F_\pi^4}\gamma_{K\pi}(t-u)\left(\overline{J}_{KK}(s)\beta_{KK}(s-4m_K^2) + 2\overline{J}_{\pi\pi}(s)\beta_{\pi\pi}(s-4m_\pi^2)\right) \\
&+ \Bigg[\frac{1}{96F_\pi^4}\left(Y^{K\pi}_{K\pi ch}(t,u)\overline{J}_{K\pi}(t) + Y^{K\eta}_{K\pi ch}(t,u)\overline{J}_{K\eta}(t)\right) \\
&\quad + \frac{1}{32F_\pi^4}\frac{1}{t}\left(X^{K\pi}_{K\pi ch}(u)\overline{J}_{K\pi}(t) + X^{K\eta}_{K\pi ch}(u)\overline{J}_{K\eta}(t)\right) \\
&\quad\quad + \frac{1}{16F_\pi^4}\frac{1}{t^2}\Delta^2_{K\pi}\left(W^{K\pi}_{K\pi ch}\overline{\overline{J}}_{K\pi}(t) + W^{K\eta}_{K\pi ch}\overline{\overline{J}}_{K\eta}(t)\right)\Bigg] - [t\leftrightarrow u] + O(p^6).
\end{aligned} \tag{4.44}$$

- $\overline{K^0}K^0 \to \eta\eta$

$$\begin{aligned}
A_{K\eta} &= \frac{1}{4F_\pi^2}\left(\beta_{K\eta}(3s-2m_K^2-2m_\eta^2) + \alpha_{K\eta}\left(2m_\eta^2 - \frac{2}{3}m_K^2\right)\right) \\
&+ \frac{1}{4F_\pi^4}\left(\delta_{K\eta}(s-2m_\eta^2)(s-2m_K^2) + \varepsilon_{K\eta}\left((t-\Sigma_{K\eta})^2 + (u-\Sigma_{K\eta})^2\right)\right) \\
&+ \frac{1}{24F_\pi^4}\left(Z^{KK}_{K\eta}(s)\overline{J}_{KK}(s) + Z^{\eta\eta}_{K\eta}(s)\overline{J}_{\eta\eta}(s) + Z^{\pi\pi}_{K\eta}(s)\overline{J}_{\pi\pi}(s)\right) \\
&+ \Bigg[\frac{1}{32F_\pi^4}\left(Y^{K\eta}_{K\eta}(t,u)\overline{J}_{K\eta}(t) + Y^{K\pi}_{K\eta}(t,u)\overline{J}_{K\pi}(t)\right) \\
&\quad - \frac{3}{32F_\pi^4}\frac{1}{t}\left(X^{K\eta}_{K\eta}(u)\overline{J}_{K\eta}(t) + X^{K\pi}_{K\eta}(u)\overline{J}_{K\pi}(t)\right) \\
&\quad\quad + \frac{3}{16F_\pi^4}\frac{1}{t^2}\Delta^2_{K\eta}\left(W^{K\eta}_{K\eta}\overline{\overline{J}}_{K\eta}(t) + W^{K\pi}_{K\eta}\overline{\overline{J}}_{K\pi}(t)\right)\Bigg] + [t\leftrightarrow u] + O(p^6).
\end{aligned} \tag{4.45}$$

- $K^-K^+ \to \overline{K^0}K^0$

$$\begin{aligned}
A_{KK} &= \frac{1}{6F_\pi^2}\left(\beta_{KK}\left(4m_K^2 - 3u\right) + 3\gamma_{KK}(s-t) + 2\alpha_{KK}m_K^2\right) \\
&+ \frac{1}{6F_\pi^4}\left(\delta_{KK}(s-2m_K^2)^2 + \varepsilon_{KK}(t-2m_K^2)^2 + \varphi_{KK}(u-2m_K^2)^2\right) \\
&+ \frac{1}{288F_\pi^4}\Big(Z^{KK}_{KK}(s,t)\overline{J}_{KK}(s) + Z^{\eta\eta}_{KK}(s)\overline{J}_{\eta\eta}(s) + Z^{\eta\pi}_{KK}(s)\overline{J}_{\eta\pi}(s) + Z^{\pi\pi}_{KK}(s,t)\overline{J}_{\pi\pi}(s)\Big) \\
&+ \frac{1}{72F_\pi^4}\left(Y^{KK}_{KK}(s,t)\overline{J}_{KK}(t) + Y^{\eta\pi}_{KK}(t)\overline{J}_{\eta\pi}(t) + Y^{\pi\pi}_{KK}(s,t)\overline{J}_{\pi\pi}(t)\right) \\
&+ \frac{1}{36F_\pi^4}\overline{J}_{KK}(u)\left(3\beta_{KK}u - 2(\alpha_{KK}+2\beta_{KK})m_K^2\right)^2 + O(p^6).
\end{aligned} \tag{4.46}$$

4.4.1 Divergent part of the chiral logarithms

In Section 3.3 we have presented a method how one obtains also the divergent part of the chiral logarithms appearing in the polynomial $R(s,t,u)$. These divergences have to cancel the divergences of the unitarity part in the chiral limit that are easy to obtain from relations (3.21) and (3.22). We have also discussed there that just on the grounds of the finiteness of the amplitude in the chiral limit we cannot determine the masses appearing in the arguments of these logarithms since it can be divided by any number which has a finite logarithm, i.e. also by any ratio of pseudoscalar masses. In the case of the divergence stemming from the single-mass one-loop function it is, however, natural to put there precisely this mass. Further, in the case of two different masses, it is useful to add a finite constant to obtain the logarithm in the form

$$\frac{1}{\Delta_{yz}}\left(m_y^2\log\frac{m_y^2}{\Lambda^2}-m_z^2\log\frac{m_z^2}{\Lambda^2}\right)=\log\frac{m_y^2}{\Lambda^2}-\frac{2m_ym_z}{\Delta_{yz}}\log\frac{m_z}{m_y}\,, \tag{4.47}$$

which coincides with the divergent one-loop contribution $J_{yz}(0)$ determined by the usual Feynman integration of one-loop diagrams.

In accordance to the standard definition [74], in the following we use the notation

$$\mu_i=\frac{m_i^2}{32\pi^2F_\pi^2}\log\frac{m_i^2}{\Lambda^2}\qquad\text{with } i=\pi,K,\eta. \tag{4.48}$$

The divergent contributions of our polynomial parameters are then given by relations

$$\delta_{\pi\pi}\to-\frac{2}{3}\beta_{\pi\pi}^2\frac{\mu_\pi}{m_\pi^2}-\frac{1}{12}(3\beta_{K\pi}^2-2\gamma_{K\pi}^2)\frac{\mu_K}{m_K^2}\,, \tag{4.49}$$

$$\varepsilon_{\pi\pi}\to-\frac{2}{3}\beta_{\pi\pi}^2\frac{\mu_\pi}{m_\pi^2}-\frac{1}{12}\gamma_{K\pi}^2\frac{\mu_K}{m_K^2}\,, \tag{4.50}$$

$$\delta_{\eta\eta}\to-\frac{27}{4}\beta_{K\eta}^2\frac{\mu_K}{m_K^2}\,, \tag{4.51}$$

$$\delta_{\eta\pi}\to-\frac{9}{4}\beta_{K\eta\pi}^2\frac{\mu_K}{m_K^2}\,, \tag{4.52}$$

$$\varepsilon_{\eta\pi}\to-\frac{9}{4}\beta_{K\eta}\beta_{K\pi}\frac{\mu_K}{m_K^2}\,, \tag{4.53}$$

$$\delta_{K\eta}\to-\frac{3}{4}\left(6\beta_{KK}\beta_{K\eta}\frac{\mu_K}{m_K^2}-\beta_{K\eta}^2\frac{\mu_K-\mu_\eta}{m_K^2-m_\eta^2}-\beta_{K\eta\pi}^2\frac{\mu_K-\mu_\pi}{m_K^2-m_\pi^2}\right), \tag{4.54}$$

$$\varepsilon_{K\eta}\to-\frac{3}{2}\left(\beta_{K\eta}^2\frac{\mu_K-\mu_\eta}{m_K^2-m_\eta^2}+\beta_{K\eta\pi}^2\frac{\mu_K-\mu_\pi}{m_K^2-m_\pi^2}\right), \tag{4.55}$$

$$\delta_{K\eta\pi}\to\frac{1}{4}\beta_{K\eta\pi}\left(-6\beta_{KK}\frac{\mu_K}{m_K^2}+3\beta_{K\eta}\frac{\mu_K-\mu_\eta}{m_K^2-m_\eta^2}+(\beta_{K\pi}+\gamma_{K\pi})\frac{\mu_K-\mu_\pi}{m_K^2-m_\pi^2}\right), \tag{4.56}$$

$$\varepsilon_{K\eta\pi}\to-\frac{1}{2}\beta_{K\eta\pi}\left(3\beta_{K\eta}\frac{\mu_K-\mu_\eta}{m_K^2-m_\eta^2}+(\beta_{K\pi}-4\gamma_{K\pi})\frac{\mu_K-\mu_\pi}{m_K^2-m_\pi^2}\right), \tag{4.57}$$

$$\delta_{K\pi} \to \frac{1}{4}\left(-6\beta_{K\pi}\left(3\beta_{KK}\frac{\mu_K}{m_K^2}+4\beta_{\pi\pi}\frac{\mu_\pi}{m_\pi^2}\right)+3\beta_{K\eta}^2\frac{\mu_K-\mu_\eta}{m_K^2-m_\eta^2}+(\beta_{K\pi}^2+2\gamma_{K\pi}^2)\frac{\mu_K-\mu_\pi}{m_K^2-m_\pi^2}\right), \tag{4.58}$$

$$\varepsilon_{K\pi} \to -\frac{1}{2}\left(3\beta_{K\eta}^2\frac{\mu_K-\mu_\eta}{m_K^2-m_\eta^2}+(\beta_{K\pi}^2+14\gamma_{K\pi}^2)\frac{\mu_K-\mu_\pi}{m_K^2-m_\pi^2}\right), \tag{4.59}$$

$$\begin{aligned}\varphi_{K\pi} \to \frac{1}{12}\Bigg(&-2\gamma_{K\pi}\left(\beta_{KK}\frac{\mu_K}{m_K^2}+2\beta_{\pi\pi}\frac{\mu_\pi}{m_\pi^2}\right)+3\beta_{K\eta}^2\frac{\mu_K-\mu_\eta}{m_K^2-m_\eta^2}\\ &+\gamma_{K\pi}(13\gamma_{K\pi}-10\beta_{K\pi})\frac{\mu_K-\mu_\pi}{m_K^2-m_\pi^2}\Bigg),\end{aligned} \tag{4.60}$$

$$\delta_{KK} \to \frac{1}{8}\left(-27\beta_{K\eta}^2\frac{\mu_\eta}{m_\eta^2}-22\beta_{KK}^2\frac{\mu_K}{m_K^2}+(4\gamma_{K\pi}^2-9\beta_{K\pi}^2)\frac{\mu_\pi}{m_\pi^2}+18\beta_{K\eta\pi}^2\frac{\mu_\eta-\mu_\pi}{m_\eta^2-m_\pi^2}\right), \tag{4.61}$$

$$\varepsilon_{KK} \to \frac{1}{4}\left(\beta_{KK}^2\frac{\mu_K}{m_K^2}-\gamma_{K\pi}^2\frac{\mu_\pi}{m_\pi^2}-18\beta_{K\eta\pi}^2\frac{\mu_\eta-\mu_\pi}{m_\eta^2-m_\pi^2}\right), \tag{4.62}$$

$$\varphi_{KK} \to -\frac{1}{4}\left(17\beta_{KK}^2\frac{\mu_K}{m_K^2}+\gamma_{K\pi}^2\frac{\mu_\pi}{m_\pi^2}\right). \tag{4.63}$$

4.5 Connection with chiral perturbation theory

The results of amplitudes in particular models can be obtained by taking specific choices of the parameters. As an illustration we compare our results with the ones of the standard one-loop χPT computation presented in [78]. As was discussed in Section 3.6, in order to reproduce these results exactly, it is natural to use the order-by-order approach to our parameters, where the comparison proceeds in the following steps. The $O(p^2)$ chiral amplitude is exactly reproduced by the appropriate leading order polynomial from Section 4.3 with the standard $O(p^2)$ χPT values of its polynomial parameters listed in (4.29)–(4.32). The one-loop chiral result should be described by the parametrization obtained in Section 4.4. By taking the standard $O(p^2)$ values of our parameters in its unitarity part, we completely reproduce the non-polynomial part of [78] (up to a different sign convention[2]). The comparison of the polynomial parts then yields $O(p^4)$ corrections to our parameters in terms of the low-energy constants (LEC) of the standard χPT.

These $O(p^4)$ values of our parameters [in the particular renormalization scheme that was used in [78]] are listed in Appendix D. One can also verify that their divergent parts in chiral limit are indeed given by expressions (4.49)–(4.63), where we insert the $O(p^2)$ values of the parameters. It is also worth mentioning that thanks to the form of the second order polynomial of our parametrization (each term of the second order vanishes at the particular initial- and final-state thresholds of the amplitude), the $O(p^4)$ expressions for the parameters of the first-order terms, viz. α's, β's and γ's, do not contain (in the subtraction

[2]In addition, one should pay attention to their label of the 4-kaon process $\overline{K^0}K^0 \to K^+K^-$, which can give the false illusion about the definition of the Mandelstam variables, whereas the right one consistent with the notation (2.1) would be better evoked by the caption $\overline{K^0}K^0 \to K^-K^+$.

	Fit10	Fit10p4	FitAll	FitAllp4
$10^3 L_1^r$	0.39 ± 0.12	0.38	0.88 ± 0.09	1.12
$10^3 L_2^r$	0.73 ± 0.12	1.59	0.61 ± 0.20	1.23
$10^3 L_3$	-2.34 ± 0.37	-2.91	-3.04 ± 0.43	-3.98
$10^3 L_4^r$	0	0	0.75 ± 0.75	1.5
$10^3 L_5^r$	0.97 ± 0.11	1.46	0.58 ± 0.13	1.21
$10^3 L_6^r$	0	0	0.29 ± 0.85	1.17
$10^3 L_7$	-0.30 ± 0.15	-0.49	-0.11 ± 0.15	-0.36
$10^3 L_8^r$	0.6 ± 0.2	1.0	0.18 ± 0.18	0.62

Table 1: Values of the low-energy constants L_i coming from "fit10" [10] and "fitAll" [34]. Fit10p4 and FitAllp4 correspond to the fits where one uses just NLO expressions. We quote here the numbers for "fit10" obtained in [34] by redoing the original fit (the quoted numbers differ slightly to the original ones given in [10]).

scheme of [78]) the low-energy constants L_1^r, L_2^r, and L_3, i.e. the LECs of the operators that have four derivatives in the $O(p^4)$ Lagrangian of [74]. By inserting these $O(p^4)$ values of α, β and γ also into the unitarity part we would obtain a part of the $O(p^6)$ corrections to the amplitudes. However, in order to gain the complete $O(p^6)$ results, the second iteration of the reconstruction procedure would be required.

Instead of it, we return back to the chiral $O(p^4)$ expressions of our parameters and illustrate on them a few of the practical applications of our parametrization. By comparison of the experimentally determined values of our parameters with those predicted by some theoretical calculation, we can verify the assumptions made in that calculation. The advantage of the parametrization is that it reduces the number of parameters, while at the same time it preserves the analytic structure of the amplitude dictated by the unitarity.

We ignore for the moment the appearance of resonances in kinematic regions of many of the discussed processes, which reduces physical applicability of our results for such processes as is discussed in the next section. Assuming that the one-loop amplitude of a considered process reasonably approximates its physical amplitude, by studying the dependence of our parameters on chiral LECs, we can determine which of the parameters would be particularly suitable for constraining the values of these LECs. Furthermore, we can study the stability of the parameters with respect to their chiral expansion — a possible instability would indicate either a bad choice of the subtraction scheme (=parametrization) or a problem with the chiral expansion of the amplitude itself.

The phenomenologically most successful determination of the χPT LECs L_i is the ten-year old "fit10" from [10]. Recently, there has appeared a new fit [34] taking into account also more recent experimental determinations and computations, which however exposed large deviations from the values that were expected from large N_c considerations and from

some results obtained by lattice. Both the fits use NNLO chiral results but present also the values of L_i that reproduce best experimental data in the case one employs just the NLO expressions — what is our current case. However, since these values are not supplemented by their error bars, we use also the values from the NNLO results in order to investigate the magnitude of the possible errors. We list all these sets of values of L_i's in Table 1.

In the expressions for our polynomial parameters from Appendix D there appear also masses of pseudoscalar mesons and pion decay constant F_π. In correspondence with [34] we take them to be equal

$$m_\pi = 134.9766\,\mathrm{MeV}, \qquad m_K = 494.50\,\mathrm{MeV}, \tag{4.64}$$

$$m_\eta = 547.853\,\mathrm{MeV}, \qquad F_\pi = (92.2 \pm 0.2)\,\mathrm{MeV} \tag{4.65}$$

and we set the logarithmic scale Λ from (4.48) to $m_\rho \approx 770\,\mathrm{MeV}$. Nevertheless, since the values of L_i's in "fit10" were obtained using slightly different masses and moreover, the relations of the isospin masses used in our computation with the one experimentally measured (in the world where the isospin is not a preserved symmetry) are ambiguous, in the plots in Tables 2(a) and 3(a) we display [Note that the scale of these plots is logarithmic.] also the dependence of our parameters on the variation in masses in intervals

$$m_\pi = (134.9764 \div 139.56995)\,\mathrm{MeV}, \qquad m_K = (493.677 \div 497.672)\,\mathrm{MeV}, \tag{4.66}$$

$$m_\eta = (547.30 \div 547.853)\,\mathrm{MeV}. \tag{4.67}$$

This brings us interesting information on the dependence of our parameters on the particular choice of the isospin masses. This effect is directly observable from the error bars of the values corresponding to "fit10p4" and to "fitAllp4" since for them we have included no under uncertainties. We observe that e.g. the parameters $\alpha_{K\pi}$, $\beta_{K\pi}$ or α_{KK} and β_{KK} are very sensitive to the exact value of the masses we take. Taking these uncertainties into account we see that with the exception of $\epsilon_{\eta\pi}$ all the parameters corresponding to "fit10" at least partially overlay with those determined using "fitAll". However, by using the pure $O(p^4)$ values of L_i's in these two fits, some of the parameters have even the opposite sign of the one-loop contributions (e.g. ϵ_{KK}, $\beta_{K\eta}$). On the plots we can also study chiral convergence of our parameters — in the case the one-loop contribution to a given parameter is well above $0.1 \div 0.3$ one doubts a good chiral behavior/convergence of that parameter. This occurs for $\alpha_{K\pi}$, $\beta_{K\pi}$ and $\beta_{K\eta\pi}$.

In parts (b) of Tables 2 and 3 we list the ranges of parameters corresponding to "fit10" [and to the values of the masses and of F_π from (4.64)–(4.64)] together with the percentage of that ranges that is due to uncertainties in the particular L_is. Ignoring still the effect of resonances and the further particles not explicitly taken into account and the effects of higher loops, these numbers in the tables would mean that if we had measured some parameter with its precision better than the one quoted in the columns $\Delta\rho$, we would obtain a constraint on the L_i's better than "fit10" gives, especially on those L_i's quoted in the ultimate columns of that tables. Since in "fit10" the values of L_4^r and L_6^r are set to the large-N_c-inspired value = 0, the influence of these constants is invisible in these tables. We

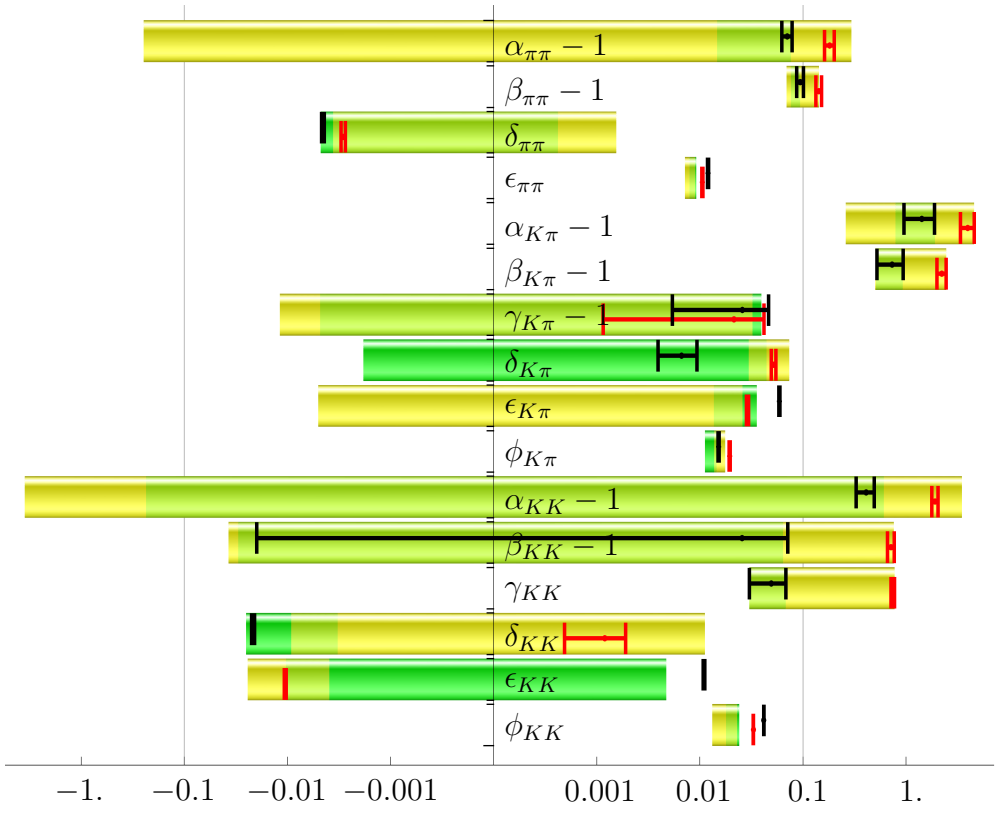

(a) with uncertainty in pseudoscalar masses included

ρ	$\Delta\rho$	Contribution of L_is	
$\alpha_{\pi\pi}-1$	$2\cdot10^{-2}\star$	L_8^r:0.82	L_5^r:0.15
$\beta_{\pi\pi}-1$	$3\cdot10^{-3}$	L_5^r:0.74	L_4^r
$\delta_{\pi\pi}$	$3\cdot10^{-3}$	L_3:0.59	L_1^r:0.38
$\epsilon_{\pi\pi}$	$5\cdot10^{-4}$	L_2^r:0.88	
$\alpha_{K\pi}-1$	$0.1\star$	L_8^r:0.68	L_5^r:0.15
$\beta_{K\pi}-1$	$2\cdot10^{-2}$	L_5^r:0.10	L_4^r
$\gamma_{K\pi}-1$	$1\cdot10^{-2}$	L_5^r:0.16	
$\delta_{K\pi}$	$2\cdot10^{-2}$	L_1^r:0.56	L_3:0.44
$\epsilon_{K\pi}$	$1\cdot10^{-2}$	L_2^r:0.56	L_3:0.44
$\phi_{K\pi}$	$1\cdot10^{-3}$	L_3:1.00	
$\alpha_{KK}-1$	$0.4\star$	L_8^r:0.76	L_5^r:0.21
$\beta_{KK}-1$	$6\cdot10^{-3}$	L_5^r:0.34	L_4^r
γ_{KK}	$3\cdot10^{-3}$	L_4^r	
δ_{KK}	$1\cdot10^{-2}$	L_1^r:0.56	L_3:0.44
ϵ_{KK}	$7\cdot10^{-3}$	L_3:0.61	L_2^r:0.39
ϕ_{KK}	$3\cdot10^{-3}$	L_2^r:1.00	

(b) without uncertainty in M_P

Table 2: Dependence of our parameters of meson-meson scattering processes on the values of $O(p^4)$ LECs L_i of χPT — first part. On the plot the value of our parameters for the following sets is depicted (note that the x-axes is logarithmic): full green corresponds to "fit10"; yellow to "fitAll"; black one to "fit10p4" and finally the red one to "fitAllp4". The uncertainties are due to uncertainties of L_i's quoted in Table 1 and the uncertainties in the pseudoscalar masses and in F_π (4.66)–(4.67). In the table part we list the uncertainties only due to L_i's and F_π. In the last columns the low-energy constants with the dominant contribution to this uncertainty are listed together with the corresponding fraction (the remaining uncertainty is mainly due to the error bar of F_π). We have denoted also the parameters depending on L_4^r and L_6^r by $\star$.

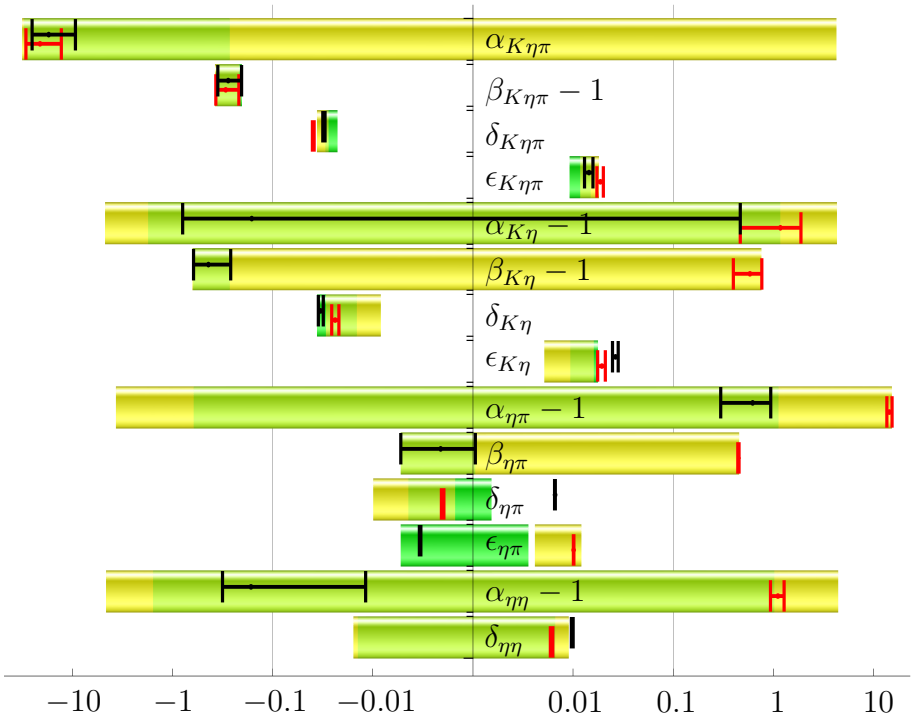

(a) with uncertainty in pseudoscalar masses included

ρ	$\Delta\rho$	Contribution of L_is		
$\alpha_{K\eta\pi}$	8.2	L_7:0.51	L_8^r:0.34	L_3:0.10
$\beta_{K\eta\pi} - 1$	$2 \cdot 10^{-2}$	L_3:0.20	L_5^r:0.11	
$\delta_{K\eta\pi}$	$3 \cdot 10^{-3}$	L_3:1.00		
$\epsilon_{K\eta\pi}$	$1 \cdot 10^{-3}$	L_3:1.00		
$\alpha_{K\eta} - 1$	0.9 $\star$	L_8^r:0.51	L_7:0.36	L_5^r:0.09
$\beta_{K\eta} - 1$	$1 \cdot 10^{-2}$	L_5^r:0.16	L_4^r	
$\delta_{K\eta}$	$9 \cdot 10^{-3}$	L_3:0.56	L_1^r:0.44	
$\epsilon_{K\eta}$	$2 \cdot 10^{-3}$	L_2^r:0.80	L_3:0.20	
$\alpha_{\eta\pi} - 1$	0.6 $\star$	L_7:0.80	L_5^r:0.10	L_8^r:0.03
$\beta_{\eta\pi}$	$1 \cdot 10^{-3}$	L_4^r		
$\delta_{\eta\pi}$	$3 \cdot 10^{-3}$	L_3:0.51	L_2^r:0.49	
$\epsilon_{\eta\pi}$	$4 \cdot 10^{-3}$	L_1^r:0.66	L_3:0.34	
$\alpha_{\eta\eta} - 1$	1.2 $\star$	L_8^r:0.50	L_7^r:0.41	L_5^r:0.08
$\delta_{\eta\eta}$	$1 \cdot 10^{-2}$	L_3:0.44	L_1^r:0.28	L_2^r:0.28

(b) without uncertainty in M_P

Table 3: Dependence of our parameters of meson-meson scattering processes on the values of $O(p^4)$ LECs L_i of χPT — second part. On the plot the value of our parameters for the following sets is depicted (note that the x-axes is logarithmic): full green corresponds to "fit10"; yellow to "fitAll"; black one to "fit10p4" and finally the red one to "fitAllp4". The uncertainties are due to uncertainties of L_i's quoted in Table 1 and the uncertainties in the pseudoscalar masses and in F_π (4.66)–(4.67). In the table part we list the uncertainties only due to L_i's and F_π. In the last columns the low-energy constants with the dominant contribution to this uncertainty are listed together with the corresponding fraction (the remaining uncertainty is mainly due to the error bar of F_π). We have denoted also the parameters depending on L_4^r and L_6^r by $\star$.

have therefore marked the parameters depending on them — L_4^r is listed in the ultimate columns of the tables and the dependence on both the L_4^r and L_6^r is denoted by star at the corresponding range.

4.6 Discussions and summary

The generic procedure from the previous chapter was used here for constructing a general form of the meson-meson scattering amplitudes valid to one-loop order. The major part of our results (published in all detail in [I] and [II]) were not computed in such a general form before. However, the practical significance of many of these results hinges on the fact that our method assumes working far below the region where the further particles different to the pseudoscalar mesons (e.g. resonances) appear. However, in the case of these processes with the exception of $\pi\pi \to \pi\pi$ and $\pi K \to \pi K$, this range is very narrow or does not even exist (e.g. in the process $KK \to KK$ with the kinematic threshold of 990 MeV, there can appear ρ resonance with its mass of 770 MeV). Nevertheless, besides the illustration of the elegance of our construction due to its intrinsic self-consistency, also the results for such processes can become useful for a check of complicated models or simulations, where it is possible to separate (or completely turn off) the effects of these resonances. The advantage is that even in the most general case in (to and excluding) $O(p^8)$ order, there is a small number (= 47) of parameters, coupling different processes together, and the analytic form of the two-loop result provides an easier survey than the usual Feynman-diagram-based computation. Naturally, to that end one should, however, complete the second iteration, which is a straightforward task (using the recipe from the previous chapter) but because of the appearance of three different masses in the NLO partial waves, the results are more complicated than in the isospin 2-flavor $\pi\pi$ amplitudes (where only one mass appears) of [95]. This is beyond the scope of this text. Nevertheless, we refer the interested reader to the following chapters where we perform the second iteration in the cases of isospin breaking $\pi\pi$ scattering and the $K, \eta \to 3\pi$ decays. From there one can gain the experience how to obtain the two-loop result also here. Moreover, since a part of the one-loop results from Section 4.4 has a similar form as the one-loop results of Chapters 5, 7 and 8, it is also possible to restore at least a part of the two-loop results from the two-loop results of those three chapters by a simple change of the masses and of the polynomial parameters appearing there.

Our final note is about the applicability of our results in the case of the power-countings where also odd chiral orders appear. One example of them is the generalized power-counting [97] which was closely connected with the original motivation of formulation of the reconstruction theorem [125, 95]. If such scheme turned out to be necessary for the description of these scattering processes, the only change we would need to make would be in shifting the chiral orders of our polynomials (together with changing their interpretations). Then, the input polynomial amplitudes would be of $O(p^3)$ order, and so after the first iteration we would obtain the $O(p^5)$ result whereas after the second one we would end up with the $O(p^7)$ order results.

Part II

$\pi\pi$ scattering

Chapter 5

$\pi\pi$ scattering

Now, we focus our interest on the most important process of chiral perturbation theory, on the pion-pion scattering.

5.1 Notation

The main aim of the present and the following chapters is the construction of amplitudes that includes the isospin breaking induced by different masses of the mesons belonging to the same isomultiplet. This leads to the necessity of distinguishing such different states. If we wanted to keep an explicit notation, it would be overburden and probably also not providing an easy survey. There is therefore a need for a shorthand notation.

We have decided to label the following $\pi\pi$ scattering processes using the one-character lower index according to the mnemonic

$$\begin{aligned}
\pi^0\pi^0 \to \pi^0\pi^0 \qquad & 0 \quad \text{[neutral]}, && (5.1\text{n})\\
\pi^+\pi^- \to \pi^+\pi^- \qquad & c \quad \text{[charged]}, && (5.1\text{c})\\
\pi^+\pi^+ \to \pi^+\pi^+ \qquad & d \quad \text{[double charged states]}, && (5.1\text{d})\\
\pi^\pm\pi^\mp \to \pi^0\pi^0 \qquad & x \quad \text{[mixed process]}, && (5.1\text{x})\\
\pi^+\pi^0 \to \pi^+\pi^0 \qquad & t \quad \text{[t-channel to the mixed process]}. && (5.1\text{t})
\end{aligned}$$

Since we do not take into account a violation of the CP symmetry, the amplitudes of the $\pi^+\pi^0$ and the $\pi^-\pi^0$ scattering processes have to be identical and similarly for the $\pi^+\pi^+$ and the $\pi^-\pi^-$ elastic scatterings.

The combinations (2.9), (2.19) and (2.20) of the pion masses with the different charged states are written in the following without any subscripts,

$$\Delta = m_{\pi^\pm}^2 - m_{\pi^0}^2, \tag{5.2}$$

$$\Sigma = m_{\pi^\pm}^2 + m_{\pi^0}^2, \tag{5.3}$$

$$\mu^\pm = (m_{\pi^\pm} \pm m_{\pi^0})^2; \tag{5.4}$$

and the similar is true also for the Källen's quadratic form (2.10),

$$\lambda(s) = \lambda_{\pi^\pm\pi^0}(s). \tag{5.5}$$

On the contrary, the one-loop function with two different pion masses keeps its indices, $\overline{J}_{+0}(s)$.

The single mass kinematical square-roots

$$\sigma_i(s) = \sqrt{1 - \frac{4m_i^2}{s}} \tag{5.6}$$

and the appropriate one-loop functions $\overline{J}_i(s)$ have their index $i = 0$ or $+$ according to the charge of the pion appearing there.

In the isospin symmetric case (IB^0) with just one mass m_π, we return back to the lower index π. On this general level, we do not identify this mass with any of the $m_{\pi^\pm}$ or m_{π^0} masses since there is an ambiguity in its choice and different authors use various definitions of it [cf. the discussion around (4.66)]. However, the choice of Weinberg [129] that takes m_π equal to the charged one prevails in the literature.

Finally, in the results of NLO partial-waves, we employ the fraction of pion masses

$$q = \frac{m_{\pi^0}}{m_{\pi^\pm}} \approx 0.97 < 1. \tag{5.7}$$

We remind the reader that in the whole work we use the same choice of phase convention bringing one minus sign for each charged particle in the final state and thereby also changing the sign of amplitude every time crossing a charged particle between the final and the initial states.

5.2 Symmetries

We begin noting that even if we take the isospin violation into account, not all of the amplitudes (5.1) are independent. The crossing property gives

$$A_t(s,t,u) = -A_x(t,s,u), \quad A_d(s,t,u) = A_c(u,t,s). \tag{5.8}$$

In addition, in the isospin symmetric case the following relations [cf. (4.5)–(4.7)]

$$A_c^{IB^0}(s,t,u) = -A_x^{IB^0}(s,t,u) - A_x^{IB^0}(t,s,u), \tag{5.9}$$

$$A_0^{IB^0}(s,t,u) = -A_x^{IB^0}(s,t,u) - A_x^{IB^0}(t,s,u) - A_x^{IB^0}(u,t,s) \tag{5.10}$$

tell us that in this case the amplitude $A_x^{IB^0}$ can be taken as the only independent one.

5.3 The reconstruction procedure

Performing the procedure of Chapter 3 and the justification of validity of the assumptions of the reconstruction theorem for $\pi\pi$ scattering are simple tasks and no further complication with respect to the cases discussed in the previous chapter appears also beyond the isospin limit. Moreover, for the low-energy kinematic region, in which we are interested in these amplitudes, the analyticity of the amplitude and the validity of the dispersion relation, together with the complete partial wave decomposition can be derived from the first principles of axiomatic theory similarly[1] as for those processes in Appendix C.

In Chapter 3 we have shown that for the construction of a meson-meson scattering amplitude up to two loops, we just need to count in the contributions of all the intermediate states (of all the crossed processes) that contain two mesons and possess the same quantum numbers as the initial (and the final) states of the considered processes do. However, we want to describe the $\pi\pi$ scattering only within the low-energy region far below the appearance of other than two-pion states, viz. KK, $K\pi$, $\eta\pi$, ..., and thereby also far from the singularities induced by such states. It is therefore not needed to retain all these intermediate states. Instead, we can formally expand such contributions in powers of Mandelstam variables divided by the scale corresponding to the threshold of appearance of these states and include such arisen polynomials into the polynomial of the theorem. Assuming that this contribution is well described by the third order polynomial, the only leading order amplitudes that have to be treated as inputs for our construction are indeed the $\pi\pi$ scattering ones.

We do not take into account any electromagnetic effects other than the $\pi^+ - \pi^0$ mass difference, however, with the charged pion scattering there is always connected the effect of appearance of pionium as the electromagnetically bounded state of two pions $(\pi^+\pi^-)_\gamma$. We could try to include it by adding also this state into the set of possible intermediate states k in the unitarity relations[2] and parametrizing its decay amplitudes $(\pi^+\pi^-)_\gamma \to \pi\pi$. This would bring some new constants, thereby making the eventual fit of data more complicated. At the current level and also taking into account its narrowness, we propose not to include it and in the practical applications of our results just discard the points where it appears from the fit.

We have already noted that the choice of the first-order polynomials as the leading order amplitudes together with the choice of the polynomial of the reconstruction theorem can be important for the chiral convergence properties of the resulting parametrization and can have influence on the stability of the eventual fit to data. The usual choice of the subthreshold parametrization seems not to be particularly suitable for the description of the experimental data on $\pi\pi$ scattering. A more natural choice is the use of the scattering lengths as parameters instead, which is discussed in the following sections. Nevertheless,

[1] Actually, we can use the results of Section C.3, where we just take $m_A = m_{\pi^\pm}$ and $m_\pi = m_{\pi^0}$.

[2] Naturally, it cannot be done simply by adding the pionium into (2.18) since in the case of $1 \to 2$ processes there is no direct meaning of partial waves. The simplest way would be therefore to perform such inclusion separately.

in Section 5.9 we give transposing relations between the parametrizations, whose simple application converts our results into the parametrization using the subthreshold parameters.

5.4 Scattering-length parametrization

The scattering-length parametrization or better to say the partial-wave parametrization is connected with the behavior of partial waves of the amplitude at its physical threshold. The expansion of the real part of ℓ-th partial wave of amplitude $A_i(s,t,u)$ of process $AB \to CD$

$$\mathrm{Re}\, f_{i,\ell}(s) = P^\ell_{AB}(s) P^\ell_{CD}(s) \left(a_{i,\ell} + (s - s_{\mathrm{thr}}) \frac{r_{i,\ell}}{F_\pi^2} + \cdots \right) \tag{5.11}$$

defines[3] the scattering lengths $a_{i,\ell}$, the effective range parameters $r_{i,\ell}$ and higher parameters hidden in the dots. The 3-momenta of the particles in the initial and the final state in their center-of-mass system are given by

$$P_{AB}(s) = \frac{\lambda^{1/2}_{AB}(s)}{2\sqrt{s}}\,, \qquad P_{CD}(s) = \frac{\lambda^{1/2}_{CD}(s)}{2\sqrt{s}}\,. \tag{5.12}$$

As is discussed below, in our applications we concentrate just on the S-wave scattering lengths $a_{i,0}$ and its effective range parameters $r_{i,0}$, so for the sake of brevity, we will not explicitly write the index indicating S-wave, i.e. we just write a_i and r_i.

At the leading order we choose the parameters of the amplitude corresponding exactly to the leading order parameters of the partial-wave expansion, i.e. to the scattering length and the effective range parameter of S-wave, and where needed also to the P-wave scattering length. Going to higher order causes a necessity to use further scattering parameters and it also leads to the appearance of corrections to the parameters from the lower orders. A part of these corrections comes from the $\pi\pi$ scatterings in the original final states and appears also in the unitarity part of the theorem. Therefore, if we want to keep the physical definition (and values) of the parameters, we have to add a restoring polynomial canceling the contribution of the unitarity part into these parameters[4]. It is obvious that more parameters we want to keep at their physical value bring more complicated restoring polynomials. Nevertheless, at low energies, where we are interested in, the contribution of the higher order parameters and of their corrections is numerically small. Moreover, the motivation for using this parametrization is to have as most precise fit of the scattering lengths (and further parameters) as possible and since it is out of the reach of the current

[3]Note that our definitions of partial waves and thereby also of the scattering lengths differ from the common isospin symmetric one (cf. e.g. [73]) by a factor of 2. In addition, the effective range parameter r (normalized here with F_π^2 to be dimensionless) is in the isospin symmetric case usually defined in a slightly different way.

[4]One can understand this procedure as a subtraction of the contribution which would be otherwise double counted — once resummed in the scattering length parameter and once in the unitarity part.

experimental and fitting techniques to fit also the higher parameters so precisely, in many cases we need to use their values from outside. It is therefore meaningful to keep the physical value of just a few of the most important parameters and in the other neglect their higher order corrections. In some applications it is even more practical to use [in addition to these few partial-wave parameters in which we are interested in] any additional parameters, not necessarily corresponding to any threshold partial-wave characteristic. In the following, we discuss these two possibilities — keeping the physical value only of the scattering lengths, which will be good enough for the current precision of experiment; and keeping the physical values of all the parameters appearing already at the leading order, i.e. of parameters a_i and r_i [or b_i from (5.24) equivalently]. On the latter approach we illustrate the way the procedure would continue for keeping the physical value also of further parameters — from a few possible choices one can take, we have chosen here the one in which the crossing relations (5.61)–(5.64) have a simple linear form.

5.5 Leading order

The physical thresholds for different processes are[5]

$$s_{0,\mathrm{thr}} = 4m_{\pi^0}^2, \qquad t_{0,\mathrm{thr}} = 0, \qquad u_{0,\mathrm{thr}} = 0, \tag{5.13}$$
$$s_{x,\mathrm{thr}} = 4m_{\pi^\pm}^2, \qquad t_{x,\mathrm{thr}} = -\Delta, \qquad u_{x,\mathrm{thr}} = -\Delta, \tag{5.14}$$
$$s_{t,\mathrm{thr}} = \mu_+, \qquad t_{t,\mathrm{thr}} = 0, \qquad u_{t,\mathrm{thr}} = \mu_-, \tag{5.15}$$
$$s_{c,\mathrm{thr}} = 4m_{\pi^\pm}^2, \qquad t_{c,\mathrm{thr}} = 0, \qquad u_{c,\mathrm{thr}} = 0, \tag{5.16}$$
$$s_{d,\mathrm{thr}} = 4m_{\pi^\pm}^2, \qquad t_{d,\mathrm{thr}} = 0, \qquad u_{d,\mathrm{thr}} = 0. \tag{5.17}$$

Taking them into account together with the crossing and the Bose symmetry, the leading order parametrization (= polynomial of the first order) of the amplitudes reads

$$A_0(s,t,u) = 16\pi a_0, \tag{5.18}$$
$$A_x(s,t,u) = 16\pi\left(a_x + \frac{r_x}{F_\pi^2}(s - 4m_{\pi^\pm}^2)\right), \tag{5.19}$$
$$A_t(s,t,u) = 16\pi\left(a_t + \frac{r_t}{F_\pi^2}(s-\mu_+) + \frac{a_{t,1}}{F_\pi^2}(t - u - \frac{\mu_-}{\mu_+}\, s + 2\mu_-)\right), \tag{5.20}$$
$$A_c(s,t,u) = 16\pi\left(a_c + \frac{r_c}{F_\pi^2}(s - 4m_{\pi^\pm}^2) + \frac{a_{c,1}}{F_\pi^2}(t-u)\right), \tag{5.21}$$
$$A_d(s,t,u) = 16\pi\left(a_d + \frac{r_d}{F_\pi^2}(s - 4m_{\pi^\pm}^2)\right). \tag{5.22}$$

In these relations, we have indicated manifestly the scattering length parametrization. Nevertheless, the crossing and the Bose symmetry dictate that the P-wave scattering lengths

[5] In [44] they take a different definition of the scattering length a_0 — defined at the cusp threshold $s_{0,\mathrm{thr}} = 4m_{\pi^\pm}^2$ instead of the physical one that is used here.

$a_{t,1}$ and $a_{c,1}$ have to fulfill relations[6]

$$a_{t,1} = -\frac{\mu_+}{4m_{\pi^\pm}m_{\pi^0}}\, r_t, \qquad a_{c,1} = r_c, \tag{5.23}$$

and so we can write equivalently

$$A_t(s,t,u) = 16\pi\left(a_t - 2\frac{b_t}{F_\pi^2}\, t\right), \tag{5.20$'$}$$

$$A_c(s,t,u) = 16\pi\left(a_c - 2\frac{b_c}{F_\pi^2}\, u\right). \tag{5.21$'$}$$

For the sake of brevity, we have introduced parameters b_i as rescalled effective range parameters, where it holds

$$r_x = b_x, \quad r_t = \frac{4m_{\pi^\pm}m_{\pi^0}}{\mu_+}\, b_t, \quad r_c = b_c, \quad r_d = b_d. \tag{5.24}$$

Even then, not all the remaining parameters are independent since we have not used the crossing relations (5.8) yet. At the leading order, they relate further

$$b_x = 2b_t, \qquad b_d = -2b_c \tag{5.25}$$

and

$$a_t = \frac{4m_{\pi^\pm}^2}{F_\pi^2}\, b_x - a_x, \quad a_d = a_c - \frac{8m_{\pi^\pm}^2}{F_\pi^2}\, b_c\,. \tag{5.26}$$

This means that at the leading order we have just 5 independent parameters, which can be chosen e.g. to be the scattering lengths. However, (only) at the leading order ($O(p^2)$) all the pion scattering lengths can be expressed in terms of the two S-wave scattering lengths in the isospin limit, a_0^0 and a_0^2 from [73]. From [98] we have the following expressions[7]

$$a_0 = \frac{2}{3}\,\mathrm{a}_0^0 + \frac{4}{3}\,\mathrm{a}_0^2 - \frac{2}{3}\left(\mathrm{a}_0^0 + 2\mathrm{a}_0^2\right)\frac{\Delta}{m_{\pi^\pm}^2}\,, \tag{5.27}$$

$$a_x = -\frac{2}{3}\,\mathrm{a}_0^0 + \frac{2}{3}\,\mathrm{a}_0^2 + \mathrm{a}_0^2\,\frac{\Delta}{m_{\pi^\pm}^2}\,, \tag{5.28}$$

$$a_t = \mathrm{a}_0^2 - \mathrm{a}_0^2\,\frac{\Delta}{m_{\pi^\pm}^2}\,, \tag{5.29}$$

$$a_c = \frac{2}{3}\,\mathrm{a}_0^0 + \frac{1}{3}\,\mathrm{a}_0^2 - 2\mathrm{a}_0^2\,\frac{\Delta}{m_{\pi^\pm}^2}\,, \tag{5.30}$$

$$a_d = 2\mathrm{a}_0^2 - 2\mathrm{a}_0^2\,\frac{\Delta}{m_{\pi^\pm}^2}\,. \tag{5.31}$$

[6] Naturally, in the case we wanted to keep the physical interpretation of the P-wave scattering lengths, at higher orders, relations (5.23) would gain $O(p^4)$ corrections and during the computation we would need to distinguish between the P-wave scattering lengths and the right-hand sides of these relations, i.e. for instance between $a_{c,1}$ and r_c.

[7] We have used relations (2.18), (2.21) and (2.22) of [98] and write a_0^0 and a_0^2 instead of $\left(\mathrm{a}_0^0\right)_{\mathrm{str}}$ and $\left(\mathrm{a}_0^2\right)_{\mathrm{str}}$ from [98]. Note that the isospin limit is defined there traditionally as $m_{\pi^0} \to m_{\pi^\pm}$, i.e. the mass of the isospin pion is identified with the mass of the charged pion, $m_{\pi^\pm}$.

5.6 Next-to-leading-order result

5.6.1 Unitarity part

The first iteration of the reconstruction procedure is again simple. Taking into account the crossing symmetry of the amplitudes, their NLO form can be written as

$$A_i(s,t,u) = 16\pi \left(R_i(s,t,u) + 16\pi U_i(s,t,u)\right) + O(p^6) \tag{5.32}$$

with

$$U_0(s,t,u) = W_0^0(s) + W_0^0(t) + W_0^0(u), \tag{5.33}$$
$$U_x(s,t,u) = W_x^0(s) - W_t^0(t) - (s-u)W_t^1(t) - W_t^0(u) - (s-t)W_t^1(u), \tag{5.34}$$
$$U_t(s,t,u) = W_t^0(s) + (t-u)W_t^1(s) - W_x^0(t) + W_t^0(u) + (t-s)W_t^1(u), \tag{5.35}$$
$$U_c(s,t,u) = W_c^0(s) + (t-u)W_c^1(s) + W_c^0(t) + (s-u)W_c^1(t) + W_d^0(u), \tag{5.36}$$
$$U_d(s,t,u) = W_d^0(s) + W_c^0(t) + (u-s)W_c^1(t) + W_c^0(u) + (t-s)W_c^1(u). \tag{5.37}$$

According to (3.10) and (3.11), the dispersion integrals W_i are given by

$$W_0^0(s) = \frac{(a_0)^2}{2}\bar{J}_0(s) + \left(a_x + \frac{b_x}{F_\pi^2}(s - 4m_{\pi^\pm}^2)\right)^2 \bar{J}_\pm(s), \tag{5.38}$$

$$W_x^0(s) = \left(a_x + \frac{b_x}{F_\pi^2}(s - 4m_{\pi^\pm}^2)\right)\left(\frac{a_0}{2}\bar{J}_0(s) + \left(a_c + \frac{b_c}{F_\pi^2}(s - 4m_{\pi^\pm}^2)\right)\bar{J}_\pm(s)\right), \tag{5.39}$$

$$\begin{aligned} W_t^0(s) = {} & \bar{J}_{\pm 0}(s)\left[\left(a_t + \frac{b_t}{F_\pi^2}(s - 2\Sigma)\right)^2 + \frac{7b_t^2}{3F_\pi^4}\Delta^2 + \frac{2}{s}\frac{b_t}{F_\pi^2}\Delta^2\left(a_t - \frac{7b_t}{3F_\pi^2}\Sigma\right)\right] \\ & + \frac{4}{3}\frac{b_t^2}{F_\pi^4}\Delta^4\frac{\bar{\bar{J}}_{\pm 0}(s)}{s^2}, \end{aligned} \tag{5.40}$$

$$W_t^1(s) = \frac{1}{3}\frac{b_t^2}{F_\pi^4}\left(s - 2\Sigma + \frac{\Delta^2}{s}\right)\bar{J}_{\pm 0}(s), \tag{5.41}$$

$$W_c^0(s) = \frac{1}{2}\left(a_x + \frac{b_x}{F_\pi^2}(s - 4m_{\pi^\pm}^2)\right)^2 J_0(s) + \left(a_c + \frac{b_c}{F_\pi^2}(s - 4m_{\pi^\pm}^2)\right)^2 \bar{J}_\pm(s), \tag{5.42}$$

$$W_c^1(s) = \frac{1}{3}\frac{b_c^2}{F_\pi^4}\left(s - 4m_{\pi^\pm}^2\right)\bar{J}_\pm(s), \tag{5.43}$$

$$W_d^0(s) = \frac{1}{2}\left(a_d + \frac{b_d}{F_\pi^2}(s - 4m_{\pi^\pm}^2)\right)^2 \bar{J}_\pm(s). \tag{5.44}$$

5.6.2 Polynomial part

The only remaining ingredients for the reconstruction of the NLO $\pi\pi$ scattering amplitudes are the polynomials $R_i(s,t,u)$. We have already discussed that their form depends on how many partial-wave parameters are retained at their physical interpretation. We have

decided to show here two possibilities — keeping the physical value only of the scattering lengths and keeping them for all the scattering lengths and the effective range parameters appearing at the leading order of the parametrization, a_i, b_i.

In any case, $R_i(s,t,u)$ should be a general polynomial of second order in Mandelstam variables obeying the same $s \leftrightarrow t \leftrightarrow u$ symmetries as the complete amplitude does. We divide every such polynomial into three parts, each obeying the given s,t,u symmetry. The first part corresponds to a general first order polynomial written in the same form as the appropriate LO amplitude from (5.18)–(5.22) and its parameter a_i (and in the second case also the parameter b_i) keeps its physical interpretation also at this order. The second part contains all allowed polynomial terms of second order supplemented by the appropriate lower order terms which are chosen so that this part does not contribute to the S-wave scattering lengths [and when keeping also the definition of b_i's, it does not contribute to the rescalled S-wave effective ranges[8] as well] of the amplitudes and thereby this part is not changing the physical meaning of a_i [and b_i]. The third part, which we call the restoring polynomial, cancels the contribution of the unitarity part $U_i(s,t,u)$ to these parameters.

Keeping the physical values of the scattering lengths

In this case the restoring polynomial is directly equal to the real part of the unitarity part at the threshold. It is therefore just a constant. In accordance with the definition

$$\operatorname{Re} A_i(s,t,u)|_{\text{thr}} = 16\pi a_i, \tag{5.45}$$

we obtain

$$w_i = 16\pi \operatorname{Re} U_i(s,t,u)|_{\text{thr}}\,. \tag{5.46}$$

Their values for the particular $\pi\pi$ scattering processes are given in Appendix E.

The polynomials of the NLO results are then simply

$$R_0(s,t,u) = a_0 + 3\frac{\lambda_0}{F_\pi^4}(s^2+t^2+u^2-16m_{\pi^0}^4) - w_0, \tag{5.47}$$

$$\begin{aligned} R_x(s,t,u) = a_x &+ \frac{b_x}{F_\pi^2}(s-4m_{\pi^\pm}^2) - \frac{\lambda_x^{(1)}}{F_\pi^4}\,s(s-4m_{\pi^\pm}^2) \\ &- \frac{\lambda_x^{(2)}}{F_\pi^4}\left[(t+\Delta)(t+\Delta-4m_{\pi^\pm}^2) + u \leftrightarrow t\right] - w_x, \end{aligned} \tag{5.48}$$

$$R_t(s,t,u) = a_t - 2\frac{b_t}{F_\pi^2}\,t + \frac{\lambda_x^{(1)}}{F_\pi^4}\,t(t-4m_{\pi^\pm}^2) + \frac{\lambda_x^{(2)}}{F_\pi^4}\left[(s-\mu_+)(s-\mu_-) + u \leftrightarrow s\right] - w_t, \tag{5.49}$$

$$R_c(s,t,u) = a_c - 2\frac{b_c}{F_\pi^2}\,u + \frac{2\lambda_c^{(2)}}{F_\pi^4}\,u(u-4m_{\pi^\pm}^2) + \frac{\lambda_c^{(1)}+\lambda_c^{(2)}}{F_\pi^4}\left[s(s-4m_{\pi^\pm}^2) + t \leftrightarrow s\right] - w_c, \tag{5.50}$$

[8] Naturally, with the exception of the process $A_0(s,t,u)$ — cf. with footnote 10 on the next page.

$$R_d(s,t,u) = a_d + \frac{b_d}{F_\pi^2}(s-4m_{\pi^\pm}^2) + \frac{2\lambda_c^{(2)}}{F_\pi^4}\,s(s-4m_{\pi^\pm}^2) + \frac{\lambda_c^{(1)}+\lambda_c^{(2)}}{F_\pi^4}\left[t(t-4m_{\pi^\pm}^2)+u\leftrightarrow t\right] - w_d. \tag{5.51}$$

From the crossing relations (5.8) it follows that the coefficients λ_i appearing in the polynomials R_x and R_t are identical and the same is true also for λ_i in R_c and R_d. Their form implies also that relations (5.25) and (5.26) obtain the following NLO corrections

$$b_t = \frac{b_x}{2}\,, \tag{5.52}$$

$$b_d = -2b_c, \tag{5.53}$$

$$a_t = \frac{4m_{\pi^\pm}^2}{F_\pi^2}\,b_x - a_x - 8m_{\pi^\pm}^2\Delta\frac{\lambda_x^{(2)}}{F_\pi^4} + w_t + w_x, \tag{5.54}$$

$$a_d = a_c - \frac{8m_{\pi^\pm}^2}{F_\pi^2}\,b_c + w_d - w_c. \tag{5.55}$$

Keeping the physical values of all the leading order parameters

In the case we want to keep the physical meaning also of the other leading order parameters, the determination of the restoring polynomials proceeds in the following way. We write it as the most general polynomial obeying the given s,t,u symmetries and compute their contributions into the values of a_i and b_i which have to cancel such contributions from the corresponding unitarity part $U_i(s,t,u)$.

We could have taken these polynomials to be of first order — each would have the same number of parameters as the appropriate LO amplitude has. It means that the conditions on the coefficients of any restoring polynomial would be a linear system of two independent equations for two independent parameters[9]. Nevertheless, we have decided to demand the simple linear form of the crossing relations (5.61)–(5.64) and thus we take the restoring polynomials in the form of second-order polynomials, which in addition fulfill the simple crossing relations coming from (5.8) — namely in both R_x and R_t there appear w_x together with w_t and similarly for R_c and R_d polynomials.

We write therefore[10]

$$R_0(s,t,u) = a_0 + 3\frac{\hat\lambda_0}{F_\pi^4}(s^2+t^2+u^2-16m_{\pi^0}^4) - w_0(s) - w_0(t) - w_0(u), \tag{5.56}$$

[9]With an exception of $A_0(s,t,u)$ where retaining a_0 means just having a restoring constant equal to the contribution of the unitary part [as in the previous case, i.e. (5.46)].

[10]In the case of amplitude $A_0(s,t,u)$, the effective range parameter is in the leading order equal to zero and thus at the next-to-leading order where it is already nonzero, we have to add it into the parametrization. Instead of writing $\hat\lambda_0$ we could call this parameter $b_0 = \hat\lambda_0 = \frac{F_\pi^2}{24m_{\pi^0}^2}r_0$.

$$\begin{aligned} R_x(s,t,u) &= a_x + \frac{b_x}{F_\pi^2}(s-4m_{\pi^\pm}^2) - \frac{\hat\lambda_x^{(1)}}{F_\pi^4}(s-4m_{\pi^\pm}^2)^2 - \frac{\hat\lambda_x^{(2)}}{3F_\pi^4}\left[(t+\Delta)(3t+5\Delta)+u\leftrightarrow t\right] \\ &\quad - w_x(s) + w_t(t) + w_t(u), \end{aligned} \tag{5.57}$$

$$\begin{aligned} R_t(s,t,u) &= a_t - 2\frac{b_t}{F_\pi^2}\,t + \frac{\hat\lambda_x^{(1)}}{F_\pi^4}t^2 \\ &\quad + \frac{\hat\lambda_x^{(2)}}{F_\pi^4}\left[(s-\mu_+)(s-\mu_-) - 4(s-\Sigma)(\Sigma+m_{\pi^0}m_{\pi^\pm}) + u\leftrightarrow s\right] \\ &\quad - w_t(s) + w_x(t) - w_t(u), \end{aligned} \tag{5.58}$$

$$\begin{aligned} R_c(s,t,u) &= a_c - 2\frac{b_c}{F_\pi^2}\,u + \frac{2\hat\lambda_c^{(2)}}{F_\pi^4}u^2 \\ &\quad + \frac{\hat\lambda_c^{(1)}+\hat\lambda_c^{(2)}}{F_\pi^4}\left[s(s-4m_{\pi^\pm}^2) - 12m_{\pi^\pm}^2(s-2m_{\pi^\pm}^2) + t\leftrightarrow s\right] \\ &\quad - w_c(s) - w_c(t) - w_d(u), \end{aligned} \tag{5.59}$$

$$\begin{aligned} R_d(s,t,u) &= a_d + \frac{b_d}{F_\pi^2}(s-4m_{\pi^\pm}^2) + \frac{2\hat\lambda_c^{(2)}}{F_\pi^4}(s-4m_{\pi^\pm}^2)^2 + \frac{\hat\lambda_c^{(1)}+\hat\lambda_c^{(2)}}{F_\pi^4}\left[t^2+u^2\right] \\ &\quad - w_d(s) - w_c(t) - w_c(u). \end{aligned} \tag{5.60}$$

The restoring polynomials $w_i(s)$ are derived and listed also for this case in Appendix E. For their determination we can either use the results for S partial-waves of the unitarity parts of amplitudes given in Section 5.7.4 and expand them in powers of $(s-s_{thr})$ or we can compute them directly using the relations between derivative expansion of the amplitude at its threshold and the partial-wave parameters as discussed into detail in Appendix E.

It is obvious that the polynomials $R(s,t,u)$ constructed in this way are the most general second order polynomials obeying the required $s\leftrightarrow t\leftrightarrow u$ symmetries and that their parameters a and b keep their physical interpretation up to one loop, e.g. there holds relation (5.45).

Thanks to our requirement of the symmetric form of the polynomials, the crossing relations (5.8) imply that the parameters $\hat\lambda_i$ appearing in R_x and R_t, and similarly those appearing in R_c and R_d, are again connected as denoted in the written form of the polynomials. Relations (5.25) and (5.26) then obtain simple linear NLO corrections that read

$$b_t = \frac{b_x}{2} + 4m_{\pi^\pm}^2\frac{\hat\lambda_x^{(1)}}{F_\pi^2} + \frac{\hat\lambda_x^{(2)}}{3F_\pi^2}(13m_{\pi^\pm}^2 + 6m_{\pi^\pm}m_{\pi^0} + 5m_{\pi^0}^2), \tag{5.61}$$

$$b_d = -2b_c + 16m_{\pi^\pm}^2\frac{\hat\lambda_c^{(1)}+2\hat\lambda_c^{(2)}}{F_\pi^2}\,, \tag{5.62}$$

$$a_t = \frac{4m_{\pi^\pm}^2}{F_\pi^2}\,b_x - a_x + 16m_{\pi^\pm}^4\frac{\hat\lambda_x^{(1)}}{F_\pi^4} + 16m_{\pi^\pm}^2(2m_{\pi^\pm}^2+m_{\pi^0}^2)\frac{\hat\lambda_x^{(2)}}{3F_\pi^4}\,, \tag{5.63}$$

$$a_d = a_c - \frac{8m_{\pi^\pm}^2}{F_\pi^2}\, b_c + 16 m_{\pi^\pm}^4 \frac{3\hat{\lambda}_c^{(1)} + 5\hat{\lambda}_c^{(2)}}{F_\pi^4}\,. \tag{5.64}$$

In summary, we have 10 independent parameters describing all the $\pi\pi$ scattering processes to the one-loop level, independently on how many parameters are kept at their physical interpretation. As is discussed in Appendix E.2.3, in the case we decided to neglect the restoring polynomials but took the physical values of the scattering lengths, such neglecting would correspond to the relative error of the scattering lengths of the order indicated in relations (E.66)–(E.70), i.e. $\sim 2\%$ to 16%.

Further, using just the restoring constants that keep the physical values only of the scattering lengths, while taking numerical values of the effective range parameters equal to their physical values corresponds to having them with relative error of order given in (E.71)–(E.75), which is less[11] than 20%. Since we will not have the values of the effective range parameters with a better precision, we use in this work precisely this procedure. Nevertheless, in forthcoming numerical analyses we use also the full restoration of a_i and b_i (by changing the restoring polynomial) for examination of its influence on the obtained results.

5.7 S- and P-partial waves of NLO amplitudes

The computation of S- and P-partial waves of NLO amplitudes was outlined already in Section 3.4. We use the general formulae from there for the $\pi\pi$ scattering amplitudes obtained in the previous section. For the physical values of s, all end-points of integrations (3.30) and (3.31) are real numbers located left to the cuts of $\bar{J}_i(t)$ and so we do not need to deform the integration contours $\mathcal{C}(t_-, t_+)$. The results of integrations are therefore just the differences of the primitive functions evaluated at those two end points.

There are three different possible types of channels we need to compute (cf. Figure 3) — either integration of a channel with two particles of the same mass in both the initial and the final state, symbolically denoted as $PP \to QQ$ (Figure 3a,b,d); or $PQ \to PQ$ channel stemming from the direct process $PP \to QQ$ (Figure 3c); and finally the latter coming from the direct process $PQ \to PQ$ (Figure 3e). Let us discuss the integrations for them separately.

5.7.1 Integration in a same-mass channel $PP \to QQ$

In this case we are computing either the T channel of a process $PQ \to PQ$ or the U channel of a $PQ \to QP$ process (or even a much simpler case with all the masses equal). From relations (3.28) and (3.29) (or just from simple physical considerations), we observe that the endpoints are generally

$$t_+ = 0, \qquad t_- = -\frac{\lambda_{PQ}(s)}{s}\,. \tag{5.65}$$

[11] Note that this larger relative error occurs only for the parameter b_c, all the other have even better precision, which is less than 8%.

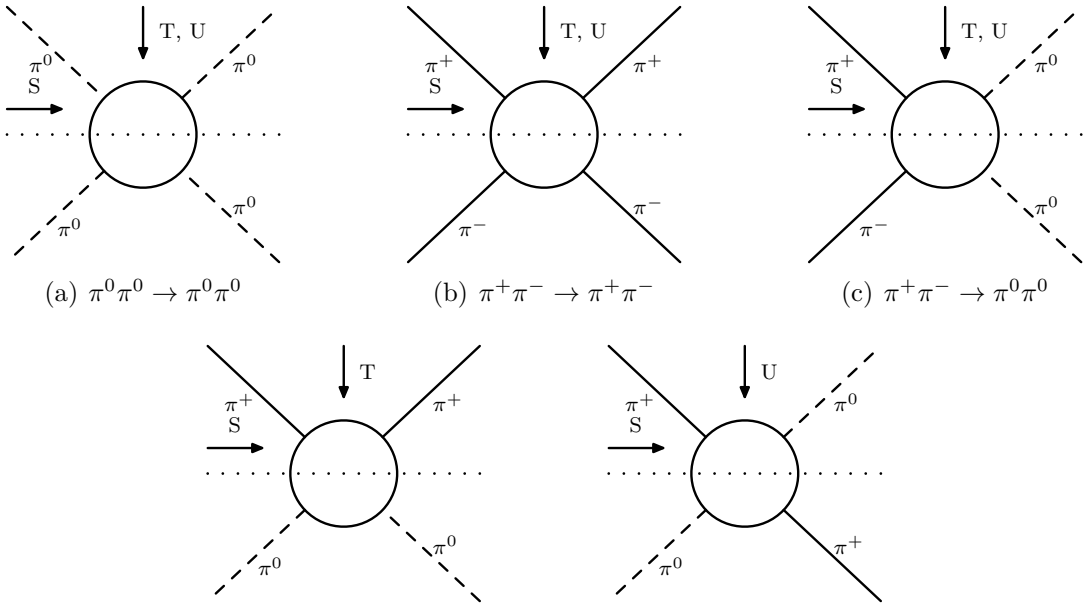

(a) $\pi^0\pi^0 \to \pi^0\pi^0$ (b) $\pi^+\pi^- \to \pi^+\pi^-$ (c) $\pi^+\pi^- \to \pi^0\pi^0$

(d) $\pi^+\pi^0 \to \pi^+\pi^0$ (T channel) (e) $\pi^+\pi^0 \to \pi^+\pi^0$ (U channel)

Figure 3: Various channels appearing in the computation of partial waves of NLO $\pi\pi$ scattering amplitudes. A dashed line corresponds to π^0, while the plain one to $\pi^\pm$ (with the line labels we have indicated charge state of the corresponding pion in S channel). With the dotted line there is denoted the unitarity cut with the appropriate intermediate states in T and U channels.

Naturally, for u integration these points are interchanged, i.e. the non-zero value is u_+.

Because two pions with different masses have also different charges and we do not violate the electric-charge conservation, the intermediate states in NLO have to be also those containing two pions of equal masses and we employ here the single-mass results (3.68)–(3.75). Since these primitive functions are chosen vanishing at $t = 0$, the results of integrations (3.30) and (3.31) are equal to linear combinations of the negative values of these primitive functions evaluated at t_- or for u integrations equal to linear combinations of these functions at u_+.

In the particular processes there appear the following functions in the results [All functions appearing in the results are summarized again in Appendix F.]

- Channel $\pi^0\pi^0 \to \pi^0\pi^0$ $\qquad (t_-(s) = 4m_{\pi^0}^2 - s)$
  – intermediate state $\pi^0\pi^0$

$$T_- = \frac{s}{2m_{\pi^0}^2}, \tag{5.66}$$

$$\sigma_{T_-} = \frac{1}{\sigma_0(t_-)} = \sigma_0(s), \tag{5.67}$$

$$L_{T_-} = \log \tau_0(t_-) = L_0(s) := \log \frac{1-\sigma_0(s)}{1+\sigma_0(s)}\,, \tag{5.68}$$

– intermediate state $\pi^+\pi^-$

$$T_- = \frac{s+4\Delta}{2m_{\pi^\pm}^2}, \tag{5.69}$$

$$\sigma_{T_-} = \frac{1}{\sigma_+(t_-)} = \sigma_\nabla(s) := \sqrt{\frac{s-4m_{\pi^0}^2}{s+4\Delta}}\,, \tag{5.70}$$

$$L_{T_-} = \log\tau_+(t_-) = L_\nabla(s) := \log\frac{1-\sigma_\nabla(s)}{1+\sigma_\nabla(s)}\,. \tag{5.71}$$

- Channel $\pi^\pm\pi^\pm \to \pi^\pm\pi^\pm$ or $\pi^\pm\pi^\mp \to \pi^\pm\pi^\mp$ $\qquad (t_-(s) = 4m_{\pi^\pm}^2 - s)$

  – intermediate state $\pi^+\pi^\pm$

$$T_-(s) = \frac{s}{2m_{\pi^\pm}^2}, \tag{5.72}$$

$$\sigma_{T_-} = \frac{1}{\sigma_+(t_-)} = \sigma_+(s), \tag{5.73}$$

$$L_{T_-} = \log\tau_+(t_-) = L_+(s) := \log\frac{1-\sigma_+(s)}{1+\sigma_+(s)}\,, \tag{5.74}$$

  – intermediate state $\pi^0\pi^0$

$$T_-(s) = \frac{s-4\Delta}{2m_{\pi^0}^2}, \tag{5.75}$$

$$\sigma_{T_-} = \frac{1}{\sigma_0(t_-)} = \sigma_\Delta(s) := \sqrt{\frac{s-4m_{\pi^\pm}^2}{s-4\Delta}}\,, \tag{5.76}$$

$$L_{T_-} = \log\tau_0(t_-) = L_\Delta(s) := \log\frac{1-\sigma_\Delta(s)}{1+\sigma_\Delta(s)}\,. \tag{5.77}$$

- Channel $\pi^\pm\pi^\mp \to \pi^0\pi^0$ $\qquad (t_-(s) = -\frac{\lambda(s)}{s})$

  – intermediate state $\pi^0\pi^0$

$$T_-(s) = \frac{(s-\Delta)^2}{2sm_{\pi^0}^2}, \tag{5.78}$$

$$\sigma_{T_-} = \frac{1}{\sigma_0(t_-)} = \sigma_\odot(s) := \frac{\lambda^{1/2}(s)}{s-\Delta}\,, \tag{5.79}$$

$$L_{T_-} = \log\tau_0(t_-) = L_\odot(s) := \log\frac{1-\sigma_\odot(s)}{1+\sigma_\odot(s)}\,, \tag{5.80}$$

  – intermediate state $\pi^+\pi^-$

$$T_-(s) = \frac{(s+\Delta)^2}{2sm_{\pi^\pm}^2}, \tag{5.81}$$

$$\sigma_{T_-} = \frac{1}{\sigma_+(t_-)} = \sigma_\oplus(s) := \frac{\lambda^{1/2}(s)}{s+\Delta}\,, \tag{5.82}$$

$$L_{T_-} = \log\tau_+(t_-) = L_\oplus(s) := \log\frac{1-\sigma_\oplus(s)}{1+\sigma_\oplus(s)}\,. \tag{5.83}$$

5.7.2 Integration in a $PQ \to PQ$ channel originating from $PP \to QQ$ process

The second type of processes is a $PQ \to PQ$ channel coming from S-channel process $PP \to QQ$. In order to take advantage of our short-hand notation, we identify already from the beginning $P \leftrightarrow \pi^\pm$ and $Q \leftrightarrow \pi^0$ and use the fact that we need the partial waves of this process only for the physical values of s, $s > 4m_{\pi^\pm}^2 > 4m_{\pi^0}^2$, i.e. in the region where both $\sigma_+(s)$ and $\sigma_0(s)$ have real values. The relations for endpoints of integrations read

$$t_\pm(s) = \Sigma - \frac{s}{2}\left(1 \mp \sigma_0(s)\sigma_+(s)\right). \tag{5.84}$$

Because of the conservation of electric-charge, the only intermediate state appearing here is the $\pi^\pm\pi^0$ one and so we need to evaluate the primitive functions (3.51)–(3.56) for one-loop functions of this two-pion state. The triangle function which appear in these relations evaluated at those end-points simplifies into [cf. (3.16)]

$$\lambda^{1/2}(t_\pm) = -\frac{s}{2}\left(\sigma_0(s) \mp \sigma_+(s)\right), \tag{5.85}$$

which implies the arguments of the logarithms (3.36) equaling to

$$\tau(t_\pm) = \frac{1}{q}\frac{1-\sigma_0(s)}{1\mp\sigma_+(s)} = \frac{s}{4m_{\pi^0}m_{\pi^\pm}}\big(1-\sigma_0(s)\big)\big(1\pm\sigma_+(s)\big). \tag{5.86}$$

Thus, we have relations between the arguments for t_+ and t_-

$$\frac{\tau(t_+)}{\tau(t_-)} = \frac{1+\sigma_+(s)}{1-\sigma_+(s)}\,, \tag{5.87}$$

$$\tau(t_+)\tau(t_-) = \frac{1-\sigma_0(s)}{1+\sigma_0(s)}\,, \tag{5.88}$$

which simplify the combinations of logarithms appearing in the results into [The functions $L_0(s)$ and $L_+(s)$ are defined in (5.68) and (5.74).]

$$\log\tau(t_+) - \log\tau(t_-) = -L_+(s), \tag{5.89}$$

$$\log\tau(t_+) + \log\tau(t_-) = L_0(s), \tag{5.90}$$

$$\log^2\tau(t_+) - \log^2\tau(t_-) = -L_+L_0(s), \tag{5.91}$$

$$\lambda^{1/2}(t_+)\log\tau(t_+) - \lambda^{1/2}(t_-)\log\tau(t_-) = \frac{s}{2}\left(\sigma_0(s)L_+(s) + \sigma_+(s)L_0(s)\right), \tag{5.92}$$

$$\lambda^{1/2}(t_+)\log\tau(t_+) + \lambda^{1/2}(t_-)\log\tau(t_-) = -\frac{s}{2}\left(\sigma_0(s)L_0(s) + \sigma_+(s)L_+(s)\right). \tag{5.93}$$

Consequently, using the notation of functions $\mathcal{M}_i$ from Appendix F, the differences of primitive functions evaluated at these endpoints [i.e. the results of integrations along $C(t_-, t_+)$] are

$$\begin{aligned}
\frac{I_1(t)}{s\sigma_0\sigma_+}\Big|_{t_-}^{t_+} &= \frac{2m_{\pi^\pm}^2 m_{\pi^0}^2}{\Sigma}\mathcal{M}_{2n+}(s) - \frac{1}{4}\left(s - 2m_{\pi^\pm}^2\right)\mathcal{M}_{1+}(s) \\
&\quad - \frac{1}{4}\left(s - 2m_{\pi^0}^2\right)\mathcal{M}_{1n}(s) - \frac{1}{4}(3s - 4\Sigma) - \frac{1}{2}\Big(s - \frac{8m_{\pi^\pm}^2 m_{\pi^0}^2}{\Sigma}\Big)\mathcal{M}_{0q}(s),
\end{aligned} \tag{5.94}$$

$$\begin{aligned}
\frac{I_2(t)}{s\sigma_0\sigma_+}\Big|_{t_-}^{t_+} &= 2m_{\pi^\pm}^2 m_{\pi^0}^2\mathcal{M}_{2n+}(s) + \frac{1}{12}\left(2s^2 - s(9m_{\pi^\pm}^2 + 5m_{\pi^0}^2) + 6m_{\pi^\pm}^2\Sigma\right)\mathcal{M}_{1+}(s) \\
&\quad + \frac{1}{12}\left(2s^2 - s(5m_{\pi^\pm}^2 + 9m_{\pi^0}^2) + 6m_{\pi^0}^2\Sigma\right)\mathcal{M}_{1n}(s) \\
&\quad + \frac{1}{36}\left(16s^2 - 61s\Sigma + 36\Sigma^2 + 16m_{\pi^\pm}^2 m_{\pi^0}^2\right) \\
&\quad + \frac{1}{6}\Big(2s^2 - s\Big(5\Sigma + \frac{12m_{\pi^\pm}^2 m_{\pi^0}^2}{\Sigma}\Big) + 32m_{\pi^\pm}^2 m_{\pi^0}^2\Big)\mathcal{M}_{0q}(s),
\end{aligned} \tag{5.95}$$

$$\begin{aligned}
\frac{I_3(t)}{s\sigma_0\sigma_+}\Big|_{t_-}^{t_+} &= 2m_{\pi^\pm}^2 m_{\pi^0}^2\Big(\Sigma + \frac{m_{\pi^\pm}^2 m_{\pi^0}^2}{\Sigma}\Big)\mathcal{M}_{2n+}(s) \\
&\quad - \frac{1}{24}\big(3s^3 - 2s^2(10m_{\pi^\pm}^2 + 7m_{\pi^0}^2) + 2s\left(7\Sigma^2 + m_{\pi^\pm}^2(11m_{\pi^\pm}^2 + 20m_{\pi^0}^2)\right) \\
&\qquad - 12m_{\pi^\pm}^2\left(\Sigma^2 + m_{\pi^\pm}^2 m_{\pi^0}^2\right)\big)\mathcal{M}_{1+}(s) \\
&\quad - \frac{1}{24}\big(3s^3 - 2s^2(7m_{\pi^\pm}^2 + 10m_{\pi^0}^2) + 2s\left(7\Sigma^2 + m_{\pi^0}^2(20m_{\pi^\pm}^2 + 11m_{\pi^0}^2)\right) \\
&\qquad - 12m_{\pi^0}^2\left(\Sigma^2 + m_{\pi^\pm}^2 m_{\pi^0}^2\right)\big)\mathcal{M}_{1n}(s) \\
&\quad - \frac{1}{144}\big(45s^3 - 266s^2\Sigma + 4s\left(107\Sigma^2 + 81m_{\pi^\pm}^2 m_{\pi^0}^2\right) \\
&\qquad - 16\Sigma\left(9\Sigma^2 + 20m_{\pi^\pm}^2 m_{\pi^0}^2\right)\big) \\
&\quad - \frac{1}{12}\Big(3s^3 - 2s^2\Big(7\Sigma + \frac{8m_{\pi^\pm}^2 m_{\pi^0}^2}{\Sigma}\Big) + 2s\left(7\Sigma^2 + 44m_{\pi^\pm}^2 m_{\pi^0}^2\right) \\
&\qquad - 16m_{\pi^\pm}^2 m_{\pi^0}^2\Big(5\Sigma + \frac{4m_{\pi^\pm}^2 m_{\pi^0}^2}{\Sigma}\Big)\Big)\mathcal{M}_{0q}(s),
\end{aligned} \tag{5.96}$$

$$\frac{I_0(t)}{s\sigma_0\sigma_+}\Big|_{t_-}^{t_+} = \mathcal{M}_{2n+}(s) - \mathcal{M}_{7x}(s) + \frac{1}{2}\big(\mathcal{M}_{1+}(s) + \mathcal{M}_{1n}(s)\big) + 2 + \mathcal{M}_{0q}(s), \tag{5.97}$$

$$\frac{I_{-1}(t)}{s\sigma_0\sigma_+}\Big|_{t_-}^{t_+} = -\frac{1}{\Sigma}\mathcal{M}_{2n+}(s) + \frac{\Sigma}{\Delta^2}\mathcal{M}_{7x}(s) + \frac{1}{2\Delta}\left(\mathcal{M}_{1+}(s) - \mathcal{M}_{1n}(s)\right) - \frac{1}{\Sigma}\mathcal{M}_{0q}(s), \tag{5.98}$$

$$\begin{aligned}
\frac{I_{-2}(t)}{s\sigma_0\sigma_+}\Big|_{t_-}^{t_+} &= \frac{2m_{\pi^\pm}^2 m_{\pi^0}^2}{\Delta^4}\mathcal{M}_{7x}(s) - \frac{s - 2m_{\pi^\pm}^2}{4\Delta^3}\mathcal{M}_{1+}(s) + \frac{s - 2m_{\pi^0}^2}{4\Delta^3}\mathcal{M}_{1n}(s) \\
&\quad + \frac{1}{2\Delta^2} + \frac{s}{2\Sigma\Delta^2}\mathcal{M}_{0q}(s).
\end{aligned} \tag{5.99}$$

For the sake of brevity, we have suppressed the explicit indication of the dependence of functions σ_0 and σ_+ on s.

5.7.3 Integration in a $PQ \to PQ$ channel originating from $PQ \to PQ$ process

The last type of contributions comes from the U channel of a process $PQ \to PQ$. [Again we perform the identification $P \leftrightarrow \pi^{\pm}$ and $Q \leftrightarrow \pi^0$ already from the beginning.]

Proceeding similarly as in the previous case, we obtain for $s > 4m_{\pi^\pm}^2$ in turn,

$$u_+(s) = 2\Sigma - s, \qquad u_-(s) = \frac{\Delta^2}{s}, \tag{5.100}$$

the values of triangle function at these points

$$\lambda^{1/2}(u_+) = -\lambda^{1/2}(s), \qquad \lambda^{1/2}(u_-) = -\frac{\Delta}{s}\lambda^{1/2}(s) \tag{5.101}$$

and consequently the arguments of the logarithms (3.36)

$$\tau(u_+) = \frac{s - \Sigma - \lambda^{1/2}(s)}{2m_{\pi^0}m_{\pi^\pm}}, \qquad \tau(u_-) = \frac{s\Sigma - \Delta^2 - \Delta\lambda^{1/2}(s)}{2sm_{\pi^0}m_{\pi^\pm}}. \tag{5.102}$$

They fulfill relations

$$\frac{\tau(u_+)}{\tau(u_-)} = \frac{1 - \sigma_\oplus(s)}{1 + \sigma_\oplus(s)}, \qquad \tau(u_+)\tau(u_-) = \frac{1 - \sigma_\odot(s)}{1 + \sigma_\odot(s)} \tag{5.103}$$

with $\sigma_\odot$ and $\sigma_\oplus$ as well as $L_\odot$ and $L_\oplus$ defined in (5.79)–(5.83), from which there follows

$$\log\tau(u_+) - \log\tau(u_-) = L_\oplus(s), \tag{5.104}$$

$$\log\tau(u_+) + \log\tau(u_-) = L_\odot(s), \tag{5.105}$$

$$\log^2\tau(u_+) - \log^2\tau(u_-) = L_\oplus L_\odot(s), \tag{5.106}$$

$$\lambda^{1/2}(u_+)\log\tau(u_+) - \lambda^{1/2}(u_-)\log\tau(u_-) = -\frac{\lambda(s)}{2s}\left(\frac{L_\oplus(s)}{\sigma_\oplus(s)} + \frac{L_\odot(s)}{\sigma_\odot(s)}\right), \tag{5.107}$$

$$\lambda^{1/2}(u_+)\log\tau(u_+) + \lambda^{1/2}(u_-)\log\tau(u_-) = -\frac{\lambda(s)}{2s}\left(\frac{L_\oplus(s)}{\sigma_\odot(s)} + \frac{L_\odot(s)}{\sigma_\oplus(s)}\right). \tag{5.108}$$

We can therefore write the results in one of the sets of functions, either using $L_\odot(s)$ and $L_\oplus(s)$, or using the functions

$$L_\uparrow := \log\tau(u_+), \qquad L_\downarrow := \log\tau(u_-). \tag{5.109}$$

Between these sets we can transfer easily by using relations (5.104)–(5.105). For the sake of the shortest possible form of the results we use the following mixed notation [Functions $\mathcal{M}_i(s)$ can be found in Appendix F.]

$$\begin{aligned} s\frac{I_1(t)}{\lambda(s)}\Big|_{u_-}^{u_+} = &-\frac{2m_{\pi^\pm}^2 m_{\pi^0}^2}{\Sigma}\mathcal{M}_{2\odot\oplus}(s) + \frac{1}{2}(s-\Sigma)\mathcal{M}_{1\uparrow}(s) - \frac{1}{2}\Big(\Sigma - \frac{\Delta^2}{s}\Big)\mathcal{M}_{1\downarrow}(s) \\ &+ \frac{3}{4}\Big(s - \frac{\Delta^2}{s}\Big) - \Sigma + \frac{1}{2}\Big(s - \frac{8m_{\pi^\pm}^2 m_{\pi^0}^2}{\Sigma} - \frac{\Delta^2}{s}\Big)\mathcal{M}_{0q}(s), \end{aligned} \tag{5.110}$$

$$
\begin{aligned}
s\frac{I_2(t)}{\lambda(s)}\Big|_{u_-}^{u_+} &= -2m_{\pi^\pm}^2 m_{\pi^0}^2 \mathcal{M}_{2\odot\oplus}(s) - \frac{1}{6}\left(2s^2 - 7\Sigma s + 5\Delta^2 + 12m_{\pi^\pm}^2 m_{\pi^0}^2\right)\mathcal{M}_{1\uparrow}(s) \\
&\quad - \frac{1}{6}\Big(\Delta^2 + 12m_{\pi^\pm}^2 m_{\pi^0}^2 + \Sigma\frac{\Delta^2}{s} - 2\frac{\Delta^4}{s^2}\Big)\mathcal{M}_{1\downarrow}(s) \\
&\quad - \frac{1}{36}\Big(16s^2 - 61s\Sigma + 4(9\Sigma^2 + 4m_{\pi^\pm}^2 m_{\pi^0}^2) + 29\Sigma\frac{\Delta^2}{s} + 16\frac{\Delta^4}{s^2}\Big) \\
&\quad - \frac{1}{6}\Big(2s^2 - s\Big(5\Sigma + \frac{12m_{\pi^\pm}^2 m_{\pi^0}^2}{\Sigma}\Big) + 32m_{\pi^\pm}^2 m_{\pi^0}^2 \\
&\qquad + \Big(\Sigma + \frac{12m_{\pi^\pm}^2 m_{\pi^0}^2}{\Sigma}\Big)\frac{\Delta^2}{s} + 2\frac{\Delta^4}{s^2}\Big)\mathcal{M}_{0q}(s),
\end{aligned}
\tag{5.111}
$$

$$
\begin{aligned}
s\frac{I_3(t)}{\lambda(s)}\Big|_{u_-}^{u_+} &= -m_{\pi^\pm}^2 m_{\pi^0}^2\Big(\Sigma + \frac{m_{\pi^\pm}^2 m_{\pi^0}^2}{\Sigma}\Big)\mathcal{M}_{2\odot\oplus}(s) \\
&\quad + \frac{1}{12}\big(3s^3 - 17s^2\Sigma + s(31\Sigma^2 - 6m_{\pi^\pm}^2 m_{\pi^0}^2) - \Sigma(17\Delta^2 + 30m_{\pi^\pm}^2 m_{\pi^0}^2)\big)\mathcal{M}_{1\uparrow}(s) \\
&\quad - \frac{1}{12}\Big(\Sigma(\Delta^2 + 30m_{\pi^\pm}^2 m_{\pi^0}^2) + (\Sigma^2 + 6m_{\pi^\pm}^2 m_{\pi^0}^2)\frac{\Delta^2}{s} + \Sigma\frac{\Delta^4}{s^2} - 3\frac{\Delta^6}{s^3}\Big)\mathcal{M}_{1\downarrow}(s) \\
&\quad + \frac{1}{144}\Big(45s^3 - 266s^2\Sigma + s(473\Sigma^2 + 144m_{\pi^\pm}^2 m_{\pi^0}^2) - 16\Sigma(9\Sigma^2 + 20m_{\pi^\pm}^2 m_{\pi^0}^2) \\
&\qquad - (121\Sigma^2 + 144m_{\pi^\pm}^2 m_{\pi^0}^2)\frac{\Delta^2}{s} - 86\Sigma\frac{\Delta^4}{s^2} - 45\frac{\Delta^6}{s^3}\Big) \\
&\quad + \frac{1}{12}\Big(3s^3 - 2s^2\Big(7\Sigma + \frac{8m_{\pi^\pm}^2 m_{\pi^0}^2}{\Sigma}\Big) + s(17\Sigma^2 + 86m_{\pi^\pm}^2 m_{\pi^0}^2) - 2\Big(\Sigma + \frac{8m_{\pi^\pm}^2 m_{\pi^0}^2}{\Sigma}\Big)\frac{\Delta^4}{s^2} \\
&\qquad - 16m_{\pi^\pm}^2 m_{\pi^0}^2\Big(5\Sigma + \frac{4m_{\pi^\pm}^2 m_{\pi^0}^2}{\Sigma}\Big) - (\Sigma^2 + 44m_{\pi^\pm}^2 m_{\pi^0}^2)\frac{\Delta^2}{s} - 3\frac{\Delta^6}{s^3}\Big)\mathcal{M}_{0q}(s),
\end{aligned}
\tag{5.112}
$$

$$
s\frac{I_0(t)}{\lambda(s)}\Big|_{u_-}^{u_+} = -\mathcal{M}_{2\odot\oplus}(s) - \mathcal{M}_{7t}(s) - \mathcal{M}_{1\uparrow}(s) + \mathcal{M}_{1\downarrow}(s) - 2 - \mathcal{M}_{0q}(s), \tag{5.113}
$$

$$
s\frac{I_{-1}(t)}{\lambda(s)}\Big|_{u_-}^{u_+} = \frac{1}{\Sigma}\mathcal{M}_{2\odot\oplus}(s) + \frac{\Sigma}{\Delta^2}\mathcal{M}_{7t}(s) - \frac{s}{\Delta^2}\mathcal{M}_{1\downarrow}(s) + \frac{1}{\Delta}\mathcal{M}_{8t}(s), \tag{5.114}
$$

$$
s\frac{I_{-2}(t)}{\lambda(s)}\Big|_{u_-}^{u_+} = \frac{2m_{\pi^\pm}^2 m_{\pi^0}^2}{\Delta^4}\mathcal{M}_{7t}(s) - \frac{s(s-\Sigma)}{2\Delta^4}\mathcal{M}_{1\downarrow}(s) + \frac{s}{2\Sigma\Delta^2}\mathcal{M}_{0q}(s) + \frac{1}{\Delta^2}\mathcal{M}_{9t}(s). \tag{5.115}
$$

5.7.4 Results for partial waves of NLO $\pi\pi$ amplitudes

By employing the formulae from Section 3.4 together with the ones from the previous subsection, it is an easy (although tedious) task to obtain the partial waves of the NLO $\pi\pi$ scattering amplitudes in the form (3.76). The partial waves of the particular processes are[12]

[12]Note that $\varphi_{i,\ell}$ is just the NLO part of the partial wave.

- $\pi^0\pi^0 \to \pi^0\pi^0$

$$\varphi_{0;0}(s) = p_\lambda^{0;0}(s) + p_w^{0;0}(s) + \frac{1}{\pi}\sum_i p_i^{0;0}(s)\mathcal{M}_i(s) \text{ with } i = 0, 1\mathrm{n}, 1\nabla, 2\mathrm{n}, 2\nabla, 3\mathrm{n}, 3+. \tag{5.116}$$

- $\pi^\pm\pi^\mp \to \pi^\pm\pi^\mp$

$$\varphi_{c;0}(s) = p_\lambda^{c;0}(s) + p_w^{c;0}(s) + \frac{1}{\pi}\sum_i p_i^{c;0}(s)\mathcal{M}_i(s) \text{ with } i = 0, 1+, 1\Delta, 2+, 2\Delta, 3\mathrm{n}, 3+, \tag{5.117}$$

$$\varphi_{c;1}(s) = s\sigma_+^2(s)\Big(p_\lambda^{c;1}(s) + p_w^{c;1}(s) + p_{3+}^{c;1}(s)\mathcal{M}_{3+}(s)\Big) + \frac{m_{\pi^\pm}^2}{\pi s\sigma_+^2(s)}\sum_i p_i^{c;1}(s)\mathcal{M}_i(s), \quad i = 0, 1+, 1\Delta, 2+, 2\Delta. \tag{5.118}$$

- $\pi^\pm\pi^\pm \to \pi^\pm\pi^\pm$

$$\varphi_{d;0}(s) = p_\lambda^{d;0}(s) + p_w^{d;0}(s) + \frac{1}{\pi}\sum_i p_i^{d;0}(s)\mathcal{M}_i(s), \ i = 0, 1+, 1\Delta, 2+, 2\Delta, 3+. \tag{5.119}$$

- $\pi^\pm\pi^\mp \to \pi^0\pi^0$

$$\varphi_{x;0}(s) = p_\lambda^{x;0}(s) + p_w^{x;0}(s) + \frac{1}{\pi}\sum_i p_i^{x;0}(s)\mathcal{M}_i(s), \ i = 0, 0q, 1\mathrm{n}, 1+, 2\mathrm{n}+, 3\mathrm{n}, 3+, 7x. \tag{5.120}$$

- $\pi^\pm\pi^0 \to \pi^\pm\pi^0$

$$\varphi_{t;0}(s) = p_\lambda^{t;0}(s) + p_w^{t;0}(s) + \frac{1}{\pi}\sum_i p_i^{t;0}(s)\mathcal{M}_i(s), \quad i = 0, 0q, 1\uparrow, 1\downarrow, 2\odot, 2\oplus, 2\odot\oplus, 3\uparrow, 7t, 8t, 9t, \tag{5.121}$$

$$\varphi_{t;1}(s) = \frac{\lambda(s)}{s}\Big(p_\lambda^{t;1}(s) + p_w^{t;1}(s) + p_{3\uparrow}^{t;1}(s)\mathcal{M}_{3\uparrow}(s)\Big) + \frac{s\Sigma}{2\pi\lambda(s)}\sum_i p_i^{t;1}(s)\mathcal{M}_i(s) \quad i = 0, 0q, 1\uparrow, 1\downarrow, 2\odot, 2\oplus, 2\odot\oplus, 7t, 8t, 9t. \tag{5.122}$$

The polynomials $p_i^j(s)$ are given in Appendix G whereas the dimensionless kinematic functions $\mathcal{M}_i(s)$ are defined in Appendix F.

5.8 Second iteration

Having all NLO partial waves at hand enables us a simple computation of the NNLO amplitudes of various processes, such as the NNLO $\pi\pi$ scattering amplitudes or the $\pi\pi$ form-factors. However, since our main interest of this work is concentrated only on its influence on the $K \to 3\pi$ and $\eta \to 3\pi$ decay processes and the results of second iteration are very extensive, we do not present here the results explicitly (but they can be obtained from the author on demand).

As an illustration for the interested reader, we present here the form of the result for $\pi^0\pi^0 \to \pi^0\pi^0$ scattering process

$$A_0(s,t,u) = 16\pi \left(R_0(s,t,u) + 16\pi (W_0^0(s) + W_0^0(t) + W_0^0(u)) \right), \tag{5.123}$$

where

$$R_0(s,t,u) = a_0 + 3\frac{\lambda_0}{F_\pi^4}\left(s^2+t^2+u^2-16m_{\pi^0}^4\right) + 3\frac{\lambda_0^{(3)}}{F_\pi^4}\left(s^3+t^3+u^3-64m_{\pi^0}^6\right) - w_0', \tag{5.124}$$

$$w_0' = 16\pi \,\mathrm{Re}\, U_0(s,t,u)|_{\mathrm{thr}} \tag{5.125}$$

and the unitarity part

$$W_0^0(s) = \sum_i \mathcal{P}_i \mathcal{H}_i \tag{5.126}$$

can be obtained from the result (8.44) of the process $K_L\pi^0 \to \pi^0\pi^0$ by performing limit $m_{K_L} \to m_{\pi^0}$, replacing $\mathcal{C} \to 16\pi$ and by an appropriate replacement of the kaon subtraction constants $\tilde{A}, \tilde{B}$ by the pion ones. It contains 13 Hilbert transforms of the functions resulting from multiplications of σ_0 with $\mathcal{M}_0$, $\mathcal{M}_{1n}$, $\mathcal{M}_{1\nabla}$, $\mathcal{M}_{2n}$, $\mathcal{M}_{2\nabla}$, $\mathcal{M}_{3n}$, $\mathcal{M}_{3+}$; and of σ_+ with $\mathcal{M}_0$, $\mathcal{M}_{0q}$, $\mathcal{M}_{1n}$, $\mathcal{M}_{1+}$, $\mathcal{M}_{2n+}$, $\mathcal{M}_{3n}$, $\mathcal{M}_{3+}$, $\mathcal{M}_{7x}$. Note that $\sigma_i\mathcal{M}_{3i}$ gives $\left(1-\frac{4m_i}{s}\right)L_i$, i.e. a similar function as was obtained from $\sigma_i\mathcal{M}_{1i}$ and $\sigma_0\mathcal{M}_{3+}$ combines with $\sigma_+\mathcal{M}_{3n}$ into one function as is discussed around relation (8.38) and on Figure 13.

5.9 Subthreshold parametrization

The parametrization usually employed in the literature in connection with the reconstruction theorem (mainly in the isospin limit case) is the subthreshold parametrization using the value of the amplitude, its slope and further characteristics in the center of Dalitz plot $s = t = u = s_i^0$ as its parameters. Such parametrization was also employed to describe the amplitudes of meson-meson scattering processes in isospin limit in the previous chapter. The NLO $\pi\pi$ scattering amplitudes (when retaining the different $m_{\pi^\pm}$ and m_{π^0} masses) look in this parametrization again like

$$A_i(s,t,u) = R_i(s,t,u) + U_i(s,t,u) + O(p^6), \tag{5.127}$$

where this time the polynomials $R_i(s,t,u)$ read

$$R_0 = \frac{\alpha_{00} m_{\pi^0}^2}{F_\pi^2} + 3\frac{\lambda_{00}}{F_\pi^4}\left((s-2m_{\pi^0}^2)^2 + (t-2m_{\pi^0}^2)^2 + (u-2m_{\pi^0}^2)^2\right), \tag{5.128}$$

$$\begin{aligned} R_c = {} & \frac{\beta_{+-}}{F_\pi^2}\left(\frac{4}{3}m_{\pi^\pm}^2 - u\right) + \frac{2\alpha_{+-}m_{\pi^0}^2}{3F_\pi^2} + \frac{\lambda_{+-}^{(1)} + \lambda_{+-}^{(2)}}{F_\pi^4}\left((s-2m_{\pi^\pm}^2)^2 + (t-2m_{\pi^\pm}^2)^2\right) \\ & + \frac{2\lambda_{+-}^{(2)}}{F_\pi^4}(u-2m_{\pi^\pm}^2)^2, \end{aligned} \tag{5.129}$$

$$\begin{aligned} R_x = {} & \frac{\beta_{\pm 0}}{3F_\pi^2}(2\Sigma - 3s) - \frac{m_{\pi^0}^2\alpha_{\pm 0}}{3F_\pi^2} - \frac{\lambda_{\pm 0}^{(1)}}{F_\pi^4}(s-2m_{\pi^\pm}^2)(s-2m_{\pi^0}^2) \\ & - \frac{\lambda_{\pm 0}^{(2)}}{F_\pi^4}\left((t-\Sigma)^2 + (u-\Sigma)^2\right). \end{aligned} \tag{5.130}$$

The amplitudes A_d and A_t are simple to obtain from a direct application of crossing relations (5.8).

In order to obtain the NLO unitarity parts $U_i(s,t,u)$, expressions for the NLO partial waves of the amplitudes and also the NNLO result, one does not need to repeat the whole procedure of the previous sections. Since the kinematical structure of the amplitude remains the same, the kinematical functions appearing in the unitarity part and then also those appearing in the NLO partial waves are identical to those of the partial-wave parametrization. Therefore, we can obtain all results in this parametrization simply by performing the following replacement in the corresponding results in the partial-wave parametrization

$$16\pi a_0 = \frac{\alpha_{00} m_{\pi^0}^2}{F_\pi^2} + 36\frac{\lambda_{00} m_{\pi^0}^4}{F_\pi^4}, \tag{5.131}$$

$$16\pi\lambda_0 = \lambda_{00}, \tag{5.132}$$

$$16\pi a_c = \frac{4\beta_{+-}m_{\pi^\pm}^2}{3F_\pi^2} + \frac{2\alpha_{+-}m_{\pi^0}^2}{3F_\pi^2} + \frac{8(\lambda_{+-}^{(1)} + 2\lambda_{+-}^{(2)})m_{\pi^\pm}^4}{F_\pi^4}, \tag{5.133}$$

$$16\pi b_c = \frac{1}{2}\beta_{+-}, \tag{5.134}$$

$$16\pi\lambda_c^{(1)} = \lambda_{+-}^{(1)}, \tag{5.135}$$

$$16\pi\lambda_c^{(2)} = \lambda_{+-}^{(2)}, \tag{5.136}$$

$$16\pi a_d = -\frac{8\beta_{+-}m_{\pi^\pm}^2}{3F_\pi^2} + \frac{2\alpha_{+-}m_{\pi^0}^2}{3F_\pi^2} + \frac{8(\lambda_{+-}^{(1)} + 2\lambda_{+-}^{(2)})m_{\pi^\pm}^4}{F_\pi^4}, \tag{5.137}$$

$$16\pi b_d = -\beta_{+-}, \tag{5.138}$$

$$16\pi a_x = -\frac{2\beta_{\pm 0}}{3F_\pi^2}(5m_{\pi^\pm}^2 - m_{\pi^0}^2) - \frac{m_{\pi^0}^2\alpha_{\pm 0}}{3F_\pi^2} - \frac{4\lambda_{\pm 0}^{(1)}}{F_\pi^4}m_{\pi^\pm}^2(2m_{\pi^\pm}^2 - m_{\pi^0}^2) - 8\frac{\lambda_{\pm 0}^{(2)}}{F_\pi^4}m_{\pi^\pm}^4, \tag{5.139}$$

$$16\pi b_x = -\beta_{\pm 0} - 2\frac{\lambda_{\pm 0}^{(1)}}{F_\pi^2}\Delta, \tag{5.140}$$

$$16\pi\lambda_x^{(1)} = \lambda_{\pm 0}^{(1)}, \tag{5.141}$$

$$16\pi\lambda_x^{(2)} = \lambda_{\pm 0}^{(2)}, \tag{5.142}$$

$$16\pi a_t = -\frac{2\beta_{\pm 0}}{3F_\pi^2}\Sigma + \frac{m_{\pi^0}^2\alpha_{\pm 0}}{3F_\pi^2} + \frac{4(\lambda_{\pm 0}^{(1)} + 2\lambda_{\pm 0}^{(2)})}{F_\pi^4} m_{\pi^\pm}^2 m_{\pi^0}^2, \tag{5.143}$$

$$16\pi b_t = -\frac{1}{2}\beta_{\pm 0} - \frac{\lambda_{\pm 0}^{(1)}}{F_\pi^2}\Delta. \tag{5.144}$$

Naturally, in order to obtain the exact form of the result in this parametrization, we have to respect strictly the chiral orders of the parameters and when replacing leading orders of the parameters $a_i^{(2)}, b_i^{(2)}$, we have to abandon the higher-order terms (those containing λ's) in the appropriate replacement. Otherwise, we would compute also a part of the higher order contributions. Let us remind the reader that in this case there is no need for the restoring polynomials and we take all $w_i = 0$.

5.10 Isospin symmetric case

5.10.1 Scattering-length parametrization

For some of the analyses we are going to perform, it will be enough to use just the much simpler results valid in the case we neglect the violation of the isospin symmetry. The only independent isospin symmetric amplitude $A_x^{IB^0}$ in the leading order reads

$$A_x^{IB^0}(s,t,u) = 16\pi\left(\mathrm{a} + \frac{\mathrm{b}}{F_\pi^2}(s - 4m_\pi^2)\right). \tag{5.145}$$

Our isospin partial-wave parameters a and b are related to the S-partial-wave scattering lengths from [73]. The leading order relations for them are

$$\mathrm{a} = \frac{2}{3}(\mathrm{a}_0^2 - \mathrm{a}_0^0), \tag{5.146}$$

$$\mathrm{b} = \frac{F_\pi^2}{12m_\pi^2}(5\mathrm{a}_0^2 - 2\mathrm{a}_0^0). \tag{5.147}$$

Similarly to the isospin violating case, we obtain the NLO parametrization of this amplitude in the form

$$A_x^{IB^0}(s,t,u) = 16\pi\left(R_x^{IB^0}(s,t,u) + 16\pi U_x^{IB^0}(s,t,u)\right) + O(p^6), \tag{5.148}$$

where

$$\begin{aligned} U_x^{IB^0}(s,t,u) = {} & W_x^{IB^0;0}(s) - W_t^{IB^0;0}(t) - (s-u)W_t^{IB^0;1}(t) - W_t^{IB^0;0}(u) \\ & - (s-t)W_t^{IB^0;1}(u), \end{aligned} \tag{5.149}$$

$$W_x^{IB^0;0}(s) = -\frac{1}{2}\left(\mathrm{a} + \frac{\mathrm{b}}{F_\pi^2}(s-4m_\pi^2)\right)\left(7\mathrm{a} + \frac{\mathrm{b}}{F_\pi^2}(s-20m_\pi^2)\right)\bar{J}_\pi(s), \tag{5.150}$$

$$W_t^{IB^0;0}(s) = \left(\mathrm{a} - \frac{\mathrm{b}}{2F_\pi^2}(s+4m_\pi^2)\right)^2\bar{J}_\pi(s), \tag{5.151}$$

$$W_t^{IB^0;1}(s) = \frac{\mathrm{b}^2}{12F_\pi^4}(s-4m_\pi^2)\bar{J}_\pi(s), \tag{5.152}$$

$$R_x^{IB^0}(s,t,u) = \mathrm{a} + \frac{\mathrm{b}}{F_\pi^2}(s-4m_\pi^2) - \frac{\hat{\lambda}_1}{F_\pi^4}(s-4m_\pi^2)^2 - \frac{\hat{\lambda}_2}{F_\pi^4}\left(t^2+u^2\right) - w(s,t,u). \tag{5.153}$$

As was discussed for the isospin breaking case in the previous sections, the particular form of the restoring polynomial $w(s,t,u)$ depends on the choice of how many parameters are demanded to keep their physical values and on the additional conditions we attach to them. Since in the isospin limit the restoring polynomial has a simple expression also when we restore the physical interpretation of both a and b, we display it in its full form without a need of restricting ourselves to the simplified case of keeping the physical interpretation just of the scattering length. (This is indicated also by writing the hats over λ's in the polynomial part of the amplitude.)

Provided we write the restoring polynomial in the form

$$w(s,t,u) = w_x^0(s) - w_t^0(t) - w_t^0(u), \tag{5.154}$$

$$w_x^0(s) = \frac{s^2}{72\pi}\left(81\frac{\mathrm{a}^2}{m_\pi^4} - 264\frac{\mathrm{a}}{m_\pi^2}\frac{\mathrm{b}}{F_\pi^2} + 88\frac{\mathrm{b}^2}{F_\pi^4}\right) - \frac{5sm_\pi^2}{12\pi}\left(17\frac{\mathrm{a}^2}{m_\pi^4} - 40\frac{\mathrm{a}}{m_\pi^2}\frac{\mathrm{b}}{F_\pi^2} - 16\frac{\mathrm{b}^2}{F_\pi^4}\right), \tag{5.155}$$

$$w_t^0(s) = \frac{s^2}{18\pi}\left(6\frac{\mathrm{a}^2}{m_\pi^4} - 9\frac{\mathrm{a}}{m_\pi^2}\frac{\mathrm{b}}{F_\pi^2} - 16\frac{\mathrm{b}^2}{F_\pi^4}\right) - \frac{m_\pi^4}{9\pi}\left(15\frac{\mathrm{a}^2}{m_\pi^4} + 36\frac{\mathrm{a}}{m_\pi^2}\frac{\mathrm{b}}{F_\pi^2} - 208\frac{\mathrm{b}^2}{F_\pi^4}\right), \tag{5.156}$$

the isospin conserved amplitudes correspond exactly[13] to the isospin limit of the results of the previous subsection with the following limits of the parameters [cf. with (5.9), (5.10) and (5.61)–(5.64)]

$$a_x \to \mathrm{a}; \qquad b_x \to \mathrm{b}; \qquad \hat{\lambda}_x^{(1)} \to \hat{\lambda}_1; \qquad \hat{\lambda}_x^{(2)} \to \hat{\lambda}_2; \tag{5.157}$$

$$a_0 \to -3\mathrm{a} + 8\frac{m_\pi^2}{F_\pi^2}\,\mathrm{b} + 32\frac{m_\pi^4}{F_\pi^4}\left(\hat{\lambda}_1+\hat{\lambda}_2\right); \qquad \hat{\lambda}_0 \to \frac{1}{3}(\hat{\lambda}_1+2\hat{\lambda}_2); \tag{5.158}$$

$$a_t \to -\mathrm{a} + 4\frac{m_\pi^2}{F_\pi^2}\,\mathrm{b} + 16\frac{m_\pi^4}{F_\pi^4}\left(\hat{\lambda}_1+\hat{\lambda}_2\right); \qquad b_t \to \frac{\mathrm{b}}{2} + 4\frac{m_\pi^2}{F_\pi^2}\left(\hat{\lambda}_1+2\hat{\lambda}_2\right); \tag{5.159}$$

[13] However, there could appear potential differences of higher orders in the case we do not strictly respect chiral orders of the individual contributions. For instance, it manifests itself in the restoring polynomial — if we include full expressions for scattering lengths in their limit from the isospin breaking results (including λ_1 and λ_2 contributions) instead of using only their leading orders (from Appendix E), we obtain the restoring polynomial dependent also on these λ's.

$$a_c \to -2\mathrm{a} + 4\frac{m_\pi^2}{F_\pi^2}\,\mathrm{b} + 16\frac{m_\pi^4}{F_\pi^4}\left(\hat{\lambda}_1 + \hat{\lambda}_2\right); \qquad b_c \to -\frac{\mathrm{b}}{2} + 4\frac{m_\pi^2}{F_\pi^2}\left(\hat{\lambda}_1 + 2\hat{\lambda}_2\right); \tag{5.160}$$

$$\hat{\lambda}_c^{(1)} \to \hat{\lambda}_1; \qquad \hat{\lambda}_c^{(2)} \to \hat{\lambda}_2; \tag{5.161}$$

$$a_d \to -2\mathrm{a} + 8\frac{m_\pi^2}{F_\pi^2}\,\mathrm{b} + 32\frac{m_\pi^4}{F_\pi^4}\left(\hat{\lambda}_1 + \hat{\lambda}_2\right) \qquad b_d \to \mathrm{b} + 8\frac{m_\pi^2}{F_\pi^2}\left(\hat{\lambda}_1 + 2\hat{\lambda}_2\right). \tag{5.162}$$

In the case we wanted to obtain these results from the limit of the isospin violating amplitudes where the physical interpretation of just the scattering lengths was restored, in the above expressions we just throw away the hats with the exception of the following parameters that have different limits,

$$b_x \to \mathrm{b} + 4\frac{m_\pi^2}{F_\pi^2}\left(\lambda_1 + \lambda_2\right); \qquad b_t \to \frac{\mathrm{b}}{2} + 2\frac{m_\pi^2}{F_\pi^2}\left(\lambda_1 + \lambda_2\right); \tag{5.163}$$

$$b_c \to -\frac{\mathrm{b}}{2} - 2\frac{m_\pi^2}{F_\pi^2}\left(\lambda_1 + \lambda_2\right); \qquad b_d \to \mathrm{b} + 4\frac{m_\pi^2}{F_\pi^2}\left(\lambda_1 + \lambda_2\right). \tag{5.164}$$

Alternatively, we can also abandon the simple form of this limit[14] and just subtract the following simple polynomial

$$w(s,t,u) = \frac{\mathrm{a}}{\pi}\left(-7\mathrm{a} + 16m_\pi^2\frac{\mathrm{b}}{F_\pi^2}\right) + \frac{s-4m_\pi^2}{36\pi}\,m_\pi^2\left(69\frac{\mathrm{a}^2}{m_\pi^4} - 456\frac{\mathrm{a}}{m_\pi^2}\frac{\mathrm{b}}{F_\pi^2} + 592\frac{\mathrm{b}^2}{F_\pi^4}\right). \tag{5.165}$$

The partial waves computed for all NLO $\pi\pi$ scattering processes are equal to

$$\varphi_{i;0}(s) = p_\lambda^{i;0}(s) + \frac{1}{\pi}p_w^{i;0}(s) + \frac{1}{\pi}\sum_{j=0}^{3} p_j^{i;0}(s)\mathcal{M}_j(s), \tag{5.166}$$

$$\varphi_{i;1}(s) = s\sigma_\pi^2(s)\left(p_\lambda^{i;1}(s) + \frac{1}{\pi}p_w^{i;1}(s) + \frac{1}{\pi}p_3^{i;1}(s)\mathcal{M}_3(s)\right) + \frac{m_\pi^2}{\pi s\sigma_\pi^2(s)}\sum_{j=0}^{2} p_j^{i;1}(s)\mathcal{M}_j(s) \tag{5.167}$$

with kinematical functions $\mathcal{M}_j(s)$ from Appendix F. Polynomials $p_j^{i;\ell}$ are listed in Appendix G. The distinct choices of the restoring polynomials differ just in the polynomials $p_w^{i,\ell}$ as is also indicated there.

Two-loop result

Thanks to its simple form, we will also write here the result of second iteration of this amplitude explicitly. The two-loop amplitude reads

$$A_x^{IB^0}(s,t,u) = 16\pi\left(R_x^{IB^0}(s,t,u) + 16\pi U_x^{IB^0}(s,t,u)\right) + O(p^8), \tag{5.168}$$

[14]Naturally, all the other parts of the amplitudes (other than the restoring polynomial) remain equal to the displayed limit of their isospin breaking counterpart also in this case.

with its polynomial part equal to

$$\begin{aligned} R_x^{IB^0}(s,t,u) &= \mathrm{a} + \frac{\mathrm{b}}{F_\pi^2}(s-4m_\pi^2) - \frac{\hat\lambda_1}{F_\pi^4}(s-4m_\pi^2)^2 - \frac{\hat\lambda_2}{F_\pi^4}\left(t^2+u^2\right) \\ &\quad - \frac{\hat\lambda_3}{F_\pi^6}(s-4m_\pi^2)^3 - \frac{\hat\lambda_4}{F_\pi^6}\left(t^3+u^3\right) - w_6(s,t,u), \end{aligned} \tag{5.169}$$

$$\begin{aligned} w_6(s,t,u) &= w(s,t,u) + 64\mathrm{a}\,\frac{m_\pi^4}{\pi F_\pi^4}\left(\hat\lambda_1+\hat\lambda_2\right) \\ &\quad + \mathrm{a}^3\left(-\frac{113}{6}+\frac{214}{3\pi^2}\right) + 2\mathrm{ab}^2\,\frac{m_\pi^4(2084-385\pi^2)}{3\pi^2F_\pi^4} - 2\mathrm{a}^2\mathrm{b}\,\frac{m_\pi^2(824-183\pi^2)}{3\pi^2F_\pi^2} \\ &\quad + 8\mathrm{b}^3\,\frac{m_\pi^6(-384+65\pi^2)}{3\pi^2F_\pi^6} \\ &\quad + (s-4m_\pi^2)\left(\frac{16m_\pi^2}{9\pi F_\pi^4}\left(\mathrm{a}\,(8\hat\lambda_2-\hat\lambda_1)+37\mathrm{b}\,\frac{m_\pi^2}{F_\pi^2}(\hat\lambda_1+\hat\lambda_2)\right)\right. \\ &\qquad + \mathrm{a}^3\,\frac{2056-163\pi^2}{144\pi^2m_\pi^2} + \mathrm{a}^2\mathrm{b}\,\frac{326-885\pi^2}{108\pi^2F_\pi^2} \\ &\qquad \left. + 2\mathrm{ab}^2\,\frac{m_\pi^2(-8284+2253\pi^2)}{81\pi^2F_\pi^4} + \mathrm{b}^3\,\frac{m_\pi^4(28529-6024\pi^2)}{81\pi^2F_\pi^6}\right), \end{aligned} \tag{5.170}$$

where we have explicitly displayed just the simpler form of the restoring polynomial, having the $O(p^4)$ part equal to $w(s,t,u)$ from (5.165). The unitarity part is of the form

$$\begin{aligned} U_x^{IB^0}(s,t,u) &= W_x^{IB^0;0}(s) - W_t^{IB^0;0}(t) - (s-u)W_t^{IB^0;1}(t) - W_t^{IB^0;0}(u) \\ &\quad - (s-t)W_t^{IB^0;1}(u), \end{aligned} \tag{5.171}$$

$$W_x^{IB^0;0}(s) = \mathcal{P}_1^{x;0}(s)\mathcal{G}_1^{(1)}(s) + \mathcal{P}_2^{x;0}(s)\mathcal{G}_2^{(1)}(s) + \mathcal{P}_3^{x;0}(s)\mathcal{G}_3^{(0)}(s), \tag{5.172}$$

$$W_t^{IB^0;0}(s) = \mathcal{P}_1^{t;0}(s)\mathcal{G}_1^{(1)}(s) + \mathcal{P}_2^{t;0}(s)\mathcal{G}_2^{(1)}(s) + \mathcal{P}_3^{t;0}(s)\mathcal{G}_3^{(0)}(s), \tag{5.173}$$

$$\begin{aligned} W_t^{IB^0;1}(s) &= \mathcal{P}_1^{t;1}(s)\mathcal{G}_1^{(1)}(s) + \mathcal{P}_2^{t;1}(s)\mathcal{G}_2^{(1)}(s) + \mathcal{P}_{1\sigma}^{t;1}(s)\mathcal{G}_1^{\sigma;(0)}(s) + \mathcal{P}_{2\sigma}^{t;1}(s)\mathcal{G}_2^{\sigma;(0)}(s) \\ &\quad + \mathcal{P}_{3\sigma}^{t;1}(s)\mathcal{G}_3^{\sigma;(0)}(s). \end{aligned} \tag{5.174}$$

Kinematical functions $\mathcal{G}_i(s)$ are listed in Appendix F.2 and the polynomials multiplying them,

$$\begin{aligned} \mathcal{P}_1^{x;0}(s) &= \frac{1}{2}\left(\alpha_x(s)\left(\alpha_0(s)+p_\lambda^{0;0}+\frac{1}{\pi}p_w^{0;0}+\frac{1}{\pi}p_0^{0;0}\right)+\alpha_0(s)\left(p_\lambda^{x;0}+\frac{1}{\pi}p_w^{x;0}+\frac{1}{\pi}p_0^{x;0}\right)\right) \\ &\quad + \alpha_c(s)\left(\alpha_x(s)+p_\lambda^{x;0}+\frac{1}{\pi}p_w^{x;0}+\frac{1}{\pi}p_0^{x;0}\right)+\alpha_x(s)\left(p_\lambda^{c;0}+\frac{1}{\pi}p_w^{c;0}+\frac{1}{\pi}p_0^{c;0}\right), \end{aligned} \tag{5.175}$$

$$\begin{aligned}\mathcal{P}_2^{x;0}(s) &= \frac{1}{2}\frac{1}{\pi}\bigg(\alpha_x(s)p_1^{0;0} + \alpha_0(s)p_1^{x;0} + 2\,\frac{1}{s}\,(s-4m_\pi^2)\alpha_0(s)p_3^{x;0}\bigg)\\ &\quad + \frac{1}{\pi}\bigg(\alpha_c(s)p_1^{x;0} + \alpha_x(s)p_1^{c;0} + 2\,\frac{1}{s}\,(s-4m_\pi^2)\alpha_c(s)p_3^{x;0}\bigg),\end{aligned} \tag{5.176}$$

$$\mathcal{P}_3^{x;0}(s) = \frac{1}{2}\frac{1}{\pi}\left(\alpha_x(s)p_2^{0;0} + \alpha_0(s)p_2^{x;0}\right) + \frac{1}{\pi}\left(\alpha_c(s)p_2^{x;0} + \alpha_x(s)p_2^{c;0}\right), \tag{5.177}$$

$$\mathcal{P}_1^{t;0}(s) = \alpha_t(s)^2 + 2\alpha_t(s)\Big(p_\lambda^{t;0} + \frac{1}{\pi}p_w^{t;0} + \frac{1}{\pi}p_0^{t;0}\Big), \tag{5.178}$$

$$\mathcal{P}_1^{t;1}(s) = (s-4m_\pi^2)\bigg(\frac{1}{3}\beta_t^2 + 2\beta_t\Big(p_\lambda^{t;1} + \frac{1}{\pi}p_w^{t;1}\Big)\bigg), \tag{5.179}$$

$$\mathcal{P}_{1\sigma}^{t;1}(s) = \frac{2}{\pi}\beta_t p_0^{t;1}, \tag{5.180}$$

$$\mathcal{P}_2^{t;0}(s) = \frac{2}{\pi}\alpha_t(s)\left(p_1^{t;0} + \frac{1}{s}\,(s-4m_\pi^2)p_3^{t;0}\right), \tag{5.181}$$

$$\mathcal{P}_2^{t;1}(s) = \frac{2}{\pi}\frac{1}{s}\,(s-4m_\pi^2)^2\beta_t p_3^{t;1}, \tag{5.182}$$

$$\mathcal{P}_{2\sigma}^{t;1}(s) = \frac{2}{\pi}\beta_t p_1^{t;1}, \tag{5.183}$$

$$\mathcal{P}_3^{t;0}(s) = \frac{2}{\pi}\,\alpha_t(s)p_2^{t;0}, \tag{5.184}$$

$$\mathcal{P}_{3\sigma}^{t;1}(s) = \frac{2}{\pi}\,\beta_t p_2^{t;1}, \tag{5.185}$$

are easily to obtain from multiplications of [cf. (3.1)]

$$\alpha_x(s) = \mathrm{a} + \frac{\mathrm{b}}{F_\pi^2}(s-4m_\pi^2), \quad \beta_x = 0, \quad \alpha_t(s) = \frac{\mathrm{b}}{2F_\pi^2}(s+4m_\pi^2) - \mathrm{a}, \quad \beta_t = -\frac{\mathrm{b}}{2F_\pi^2} \tag{5.186}$$

with the polynomials $p_a^{i;\ell}(s)$ appearing in the NLO partial waves (5.166)–(5.167). Note that in these relations we have suppressed the explicit indication of the dependence of these polynomials on s.

5.10.2 Subthreshold parametrization

In order to benefit from the previous analyses of $\pi\pi$ scattering amplitudes by Stern et al. [125, 94, 95, 56] it is convenient to use also isospin subthreshold parametrization, in which the polynomial part of the amplitude A_x from (5.127) looks like

$$\begin{aligned}R_x &= \frac{\beta}{3F_\pi^2}(4m_\pi^2 - 3s) - \frac{m_\pi^2\alpha}{3F_\pi^2} - \frac{\lambda_1}{F_\pi^4}(s-2m_\pi^2)^2 - \frac{\lambda_2}{F_\pi^4}\big((t-2m_\pi^2)^2 + (u-2m_\pi^2)^2\big)\\ &\quad - \frac{\lambda_3}{F_\pi^6}(s-2m_\pi^2)^3 - \frac{\lambda_4}{F_\pi^6}\big((t-2m_\pi^2)^3 + (u-2m_\pi^2)^3\big).\end{aligned} \tag{5.187}$$

All the other expressions can be obtained from those written for partial-wave parametrization by replacing

$$16\pi \mathrm{a} \to -\frac{8\beta m_\pi^2}{3F_\pi^2} - \frac{m_\pi^2\alpha}{3F_\pi^2} - \frac{4m_\pi^4}{F_\pi^4}(\lambda_1+2\lambda_2), \qquad 16\pi \mathrm{b} \to -\beta_{\pm 0} - \frac{4m_\pi^4}{F_\pi^4}(\lambda_1+\lambda_2), \quad (5.188)$$

$$16\pi\hat{\lambda}_1 \to \lambda_1, \qquad 16\pi\hat{\lambda}_2 \to \lambda_2, \qquad 16\pi\hat{\lambda}_3 \to \lambda_3, \qquad 16\pi\hat{\lambda}_4 \to \lambda_4. \quad (5.189)$$

Note that the one-loop result can be obtain also from the result (4.33) of Chapter 4 [where the subtraction parameters are denoted according to $\alpha_{\pi\pi}=\alpha, \beta_{\pi\pi}=\beta, \gamma_{\pi\pi}=\lambda_1, \delta_{\pi\pi}=\lambda_2$] by expanding the loops containing KK or $\eta\eta$ in powers of $\frac{s}{4m_K^2}$ or $\frac{s}{4m_\eta^2}$ and the subsequent inclusion of such terms into the polynomial of the theorem (since we assume working far below the unitarity cuts corresponding to these intermediate states). Note, however, that $\overline{J}_{PP}(s)$ behaves for $s \ll 4m_P^2$ as

$$\overline{J}_{PP}(s) = \frac{1}{96\pi^2}\frac{s}{4m_P^2} + O\left(\left(\frac{s}{4m_P^2}\right)^2\right), \quad (5.190)$$

i.e. by counting such $2m_P$ as a quantity of order Λ, to a given order such loop function contributes only through its scale dependent part $J_{PP}^r(0)$, which is already included in the polynomial. Thus, we can use the standard one-loop expressions for the values of the parameters from Appendix D.

For our further applications we also use the results from [125, 94, 95, 56]. However, when comparing to them, one should remember that our choice of the subtraction scheme for the NNLO amplitude differs slightly to the NNLO amplitude used there, i.e these amplitudes differ in their polynomial parts. Denoting their parameters with subscript $\star$, the corresponding values of our parameters that lead to the same amplitude read

$$\alpha = \alpha_\star - \frac{m_\pi^4\left(\left(37\pi^2-282\right)\alpha_\star^3 - 8\pi^2\alpha_\star^2\beta_\star + 4\left(144+19\pi^2\right)\alpha_\star\beta_\star^2 + 24\left(8+\pi^2\right)\beta_\star^3\right)}{13824\pi^4F_\pi^4}, \quad (5.191)$$

$$\beta = \beta_\star + \beta_\star\frac{m_\pi^4\left(5\left(108-\pi^2\right)\alpha_\star^2 + 40\left(78-5\pi^2\right)\alpha_\star\beta_\star - 2\left(388-53\pi^2\right)\beta_\star^2\right)}{27648\pi^4F_\pi^4}, \quad (5.192)$$

$$\lambda_1 = \lambda_{1\star} + \beta_\star^2\frac{m_\pi^2\left(\left(434-15\pi^2\right)\alpha_\star + 2\left(118+9\pi^2\right)\beta_\star\right)}{13824\pi^4F_\pi^2}, \quad (5.193)$$

$$\lambda_2 = \lambda_{2\star} + \beta_\star^2\frac{m_\pi^2\left(\left(15\pi^2-2\right)\alpha_\star - 20\beta_\star\right)}{27648\pi^4F_\pi^2}, \quad (5.194)$$

$$\lambda_3 = \lambda_{3\star} + \beta_\star^3\frac{988-3\pi^2}{82944\pi^4}, \quad (5.195)$$

$$\lambda_4 = \lambda_{4\star} + \beta_\star^3\frac{3\pi^2-340}{165888\pi^4}. \quad (5.196)$$

5.11 Determination of parameters of $\pi\pi$ scattering

For various numerical analyses we would need the values of our parameters which reproduce well the physical amplitudes or the values of the parameters corresponding to χPT computations. To the best author's knowledge there exists no analysis including full isospin breaking in $\pi\pi$ scattering that would give us particular numbers for its physical amplitude or for its chiral amplitude. We therefore determine the values of our parameters in the isospin breaking case by using just the leading-order isospin-breaking relations (5.27)–(5.31) from [98] and the values obtained in the isospin limit.

In the isospin symmetric case the situation is better since the $\pi\pi$ scattering is one of the most important processes and has been measured by various methods and there also exists a result in χPT including two-loop effects [30, 31]. As was already stated we do not need to repeat all the comparisons of our parametrization with these result but can also use the outcome of such comparisons performed in [94] with the two-loop χPT computation and in [56] with the physical measurements of the $\pi\pi$ phase-shifts (for more details see Section 5.11.1). Note that in these cases one needs to perform the transformation of variables from (5.191)–(5.196) due to the different subtraction scheme used there.

Let us start with the χPT values. For this comparison we use the order-by-order interpretation of the polynomial parameters and it is therefore more natural to work in the subthreshold parametrization [the values of the parameters for the scattering-length parametrization can be then obtained from (5.188)–(5.189)]. The tree level χPT amplitude corresponds to the LO polynomial with the values of parameters $\alpha = \beta = 1$ [cf. (4.29)–(4.32)]. For reproducing the one-loop result we use the result of first iteration and for the particular values of the parameters that reproduce exactly the standard one-loop calculation we can employ the analysis of Section 4.5. We remind the reader that in Appendix D we have listed the expressions for our parameters in terms of pseudoscalar masses and low-energy constants of χPT L_i, for whose values there exist two complete determinations, fit10 from [10] and fitAll from [34], which are displayed in Table 1. In Section 4.5 we have studied also the variations of the parameters with the particular choices/definitions of the isospin masses m_π, m_K and m_η and of the value of the pion decay constant. For the purpose of our analysis of $\eta \to 3\pi$ decay in Chapter 9 (cf. Section 9.4) we display here the numbers corresponding to these masses and the decay constant equal to

$$m_\pi = 138.0558\,\mathrm{MeV}, \quad m_K = 494.53\,\mathrm{MeV}, \quad m_\eta = 547.3\,\mathrm{MeV}, \quad F_\pi = 92.4\,\mathrm{MeV} \quad (5.197)$$

and all the presented error bars are just due to the uncertainties in L_is. In order to reproduce the two-loop chiral result, we need $O(p^6)$ values of the parameters appearing in the real (polynomial) part of the amplitude. Since in this work we are not going to perform the numerical two-loop analyses of $\pi\pi$ scattering and in the parametrization of $K/\eta \to 3\pi$ decays, which are of the main interest of this work, there appear just the parameters from the first iteration for the $\pi\pi$ scattering, we present here the numerical results for NNLO $\pi\pi$ scattering just for the illustration and before one uses them in some other application, a more complete analysis would be required. For this purpose, it is enough to obtain the

		α	β	$10^3\lambda_1$	$10^3\lambda_2$	$10^4\lambda_3$	$10^4\lambda_4$	a_0	$10^2 a_2$	$10^2 m_\pi^2 a_1$
ObO	p^2	1	1					0.155	-4.44	4.4
	p^4	1.05(2)	1.085(2)	−1.6(1.8)	8.4(5)			0.198	-4.15	5.2
	p^6	1.06	1.116	−5.6	9.7	2.2	−1.6	0.206	-4.25	5.5
	p^4 [34]	1.02(19)	1.11(3)	−0.7(1.9)	7.9(8)			0.199	-4.31	5.2
Resummed polyn.	ResPh	1.37(25)	1.09(3)	−2.8(5)	9.2(1)	3.7(2)	−1.64(6)	0.225	-3.76	5.4
	Res4Ph	1.37(25)	1.09(3)	−2.8(5)	9.2(1)			0.217	-3.64	5.3
	Resp6	1.06	1.116	−5.6	9.7	2.2	−1.6	0.212	-4.40	5.6
	Resp4λ	1.05(2)	1.085(2)	−1.6(1.8)	8.4(5)	3.7(2)	−1.64(6)	0.209	-4.23	5.3
	Res4p4	1.05(2)	1.085(2)	−1.6(1.8)	8.4(5)			0.201	-4.10	5.2
	Fit4	1.352(22)	1.253(3)	−10.0(3)	17.5(1)			0.223	-4.43	5.7

Table 4: Various sets of parameters describing $\pi\pi$ scattering together with the corresponding values of the standard a_0, a_2 and a_1 scattering lengths. The rows labeled by ObO refer to the order-by-order interpretation of the parameters, i.e. e.g. in $O(p^6)$ amplitude there appear parameter α in three different orders, its $O(p^2)$ value appears in the row labeled by p^2, its $O(p^4)$ value in the p^4 row and finally the $O(p^6)$ value is displayed in the p^6 row. The sets with resummed interpretation of the polynomials are given in the lower part of the table. Any of the parameters appearing appears as one entity in the parametrization and their values are listed in the particular row. The labels of various resummed sets are described in the main text.

$O(p^6)$ parameters by comparison of relations (48) from [94] for the constants b_i of the standard two-loop amplitudes (cf. [30]) in terms of the subthreshold parameters with their values stemming from the two-loop χPT computation [31] (Table 3 there).

All the determined values of our parameters together with the corresponding values of the scattering lengths a_0, a_2 and a_1 (which are usually quoted in the analyses of $\pi\pi$ scatterings) are listed in the upper part of Table 4. We have also constructed the corresponding parametrizations where we do not distinguish various orders of the parameters appearing there, which we call the resummed interpretation of the polynomial parameters or resummed parametrization for short (cf. Section 3.6). The most important for us is the two-loop representation ResPh, which corresponds to the result of [56], where they matched their dispersive parametrization with the solutions of Roy equations from [13] supplemented by measurements of $\pi\pi$ phases by E865 [116] — we refer to this amplitude also as the "physical amplitude" and use it for an illustration how the other representations differ from the physically measured amplitude (note, however, that this representation of the genuine physical amplitude is also limited as is shortly discussed in Section 5.11.1 and manifests itself with the value of a_2 coming from this representation $a_2 = -0.0376 \pm 0.037$ which has almost 2σ deviation from the current experimental value.). In Resp6 we take the complete two-loop parametrization with all the parameters equal to their chiral $O(p^6)$

values[15]. For the illustration of the effects of second iteration and also of changing λ_3 and λ_4 we have used the choice denoted by Resp4λ, where in the resummed parametrization we take α, β, λ_1, λ_2 equal to their chiral $O(p^4)$ values and add λ_3, λ_4 from ResPh.

As we have already stated, in our further applications the more relevant $\pi\pi$ parametrizations are those coming from the first iteration. We therefore add into our sets of various choices also such parametrizations: Res4Ph, where the values of all the parameters appearing in the first iteration are set to the "physical values" from ResPh; and similarly Res4p4 is first order parametrization with parameters equal to the chiral $O(p^4)$ values. Finally, as described in Section 5.11.1 we have performed a fit of the recent $\pi\pi$ results to the one-loop parametrization and obtained so Fit4 — this fit uses scattering length parametrization, so the values of α, β, λ_1, λ_2 quoted in Table 4 are just approximate and the amplitude that woudl be constructed by using these values is different to the original Fit4 one as used below (we remind however that the difference is of higher chiral orders).

On Figure 4 we have plotted the real and the imaginary parts of the amplitude $A_x(s,t,u)$ corresponding to various choices of the values (and the interpretations) of the parameters in comparison to the "physical amplitude" on the cut $t = u$. We plot them in region $s \lesssim (0.77\text{GeV})^2$, above which χPT and also the parametrization ResPh cease to reproduce well the physics because of the appearance of ρ resonance, and then we have also zoomed in on the region near the physical threshold $s = 4m_\pi^2$, which is of particular importance for us. The datasets whose label contains the shortcut "er." include their error bars in their plots. Taking into account such error bars, we observe that the tree and the one-loop chiral amplitude reproduce the real part of the "physical amplitude" only in the region $\sim (0.25 \div 0.45)\,\text{GeV}^2$, while, as expected, they completely miss the physical imaginary part. The two-loop chiral amplitude can be considered to reproduce both of the real and the imaginary parts very well. What is a little bit surprising is that the parametrization Resp4λ reproduces it at best. It shows us the importance of parameters λ_3 and λ_4 and of the two-loop effects.

For our further analyses (mainly of $\eta \to 3\pi$ decay) the parametrizations stemming from first iteration will be more important. It is because we will construct such processes to the two-loop level and therefore the $\pi\pi$ scattering parameters appear there at the one-loop level. We would therefore need a good one-loop parametrization of the physical amplitude. Fortunately, as we have emphasized in the construction of our parametrization, the advantage of our choice of the dispersive representation is that we do not need to reproduce the physics for all energies but only in the low-energy region up to some cut-off Λ that is an integral part of our parametrization. The value of such Λ (together with the precision with which we reproduce the physical amplitudes entering the analysis) then provides us with the estimate of the precision of the resulting parametrization. On Figure 5 we have plotted various one-loop parametrizations in the region $s \in (4m_\pi^2, 180\,\text{MeV})$. We

[15]Note that the usage of the polynomial parameters in [94] is more consistent with our resummed interpretation and so strictly speaking the genuine chiral two-loop amplitude should be somewhere in between the result of this and the $O(p^6)$ order-by-order parametrizations. The chiral $O(p^6)$ imaginary part should be naturally equal to the one from the order-by-order approach, whereas the quoted $O(p^6)$ values of the parameters were obtained from the matching with the resummed parametrization used in [94].

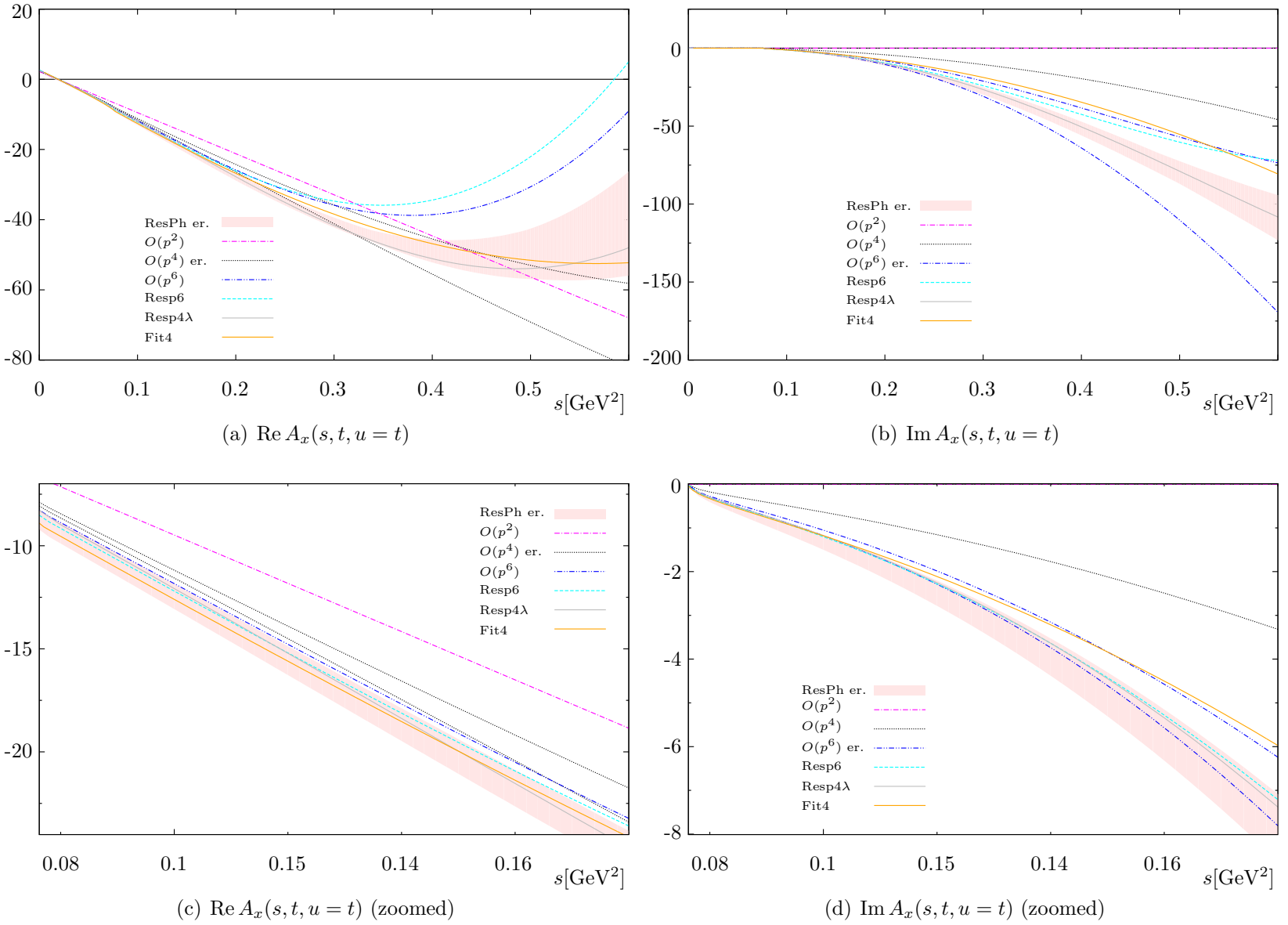

(a) Re $A_x(s,t,u=t)$ (b) Im $A_x(s,t,u=t)$

(c) Re $A_x(s,t,u=t)$ (zoomed) (d) Im $A_x(s,t,u=t)$ (zoomed)

Figure 4: Course of $A_x(s,t,u)$ in isospin limit for various sets of $\pi\pi$ scattering parameters — described in the main text.

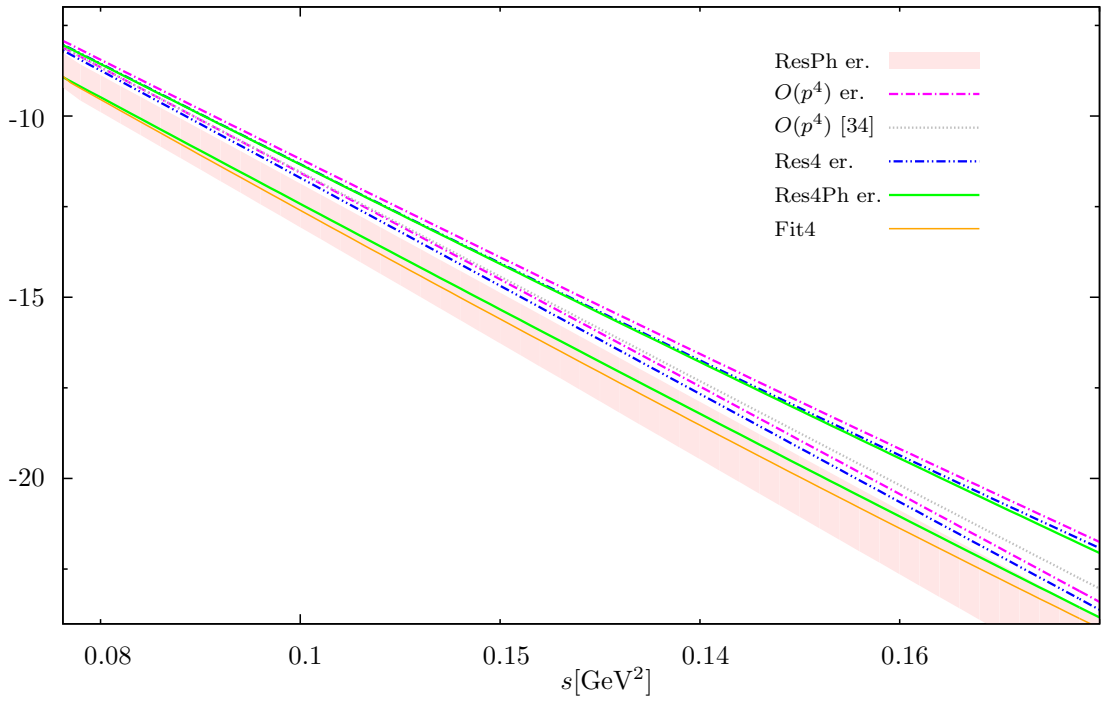

(a) Re $A_x(s,t,u=t)$

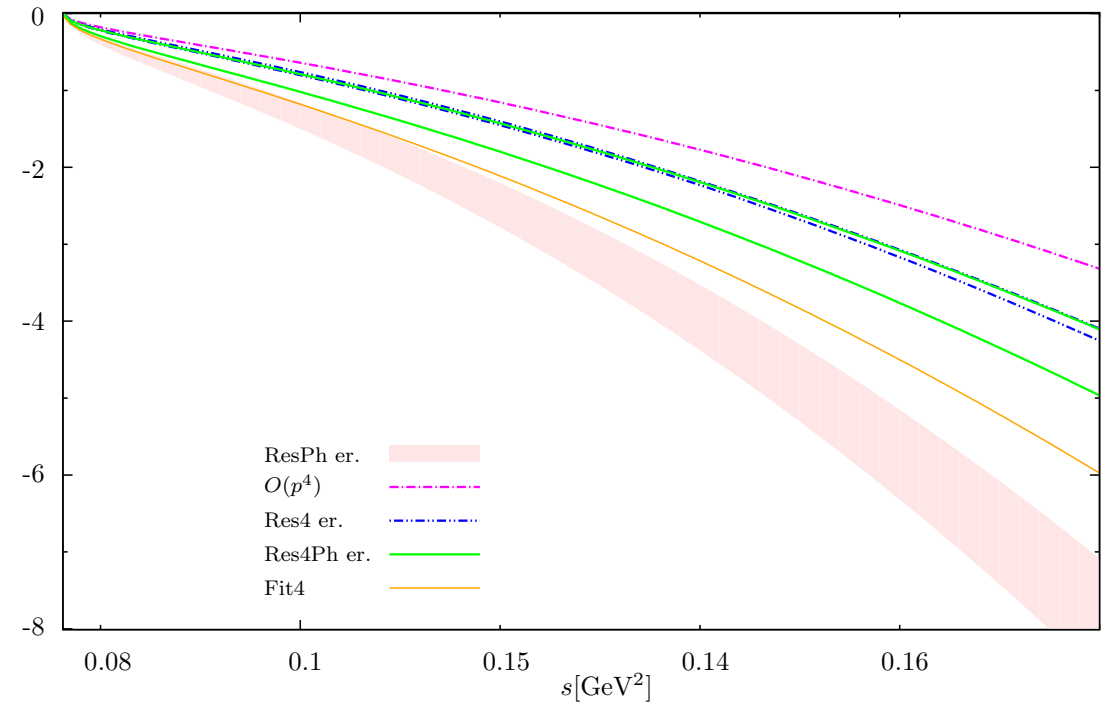

(b) Im $A_x(s,t,u=t)$

Figure 5: Course of the amplitude $A_x(s,t,u)$ in isospin limit for various sets of $\pi\pi$ scattering parameters in the parametrization from the first iteration — description given in the main text.

observe that while the real part in all the cases is reproduced quite well, the imaginary part seems to be problematic. Naturally as is illustrated with the parametrization Res4Ph, the situation can be saved by two-loop corrections, which will be included in the analyzed processes. There appears therefore the natural question, in what extent our one-loop amplitude should reproduce the physical one, in order to prevent such double-counting. Fortunately, we have at hand also the scattering length parametrizations, which does not suffer of such effects. Therefore, we have decided to find a one-loop scattering length parametrization reproducing the known physical data on $\pi\pi$ scattering in the low-energy region as well as possible. (However, for the moment we will use it just for an estimate of the magnitude of the error of $\pi\pi$ inputs in our further analyses.)

5.11.1 Search for one-loop parametrization reproducing physical $\pi\pi$ phase shifts

The experimental knowledge on the $\pi\pi$ scattering is usually presented in terms of the $\pi\pi$ phase shifts of the amplitudes with the specific values of isospin. These amplitudes are related to our amplitudes containing physical states by relations (cf. Section 4.2 and [I]):

$$T^0(s,t,u) = -3A_x(s,t,u) - A_x(t,s,u) - A_x(u,t,s), \tag{5.198}$$
$$T^1(s,t,u) = -A_x(t,s,u) + A_x(u,t,s), \tag{5.199}$$
$$T^2(s,t,u) = -A_x(t,s,u) - A_x(u,t,s). \tag{5.200}$$

The partial wave expansion usually written for them defines the corresponding partial waves [cf. (2.14) with $N = 2$]

$$T^I(s,t,u) = 32\pi \sum_\ell (2\ell+1) t_\ell^I(s) P_\ell(\cos\theta), \tag{5.201}$$

where $P_\ell(x)$ are Legendre polynomials. By taking into account the conservation of isospin, the unitarity relation (2.18) below all inelastic channels ($s < 16m_\pi^2$) reads (note that $S = 2$ for identical particles)

$$\operatorname{Im} t_\ell^I(s) = \sigma(s) \left|t_\ell^I(s)\right|^2 \theta(s - 4m_\pi^2). \tag{5.202}$$

This means that in the interval $s \in (4m_\pi^2, 16m_\pi^2)$ the phase of the partial wave $\delta_\ell^I(s)$ fulfills

$$\sin\delta_\ell^I(s) = 2\sigma(s) \left|t_\ell^I(s)\right| \tag{5.203}$$

and the partial wave can be written in the form

$$t_\ell^I(s) = \frac{1}{\sigma(s)} \sin\delta_\ell^I(s)\, e^{i\delta_\ell^I(s)} = \frac{1}{2i\sigma(s)} \left(e^{2i\delta_\ell^I(s)} - 1\right). \tag{5.204}$$

We arrive at the definition of the phase shift for any s in the form

$$t_\ell^I(s) = \frac{1}{2i\sigma(s)} \left(\eta_\ell^I(s) e^{2i\delta_\ell^I(s)} - 1\right), \tag{5.205}$$

where $\eta_\ell^I(s)$ is the inelasticity parameter equal to 1 in the case of appearance of no inelasticity.

Note that the symmetry[16] of $A_x(s,t,u)$ in $t \leftrightarrow u$ exchange implies the same symmetry for amplitudes $T^0(s,t,u)$ and $T^2(s,t,u)$; and the antisymmetry of $T^1(s,t,u)$ with respect to this exchange. Restricting ourselves to $\ell = 0, 1$, the only non-zero partial waves in these processes are thus S-waves for $I = 0, 2$ and P-wave for $I = 1$. Therefore, the usually presented $\pi\pi$ phase shifts are

$$\delta_0^0 = \frac{1}{2}\arg\left(1 + \frac{i\sigma(s)}{32\pi}\int_{-1}^{1} \mathrm{d}(\cos\theta) T^0(s,\cos\theta)\right), \tag{5.206}$$

$$\delta_1^1 = \frac{1}{2}\arg\left(1 + \frac{i\sigma(s)}{32\pi}\int_{-1}^{1} \mathrm{d}(\cos\theta)\ \cos\theta\, T^1(s,\cos\theta)\right), \tag{5.207}$$

$$\delta_0^2 = \frac{1}{2}\arg\left(1 + \frac{i\sigma(s)}{32\pi}\int_{-1}^{1} \mathrm{d}(\cos\theta) T^2(s,\cos\theta)\right). \tag{5.208}$$

Schenk [120] has proposed the following parametrization of their energy dependence

$$\tan\delta_\ell^I(s) = \sigma(s) P^{2\ell}\left(A_\ell^I + B_\ell^I P^2 + C_\ell^I P^4 + D_\ell^I P^6 + \dots\right)\left(\frac{4m_\pi^2 - s_\ell^I}{s - s_\ell^I}\right), \tag{5.209}$$

where $P = \frac{\sqrt{s}}{2}\sigma(s)$ is 3-momenta of the pions in center-of-mass system [cf. (5.12)] and s_ℓ^I specify the values of s where $\tan\delta_\ell^I(s)$ diverge, i.e. where $\delta_\ell^I(s)$ go through 90°. Since $\tan x \approx x$ for small x, the parameter A_ℓ^I corresponds to the appropriate scattering length a_ℓ^I and similarly B_ℓ^I is related to the effective range [cf. (5.11)].

In [118] Roy has written for the partial waves of $\pi\pi$ scattering an infinite set of twice[17] subtracted dispersion relations, known as Roy equations. The required subtraction constants can be identified with a_0 and a_2. In [13] these equations were used together with experimental data on phase shifts at high energies and with the theoretical values of scattering lengths from [49] and determined the corresponding Schenk parametrization. In [56] this analysis was extended by using new experimental measurement also for the scattering lengths. In the same paper the matching of the dispersive representation we are using for ResPh was made. In [69] it was pointed out that Schenk parametrization is not physical and the alternative representation of the $\pi\pi$ phase-shifts was proposed (using physical positions of unelastic thresholds and it also parametrizes the region for energies higher than 800 MeV.). In the following we take unconstrained fits to data (UFD) fit from there, which gives

$$a_0^0 = 0.218 \pm 0.009, \quad a_0^2 = -0.052 \pm 10, \quad a_1^1 = (37.3 \pm 1.2)\cdot 10^{-3} m_\pi^{-2}. \tag{5.210}$$

[16]Note that this symmetry originates in isospin symmetry connected with Bose/crossing symmetry, i.e. just by using them we can come to the same conclusions for $T^I(s,t,u)$ directly.

[17]Note that if we do not introduce the cut-off into the dispersion relations, we can use the Froissart bound [66] together with analysis of Jin and Martin [85] and find that two subtraction are sufficient.

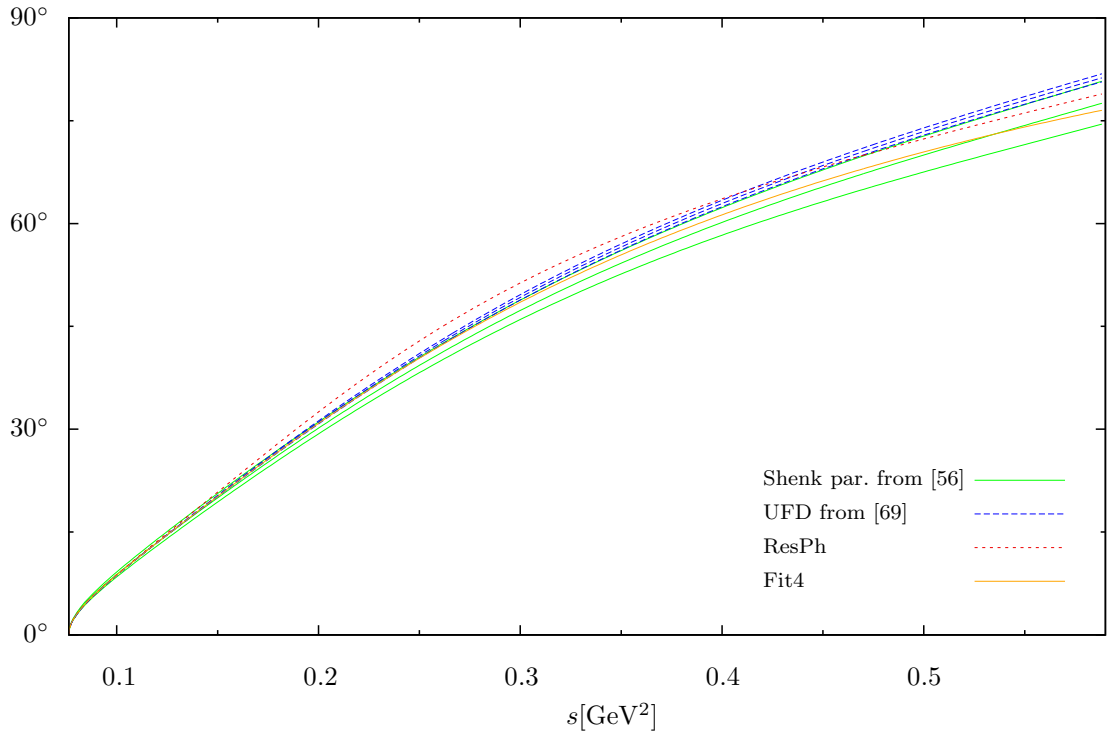

Figure 6: Comparison of various analyses for $\pi\pi$ phase shift δ_0^0. We have included Schenk parametrization obtained from [56] and dispersive parametrization matched to it ResPh, the unconstrained fits to data analysis from [69] and finally our one-loop fit to this result Fit4.

We show the corresponding functional behavior corresponding to these two recent determinations from [56] and [69] on Figures 6, 7 and 8. We see that to a good precision level it is still enough to take the values from [56] supplemented by their error-bars. However, visible differences between these two parametrizations occur around $(0.3 \div 0.4)\,\mathrm{GeV}^2$. We have added into the pictures also the phase shifts stemming from the amplitude ResPh, which is connected with the Schenk parametrization of [56] as explained above.

After we have everything prepared we can return to the original motivation of this section and find the one-loop representation reproducing well these phase shifts. As was explained above, we have chosen to fit the scattering-length parametrization since such fit is stable at the threshold with respect to higher order corrections, and it has shown up that the representation with the restoring polynomial (5.154) that takes into account the crossing properties works better that the one with the simpler form of this polynomial. Since our representation should work for low-energies and for larger energies it can be worse, we have weighted the fit of the individual phase shifts by choosing the points of data set with exponentially increasing distances (the number of fitted points in a interval of s at the threshold is more than the interval of the same size for larger energies and this number for the interval of fixed size decreases exponentially) — naturally, the result of the fit depends on the exact choice of this prescription for choosing the fitting points. The

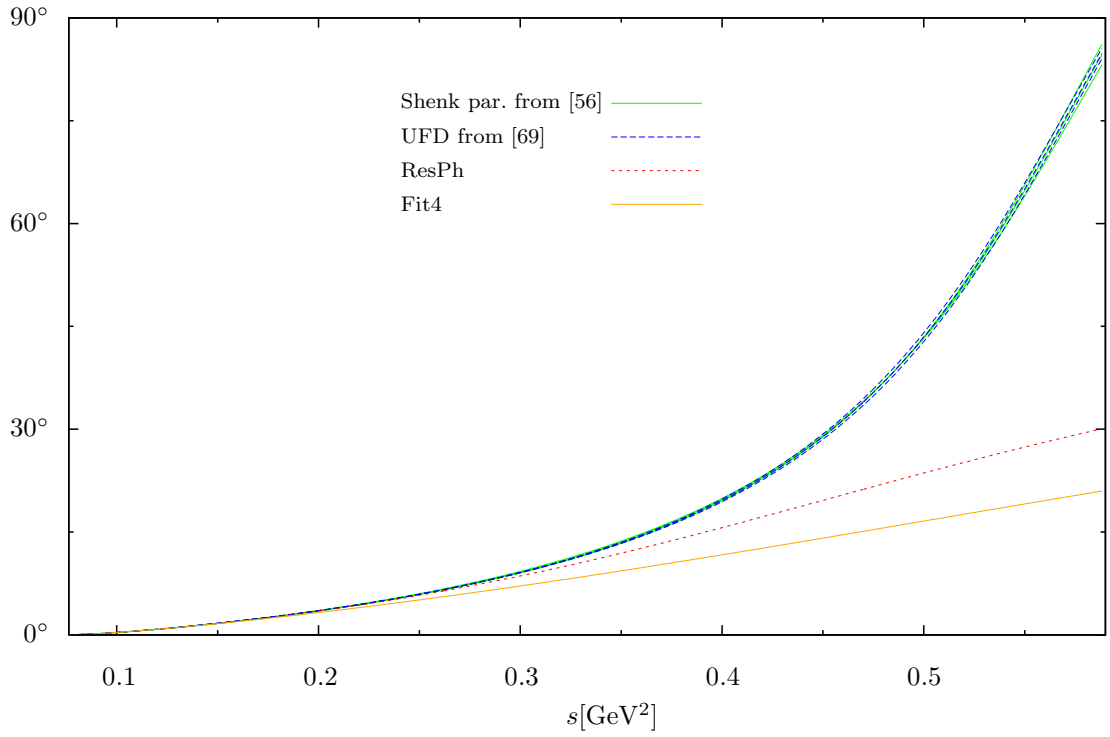

Figure 7: Comparison of various analyses for $\pi\pi$ phase shift δ_1^1. The included data sets are the same as on the previous Figure.

fitting procedure is affected also by the fact that we have to perform coupled fit on three data-sets δ_0, δ_1 and δ_2. Since the value of δ_0 for fixed s is larger than those of δ_1 and δ_2, we have decided to use weights of the datasets $(w_0, w_1, w_2) = (1, 5, 5)$. This choice is another source of ambiguity which can change the fitting result. However, at the current level of precision and since we use this result rather for determination of error connected with the $\pi\pi$ inputs in our further analysis, the result of such procedure is sufficient for our purposes.

The fit of the UFD parametrization [69] was performed in Wolfram Mathematica and we have obtained

$$\mathrm{a} = -0.1783(2), \quad \mathrm{b} = -0.02626(3), \quad 10^3\hat{\lambda}_1 = -0.198(7), \quad 10^3\hat{\lambda}_2 = 0.347(2) \tag{5.211}$$

with the correlation matrix

	a	b	$\hat{\lambda}_1$	$\hat{\lambda}_2$
a	1	−0.61	0.87	−0.77
b		1	−0.81	0.60
$\hat{\lambda}_1$			1	−0.94
$\hat{\lambda}_2$				1

(5.212)

and adjusted r-squared 0.99994 on 284 degrees of freedom. We refer to the result of this fit as Fit4. We have added it into plots on Figures 4–8. We see that this fit reproduces

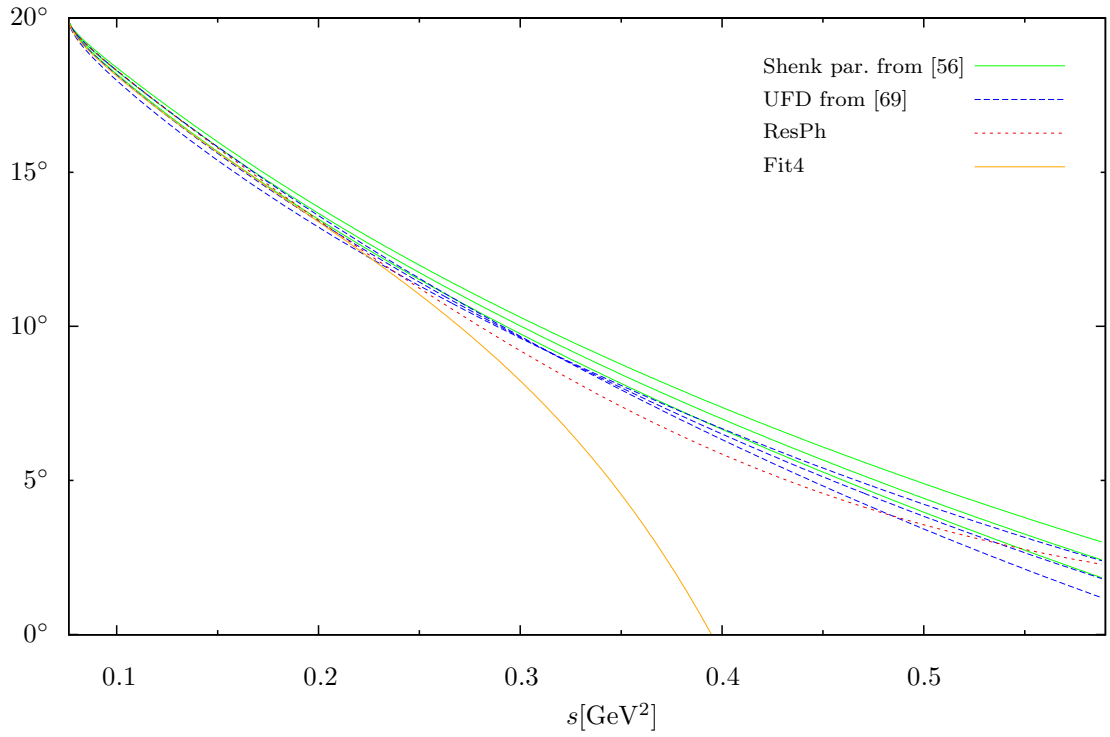

Figure 8: Comparison of various analyses for $\pi\pi$ phase shift δ_0^2. The included data sets are the same as on the previous two Figures.

well the δ_0^0 from [69] on whole the kinematic region (even better than ResPh) while δ_1^1 with δ_0^2 are reproduces only up to $\sim 0.22\,\mathrm{GeV}^2$ (for these two phase shifts ResPh that includes also two-loop effects is more reliable). Similarly, the real parts of $A_x(s,t,t)$ corresponding to Fit4 and ResPh are in agreement, whereas for their imaginary parts there occurs a deviation already at low energies. Nevertheless, Fit4 works best of all parametrizations that include just one-loop effects.

5.12 Conclusions for $\pi\pi$ scattering amplitudes

We have constructed parametrization of $\pi\pi$ scattering amplitudes that takes into account two-loop effects and the full isospin breaking connected with $m_{\pi^\pm} \neq m_{\pi^0}$. It can be written in terms of physical scattering lengths or in terms of subthreshold parameters.

This parametrization can be used as starting point for many phenomenological analyses, such as analysis of the physical $\pi\pi$ scattering amplitudes or of $\pi\pi$ form-factors. However, as was already stated, our main purpose of the construction of $\pi\pi$ scattering processes is the analysis of its influence on the $K \to 3\pi$ and $\eta \to 3\pi$ decay processes. Moreover, the numerical analysis performed in this work concerns only the latter process and therefore we have determined the values of the parameters just in the case of isospin conservation. Nevertheless, the numerical analysis of the isospin breaking effects is also in progress.

Part III

$K \to 3\pi$ and $\eta \to 3\pi$ decay

Chapter 6

$K \to 3\pi$ and $\eta \to 3\pi$ decays. General properties.

Our next task (and also the one we are most interested in) will be the dispersive construction of the amplitudes of $K \to 3\pi$ and $\eta \to 3\pi$ decay processes [in the case we want to speak about both of these processes, we denote them generically as $P \to 3\pi$]. Our final aim is to include the isospin breaking effects induced by the mass difference between the mesons belonging to the same isomultiplet. For the sake of brevity we have divided the analysis into several steps. A discussion of general properties of all these processes and a presentation of motivation for their studies is given in the rest of this chapter. In the next chapter we address the computation in the lowest order in the isospin symmetry breaking. As is discussed further on, it means an isospin symmetric computation (IB^0) in the case of $K \to 3\pi$ decays; whereas for $\eta \to 3\pi$ processes, which are forbidden in IB^0, the lowest (non-zero) order corresponds to the first order in the isospin breaking (IB^1). Finally, in Chapter 8 we take into account the complete isospin violation induced by the mass differences of the charged and the neutral pions (and kaons). There we perform the second iteration of our construction procedure (leading to NNLO results) only for the $P \to 3\pi^0$ decay processes of the neutral mesons P^0 since in all the other cases there appear further complications, which will be addressed in our next work.

6.1 Motivation

Our experimental knowledge of the processes $P \to 3\pi$ has greatly improved during the recent years, and is likely to improve further still in the near future. The sizes of the collected data-samples in the case of kaons, for instance, outgrow by orders of magnitude those that were available before. This increase in statistics has prompted various theoretical studies [27,43,44,68,47,36,37,33,39,82,50,122] of these decay modes, often with emphasis on isospin breaking contributions. Indeed, from the theoretical point of view, these processes are interesting because they provide access to fundamental quantities. For instance, the rates for the decays $\eta \to 3\pi$, which are forbidden in the isospin limit, offer a good possibility

to obtain the value of the quark mass ratio

$$R = \frac{m_s - \bar{m}}{m_d - m_u}. \tag{6.1}$$

We perform such analysis in Chapter 9.

Furthermore, the processes with two neutral pions in the final state exhibit the so-called cusp effect, which contains information on the $\pi\pi$ scattering lengths in the S-wave. In particular, decays $K^\pm \to \pi^\pm\pi^0\pi^0$ and $K_L \to 3\pi^0$ have already been studied from this point of view by NA48 [77] and KTeV [3] collaborations.

Traditionally, these processes have most of the time been analyzed with a polynomial parametrization in terms of slopes and curvatures of the particular amplitude, usually referred as Dalitz plot parametrization (which is discussed in Section 6.4), and theoretical expressions have often been given in this form. It is clear that the study of non-analytic features of the amplitudes (mainly beyond the $m_{\pi^\pm} = m_{\pi^0}$ limit), such as a cusp, cannot be done within such a simple framework. The aim of the following chapters is therefore to construct a model independent form of two-loop amplitudes of the processes mentioned above exhibiting the correct unitarity parts coming from the $\pi\pi$ intermediate states.

As was discussed in Section 5.3, these are the only states that, up to two loops in the chiral expansion, give rise to non-analytic structures to the amplitudes inside the decay region. Other two-meson intermediate states, such as $K\pi$, $\eta\pi$ or KK, correspond to more remote thresholds. Inside the decay region (i.e. sufficiently far below them), their effects can be appropriately approximated and described by a polynomial with the terms up to the third order in Mandelstam variables [cf. also Figure 9]. Let us recall that intermediate states with more than two mesons contribute only into higher orders in the chiral expansion, and are not considered in the analysis (also their numerical effects are tiny as is illustrated on the $\eta \to 3\pi$ decay in Chapter 9). Note that this is a direct consequence of the reconstruction theorem and the validity of these arguments rests among others on three subtractions we have taken there. In general, if we took a somehow simplified form of the theorem (e.g. with less subtractions) without imposing some additional assumptions on the amplitudes, we could miss some contribution to them. It is still possible that the genuine physical amplitudes fulfill such assumptions, but if we want to be cautious and base our analysis only on the assumptions of Chapter 2, we have to employ the theorem in the form it was proved there.

The dispersive construction is just an adaptation of the methods of the reconstruction theorem from the previous chapters on a slightly more complicated case corresponding to the amplitudes of the scattering processes $P\pi \to \pi\pi$ in the threshold region. The amplitudes for the decay processes $P \to 3\pi$ are then obtained by an analytic continuation inside the physical decay region in the Mandelstam plane.

In the current work, we do not include real or virtual photons, and all the isospin breaking is given just by the difference in the physical masses of $\pi^\pm$ and π^0. We also do not address the possible violation of CP invariance.

6.2 Processes in question

Our analysis considers the following processes

$$K^\pm \to \pi^0\pi^0\pi^\pm, \qquad [\tilde{\mathcal{M}}_x^\pm] \tag{6.2a}$$
$$K^\pm \to \pi^\pm\pi^\pm\pi^\mp, \qquad [\tilde{\mathcal{M}}_c^\pm] \tag{6.2b}$$
$$K_L \to \pi^0\pi^0\pi^0, \qquad [\tilde{\mathcal{M}}_0^L] \tag{6.2c}$$
$$K_L \to \pi^+\pi^-\pi^0, \qquad [\tilde{\mathcal{M}}_x^L] \tag{6.2d}$$
$$K_S \to \pi^+\pi^-\pi^0, \qquad [\tilde{\mathcal{M}}_x^S] \tag{6.2e}$$
$$\eta \to \pi^0\pi^0\pi^0, \qquad [\tilde{\mathcal{M}}_0^\eta] \tag{6.2f}$$
$$\eta \to \pi^+\pi^-\pi^0, \qquad [\tilde{\mathcal{M}}_x^\eta] \tag{6.2g}$$

neglecting CP-violating effects. A natural framework for description of these processes has evolved to be chiral perturbation theory, in the case of K decays extended to include also weak non-leptonic decays [88]. Nevertheless, technical complications in computation of the higher and higher orders together with an increasing number of need-to-be-determined constants have contributed to a wider interest also in alternative phenomenological methods. Among them the most favorable are the ones using unitarity properties of the amplitudes or the methods inspired by non-relativistic effective theories.

We are going to describe the decays of the following three types.

$K^\pm$ and K_L^0 decays

Since kaons are the lightest particles carrying strangeness and this quantum number is conserved by strong interactions, their decay have to be mediated by weak interactions. Inclusion of the non-leptonic weak interactions into χPT was done by Kambor, Missimer and Wyler [88] already in 1989 by adding operators changing isospin by $1/2$ and $3/2$ into the chiral Lagrangian. Using their framework, in [89] they have computed amplitudes of these decays up to the next-to-leading order, at that time ignoring all the isospin breaking effects (cf. also [32]). The most complete work in including them but still ending at NLO is a sequence of papers by Bijnens and Borg [27, 28, 29].

The importance of these processes has arisen after the discovery of the cusp effect in $K^\pm \to \pi^\pm\pi^0\pi^0$ decay by NA48 collaboration [20], which has been proposed by Cabibbo to be a potentially clear method for the determination of the $\pi\pi$ scattering lengths $a_0 - a_2$ [43]. In the same paper he sketched a simple toy-model description of this process using unitarity properties and so explained the appearance of the cusp. We reformulate his argumentation in Section 6.5.

A continuation of his ideas and a completion of the NNLO computation is given in [44]. By assuming a simplified analytic structure of the amplitude and using unitarity of scattering matrix, the decay amplitude in the vicinity of the cusp is expressed there as an expansion in scattering lengths a_i. In [68] the same assumptions are made but in addition

to them the isospin symmetric NLO result of χPT is used as an input for the real parts of the amplitudes.

It was pointed out by the authors of [47] that the correct analytic structure of these amplitudes is more complicated and they presented a method inspired by non-relativistic effective field theory (NREFT) based on a combined expansion in a_i and in formal non-relativistic parameter ε. They use a computation done in modified NREFT with non-local Lagrangian (which obeys the Lorentz invariance) supplemented by the threshold expansion of the amplitudes for the construction of the non-analytical parts of the $P \to 3\pi$ amplitudes induced by $\pi\pi$ rescatterings. The polynomial part of the amplitudes is absorbed into a redefinition of the parameters of the Lagrangian. With that they succeeded in a continuation of the non-relativistic expansion to the whole decay region, even though this formal expansion would diverge at the edge of this region, where the outgoing π is relativistic. One of the profits of using NREFT based computation is the fact that the amplitudes have there a very simple expansion in a_i. For more details see [72]. Finally, they took advantage of having a Lagrangian formulation and introduced into computations also real and virtual photons, having so in this aspect the most advanced result [37].

η decays

$\eta \to 3\pi$ decays violate G-parity[1]. Therefore, they have to proceed via isospin breaking effects. There are two mechanisms of this breaking, either through the electromagnetic (EM) interactions, which are proportional to the electric charge squared,

$$\mathcal{H}^{\mathrm{IB}}_{\mathrm{QED}}(x) = -\frac{1}{2}e^2 \int dy D^{\mu\nu}(x-y)\, T(j_\mu(x) j_\nu(y))\,, \tag{6.4}$$

where $D^{\mu\nu}(x-y)$ is the photon propagator, T denotes the operator of time-ordering and $j_\mu(s)$ is the current density containing the fields corresponding to the charged particles of the theory; or through the isospin breaking mass difference between u and d quarks,

$$\mathcal{H}^{\mathrm{IB}}_{\mathrm{QCD}}(x) = \frac{m_d - m_u}{2}\left(\bar{d}(x)d(x) - \bar{u}(x)u(x)\right). \tag{6.5}$$

However, even though the EM interactions have a large effect on the $m_{\pi^\pm} - m_{\pi^0}$ difference and on the pion decay constant F_π, it has turned out that their influence on the

[1]G-parity (isotopic parity) is a combination of charge conjugation and an isospin rotation by π about the second axis,

$$\mathcal{G} = \mathcal{C}e^{i\pi T_2}. \tag{6.3}$$

G-partity of η is even, whereas the one of π is odd. A system of n pions obeys G-parity $\eta_G = (-1)^n$.

We can deduce the impossibility of the decay as a result of isospin conservation and charge conjugation invariance (C-invariance) without even introducing G-parity. Indeed, the final state has to have the total isospin $I = 0$ and is therefore totally antisymmetric with respect to the permutation of the three pions (the only allowed state is then $\pi^+\pi^-\pi^0$). Due to Bose symmetry, the corresponding amplitude is then totally antisymmetric under exchanges of the momenta of these three pions. On the other hand, according to C-invariance, the amplitude has to be symmetric with respect to the exchange of the momenta of the π^+ and the π^-, which implies that the amplitude is zero.

$\eta \to 3\pi$ decay amplitudes is very small [126, 23, 59]. Hence, $\mathcal{H}^{\mathrm{IB}}_{\mathrm{QCD}}$ represents the dominant contribution and the amplitude is proportional to $m_u - m_d$. The leading behavior is given by the results computed to the first order in this isospin breaking parameter, in IB[1].

Passing over the early computations using the PCAC methods (e.g. [24, 51, 115]), the first computation of these amplitudes using chiral perturbation theory to NLO [75] was performed already immediately after the formulation of $SU(3)$ χPT in [74].

Quite recently the NNLO computation has been published [33]. There is included also the comparison of these IB[1] results together with experimental data, the result of which is used by many authors as the most precise determination of the isospin breaking parameters R and Q, even though there are still sign discrepancies in the determination of Dalitz parameters describing the energy dependence of the η decay amplitudes between experiment and this analysis (cf. also Section 6.4). This discrepancy is one part of the motivation for our analysis performed in Chapter 9, which uses our dispersive parametrization of the next section in order to put together consistently the information we have from the experiment with the information coming from the analysis of [33], resulting in a better determination of the parameter R. But for now, let us return back to this historical overview of the computations of $\eta \to 3\pi$ amplitudes.

By comparison of these three successive orders in the chiral expansion one observes that $\eta \to 3\pi$ represents a case where the chiral corrections are large [26]. This is connected with the higher importance of the $\pi\pi$ rescattering effects. Already at the one-loop level (before the appearance of the paper [33]) this observation led [90, 17] to abandon, in a certain sense, the strict chiral counting, attempting instead to obtain the amplitudes with two-pion rescattering effects formally included to all orders. These approaches employ a restricted version of unitarity (taking into account just the $\pi\pi$ intermediate states) and construct dispersion relations of Khuri-Treiman type neglecting the $l \geq 2$ partial waves (and the other intermediate states). The resulting amplitudes are obtained by finding fixed-point solution of those dispersion relations numerically together with the determination of the values of subtraction constants from the matching with NLO χPT results at specific points. Thereby the numerical resummation of all the contributions with any number of subsequent two-pion rescatterings is performed[2]. Although the ideas used in both the papers are in many concepts the same, the formalisms in which they were written are different. The main phenomenological difference between them is that in [90] the validity of the chiral expansion is assumed whereas in [17] the chiral counting is believed to converge only in the vicinity of the Adler zero (for the discussion of the specialties of this point see Section II.C in [VI]). On the other hand, in [17] a simple high-energy behavior of the amplitudes leading to the possibility to consider the higher partial waves for any energy negligible to a considered precision is assumed, and hence just two subtractions are taken; while in [90] no such additional premises are added and three subtractions are taken (cf. our discussion of a need for at least 3 subtractions within the proof of the reconstruction

[2]Note that some authors use the name "dispersive methods" solely for the computations that resum such rescatterings to an infinite order. This can lead to some misunderstanding of the work that the reader is currently reading. Here the word "dispersive" is deduced from and refers to the use of dispersion relations.

theorem in Section 2.4). Recently, there appeared an attempt [50] to redo the analysis of [17]; eventually also with obtaining the subtraction constants by matching to the new NNLO χPT results [33].

As we have already noted, all these studies compute their results in IB[1] order and exactly the same is true for our NNLO result of the next chapter. Nevertheless, although the $\eta \to 3\pi$ processes have a different physical background than the weak $K_L \to 3\pi$ decays, by a simple change of the interpretation of the constants appearing in that amplitude we obtain the complete isospin breaking (IB) results of the η decays, including also description of the cusp effect in $\eta \to 3\pi^0$. This will be discussed in Chapter 8.

The similar fact is true also for the non-relativistic approach. Changing the interpretation of the constants in the analysis of $K_L \to 3\pi$ decay [36], in [82] there was also made a prediction of the strength of the cusp effect there. The NREFT formalism was also use in order to attempt to shed light on the Dalitz parameter α discrepancy [122]. Note, however, that in this case the non-relativistic parameter is even more formal. [In the center of Dalitz plot the momenta of the outgoing pions in the rest-frame of the decaying particle (counted in their expansion as $O(\varepsilon)$) are 90% of their rest energy (counted as $O(1)$).]

There exist also further approaches using different methods, such as the parametrization inspired by the Bethe-Salpeter equation within the unitarised χPT [39].

In Chapter 9 we recall some further arguments leading to the conclusions that our approach can improve the determination of the m_u and m_d masses and such analysis is also performed there.

K_S decay

Our procedure can be easily modified in order to obtain also the CP even part of the decay amplitude $K_S \to 3\pi$ (it means the contributions of the isospin states $I = 0$ and $I = 2$ to this process). Nevertheless, its branching ratio is very small, and so the only parameter connected with the energy dependence of this process usually measured in the recent experiments (e.g. [16, 21]) is the interference parameter λ between $K_L \to 3\pi$ and $K_S \to 3\pi$ processes,

$$\lambda = \frac{\int dy\, dx \tilde{\mathcal{M}}_x^{L*} \tilde{\mathcal{M}}_x^S}{\int dy\, dx |\tilde{\mathcal{M}}_x^{L*}|^2}\,, \tag{6.6}$$

where the integrations are taken over the whole decay region. However, there already exist first measurements of the parameters of energy dependence (6.25) even though with a large error of them (e.g. [15], see also Table 6).

From the theoretical point of view, this process is also covered by the χPT computations up to NLO by Bijnens and his collaborators [32, 27, 28, 29].

6.3 Kinematics

Before the completion of all the motivational topics, we write a few words about kinematics of the discussed processes and we introduce the rest of our notation, which will be used

also in the following motivational sections. We start with our notation for the masses. The masses of the pions are denoted in the same way as in Chapter 5, the masses of $K^\pm$, K_L and K_S are denoted by $m_{K^\pm}$, m_{K^L} and m_{K^S}, respectively, and finally m_η denotes the mass of η. In addition, we use the generic mass m_P when talking about the mass of any P.

As was mentioned above, we obtain the amplitude $\tilde{\mathcal{M}}_i^c$ of (6.2) that describes the decay process[3]

$$P^c(k) \to \pi^a(p_1)\pi^b(p_2)\pi^e(p_3) \tag{6.7}$$

by analytic continuation of the amplitudes of the corresponding scattering process

$$P^c(k)\pi^d(p) \to \pi^a(p_1)\pi^b(p_2) \tag{6.8}$$

by taking $p = -p_3$ and π^d as the charge conjugated pion to π^e.

Unlike for the pion-pion scattering case, the scattering amplitudes are denoted here by the more explicit notation $\tilde{A}^c_{ab}$ with ab corresponding to the charge states of the pions in the final state, and c being $\pm$ for decaying $K^\pm$, L or S for $K_{L,S}$ and η for $P = \eta$. However, the notation for the decay amplitudes and for the polynomial constants appearing in the processes is given again by the one-letter lower indices 0, c and x according to the mnemonics similar to the pion case (5.1). These three indices are sufficient thanks to the fact that we exploit the crossing relations relating different scattering amplitudes containing the same particle P and the same number of charged pions. As we do not take in the unitarity relations into account the intermediate states involving particles P, in every relation there always appears just one specific particle P (i.e. for instance in the relations for a process with K_L there never appears any particle K^+), so there is no need to indicate explicitly for every variable the specific index P. For the sake of shorter notation we have decided to omit these indices on the right-hand-sides of all relations in such cases. To avoid confusion of some of the quantities connected to processes containing particle P with the one related to the $\pi\pi$ scattering, we use a tilde above the P quantities where such confusion could occur.

Depending on the particular phase convention used for various states, in the analytic continuation connected with the crossing relation

$$\tilde{\mathcal{M}}_i^c(k, p_1, p_2, p_3) = \epsilon \tilde{A}^c_{ab}(k, p = -p_3, p_1, p_2) \tag{6.9}$$

the residual phase factor ϵ might appear. The convention that we use in the whole of this work implies ϵ to be minus sign in the case of crossing charged pion between the final and the initial states (in the S-channel it corresponds to a charged π^e) and plus in all the other cases.

We use the usual Mandelstam variables, in the scattering region

$$s = (k+p)^2, \qquad t = (k-p_1)^2, \qquad u = (k-p_2)^2, \tag{6.10}$$

while in the decay region

$$s_j = (k-p_j)^2. \tag{6.11}$$

[3] As is usual in the literature, we denote the odd pion as the third one [cf. (6.2) and Table 5].

Decay amplitude	S	T	U	$\tilde{s}_i^c$
$\tilde{\mathcal{M}}_x^+$: $K^+ \to \pi^0\pi^0\pi^+$	$-\tilde{A}_{00}^+$	$\tilde{A}_{+0}^+$	$\tilde{A}_{0+}^+$	$3\tilde{s}_x = m_{K^\pm}^2 + 2m_{\pi^0}^2 + m_{\pi^\pm}^2$
$\tilde{\mathcal{M}}_c^+$: $K^+ \to \pi^+\pi^+\pi^-$	$-\tilde{A}_{++}^+$	$-\tilde{A}_{-+}^+$	$-\tilde{A}_{+-}^+$	$3\tilde{s}_c = m_{K^\pm}^2 + 3m_{\pi^\pm}^2$
$\tilde{\mathcal{M}}_0^L$: $K_L \to \pi^0\pi^0\pi^0$	$\tilde{A}_{00}^L$	$\tilde{A}_{00}^L$	$\tilde{A}_{00}^L$	$3\tilde{s}_0 = m_{K^L}^2 + 3m_{\pi^0}^2$
$\tilde{\mathcal{M}}_x^L$: $K_L \to \pi^+\pi^-\pi^0$	$\tilde{A}_{+-}^L$	$-\tilde{A}_{0-}^L$	$-\tilde{A}_{+0}^L$	$3\tilde{s}_x = m_{K^L}^2 + 2m_{\pi^\pm}^2 + m_{\pi^0}^2$
$\tilde{\mathcal{M}}_x^S$: $K_S \to \pi^+\pi^-\pi^0$	$\tilde{A}_{+-}^S$	$-\tilde{A}_{0-}^S$	$-\tilde{A}_{+0}^S$	$3\tilde{s}_x = m_{K^S}^2 + 2m_{\pi^0}^2 + m_{\pi^\pm}^2$
$\tilde{\mathcal{M}}_0^\eta$: $\eta \to \pi^0\pi^0\pi^0$	$\tilde{A}_{00}^\eta$	$\tilde{A}_{00}^\eta$	$\tilde{A}_{00}^\eta$	$3\tilde{s}_0 = m_\eta^2 + 3m_{\pi^0}^2$
$\tilde{\mathcal{M}}_x^\eta$: $\eta \to \pi^+\pi^-\pi^0$	$\tilde{A}_{+-}^\eta$	$-\tilde{A}_{0-}^\eta$	$-\tilde{A}_{+0}^\eta$	$3\tilde{s}_x = m_\eta^2 + 2m_{\pi^\pm}^2 + m_{\pi^0}^2$

Table 5: Crossing processes belonging to the individual $P \to 3\pi$ decay processes. With S we denote the S-channel that can be obtained by the crossing (s_3, s_1, s_2) to (s, t, u). The T- and the U-channels result from the crossing (s_3, s_1, s_2) to (t, s, u) and (u, t, s), respectively. $\tilde{s}_i^c$ corresponds to the center of the Dalitz plot of the particular process (for the sake of simpler notation we do not repeat there the upper index c).

These variables satisfy

$$s + t + u = 3\tilde{s}_i^c = s_1 + s_2 + s_3, \tag{6.12}$$

where $s = t = u = \tilde{s}_i^c$, with[4]

$$3\tilde{s}_i^c = m_P^2 + m_{\pi^a}^2 + m_{\pi^b}^2 + m_{\pi^e}^2 \tag{6.13}$$

corresponds to the center of the Dalitz plot.

Up to the phase factor the crossing relation then means a substitution of the variables (s, t, u) by (s_3, s_1, s_2) together with the appropriate analytic continuation from the scattering to the decay region. We summarize the crossed amplitudes belonging to each of the considered decay amplitudes in Table 5. Note that the decay amplitudes of K^- are equal to the ones of K^+ thanks to CP symmetry, violation of which is not considered in our approach.

The constraints (6.12) tell us that just of the kinematic variables are independent. We can choose them to be, for instance, $s_3 = s$ and $s_1 = t$. The plot of the dependence of the decay amplitudes on these variables is called Dalitz plot. The physically allowed kinematic regions for the different crossed amplitudes are constrained by kinematic limits arising from the condition that the energy of a real particle has to be at least equal to its rest energy. Therefore, for a decay process the variable s_3 is bounded by

$$(m_{\pi^a} + m_{\pi^b})^2 \leq (p_1 + p_2)^2 = s_3 = (k - p_3)^2 \leq (m_P - m_{\pi^e})^2, \tag{6.14}$$

whereas for a scattering in the S-channel

$$s \geq (m_P + m_{\pi^d})^2. \tag{6.15}$$

[4]Note that in some relations we suppress the index c identifying the particle P.

[N.B. $m_P > m_{\pi^a} + m_{\pi^b} + m_{\pi^d}$ otherwise the decay would be impossible.]

In both cases for a fixed value of s_3 we can obtain bounds for s_1 using the following arguments. s_1 is an invariant quantity, therefore, it is enough to find the bounds in any frame of reference. We choose the rest frame of the system $p_1 + p_2$. In this system the energies of the particle with the momenta p_2 a the one with p_3 are fixed,

$$E_2^{(12)} = \frac{s_3 + m_{\pi^b}^2 - m_{\pi^a}^2}{2\sqrt{s_3}}, \qquad E_3^{(12)} = \frac{m_P^2 - m_{\pi^d}^2 - s_3}{2\sqrt{s_3}}. \tag{6.16}$$

The minimal and the maximal value of the quantity $(p_2 + p_3)^2$ for some real particles are then settled by the situations in which they move parallel or antiparallel to each other. After some simple algebra we find the bounds for s_1 to be

$$s_1^-(s_3) \leq s_1 \leq s_1^+(s_3) \tag{6.17}$$

with

$$s_1^\pm(s_3) = \frac{3\tilde{s}_i^c - s_3}{2} - \frac{\tilde{\Delta}_{P\pi^d}\Delta_{\pi^a\pi^b}}{2s_3} \pm \frac{\tilde{\lambda}_{P\pi^d}^{1/2}(s_3)\lambda_{\pi^a\pi^b}^{1/2}(s_3)}{2s_3}, \tag{6.18}$$

where we have already used the tilde denoting the variable containing the particle P. [Naturally, these limits coincide with the boundary values from (3.28).] From the crossing we simply obtain the regions also for the T- and the U-crossed amplitudes. In Figure 9 we plot these kinematic regions in the case of $K^+ \to \pi^0\pi^0\pi^+$ decay. The figures for the other processes look similarly. As an illustration supporting the arguments of the discussion from page 102 regarding the intermediate states that has to be taken into account, we have indicated on this figure also the position where the kinematic variables equal $m_{K^\pm}^2$. Any intermediate state that contains this particle has to have its threshold behind one of the dotted line (in the sense outside from the center of the triangle). In the picture we verify that the decay region is far away from such thresholds, which indicates that a polynomial expansion of their contributions describes them with a very good accuracy.

In addition to the pion quantities we have defined in the previous chapter, we introduce the following further useful notation

$$\tilde{\Delta}_+ = m_P^2 - m_{\pi^\pm}^2, \qquad \tilde{\Delta}_0 = m_P^2 - m_{\pi^0}^2, \qquad \tilde{\Delta} = m_P^2 - m_\pi^2, \tag{6.19}$$

$$\tilde{\mu}_c^\pm = (m_P \pm m_{\pi^\pm})^2, \qquad \tilde{\mu}_0^\pm = (m_P \pm m_{\pi^0})^2, \qquad \tilde{\mu}^\pm = (m_P \pm m_\pi)^2. \tag{6.20}$$

A similar philosophy is followed also by the notation for the Källen's quadratic form (2.10),

$$\tilde{\lambda}_+(s) = \tilde{\lambda}_{P\pi^\pm}(s), \qquad \tilde{\lambda}_0(s) = \tilde{\lambda}_{P\pi^0}(s), \qquad \tilde{\lambda}_\pi(s) = \tilde{\lambda}_{P\pi}(s). \tag{6.21}$$

6.4 Dalitz plot parametrization

The standard parametrization of a decay process $P \to 3\pi$ is called a Dalitz plot parametrization (cf. [110]). It is a polynomial expansion of $|M_i^c(s_1, s_2, s_3)|^2$ around the center of

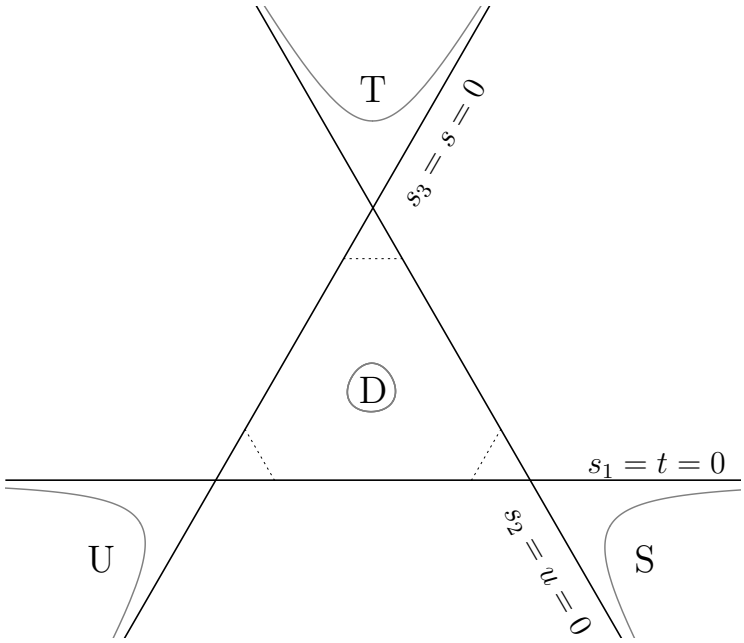

Figure 9: Kinematic regions in the Dalitz plot of $K^+ \to \pi^0\pi^0\pi^+$. D denotes the decay region and S, T and U are the scattering regions in the corresponding crossing channels. On the solid lines the individual kinematic variables equal to zero. By the dotted lines we have indicated the positions where these variables equal to $m^2_{K^\pm}$.

the Dalitz plot

$$\frac{|\tilde{\mathcal{M}}_i^c(s_1,s_2,s_3)|^2}{|\tilde{\mathcal{M}}_i^c(\tilde{s}_i^c)|^2} = 1+a(s_3-\tilde{s}_i^c)+b(s_3-\tilde{s}_i^c)^2+c(s_2-s_1)+d(s_2-s_1)^2+e(s_3-\tilde{s}_i^c)(s_2-s_1)+\cdots . \tag{6.22}$$

The parameters are usually normalized in order to be dimensionless. Such normalization and the labels used for the parameters differ for K and for η decays, so we discuss them separately.

For theoretical comparisons it is sometimes useful to introduced also the *linear* Dalitz parametrization of the amplitude itself which is discussed and employed in Appendix H.

6.4.1 Dalitz plot parametrization for $K \to 3\pi$ decays

In the case of $K \to 3\pi$ decays, the normalization factor is chosen to be the mass of the pion in the isospin limit m_π^2. Its physical value is defined by various authors differently, but the most common choice is to take it equal to the mass of the charged pion $m^2_{\pi^\pm}$. Using the kinematic variables

$$x = \frac{s_2 - s_1}{m^2_{\pi^\pm}}\,, \qquad y = \frac{s_3 - \tilde{s}_i^c}{m^2_{\pi^\pm}} \tag{6.23}$$

Decay	Parameter	Exp.	χPT
$K^+ \to \pi^0\pi^0\pi^+$	g	0.626 ± 0.007	0.638
	h	0.052 ± 0.008	0.074
	k	0.0054 ± 0.0035	0.0045
$K^+ \to \pi^+\pi^+\pi^-$	g	-0.21134 ± 0.00017	-0.216
	h	0.01848 ± 0.00040	0.012
	k	-0.00463 ± 0.00014	-0.0052
$K_L \to \pi^0\pi^0\pi^0$	h (KTeV [3])	0.00059 ± 0.00119	-0.0072
	h (NA48 [101])	-0.0061 ± 0.0010	
$K_L \to \pi^+\pi^-\pi^0$	g	0.678 ± 0.008	0.677
	h	0.076 ± 0.006	0.085
	k	0.0099 ± 0.0015	0.0055
$K_S \to \pi^+\pi^-\pi^0$	γ	$(3.3 \pm 0.5)\cdot 10^{-8}$	$3.4 \cdot 10^{-8}$
	ξ	$(0.4 \pm 0.8)\cdot 10^{-8}$	$-0.2 \cdot 10^{-8}$

Table 6: Dalitz parameters for $K \to 3\pi$ decays. The experimental values are taken from [110] with the exception of K_S parameters that are from [15]. In the last column there are given results of χPT fit from [32].

the parametrization then reads

$$\frac{|\tilde{\mathcal{M}}_i^c(s_1, s_2, s_3)|^2}{|\tilde{\mathcal{M}}_i^c(\tilde{s}_i^c)|^2} = 1 + gy + hy^2 + jx + kx^2 + fxy + \cdots . \tag{6.24}$$

Note that in the processes $K^\pm \to \pi^\pm\pi^\pm\pi^\mp$, $K^\pm \to \pi^0\pi^0\pi^\pm$ and $K_L \to 3\pi^0$, Bose symmetry dictates the quantities that are odd in x to be zero. Similarly, since we consider also CP symmetry to be conserved, it has to be true also for the decay $K_L \to \pi^+\pi^-\pi^0$. Therefore, $j = f = 0$ for all these processes.

For the same reason, the amplitude $K_S \to \pi^+\pi^-\pi^0$ has to contain only the terms with odd powers of x. With this fact there is connected the usual alternative parametrization of this process (the *linear* one) in the way

$$\tilde{\mathcal{M}}_x^S = \gamma_x^S x - \xi_x^S xy + \cdots . \tag{6.25}$$

But let us return to the parametrization (6.24). Since the process $K_L \to 3\pi^0$ obeys also additional (Bose) symmetries, further constraints appear, $g = 0$ and $k = \frac{h}{3}$. Finally, imposing the isospin symmetry (cf. Appendix I) there will appear some (in)equalities between the parameters similar to the ones derived in Appendix H for η.

In Table 6 we list experimental values of the parameters from PDG [110]. These values are compared with the calculation in NLO χPT [32].

Recently there appeared new empirical parametrizations that try to include the existence of cusp-like structures in the amplitudes. One such parametrization is the one from NA48/2 group [22]

$$\frac{d|\tilde{\mathcal{M}}_i^c(x,y)|^2}{dydx} \propto \left(1 + \frac{g}{2}y + \frac{h}{2}y^2 + \frac{k}{2}x^2 + a(y_t - y)^q\theta(y_t - y) + b(y - y_t)^q\theta(y - y_t)\right)^2 f(y), \tag{6.26}$$

where $y = y_t \equiv \frac{4m_{\pi^\pm}^2 - \tilde{s}_i^c}{m_{\pi^\pm}^2}$ is the cusp point, $\theta(y)$ denotes the Heaviside step function and the function $f(y) = 1 + pw\delta(y - y_t)$ takes into account additional contributions from the $\pi^+\pi^-$ bound states and similar electromagnetic effects in the vicinity of the cusp. Their analysis then leads to the following values of these parameters

$$g = 0.672 \pm 0.011, \tag{6.27}$$
$$h = -0.027 \pm 0.011, \tag{6.28}$$
$$k = 0.0081 \pm 0.0005, \tag{6.29}$$
$$a = -0.130 \pm 0.007, \tag{6.30}$$
$$b = 0.07 \pm 0.03, \tag{6.31}$$
$$q = 0.45 \pm 0.06. \tag{6.32}$$

6.4.2 Dalitz parametrization of $\eta \to 3\pi$ decays

In the parametrization of $\eta \to \pi^+\pi^-\pi^0$ there appears the energy of reaction

$$Q_\eta = m_\eta - 2m_{\pi^\pm} - m_{\pi^0}. \tag{6.33}$$

The variables of standard use for this decay are then

$$x = \sqrt{3}\,\frac{T_1 - T_2}{Q_\eta} = \frac{\sqrt{3}\,(s_2 - s_1)}{2m_\eta Q_\eta}, \quad y = \frac{3T_3}{Q_\eta} - 1 = \frac{3}{2m_\eta Q_\eta}\left((m_\eta - m_{\pi^0})^2 - s_3\right) - 1, \tag{6.34}$$

where T_j is the kinetic energy of the j-th pion in the rest frame of η. In the case we use in this definition the physical values of the masses, the point $x = y = 0$, around which we expand the amplitude, does not coincide exactly with the center of the Dalitz plot. It is shifted slightly in the s_3 direction to

$$s_3(x = 0, y = 0) = \tilde{s}_x^\eta + \frac{2}{3}\,(m_{\pi^\pm} - m_{\pi^0})\,(2m_\eta - m_{\pi^\pm} - m_{\pi^0})\,. \tag{6.35}$$

However, in the isospin limit,

$$y = \frac{3}{2m_\eta Q_\eta}(\tilde{s}_x^\eta - s_3) \tag{6.36}$$

and the center of the expansion $x = y = 0$ matches the center of the Dalitz plot.

	a	b	d	f
Gormley et al. [79]	-1.17 ± 0.02	0.21 ± 0.03	0.06 ± 0.04	
Layter et al. [104]	-1.08 ± 0.014	0.034 ± 0.027	0.046 ± 0.031	
Crystal Barrel [2]	-1.22 ± 0.07	0.22 ± 0.11	0.06 ± 0.04	
KLOE [8]	-1.090 ± 0.020	0.124 ± 0.012	0.057 ± 0.017	0.14 ± 0.02
χPT NNLO [33]	-1.271 ± 0.075	0.394 ± 0.102	0.055 ± 0.057	0.025 ± 0.160
χPT + Unitarity [90]	-1.33	0.26	0.10	
NREFT [122]	-1.213 ± 0.014	0.308 ± 0.023	0.050 ± 0.003	0.083 ± 0.019

Table 7: Values of the Dalitz plot parameters of the $\eta \to \pi^+\pi^-\pi^0$ decay coming from various experimental and theoretical determinations.

The parameters are usually labeled according to

$$|\tilde{\mathcal{M}}_x^\eta(s_1, s_2, s_3)|^2 = |A|^2 \left(1 + ay + by^2 + cx + dx^2 + exy + fy^3 + gx^2y + \cdots\right), \qquad (6.37)$$

where A is the value of the amplitude $\tilde{\mathcal{M}}_x^\eta$ in the point $x = y = 0$. Charge conjugation forbids the appearance of terms containing odd powers of x in this expansion, and so $c = e = 0$.

The values of the parameters obtained by various experiments and by a few theoretical determinations are listed in Table 7. All of the experiments find the values of c and e compatible with zero. From the table it is obvious that the precision of the determination from KLOE [8] exceeds significantly the precision of all the others, which are more than ten years older. It is also up to now the only experiment that has determined the parameter f with a reasonable precision.

At leading order, the parametrization of the $\eta \to 3\pi^0$ differential decay rate depends only on the kinematic variable

$$z = \frac{3}{2m_\eta^2(m_\eta - 3m_\pi)^2} \sum_j (s_j - \tilde{s}_0^\eta)^2 = \frac{3}{2m_\eta^2(m_\eta - 3m_\pi)^2} \left(s_1^2 + s_2^2 + s_3^2 - 3(\tilde{s}_0^\eta)^2\right), \quad (6.38)$$

which denotes the distance from the center of the Dalitz plot, normalized to one at the edge of the decay region. However, higher-order corrections do not preserve this accidental rotational symmetry, and we need again x and/or y from relations (6.34) with $m_{\pi^\pm} \to m_{\pi^0}$. Note that the relation

$$z = x^2 + y^2 \qquad (6.39)$$

holds. The Dalitz plot parametrization of this process reads

$$\frac{|\tilde{\mathcal{M}}_n^\eta(s_1, s_2, s_3)|^2}{|\tilde{\mathcal{M}}_n^\eta(s_0^\eta)|^2} = 1 + 2\alpha z + 2\beta y(3z - 4y^2) + \gamma z^2 + \cdots . \qquad (6.40)$$

The factor of 2 in front of α and β is a mere convention to stress the connection with the direct *linear* Dalitz parametrization of the amplitude (see Appendix H). For a better visualization of the violation of the (x, y) rotational symmetry at higher orders, it is convenient

	α
Crystal Barrel [1]	-0.052 ± 0.020
Crystal Ball [127]	-0.031 ± 0.004
WASA/CELSIUS [19]	-0.026 ± 0.014
Crystal Ball @ MAMI-B [128]	-0.032 ± 0.003
Crystal Ball @ MAMI-C [117]	-0.0322 ± 0.0025
KLOE [9]	-0.0301 ± 0.0050
WASA @ COSY [5]	-0.027 ± 0.009
χPT NLO [75]	0.015
χPT NNLO [33]	0.013 ± 0.032
χPT + Unitarity [90]	$-0.014 \div -0.007$
U(3) χPT + Bethe-Salpeter [39]	-0.031 ± 0.003
NREFT [122]	-0.025 ± 0.005

Table 8: Experimental and theoretical values of the slope parameter α of the $\eta \to 3\pi^0$ decay.

to introduce the polar coordinates, $x = \rho \cos\phi$, $y = \rho \sin\phi$ with the distance $\rho^2 = z$, for which we have $y(3z - 4y^2) = \rho^3 \sin(3\phi)$.

Various experimental and theoretical determinations of the parameter α are given in Table 8. Note the sign discrepancy between the pure χPT determinations (with however large error bars) and the other determinations, both the theoretical and the experimental ones, which we address in Chapter 9. Up to now, no experiment has so far published any constraint on the other parameters, such as β.

In Appendix H we show a derivation of the following relation between Dalitz parameters that results from the isospin symmetry,

$$\alpha \leq \frac{1}{4}\left(b + d - \frac{a^2}{4}\right). \tag{6.41}$$

6.5 Cusp

We have already mentioned that in the processes with two neutral pions in their final state, the cusp effect caused by different $\pi^+ - \pi^0$ masses can appear. It is connected with the contributions of $\pi^+\pi^-$ intermediate states rescattering to $\pi^0\pi^0$. Such a state generates a square root singularity, which resides at $4m_{\pi^\pm}^2$. In the case that the masses of the charged and the neutral pions are different, it lies above the physical threshold, $4m_{\pi^0}^2$, and the cusp is a result of the interference between the part of the amplitude containing this singularity and the rest without it.

We illustrate this situation at the one-loop level. The contribution of the $\pi^+\pi^-$ intermediate state in the S channel is represented by the Feynman diagram depicted on

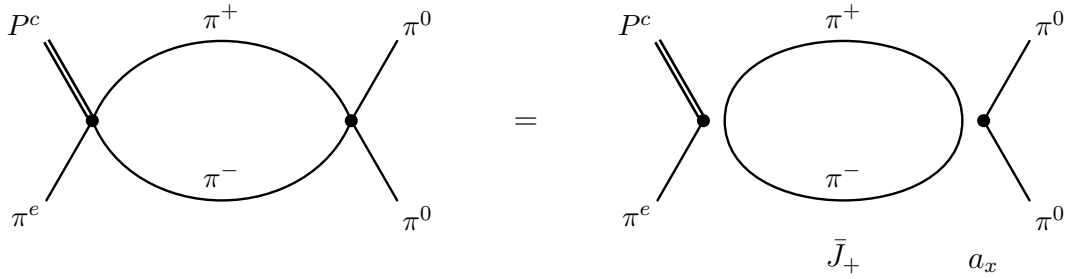

Figure 10: Feynman diagram connected with the appearance of the cusp in the process $P^c \to \pi^0\pi^0\pi^c$ ($P^c\pi^e \to \pi^0\pi^0$) at the one-loop level. The appearance of the square-root singularity at $4m^2_{\pi^\pm}$ in this diagram is connected with $\bar{J}_+(s)$. Contribution of this diagram at that singularity point is proportional to the scattering length a_x.

Figure 10. In its expression there appears one-loop function $\bar{J}_+(s)$ [from (3.13)] behaving in the vicinity of $s = 4m^2_{\pi^\pm}$ like $i\pi\sigma_+(s)$ plus some analytic part. It means that around that point the amplitude behaves as

$$\tilde{\mathcal{M}}(s) = R(\sigma_+^2) + \pi S(\sigma_+^2) \begin{cases} i\sqrt{1 - \frac{4m^2_{\pi^\pm}}{s}}, & s > 4m^2_{\pi^\pm} \\ -\sqrt{\frac{4m^2_{\pi^\pm}}{s} - 1}, & s < 4m^2_{\pi^\pm} \end{cases} , \tag{6.42}$$

where the functions $R(\sigma_+^2)$ and $S(\sigma_+^2)$ can be expressed as convergent series in $\left(s - 4m^2_{\pi^\pm}\right)$ in the physical region of the $P^c \to \pi^0\pi^0\pi^c$ decay. The modulus square of the scattering amplitude will then look near this singularity like

$$|\tilde{\mathcal{M}}|^2 = \begin{cases} \bar{R}^2 + S^2\pi^2\left(1 - \frac{4m^2_{\pi^\pm}}{s}\right), & s > 4m^2_{\pi^\pm} \\ \bar{R}^2 + S^2\pi^2\left(\frac{4m^2_{\pi^\pm}}{s} - 1\right) - 2\bar{R}S\pi\sqrt{\frac{4m^2_{\pi^\pm}}{s} - 1}, & s < 4m^2_{\pi^\pm} \end{cases} , \tag{6.43}$$

where $\bar{R}$ now includes also regular contributions of the tree amplitude and of the other intermediate states (in our NLO case the only other intermediate state is the $\pi^0\pi^0$ one). Note that a similar situation happens in all crossed channels.

It is obvious that the cusp emerges only in the $m_{\pi^0} \neq m_{\pi^\pm}$ case and its strength is sensitive to the $\pi^+\pi^- \to \pi^0\pi^0$ scattering at threshold (mainly to the scattering length of this process). This property can be used for a determination of the scattering lengths from the measurement of the cusp.

Let us try to estimate the relative sizes of the cusps in various processes where a pseudoscalar, namely K^+, K_L or η, decays into three pions. (This discussion is inspired by [44] and [58].) Because the pion rescattering part will be approximately the same for all the processes, we may consider the notion of the "visibility" of the cusp in these processes by comparing the relative ratios between the cusps and the regular parts of the amplitudes,

$$\gamma(P^c) = \left.\frac{\kappa_c|\tilde{\mathcal{M}}_{P^c\to\pi^+\pi^-\pi^c}|\ |\tilde{\mathcal{M}}_{P^c\to\pi^0\pi^0\pi^c}|}{|\tilde{\mathcal{M}}_{P^c\to\pi^0\pi^0\pi^c}|^2}\right|_{\text{cusp}} = \kappa_c \left.\frac{|\tilde{\mathcal{M}}_{P^c\to\pi^+\pi^-\pi^c}|}{|\tilde{\mathcal{M}}_{P^c\to\pi^0\pi^0\pi^c}|}\right|_{\text{cusp}} \tag{6.44}$$

where $|\tilde{\mathcal{M}}|$ is the absolute value of the matrix element of the indicated process and κ_c is a multiplicity factor corresponding to that process, equal to 2 in the case the decaying particle is charged (then two possible $\pi^+\pi^- \to \pi^0\pi^0$ scatterings are possible), and to 1 in the other cases. These ratios have to be evaluated at the cusp point $s = 4m_{\pi^\pm}^2$.

Using the measured relative decay rates and the values of Dalitz parameters from [110], we obtain for these processes,

$$\gamma(K^\pm) \sim 7.3, \qquad \gamma(K_L) \sim 0.45, \qquad \gamma(\eta) \sim 0.93. \tag{6.45}$$

From that we can estimate that the effect is approximately 16 (8) times more pronounced in the $K^\pm$ decay with respect to K_L (η) decay.

The cusp effect in $K^\pm \to \pi^\pm\pi^\pm\pi^\mp$ decay was successfully used for the determination of the $a_0 - a_2$ scattering length by NA48/2 [20]. Similar study for $K_L \to 3\pi^0$ was performed by KTeV [3] and is being performed by NA48/2 [77]. First indications of the cusp effect in the $\eta \to 3\pi^0$ decay were also already observed (cf. e.g. [117]). This effect however appears at the edge of the decay region[5] and is therefore not simple to measure. In Chapter 8 we present a parametrization of the processes $P \to 3\pi$ where the effect of the cusp is also included. Note that there we give the NLO parametrization of all these processes and the NNLO parametrization just of $K_L \to 3\pi^0$ and $\eta \to 3\pi^0$ decays.

6.6 The reconstruction procedure

For the construction of $P\pi \to \pi\pi$ amplitudes we would like to follow again the steps of the reconstruction procedure of Chapter 3. However, here one serious complication appears.

Since particle P is unstable, one cannot derive dispersion relations, which are the basic premise of the procedure, for such processes in the usual way. One way how to evade this problem is to start with the mass of P such that this particle is stable (i.e. $m_P < m_1 + m_2 + m_3$), in the following we refer to this situation as the "stable m_P" case. For such P all the arguments and the statements described before (and used for the $\pi\pi$ scattering) remain valid and there appears no additional complication in the reconstruction procedure of the amplitudes.

Nevertheless, in order to obtain results with some practical physical importance we would need to find them for the physical value of m_P. In some cases one can find an analytic continuation in the parameter m_P of such amplitude (obtained for stable m_P) that leads to the correct physical amplitude (with the physical mass of m_P). However, it is important to stress once more that even thought the dispersion relations can be derived and the amplitudes can be constructed for all the studied processes for the stable m_P, the existence of such analytic continuation (leading to the correct physical result) is not

[5] In the (x, y) plane, the cusp is located on the segment $y = y(4m_{\pi^\pm}^2) \sim 0.773$ and on two other segments obtained by $s \leftrightarrow t$ and $s \leftrightarrow u$ (i.e. obtained by rotation of the original one by $\pm 120^\circ$ around the center of the Dalitz plot). Its position thus does not respect the accidental rotation symmetry, and depending on its direction in the (x, y) plane, the corresponding value of z changes from 0.597 to 0.883 as $\frac{0.597}{\cos(\phi - \phi_0)}$, with $\phi_0 = 0^\circ, \pm 120^\circ$.

guarantied. Fortunately, in our applications such analysis is simplified by the fact that we deal only with the amplitudes within the regions of kinematic variables where the chiral expansion of the amplitudes makes sense. Thus, we can use the analytic properties of the usual Feynman diagram method in the field theoretical framework of chiral perturbation theory for the study of the existence and eventually also as a guiding line for writing the correct form of such analytic continuation.

At the one-loop level, i.e. by performing the first iteration, the only non-analytic structure of the amplitude is induced by the bubble diagram (cf. Figure 30f) which leads to the normal threshold singularity. On the other side, since the leading order amplitudes are simply polynomials in Mandelstam variables, there is no ambiguity in the analytic continuation of their partial waves and thereby of the one-loop discontinuities of the amplitudes and the physical result for the physical value of m_P can be written directly. Naturally, this leads to the correct analytic structure of the one-loop amplitudes.

The situation for the second iteration is more involved. The case in which the masses of the charged and the neutral pions are the same, i.e. if we want to compute the amplitudes only to the leading order in the isospin breaking, was studied by Kacser and Bronzan [86,40] resulting with the prescription for such analytic continuation in m_P giving the correct physical singularities. In Appendix J we recall the important steps of their analysis and show that even for different masses of $m_{\pi^\pm}$ and m_{π^0} in the case of $P^0\pi^0 \to \pi^0\pi^0$ processes the same Kacser prescription for the analytic continuation works. For these processes there appears no principal complication and one can compute quite straightforwardly the amplitudes also for them. The remaining cases are however more complicated — for instance there appears an anomalous threshold and one can not avoid deforming the contour of the dispersion relations. This leads us to the decision to leave their studies in the full isospin breaking for our next work.

Therefore in this work we are in fact computing the second iteration only of the amplitudes of the processes where the masses of all the pions in the initial and in the final states are the same, either because we work in the isospin limit or because they are the same pion states.

For these processes the Kacser prescription suggest to compute the amplitudes for stable m_P and thereafter perform the analytic continuation of the results by taking

$$m_P^2 \to \left(m_P^2\right)_{\text{physical}} + i\varepsilon. \tag{6.46}$$

By that we obtain the correct form of the results for the physical masses. However, in the general discussion of the second iteration in Section 3.5 we have gain its result in the integral form (3.81)–(3.82) [where there appear only integrals in one variable]. Therefore, there suggest itself the possibility to make the analytic continuation already on the base of these integrals by the knowledge of the analytic continuation of the integrand. It is even unavoidably the only way for obtaining it for the parts of the result where we do not have the results of integration in terms of functions with known analytic continuations. To that end, it will be very handy to know the results of continuation (6.46) of the partial waves. This is why we discuss their computation in Appendix K.

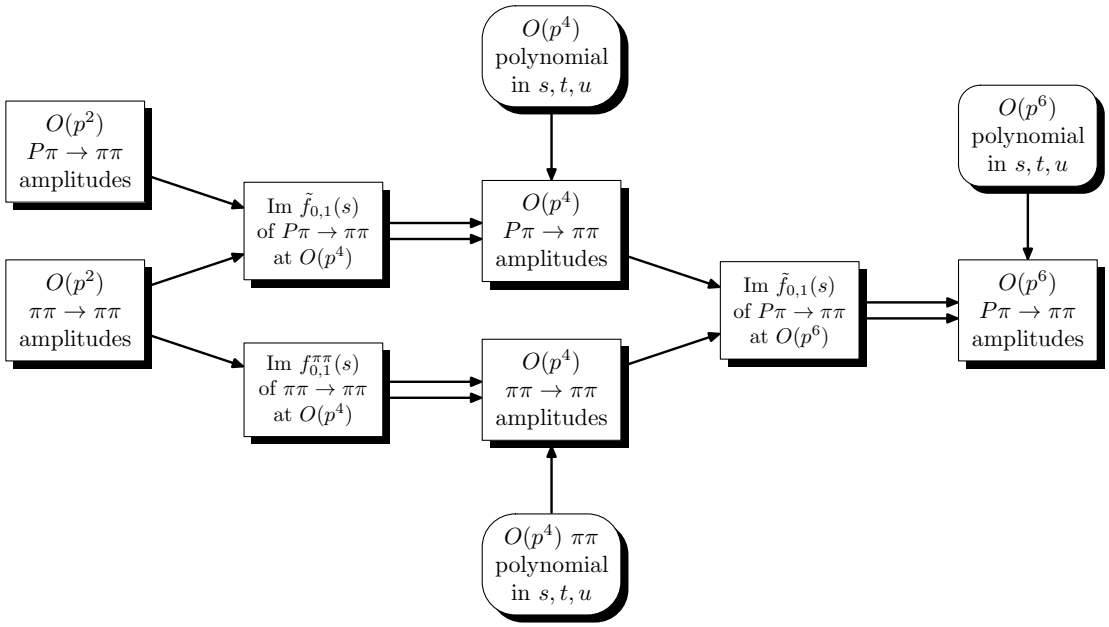

Figure 11: Schematic representation of the iterative two-step reconstruction procedure for the $P\pi \to \pi\pi$ amplitude. For the construction one needs to perform this procedure simultaneously also for the $\pi\pi$ scattering amplitudes appearing as the intermediate processes in the original $P\pi \to \pi\pi$ process.

6.6.1 Parametrization of polynomials

As was discussed already on few places of this work, the choice of the polynomial parametrization of the theorem can be crucial for its convergence properties. Inspired by the Dalitz plot parametrization, we use for $P\pi \to \pi\pi$ processes an expansion around the center of Dalitz plot, although there could exist some better choices.

As is obvious from the reconstruction scheme on Figure 11, during the construction of the $P\pi \to \pi\pi$ processes we employ also the parametrization of the $\pi\pi$ scattering amplitudes. We have constructed it in Chapter 5, where we have presented two possible forms of it — either the partial-wave (scattering-length) parametrization or the subthreshold parametrization similar to the one we have chosen for $P\pi \to \pi\pi$ scattering. We can use either of them and it is even possible to convert one into the other using relations from Section 5.9. We have discussed there that the conversion from the subthreshold into the partial-wave parametrization is more complicated than the other direction since then we have to track down all uses of crossing relations to distinguish for example between a_x and a_t.

For the full isospin breaking results of chapter 8 describing the cusp it is natural to use the scattering lengths as the parameters — actually, it was the reason why we have started with this parametrization of the $\pi\pi$ scattering amplitudes.

For the parametrization of the isospin $\pi\pi$ amplitudes used in the results of $P\pi \to \pi\pi$

amplitudes in the limit $m_{\pi^\pm} = m_{\pi^0}$ we have chosen also the partial-wave parametrization. It has two advantages, we can check these results simply by performing limit $m_{\pi^\pm} \to m_{\pi^0}$ and by using the relations (5.157)–(5.162); and the results in the subthreshold parametrization are simpler to obtain from them than when doing so from the other direction. The partial-wave parametrization could be useful also in this case since its better description of the $\pi\pi$ scattering data can lead to a better description of the $P \to 3\pi$ decay processes.

A special advantage of the partial-wave parametrization will occur when analyzing $\eta \to 3\pi$ decays once we will have obtained the scattering lengths exactly from the parametrization of the $K \to 3\pi$ cusps — in our parametrizations of both of the processes there appear the same $\pi\pi$ parameters and so the theoretical error induced by their uncertainties can be reduced.

Nevertheless, for a simpler comparison and a check with χPT results (for $\eta \to 3\pi$ decays with [33]) and to benefit from the analysis of $\pi\pi$ scattering for the subthreshold parameters by Stern et al. [95, 56], the subthreshold parametrization for $\pi\pi$ scattering is more useful and is explored for $\eta \to 3\pi$ in Chapter 9 in more detail.

6.6.2 Normalization of the amplitudes

Both the dispersive and the unitarity relations[6] do not depend on the normalization of the amplitudes and so using a dispersive method, which is based on these relations, we cannot determine their normalization. It has to be fixed by matching of our parametrization of the amplitude to the result of some theory that determines the scale, such as χPT. In order to simplify such matching, we introduce the overall normalization parameter $\mathcal{C}$ [similarly as in (3.1)] with some fixed value. The arbitrariness of the scale is then reflected in the arbitrariness of the scale of the subthreshold parameters of $P\pi \to \pi\pi$ that are obtained by such matching.

Since the kaon decay is a flavour-changing weak decay, it should be proportional to CKM matrix element squared and to Fermi constant G_F. For all kaon processes we take

$$\mathcal{C}^K = -\frac{3}{5} V_{us}^* V_{ud} \frac{G_F}{\sqrt{2}} \,. \tag{6.47}$$

Already around relation (6.5) we have discussed that the η decay amplitude should be proportional to $m_u - m_d$. The natural choice of the normalization constant for η decay processes is therefore for instance

$$\mathcal{C}^\eta = \frac{\sqrt{3}}{4} \frac{1}{R} \,, \tag{6.48}$$

[6] Naturally, if we have computed also with some other intermediate states than are the two-pion ones, such as $P\pi$, in the unitarity relations there would appear the relative normalization of these two amplitudes ($\pi\pi \to \pi\pi$ and $P\pi \to \pi\pi$). Then by measuring of the effects of those intermediate states, we could determine this relative normalization. However, as we have already discussed, the effect of such intermediate states is very small — negligible and this determination cannot be performed.

where the isospin breaking parameter

$$R = \frac{m_s - \hat{m}}{m_d - m_u} \tag{6.49}$$

depends on quark masses m_u, m_d and m_s and the isospin averaged mass $\hat{m} = 1/2(m_u + m_d)$.

Note that $\mathcal{C}^\eta$ vanishes in the isospin limit. Therefore, if we compute the amplitude in the leading order in isospin breaking IB[1] (the $m_{\pi^\pm} = m_{\pi^0}$ case), by factoring this isospin breaking quantity out of the amplitude the rest remains isospin conserving and from this there follows why one usually loosely calls also this case as the isospin symmetric one.

Chapter 7

$K \to 3\pi$ for isospin conservation. $\eta \to 3\pi$ in first order in isospin breaking.

After the general discussions of the previous chapter, we start with the studies of the $P \to 3\pi$ decay processes in the leading order in the isospin breaking. We have already explained there that in the case of η these decays are forbidden in the isospin limit and so the leading order is the first one in the isospin breaking. Nevertheless, in the dispersive approach, this just means that the leading order amplitude is nonzero and we can include all the isospin breaking into the overall normalization constant and continue further with the computation using an isospin conserving procedure (with taking isospin symmetry of the amplitudes, the same masses of charged and neutral pions, etc.) as is the case of the leading order for kaons.

This chapter is not only an easier step (or preparation) before we proceed to the full isospin-breaking but already on this level of computation one can draw important physical conclusions. Especially for the η decays, the assumption of the same masses of pions is still a very good approximation with respect to the present-day experimental uncertainties of their measurements and for instance in Chapter 9 it is used for the most precise determination of the masses of the lightest quarks, m_u and m_d.

Naturally, this analysis cannot cover the effect of cusp and if we expand our result for squared modulus of an amplitude into polynomial, we will obtain nothing more than its Dalitz plot parametrization from Section 6.4. But since our parametrization contains explicitly the unitarity relations, it should be more natural to match to various quantum field theoretical methods, especially to χPT, which is up to the contributions we have neglected, exactly reproduced by a specific choice of our parameters. The form of our parametrization also enables us to resign on the exact chiral power-counting and try to re-sum partially higher unitarity contributions. Also this is discussed in more detail in Chapter 9.

7.1 Symmetries

We have already listed some of the crossing symmetries of the amplitudes in Table 5 on page 108. Together with Bose symmetry they relate all amplitudes $P\pi \to \pi\pi$ with the same particle P and the same number of charged pions and dictate also some s,t,u symmetries that each amplitude has to obey. Taking the isospin conservation into account results in more relations between them.

In Appendix I we show that in the case of $K\pi \to \pi\pi$ scattering the amplitudes fulfill

$$\tilde{A}^{+}_{++}(s,t,u) = \tilde{A}^{S}_{+-}(t,s,u) - \tilde{A}^{S}_{+-}(u,t,s) - \tilde{A}^{+}_{00}(t,s,u) - \tilde{A}^{+}_{00}(u,t,s), \tag{7.1}$$

$$\tilde{A}^{L}_{00}(s,t,u) = -\left(\tilde{A}^{L}_{+-}(s,t,u) + \tilde{A}^{L}_{+-}(t,s,u) + \tilde{A}^{L}_{+-}(u,t,s)\right) \tag{7.2}$$

with $\tilde{A}^{+}_{00}$, $\tilde{A}^{+}_{++}$, $\tilde{A}^{L}_{+-}$ and $\tilde{A}^{L}_{00}$ being symmetric with respect to $t \leftrightarrow u$ exchange [the last one even totally symmetric in s,t,u], whereas $\tilde{A}^{S}_{+-}$ has to be $t-u$ antisymmetric.

In the processes with K_L, it is therefore natural to take $\tilde{A}^{L}_{+-}$ as the only independent amplitude and to compute all the other amplitudes from the relation (7.2) and the crossing symmetry. The situation in the $K^{\pm}$ processes is more complicated since the process $\tilde{A}^{S}_{+-}$ mixes in and this process is not measured with such a high precision as the $K^{\pm}$ processes are. We will therefore treat these amplitudes as independent and regard the relation (7.1) as an additional constraint on their parameters. Note that CP symmetry together with the one of Bose forbid the existence of the process $K_S\pi^0 \to \pi^0\pi^0$.

In the case of η the situation is simpler since after extracting the $\pi - \eta^0$ mixing angle, which is of the first order in isospin breaking, the rest of the amplitude can be in the considered level of computation taken in the isospin limit and so the isospin structure of the $\eta \to 3\pi$ amplitudes is the same as the structure of the $\pi\pi$ scattering amplitudes (5.10) with η replaced by π^0,

$$\tilde{A}^{\eta}_{00}(s,t,u) = -\tilde{A}^{\eta}_{+-}(s,t,u) - \tilde{A}^{\eta}_{+-}(t,s,u) - \tilde{A}^{\eta}_{+-}(u,t,s). \tag{7.3}$$

From charge conjugation there follows that the amplitude $\tilde{A}^{\eta}(s,t,u)$ is $t \leftrightarrow u$ symmetric,

$$\tilde{A}^{\eta}_{+-}(s,t,u) = \tilde{A}^{\eta}_{+-}(s,u,t). \tag{7.4}$$

Since the symmetries of the processes containing η and those containing K^L are the same and on top of it we consider just the $\pi\pi$ intermediate states, the amplitudes of these two processes will look in our reconstruction identical and the only difference between them will be just a different physical interpretation of the parameters appearing there. In the following we will therefore write the results only in the form for K^L and just discuss potential differences that can appear for η.

7.2 Leading order of amplitudes

The amplitudes in the leading order are first order polynomials. Taking into account their symmetries from the previous section, we parametrize them in the form

$$\tilde{A}^{+}_{++} = \mathcal{C}\left(A_c + \frac{B_c}{F_\pi^2}(s-\tilde{s}_0)\right), \tag{7.5}$$

$$\tilde{A}^{+}_{00} = \mathcal{C}\left(A_x + \frac{B_x}{F_\pi^2}(s-\tilde{s}_0)\right), \tag{7.6}$$

$$\tilde{A}^{L}_{+-} = \mathcal{C}\left(A_x + \frac{B_x}{F_\pi^2}(s-\tilde{s}_0)\right), \tag{7.7}$$

$$\tilde{A}^{S}_{+-} = \mathcal{C}\frac{B_x}{F_\pi^2}(t-u). \tag{7.8}$$

Note that on the right-hand side of the relations we suppress the upper index determining the particle P. Moreover, in the isospin limit there is no need to distinguish the different centers of Dalitz plot since all of them are equal to

$$\tilde{s}_i^c = \frac{1}{3}m_P^2 + m_\pi^2 \equiv \tilde{s}_0. \tag{7.9}$$

As is discussed in Section 6.6.2, we take normalization factor $\mathcal{C}$ for all the processes with kaons from (6.47), while for the processes with η we take the value (6.48).

The amplitude $\tilde{A}^L_{00}$ can be obtained from $\tilde{A}^L_{+-}$ using (7.2)

$$\tilde{A}^L_{00} = -3\mathcal{C}A_x \tag{7.10}$$

and the relation (7.1) constrains the parameters in the following way

$$A_c^+ + 2A_x^+ + \left(B_c^+ - B_x^+ - 3B_x^S\right)\frac{s-\tilde{s}_0}{F_\pi^2} = 0. \tag{7.11}$$

Since this relation should hold for any value of s, it leads to

$$A_c^+ = -2A_x^+, \tag{7.12}$$

$$3B_x^S = B_c^+ - B_x^+. \tag{7.13}$$

Since we take the polynomial parameters in such form that these relations remain valid, we can use them for expressing A_c^+ and B_x^S in the results.

7.3 Next-to-leading order result

First iteration of our reconstruction procedure supplemented with the symmetries of the particular amplitudes leads to the following form of the NLO expressions for the amplitudes

$$\tilde{A}^c_{ab}(s,t,u) = \mathcal{C}^c\left(\tilde{R}^c_{ab}(s,t,u) + 16\pi\tilde{U}^c_{ab}(s,t,u)\right) + O(p^6) \tag{7.14}$$

with

$$\tilde{U}^+_{++}(s,t,u) = \tilde{W}^+_{++}(s) + \tilde{W}^{+;0}_{+-}(t) + (u-s)\tilde{W}^{+;1}_{+-}(t) + \tilde{W}^{+;0}_{+-}(u) + (t-s)\tilde{W}^{+;1}_{+-}(u), \quad (7.15)$$

$$\tilde{U}^+_{00}(s,t,u) = \tilde{W}^+_{00}(s) - \tilde{W}^{+;0}_{+0}(t) - (s-u)\tilde{W}^{+;1}_{+0}(t) - \tilde{W}^{+;0}_{+0}(u) - (s-t)\tilde{W}^{+;1}_{+0}(u), \quad (7.16)$$

$$\tilde{U}^L_{+-}(s,t,u) = \tilde{W}^L_{+-}(s) - \tilde{W}^{L;0}_{0+}(t) - (s-u)\tilde{W}^{L;1}_{0+}(t) - \tilde{W}^{L;0}_{0+}(u) - (s-t)\tilde{W}^{L;1}_{0+}(u), \quad (7.17)$$

$$\tilde{U}^S_{+-}(s,t,u) = (t-u)\tilde{W}^S_{+-}(s) + \tilde{W}^{S;0}_{0+}(t) + (s-u)\tilde{W}^{S;1}_{0+}(t) - \tilde{W}^{S;0}_{0+}(u) - (s-t)\tilde{W}^{S;1}_{0+}(u). \quad (7.18)$$

According to (3.10) and (3.11), the dispersion integrals $\tilde{W}^{c;\ell}_{ab}$ are given by

$$\tilde{W}^+_{++}(s) = \left(2A_x - \frac{B_c}{F_\pi^2}(s-\tilde{s}_0)\right)\left(a - \frac{b}{2F_\pi^2}(s+4m_\pi^2)\right)\bar{J}_\pi(s), \quad (7.19)$$

$$\tilde{W}^{+;0}_{+-}(s) = \frac{1}{2}\Bigg(A_x\Big(9a + \frac{b}{F_\pi^2}(3s-28m_\pi^2)\Big) + \frac{B_x}{F_\pi^2}(s-\tilde{s}_0)\Big(a + \frac{b}{F_\pi^2}(s-4m_\pi^2)\Big) + \frac{B_c}{F_\pi^2}(s-\tilde{s}_0)\Big(2a + \frac{b}{2F_\pi^2}(s-12m_\pi^2)\Big)\Bigg)\bar{J}_\pi(s), \quad (7.20)$$

$$\tilde{W}^{+;1}_{+-}(s) = \frac{B_c}{F_\pi^2}\frac{b}{12F_\pi^2}(s-4m_\pi^2)\bar{J}_\pi(s), \quad (7.21)$$

$$\tilde{W}^+_{00}(s) = -\frac{1}{2}\Bigg(A_x\Big(7a + 4\frac{b}{F_\pi^2}(s-6m_\pi^2)\Big) + \frac{B_x}{F_\pi^2}(s-\tilde{s}_0)\Big(3a - 8\frac{b}{F_\pi^2}m_\pi^2\Big) + \frac{B_c}{F_\pi^2}(s-\tilde{s}_0)\Big(a + \frac{b}{F_\pi^2}(s-4m_\pi^2)\Big)\Bigg)\bar{J}_\pi(s), \quad (7.22)$$

$$\tilde{W}^{+;0}_{+0}(s) = \left(A_x - \frac{B_x}{2F_\pi^2}(s-\tilde{s}_0)\right)\left(a - \frac{b}{2F_\pi^2}(s+4m_\pi^2)\right)\bar{J}_\pi(s), \quad (7.23)$$

$$\tilde{W}^{+;1}_{+0}(s) = \frac{B_x}{F_\pi^2}\frac{b}{12F_\pi^2}(s-4m_\pi^2)\bar{J}_\pi(s), \quad (7.24)$$

$$\tilde{W}^L_{+-}(s) = -\frac{1}{2}\left(A_x\left(7a + 4\frac{b}{F_\pi^2}(s-6m_\pi^2)\right) + \frac{B_x}{F_\pi^2}(s-\tilde{s}_0)\left(4a + \frac{b}{F_\pi^2}(s-12m_\pi^2)\right)\right)\bar{J}_\pi(s), \quad (7.25)$$

$$\tilde{W}^{L;0}_{0+}(s) = \left(A_x - \frac{B_c}{2F_\pi^2}(s-\tilde{s}_0)\right)\left(a - \frac{b}{2F_\pi^2}(s+4m_\pi^2)\right)\bar{J}_\pi(s), \quad (7.26)$$

$$\tilde{W}^{L;1}_{0+}(s) = \frac{B_x}{F_\pi^2}\frac{b}{12F_\pi^2}(s-4m_\pi^2)\bar{J}_\pi(s), \quad (7.27)$$

$$\tilde{W}^S_{+-}(s) = -\frac{B_x}{F_\pi^2}\frac{b}{6F_\pi^2}(s-4m_\pi^2)\bar{J}_\pi(s), \quad (7.28)$$

$$\tilde{W}^{S;0}_{0+}(s) = -\frac{3B_x}{2F_\pi^2}(s-\tilde{s}_0)\left(a - \frac{b}{2F_\pi^2}(s+4m_\pi^2)\right)\bar{J}_\pi(s), \quad (7.29)$$

$$\tilde{W}^{S;1}_{0+}(s) = -\frac{B_x}{F_\pi^2}\frac{b}{12F_\pi^2}(s-4m_\pi^2)\bar{J}_\pi(s). \quad (7.30)$$

and the polynomials

$$\tilde{R}^{+}_{++}(s,t,u) = A_c + \frac{B_c}{F_\pi^2}(s-\tilde{s}_0) + \frac{C_c}{F_\pi^4}(s-\tilde{s}_0)^2 + \frac{D_c}{F_\pi^4}\left((t-\tilde{s}_0)^2 + (u-\tilde{s}_0)^2\right), \tag{7.31}$$

$$\tilde{R}^{+}_{00}(s,t,u) = A_x + \frac{B_x}{F_\pi^2}(s-\tilde{s}_0) + \frac{C_x}{F_\pi^4}(s-\tilde{s}_0)^2 + \frac{D_x}{F_\pi^4}\left((t-\tilde{s}_0)^2 + (u-\tilde{s}_0)^2\right), \tag{7.32}$$

$$\tilde{R}^{L}_{+-}(s,t,u) = A_x + \frac{B_x}{F_\pi^2}(s-\tilde{s}_0) + \frac{C_x}{F_\pi^4}(s-\tilde{s}_0)^2 + \frac{D_x}{F_\pi^4}\left((t-\tilde{s}_0)^2 + (u-\tilde{s}_0)^2\right), \tag{7.33}$$

$$\tilde{R}^{S}_{+-}(s,t,u) = \frac{B_x}{F_\pi^2}(t-u) + \frac{C_x}{F_\pi^4}(s-\tilde{s}_0)(t-u). \tag{7.34}$$

In the unitarity parts of the results, we have already expressed A_c^+ using (7.12).

From the validity of the isospin relation (7.1) for any value of s and t in addition to the relations (7.12) and (7.13) we obtain the following relations between the parameters

$$A_c^+ = -2A_x^+, \tag{7.35}$$

$$3B_x^S = B_c^+ - B_x^+, \tag{7.36}$$

$$2D_c^+ = -C_c^+ - 2C_x^+ - 4D_x^+, \tag{7.37}$$

$$2C_x^S = -C_c^+ - 2D_x^+. \tag{7.38}$$

Note that provided the lower order isospin relations (7.12) and (7.13) are fulfilled, the unitarity parts satisfy the isospin relation (7.1) automatically.

7.4 Results for partial waves of NLO $P\pi \to \pi\pi$ amplitudes

Before we can proceed to the second iteration of our construction of the $P\pi \to \pi\pi$ amplitudes leading to the full NNLO results, we need to compute the S- and the P- partial waves of the NLO amplitudes of these processes.

In Section 6.6 we have discussed the fact that since P is an unstable particle, the situation in the case of these processes is more complicated than it was in the case of $\pi\pi \to \pi\pi$ scattering. Nevertheless, we have also discussed there the way, how one can avoid these problems by employing an analytic continuation in m_P. Using such procedure for $m_{\pi^\pm} = m_{\pi^0}$ in Appendix K.4, we have computed integrals $I_n(s)$ from (3.32)–(3.33) appearing in the relations for the S- and the P-waves of the amplitudes from Section 3.4. Employing them, we obtain all the S-partial waves in the form[1]

$$\tilde{\varphi}_{a;0}(s) = \frac{\mathcal{C}}{16\pi}\left(\tilde{p}^{a;0}_{\lambda}(s) + \frac{1}{\pi}\sum_{j=0,1,1\mathrm{P},2\mathrm{P},3}\tilde{p}^{a;0}_{j}(s)\mathcal{M}_j(s)\right) \tag{7.39}$$

with the dimensionless kinematic functions $\mathcal{M}_j(s)$ from Appendix F.1.3. We list the Laurent polynomials $\tilde{p}^{a;0}_j(s)$ for individual processes in Appendix L. Note that because of the CP symmetry, the S-wave of the process $K^S\pi^0 \to \pi^+\pi^-$ is identically equal to zero.

[1]Note that $\tilde{\varphi}_{a,\ell}$ denotes just the NLO part of the partial wave.

The P-waves $\tilde{\varphi}_{a;1}(s)$ of the $P\pi \to \pi\pi$ processes are non-zero only for processes $K^\pm\pi^\mp \to \pi^\pm\pi^\mp$, $K^\pm\pi^0 \to \pi^\pm\pi^0$, $K^L\pi^\pm \to \pi^0\pi^\pm$, $K^S\pi^0 \to \pi^+\pi^-$, and $K^S\pi^+ \to \pi^0\pi^+$. We can write them in the form

$$\tilde{\varphi}_{a;1}(s) = \frac{\mathcal{C}}{16\pi}\left(\sigma_\pi \tilde{\lambda}_\pi^{1/2}\left(\tilde{p}_\lambda^{a;1} + \frac{1}{\pi}\tilde{p}_3^{a;1}(s)\mathcal{M}_3(s)\right) + \frac{m_\pi^2}{\pi\sigma_\pi\tilde{\lambda}_\pi^{1/2}}\sum_{j=0,1,1\mathrm{P},2\mathrm{P}}\tilde{p}_j^{a;1}(s)\mathcal{M}_j(s)\right) \tag{7.40}$$

with the same kinematic functions $\mathcal{M}_j(s)$ as appear in the expression for S-waves. The polynomials $\tilde{p}_j^{a;1}(s)$ for these processes are listed again in Appendix L.

7.5 Second iteration for $P\pi \to \pi\pi$ amplitudes

Having all the ingredients prepared it is a straightforward task to obtain the NNLO amplitudes of the $P\pi \to \pi\pi$ processes. From the reconstruction theorem it is obvious that also the NNLO amplitudes are obtained in the form similar to (7.14),

$$\tilde{A}_{ab}^c(s,t,u) = \mathcal{C}^c\left(\tilde{R}_{ab}^c(s,t,u) + 16\pi\tilde{U}_{ab}^c(s,t,u)\right) + O(p^8), \tag{7.41}$$

where the unitarity parts $\tilde{U}_{ab}^c(s,t,u)$ are expressed in terms of single variable dispersion integrals $\tilde{W}_{ab}^c(s)$ according to the relations (7.15)–(7.18). For the determination of these integrals $\tilde{W}_{ab}^c(s)$ we just need to follow the lines of Section 3.5.

7.5.1 Construction of the NNLO amplitude of the process $K^\pm\pi^\pm \to \pi^\pm\pi^\pm$

The second iteration proceeds similarly for all the $P\pi \to \pi\pi$ processes. In order not to lose ourselves in the ample amount of general indices, we deal here specifically with the process $K^+\pi^+ \to \pi^+\pi^+$. The transcription of the formulas of this section into expressions for the other processes should be then obvious.

We begin with the simpler task — the determination of the polynomial part. The polynomial $\tilde{R}_{++}^+(s,t,u)$ has to be now the third order polynomial compatible with the symmetries of the amplitude $\tilde{A}_{++}^+(s,t,u)$. We can take it in the form where we simply add some particular third order terms to the second order polynomial of (7.31), namely

$$\begin{aligned}\tilde{R}_{++}^+(s,t,u) = A_c + \frac{B_c}{F_\pi^2}(s-\tilde{s}_0) + \frac{C_c}{F_\pi^4}(s-\tilde{s}_0)^2 + \frac{D_c}{F_\pi^4}\left((t-\tilde{s}_0)^2 + (u-\tilde{s}_0)^2\right)\\ + \frac{E_c}{F_\pi^6}(s-\tilde{s}_0)^3 + \frac{F_c}{F_\pi^6}\left((t-\tilde{s}_0)^3 + (u-\tilde{s}_0)^3\right).\end{aligned} \tag{7.42}$$

Naturally, the $O(p^6)$ corrections with respect to the polynomial (7.31) are included not only in the new terms with the parameters E_c and F_c, but also in the $O(p^6)$ corrections to the constants $A_c, \ldots, D_c$. We explicate this aspect in Section 9.4, where we discuss the relation of our parametrization of the $\eta \to 3\pi$ amplitude to the χPT results for it.

Now let us proceed to the unitarity part. Since the only intermediate states we take into account in the unitarity relations are those containing two pions and in this chapter we work in the limit $m_{\pi^\pm} = m_{\pi^0}$, these relations imply for the imaginary part of the $O(p^6)$ partial waves

$$\mathrm{Im}\,\psi_\ell^{i\to f}(s) = \sum_k \frac{1}{S_k}\,\sigma_\pi(s)\left[\tilde\phi_\ell^{i\to k}(s)\left(\varphi_\ell^{f\to k}(s)\right)^\star + \tilde\varphi_\ell^{i\to k}(s)\left(\phi_\ell^{f\to k}(s)\right)^\star\right]\theta(s-4m_\pi^2), \quad (7.43)$$

where the sum goes over all the possible two-pion intermediate states with the symmetry factor S_k ($S_k = 2$ for two identical pions in k, otherwise $S_k = 1$).

Note that the unitarity relation holds in this form only in the stable mass $m_P < 3m_\pi$ case — then all the functions $\mathcal{M}_j(s)$ with the exception of $\mathcal{M}_3(s)$ are real and therefore also the right-hand side of this relation is real. This remains true also after inclusion of functions $\mathcal{M}_3(s)$ thanks to the mechanism discussed below near relation (7.57) and Figure 12. However, after analytic continuation of the relations to physical mass m_P, the functions $\mathcal{M}_{1P}(s)$ and $\mathcal{M}_{2P}(s)$ start to be imaginary in the interval $\big(4m_\pi^2, (m_P-m_\pi)^2\big)$ and such continuation means allowing the discontinuity to be complex — we should thus write in all the relations $\frac{1}{2}\,\mathrm{Disc}$ instead of Im. Nevertheless, keeping this fact and the analytic continuation in mind, we will not complicate the notation and denote all the quantities as they appear in the stable mass m_P scenario. Note also that since the complex conjugation in (7.43) is connected with the partial waves of $\pi\pi$ scattering, in the unitarity relations there also appear these complicated functions but never their complex conjugations and the only case, where we take care with the conjugation is just the function $\mathcal{M}_3(s)$.

In correspondence with Section 3.1, we denote with $\alpha_a(s)$ and β_a the following parts of the leading order amplitudes

$$A_{\pi\pi\to\pi\pi}(s,t,u) = 16\pi\big(\alpha_a(s) + \beta_a\,(t-u)\big), \quad (7.44)$$

$$\tilde A_{P\pi\to\pi\pi}(s,t,u) = 16\pi\big(\tilde\alpha_a(s) + \tilde\beta_a\,(t-u)\big), \quad (7.45)$$

where the formal index a corresponds to our usual indices denoting charge states of the particles. In this notation the leading order partial waves of the corresponding processes (in the limit $m_{\pi^\pm} = m_{\pi^0}$) read simply

$$\phi_{a;0}(s) = \alpha_a(s), \qquad \phi_{a;1}(s) = \frac{1}{3}\beta_a\, s\sigma_\pi^2(s), \quad (7.46)$$

$$\tilde\phi_{a;0}(s) = \frac{C}{16\pi}\,\tilde\alpha_a(s), \qquad \tilde\phi_{a;1}(s) = \frac{C}{48\pi}\,\tilde\beta_a\sigma_\pi(s)\tilde\lambda_\pi^{1/2}(s). \quad (7.47)$$

Note that the leading order parameters of our amplitudes are real (e.g. $\alpha_a^\star = \alpha_a$).

Dispersive integrals of the direct process $K^\pm\pi^\pm \to \pi^\pm\pi^\pm$ (S-wave integration)

For the imaginary part of the S-wave of the process $K^\pm\pi^\pm \to \pi^\pm\pi^\pm$ we obtain (the only possible intermediate state here is $\pi^\pm\pi^\pm$)

$$\mathrm{Im}\,\tilde{\psi}_{Cd;0}(s) = \frac{1}{2}\,\frac{C}{16\pi}\,\sigma_\pi(s)\left[\tilde{\alpha}_{Cd}(s)\left(p_\lambda^{d;0}(s)+\frac{1}{\pi}p_w^{d;0}(s)+\frac{1}{\pi}\sum_{j=0}^{3}p_j^{d;0}(s)\mathcal{M}_j(s)\right)^\star + \alpha_d^\star(s)\left(\tilde{p}_\lambda^{Cd;0}(s)+\frac{1}{\pi}\sum_{j=0,1,1\mathrm{P},2\mathrm{P},3}\tilde{p}_j^{Cd;0}(s)\mathcal{M}_j(s)\right)\right]\theta(s-4m_\pi^2) \quad (7.48)$$

and the P-wave is identically zero.

Introducing this expression into (2.23), for the integral $\tilde{W}_{++}^+(s)$ we obtain schematically

$$\tilde{W}_{++}^+(s) = \frac{C}{\pi}\int_{4m_\pi^2}^{\Lambda^2}\frac{s^3}{x^3}\frac{dx}{x-s}\sigma_\pi(x)\,\frac{1}{2}\left(\alpha\Big(p+\frac{1}{\pi}p_j\mathcal{M}_j\Big)\right). \quad (7.49)$$

It is therefore of the form (2.73)

$$\tilde{W}_{++}^+(s) = \frac{C}{\pi}\int_{4m_\pi^2}^{\Lambda^2}\frac{s^3}{x^3}\frac{dx}{x-s}\,\mathcal{P}_j(x)\mathcal{F}_j(x) \quad (7.50)$$

with $\mathcal{F}_j(x)$ being dimensionless functions originating from products of $\sigma_\pi(x)$ with various $\mathcal{M}_j(x)$; and $\mathcal{P}_j(x)$ are some Laurent polynomials. Thus, we can employ the simplifications collected in Section 2.5 and obtain these integrals as

$$\tilde{W}_{++}^+(s) = \frac{C}{\pi}\mathcal{P}_j(s)\mathcal{G}_j(s), \quad (7.51)$$

where the functions $\mathcal{G}_j(s)$ are Hilbert transforms of $\mathcal{F}_j(s)$. We list here the functions appearing in the results together with the corresponding polynomials (the functions and some additional information on their properties are discussed in Appendix F.2).

Function $\mathcal{G}_1(s)$

This function is Hilbert transform of function

$$\mathcal{F}_1(s) = \sigma_\pi(s). \quad (7.52)$$

The high-energy asymptotics of this function is $F_1(s) \sim s^0$ for $s \to \infty$. Condition (2.71) thus implies that the corresponding Hilbert transform exists for the number of subtractions $n \geq 1$.

This function arises in the integrand from the product of $\sigma_\pi(s)$ and $\mathcal{M}_0(s) = 1$. The polynomial that multiplies it is therefore equal to

$$\mathcal{P}_1(s) = \frac{1}{2}\left(\tilde{\alpha}_{Cd}(s)\alpha_d(s)+\tilde{\alpha}_{Cd}(s)\Big(p_\lambda^{d;0}(s)+\frac{1}{\pi}p_w^{d;0}(s)+\frac{1}{\pi}p_0^{d;0}(s)\Big)+\alpha_d(s)\Big(\tilde{p}_\lambda^{Cd;0}(s)+\frac{1}{\pi}\tilde{p}_0^{Cd;0}(s)\Big)\right). \quad (7.53)$$

We have included here also the $O(p^4)$ part $\frac{1}{2}\tilde{\alpha}\alpha$, which is also of this type and was discussed in Section 3.1 [cf. the NLO result (7.19)]. It remains to determine the number of

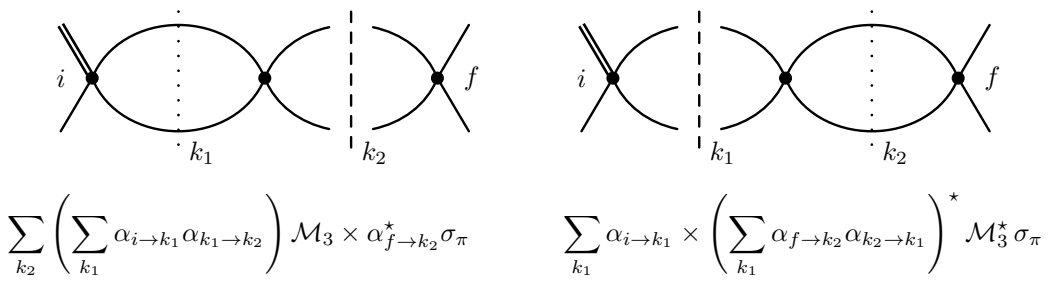

Figure 12: Illustration of the symmetry between the contributions with $\mathcal{M}_3(s)$ coming from the NLO $P\pi \to \pi\pi$ processes with those from the NLO $\pi\pi$ scattering processes. The real tree-order parameters α are defined in (7.44)–(7.45).

subtractions n of $\mathcal{G}_1(s)$ needed for the $O(p^6)$ part. Any term of m-th polynomial order has to be multiplied by $\mathcal{G}_1^{(n)}(s)$ with n from the interval (2.76)

$$\max(1, -m) \le n \le 4 - m. \tag{7.54}$$

Since the polynomial $\mathcal{P}_1(s)$ contains only terms with $m \in \langle -1, 3\rangle$, we can take for each of them $n = 1$ and we need just the function

$$\mathcal{G}_1^{(1)}(s) = 16\pi^2 \bar{J}_\pi(s) = 2 + \sigma_\pi \mathcal{L}_\pi(s). \tag{7.55}$$

Function $\mathcal{G}_2(s)$

The asymptotics of the function

$$\mathcal{F}_2(s) = L_\pi(s) \tag{7.56}$$

is $F_2(s) \sim s^0 \log s$ for $s \to \infty$, and so the Hilbert transform of this function exists for all $n \ge 1$. The interval for the possible number of subtractions of functions multiplying an $O(p^6)$ term with the polynomial order m is therefore again (7.54).

This function appears in the integrand as the result of multiplication of $\sigma_\pi(s)$ with $\mathcal{M}_1(s)$. In addition, there occurs also a contribution from the multiplication with $\mathcal{M}_3(s)$. One should remind that the appearance of $\mathcal{M}_3(s)$ in the partial waves stems from the integration of the s-dependent part — it comes from the one-loop contribution to the direct process. We can thus compare the contributions coming from the intermediate process of NLO $P\pi \to \pi\pi$ amplitude and LO $\pi\pi$ scattering amplitude with the one from NLO $\pi\pi$ scattering with LO $P\pi \to \pi\pi$ intermediate amplitudes as is illustrated on Figure 12. Since in our cases α's are real and the considered T-invariance means $\alpha_{i\to f} = \alpha_{f\to i}$, the coefficient standing in front of $\mathcal{M}_3\sigma_\pi$ in the contribution of the first diagram is the same as the coefficient standing in front of $\mathcal{M}_3^\star\sigma_\pi$ in the contribution of the second diagram. In the integration region $s > 4m_\pi^2$

$$\sigma_\pi(s)\mathcal{M}_3(s) = \sigma_\pi^2(s)\mathcal{F}_2(s) \mp i\pi\sigma_\pi^2(s) = \frac{1}{s}(s - 4m_\pi^2)\mathcal{F}_2(s) \mp i\pi\sigma_\pi^2(s). \tag{7.57}$$

The upper sign corresponds to taking the physical value of the function with s from below.

Therefore, the imaginary parts of the two contributions cancel and their real parts contribute equally into $\mathcal{P}_2\mathcal{G}_2$.

In total,

$$\mathcal{P}_2(s) = \frac{1}{2}\frac{1}{\pi}\left(\tilde{\alpha}_{Cd}(s)p_1^{d;0}(s) + \alpha_d(s)\tilde{p}_1^{Cd;0}(s) + 2\,\frac{1}{s}\,(s-4m_\pi^2)\tilde{\alpha}_{Cd}(s)p_3^{d;0}(s)\right). \tag{7.58}$$

This polynomial contains again only the terms with $m \in \langle -1, 3\rangle$, so it is sufficient to use just the once subtracted function

$$\mathcal{G}_2^{(1)}(s) = \frac{1}{2}\mathcal{L}_\pi^2(s). \tag{7.59}$$

Function $\mathcal{G}_3(s)$

By multiplication of $\sigma_\pi(s)$ with $\mathcal{M}_2(s)$ we obtain the function

$$\mathcal{F}_3(s) = -m_\pi^2\frac{L_\pi^2(s)}{s\sigma_\pi(s)}\,. \tag{7.60}$$

Its asymptotics is $F_3(s) \sim \frac{\log^2 s}{s}$ for $s \to \infty$, and so its Hilbert transform exists also without a need for subtractions. This time the number of subtraction of the function $\mathcal{G}_3^{(n)}(s)$ that can multiply a term with the polynomial power m lies in the interval (2.76)

$$\max(0, -m) \le n \le 4 - m. \tag{7.61}$$

The polynomial

$$\mathcal{P}_3(s) = \frac{1}{2}\frac{1}{\pi}\,\tilde{\alpha}_{Cd}(s)p_2^{d;0}(s) \tag{7.62}$$

contains terms with $m \in \langle 0, 2\rangle$, so we manage with

$$\mathcal{G}_3^{(0)}(s) = -\frac{m_\pi^2}{3s\sigma_\pi(s)}\,\mathcal{L}_\pi(s)\Big(\mathcal{L}_\pi^2(s) + \pi^2\Big). \tag{7.63}$$

Function $\mathcal{G}_4(s)$

A little bit more complicated situation occurs for

$$\mathcal{F}_4(s) = s\sigma_\pi(s)\frac{M_0(s)}{\tilde{\lambda}_\pi^{1/2}(s)}, \tag{7.64}$$

which originates from the product of $\sigma_\pi(s)$ with $\mathcal{M}_{1P}(s)$.

Its asymptotics is $F_4(s) \sim \log s$ for $s \to \infty$ and for the existence of its Hilbert transform we need at least one subtraction. However, the polynomial

$$\mathcal{P}_4(s) = \frac{1}{2}\frac{1}{\pi}\,\alpha_d(s)\tilde{p}_{1P}^{Cd;0}(s) \tag{7.65}$$

contains terms with $m \in \langle -2, 3\rangle$. Thus, the term with $m = -2$ does not satisfy the condition (7.54) with $n = 1$ and we need to take for this term $n = 2$. (Note that with this choice we satisfy our conventional requirement of taking the minimal positive number of subtractions for each term.)

In order to simplify the notation of the results, we introduce the following operator

$$\left\langle \sum_i a_i s^i \right\rangle_m := a_m s^m \tag{7.66}$$

picking up the term with a given polynomial order out of a polynomial and the operator

$$\left\langle \sum_i a_i s^i \right\rangle_{\not m} := \sum_i a_i s^i - \left\langle \sum_i a_i s^i \right\rangle_m = \sum_{i \neq m} a_i s^i \tag{7.67}$$

dropping such polynomial term.

The contribution related to the function $\mathcal{F}_4(s)$ then reads

$$\left\langle \mathcal{P}_4(s) \right\rangle_{\not -2} \mathcal{G}_4^{(1)}(s) + \left\langle \mathcal{P}_4(s) \right\rangle_{-2} \mathcal{G}_4^{(2)}(s). \tag{7.68}$$

Function $\mathcal{G}_5(s)$

Finally, the last function appearing in the integrands of the S-waves is

$$\mathcal{F}_5(s) = -m_\pi^2 L_\pi(s) \frac{M_0(s)}{\tilde{\lambda}_\pi^{1/2}(s)}, \tag{7.69}$$

originating from the product of $\sigma_\pi(s)$ with $\mathcal{M}_{2P}(s)$. Its asymptotics is similar to $F_3(s)$ and so the number of subtractions has to fulfill the condition (7.61). Similarly as for that case, the polynomial

$$\mathcal{P}_5(s) = \frac{1}{2}\frac{1}{\pi}\alpha_d(s)\tilde{p}_{2P}^{Cd;0}(s) \tag{7.70}$$

contains only terms with $m \in \langle 0, 2\rangle$ and so it is sufficient to introduce

$$\mathcal{G}_5^{(0)} = \int_{4m_\pi^2}^\infty \frac{dx}{x - s}\mathcal{F}_5(x). \tag{7.71}$$

Dispersive integrals of the crossed process $K^\pm\pi^\mp \to \pi^\pm\pi^\mp$ (P-wave integration)

For the crossed channel $K^\pm\pi^\mp \to \pi^\pm\pi^\mp$ the S-wave have a similar form, with a small additional complication that the possible intermediate states are both $\pi^+\pi^-$ and $\pi^0\pi^0$. Nevertheless, all the other facts described for the direct process remain valid and so the result for S-wave dispersion integral $\tilde{W}_{+-}^{+;0}(s)$ can be again written using the functions $\mathcal{F}_{1,2,4}^{(1)}(s)$, $\mathcal{F}_{3,5}^{(0)}(s)$, $\mathcal{F}_4^{(2)}(s)$ and the corresponding polynomials.

For this process the P-wave is nonzero and one gets[2]

$$\begin{aligned}&\operatorname{Im}\psi_{Cc;1}(s)\\&= \frac{C}{48\pi}\, s\sigma_\pi^4 \tilde\lambda_\pi^{1/2}\left[\tilde\beta_{Cc}\left(p_\lambda^{c;1}(s)+\frac{1}{\pi}p_w^{c;1}(s)+\frac{1}{\pi}p_3^{c;1}(s)\mathcal{M}_3(s)+\frac{m_\pi^2}{\pi s^2\sigma_\pi^4}\sum_{j=0}^{2}p_j^{c;1}(s)\mathcal{M}_j(s)\right)^\star\right.\\&\left.+\,\beta_c^\star\left(\tilde p_\lambda^{Cc;1}(s)+\frac{1}{\pi}\tilde p_3^{Cc;1}(s)\mathcal{M}_3(s)+\frac{m_\pi^2}{\pi\sigma_\pi^2\tilde\lambda_\pi}\sum_{j=0,1,1\mathrm{P},2\mathrm{P}}\tilde p_j^{Cc;1}(s)\mathcal{M}_j(s)\right)\right]\theta(s-4m_\pi^2).\end{aligned}\tag{7.72}$$

From (2.24) we obtain the dispersion integral $\tilde W_{+-}^{+;1}(s)$ in the (schematic) form

$$\begin{aligned}\tilde W_{+-}^{+;1}(s) = \frac{C}{\pi}\int_{4m_\pi^2}^{\Lambda^2}\frac{s^2}{x^2}\frac{dx}{x-s}\,\sigma_\pi(x)\Bigg(\tilde\beta\Bigg(x\sigma_\pi^2(x)p(x)\mathcal{M}(x)+\frac{1}{\pi}p_j(x)\frac{m_\pi^2\mathcal{M}_j(x)}{x\sigma_\pi^2(x)}\Bigg)\\+\,\beta\Bigg(x\sigma_\pi^2(x)\tilde p(x)\mathcal{M}(x)+\frac{1}{\pi}\tilde p_j\frac{m_\pi^2 x\mathcal{M}_j(x)}{\tilde\lambda_\pi(x)}\Bigg)\Bigg).\end{aligned}\tag{7.73}$$

It means, it is in the form (2.77)

$$\tilde W_{+-}^{+;1}(s) = \frac{C}{\pi}\int_{4m_\pi^2}^{\Lambda^2}\frac{s^2}{x^2}\frac{dx}{x-s}\,\mathcal{P}_j^{1;\kappa}(x)\mathcal{F}_j^\kappa(x),\tag{7.74}$$

which again allows for employing the simplifications of Section 2.5 and we obtain these integrals as

$$\tilde W_{+-}^{+;1}(s) = \frac{C}{\pi}\mathcal{P}_j^{1;\kappa}(s)\mathcal{G}_j^\kappa(s),\tag{7.75}$$

where the functions $\mathcal{G}_j^\kappa(s)$ are Hilbert transforms of $\mathcal{F}_j^\kappa(s)$. As is obvious from the introduction of the further index κ, the set of functions appearing in P waves is more complex than it was in the case of S waves. Nevertheless, by comparing (7.73) with (7.50) one discovers that the additional functions appearing here are related to the original ones,

$$\mathcal{F}_j^\sigma(s) = m_\pi^2\frac{\mathcal{F}_j(s)}{s\sigma_\pi^2(s)} \qquad \text{or} \qquad \mathcal{F}_j^{\tilde\lambda}(s) = m_\pi^2 s\,\frac{\mathcal{F}_j(s)}{\tilde\lambda_\pi(s)}\,,\tag{7.76}$$

and their Hilbert transforms can be derived from the knowledge of the Hilbert transform of the original function $\mathcal{F}_j(s)$ using relations from Appendix B. These derived functions are discussed in Appendix F.2.3. In the following, we discuss the polynomials multiplying these functions in the result of $\tilde W_{+-}^{+;1}(s)$.

Function $\mathcal{G}_1(s)$

From (7.73) we see that the contributions to $\tilde W_{+-}^{+;1}(s)$ of the parts appearing in the P-wave with $\mathcal{M}_0(s) = 1$ separate into three parts.

[2]Note that the part with the intermediate state $\pi^0\pi^0$ has again a vanishing P-wave.

First of them is the part corresponding to the original $\mathcal{F}_1(s)$ function with the polynomial

$$\mathcal{P}_1(s) = s\sigma_\pi^2(s)\left(\frac{1}{3}\tilde{\beta}_{Cc}\beta_c + \tilde{\beta}_{Cc}\Big(p_\lambda^{c;1}(s) + \frac{1}{\pi}p_w^{c;1}(s)\Big) + \beta_c\tilde{p}_\lambda^{Cc;1}(s)\right), \tag{7.77}$$

in which we can include also the NLO part $\frac{1}{3}\tilde{\beta}\beta\, s\sigma_\pi^2$ that was discussed in Section 3.1. The part of the polynomial contributing to the NNLO ($O(p^6)$) amplitude is of the chiral order[3] $O(p^4)$. The interval for the number of subtraction of the Hilbert transforms multiplying polynomial term of m-th order is therefore shifted with respect to (7.54). Here,

$$\max(1, -m) \le n \le 3 - m. \tag{7.78}$$

Nevertheless, polynomial (7.77) contains only terms with $m \in \langle 0, 2\rangle$ and we manage with the once subtracted $\mathcal{G}_1^{(1)}(s)$.

The second part contains the function $\mathcal{F}_1^\sigma(s)$ multiplied by

$$\mathcal{P}_{1\sigma}(s) = \frac{1}{\pi}\tilde{\beta}_{Cc}p_0^{c;1}(s). \tag{7.79}$$

Hilbert transform of function $\mathcal{F}_1^\sigma(s)$ exists with the number of subtraction $n \ge 0$ (by dividing the original function with $s - 4m_\pi^2$ we have added a subtraction with respect to it). The polynomial $\mathcal{P}_{1\sigma}(s)$ is again of order $O(p^4)$ and contains terms with $m \in \langle 0, 3\rangle$, we thus need to introduce just $\mathcal{G}_1^{\sigma;(0)}(s)$ from (F.61).

Finally, from the NLO $P\pi \to \pi\pi$ contribution with $\mathcal{M}_0(s)$ we obtain the third type of contributions,

$$\mathcal{P}_{1\tilde{\lambda}}(s) = \frac{1}{\pi}\beta_c\tilde{p}_0^{Cc;1}(s). \tag{7.80}$$

multiplied by $\mathcal{F}_1^{\tilde{\lambda}}(s)$. From the same reasons as there occurred for $\mathcal{F}_1^\sigma(s)$, Hilbert transform of this function also needs n subtractions with

$$\max(0, -m) \le n \le 3 - m. \tag{7.81}$$

However, in the opposite to the situation of $\mathcal{F}_1^\sigma(s)$ the polynomial $\mathcal{P}_{1\tilde{\lambda}}(s)$ contains terms with $m \in \langle -1, 3\rangle$, we therefore need to introduce not only $\mathcal{G}_1^{\tilde{\lambda};(0)}(s)$ but also $\mathcal{G}_1^{\tilde{\lambda};(1)}(s)$ and the correspondent contribution reads

$$\Big\langle \mathcal{P}_{1\tilde{\lambda}}(s)\Big\rangle_{\not{-1}}\mathcal{G}_1^{\tilde{\lambda};(0)}(s) + \Big\langle \mathcal{P}_{1\tilde{\lambda}}(s)\Big\rangle_{-1}\mathcal{G}_1^{\tilde{\lambda};(1)}(s). \tag{7.82}$$

Function $\mathcal{G}_2(s)$

In the result of multiplication of $\sigma_\pi(s)$ with $\mathcal{M}_3(s)$ there appears another function from the original set, $\mathcal{F}_2(s)$. Its appearance in the P partial waves is connected with the integration

[3] As was reminded also in Section 2.5, it is connected with the fact that this polynomial appears in the amplitude multiplied by $(t - u)$.

of the P-wave of the original direct process. Thus, repeating the discussion of the text above relation (7.57), which was illustrated also on Figure 12, we verify that the contribution to $\mathcal{P}_2(s)$ from both the NLO $P\pi \to \pi\pi$ and the NLO $\pi\pi$ scattering amplitudes are the same $\frac{1}{9\pi}\tilde{\beta}_{Cc}\beta_c^2 s^2 \sigma_\pi^6(s)$. It means

$$\mathcal{P}_2(s) = \frac{2}{\pi}\tilde{\beta}_{Cc} p_3^{c;1}(s)\, s\, \sigma_\pi^4(s). \tag{7.83}$$

This polynomial contains terms with $m \in \langle -1, 2\rangle$, which fulfill the inequality (7.78) with $n = 1$ and we need no other function than $\mathcal{G}_2^{(1)}(s)$.

All the other contributions contain either $\mathcal{F}_j^\sigma(s)$ in the case of taking the NLO part from $\pi\pi$ scattering or $\mathcal{F}_j^{\tilde{\lambda}}(s)$ when we take NLO $P\pi \to \pi\pi$ with the LO part of $\pi\pi \to \pi\pi$. Both of the Hilbert transforms are convergent already with one less subtractions than the corresponding original function. In the case of $\mathcal{F}_2^\kappa(s)$, the range of possible number of subtractions is thus again (7.81).

Since

$$\mathcal{P}_{2\sigma}(s) = \frac{1}{\pi}\tilde{\beta}_{Cc} p_1^{c;1}(s) \tag{7.84}$$

contains terms with $m \in \langle 0, 3\rangle$, we need only $\mathcal{G}_2^{\sigma;(0)}(s)$, while for

$$\mathcal{P}_{2\tilde{\lambda}}(s) = \frac{1}{\pi}\beta_c \tilde{p}_1^{Cc;1}(s) \tag{7.85}$$

the situation is more complicated as it possesses all terms with $m \in \langle -2, 3\rangle$, therefore we have to use the set of functions $\mathcal{G}_2^{\tilde{\lambda};(0)}(s)$, $\mathcal{G}_2^{\tilde{\lambda};(1)}(s)$, $\mathcal{G}_2^{\tilde{\lambda};(2)}(s)$. The total contribution of $\mathcal{F}_2^{\tilde{\lambda}}(s)$ then has the form

$$\left\langle \mathcal{P}_{2\tilde{\lambda}}(s)\right\rangle_{\not{-1}\not{-2}} \mathcal{G}_2^{\tilde{\lambda};(0)}(s) + \left\langle \mathcal{P}_{2\tilde{\lambda}}(s)\right\rangle_{-1} \mathcal{G}_2^{\tilde{\lambda};(1)}(s) + \left\langle \mathcal{P}_{2\tilde{\lambda}}(s)\right\rangle_{-2} \mathcal{G}_2^{\tilde{\lambda};(2)}(s). \tag{7.86}$$

Function $\mathcal{G}_3(s)$

The contribution coming from $\mathcal{F}_3^\sigma(s)$ is again simple since

$$\mathcal{P}_{3\sigma}(s) = \frac{1}{\pi}\tilde{\beta}_{Cc} p_2^{c;1}(s) \tag{7.87}$$

contains only $m \in \langle 0, 2\rangle$ and the condition

$$\max(-1, -m) \le n \le 3 - m \tag{7.88}$$

is fulfilled with $\mathcal{G}_3^{\sigma;(0)}(s)$.

Function $\mathcal{G}_4(s)$

More complications occur again for $\mathcal{F}_4^{\tilde{\lambda}}(s)$. Polynomial

$$\mathcal{P}_{4\tilde{\lambda}}(s) = \frac{1}{\pi}\beta_c \tilde{p}_{1P}^{Cc;1}(s) \tag{7.89}$$

possesses terms with $m \in \langle -2, 3\rangle$, which together with (7.81) imply the following form of its total contribution to the integral $\tilde{W}_{+-}^{+;1}(s)$,

$$\left\langle \mathcal{P}_{4\tilde{\lambda}}(s)\right\rangle_{\not{-1}\not{-2}} \mathcal{G}_4^{\tilde{\lambda};(0)}(s) + \left\langle \mathcal{P}_{4\tilde{\lambda}}(s)\right\rangle_{-1} \mathcal{G}_4^{\tilde{\lambda};(1)}(s) + \left\langle \mathcal{P}_{4\tilde{\lambda}}(s)\right\rangle_{-2} \mathcal{G}_4^{\tilde{\lambda};(2)}(s). \tag{7.90}$$

Function $\mathcal{G}_5(s)$

Finally, with the last function $\mathcal{F}_5^{\tilde{\lambda}}(s)$, we are back at (7.88) and $m \in \langle 0, 2\rangle$. Polynomial

$$\mathcal{P}_{5\tilde{\lambda}}(s) = \frac{1}{\pi}\beta_c \tilde{p}_{2P}^{Cc;1}(s) \tag{7.91}$$

is thus multiplied by $\mathcal{G}_5^{\tilde{\lambda};(0)}(s)$.

7.5.2 Results of the second iteration

One can show that the situation for all the considered processes $P\pi \to \pi\pi$ in the limit $m_{\pi^\pm} = m_{\pi^0}$ is the same and their dispersively constructed $O(p^6)$ amplitudes read

$$\tilde{A}_{ab}^c(s,t,u) = \mathcal{C}^c\left(\tilde{R}_{ab}^c(s,t,u) + 16\pi \tilde{U}_{ab}^c(s,t,u)\right) + O(p^8), \tag{7.92}$$

with the polynomials

$$\begin{aligned}\tilde{R}_{ab}^c(s,t,u) = A_z + \frac{B_z}{F_\pi^2}(s-\tilde{s}_0) + \frac{C_z}{F_\pi^4}(s-\tilde{s}_0)^2 + \frac{D_z}{F_\pi^4}\left((t-\tilde{s}_0)^2 + (u-\tilde{s}_0)^2\right) \\ + \frac{E_z}{F_\pi^4}(s-\tilde{s}_0)^3 + \frac{F_z}{F_\pi^4}\left((t-\tilde{s}_0)^3 + (u-\tilde{s}_0)^3\right)\end{aligned} \tag{7.93}$$

for $\tilde{R}_{++}^+(s,t,u)$, $\tilde{R}_{00}^+(s,t,u)$ and $\tilde{R}_{+-}^L(s,t,u)$ with the corresponding index of the coefficient z being c, x and x respectively; for the process $K_S\pi^0 \to \pi^+\pi^-$ the polynomial is of the form

$$\tilde{R}_{+-}^S(s,t,u) = (t-u)\left(\frac{B_x}{F_\pi^2} + \frac{C_x}{F_\pi^4}(s-\tilde{s}_0) + \frac{E_x}{F_\pi^6}(s-\tilde{s}_0)^2 + \frac{F_x}{F_\pi^6}\left((t-\tilde{s}_0)^2 + (u-\tilde{s}_0)^2\right)\right). \tag{7.94}$$

The isospin relation (7.1) relates again together the following parameters[4]

$$A_c^+ = -2A_x^+, \tag{7.95}$$

$$3B_x^S = B_c^+ - B_x^+, \tag{7.96}$$

$$2D_c^+ = -C_c^+ - 2C_x^+ - 4D_x^+, \tag{7.97}$$

[4]Note that thanks to exact choice of the polynomials the NLO relations (7.35)–(7.38) obtains no higher order corrections.

$$2C_x^S = -C_c^+ - 2D_x^+, \tag{7.98}$$
$$2F_c^+ = -E_c^+ - 2E_x^+ - 4F_x^+, \tag{7.99}$$
$$10F_x^S = 3E_c^+ + 6F_x^+ - 2E_x^S. \tag{7.100}$$

The unitarity parts $\tilde{U}_{ab}^c(s,t,u)$ are expressed in terms of single variable dispersion integrals $\tilde{W}_{ab}^c(s)$ according to the relations (7.15)–(7.18) and these integrals are

$$\begin{aligned}
\tilde{W}_{ab}^{c;0}(s) &= \mathcal{P}_1^{z;0}(s)\mathcal{G}_1^{(1)}(s) + \mathcal{P}_2^{z;0}(s)\mathcal{G}_2^{(1)}(s) + \mathcal{P}_3^{z;0}(s)\mathcal{G}_3^{(0)}(s) + \mathcal{P}_5^{z;0}(s)\mathcal{G}_5^{(0)}(s) \\
&\quad + \left\langle \mathcal{P}_4^{z;0}(s) \right\rangle_{\not{2}} \mathcal{G}_4^{(1)}(s) + \left\langle \mathcal{P}_4^{z;0}(s) \right\rangle_{-2} \mathcal{G}_4^{(2)}(s),
\end{aligned} \tag{7.101}$$

$$\begin{aligned}
\tilde{W}_{ab}^{c;1}(s) &= \mathcal{P}_1^{z;1}(s)\mathcal{G}_1^{(1)}(s) + \mathcal{P}_2^{z;1}(s)\mathcal{G}_2^{(1)}(s) + \mathcal{P}_{1\sigma}^{z;1}(s)\mathcal{G}_1^{\sigma;(0)}(s) + \mathcal{P}_{2\sigma}^{z;1}(s)\mathcal{G}_2^{\sigma;(0)}(s) \\
&\quad + \mathcal{P}_{3\sigma}^{z;1}(s)\mathcal{G}_3^{\sigma;(0)}(s) + \left\langle \mathcal{P}_{1\tilde{\lambda}}^{z;1}(s) \right\rangle_{\not{2}} \mathcal{G}_1^{\tilde{\lambda};(0)}(s) + \left\langle \mathcal{P}_{1\tilde{\lambda}}^{z;1}(s) \right\rangle_{-1} \mathcal{G}_1^{\tilde{\lambda};(1)}(s) \\
&\quad + \left\langle \mathcal{P}_{2\tilde{\lambda}}^{z;1}(s) \right\rangle_{\not{2}\not{1}\not{0}} \mathcal{G}_2^{\tilde{\lambda};(0)}(s) + \left\langle \mathcal{P}_{2\tilde{\lambda}}^{z;1}(s) \right\rangle_{-1} \mathcal{G}_2^{\tilde{\lambda};(1)}(s) + \left\langle \mathcal{P}_{2\tilde{\lambda}}^{z;1}(s) \right\rangle_{-2} \mathcal{G}_2^{\tilde{\lambda};(2)}(s) \\
&\quad + \left\langle \mathcal{P}_{4\tilde{\lambda}}^{z;1}(s) \right\rangle_{\not{2}\not{1}\not{0}} \mathcal{G}_4^{\tilde{\lambda};(0)}(s) + \left\langle \mathcal{P}_{4\tilde{\lambda}}^{z;1}(s) \right\rangle_{-1} \mathcal{G}_4^{\tilde{\lambda};(1)}(s) + \left\langle \mathcal{P}_{4\tilde{\lambda}}^{z;1}(s) \right\rangle_{-2} \mathcal{G}_4^{\tilde{\lambda};(2)}(s) \\
&\quad + \mathcal{P}_{5\tilde{\lambda}}^{z;1}(s)\mathcal{G}_5^{\tilde{\lambda};(0)}(s)
\end{aligned} \tag{7.102}$$

with the polynomials $\mathcal{P}_{j\kappa}^{z;\ell}(s)$ constructed using the procedure described in the previous subsection, the picking up $\left\langle \sum_i a_i s^i \right\rangle_m$ and the dropping operator $\left\langle \sum_i a_i s^i \right\rangle_{\not{m}}$ are defined in (7.66) and (7.67) respectively and functions $\mathcal{G}_j^\kappa(s)$ are listed in Appendix F.2.

For concreteness, we list here the polynomials (with the correct indices) for $K_L\pi^0 \to \pi^+\pi^-$ explicitly since this amplitude is used in Chapter 9 for numerical analysis of $\eta \to 3\pi$ decay. From (7.17) in its unitarity part there appear three dispersion integrals $\tilde{W}_{+-}^L(s)$, $\tilde{W}_{0+}^{L;0}(s)$ and $\tilde{W}_{0+}^{L;1}(s)$. They contain the following polynomials

$$\begin{aligned}
\mathcal{P}_1^{+-}(s) &= \frac{1}{2}\tilde{\alpha}_{Ln}(s)\alpha_x(s) + \tilde{\alpha}_{Lx}(s)\alpha_c(s) \\
&\quad + \frac{1}{2}\left(\tilde{\alpha}_{Ln}(s)\left(p_\lambda^{x;0} + \frac{1}{\pi}p_w^{x;0} + \frac{1}{\pi}p_0^{x;0}\right) + \alpha_x(s)\left(\tilde{p}_\lambda^{Ln;0} + \frac{1}{\pi}\tilde{p}_0^{Ln;0}\right)\right) \\
&\quad + \tilde{\alpha}_{Lx}(s)\left(p_\lambda^{c;0} + \frac{1}{\pi}p_w^{c;0} + \frac{1}{\pi}p_0^{c;0}\right) + \alpha_c(s)\left(\tilde{p}_\lambda^{Lx;0} + \frac{1}{\pi}\tilde{p}_0^{Lx;0}\right),
\end{aligned} \tag{7.103}$$

$$\begin{aligned}
\mathcal{P}_2^{+-}(s) &= \frac{1}{2}\frac{1}{\pi}\left(\tilde{\alpha}_{Ln}(s)p_1^{x;0} + \alpha_x(s)\tilde{p}_1^{Ln;0} + 2\,\frac{1}{s}\,(s-4m_\pi^2)\tilde{\alpha}_{Ln}(s)p_3^{x;0}\right) \\
&\quad + \frac{1}{\pi}\left(\tilde{\alpha}_{Lx}(s)p_1^{c;0} + \alpha_c(s)\tilde{p}_1^{Lx;0} + 2\,\frac{1}{s}\,(s-4m_\pi^2)\tilde{\alpha}_{Lx}(s)p_3^{c;0}\right),
\end{aligned} \tag{7.104}$$

$$\mathcal{P}_3^{+-}(s) = \frac{1}{2}\,\frac{1}{\pi}\,\tilde{\alpha}_{Ln}(s)p_2^{x;0} + \frac{1}{\pi}\,\tilde{\alpha}_{Lx}(s)p_2^{c;0}, \tag{7.105}$$

$$\mathcal{P}_4^{+-}(s) = \frac{1}{2}\,\frac{1}{\pi}\,\alpha_x(s)\tilde{p}_{1P}^{Ln;0} + \frac{1}{\pi}\,\alpha_c(s)\tilde{p}_{1P}^{Lx;0}, \tag{7.106}$$

$$\mathcal{P}_5^{+-}(s) = \frac{1}{2}\frac{1}{\pi}\,\alpha_x(s)\tilde{p}_{2P}^{Ln;0} + \frac{1}{\pi}\,\alpha_c(s)\tilde{p}_{2P}^{Lx;0}, \tag{7.107}$$

$$\mathcal{P}_1^{0+;0}(s) = \tilde{\alpha}_{Lt}(s)\alpha_t(s) + \tilde{\alpha}_{Lt}(s)\Big(p_\lambda^{t;0} + \frac{1}{\pi}p_w^{t;0} + \frac{1}{\pi}p_0^{t;0}\Big) + \alpha_t(s)\Big(\tilde{p}_\lambda^{Lt;0} + \frac{1}{\pi}\tilde{p}_0^{Lt;0}\Big), \tag{7.108}$$

$$\mathcal{P}_2^{0+;0}(s) = \frac{1}{\pi}\bigg(\tilde{\alpha}_{Lt}(s)p_1^{t;0} + \alpha_t(s)\tilde{p}_1^{Lt;0} + 2\,\frac{1}{s}\,(s-4m_\pi^2)\tilde{\alpha}_{Lt}(s)p_3^{t;0}\bigg), \tag{7.109}$$

$$\mathcal{P}_3^{0+;0}(s) = \frac{1}{\pi}\,\tilde{\alpha}_{Lt}(s)p_2^{t;0}, \tag{7.110}$$

$$\mathcal{P}_4^{0+;0}(s) = \frac{1}{\pi}\,\alpha_t(s)\tilde{p}_{1P}^{Lt;0}, \tag{7.111}$$

$$\mathcal{P}_5^{0+;0}(s) = \frac{1}{\pi}\,\alpha_t(s)\tilde{p}_{2P}^{Lt;0}, \tag{7.112}$$

$$\mathcal{P}_1^{0+;1}(s) = s\sigma_\pi^2(s)\bigg(\frac{1}{3}\tilde{\beta}_{Lt}\beta_t + \tilde{\beta}_{Lt}\Big(p_\lambda^{t;1} + \frac{1}{\pi}p_w^{t;1}\Big) + \beta_t\tilde{p}_\lambda^{Lt;1}\bigg), \tag{7.113}$$

$$\mathcal{P}_{1\sigma}^{0+;1}(s) = \frac{1}{\pi}\tilde{\beta}_{Lt}p_0^{c;1}, \tag{7.114}$$

$$\mathcal{P}_{1\tilde{\lambda}}^{0+;1}(s) = \frac{1}{\pi}\beta_t\tilde{p}_0^{Lt;1}, \tag{7.115}$$

$$\mathcal{P}_2^{0+;1}(s) = \frac{2}{\pi}\tilde{\beta}_{Lt}p_3^{c;1}(s)\,s\,\sigma_\pi^4, \tag{7.116}$$

$$\mathcal{P}_{2\sigma}^{0+;1}(s) = \frac{1}{\pi}\tilde{\beta}_{Lt}p_1^{c;1}, \tag{7.117}$$

$$\mathcal{P}_{2\tilde{\lambda}}^{0+;1}(s) = \frac{1}{\pi}\beta_t\tilde{p}_1^{Lt;1}, \tag{7.118}$$

$$\mathcal{P}_{3\sigma}^{0+;1}(s) = \frac{1}{\pi}\tilde{\beta}_{Lt}p_2^{c;1}, \tag{7.119}$$

$$\mathcal{P}_{4\tilde{\lambda}}^{0+;1}(s) = \frac{1}{\pi}\beta_t\tilde{p}_{1P}^{Lt;1}, \tag{7.120}$$

$$\mathcal{P}_{5\tilde{\lambda}}^{0+;1}(s) = \frac{1}{\pi}\beta_t\tilde{p}_{2P}^{Lt;1}, \tag{7.121}$$

where there appear polynomials $\tilde{p}_j^{a;\ell}(s)$ from Appendix L and polynomials $p_j^{i;\ell}(s)$ from Appendix G [we have suppressed denoting their dependence on s in these relations]. Polynomials $\alpha_a(s)$, $\tilde{\alpha}_a(s)$ and constants β_a, $\tilde{\beta}_a$ are parts of the leading order amplitudes [cf. (7.45)–(7.45)]

$$\alpha_x(s) = \quad \mathrm{a} + \frac{\mathrm{b}}{F_\pi^2}(s-4m_\pi^2), \qquad \alpha_c(s) = -2\mathrm{a} - \frac{\mathrm{b}}{2F_\pi^2}(s-12m_\pi^2), \tag{7.122}$$

$$\alpha_t(s) = -\mathrm{a} + \frac{\mathrm{b}}{2F_\pi^2}(s+4m_\pi^2), \qquad \beta_t = -\frac{\mathrm{b}}{2F_\pi^2}\,, \tag{7.123}$$

$$\tilde{\alpha}_{Ln}(s) = -3A_x, \qquad \tilde{\alpha}_{Lx}(s) = \quad A_x + \frac{B_x}{F_\pi^2}(s-\tilde{s}_0), \tag{7.124}$$

$$\tilde{\alpha}_{Lt}(s) = -A_x + \frac{B_x}{2F_\pi^2}(s-\tilde{s}_0), \qquad \tilde{\beta}_{Lt} = -\frac{B_x}{2F_\pi^2}\,. \tag{7.125}$$

7.6 Conclusions for $P\pi \to \pi\pi$ scattering in the limit $m_{\pi^\pm} = m_{\pi^0}$

We have constructed all the considered amplitudes in the limit $m_{\pi^\pm} = m_{\pi^0}$ including the two-loop effects. The results are presented in Section 7.5 in the form where the $\pi\pi$ scattering amplitudes are parametrized using the scattering-length parametrization. In order to obtain the result the $\pi\pi$ scatterign parametrized by the subthreshold parameters, we just need to use the transformations (5.188)–(iso sub-scatt relation last).

All parametrizations are prepared for numerical analyses. In this work we perform such analysis only for $\eta \to 3\pi$ decay (which has the same structure as $K_L \to 3\pi$ decay) in Chapter 9.

Chapter 8

$K \to 3\pi$ and $\eta \to 3\pi$ for isospin breaking

In this chapter we use all the knowledge we have accumulated so far and construct the amplitudes of $P \to 3\pi$ decays that take into account all the isospin breaking connected with the different masses of pseudoscalar mesons belonging to the same isomultiplet. Without isospin symmetry at hand there is no connection between the amplitudes concerning different charge states and we need to compute all the amplitudes $\tilde{A}^+_{++}$, $\tilde{A}^+_{00}$, $\tilde{A}^L_{+-}$, $\tilde{A}^L_{00}$, $\tilde{A}^S_{+-}$ separately. Note that the identity of the analytic structure of the processes with K_L and those with η remains also without isospin symmetry and so the results obtained for K_L are valid also for η, where we just need to change the interpretation of the parameters (and normalization constant) appearing there.

8.1 Leading order of amplitudes

The crossing and the Bose symmetries dictate the following form of leading orders of the particular amplitudes (which have to be first order polynomials),

$$\tilde{A}^+_{++} = \mathcal{C}\left(A_c + \frac{B_c}{F_\pi^2}(s - \tilde{s}_c)\right), \tag{8.1}$$

$$\tilde{A}^+_{00} = \mathcal{C}\left(A_x + \frac{B_x}{F_\pi^2}(s - \tilde{s}_x)\right), \tag{8.2}$$

$$\tilde{A}^L_{+-} = \mathcal{C}\left(A_x + \frac{B_x}{F_\pi^2}(s - \tilde{s}_x)\right), \tag{8.3}$$

$$\tilde{A}^L_{00} = \mathcal{C}A_0, \tag{8.4}$$

$$\tilde{A}^S_{+-} = \mathcal{C}\frac{B_x}{F_\pi^2}(t - u). \tag{8.5}$$

We have again suppressed the upper index determining the particle P on the right-hand side of the expressions. The normalization factor $\mathcal{C}$ was discussed in Section 6.6.2 and the values corresponding to the center of Dalitz plot $\tilde{s}_i^c$ for the particular processes are listed in Table 5.

8.2 Next-to-leading order result

The first iteration of our reconstruction procedure brings no complications to the general prescriptions of Section 3.1.

$$\tilde{A}^c_{ab}(s,t,u) = \mathcal{C}^c\left(\tilde{R}^c_{ab}(s,t,u) + 16\pi\tilde{U}^c_{ab}(s,t,u)\right) + O(p^6) \tag{8.6}$$

with

$$\tilde{U}^+_{++}(s,t,u) = \tilde{W}^+_{++}(s) + \tilde{W}^{+;0}_{+-}(t) + (u-s)\tilde{W}^{+;1}_{+-}(t) + \tilde{W}^{+;0}_{+-}(u) + (t-s)\tilde{W}^{+;1}_{+-}(u), \tag{8.7}$$

$$\tilde{U}^+_{00}(s,t,u) = \tilde{W}^+_{00}(s) - \tilde{W}^{+;0}_{+0}(t) - (s-u)\tilde{W}^{+;1}_{+0}(t) - \tilde{W}^{+;0}_{+0}(u) - (s-t)\tilde{W}^{+;1}_{+0}(u), \tag{8.8}$$

$$\tilde{U}^L_{+-}(s,t,u) = \tilde{W}^L_{+-}(s) - \tilde{W}^{L;0}_{0+}(t) - (s-u)\tilde{W}^{L;1}_{0+}(t) - \tilde{W}^{L;0}_{0+}(u) - (s-t)\tilde{W}^{L;1}_{0+}(u), \tag{8.9}$$

$$\tilde{U}^L_{00}(s,t,u) = \tilde{W}^L_{00}(s) + \tilde{W}^L_{00}(t) + \tilde{W}^L_{00}(u), \tag{8.10}$$

$$\tilde{U}^S_{+-}(s,t,u) = (t-u)\tilde{W}^S_{+-}(s) + \tilde{W}^{S;0}_{0+}(t) + (s-u)\tilde{W}^{S;1}_{0+}(t) - \tilde{W}^{S;0}_{0+}(u) - (s-t)\tilde{W}^{S;1}_{0+}(u). \tag{8.11}$$

According to (3.10) and (3.11), the dispersion integrals $\tilde{W}^{c;\ell}_{ab}$ are given by

$$\tilde{W}^+_{++}(s) = \frac{1}{2}\left(A_c + \frac{B_c}{F_\pi^2}(s-\tilde{s}_c)\right)\left(a_d + \frac{b_d}{F_\pi^2}(s-4m^2_{\pi^\pm})\right)\bar{J}_+(s), \tag{8.12}$$

$$\begin{aligned}\tilde{W}^{+;0}_{+-}(s) = {}& \frac{1}{2}\left(A_x + \frac{B_x}{F_\pi^2}(s-\tilde{s}_x)\right)\left(a_x + \frac{b_x}{F_\pi^2}(s-4m^2_{\pi^\pm})\right)\bar{J}_0(s)\\ &+ \left(A_c - \frac{B_c}{2F_\pi^2}(s-\tilde{s}_c)\right)\left(a_c + \frac{b_c}{F_\pi^2}(s-4m^2_{\pi^\pm})\right)\bar{J}_+(s),\end{aligned} \tag{8.13}$$

$$\tilde{W}^{+;1}_{+-}(s) = -\frac{b_c B_c}{6F_\pi^4}(s-4m^2_{\pi^\pm})\bar{J}_+(s), \tag{8.14}$$

$$\begin{aligned}\tilde{W}^+_{00}(s) = {}& \frac{1}{2}a_0\left(A_x + \frac{B_x}{F_\pi^2}(s-\tilde{s}_x)\right)\bar{J}_0(s)\\ &+ \left(A_c - \frac{B_c}{2F_\pi^2}(s-\tilde{s}_c)\right)\left(a_x + \frac{b_x}{F_\pi^2}(s-4m^2_{\pi^\pm})\right)\bar{J}_+(s),\end{aligned} \tag{8.15}$$

$$\begin{aligned}\tilde{W}^{+;0}_{+0}(s) = {}& \left(\frac{B_x}{2F_\pi^2}\left(\frac{b_t}{3F_\pi^2}\left(3(s-\tilde{s}_x)(s-2\Sigma) + \Delta(3\Delta+4\tilde{\Delta}_0) - (8\Sigma\tilde{\Delta}_0 + 3\tilde{s}_x\Delta)\frac{\Delta}{s}\right)\right.\right.\\ &\left.\left. + a_t\left(s - \tilde{s}_x + \frac{\tilde{\Delta}_0\Delta}{s}\right)\right) - A_x\left(a_t + \frac{b_t}{F_\pi^2}\frac{\lambda(s)}{s}\right)\right)\bar{J}_{+0}(s)\\ &+ \frac{2}{3}\frac{b_t B_x}{F_\pi^4}\frac{\Delta^3\tilde{\Delta}_0}{s^2}\bar{\bar{J}}_{+0}(s),\end{aligned} \tag{8.16}$$

$$\tilde{W}^{+;1}_{+0}(s) = \frac{b_t B_x}{6F_\pi^4}\frac{\lambda(s)}{s}\bar{J}_{+0}(s), \tag{8.17}$$

$$\begin{aligned}\tilde{W}^L_{+-}(s) &= \frac{1}{2}A_0\left(a_x + \frac{b_x}{F_\pi^2}(s-4m^2_{\pi^\pm})\right)\bar{J}_0(s)\\ &\quad + \left(A_x + \frac{B_x}{F_\pi^2}(s-\tilde{s}_x)\right)\left(a_c + \frac{b_c}{F_\pi^2}(s-4m^2_{\pi^\pm})\right)\bar{J}_+(s),\end{aligned} \tag{8.18}$$

$$\begin{aligned}\tilde{W}^{L;0}_{0+}(s) &= \left(\frac{B_x}{2F_\pi^2}\Big(\frac{b_t}{3F_\pi^2}\Big(3(s-\tilde{s}_x)(s-2\Sigma)+\Delta(3\Delta-4\tilde{\Delta}_+)+(8\Sigma\tilde{\Delta}_+-3\tilde{s}_x\Delta)\frac{\Delta}{s}\Big)\right.\\ &\qquad \left. + a_t\Big(s-\tilde{s}_x-\frac{\tilde{\Delta}_+\Delta}{s}\Big)\Big) - A_x\left(a_t+\frac{b_t}{F_\pi^2}\frac{\lambda(s)}{s}\right)\right)\bar{J}_{+0}(s)\\ &\quad - \frac{2}{3}\frac{b_tB_x}{F_\pi^4}\frac{\Delta^3\tilde{\Delta}_+}{s^2}\bar{\bar{J}}_{+0}(s),\end{aligned} \tag{8.19}$$

$$\tilde{W}^{L;1}_{0+}(s) = \frac{b_tB_x}{6F_\pi^4}\frac{\lambda(s)}{s}\bar{J}_{+0}(s), \tag{8.20}$$

$$\tilde{W}^L_{00}(s) = \frac{1}{2}a_0A_0\bar{J}_0(s) + \left(A_x+\frac{B_x}{F_\pi^2}(s-\tilde{s}_x)\right)\left(a_x+\frac{b_x}{F_\pi^2}(s-4m^2_{\pi^\pm})\right)\bar{J}_+(s), \tag{8.21}$$

$$\tilde{W}^S_{+-}(s) = \frac{b_cB_x}{3F_\pi^4}(s-4m^2_{\pi^\pm})\bar{J}_+(s), \tag{8.22}$$

$$\begin{aligned}\tilde{W}^{S;0}_{0+}(s) &= \left(\frac{B_x}{2F_\pi^2}\Big(\frac{b_t}{3F_\pi^2}\Big(9(s-\tilde{s}_x)(s-2\Sigma)+\Delta(9\Delta+4\tilde{\Delta}_+)-(8\Sigma\tilde{\Delta}_+ + 9\tilde{s}_x\Delta)\frac{\Delta}{s}\Big)\right.\\ &\qquad \left. + a_t\Big(3s-3\tilde{s}_x+\frac{\tilde{\Delta}_+\Delta}{s}\Big)\Big) + \frac{2}{3}\frac{b_tB_x}{F_\pi^4}\frac{\Delta^3\tilde{\Delta}_+}{s^2}\bar{\bar{J}}_{+0}(s),\end{aligned} \tag{8.23}$$

$$\tilde{W}^{S;1}_{0+}(s) = -\frac{b_tB_x}{6F_\pi^4}\frac{\lambda(s)}{s}\bar{J}_{+0}(s). \tag{8.24}$$

and the NLO polynomial parts are written in the expected form

$$\tilde{R}^+_{++}(s,t,u) = A_c + \frac{B_c}{F_\pi^2}(s-\tilde{s}_c) + \frac{C_c}{F_\pi^4}(s-\tilde{s}_c)^2 + \frac{D_c}{F_\pi^4}\left((t-\tilde{s}_c)^2+(u-\tilde{s}_c)^2\right), \tag{8.25}$$

$$\tilde{R}^+_{00}(s,t,u) = A_x + \frac{B_x}{F_\pi^2}(s-\tilde{s}_x) + \frac{C_x}{F_\pi^4}(s-\tilde{s}_x)^2 + \frac{D_x}{F_\pi^4}\left((t-\tilde{s}_x)^2+(u-\tilde{s}_x)^2\right), \tag{8.26}$$

$$\tilde{R}^L_{+-}(s,t,u) = A_x + \frac{B_x}{F_\pi^2}(s-\tilde{s}_x) + \frac{C_x}{F_\pi^4}(s-\tilde{s}_x)^2 + \frac{D_x}{F_\pi^4}\left((t-\tilde{s}_x)^2+(u-\tilde{s}_x)^2\right), \tag{8.27}$$

$$\tilde{R}^L_{00}(s,t,u) = A_0 + \frac{C_0}{F_\pi^4}\left(s^2+t^2+u^2-3\tilde{s}_0^2\right), \tag{8.28}$$

$$\tilde{R}^S_{+-}(s,t,u) = \frac{B_x}{F_\pi^2}(t-u) + \frac{C_x}{F_\pi^4}(s-\tilde{s}_x)(t-u). \tag{8.29}$$

8.3 Second iteration for $P^0\pi^0 \to \pi^0\pi^0$

In Section 6.6 we have discussed the complications that appear in the reconstruction procedure of $P\pi \to \pi\pi$ processes because of the instability of the particle P. From that

discussion there followed the observation that the complications do not manifest themselves in the first iteration. However, when one wants to perform the second iteration we have to pay attention to them. One possible way how to deal with them is to compute the amplitude for $m_P < 3m_\pi$ (which can be done for any of the considered processes) and try to find an analytic continuation in m_P that will lead to the physical result also for the physical mass m_P. In many cases such analytic continuation needs deformations of the contour of the dispersion relations and one needs to perform it very carefully. However, as is discussed in Appendix J this is not the case for the process $P^0\pi^0 \to \pi^0\pi^0$ even if we take $m_{\pi^\pm} \neq m_{\pi^0}$. By coincidence that are two of the most important processes for our analyses, $\eta \to 3\pi^0$ and $K_L \to 3\pi^0$ containing the cusp effect. In order to shorten the current discussion and to simplify the computation, we have therefore decided to perform in this work the second iteration only for these two processes and the computation for the other processes will be discussed elsewhere.

8.3.1 Computation of NLO partial waves contributing to $P^0\pi^0 \to \pi^0\pi^0$

The Bose symmetry (together with the crossing property) dictates this amplitude to be symmetric with respect to the exchange of all the Mandelstam variables. It means that the amplitude remain the same in all the crossed channels and in addition it has to be $t-u$ symmetric. Consequently, it possesses only the S-waves and we need to compute just the NLO S-waves of $P^0\pi^0 \to \pi^0\pi^0$ and of $P^0\pi^0 \to \pi^+\pi^-$. We have already discussed that instead of starting the computation of the complete amplitude for $m_P < 3m_\pi$ and performing the analytic continuation using the Kacser prescription not until such amplitude is computed, we can use the integral representation of the second iteration we have given in Section 3.5 and perform such continuation already in the partial waves. In Appendix K we have computed the integrals (3.32) of the one-loop functions appearing in NLO $P^0\pi^0 \to \pi^0\pi^0$ and $P^0\pi^0 \to \pi^+\pi^-$ amplitudes. It is therefore a straightforward task to put all these relations together and obtain the partial waves desired.

We write them again in the form[1]

$$\tilde{\varphi}_{Ln;0}(s) = \frac{\mathcal{C}}{16\pi}\left(\tilde{p}_\lambda^{Ln;0}(s) + \frac{1}{\pi}\sum_j \tilde{p}_j^{Ln;0}(s)\mathcal{M}_j(s)\right) \text{ with } j = \begin{cases} 0, 1n, 1\mathrm{L}, 2\mathrm{L}n, 3n, \\ 3+, 11\mathrm{L}, 12\mathrm{L}, 13\mathrm{L} \end{cases}, \quad (8.30)$$

$$\tilde{\varphi}_{Lx;0}(s) = \frac{\mathcal{C}}{16\pi}\left(\tilde{p}_\lambda^{Lx;0}(s) + \frac{1}{\pi}\sum_j \tilde{p}_j^{Lx;0}(s)\mathcal{M}_j(s)\right) \text{ with } j = \begin{cases} 0, 0q, 1+, 1\mathrm{L}, 2\mathrm{L}+, \\ 3n, 3+, 7\mathrm{L}x \end{cases}. \quad (8.31)$$

The polynomials $\tilde{p}_j^{a;0}(s)$ are listed in Appendix L.2 and the dimensionless functions $\mathcal{M}_j(s)$ in Appendix F.

[1]Note that the amplitude $P^0\pi^0 \to \pi^+\pi^-$ possesses also the P-wave. However, we will not need it in our computation and therefore will not write explicitly.

8.3.2 Computation of the second iteration

The reconstruction theorem shows that the NNLO amplitude $P^0\pi^0 \to \pi^0\pi^0$ can be obtained in the form

$$\tilde{A}^L_{00}(s,t,u) = \mathcal{C}\left(\tilde{R}^L_{00}(s,t,u) + 16\pi\tilde{U}^L_{00}(s,t,u)\right) + O(p^8). \tag{8.32}$$

We write the polynomial part in the form

$$\tilde{R}^L_{00}(s,t,u) = A_0 + \frac{C_0}{F_\pi^4}\left(s^2+t^2+u^2-3\tilde{s}_0^2\right) + \frac{E_0}{F_\pi^6}\left(s^3+t^3+u^3-3\tilde{s}_0^3\right) \tag{8.33}$$

and the single variable dispersion integral $\tilde{W}^L_{00}(s)$ appearing in the unitarity part

$$\tilde{U}^L_{00}(s,t,u) = \tilde{W}^L_{00}(s) + \tilde{W}^L_{00}(t) + \tilde{W}^L_{00}(u) \tag{8.34}$$

is computed in the following.

Similarly as in the isospin case from the previous chapter, this integral is of the form (2.73) and we can employ the simplifications of Section 2.5 and obtain the result in the form

$$\tilde{W}^L_{00}(s) = \frac{\mathcal{C}}{\pi}\mathcal{P}_j(s)\mathcal{H}_j(s), \tag{8.35}$$

where $\mathcal{H}_j(s)$ are Hilbert transforms of dimensionless functions appearing in the integrands of $\tilde{W}^L_{00}(s)$ and $\mathcal{P}_j(s)$ are polynomials in s.

Since we have explained the computation in great detail on the case of isospin symmetric result of Chapter 7, we can be brief now. The richer set of the functions $\mathcal{M}_j(s)$ in the partial waves means also a richer set of kinematic functions $\mathcal{K}_j(s)$ appearing in the integrand of $\tilde{W}^L_{00}(s)$. We list them together with some of their properties in Tables 9 and 10. In Table 9 there are given the functions appearing in the contribution of $\pi^0\pi^0$ intermediate state, whereas in Table 10 those from contribution of $\pi^+\pi^-$ are listed. The limits of functions $\mathcal{K}_{11}$ and $\mathcal{K}_{12}$ are

$$\mathcal{K}_{11}(s) \to \mathcal{K}^{q=1}_{11}(s) = \frac{\tilde{\Delta}-s}{m_\pi^2}\sigma_\pi^2(s)\mathcal{F}_2(s) - \frac{1}{sm_\pi^2}\tilde{\lambda}(s)\mathcal{F}_4(s), \tag{8.36}$$

$$\mathcal{K}_{12}(s) \to \mathcal{K}^{q=1}_{12}(s) = \mathcal{F}_2(s) + \left(1-\frac{\tilde{\Delta}}{s}\right)\mathcal{F}_4(s). \tag{8.37}$$

As was discussed below the unitarity relations (7.43) even though the various functions $\mathcal{M}_j(s)$ (and thereby also $\mathcal{K}_j(s)$) are for the physical mass m_P complex, the only functions that need specific care are functions $\mathcal{M}_{3n}(s)$ and $\mathcal{M}_{3+}(s)$ that are complex even for $m_P < 3m_\pi$ and because of the complex conjugation in (7.43) they appear in the integrand once in the direct and once in the complex conjugated form. It should be obvious that for the contribution of $\mathcal{M}_{3n}(s)$ in $\pi^0\pi^0$ intermediate state, i.e. for the direct contribution of $P\pi^0 \to \pi^0\pi^0 \to \pi^0\pi^0$ rescatterings, there occur the same mechanism as in the isospin symmetric computation (cf. (7.57) and Figure 12). It means that there contribute only real part of this function, which is in the integration region equal to $\sigma_0^2(s)L_0(s)$, and

$\mathcal{K}_j$	$\mathcal{M}_j$	Asympt.	$n_{\min}$	$\mathcal{P}_j$	m	n	$q \to 1$
$\mathcal{K}_{1n} = \sigma_0$	$\mathcal{M}_0$	s^0	1	$\mathcal{P}_{1n}$	$\langle -1, 2\rangle$	1	$\to \mathcal{F}_1$
$\mathcal{K}_{2n} = L_0$	$\mathcal{M}_{1n}, \mathcal{M}_{3n}$	$\log s$	1	$\mathcal{P}_{2n}$	$\langle -1, 0\rangle$	1	$\to \mathcal{F}_2$
$\mathcal{K}_{2n\nabla} = \sigma_0 \frac{L_\nabla}{\sigma_\nabla}$	$\mathcal{M}_{1\nabla}$	$\log s$	1	$\mathcal{P}_{2n\nabla}$	$\langle 0, 2\rangle$	1	$\to \mathcal{F}_2$
$\mathcal{K}_{3n} = -m_{\pi^0}^2 \frac{L_0^2}{s\sigma_0}$	$\mathcal{M}_{2n}$	$\frac{1}{s}\log^2 s$	0	$\mathcal{P}_{3n}$	0	0	$\to \mathcal{F}_3$
$\mathcal{K}_{3n\nabla} = -m_{\pi^\pm}^2 \frac{L_\nabla^2}{s\sigma_0}$	$\mathcal{M}_{2\nabla}$	$\frac{1}{s}\log^2 s$	0	$\mathcal{P}_{3n\nabla}$	0	0	$\to \mathcal{F}_3$
$\mathcal{K}_{4n} = s\sigma_0 \frac{M_0}{\tilde\lambda_0^{1/2}}$	$\mathcal{M}_{1\mathrm{L}}$	$\log s$	1	$\mathcal{P}_{4n}$	$\langle -1, 0\rangle$	1	$\to \mathcal{F}_4$
$\mathcal{K}_{5n} = -m_{\pi^0}^2 L_0 \frac{M_0}{\tilde\lambda_0^{1/2}}$	$\mathcal{M}_{2\mathrm{L}n}$	$\frac{1}{s}\log^2 s$	0	$\mathcal{P}_{5n}$	0	0	$\to \mathcal{F}_5$
$\mathcal{K}_{6\nabla} = \mathrm{Re}\,\sigma_0\sigma_+\mathcal{L}_+$	$\mathcal{M}_{3+}$	$\log s$	1	$\mathcal{P}_{6\nabla}$	$\langle 0, 2\rangle$	1	$\to \sigma_\pi^2\mathcal{F}_2$
$\mathcal{K}_{11} = 2\sigma_0(\omega(\tau_+^{\mathrm{L}n}) + \omega(\tau_-^{\mathrm{L}n}))$	$\mathcal{M}_{11\mathrm{L}n}$	$s\log s$	2	$\mathcal{P}_{11}$	$\langle 0, 1\rangle$	2	$\to \mathcal{K}_{11}^{q=1}$
$\mathcal{K}_{12} = 2m_{\pi^\pm}^2 \frac{\omega(\tau_+^{\mathrm{L}n}) - \omega(\tau_-^{\mathrm{L}n})}{\tilde\lambda_0^{1/2}}$	$\mathcal{M}_{12\mathrm{L}n}$	$\log s$	1	$\mathcal{P}_{12}$	$\langle -1, 2\rangle$	1	$\to \mathcal{K}_{12}^{q=1}$
$\mathcal{K}_{13} = m_{\pi^\pm}^2 \frac{\log^2\tau_+^{\mathrm{L}n} - \log^2(\tau_-^{\mathrm{L}n})}{\tilde\lambda_0^{1/2}}$	$\mathcal{M}_{13\mathrm{L}n}$	$\frac{1}{s}\log^2 s$	0	$\mathcal{P}_{13}$	0	0	$\to \mathcal{F}_5$

Table 9: Kinematic functions $\mathcal{K}_j$ appearing in the integrand of $\tilde W_{00}^L(s)$ stemming from $\pi^0\pi^0$ intermediate state, i.e. originating as $\sigma_0\mathcal{M}_j$. The expressions for $\mathcal{M}_j$ and further functions used in the table are given in Appendix F. The third column denote asymptotics of the particular function for $s \to \infty$, from which it follows the minimal number of subtraction $n_{\min}$ of its Hilbert transform. In the sixth column there are listed powers of s appearing in the polynomial $\mathcal{P}_j$ multiplying the function in question. Using these two numbers together with the inequality (2.76) we determine the number of subtraction needed for $\mathcal{H}_j^{(n)}$ given in the penultimate column. The ultimate column contains limit of $\mathcal{K}_j$ for $m_{\pi^0} = m_{\pi^\pm}$ — for the sake of space the more dense limit are labeled here and expressions for them are given in the main text.

such contribution can be included into $\mathcal{P}_{2n}(s)$. The similar discussion applies also for the contribution of $\mathcal{M}_{3+}(s)$ in $\pi^+\pi^-$ intermediate state. A more complex situation appears in the crossed contributions. As is depicted on Figure 13 (thanks to the T-invariance) such crossed contribution in $\pi^0\pi^0$ intermediate state is for $s > 4m_{\pi^0}^2$

$$\frac{1}{2}\alpha_x(s)\sigma_0(s)\Big(\tilde\alpha_x(s)\alpha_0(s)\sigma_+(s)\mathcal{L}_+(s) + \tilde\alpha_0(s)\alpha_x(s)\sigma_+^\star(s)\mathcal{L}_+^\star(s)\Big). \tag{8.38}$$

For $s > 4m_{\pi^\pm}^2$ it simplifies ($\sigma_+(s) > 0$ and $L_+(s)$ is real) into

$$\frac{1}{2}\alpha_x(s)\sigma_0(s)\sigma_+(s)\Big(\big(\tilde\alpha_x(s)\alpha_0(s)+\tilde\alpha_0(s)\alpha_x(s)\big)L_+(s)\mp i\pi\big(\tilde\alpha_x(s)\alpha_0(s)-\tilde\alpha_0(s)\alpha_x(s)\big)\Big), \tag{8.39}$$

where the upper sign corresponds to the usual physical choice (continuation in s from below), whereas for $s \in (4m_{\pi^0}^2, m_{\pi^\pm}^2)$ the contribution looks like

$\mathcal{K}_j$	$\mathcal{M}_j$	Asympt.	$n_{\min}$	$\mathcal{P}_j$	m	n	$q \to 1$
$\mathcal{K}_{1+} = \sigma_+$	$\mathcal{M}_0$	s^0	1	$\mathcal{P}_{1+}$	$\langle -1, 3\rangle$	1	$\to \mathcal{F}_1$
$\mathcal{K}_{1q} = -\frac{\Sigma}{\Delta}\log q\,\sigma_+$	$\mathcal{M}_{0q}$	s^0	1	$\mathcal{P}_{1q}$	$\langle -1, 3\rangle$	1	$\to \mathcal{F}_1$
$\mathcal{K}_{2+} = L_+$	$\mathcal{M}_{1+}, \mathcal{M}_{3+}$	$\log s$	1	$\mathcal{P}_{2+}$	$\langle -1, 3\rangle$	1	$\to \mathcal{F}_2$
$\mathcal{K}_{2+n} = \sigma_+\frac{L_0}{\sigma_0}$	$\mathcal{M}_{1n}$	$\log s$	1	$\mathcal{P}_{2+n}$	$\langle 0, 3\rangle$	1	$\to \mathcal{F}_2$
$\mathcal{K}_{3n+} = -\frac{\Sigma}{2}\frac{L_+L_0}{s\sigma_0}$	$\mathcal{M}_{2n+}$	$\frac{1}{s}\log^2 s$	0	$\mathcal{P}_{3n+}$	$\langle 0, 2\rangle$	0	$\to \mathcal{F}_3$
$\mathcal{K}_{4+} = s\sigma_+\frac{M_0}{\tilde{\lambda}_0^{1/2}}$	$\mathcal{M}_{1\mathrm{L}}$	$\log s$	1	$\mathcal{P}_{4+}$	$\langle -1, 3\rangle$	1	$\to \mathcal{F}_4$
$\mathcal{K}_{4+}$				$\mathcal{P}_{4+}$	-2	2	$\to \mathcal{F}_4$
$\mathcal{K}_{5+} = -\frac{\Sigma}{2}L_+\frac{M_0}{\tilde{\lambda}_0^{1/2}}$	$\mathcal{M}_{2\mathrm{L}+}$	$\frac{1}{s}\log^2 s$	0	$\mathcal{P}_{5+}$	$\langle 0, 2\rangle$	0	$\to \mathcal{F}_5$
$\mathcal{K}_{6\Delta} = \mathrm{Re}\,\sigma_0\sigma_+\mathcal{L}_0$	$\mathcal{M}_{3n}$	$\log s$	1	$\mathcal{P}_{6\delta}$	$\langle 0, 2\rangle$	1	$\to \sigma_\pi^2\mathcal{F}_2$
$\mathcal{K}_{7x} = \Delta\frac{\mathcal{J}(\tau_+^x)-\mathcal{J}(\tau_-^x)}{s\sigma_0}$	$\mathcal{M}_{7x}$	$\frac{1}{s}\log s$	0	$\mathcal{P}_{7x}$	$\langle 0, 2\rangle$	0	$\to 0$
$\mathcal{K}_{7\mathrm{L}x} = \Delta\frac{\mathcal{J}(\tau_+^{\mathrm{L}x})-\mathcal{J}(\tau_-^{\mathrm{L}x})}{\tilde{\lambda}_0^{1/2}}$	$\mathcal{M}_{7\mathrm{L}x}$	$\frac{1}{s}\log s$	0	$\mathcal{P}_{7\mathrm{L}x}$	$\langle 0, 2\rangle$	0	$\to 0$
$\mathcal{K}_{8\mathrm{L}x} = \sigma_+\mathcal{M}_{8\mathrm{L}x}$	$\mathcal{M}_{8\mathrm{L}x}$	$\frac{1}{s}\log s$	0	$\mathcal{P}_{8\mathrm{L}x}$	$\langle 0, 2\rangle$	0	$\to -\mathcal{F}_2 + \mathcal{F}_4$
$\mathcal{K}_{9\mathrm{L}x} = \sigma_+\mathcal{M}_{9\mathrm{L}x}$	$\mathcal{M}_{9\mathrm{L}x}$	$\frac{1}{s}$	0	$\mathcal{P}_{9\mathrm{L}x}$	$\langle 0, 1\rangle$	1	$\to 0$

Table 10: Kinematic functions $\mathcal{K}_j$ appearing in the integrand of $\tilde{W}_{00}^L(s)$ stemming from $\pi^+\pi^-$ intermediate state, i.e. originating as $\sigma_+\mathcal{M}_j$. The expressions for $\mathcal{M}_j$ and further functions used in the table are given in Appendix F. The other columns contain the similar quantities as it was the case in the previous table. Note that for $\mathcal{K}_{4+}$ we need two Hilbert transforms, once with one subtraction and once with two of them.

$$\pm\frac{1}{2}\alpha_x(s)i\sigma_0(s)|\sigma_+(s)|\Big(\tilde{\alpha}_x(s)\alpha_0(s)\mathcal{L}_+(s) - \tilde{\alpha}_0(s)\alpha_x(s)\mathcal{L}_+^\star(s)\Big)$$
$$= \frac{1}{2}\alpha_x(s)\sigma_0(s)|\sigma_+(s)|\Big(\tilde{\alpha}_x(s)\alpha_0(s) + \tilde{\alpha}_0(s)\alpha_x(s)\Big)\left(\arctan\frac{2|\sigma_+(s)|}{1-\sigma_+^2(s)} - \pi\right) \quad (8.40)$$

independently on the choice of the sign since $\sigma_+(s)$ is on this interval purely imaginary and the argument of the logarithm is then with its norm equal to 1. In conclusion this contribution splits into the real part, whose polynomial is obtained as adding of two parts contributing and the imaginary part that starts for $s > 4m_{\pi^\pm}^2$ with polynomial containing difference.

Similarly the crossed contribution in $\pi^+\pi^-$ intermediate state for $s > 4m_{\pi^\pm}^2$ (the one-half appearing there is from $p_{3n}(s)$)

$$\frac{1}{2}\alpha_x(s)\sigma_0(s)\sigma_+(s)\Big(\tilde{\alpha}_x(s)\alpha_0(s)\mathcal{L}_0^\star(s) + \tilde{\alpha}_0(s)\alpha_x(s)\mathcal{L}_0(s)\Big)$$
$$= \frac{1}{2}\alpha_x(s)\sigma_0(s)\sigma_+(s)\Big(\big(\tilde{\alpha}_x(s)\alpha_0(s) + \tilde{\alpha}_0(s)\alpha_x(s)\big)L_0(s) \pm i\pi\big(\tilde{\alpha}_x(s)\alpha_0(s) - \tilde{\alpha}_0(s)\alpha_x(s)\big)\Big). \quad (8.41)$$

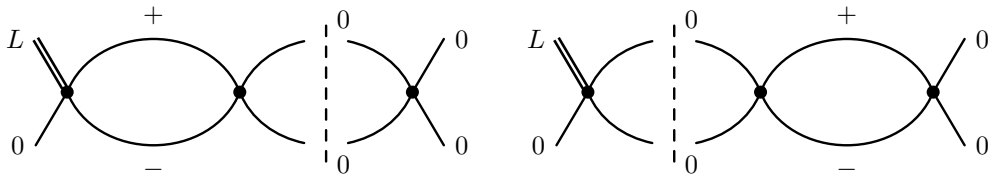

$$\frac{1}{2}\left(\tilde{\alpha}_x(s)\mathcal{M}_{3+}(s)\alpha_x(s)\right)\times\alpha_0^\star(s)\sigma_0(s) \qquad \frac{1}{2}\tilde{\alpha}_0(s)\times\left(\alpha_x(s)\mathcal{M}_{3+}(s)\alpha_x(s)\right)^\star\sigma_0(s)$$

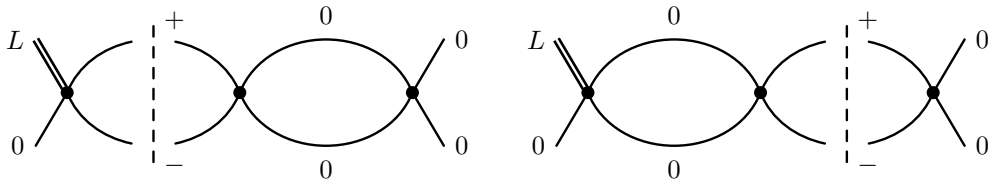

$$\frac{1}{2}\tilde{\alpha}_x(s)\times\left(\alpha_x(s)\mathcal{M}_{3n}(s)\alpha_0(s)\right)^\star\sigma_+(s) \qquad \frac{1}{2}\left(\tilde{\alpha}_0(s)\mathcal{M}_{3n}(s)\alpha_x(s)\right)\times\alpha_x^\star(s)\sigma_+(s)$$

Figure 13: Illustration of the symmetry of the crossed contributions with $\mathcal{M}_3$ to NNLO $P\pi^0 \to \pi^0\pi^0$ amplitude. In the first line there are diagrams containing $\mathcal{M}_{3+}$ in the contribution with $\pi^0\pi^0$ intermediate state. The second line contains contributions with $\mathcal{M}_{3n}$ from the $\pi^+\pi^-$ intermediate state.

Since both of the imaginary parts are non-zero for $s > 4m_{\pi^\pm}^2$ and of different sign, they cancel and only the real parts of the contributions remain, moreover, both with the same polynomial coefficient. It is not unexpected since the discontinuity of

$$\mathcal{H}_6^{(1)}(s) = \sigma_0(s)\mathcal{L}_0(s)\sigma_+(s)\mathcal{L}_+(s) - 4 = \left(16\pi^2\bar{J}_0(s) - 2\right)\left(16\pi^2\bar{J}_+(s) - 2\right) - 4 \tag{8.42}$$

is equal to

$$\operatorname{Disc}\mathcal{H}_6^{(1)}(s) = \operatorname{Re}\sigma_0(s)\sigma_+(s)\Big(\mathcal{L}_0(s)\theta(s-4m_{\pi^\pm}^2) + \mathcal{L}_+(s)\theta(s-4m_{\pi^0}^2)\Big). \tag{8.43}$$

It means that our formal $\mathcal{H}_{6\Delta}^{(1)}(s)$ and $\mathcal{H}_{6\nabla}^{(1)}(s)$ combine into this function which is multiplication of two one-loop functions.

In summary, the single variable dispersion integral is

$$\begin{aligned}\tilde{W}_{00}^L(s) = \frac{\mathcal{C}}{\pi}\Big(&\mathcal{P}_{1n}(s)\mathcal{G}_{1n}^{(1)}(s) + \mathcal{P}_{1+}(s)\mathcal{G}_{1+}^{(1)}(s) + \mathcal{P}_{1q}(s)\mathcal{G}_{1q}^{(1)}(s) + \mathcal{P}_{2n}(s)\mathcal{G}_{2n}^{(1)}(s)\\
&+ \mathcal{P}_{2+}(s)\mathcal{G}_{2+}^{(1)}(s) + \mathcal{P}_{2+n}(s)\mathcal{G}_{2+n}^{(1)}(s) + \mathcal{P}_{2n\nabla}(s)\mathcal{G}_{2n\nabla}^{(1)}(s) + \mathcal{P}_{3n}(s)\mathcal{G}_{3n}^{(0)}(s)\\
&+ \mathcal{P}_{3n+}(s)\mathcal{G}_{3n+}^{(0)}(s) + \mathcal{P}_{3n\nabla}(s)\mathcal{G}_{3n\nabla}^{(0)}(s) + \mathcal{P}_{4n}(s)\mathcal{G}_{4n}^{(1)}(s) + \mathcal{P}_{5n}(s)\mathcal{G}_{5n}^{(0)}(s)\\
&+ \mathcal{P}_{5+}(s)\mathcal{G}_{5+}^{(0)}(s) + \mathcal{P}_6(s)\mathcal{G}_6^{(1)}(s) + \mathcal{P}_{7x}(s)\mathcal{G}_{7x}^{(0)}(s) + \mathcal{P}_{7\mathrm{L}x}(s)\mathcal{G}_{7\mathrm{L}x}^{(0)}(s)\\
&+ \mathcal{P}_{8\mathrm{L}x}(s)\mathcal{G}_{8\mathrm{L}x}^{(0)}(s) + \mathcal{P}_{9\mathrm{L}x}(s)\mathcal{G}_{9\mathrm{L}x}^{(1)}(s) + \mathcal{P}_{11}(s)\mathcal{G}_{11}^{(2)}(s) + \mathcal{P}_{12}(s)\mathcal{G}_{12}^{(1)}(s)\\
&+ \mathcal{P}_{13}(s)\mathcal{G}_{13}^{(0)}(s) + \Big\langle\mathcal{P}_{4+}(s)\Big\rangle_{\not{2}}\mathcal{G}_{4+}^{(1)}(s) + \Big\langle\mathcal{P}_{4+}(s)\Big\rangle_{-2}\mathcal{G}_{4+}^{(2)}(s)\Big),\end{aligned} \tag{8.44}$$

where we have again used the picking up $\left\langle \sum_i a_i s^i \right\rangle_m$ and the dropping $\left\langle \sum_i a_i s^i \right\rangle_{\not m}$ operators from (7.66) and (7.67) respectively.

The polynomials multiplying these kinematic functions are simply

$$\mathcal{P}_{1n}(s) = \frac{a_0\,A_0}{2} + \frac{A_0}{2}\Big(p_\lambda^{0;0}(s) + \frac{1}{\pi}p_w^{0;0} + \frac{1}{\pi}p_0^{0;0}(s)\Big) + \frac{a_0}{2}\Big(\tilde{p}_\lambda^{Ln;0}(s) + \frac{1}{\pi}\tilde{p}_0^{Ln;0}(s)\Big), \tag{8.45}$$

$$\mathcal{P}_{2n}(s) = \frac{1}{2}\frac{1}{\pi}\Big(A_0\,p_{1n}^{0;0}(s) + a_0\,\tilde{p}_{1n}^{Ln;0}(s) + 2\sigma_0^2(s)A_0\,p_{3n}^{0;0}(s)\Big), \tag{8.46}$$

$$\mathcal{P}_{2n\nabla}(s) = \frac{1}{2}\frac{1}{\pi}\,A_0\,p_{1\nabla}^{0;0}(s), \tag{8.47}$$

$$\mathcal{P}_{3n}(s) = \frac{1}{2}\frac{1}{\pi}\,A_0\,p_{2n}^{0;0}(s), \tag{8.48}$$

$$\mathcal{P}_{3n\nabla}(s) = \frac{1}{2}\frac{1}{\pi}\,A_0\,p_{2\nabla}^{0;0}(s), \tag{8.49}$$

$$\mathcal{P}_{4n}(s) = \frac{1}{2}\frac{1}{\pi}\,a_0\,\tilde{p}_{1\mathrm{L}}^{Ln;0}(s), \tag{8.50}$$

$$\mathcal{P}_{5n}(s) = \frac{1}{2}\frac{1}{\pi}\,a_0\,\tilde{p}_{2\mathrm{L}n}^{Ln;0}(s), \tag{8.51}$$

$$\mathcal{P}_{6}(s) = \frac{1}{2}\frac{1}{\pi}\Big(A_0\,p_{3+}^{0;0}(s) + a_0\,\tilde{p}_{3+}^{Ln;0}(s)\Big), \tag{8.52}$$

$$\mathcal{P}_{11}(s) = \frac{1}{2}\frac{1}{\pi}\,a_0\,\tilde{p}_{11\mathrm{L}n}^{Ln;0}(s), \tag{8.53}$$

$$\mathcal{P}_{12}(s) = \frac{1}{2}\frac{1}{\pi}\,a_0\,\tilde{p}_{12\mathrm{L}n}^{Ln;0}(s), \tag{8.54}$$

$$\mathcal{P}_{13}(s) = \frac{1}{2}\frac{1}{\pi}\,a_0\,\tilde{p}_{13\mathrm{L}n}^{Ln;0}(s), \tag{8.55}$$

$$\mathcal{P}_{1+}(s) = \alpha_x(s)\tilde{\alpha}_x(s) + \tilde{\alpha}_x(s)\Big(p_\lambda^{x;0}(s) + \frac{1}{\pi}p_w^{x;0} + \frac{1}{\pi}p_0^{x;0}(s)\Big) + \alpha_x(s)\Big(\tilde{p}_\lambda^{Lx;0}(s) + \frac{1}{\pi}\tilde{p}_0^{Lx;0}(s)\Big), \tag{8.56}$$

$$\mathcal{P}_{1q}(s) = \frac{1}{\pi}\Big(\tilde{\alpha}_x(s)p_{0q}^{x;0}(s) + \alpha_x(s)\tilde{p}_{0q}^{Lx;0}(s)\Big), \tag{8.57}$$

$$\mathcal{P}_{2+}(s) = \frac{1}{\pi}\Big(\tilde{\alpha}_x(s)p_{1+}^{x;0}(s) + \alpha_x(s)\tilde{p}_{1+}^{Lx;0}(s) + 2\sigma_+^2(s)\tilde{\alpha}_x(s)p_{3+}^{x;0}(s)\Big), \tag{8.58}$$

$$\mathcal{P}_{2+n}(s) = \frac{1}{\pi}\,\tilde{\alpha}_x(s)p_{1n}^{x;0}(s), \tag{8.59}$$

$$\mathcal{P}_{3n+}(s) = \frac{1}{\pi}\,\tilde{\alpha}_x(s)p_{2n+}^{x;0}(s), \tag{8.60}$$

$$\mathcal{P}_{4+}(s) = \frac{1}{\pi}\,\alpha_x(s)\tilde{p}_{1\mathrm{L}}^{Lx;0}(s), \tag{8.61}$$

$$\mathcal{P}_{5+}(s) = \frac{1}{\pi}\,\alpha_x(s)\tilde{p}_{2\mathrm{L}+}^{Lx;0}(s), \tag{8.62}$$

$$\mathcal{P}_{7x}(s) = \frac{1}{\pi}\,\alpha_x(s)\tilde{p}_{7x}^{Lx;0}(s), \tag{8.63}$$

$$\mathcal{P}_{7\mathrm{L}x}(s) = \frac{1}{\pi}\,\tilde{\alpha}_x(s) p^{Lx;0}_{7\mathrm{L}x}(s), \tag{8.64}$$

$$\mathcal{P}_{8\mathrm{L}x}(s) = \frac{1}{\pi}\,\alpha_x(s) \tilde{p}^{Lx;0}_{8\mathrm{L}x}(s), \tag{8.65}$$

$$\mathcal{P}_{9\mathrm{L}x}(s) = \frac{1}{\pi}\,\alpha_x(s) \tilde{p}^{Lx;0}_{9\mathrm{L}x}(s), \tag{8.66}$$

where we have again denoted with $\alpha(s)$ and $\tilde{\alpha}(s)$ the LO amplitudes of $A_x(s,t,u)$ and $\tilde{A}^L_{+-}(s,t,u)$ respectively,

$$\alpha_x(s) = a_x + \frac{b_x}{F_\pi^2}(s - 4m^2_{\pi^\pm}), \quad \tilde{\alpha}_x(s) = A_x + \frac{B_x}{F_\pi^2}(s - \tilde{s}_x). \tag{8.67}$$

For completeness, let us remind that the polynomials $\tilde{p}^{a;\ell}_j(s)$ and $p^{i;\ell}_j(s)$ can be found in Appendix L and Appendix G.

8.3.3 Using the result for obtaining other amplitudes

As was already noted above by performing two distinct limits of the amplitude, we can obtain the result of the amplitude $P\pi^0 \to \pi^0\pi^0$ in the isospin limit or isospin breaking result for $\pi^0\pi^0$ scattering. In order to obtain the isospin limit of this result, we just need to perform the limit of the kinematic functions which were already given in Tables 9 and 10 and in the polynomial part we limit $m_{\pi^\pm} \to m_{\pi^0}$ together with the limit in the $\pi\pi$ parameters from (5.157)–(5.162) and the following change in the parameters of $P\pi \to \pi\pi$ amplitudes

$$A^L_0 = -3A^L_x, \qquad C^L_0 = -C^L_x - 2D^L_x, \qquad E^L_0 = -E^L_x - 2F^L_x\,. \tag{8.68}$$

We have verified that we obtain the same result as from the computation of the previous chapter.

Similarly by performing the limit $m_P \to m_{\pi^0}$, we can obtain the isospin breaking result for $\pi^0\pi^0$ scattering. In this case the kinematic functions have limits

$$\mathcal{K}_{4n} \to \mathcal{K}_{2n}, \qquad \mathcal{K}_{4+} \to \mathcal{K}_{2+}, \tag{8.69}$$

$$\mathcal{K}_{5n} \to \mathcal{K}_{3n}, \qquad \mathcal{K}_{5+} \to \mathcal{K}_{3+}, \tag{8.70}$$

$$\mathcal{K}_{7\mathrm{L}x} \to \mathcal{K}_{7x}, \qquad \mathcal{K}_{11} \to -2\,\frac{s - 4m^2_{\pi^0}}{m^2_{\pi^\pm}}\,\mathcal{K}_{2n\nabla}, \tag{8.71}$$

$$\mathcal{K}_{12} \to 2\mathcal{K}_{2n\nabla}, \qquad \mathcal{K}_{13} \to \mathcal{K}_{3n\nabla}, \tag{8.72}$$

$$\mathcal{K}_{8\mathrm{L}x} \to \frac{\Delta}{\Sigma}\mathcal{K}_{1q} - \frac{1}{2}\mathcal{K}_{2+} + \frac{1}{2}\mathcal{K}_{2+n}, \tag{8.73}$$

$$\mathcal{K}_{9\mathrm{L}x} \to \left(1 - \frac{s}{\Sigma}\right)\mathcal{K}_{1q} + \frac{s - 4m^2_{\pi^\pm} + \Delta}{2\Delta}\mathcal{K}_{2+} - \frac{s - 4m^2_{\pi^0} - \Delta}{2\Delta}\mathcal{K}_{2+n} - 1 \tag{8.74}$$

and the remaining functions leave the same. In the polynomial part it is easier to obtain the subthreshold parametrization by changing

$$A_0^L \to \frac{\alpha_{00} m_{\pi^0}^2}{F_\pi^2}, \qquad A_x^L \to -\frac{\alpha_{\pm 0} m_{\pi^0}^2}{3F_\pi^2}, \qquad B_x^L \to -\frac{\beta_{\pm 0}}{3} \tag{8.75}$$

and some more complicated changes in C_x^L, D_x^L and E_0^L (this is connected with the fact that λ's in subthreshold parametrization of $\pi\pi$ scattering from Section 5.9 were not expanded around the center of the Dalitz plot but instead at the thresholds).

8.4 Conclusions for $P\pi \to \pi\pi$ scattering with $m_{\pi^\pm} \neq m_{\pi^0}$

We have constructed all $K \to 3\pi$ and $\eta \to 3\pi$ amplitudes taking into account all the isospin breaking effects connected with $m_{\pi^\pm} \neq m_{\pi^0}$ at the one-loop level and the amplitudes $K_L \to 3\pi^0$ and $\eta \to 3\pi^0$ at the two-loop level. These results are prepared for the phenomenological analyses. Thanks to the inclusion of the isospin breaking effects it is especially useful for the analyses of the cusp. Note however that at the current level we do not include photons, which can be missing in the analysis of K decays. Nevertheless, thanks to the suppression of the electromagnetic effects in $\eta \to 3\pi$ decays, it seems that our amplitude will be very suitable for the analysis of cusp effect in $\eta \to 3\pi^0$, whose first indications are already observed (cf. [117]).

Part IV

Phenomenological applications of the construction

Chapter 9

Determination of the m_u and the m_d masses from $\eta \to 3\pi$ decays

In the previous chapters we have already discussed some of the possible phenomenological applications of the amplitudes constructed using the reconstruction theorem and stated that they are prepared for such studies. The only study we have already performed is the determination of the isospin breaking parameter R [from (6.1)] connected to the light quark masses from the $\eta \to 3\pi$ decay. Nevertheless, also in this case the analysis is incomplete as we still do not have an access to the physically measured data [cf. Section 9.6]. Before we describe our analysis, we recall in the next section, the importance of the χPT-inspired studies for the determination of the light quark masses.

9.1 Introduction

Quark masses are fundamental free parameters of the Standard model. Because of the QCD phenomenon of color confinement, quarks are bounded inside hadrons and their masses cannot be directly measured. The only method for their determination is a comparison of a theoretical prediction of some observable depending on the masses in some theoretical framework with the corresponding experimental value. For that end we thus need a framework, in which the quark masses explicitly occur and which can make predictions of such observable with a sufficient precision. Naturally, such definition of the masses can depend on the particular framework used. In the following we deal with the *current quark masses*, which are the masses occurring in the QCD Lagrangian. However, because of the quark confinement and the fact that the light quark masses (m_u, m_d, m_s) are very small in comparison to the typical hadron scales, the perturbative QCD cannot be used for their determination and we need to employ non-perturbative methods of QCD. Nowadays, the natural candidates for them are sum rules, lattice QCD and chiral perturbation theory.

QCD sum rules are based on dispersion relations stemming from analytic properties of some observables (such as differential decay rate of τ). They connect together the hadron world measured in experiments with the perturbative QCD in terms of operator

product expansion. For the recent review on the sum-rule results on light quark masses we refer to [110, 60]. Note that a computation of electromagnetic corrections within sum-rule methods would be very difficult since an inclusion of long-range interactions changes significantly analytic properties of the amplitudes, which makes it impossible to write dispersion relations in the regular form.

Numerical simulations on lattice have achieved in recent years a considerable progress — the current day simulations are performed with $2 + 1$ dynamical quarks, moreover, with m_s near its physical value. However, in order to reach the physical point in $m_{u,d}$, chiral extrapolation is predominantly still necessary. Again the inclusion of electromagnetic interactions on the lattice is very involved for their long-range character, nevertheless, even in this aspect, there is some progress as quenched QED simulations are already performed (e.g. [38]). In recent years there appeared two attempts [46, 102] to review and average existing lattice calculations of various quantities, including m_q, where more details can be found.

Both of these methods independently determined the values of m_s and of the isospin averaged mass $\hat{m} = \frac{m_u+m_d}{2}$ with a reasonable precision with more-or-less compatible results. But since the isospin breaking effects generated by electromagnetic interactions are of the same order as those stemming from $m_u - m_d$ difference and there occur the above mentioned problems with the direct inclusion of the electromagnetic corrections into the nowadays studies within both of these frameworks, for the determination of the individual masses m_u and m_d they both need an additional input[1].

A framework that can provide such an input is chiral perturbation theory. We recall that for the determination of the quark masses, χPT alone is insufficient. It is so because in all physical results, the quark masses occur multiplied by the scalar quark condensate B_0 and thus rescaling both of them does not change the physics. In addition, starting at next-to-leading order in chiral counting, there exists the following transformation of the masses [92]

$$m'_u = m_u + \lambda m_d m_s, \quad m'_d = m_d + \lambda m_s m_u, \quad m'_s = m_s + \lambda m_u m_d, \tag{9.1}$$

which together with the corresponding shifts in low-energy constants

$$L'_6 = L_6 - \lambda \frac{F_0^2}{32B_0}, \quad L'_7 = L_7 - \lambda \frac{F_0^2}{32B_0}, \quad L'_8 = L_8 + \lambda \frac{F_0^2}{16B_0} \tag{9.2}$$

and similar shifts in some of the NNLO constants C_i leave the pseudoscalar masses, scattering amplitudes and matrix elements containing vector or axial vector currents invariant. Thus, using only experimental measurements we cannot fix this so-called Kaplan-Manohar ambiguity. Consequently, χPT can determine only quark mass ratios and needs some external theoretical input in order to fix the physical definition of the masses (otherwise the

[1]Even for a precise determination of m_s, electromagnetic interactions cannot be neglected. However, since they are here less important, at the current level of precision of the determination of m_s it is enough to take an estimate of them.

χPT masses could be different with respect to the current quark masses we want to determine). For a review of χPT NLO determinations of light quark masses, we refer to [107]. In addition, in [10] the employment of NNLO meson mass formulae is included.

For a more precise determination of light quark masses it is therefore useful to combine isospin symmetric results of the lattice QCD and the sum-rules with some isospin-breaking study performed in χPT. A very suitable process for such a study is $\eta \to 3\pi$ decay[2], which is possible only in the isospin breaking world. Moreover, as was discussed in Section 6.2 the electromagnetic contributions to this decay are very small and thus its amplitude is to a good approximation directly proportional to $m_d - m_u$. We pull out the following normalization factor out of the amplitude [cf. (6.48)]

$$\tilde{\mathcal{M}}(s,t,u) = \frac{\sqrt{3}}{4R}\tilde{M}(s,t,u), \quad \text{with} \quad R = \frac{m_s - \hat{m}}{m_d - m_u}\,. \tag{9.3}$$

By a computation of the so defined $\tilde{M}(s,t,u)$ in χPT and its comparison to the measured decay rate of this decay Γ, one can determine the parameter R. As we have already discussed, after pulling out this isospin breaking parameter we can perform isospin limit in the rest of the amplitude $\tilde{M}(s,t,u)$, which provides a very good approximation.

9.2 Recent theoretical approaches to $\eta \to 3\pi$

In Section 6.2 we have summarized all the recent computations of $\eta \to 3\pi$ amplitude. We recall that the two-loop computation within χPT exists [33] but there are several hints questioning the value of R deduced from this computation.

First of them is connected with the observed large chiral corrections in the first three successive orders — we can illustrate it on Figure 14, where we have plotted the squared amplitudes stemming from LO, NLO and NNLO computations in χPT, or on the values of R which follow from these amplitudes if we combine them with the experimental value of the decay rate of the charged process $\Gamma = 295(16)\,\mathrm{eV}$ [110]

$$R_{\mathrm{LO}} = 19.1, \quad R_{\mathrm{NLO}} = 31.8, \quad R_{\mathrm{NNLO}} = 41.3. \tag{9.4}$$

The second hint is connected with the observed discrepancies between the experimentally measured values of Dalitz parameters and the values predicted from [33] — cf. Tables 7 and 8. For a better quantification of the difference between experiment and theory, we can introduce

$$\chi^2 = \left(\frac{\mathrm{exp} - \mathrm{theor}}{\sigma[\mathrm{exp}]}\right)^2, \tag{9.5}$$

where exp and σ[exp] are the central value and the error bars of the experimentally measured value and theor is the value of the considered quantity predicted by the theory.

[2] In addition to the studies referred in Section 6.2, we refer also to [45], which was one of the first studies taking seriously into account the results of $\eta \to 3\pi$ decay together with the first lattice determinations in order to put constraints on the quark masses.

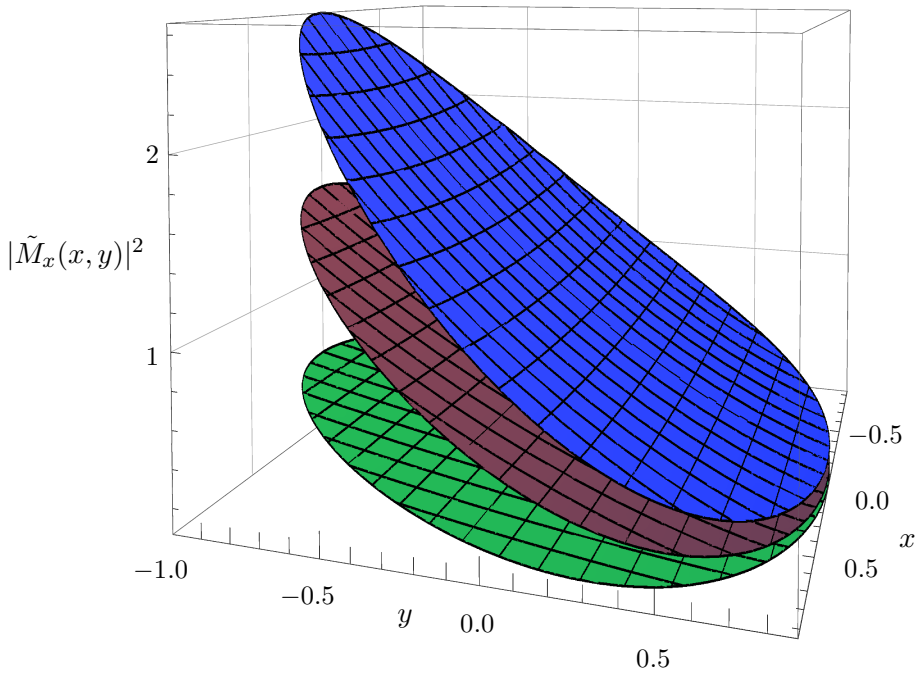

Figure 14: The squared amplitudes of the charged $\eta \to 3\pi$ decay stemming from χPT computation in the first three chiral orders. The green, red and blue surfaces correspond to LO, NLO and NNLO amplitudes, respectively. The plot is normalized by taking the NNLO amplitude in the center of the Dalitz plot equal to one.

For the neutral parameter α, which is most often put forward in this aspect, we obtain a huge difference of $\chi^2 = 225$. However, there is a parameter with even more apparent discrepancy, namely b with $\chi^2 \sim 500$.

A third hint questioning the accurateness of the R determination from the two-loop χPT computation as well as a possible explanation of the discrepancies in Dalitz parameters is the poor knowledge of the $O(p^6)$ low-energy constants (LECs) C_i. Two-loop amplitudes depend on subsets of 102 C_is, whose determination is needed before any reliable prediction. However, nowadays we are far from a determination of all required LECs from experiment (or lattice), and hence for many of them we have to rely on some estimates, predominantly of the resonance saturation type [64, 63, 109, 96]. This brings an unknown error into the game — the error presented in [33] is an estimate by the authors obtained by taking the uncertainty of the amplitudes equal to one half of the two-loop contributions.

These complications impose the following questions: What is the origin of the Dalitz parameters discrepancy? How do this discrepancy together with the slow chiral convergence and the poor knowledge of the C_i's influence the determination of the isospin breaking ratio R?

This has inspired various theoretical studies exploring possible explanations of the discrepancy, namely the effect of higher order final state rescattering [90, 17, 50], the influence

of slow chiral convergence of $\pi\pi$ scattering or of $\eta \to 3\pi$ amplitude itself [122, 99], unexpectedly large electromagnetic corrections [112, 111], effects of resonances or with that connected possibility of incorrectly estimated values of C_i's [99].

We have discussed some of these studies already in Section 6.2, so we emphasize here only their aspects related to the extraction of the information on the quark masses. From these four types of studies, quark masses appear explicitly only in two of them [99,112,111] as these two are using chiral perturbation theory.

In [112, 111] the authors have pointed out that the electromagnetic corrections coming from their partial two-loop computation (taking into account only a subset of the diagrams contributing at the $O(e^2p^4)$ order) have in their particular renormalization scheme at the particular scale they are computing unexpectedly large value and it can happen that these contributions will not be canceled by the counter terms and the further diagrams not yet computed. [Note that such cancellation has happened at the electromagnetic one-loop level [59].] These partial results therefore send an alert that the smallness of the electromagnetic corrections is not automatic as one would naively expect. Hopefully, after the completion of the analysis it will answer the question, whether the complete two-loop electromagnetic contribution is large enough to explain the observed discrepancies in Dalitz plot parameters or whether the largeness of the partial results presented in [112, 111] was just due to an inappropriate choice of the regularization/renormalization scheme (leading to large cancellation of the individual contributions in the total correction).

The study [99] uses the framework of resummed[3] chiral perturbation theory [57, 55] changing the usual treatment of chiral series and of their remainders. The preliminary studies of [99] show that whereas the discrepancy in b can be accommodated by higher chiral orders of the expected small size, the experimentally observed value of α cannot be explained by the higher chiral orders if we assume good convergence properties of both the chiral amplitudes themselves and of their derivatives (one have to weaken at least the second requirement). The results of partial studies of the effects of resonances and of the higher $\pi\pi$ rescattering are also discussed in [99] but the satisfactory explanation of the Dalitz parameter discrepancies was not found yet.

Putting aside these two ongoing studies, which do not deal directly with the quark mass determination yet, we are left with two alternatives to χPT, the dispersive methods [90, 17, 50] and the non-relativistic effective field theory [72, 82, 122]. In order to understand their relative advantages and disadvantages, let us recall a few basic properties they share. All these approaches are constructed as effective field theories that on the basis of some assumptions (usually represented by some expansion of the amplitude) divide the phase-space of each amplitude into the "low-energy part" that is included in the computation and the "high-energy part" that is not known or at least less known. At tree-level one simply uses the amplitudes only in the low-energy region and is not concerned by what lies above the cut-off. In order to work consistently, one needs to introduce a mechanism

[3]This adjective "resummed" denoting the framework introduced in [57,55] should not be confused with the adjective "resummed" denoting one of the possible approaches to the polynomial appearing in the reconstruction theorem from Section 3.6.

that picks up the contributions that contribute with the same importance to a given order, usually represented by a power-counting. Then, when computing the amplitude to the higher order, one needs to include also loop contributions (either by means of taking into account loop Feynman diagrams, as a unitarity contribution, or by any other method), where one has to integrate also over the high-energy part of the intermediate amplitudes (over higher momenta of the intermediate virtual particles). By using the "power-counting mechanism" or by adding some further assumptions, part of these contributions are considered negligible, but there always remains a part that is finite and unknown and has to be parametrized somehow — usually there occur new effective parameters in the model and the old ones are renormalized or shifted. Note that in χPT (representing a Lagrangian effective field theory) the power-counting mechanism is given by the chiral counting, which also monitors the number of LECs (effectively containing the contribution of the physics above the chiral cut-off — the hadronic scale) appearing at a given order.

In the usual dispersive approaches [90, 17, 50], which attempt to obtain the amplitudes with two-pion rescattering effects formally included to all orders, the mechanism assigning the importance to a given contribution is based on the assumption that the two-pion rescattering effects are dominant. In the low-energy part of the amplitudes, the unitarity contribution of the physics above the threshold, where further intermediate states contribute and where the S and P partial waves of the considered amplitudes cease to be the dominant ones, are taken into account through subtraction constants. However, in order to restrict their number to a reasonable amount, one needs to impose some assumptions on the high-energy region (of both the physical amplitudes and of the amplitude constructed iteratively by the numerical method). In [17, 50] these assumptions are specified by the requirement to have only four[4] of them.

The methods based on the modified non-relativistic effective field theory (NREFT) [72, 82, 122] implement instead of the usual chiral expansion a combined expansion in powers of a formal non-relativistic parameter ϵ and of a formal partial-wave $\pi\pi$ scattering-characteristics parameter a (representing scattering lengths and higher threshold shape parameters). The amplitude is then computed to the two-loop order in the NREFT Lagrangian formalism. The power-counting scheme is therefore based on the non-relativistic expansion together with the loop expansion (which is equivalent in this case to the expansion in the pion scattering parameters). In [122] the results are presented including the orders up to $O(\epsilon^4), O(a\epsilon^5), O(a^2\epsilon^4)$, and partially also $O(a^2\epsilon^6)$ and $O(a^2\epsilon^8)$. By assuming that the included orders are dominant, the contribution of the intermediate states other than the two-pion ones have to be included through four parameters [cf. footnote 4] coming from local interaction terms.

Naturally, the reasonable question that has to be addressed in the future is whether each set of assumptions (either of χPT, of the dispersive approaches, or of the modified NREFT) adequately describes the physics, and whether a possible drawback in this respect

[4]Here we classify the number of parameters appearing in the case we take masses of the charged and the neutral pions equal, $m_{\pi^\pm} = m_{\pi^0}$. Note that from our analysis it is obvious that in two-loop χPT results there occur at least six independent combinations of LECs.

in any of them is paid off by the other advantages it possesses. The advantages and the disadvantages of these approaches were nicely summarized in [100]. We emphasize only that NREFT provides analytic results that are easy to extent beyond the $m_{\pi^\pm} = m_{\pi^0}$ limit, while the dispersive methods [90, 17, 50] proceed numerically and their extension to full isospin breaking was never studied. On the other hand, whereas the NREFT expansion in ϵ is safe only inside the Dalitz region, the results of the dispersive approaches should work also in some larger regions beyond it. Both types of approaches have in common that, in contrast to χPT, they directly use the physically measured $\pi\pi$ scattering parameters as inputs, but there remain four free parameters that have to be fixed from matching either to χPT or to experimental data. Moreover, since the studied decay amplitudes depend on R or Q merely just through their normalization, which is factored out in both of methods, even if those representations are fitted to experimental data, the determination of R or Q would still require to match with χPT at least at one point, thereby fixing the normalization.

The matching is not an easy task in this context. In addition to the differences in the structures of these results, since we are matching two different approaches with different power-counting schemes and assumptions, we need to find the region (or as discussed above at least one point) and the appropriate orders in both approaches in which their results are compatible. Nevertheless, thanks to the simple form of the one-loop χPT amplitude, and to the fact that the physical regions of $\eta \to 3\pi$ decays are quite small, in both approaches the matching to one-loop χPT was obtained (cf. [17, 50] and [122]).

In conclusion, in order to determine the correct value of R from $\eta \to 3\pi$ decays, one cannot avoid discussing either the accuracy of the χPT result and its possible corrections (by correcting the values of $O(p^6)$ LECs C_i or by inclusion of some higher-order corrections into the χPT calculation) or the existence of at least one point (or some region) where the current chiral result reproduces well the complete physical amplitude. For instance, the discussion of the influence of the C_i's on the results can be studied using directly the χPT amplitude, but its complexity and its extreme length together with the fact that it includes many C_i's complicates such an analysis.

9.3 The use of the analytical dispersive representation of $\eta \to 3\pi$ amplitude

The two-loop representation of $\eta \to 3\pi$ amplitude constructed in Chapter 7 contains the χPT result as a special case [the assumptions used for its construction are compatible with χPT] but have a simpler compact analytic form, therefore, there naturally offers itself the possibility to use the analytical dispersive representation for addressing the questions we have premised before, namely, whether one can obtain a reasonable agreement in the determination of the Dalitz parameters from experiment and from the NNLO χPT amplitude with the corrected set of the C_is; how such a change would influence the determination of R; possibly also whether there exists another simple way how to solve that disagreement.

Moreover, since the representation is more general than the χPT amplitude [the values

of its parameters do not need to be held fixed at the χPT values] and it is based only on the general properties of field theories and on the hierarchy of various contributions to the amplitude from Section 2.3, we do not need to work in such a close connection to the χPT amplitude[5] and fit the representation directly to the experimental data. We can thus change completely our strategy and instead of trying to correct the amplitude stemming from χPT, we use our representation as a parametrization of the data, from which we can compute the value of R. However, as was discussed above, also in this case we need to fix the normalization from χPT. For that end we would need to find a region where the chiral expansion of the amplitude converges fast, where the two-loop χPT amplitude reproduces the physics well. Thanks to the form of our representation and its simple connection to χPT, the analytic dispersive method is helpful also in this analysis, resulting with the recipe for such matching.

Before we discuss these analyses, we recall the form of the parametrization and perform its matching to the χPT result [33].

In the context of the above discussion of various approaches in effective field theory we recall that the requirement of having our representation valid to two loops in chiral counting picks up the contributions that have to be included into the computation and tells us that at the low-energy region up to this chiral order all the other effects are taken into account effectively in terms of six subtraction parameters [cf. again footnote 4]. The amplitude $\tilde{M}_x(s,t,u)$ from (9.3) in this parametrization reads

$$\tilde{M}_x(s,t,u) = \tilde{R}_x(s,t,u) + 16\pi\tilde{U}_x(s,t,u) + O(p^8), \tag{9.6}$$

where $\tilde{R}(s,t,u)$ is the polynomial containing those six (dimensionless) parameters

$$\begin{aligned}\tilde{R}_x(s,t,u) = A_x + \frac{B_x}{F_\pi^2}(s-\tilde{s}_0) + \frac{C_x}{F_\pi^4}(s-\tilde{s}_0)^2 + \frac{D_x}{F_\pi^4}\left((t-\tilde{s}_0)^2 + (u-\tilde{s}_0)^2\right) \\ + \frac{E_x}{F_\pi^6}(s-\tilde{s}_0)^3 + \frac{F_x}{F_\pi^6}\left((t-\tilde{s}_0)^3 + (u-\tilde{s}_0)^3\right)\end{aligned} \tag{9.7}$$

and the unitarity part

$$\tilde{U}_x(s,t,u) = \tilde{U}_x(s,t,u; A_x, B_x, C_x, D_x; \alpha_\pi, \beta_\pi, \lambda_1, \lambda_2) \tag{9.8}$$

is expressed in terms of single variable dispersion integrals from Section 7.5.2 and depends on the $\pi\pi$ parameters[6] and the lower order parameters of the $\eta \to 3\pi$ amplitude. As was discussed in Section 3.6, depending on our treatment of various chiral orders, the values of $A_x, \ldots, D_x$ inside the unitarity part can be taken either equal to the values appearing in the polynomial part in the case of the resummed approach, or can be taken in each

[5] In Section 2.3 we have discussed mainly the validity of the individual assumptions for χPT but from those discussions it should be obvious that we can require their validity also for a more general framework — this requirement is justified also from the previous numerical studies of $\eta \to 3\pi$.

[6] We have specified them here as the subthreshold parameters of the $\pi\pi$ scattering $\alpha_\pi, \ldots \lambda_2$, but the scattering length parameters can be used as well.

instance with the appropriate chiral order in the case we want to respect strictly the chiral counting in our order-by-order approach.

In the following, we will refer also to the results of our analysis in [VI], where we have used a slightly different parametrization. The polynomial part was taken to be

$$\tilde{R}_x(s,t,u) = \frac{1}{F_\pi^2}\Big(A'_x m_\eta^2 + B'_x(s-\tilde{s}_0) + C'_x(s-\tilde{s}_0)^2 + D'_x\left((t-\tilde{s}_0)^2+(u-\tilde{s}_0)^2\right) + E'_x(s-\tilde{s}_0)^3 + F'_x\left((t-\tilde{s}_0)^3+(u-\tilde{s}_0)^3\right)\Big). \quad (9.9)$$

Relations between these two sets of parameters are therefore

$$A_x = A'_x\,\frac{m_\eta^2}{F_\pi^2}, \qquad B_x = B'_x, \qquad C_x = C'_x\,F_\pi^2, \quad (9.10)$$

$$D_x = D'_x\,F_\pi^2, \qquad E_x = E'_x\,F_\pi^4, \qquad F_x = F'_x\,F_\pi^4. \quad (9.11)$$

However, we have taken there also a little bit different subtraction scheme in the two-loop unitarity part [7]. These two parametrizations therefore differ by a polynomial, which is in general complex. It contains the values of Hilbert transforms $\mathcal{G}_j(s)$ evaluated in various points connected with the subtraction schemes and depends on the masses m_η, m_π and on the decay constant F_π. Its form is more complicated than it was in the $\pi\pi$ case (5.191)–(5.196), we therefore display just the numerical values corresponding to the masses and F_π from (9.27)–(9.28),

$$A_x^{(6)} = A'_x\,\frac{m_\eta^2}{F_\pi^2} - 0.025 - 0.022\,i, \quad (9.12)$$

$$B_x^{(6)} = B'_x - 0.066 + 0.035\,i, \quad (9.13)$$

$$C_x^{(6)} = C'_x\,F_\pi^2 - 0.0021 + 1.3\cdot 10^{-5}\,i, \quad (9.14)$$

$$D_x^{(6)} = D'_x\,F_\pi^2 + 5.6\cdot 10^{-4} - 4.4\cdot 10^{-4}\,i, \quad (9.15)$$

$$E_x^{(6)} = E'_x\,F_\pi^4 - 2.2\cdot 10^{-4} - 1.6\cdot 10^{-4}\,i, \quad (9.16)$$

$$F_x^{(6)} = F'_x\,F_\pi^4 + 1.1\cdot 10^{-4} + 7.4\cdot 10^{-5}\,i. \quad (9.17)$$

We have labeled these parameters with the upper index "(6)" in order to indicate that these numerical shifts have to be added only in the case we work with the $O(p^6)$ order of the parameters, i.e. in the polynomial part of the NNLO parametrization in order-by-order approach or in all appearances of these parameters in the case of the resummed approach.

9.4 Connection of the analytic dispersive parametrization with χPT

Similarly, as was done for the $\pi\pi$ scattering in Section 5.11, we shall find in the following the values of our parameters corresponding to the two-loop χPT amplitude [33]. However,

[7] In the current work we have demanded dimensionless functions $\mathcal{F}_j(s)$ and each term of the polynomial is multiplied by the Hilbert transform with the minimal possible number of subtractions, which was not the case in [VI].

before doing that we have to discuss the effects that are neglected or approximated in our representation with respect to the complete standard χPT two-loop calculation from [33].

In analogy to our dispersive representation, the $O(p^6)$ χPT amplitude can also be split into a polynomial part and a non-analytic unitarity part. The former corresponds to the tree-level counterterm contributions as well as to the chiral logs and sunset diagrams (Figure 30e), while the latter takes explicitly into account the nontrivial contributions of the loops. Though this splitting is not unambiguous and depends on the particular definition of the nontrivial part of the loop graphs, the unitarity part has to reproduce the correct discontinuities of the amplitude as required by unitarity and corresponding to the two-particle intermediate states. Along with the pure pion loop contributions also the higher intermediate states are taken into account, namely, the graphs with K and η inside the loops. However, below the $\pi\eta$ threshold the contributions of discontinuities corresponding to the $\pi\eta$, KK and $\eta\eta$ intermediate states are analytic and can therefore be expanded in powers of s, t, u. Sufficiently far below these thresholds one can show that their effects can be approximated by means of only the terms up to the third order — we perform the numerical estimate of the error introduced by that in the next section. As a result we should obtain in this region an approximate χPT amplitude with the same structure as our dispersively constructed amplitude (recall that both of them include the higher non-Goldstone intermediate states contributions only effectively through the low-energy and the subtraction constants, respectively). The only difference is that the polynomial part of the $O(p^6)$ χPT amplitude is generally complex due to the contribution of the sunset diagram with three intermediate pions which develops a nonzero imaginary part. However, it has been found to be tiny in [33] and therefore can be neglected — we reverify this observation again in the next section.

We have already noted that for the matching with the χPT result the natural treatment of the various chiral orders in our representation is the order-by-order fit, in which the parameters $A_x, \dots, F_x$ are split into their $O(p^2)$, $O(p^4)$ and $O(p^6)$ parts, i.e.

$$A_x = A_x^{(2)} + \Delta A_x^{(4)} + \Delta A_x^{(6)}, \qquad B_x = B_x^{(2)} + \Delta B_x^{(4)} + \Delta B_x^{(6)}, \tag{9.18}$$

$$C_x = C_x^{(4)} + \Delta C_x^{(6)}, \qquad D_x = D_x^{(4)} + \Delta D_x^{(6)}, \tag{9.19}$$

$$E_x = E_x^{(6)}, \qquad F_x = F_x^{(6)}. \tag{9.20}$$

We determine these individual parts by the following consecutive matching procedures in each chiral order.

The $O(p^2)$ χPT amplitude is exactly reproduced by taking

$$A_x^{(2)} = \frac{m_\eta^2 - m_\pi^2}{3F_\pi^2}, \qquad B_x^{(2)} = 1 \tag{9.21}$$

in the leading order parametrization (7.7).

The imaginary part of the $O(p^4)$ χPT amplitude below the $\pi\eta$ threshold is fixed by unitarity and is thus equal to

$$\operatorname{Im} U_x^{(4)}(A_x^{(2)}, B_x^{(2)}; \alpha_\pi^{(2)}, \beta_\pi^{(2)}), \tag{9.22}$$

where

$$\alpha_\pi^{(2)} = \beta_\pi^{(2)} = 1 \tag{9.23}$$

are the leading order χPT values of the $\pi\pi \to \pi\pi$ subthreshold parameters [cf. (4.29)–(4.32)]. Hence, up to a polynomial of the second order in s, t, u, the chiral $O(p^4)$ amplitude (with the contributions of $\pi\eta$ and KK intermediate states expanded to second order polynomial as discussed above) is exactly reproduced by $U_x^{(4)}$. We therefore subtract $U_x^{(4)}$ from the chiral amplitude and obtain the desired polynomial.

Similarly to the $\pi\pi$ case, it should be possible (and in order to make the analyses of the following sections more precise also desirable) to obtain an exact analytic expression for $\Delta A_x^{(4)}, \Delta B_x^{(4)}, C_x^{(4)}$, and $D_x^{(4)}$. However, for the current level of precision it is sufficient to perform a numerical fit as is described below. This numerical analysis has also such benefit that it visualizes the effect of the choice of the fitting points to the values of the parameters.

Once these $O(p^4)$ parameters are fixed, we can proceed similarly to the $O(p^6)$ order. At this order the unitarity part obtains corrections

$$\begin{aligned}&\mathcal{U}_x^{(4)}(\Delta A_x^{(4)}, \Delta B_x^{(4)}; \alpha_\pi^{(2)}, \beta_\pi^{(2)}) + \mathcal{U}_x^{(4)}(A_x^{(2)}, B_x^{(2)}; \Delta\alpha_\pi^{(4)}, \Delta\beta_\pi^{(4)})\\ &+ \mathcal{U}_{\lambda\pi}^{(6)}(A_x^{(2)}, B_x^{(2)}; \lambda_1^{(4)}, \lambda_2^{(4)}) + \mathcal{U}_{\lambda\eta}^{(6)}(C_x^{(4)}, D_x^{(4)}; \alpha_\pi^{(2)}, \beta_\pi^{(2)}) + \mathcal{U}_{2-\mathrm{loop}}^{(6)}(A_x^{(2)}, B_x^{(2)}; \alpha_\pi^{(2)}, \beta_\pi^{(2)}),\end{aligned} \tag{9.24}$$

where the last term corresponds to the genuine 2-loop contributions (in our approximation containing terms each with one LO $\eta \to 3\pi$ parameter multiplied by the product of two LO $\pi\pi$ scattering parameters) while the other four terms correspond to the 1-loop contributions (containing terms with products of one NLO parameter and one LO parameter). In addition to the parameters known from the previous steps, there appear also the NLO corrections to the subthreshold $\pi\pi$ parameters, which we have discussed in Section 5.11. In order to keep the correspondence between the parametrization and the two-loop results of [33] as close as possible, we take their values corresponding to Fit10 [cf. Table 4]

$$\alpha_\pi^{(4)} = \alpha_\pi^{(2)} + \Delta\alpha_\pi^{(4)} = 1.05(2), \qquad \lambda_1^{(4)} = -1.6(1.8)\cdot 10^{-3}, \tag{9.25}$$

$$\beta_\pi^{(4)} = \beta_\pi^{(2)} + \Delta\beta_\pi^{(4)} = 1.085(2), \qquad \lambda_2^{(4)} = 8.4(5)\cdot 10^{-3}. \tag{9.26}$$

Again by subtracting this unitarity part from the $O(p^6)$ part of the chiral amplitude, we obtain the $O(p^6)$ polynomial depending on $\Delta A_x^{(6)}, \ldots, \Delta D_x^{(6)}$, $E_x^{(6)}$ and $F_x^{(6)}$. Since the $O(p^6)$ chiral amplitude [33] is known only numerically, in this case we cannot avoid a numerical fitting procedure.

On this place we shall specify the numerical values of the pseudoscalar masses and the pion decay constant used in the following numerical analyses. In order to be in exact correspondence with [33] we have taken

$$m_\eta = 547.3\,\mathrm{MeV}, \qquad F_\pi = 92.4\,\mathrm{MeV} \tag{9.27}$$

even thought the recent analyses indicate slightly different values $m_\eta = 547.9\,\mathrm{MeV}$ ([7]; cf. also [80]) and $F_\pi = (92.22 \pm 0.07)\,\mathrm{MeV}$ (e.g. [91]). In order to fully include these changes

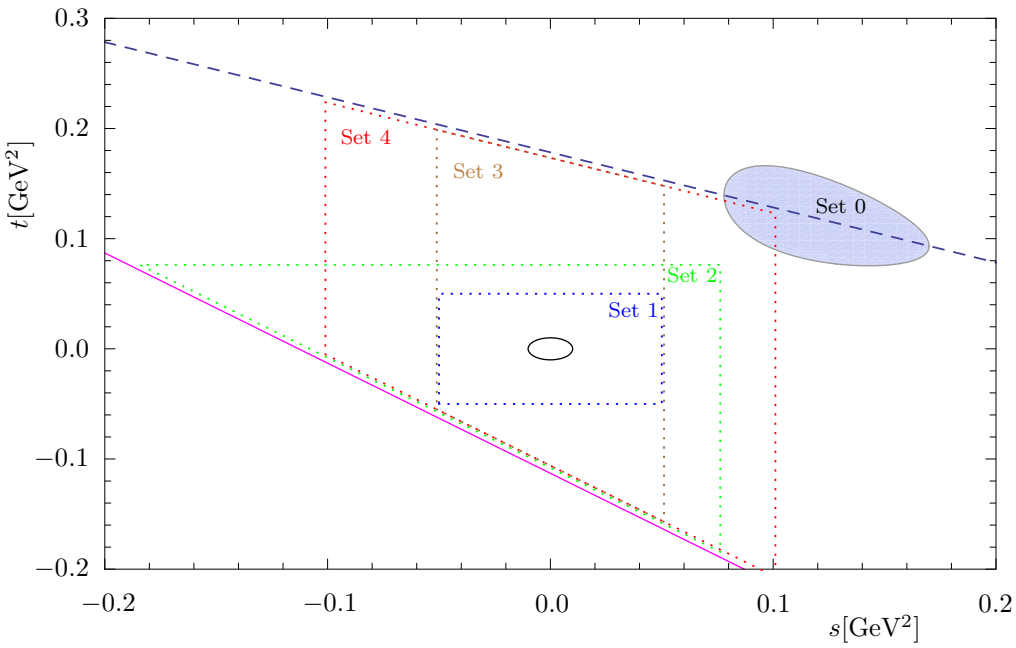

Figure 15: Various regions used for the matching procedure of the analytic dispersive parametrization for $\eta \to \pi^+\pi^-\pi^0$ amplitude with the corresponding result of NNLO χPT [33] — the individual regions denoted by dotted lines. The blue oval corresponds to the physical region. The full magenta line indicate the $\pi\eta$ threshold (where the representation ceases to be adequate. The blue dashed line represents the axis of the $t-u$ symmetry of the amplitude.

into our analyses, redoing of the computation [33], which is needed for our inputs, with the new values would be necessary. However, one should note that a mere change of these values in our final results (with the values of the subtractions parameters fixed) leads to a shift in the value of R of about 0.5%, which is negligible with respect to the other sources of errors. A slightly different situation is with the pion masses. Even though we are working in the limit $m_{\pi^\pm} = m_{\pi^0}$, it is more proper to take different numerical values of the isospin mass m_π for the charged and the neutral decays. By taking $3m_\pi^2 = 2m_{\pi^\pm}^2 + m_{\pi^0}^2$ for the charged decay (and $m_\pi = m_{\pi^0}$ for the neutral decay) we reproduce exactly the physical location of the center of the Dalitz plot and reproduce almost exactly the physical value of normalization $Q_\eta = m_\eta - 2m_{\pi^\pm} - m_{\pi^0}$ in the definition of Dalitz variables x and y from (6.34). This choice is especially important for the value of Q_η since

$$(m_\eta - 2m_{\pi^\pm} - m_{\pi^0}) : (m_\eta - 3m_\pi) : (m_\eta - 3m_{\pi^0}) = 1 : 0.9996 : 1.0690$$

and by taking the isospin mass m_π equal to m_{π^0} in the case of the charged decay, we would induce the error of Dalitz plot parameters and thereby also of the parameter R of about 7% (cf. also the discussion in [122]). For the similar reasons we take in the computation of the integration over the phase space, its boundaries equal to the physical ones. We again take the numerical values corresponding to [33] since the slight change in these values with

		A_x	B_x	$10^3 C_x$	$10^3 D_x$	$10^4 E_x$	$10^4 F_x$	$1-r^2$
Set 0 (physical)	$O(p^2)$	10.95	1.000					0
	$O(p^4)$	16.27	1.955	$-3.620(7)$	9.19			10^{-9}
	$O(p^6)$	20.27	2.357	$-0.470(4)$	13.92	1.62(1)	$-1.78(1)$	$3\cdot10^{-10}$
	$O(p^{6+p^8})$	20.27	2.356	$-0.57(1)$	13.92	1.55(1)	$-1.77(1)$	$1\cdot10^{-10}$
	Imag. parts $O(p^6)$	0.22(2)						$2\cdot10^{-3}$
		0.220	0.099					10^{-5}
		0.202	0.098	2.25(5)				$9\cdot10^{-7}$
		0.208	0.098	2.27(3)	$-0.38(2)$			$3\cdot10^{-7}$
		0.209	0.096	2.18(2)	$-0.40(1)$	1.08(8)		10^{-7}
		0.209	0.096	2.19(2)	$-0.37(1)$	1.15(7)	$-0.31(4)$	$9\cdot10^{-8}$
Set 4	$O(p^4)$	16.58(1)	1.990(2)	$-2.43(6)$	8.89			$5\cdot10^{-5}$
	$O(p^6)$	20.35	2.399(1)	1.34(9)	14.04	2.05(2)	-1.641	10^{-6}
	$O(p^{6+p^8})$	20.34	2.383(3)	$-1.3(4)$	13.98	0.5(2)	-1.61	$9\cdot10^{-7}$
	Imag. parts $O(p^6)$	$-0.78(2)$						0.05
		$-1.61(4)$	$-0.062(3)$					0.04
		$-1.13(7)$	0.03(1)	3.4(4)				0.04
		$-0.10(1)$	0.053(2)	3.92(7)	-0.93			10^{-3}
		$-0.05(2)$	0.071(6)	5.4(5)	-0.93	0.4(1)		10^{-3}
		0.24	0.104(1)	6.2(1)	-1.19	0.42(2)	0.16	$5\cdot10^{-5}$

Table 11: Values of parameters describing χPT $\eta\to3\pi$ amplitude in various chiral orders obtained from the successive fitting procedure described in the text. The error bars stemming from the fits are specified in brackets or are less than the number of significant digits presented. The corresponding values of parameters G_x, H_x, I_x for fits $O(p^{6+p^8})$, where we have added the polynomial terms of the fourth order, are listed in the text.

respect to the recent ones induce a negligible error. Numerically, for the charged decay we take

$$m_\pi = 138.0558\,\mathrm{MeV}, \qquad m_{\pi^\pm} = 139.5702\,\mathrm{MeV}, \qquad m_{\pi^0} = 134.9760\,\mathrm{MeV}. \tag{9.28}$$

9.5 Numerical determination of the values of parameters corresponding to NNLO χPT result

In [VI] we have employed FORTRAN codes[8] which produce the two-loop χPT results of [33] for generating five sets of points each inside the corresponding region depicted on Figure 15.

[8]These codes were provided to us by Hans Bijnens (one of the authors of [33]).

These sets were fitted with MINUIT package according to the procedure described in the previous section. We will not repeat here the complete analysis of [VI] but we present here only the results of the fits[9] for Sets 0 and 4 in Table 11. Set 0 represents the physical region and Set 4 is the one with the largest extent (i.e. the coefficients of the terms with higher powers can be determined with a higher precision but on the other hand the effect of the neglected contributions on them is here the largest). All of these fits were performed with Wolfram Mathematica. In the ultimate column of Table 11 the resulting adjusted r-squared describing the quality of the corresponding fit is given — the lesser number quoted in table (i.e. r^2 closer to 1) the better fit it provides.

The leading order values are included just for the verification of (9.21). We observe that both the sets of points are parametrized by the appropriate dispersive formula well, as expected the physical Set 0 better than Set 4. The differences between these two sets give us an idea about the effect of the choice of the points for which we perform the fit. With the exception of parameters C_x and E_x such error is reasonably small. The parameter C_x which contributes dominantly to the Dalitz parameters b and f depends strongly on this choice and also obtains the higher chiral order corrections [note its relation with the results of study [99]].

We have also verified two approximations made in our parametrization and studied the numerical error introduced by them to our results. The polynomial part of the two-loop parametrization should be in general complex — this is obvious also from the relations translating the values of the parameters used in [VI] to the values of the parameters used in this work. We have stated that we can simplify the parametrization in the physical region by neglecting the imaginary parts of the parameters. We have therefore performed the above fits only to the real part of the polynomial. However, in Table 11 we have also listed the results of the independent fit to the imaginary parts. We have listed consecutive fits adding an imaginary part to the individual parameters. We observe that in the physical region the quality of the fit with addition of the higher parameters does not change too strong and also the values of the imaginary parts of the parameters from the previous fits do not change significantly after inclusion of further imaginary parts. Therefore, we can approximate the imaginary contribution in the physical region by addition of just $\mathrm{Im}\, A_x^{(6)} = 0.22$. It is about two orders of magnitude smaller than the real part $A_x^{(6)}$ and as we will see in the following it introduce an error in the determination of the physical observables of order 0.7%. Naturally these simplifications are not possible for the Set 4, where the imaginary part depends on the phase-space and each inclusion of the imaginary part to a larger parameter changes significantly the quality of the fit and the values of the previously determined imaginary parts. Note however that the complete fit of imaginary parts to all the NNLO parameters leads to the values of $\mathrm{Im}\, A_x$ and $\mathrm{Im}\, B_x$ similar to the result of the fit on Set 0.

Similarly, in the representation we have neglected higher than third order polynomial terms in expansion of KK and $\pi\eta$ contributions (in the decay region). We can estimate

[9]Note that the other sets can be obtained by using relations (9.10)–(9.17) for the values presented in [VI].

the corresponding error by addition of some higher-order terms into the polynomial. The symmetries dictate that the fourth order polynomial would contain just the terms

$$\frac{G_x}{F_\pi^8}(s-\tilde{s}_0)^4+\frac{H_x}{F_\pi^8}(s-\tilde{s}_0)^2(t-\tilde{s}_0)(u-\tilde{s}_0)+\frac{I_x}{F_\pi^8}\left((t-\tilde{s}_0)^4+(u-\tilde{s}_0)^4\right). \tag{9.29}$$

From dimensional considerations, the contribution of the KK intermediate states into these parameters should be $\sim \frac{F_\pi^4}{(4\pi)^2 M_K^4} \lesssim 10^{-5}$ (and similarly for $\pi\eta$, which is however suppressed by the $SU(2)$ low-energy theorem), whereas even if all of them were $\sim 10^{-3}$ the shift in the determined R would be 0.1% as is obvious from the following paragraphs. This expectation is confirmed by fitting the extended polynomial with these terms added. The values of the parameters corresponding to these fits are included in Table 11 in the lines denoted by $O(p^{6+}p^8)$. For the physical set the fitted values of the additional parameters are

$$G_x = 4.0(5)\cdot 10^{-6}, \qquad H_x = 3.3(7)\cdot 10^{-6}, \qquad I_x = 1(3)\cdot 10^{-7}. \tag{9.30}$$

All of them are of the expected size. We also see that in the physical region the only affected parameters are C_x and E_x, which have changed their values by 20% and 4% respectively. However, note that exactly these parameters are the most sensitive ones to the change of the fitting points.

For Set 4 the values of the additional parameters read

$$G_x = 2.9(3)\cdot 10^{-6}, \qquad H_x = 3.6(4)\cdot 10^{-7}, \qquad I_x = 3.2(2)\cdot 10^{-8}. \tag{9.31}$$

From the other parameters the only one which has changed significantly is E_x.

We have illustrated the individual effects on the amplitudes on Figures 16 and 17 depicting the the real and the imaginary parts of the amplitudes corresponding to the individual sets of parameters determined from the fits along the lines $t = u$ and $s = u$ respectively. [Note that they correspond to the figures 6 and 10 from [33].] We have plotted the complete $O(p^2)$, $O(p^4)$ and $O(p^6)$ amplitudes for Set 0 as denoted on the plots, the dotted lines corresponds to the same amplitudes obtained from Set 4. In the imaginary part of the $O(p^6)$ amplitude we have included also the imaginary parts of the parameters from the corresponding fits. With the dashed line there is illustrated the effect of neglecting this imaginary part (i.e. this line corresponds to our fit $O(p^6)$.

We can also go beyond the strict respecting chiral orders of the representation and use our resummed approach, which is obtained by inserting the full $A_x^{(6)},\ldots,F_x^{(6)}$ (and the NLO $\pi\pi$ parameters) also into the unitarity part. The difference between this resummed parametrization (for Set 0) denoted as Res_0 and the original order-by-order one "$O(p^6)_0$" is of order $O(p^8)$ and contains effectively the contributions of the one and the two-loop diagrams with higher-order counterterms. It might be therefore treated as a rough estimate of the convergence of the chiral expansion.

Further effect we can study is the effect of the $\pi\pi$ parametrization we take in the unitarity part of the amplitude. In Section 5.11 we have found that for that end the suitable parametrization of the $\pi\pi$ scattering could be the scattering length parametrization denoted there as Fit4, which reproduced the physical phase shifts best from all one-loop

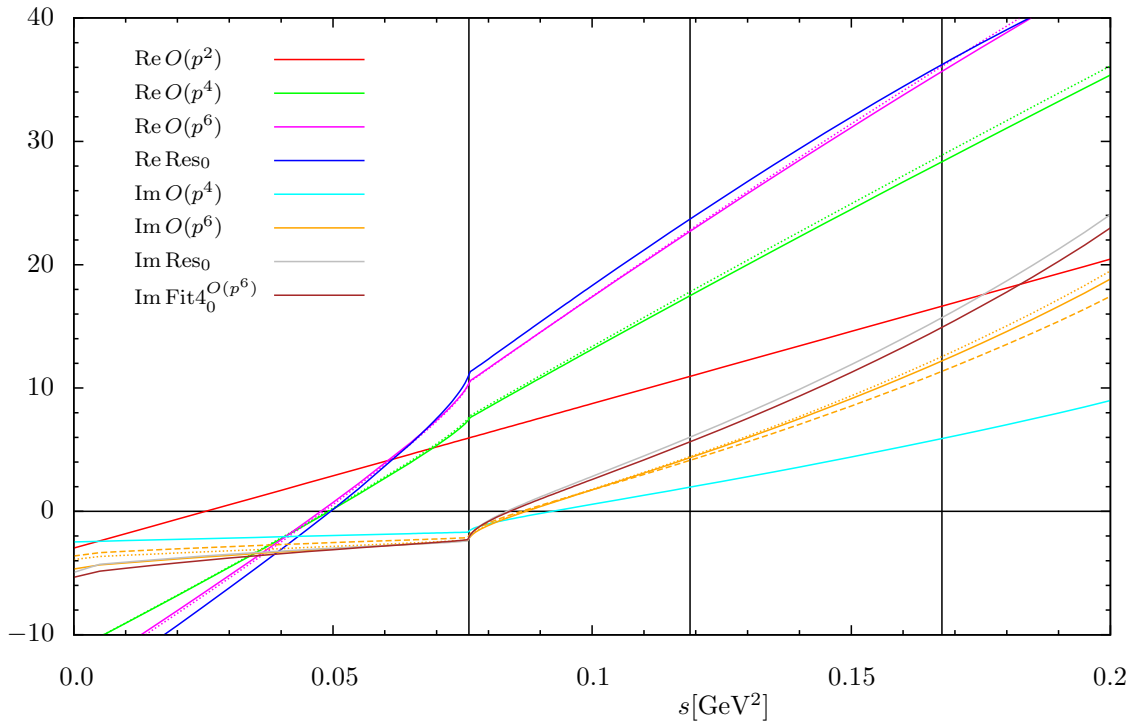

Figure 16: The real and the imaginary parts of the amplitudes of the charged $\eta \to 3\pi$ decay corresponding to various dispersive parametrizations along the line $t = u$. The vertical lines demarcate the physical region and its center.

parametrizations (and in addition is quite stable with respect to the higher order chiral corrections). We assume that this choice will not change significantly the values of parameters $A_x, \ldots, F_x$ determined from the above fit and add such constructed amplitudes, the order-by-order one $\mathrm{Fit4}_0^{O(p^6)}$ and the resummed one $\mathrm{Fit4}_0^{\mathrm{Res}}$, into our further analyses.

For the sake of clearness we have not included on Figures 16 and 17 the real part of the amplitude $\mathrm{Fit4}_0^{O(p^6)}$ which lies between $O(p^6)_0$ and Res_0; and the amplitude $\mathrm{Fit4}_0^{\mathrm{Res}}$, whose both parts lie slightly above the corresponding parts of Res_0.

More important for our further applications are the individual effects on the physical observables, in this case on the Dalitz plot parameters and the normalization imprinted in the isospin-breaking parameter R. In Table 12 are listed the values of Dalitz plot parameters and of the isospin-breaking parameter R corresponding to the various amplitudes — the order-by-order amplitudes are denoted $O(p^n)_j$, where n is the maximal chiral order included in the amplitude and subscript j corresponds to the Set j for which we have fitted the values of the corresponding parameters; we have included also the $O(p^6)$ amplitudes with the non-zero imaginary parts of the parameters $O(p^6)_0^{\mathrm{Im}}$ and with the included higher-order terms from (9.29) $O(p^6)_0^{p^8}$; further there are included the resummed amplitude Res_0 and the amplitudes with the $\pi\pi$ parameters from Fit4. For comparison we have included also the experimental fits for the Dalitz plot parameters from KLOE [8, 9].

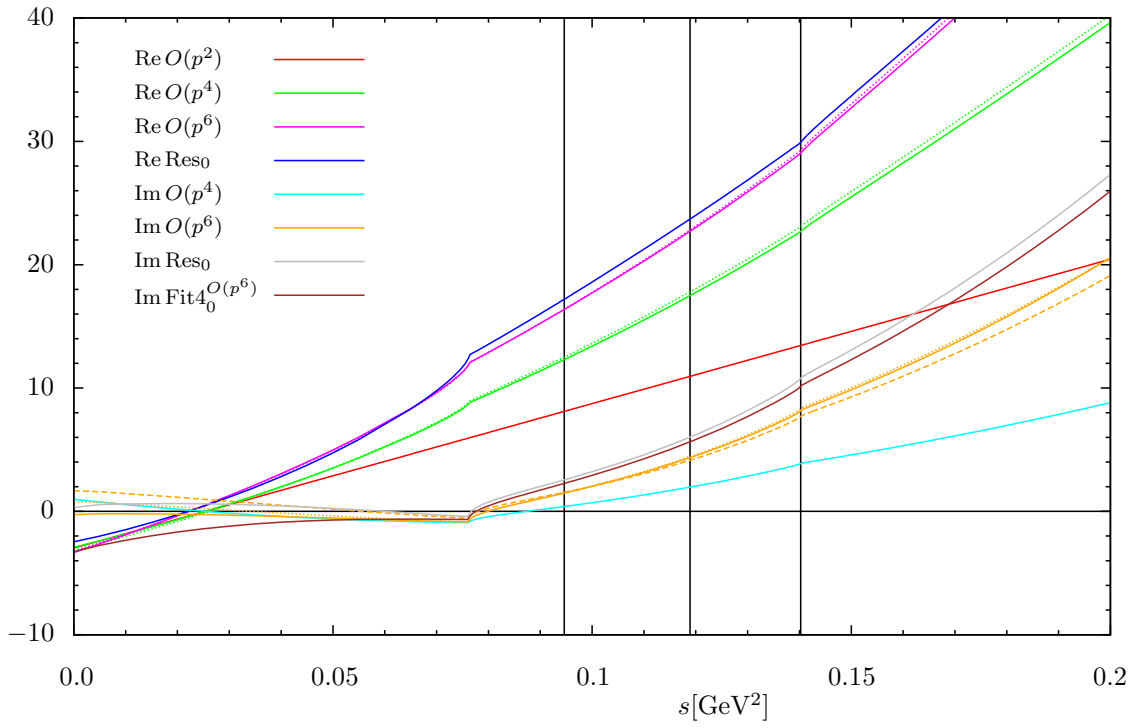

Figure 17: The real and the imaginary parts of the amplitudes of the charged $\eta \to 3\pi$ decay corresponding to various dispersive parametrizations along the line $s = u$. The vertical lines demarcate the physical region and its center.

The values of the Dalitz plot parameters in Table 12 were obtained by fitting the squared amplitudes[10] to the parametrization (6.37) and (6.40) respectively weighted by their error estimated as one half of the higher order ($O(p^n)$) contribution to the $O(p^n)$ amplitude. Note that these fits depend on the number of Dalitz plot parameters we include in the fit. For instance, the inclusion of the parameter g to the fit of $O(p^6)_0^{\rm Im}$ gives

$$A = 534.4, \quad a = -1.260, \quad b = 0.404, \quad d = 0.079, \quad f = 0.007, \quad g = -0.07. \tag{9.32}$$

Similarly, we give the values of the neutral parameter α in Table 12 only with the precision that takes into account their dependence on the choice whether we include also the parameter β.

The values of the parameter R were obtained from the computed decay rates

$$\Gamma = \frac{3}{16R^2}\,\frac{1}{256\pi^3 m_\eta^3}\int \mathrm{d}s\mathrm{d}t\,|\tilde{M}_x(s,t,u)|^2, \quad \Gamma_0 = \frac{1}{6}\,\frac{3}{16R^2}\,\frac{1}{256\pi^3 m_\eta^3}\int \mathrm{d}s\mathrm{d}t\,|\tilde{M}_0(s,t,u)|^2 \tag{9.33}$$

[10] As is common in χPT computations, we have used the complete amplitude squared even though in chiral counting for instance the effect of the squared $O(p^6)$ amplitude is of order $O(p^{12})$, i.e. the same as would be from the multiplication of the $O(p^2)$ and the $O(p^{10})$ parts of the amplitude, which we do not have at disposal in this computation.

	A	a	b	$10^2 d$	$10^2 f$	R	$10^2\alpha$	$10^4\beta$	R_0
$O(p^2)$	119.9	−1.039	0.270	0	0	19.1	0	0	19.7
$O(p^4)_0$	311.4(2)	−1.305(1)	0.406(3)	4.8(1)	3.0(4)	31.5	1.1	−5.5	31.9
$O(p^4)_4$	322.3(2)	−1.305(1)	0.409(2)	4.6(1)	2.7(3)	32.0	1.1	−5.4	32.4
$O(p^6)_0$	535.6(4)	−1.259(2)	0.378(3)	5.5(2)	3.3(4)	41.1	1.1	−17	41.8
$O(p^6)_0^{\mathrm{Im}}$	537.4(4)	−1.269(2)	0.392(3)	5.5(2)	3.0(4)	41.3	1.1	−16	41.9
$O(p^6)_0^{p^8}$	537.4(4)	−1.269(2)	0.392(3)	5.5(2)	3.0(4)	41.3	1.1	−16	41.9
$O(p^6)_4$	541.4(4)	−1.274(2)	0.393(3)	5.5(2)	2.9(4)	41.4	1.2	−15	42.1
Res_0	601.2(4)	−1.256(2)	0.367(3)	5.2(2)	4.4(5)	43.5	0.5	−22	44.2
$\mathrm{Fit4}_0^{O(p^6)}$	581.6(4)	−1.263(2)	0.381(3)	5.1(2)	3.6(4)	42.9	0.7	−19	43.5
$\mathrm{Fit4}_0^{\mathrm{Res}}$	627.7(5)	−1.235(2)	0.329(3)	5.2(2)	6.4(5)	44.3	−0.1	−26	45.0
KLOE		−1.090(5)	0.124(6)	5.7(6)	14.0(9)		−3.0(5)		

Table 12: Dalitz plot parameters corresponding to various amplitudes obtained from the dispersive parametrization together with the corresponding values of R for the experimental values of the decay rates of the charged and the neutral processes.

and the experimentally measured values

$$\Gamma = 295(16)\,\mathrm{eV}, \qquad \Gamma_0 = 423(22)\,\mathrm{eV}. \tag{9.34}$$

We observe that the neglected effects on the observables are each time smaller than the effect of the choice of the fitting points — for instance their effect on the determination of R is smaller than 0.5% whereas the effect of the choice of the fitting points is 0.7%. The partial inclusion of higher chiral-order corrections in the resummed amplitude changes significantly all the parameters with the exception of a, the parameter R obtains correction of 6%; the parameter f and the neutral parameters are changed totally. The similar situation occurs when we change the $\pi\pi$ parameters into those of Fit4. Note that both these changes move the Dalitz plot parameters in the right direction towards the physical values obtained by KLOE, the amplitude $\mathrm{Fit4}_0^{\mathrm{Res}}$ even leads to the negative value of α. However, even such change of the $\pi\pi$ scattering parameters is not sufficient in order to obtain the agreement with the experiment (moreover, the values of R are changed to higher values, which is not the preferred direction as seen from the other methods).

We thus conclude that if we want to obtain the physical values of the Dalitz plot parameters, we have to change also[11] the values of the parameters $A_x, \ldots, F_x$ of $\eta \to 3\pi$

[11] One could be tempted to draw too strong conclusions from this that the Dalitz plot parameter discrepancy cannot be explained by the physical $\pi\pi$ rescattering effects, however, one should bear in mind that our current parametrization of the $\eta \to 3\pi$ amplitude does not enable to separate the effect of the $\pi\pi$ scattering from the other effects since it influences also the values of its polynomial parameters. It is therefore still possible that the demanded change of the values of these parameters is connected mainly with the correct inclusion of the $\pi\pi$ scattering effects.

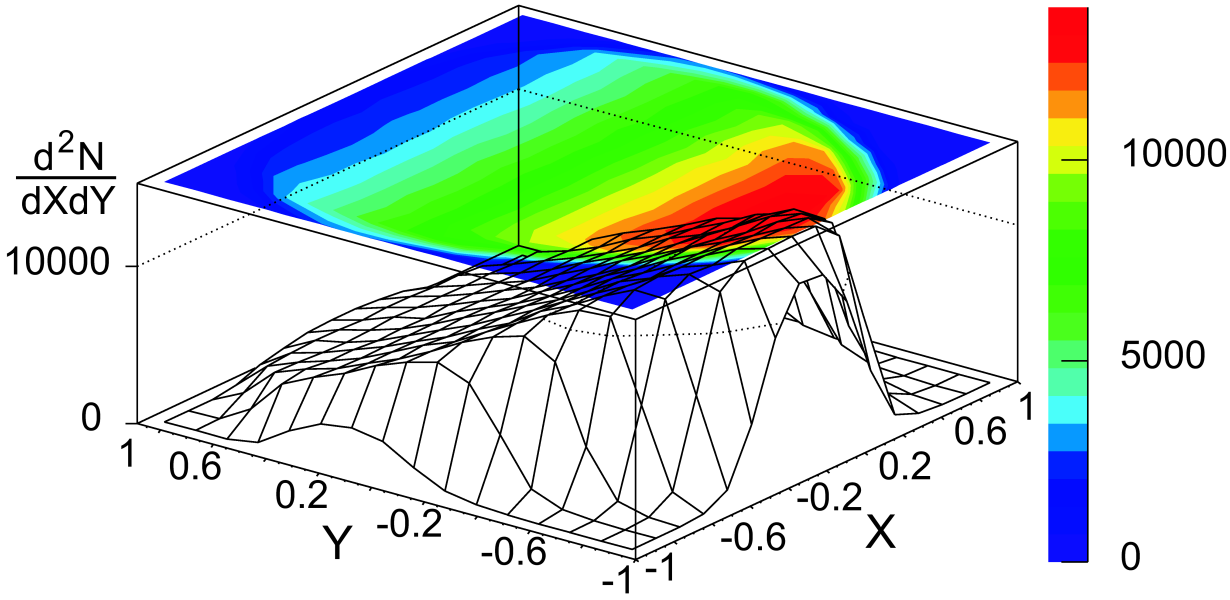

Figure 18: The Dalitz plot distribution for the charged $\eta \to 3\pi$ decay measured by KLOE. The picture taken from [8]. The capital X and Y in their notation correspond to Dalitz parameters x and y respectively.

amplitude.

9.6 Experimentally measured Dalitz plot distribution

For the following analyses we would need the access to the experimentally measured Dalitz plot distribution. Unfortunately, such information is inaccessible yet as we have at disposal only an approximate 5-parametric distribution from just one experiment [8] for the charged decay and the value of just one parameter (although independently confirmed by various experiments — cf. Table 8) for the neutral decay. However, it could change in the near future as there is currently a substantial activity on the experimental measurement of these processes at KLOE and WASA-at-COSY promising new data[12].

Therefore, for our analyses we try to construct a distribution for the charged $\eta \to 3\pi$ decay that will possess all the properties determined by KLOE [8] (we will discuss the possibility of inclusion of the information on the neutral parameter α in Section 9.9). They have obtained the Dalitz plot distribution containing 1.34 millions of events depicted

[12]See e.g. contributions of L. Caldeira Balkeståhl and P. Adlarson at the International PrimeNet Workshop 2011, Jülich.

on Figure 18 and fitted it for 154 bins ($\Delta x = \Delta y = 0.125$) to the distribution[13] [cf. (6.37)]

$$|\tilde{M}_x(x,y)|^2 = |A|^2 \left(1 + ay + by^2 + cx + dx^2 + exy + fy^3 + e_2x^3 + gx^2y + e_3xy^2\right). \quad (9.35)$$

At the confidence level 74% they have obtained consistency of the parameters c, e, e_2, e_3, g with zero (the first three are expected to be zero from C-invariance) and the further parameters equal to[14]

$$a = -1.090(5), \quad b = 0.124(6), \quad d = 0.057(6), \quad f = 0.14(1), \quad g = 0, \quad (9.36)$$

where we have included just the statistical error. The quoted correlation matrix is then

$$\begin{array}{c|cccc} & a & b & d & f \\ a & 1 & -0.226 & -0.405 & -0.795 \\ b & & 1 & 0.358 & 0.261 \\ d & & & 1 & 0.113 \\ f & & & & 1 \end{array}. \quad (9.37)$$

In [VI] we have constructed two data sets, one realistic containing 174 data points and one very optimistic with 2500 data points, both leading to Dalitz parameters from (9.36) taking into account also the errors. In the meantime we have also obtained from A. Kupść a distribution that was used in [81] and is based on information from both [8] and from the more detailed internal KLOE note [6] describing their fitting procedure.

In the following we therefore use this distribution as the physical data — we denote it as the K distribution. In order to acquire the idea of the possible precision in the upcoming experiments, we quote also the results for our optimistic data set with 2500 points, denoted as OPT.

After fitting the 154 points of the K distribution in Wolfram Mathematica weighted by the statistical uncertainties from the distribution, we obtain

$$a = -1.085(5), \quad b = 0.126(5), \quad d = 0.056(4), \quad f = 0.12(1), \quad r^2 - 1 = 1.2 \cdot 10^{-4}. \quad (9.38)$$

We obtain a compatibility of g with zero, since after releasing this condition, we get

$$a = -1.084(5), \quad b = 0.128(5), \quad d = 0.058(6), \quad f = 0.11(1), \quad r^2 - 1 = 1.2 \cdot 10^{-4} \quad (9.39)$$

and $g = -0.01(1)$.

We see that these values are compatible with the ones presented by KLOE (9.36). Another consistency check of the K distribution is the resulting correlation matrix from this fit

$$\begin{array}{c|cccc} & a & b & d & f \\ a & 1 & -0.277 & -0.369 & -0.805 \\ b & & 1 & 0.329 & -0.194 \\ d & & & 1 & 0.076 \\ f & & & & 1 \end{array}, \quad (9.40)$$

[13] Note the different notation of Dalitz parameters in [8] — e.g. for the parameter denoted in this text by g, KLOE uses symbol h.

[14] We have included the parameter g once more in order to simplify referring to these values.

	KLOE	χPT	χPT_g	NREFT	K distr.	$O(p^6)_0^{\text{Im}}$	$\left(O(p^6)_0^{\text{Im}}\right)_g$
rel_1	0.02(12)	−0.03(72)	0.15(79)	0.35(13)	0.03(13)	0.001(20)	0.17(12)
χ^2		0.1	1.2	7.6		0.03	1.6
rel_2	0.12(21)	−0.1(1.4)	0.3(2.1)	0.44(20)	−0.04(9)	−0.09(5)	0.27(4)
χ^2		1.4	0.6	2.4		1.0	0.5
$10^3\beta$	?	−2(25)	−2(25)	−4.2(7)		−1.6	−1.6

Table 13: Values of the C_i-independent combinations (9.41) of Dalitz plot parameters corresponding to determinations from KLOE [8, 9], χPT and χPT_g [33], NREFT [122]; the K distribution and the analytic dispersive parametrization $O(p^6)_0^{\text{Im}}$. The quantity χ^2 defined in (9.5) was computed for the theoretical determinations by taking the experimental value from KLOE as given in the first column.

i.e. with the exception of the $b - f$ correlation coefficient it is again consistent with the results of KLOE.

9.7 First analysis: Correcting χPT $\eta \to 3\pi$ result

9.7.1 Motivation

Our first analysis studies the effect of C_i's on the Dalitz plot parameters. Their contribution to the NNLO amplitude is linear and as they contribute just as tree-level counter-terms, it can be expanded into a real polynomial in Mandelstam variables. In addition, after a careful investigation of the $O(p^6)$ polynomial of the amplitude calculated in [33], we realize that there is no contribution of C_i's to the neutral parameter $\tilde{\beta}$ of the linear Dalitz plot expansion (H.8). From relations (H.17)–(H.18), we then obtain the following relations between Dalitz plot parameters that are independent on the values of the C_i's (they do not contribute to imaginary parts), where the subscript C denote the contribution of C_i's to the particular Dalitz plot parameter.

$$\begin{aligned} \text{rel}_1 : &\quad \left(4(b+d) - a^2 - 16\alpha\right)\big|_C = 0, \\ \text{rel}_2 : &\quad \left(a^3 - 4ab + 4ad + 8f - 8g\right)\big|_C = 0, \\ \text{rel}_3 : &\quad \beta|_C = 0. \end{aligned} \tag{9.41}$$

Note that the independence of these relations on the C_i's occur only in the case we take $m_{\pi^\pm} = m_{\pi^0}$. In Table 13 we list the values of these combinations coming from KLOE and from NNLO χPT.

This table indicates that even though the central values of the individual Dalitz parameters determined by χPT and KLOE differ, the central values of these two combinations are in a good agreement, which indicates that the incorrectly determined values of C_i could

be a possible explanation of the Dalitz parameter discrepancies. Unfortunately, the large errors of these combinations for these approaches somehow put down the importance of any conclusions. However, one should bear in mind that these values were computed just using the values and the error bars of the individual parameters that were attributed mainly from the fitting procedures and are thus strongly correlated. This can affect the positions of the central values by small changes, but primarily the error bars of these combinations are then overestimated. Note that the errors of the Dalitz parameters from ChPT are enhanced also by large systematic uncertainties of the amplitudes entering these fitting procedures. Such uncertainties were caused mainly by uncertainties of the C_is, which should be substantially eliminated in these combinations.

In order to study these effects we have computed the values of these relations also for the K distribution and for our parametrization $O(p^6)_0^{\mathrm{Im}}$, which represents our approximations for the KLOE distribution and the NNLO χPT amplitude respectively. The error bars quoted for these values take into account the correlations matrix we have obtained for these distributions in the previous sections and the effect of systematic uncertainty enters into them just through the weighting function of the fitting procedure as described above. We observe that even after reducing the resulting error bars the values remain compatible. Finally, we have illustrated in the table the effect of truncation of the Dalitz parametrization at either f or g. The values with g included corresponding to χPT computation [33] are denoted by $\chi\mathrm{PT}_g$ and the ones stemming from our parametrization $O(p^6)_0^{\mathrm{Im}}$ are listed in the ultimate column.

Since the K distribution was constructed from the condition $g = 0$, we cannot perform its addition into the fit of this distribution. Note however that if we add to the values of a, b, d, f measured by KLOE the value of $g = -0.02$ ($g = -0.04$), we would obtain an exact match of the so defined experimental[15] value of rel_2 with the value from ChPT_g (NREFT).

In this table we have also studied predictions of NREFT [122]. Since that method is built in a different way than ChPT, the combinations of the observables appearing in rel_1 and rel_2 have no special significance there. However, they are still valid combinations of observables and so nothing prevents us from using them for comparison of the predictions from any theory with the experiment. The lesser agreement of NREFT and KLOE in rel_1 was already pointed out in [122] in terms of different values of $\mathrm{Im}\,\bar{a}$ stemming from the representation of [122] and the one coming from the KLOE measurement and the relation (H.17). Together with the slight inconsistency also in rel_2 depending only on the parameters of the charged decay, this indicates that there is a problem either on the side of the current determination from the KLOE group or on the side of the NREFT representation.

In summary, a new measurement of the charged Dalitz parameters (possibly taking into account these two relations) would therefore be highly desirable. Before that, we are not able to answer the question whether it is possible to reproduce the physical Dalitz plot distribution with a better determination of the LECs C_i or whether the discrepancy between the ChPT-computed and the experimentally measured distributions has some

[15] Naturally, repeating the KLOE fit with g included would also change the values of the further parameters as is illustrated near relation (9.39) above.

	A_x	B_x	$10^3 C_x$	$10^3 D_x$	$10^4 E_x$	$10^4 F_x$	$1-r^2$	R
OPT_0	19.3(2)	1.92(4)	−61(3)	8.6(3)	−25(2)	16.0(7)	10^{-8}	38.1(4)
K_0	14.3(7.1)	1.41(76)	−50(8)	4.9(5.5)	−8.9(6.0)	14.9(3.3)	10^{-4}	$29.8^{+12.1}_{-11.5}$
K_4	14.6(7.3)	1.44(77)	−51(8)	5.0(5.6)	−9.1(6.2)	15.1(3.4)	10^{-4}	$30.4^{+12.3}_{-11.7}$
$\mathrm{K}_0^{\mathrm{Im}}$	16.0(7.7)	1.56(81)	−57(9)	6.2(5.7)	−9.5(6.7)	15.4(3.7)	10^{-4}	$32.7^{+13.1}_{-12.5}$
$\mathrm{K}_0^{\mathrm{Fit4}}$	16.0(8.3)	1.57(89)	−55(8)	6.5(6.8)	−12.3(6.1)	17.6(4.0)	10^{-4}	$34.2^{+14.0}_{-13.0}$
$O(p^4)_0$	16.27	1.955	−3.62	9.19				31.9
$O(p^6)_0$	20.27	2.357	−0.47	13.92	1.62(1)	−1.78(1)		41.8

Table 14: The corrected values of the NNLO parameters of the analytic dispersive parametrization for the chiral amplitude of the charged $\eta \to 3\pi$ decay in order to reproduce our approximations of the physical distribution from KLOE — OPT corresponds to the optimistic distribution containing 2500 data points whereas K denotes the more realistic distribution from Section 9.6.

other origin. In addition, should the experimental value confirm the values inconsistent with the predictions of [122], even if one accepts the explanation for the discrepancy of the neutral parameter α proposed in [122], the issue of the discrepancy for the charged parameter b would remain open.

Similarly, the measurement of the second neutral parameter β can provide another test of this possible explanation since to a very good precision this parameter does not depend on the values of the C_i's.

9.7.2 The numerical analysis

Now, we can proceed to the actual analysis. From the previous discussion, we are motivated to assume that all Dalitz parameter discrepancies can be included into a small real polynomial contribution (i.e. into a possible change of the values of the C_is). This means that by adding a small real polynomial ΔP to the NNLO χPT amplitude one should reproduce the data. Thanks to the form of our representation, we can obtain the corrected polynomial part of the amplitude $P_{\mathrm{cor.}} = P^{(6)} + \Delta P$ directly by repeating the procedure from Section 9.4, where we in the last step fit instead of real part of the NNLO χPT amplitude the particular KLOE-like distribution — note however that this distribution corresponds to the amplitude squared and thus this fit is more complicated.

We have performed various fits of such $P_{\mathrm{cor.}}$ — the resulting values compared to the values of parameters corresponding to χPT result [33] are listed in Table 14. The fit of the optimistic distribution OPT was discussed in more detail in [VI]. We observe that with the exception of the parameter C_x and the higher-higher order parameters[16] E_x,

[16]These higher-order parameters are nevertheless determined from the fit inside the physical region with a very low precision.

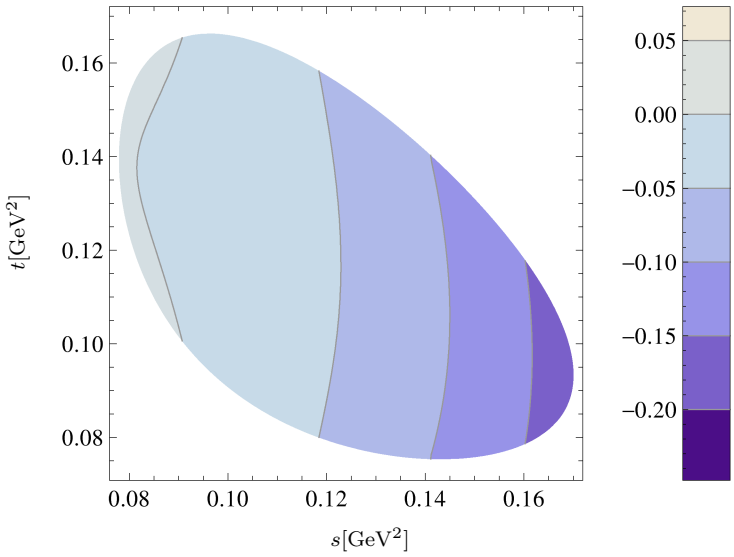

Figure 19: Relative difference between the real parts of the NNLO amplitudes obtained from two-loop χPT computation [33] and from our fit of the NNLO polynomial parameters from KLOE data on the physical region. For instance, the region with the depicted difference of -0.05 corresponds to the region where the KLOE amplitude is of 5% less than the χPT result.

F_x the parameters of the "corrected amplitude" lie between their NLO and NNLO χPT values. On Figure 19 we have plotted the change of the real part of the amplitude with respect to the NNLO χPT result. On the physical region this change is smaller than $\sim 15\%$. In summary, for the optimistic approximation of the data from KLOE, we have verified that this distribution is reproduced well by adding a small real polynomial to the two-loop χPT amplitude [33] and thus the discrepancy between the energy dependence of the physical amplitude and of the χPT result can be included into the parameters C_i. If this result were confirmed by the real physical data, from the values of the individual "corrected parameters" from Table 14 corresponding to the experimental amplitude one could construct sum rules for the C_i's and examine their compatibility with the values coming from other observables. [Note that the possibility to include the higher orders into the low-energy parameters in one process does not mean that one can perform it in the complete effective theory.]

The corresponding value of R is shifted to 38.1(4). By repeating this fit also for the values of the NLO parameters stemming from the other χPT sets, we have obtained

$$R = 37.7 \pm 2.9 \quad [\chi\text{PT+Disp.+OPT KLOE}]. \tag{9.42}$$

The quoted error is estimated conservatively by taking into account the slow convergence of the chiral expansion in the first three orders — assuming that the error of the corrected

amplitude is equal to one half of its difference to the NLO one (similarly as it was done in [33]).

However, we have performed also the analysis using the approximation of data by the K distribution and found that even though the distribution is reproduced well by the "corrected" amplitude and the polynomial is still on the physical region of a reasonably small size, the fitting procedure leads to huge uncertainties in the individual corrected parameters $A_x, \ldots, F_x$. The results of this analysis are therefore not significant and we cannot conclude any information on the explanation of the Dalitz parameter discrepancy by the incorrectly determined values of C_i's. Also the interval of the corresponding values or R is very large

$$R = 30^{+14}_{-12} \quad [\chi\text{PT+Disp.+K KLOE}]. \tag{9.43}$$

In the quoted uncertainties we have included the effect of the various choices of the values of the NLO parameters and of the description of $\pi\pi$ scattering. In Table 14 we have included the following choices — the values of the NLO parameters from Set 0 and Set 4; the addition of the C_i-independent imaginary part of the NNLO parameters from χPT and finally the different parametrization of the $\pi\pi$ scattering from Fit4.

9.8 Second analysis: Direct fit to $\eta \to 3\pi$ data

A different analysis not imposing anything about the origin of the Dalitz parameters discrepancy takes advantage of the fact that the construction of the analytic dispersive parametrization (9.6) employs just some general properties of the amplitude. We can thus assume that the physical amplitude should be also reproduced by this parametrization and the physical values of its parameters can be obtained by a direct fit to the physical amplitude. Naturally, as was discussed already a few times above, by this we do not fix the normalization. In order to perform also this task we suppose that χPT determination of the amplitude is reliable at least in the region[17] specified below.

9.8.1 Fit of the parametrization to the physical amplitude

Let us start with the easier part — fitting the physical data. In contrast to our previous fits, where respecting the chiral orders of the dispersive parameters was natural (and important), in this case keeping the different chiral orders of the parameters makes no sense. The more natural approach is using our representation in the "resummed" form — the values of the parameters in the polynomial and in the unitarity part are the same.

The fit of this general representation was performed for K distribution from Section 9.6 approximating the physical data set obtained by KLOE (which is not available). Since the overall normalization will be fixed in the next step, we can for the moment multiply the resulting values of the parameters by any number. In order to simplify the comparison

[17]Note that since we have analytic results, for fixing of the normalization one matching point would be sufficient.

	A_x	B_x	$10^3 C_x$	$10^3 D_x$	$10^4 E_x$	$10^4 F_x$	$1-r^2$
K	20.27(2)	2.03(1)	−52(2)	9.6(1.4)	−4.0(7.4)	17(5)	10^{-4}
K^{Fit4}	20.27(2)	2.07(1)	−44(2)	9.4(1.5)	1.3(7.6)	19(5)	10^{-4}
$O(p^6)_0$	20.27	2.357	−0.47	13.92	1.62(1)	−1.78(1)	
OPT_0	20.27(21)	2.02(4)	−64(3)	9.0(3)	−26(2)	16.8(7)	

Table 15: The values of the dispersive parameters obtained from the fit to the distribution K reproducing the $\eta \to 3\pi$ results from KLOE. For a comparison there are included also the values corresponding to the NNLO χPT amplitude and to the "corrected amplitude" from the previous analysis. All the sets of parameters are rescaled such that for all of them $A_x = 20.27$.

between this and the previous fits, we have decided to multiply here all these data by such numerical factor that produces the same number for parameter A_x as follows from NNLO χPT computation on Set 0, i.e. $A_x = 20.27$. The values of the so normalized dispersive parameters coming from this fit of K distribution are presented in Table 15 — we list their values for two possible choices of $\pi\pi$ scattering parameters (the value of the parameters corresponding to χPT with L_i values from Fit10 [10] and physically motivated values of the parameters coming from Fit4 from Section 5.11.1). For a comparison we have also included rescaled values of the parameters from the analysis of the previous section.

Putting aside the parameter E_x, whose determination is affected by a large error, we observe that only the parameter C_x changes significantly with the change of the $\pi\pi$ scattering parameters. Surprisingly, the same correspondence is noticeable also between these parameters and the rescaled parameters of the previous analysis (in Table 15 we have quoted the results obtained for distribution OPT since they give smaller error bars). Note that the parametrizations of the KLOE-like distributions corresponding to these two analyses possess different unitarity parts (the first one containing NLO χPT parameters, whereas the second unitarity part containing exactly the same parameters as they appear in the polynomial part).

In the following we perform the analysis for the physical values of $\pi\pi$ parameters from Fit4 and the second analysis giving similar results is used just for the estimate of the error connected with the $\pi\pi$ inputs.

9.8.2 Normalization of the parametrization

Setting the correct normalization of the parametrization of KLOE-like distribution is the main issue of the dispersive studies of this process. Without its right choice we cannot obtain a reliable value of R.

In connection with the search of the matching region to χPT in the literature there is usually employed the following coincidence. At the chiral NLO level there accidentally coincide the following three points (on the cut $s = u$):

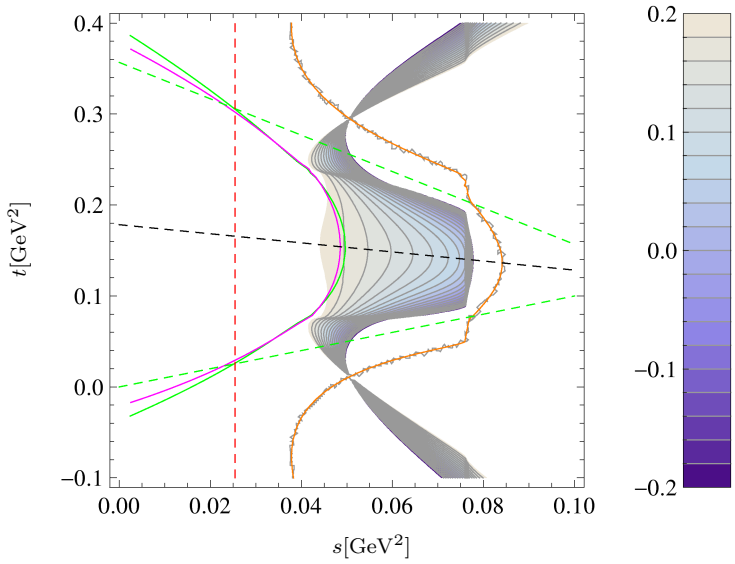

Figure 20: The relative difference between the imaginary parts of the NNLO and the NLO chiral amplitudes for the charged $\eta \to 3\pi$ decay. The ratio $1 - \mathrm{Im}\,\tilde{M}_x^{NLO}/\mathrm{Im}\,\tilde{M}_x^{NNLO}$ is plotted — only the region where the difference is less than 20% is included. The dashed black line denotes $t = u$ (around which the plot is symmetric), while the dashed green lines are the $s = t$ and $s = u$ lines. The dashed red line corresponds to the leading order Adler zero. Finally, the full green, magenta and orange lines mark the points, where $\mathrm{Re}\,O(p^4)$, $\mathrm{Re}\,O(p^6)$, $\mathrm{Im}\,O(p^6)$, respectively, are zero.

a) the point, where the amplitude is of order $O(m_\pi^2)$ (Adler zero — cf. our discussion of the Adler zero in Section II.C of [VI]),

b) the point, where $\mathrm{Re}\,M = 0$,

c) the point, where the corrections of the computed order to the slope are small.

However, this coincidence proves not to be the case at NNLO. Therefore, having the NNLO results at hand there is no reason why e.g. the amplitude at the point fulfilling condition b) should have a faster chiral convergence than at any other point (at NNLO it even seems to be the opposite). Thus, for the matching at the NNLO order we should not use this accidental NLO properties and instead we should try to find some other region.

For that end, we use the following conditions.

(i) The matching to NNLO χPT amplitude should be dependent on the values of C_i's as less as possible.

It is the reason why we use for the matching just the imaginary part of the amplitudes, which does not depend on the values of C_i's at the two-loop order.

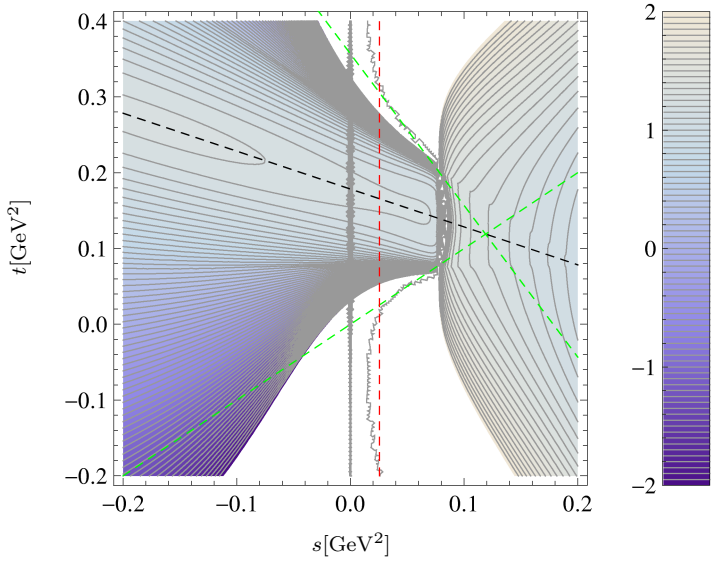

Figure 21: The ratio of the imaginary parts of the physical amplitude (obtained from the fit to K distribution) and of the NNLO chiral amplitude. The divergence at $s = 0$ is caused by a numerical instability of the approximation used for plotting. The dashed lines denoting $t = u$ (black), $s = t$ (green) and $s = u$ (green) are included similarly as in the previous plot. The dashed red line denotes the points, where the leading order amplitude is equal to zero (Adler points).

(ii) Within the matching region the chiral expansion should work well.

It means that already when going from NLO to NNLO the amplitude should not obtain too large corrections. On Figure 20 we have plotted the relative difference between the imaginary parts of the NLO and the NNLO chiral amplitudes. We discard the regions where such difference is larger than 20%. We have also added a few lines corresponding to various cuts of the phase space and denoted the positions of the points, where the real parts of the various orders of the amplitude are zero — we observe that with the exception of the neighborhood of the $t = u$ line such points are inappropriate for the matching (the NNLO corrections are there higher than the depicted 20%).

(iii) Also the higher corrections should be small within the matching region.

We assume that the resummed amplitude (containing also some of the higher order corrections) constructed from the NNLO order-by-order amplitude should not differ too much from the latter amplitude. Therefore, we match to the average of these two amplitudes and use their difference as the reference value (we use it as the weighting function of the fit).

(iv) The physical amplitude should have the similar behavior as the chiral amplitude

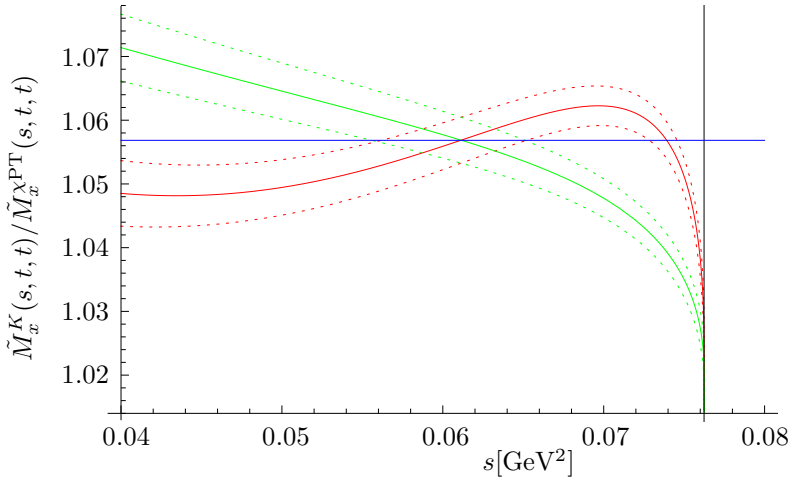

Figure 22: The ratio of the imaginary parts of the physical amplitude (K distribution) and of the NNLO chiral amplitude along the line $t = u$. The red plot corresponds to the order-by-order representation of the chiral amplitude, whereas the green plot corresponds to its resummed representation. With the dotted curves the statistical errors stemming from the fit of the K distribution are depicted. The vertical line demarcates the physical threshold. Finally, with the blue line we have depicted the result of our matching procedure.

inside this region.

As there is no theorem preferring individual points where the chiral corrections should be small (cf. the discussion of the Adler theorem in [VI]), we assume that if such point exists, it will not be an isolated point but a region where the behaviors of the NNLO χPT amplitude and of the physical amplitude are similar. Therefore, we have plotted on Figure 21 the ratio of the imaginary part of the physical amplitude with respect to the imaginary part of the NNLO chiral one[18]. If we had the physical amplitude with the right normalization, such ratio should be within the correct region close to one and there should be no steep behavior there. However, since the physical amplitude is multiplied by an unknown number, the only information we have is that this ratio should be on the correct region almost constant — we are thus looking for a plateau.

All these conditions together point towards the region around the $t = u$ line for $s \in \left(0.04\,\mathrm{GeV}^2, 4m_\pi^2\right)$. Naturally, this region is chosen just by the above arguments using the NNLO computation and it is possible that at NNNLO this prescription will again turn up

[18]In order to speed up the plotting of this graph, we have used a numerical approximation of the analytic representation of the amplitudes. This approximation diverges for $s = 0$, which created the numerical artifacts around this line visible on Figure 21. We can easily get rid of it by taking the full analytic form of the representation, which would, however, slow down the production of this plot and would change in no aspect the results of the current analysis.

Note also that the region where the imaginary part of the NNLO amplitude vanishes has moved slightly with respect to the situation on Figure 20, which is caused by neglecting here the small imaginary parts of the dispersive constants in contrast to the plot of Figure 20.

not to be the right one. But without a strong theoretical argument at hand there is no better way how to determine the correct region for matching and in this aspect we are just correcting the prescription used by the previous dispersive analyses by taking the NNLO corrections into account. Note that the conditions (iii) and (iv) from above are dependent on the subtraction scheme used, however, we have found that the region chosen above is picked up for all choices of the scheme we have performed.

On Figure 22 we have plotted the ratio between the physical amplitude and the NNLO chiral amplitude along the line $t = u$ within the considered region. It varies between $N = 1.02 \div 1.09$, which gives us the estimate of $R = 39.4 \div 42.2$. For a more precise determination of the factor we use the following procedure (taking into account the above conditions once more). We perform a fit on the $t = u$ cut for $s \in (0.04\,\mathrm{GeV}^2, 4m_\pi^2)$ (i.e. below the physical threshold) of the imaginary part of the physical amplitudes to the imaginary part of the average between the order-by-order chiral parametrization and the corresponding resummed one. The error used for the weighting within the fit is taken equal to the difference between the order-by-order and the resummed amplitudes.

The result of this fit is

$$N = 1.06 \pm 0.02, \tag{9.44}$$

where we have included the systematic error estimated from the difference between the order-by-order and the resummed amplitudes by using Figure 22 and the statistical error of the original fit of the K distribution — these two errors dominate over the error of the matching fit. (Note that this result was obvious already from Figure 22.)

By integration of the resulting parametrization and using the measured decay rate, we obtain

$$R = 40.5 \pm 1.6 \quad \text{[Match.+Disp.+K KLOE]}. \tag{9.45}$$

The quoted error includes the statistical error of the fit (~ 0.3), the error of the chiral amplitude in the matching region ($\lesssim 0.1$), the effects of the choice of the parametrization of the $\pi\pi$ scattering (~ 0.1), the effects of the choice of the subtraction scheme (~ 0.3) and finally, the effect of the choice of the matching point (~ 0.8). Note that in our case in contrast to the analysis in [VI], the errors of the first type are of the same order as the error of matching — with respect to the fit of [VI] this statistical error have been reduced here. However, it is probably just the property of the chosen KLOE-like distribution and it would be therefore again desirable to perform this analysis for the genuine physical data. In order to be more conservative we should add into our error budget also the effect of the possible inaccuracy of the "physical distribution" that was used. In [VI] we have found

$$R = 37.8 \pm 3.3 \quad \text{[Match.+Disp.+OPT KLOE]} \tag{9.46}$$

and also further slight variations we have tried on the K distribution lead to a smaller value of R. Thus, for the moment our conservative value of R following from this second analysis is

$$R = 39.6^{+2.5}_{-5.1} \quad \text{[Match.+Disp.+KLOE]}. \tag{9.47}$$

	$m_{\pi^\pm} = m_{\pi^0}$	$m_{\pi^\pm} \neq m_{\pi^0}$
$\eta \to \pi^+\pi^-\pi^0$	6	8
$\eta \to 3\pi^0$	5	7
$\eta \to 3\pi$	6	9

Table 16: Numbers of free parameters of the dispersive parametrization that are needed to be determined in various $\eta \to 3\pi$ analysis. The first two lines describe the individual studies of the charged and the neutral $\eta \to 3\pi$ decays, while the ultimate line corresponds to the combined fit of both of them.

9.9 Analysis of the neutral decay

In the previous sections we have used for the analysis just the charged $\eta \to 3\pi$ decay. Thanks to its symmetries the neutral decay is much simpler. Note that the polynomial part of the analytic dispersive representation for this decay reads

$$\tilde{R}_0(s,t,u) = A_0 + \frac{C_0}{F_\pi^4}\big[(s-\tilde{s}_0)^2 + (t-\tilde{s}_0)^2 + (u-\tilde{s}_0)^2\big] + \frac{E_0}{F_\pi^6}\big[(s-\tilde{s}_0)^3 + (t-\tilde{s}_0)^3 + (u-\tilde{s}_0)^3\big], \tag{9.48}$$

i.e. it contains just 3 independent parameters. However, these two decays are related by the 2-particle unitarity and so in the unitarity part of the $\eta \to \pi^+\pi^-\pi^0$ decay there appear 2 parameters from the neutral decay, whereas in the unitarity part of the $\eta \to 3\pi^0$ decay there appear 4 parameters from the charged one. When one takes the full isospin breaking into account there is no further connection between these two decays and one needs to determine all these parameters appearing in the considered amplitude. In the case we work in the leading order of the isospin breaking, relation (7.3) bounds these two amplitudes together and all the parameters of the neutral decay can be expressed in terms of the charged ones. The number of the parameters needed to be determined in the various studies in these two cases are given in Table 16.

From the table and the present status of the information we have from experiment on these amplitudes, it is obvious that we need to include the studies on the charged decay modes of η and work in the limit $m_{\pi^\pm} = m_{\pi^0}$. In that case we have six unknown parameters in our dispersive formula which could be saturated by five known Dalitz parameters of this decay. On the other hand, although the neutral decay is theoretically much simpler (having less parameters and there is no P-wave contribution to the unitarity part), so far only one Dalitz parameter (α) was measured for $\eta \to 3\pi^0$. The procedure elaborated in the previous section will not be thus very reliable in the case of study of the neutral decay alone.

However, we could try to include the information on α to the combined fit of both decay modes in the limit $m_{\pi^\pm} = m_{\pi^0}$ since according to the table it should just add further constraints on the charged parameters. Nevertheless, with that we come across the following disadvantage of the dispersive parametrization. We have discussed at the end of Section 9.4 that even in the $m_{\pi^\pm} = m_{\pi^0}$ limit we have to use different numerical values for the charged and the neutral decays since otherwise we would introduce the error

	$-\alpha$	$1-r^2$	$-\alpha$	β	$1-r^2$	r_η
OPT_0	$0.038^{+0.002}_{-0.001}$	$2\cdot 10^{-8}$	$0.038^{+0.002}_{-0.001}$	$0.0002^{+0.0007}_{-0.0001}$	$1.5\cdot 10^{-8}$	1.483(2)
$\mathrm{K}^{\mathrm{Fit4}}$	0.037(4)	$5\cdot 10^{-6}$	0.039(3)	0.005(3)	$1.2\cdot 10^{-8}$	1.477(1)

Table 17: The values of the neutral Dalitz parameters and of the ratio of the decay rates of the neutral and of the charged $\eta \to 3\pi$ decays corresponding to our fits to KLOE data of the previous sections.

of the incorrect normalization of Q_η (the isospin breaking effect), which would lead to about 13% smaller value of α (cf. again also the discussion in [122]). In χPT computation we are free to make this change since the other parameters, LECs, do not depend for instance on the light quark masses. However, the subtraction parameters in the dispersive approach do strongly depend on them as they include also their effects. We cannot thus simply obtain the amplitudes for a new choice of the pion masses without changing the subtraction parameters. We have decided not to introduce this error (of isospin breaking) into our analysis and just compute the parameters α and β for the amplitudes obtained from the previous sections — they are listed in Table 17. From both of the analyses, we have obtained compatible values (note that in the case of the second analysis they do not depend on the matching to χPT)

$$\alpha = -0.038(3), \tag{9.49}$$

which is in quite a good agreement with the experimental values from Table 8 (most importantly it is negative) but as expected its value is smaller than the current most precise experimental values such as MAMI-C result $\alpha = -0.032(3)$. In [VI] we have also performed the complete analysis where we took the isospin mass m_π equal to the average of the values used in the charged and the neutral decays and observed the shift of the resulting value of the expected size ($\sim$ 10%) in the right direction. Our conservative estimate including also this theoretical error (of the isospin breaking origin) into account is then

$$\alpha = -\left(0.038^{+0.005}_{-0.008}\right) \quad \text{[Disp.+KLOE]}. \tag{9.50}$$

Another interesting physical quantity connected with the neutral and the charged $\eta \to 3\pi$ decay is the ratio of their decay rates

$$r_\eta = \frac{\Gamma(\eta \to 3\pi^0)}{\Gamma(\eta \to \pi^+\pi^-\pi^0)}\,. \tag{9.51}$$

It does not depend on the overall normalization of the amplitudes and thus its determination from the analysis of Section 9.8 is completely χPT independent. We have listed the corresponding numbers for the analyses of the previous two sections in Table 17. Our expectation for this quantity including also the expected error of the isospin breaking is

$$r_\eta = 1.479(11) \quad \text{[Disp.+KLOE]}. \tag{9.52}$$

This value is in an excellent agreement with the most precise measurement of [4]: $r_\eta = 1.46(3)(9)$.

9.10 Implications for the quark masses

We return back to our original motivation of the determination of the light quark masses. Assuming that the optimistic distribution OPT describes well the physical amplitude, we have concluded in [VI] that since both of the performed analyses lead to the compatible results and both of them have different origin of the dominant errors, these two analyses can be combined into

$$R_1 = 37.7 \pm 2.2. \tag{9.53}$$

However, we have shown here that by taking the different distribution compatible with the data, the distribution K, the conclusions of the analysis of Section 9.7 are less significant and in the case we want to include the estimate of the error connected with the dependence on the "physical" distribution we take, the more conservative value would be

$$R_2 = 39.6^{+2.5}_{-5.1}. \tag{9.54}$$

We can now compare this result with the other recent analyses of the quark mass quantities.

Note that many of the analyses on the isospin breaking use instead of R the quadratic isospin breaking parameter

$$Q^2 = \frac{m_s^2 - \hat{m}^2}{m_d^2 - m_u^2}\,, \tag{9.55}$$

which is connected with R by

$$Q^2 = \frac{1}{2}\,R(r+1) \quad \text{with} \quad r = \frac{m_s}{\hat{m}}\,, \tag{9.56}$$

and use the amplitude $\tilde{M}_Q$ defined by

$$\tilde{\mathcal{M}}(s,t,u) = \frac{1}{Q^2}\,\frac{m_K^2}{m_\pi^2}\,(m_\pi^2 - m_K^2)\,\frac{\tilde{M}_Q}{3\sqrt{3}F_\pi^2} \tag{9.57}$$

rather than the amplitude $\tilde{M}$ from (9.3). Such choice is favored in the analyses based on χPT at NLO since at this order the parameter Q depends only on QCD meson masses [74] and is reasonably stable with respect to the Kaplan-Manohar transformation (9.1)–(9.2). However, at the current level of precision one includes also chiral two-loop effects, with which both of these advantages are lost since the relation between Q and the meson masses gains noticeable r-dependent corrections at NNLO (cf. [10]). When matching the amplitudes with the result of NNLO χPT [33], it is more natural to employ the normalization containing R and assume that the Kaplan-Manohar ambiguity is fixed by the values of LECs used in that computation (for instance the value of $L_6^r = 0$ stemming from large N_c considerations).

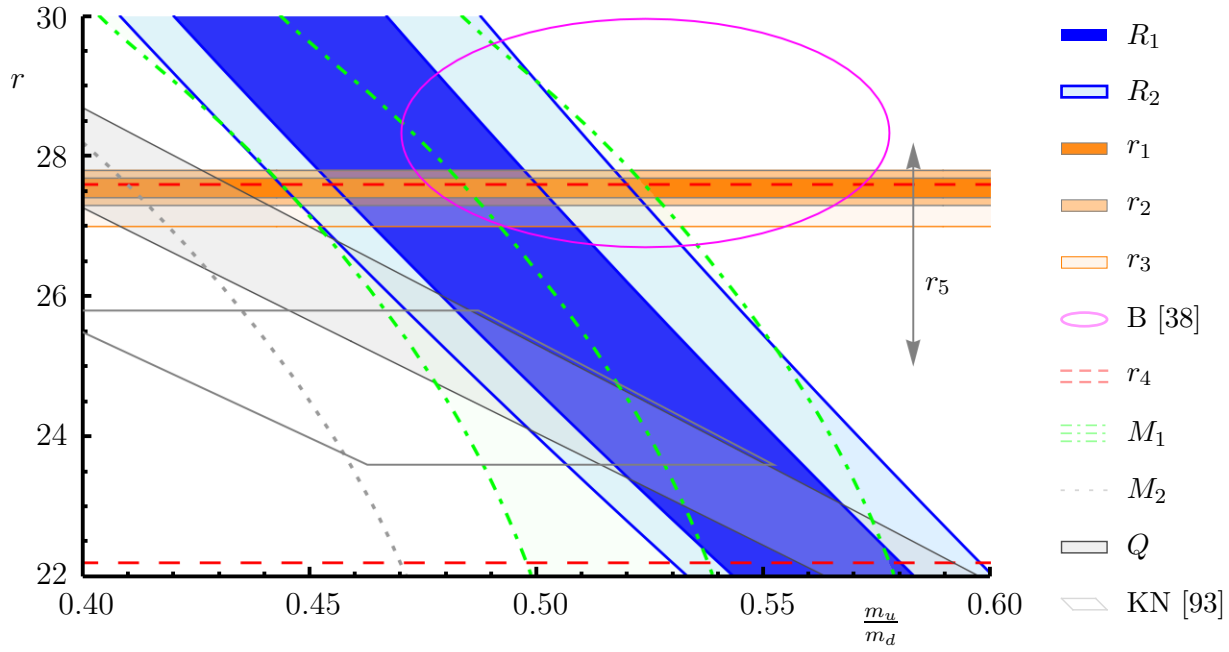

Figure 23: Various constraints on quark mass ratios (description given in the main text)

In Figure 23 we review various constraints on the light quark masses coming from recent analyses. In order to keep the plot uncluttered, we include only those which are independent and when different updates of some analysis exist, we list only the most recent one. For older results we refer to [107]. The axes of the presented plot correspond to (isospin symmetric) ratio $r = \frac{m_s}{\hat{m}}$ and to the quantitative measure of isospin violation $\frac{m_u}{m_d}$, which appear naturally in various analyses.

Our results (9.53) and (9.54) are plotted in blue and are denoted by R_1 and R_2, respectively. The result of the alternative analysis of $\eta \to 3\pi$ from [17, 50] is depicted in light gray as Q — we use the most recent result of this analysis from [103], $Q = 21.31^{+0.59}_{-0.50}$. We recall that this numeric approach uses dispersion relations of Omnès type, thereby attempting to include two-pion rescatterings to all orders. The necessary matching to the chiral amplitude is performed at the NLO Adler zero at the NLO level. For $r > 26$ it leads (similarly as χPT NLO computation) to m_u lighter than our result.

Interestingly, our result is fully compatible with one of the results of [10] which compared the experimental values for meson masses with the χPT NNLO expressions for them taking into account only the electromagnetic contributions due to Dashen [54] (its central value and error bars plotted in green and denoted by M_1), while the result of [10] that includes the violation of Dashen limit computed in [35] $x_D = 1.84$ (depicted without error bars with dotted gray line as M_2) moves m_u to noticeable smaller values. Note that if we used only the NLO expressions for the masses, our result would lie in between the determination respecting Dashen and the one with $x_D = 1.84$ — for $r < 27$ it would be more compatible with this violation of the Dashen limit, whereas for $r > 28$ the NLO result respecting the Dashen limit would be preferred by our result.

We proceed now to the recent determinations of r. Progress report on sum rules [60] quotes the value denoted by r_4 (between the dashed red lines), $r_4 = 24.9 \pm 2.7$. The method of [87], which is inspired by large N_c considerations, enables to determine r from the ratio of $\frac{\Gamma(\eta\to\gamma\gamma)}{\Gamma(\eta'\to\gamma\gamma)}$. The original number is indicated by the arrow $r_5 = 26.6 \pm 1.6$. In [93] such analysis was repeated with more recent numbers, leading to the determination of r that is significantly below all recent lattice determinations[19], $r_{\rm KN} = 24.7 \pm 1.1$. In [93] there was also used the result of [14] for Dashen violation $x_D = 1.5$ and from the experimental value of $m_{K^+} - m_{K^0}$ there was obtained $Q_{\rm KN} = 20.7 \pm 1.2$. These two results of [93] together are depicted with label KN.

The most advanced determinations of r are performed using lattice methods. Nowadays there exist two averaging attempts on lattice results. The average of Laiho et al. [102] gives $r_1 = 27.55(14)$ and isospin quark masses[20]

$$m_s^\mu = 93.6(1.1)\,\text{GeV}, \quad \hat{m}^\mu = 3.419(47)\,\text{GeV}. \tag{9.58}$$

FLAG group [46] have similar averages but in order to be more conservative, they quote estimates $r_3 = 27.4(4)$,

$$m_s^\mu = 94(3)\,\text{GeV}, \quad \hat{m}^\mu = 3.43(11)\,\text{GeV}. \tag{9.59}$$

We use FLAG numbers as our conservative choice. However, since their estimate are in some aspects very strict (e.g. not including BMW [61] yet), in order to show the precision of the current determinations we also use the average of [102] with error bars extended so that they include all the central values of the individual recent lattice determinations, $r_2 = 27.55(25)$,

$$m_s^\mu = 93.6(2.2)\,\text{GeV}, \quad \hat{m}^\mu = 3.42(9)\,\text{GeV}. \tag{9.60}$$

On Figure 23 these lattice values of r are plotted with orange regions. We have also included there the recent isospin breaking study on lattice [38] — depicted as the magenta ellipse denoted by B (note that this value is included in average [102] but not in [46]).

For completeness, let us note that baryonic determinations such as [83] give smaller quark ratio $\frac{m_u}{m_d} \lesssim 0.4$.

Taking our conservative result (9.54) together with the conservative lattice estimate (9.59), we obtain the following values of the quark mass characteristics

$$\frac{m_u}{m_d} = 0.50^{+0.02}_{-0.05}\ \ [0.48(2)]\,, \quad Q = 23.7^{+0.8}_{-1.5}\ \ [23.2(7)]\,,$$
$$m_u^{\overline{MS},\,\mu=2\,\text{GeV}} = 2.29^{+0.10}_{-0.17}\,\text{MeV}\ \ [2.21(9)\,\text{MeV}]\,,$$

[19] Note, however, that in [113] there is a possible explanation of this discrepancy as there is claimed that the higher loop diagrams not included in the recent lattice calculations can reduce also the values of r coming from lattice, i.e. it is still possible that the real physical value of r will be less than 26, which would lead to a higher mass of m_u than the one quoted at the end of this section.

[20] Unlike the mass ratios used above, m_q depend on renormalization scheme. All quoted values are in $\overline{MS}$ scheme at the scale $\mu = 2\,\text{GeV}$.

$$m_d^{\overline{MS},\,\mu=2\,\mathrm{GeV}} = 4.57^{+0.19}_{-0.14}\,\mathrm{MeV}\ \ [4.62(12)\,\mathrm{MeV}]\,.$$

In the square brackets we have quoted also the more precise values that would be valid in the case the OPT distribution described the physical $\eta \to 3\pi$ amplitude and our estimates on the isospin quark masses (9.60) were fulfilled.

Part V

Conclusions

Chapter 10

Final conclusions and outlook

We have derived the procedure that enables to construct two-loop amplitudes of processes containing four particles fulfilling the assumptions from Section 2.3 just from the knowledge of imaginary parts (discontinuities) of the S- and P- partial waves of the crossed processes along the rays starting at their thresholds. In the case when all the possible intermediate amplitudes contributing to the unitarity relations of these processes also fulfill these assumptions, this procedure enables us to construct self-consistently the amplitudes by employing the iterative two-step scheme of Figure 1 and the only undetermined part is represented by the values of a small number of subtraction constants. The resulting parametrization can be used either for the computation of the form of the unknown amplitudes, for the simplification of the complex structure of the result of some computation or for its direct fit to the physical amplitudes.

In this work we have employed such construction (with the verification of all its assumptions) for four types of amplitudes. In Chapter 4 we have constructed the pseudoscalar meson-meson scattering amplitudes in isospin-conserving strong χPT. We have shown possible applications of this construction for the understanding of the χPT processes, however, as was discussed there, such construction for the $\pi\pi$ and the $K\pi$ scatterings was already performed in [125,95] and [11,12] and in all the other processes we have very narrow regions (or for some processes such regions even do not exist), where the effects of the other particles than those included in our analysis can be neglected (very narrow regions where the chiral amplitudes describe well the physics) because of the appearance of the resonances. It was one of the main reasons, why we have not explicitly performed the second iteration for these processes.

In Chapter 5 we have constructed two-loop amplitudes (this time performing explicitly also the second step) of the $\pi\pi$ scatterings in the low-energy region where just the effects of $\pi\pi$ rescatterings are important. We have included the isospin-breaking effects connected with the different masses of $m_{\pi^\pm}$ and m_{π^0} and also derived the representation where the scattering lengths appear as its parameters. In the isospin limit we have shown its connection with the standard χPT computation and also with the experimentally measured $\pi\pi$ phase shifts. In Section 5.11.1 we have derived a one-loop parametrization that for

very low energies reproduces well the physical phase shifts (denoted as Fit4). A similar two-loop analysis and also the analysis taking into account the isospin breaking effects are prepared.

In Chapter 7, we have constructed a two-loop parametrization of the $K \to 3\pi$ and of the $\eta \to 3\pi$ amplitudes in the limit $m_{\pi^\pm} = m_{\pi^0}$. It was then used in Chapter 9 for the analysis of the $\eta \to 3\pi$ decays as we summarize below.

Finally, in Chapter 8 we have constructed one-loop parametrizations of the $K \to 3\pi$ and of the $\eta \to 3\pi$ amplitudes with taking into account the isospin breaking connected with the different masses of the particles belonging to the same isomultiplet. For the processes $K_L \to 3\pi^0$ and $\eta \to 3\pi^0$ we have presented the full two-loop results — note that for the time being there exists no computation of these amplitudes within χPT including these isospin breaking effects to the two-loop order yet (however, there exists such a computation using methods of nonrelativistic effective field theory [47, 36, 72]). These parametrizations are prepared for the phenomenological analyses, especially of the cusp effects appearing in these processes (note that this effect for $K^+ \to \pi^+\pi^0\pi^0$ decay was used for a very precise determination of the $\pi\pi$ scattering lengths).

The main advantages of our parametrization with respect to the results of chiral perturbation theory are its simple analytic form, the natural appearance of just a few scale-invariant combinations of the LECs (in terms of the subtraction constants), and the possibility to go beyond the standard power-counting (the subtraction constants do not need to be fixed to the standard χPT values) and also the possibility to perform partial resummations of the chiral expansion of some observables.

Its main disadvantages are the impossibility to determine (or at least to estimate) the subtraction constants without the matching either to some other theoretical calculation (such as the calculation in χPT) or to the experiment (note that usually this does not fix the overall normalization), the fact that their include many effects together, as for instance the dependence on the quark masses or on the properties of the intermediate processes, which cannot be simply separated. The values of the constants depend also on the subtraction scheme we choose in the dispersive parametrization and can vary a lot in different orders of computation (this affects then also the resummed interpretation of the polynomial, where we want to include partially also the higher unitarity effects). However, on the case of $\pi\pi$ scattering we have shown that the last two problems can be overcome in the case there exists natural physical observable quantities with the suitable properties that are used in the parametrization such as the scattering lengths (their values are then kept fixed at their physical values and by the addition of the "restoring polynomials" they do not obtain higher unitarity corrections).

Another natural sort of disadvantages is connected with the fact that we have not constructed the Lagrangian but used just the dispersive methods, i.e. for instance if we want to include into the computation the electromagnetic effects with the virtual photons, we have to return back to the Lagrangian formulation.

In Chapter 9 we have used our parametrization of the $\eta \to 3\pi$ amplitudes for the phenomenological analyses of the results of KLOE. Unfortunately, the genuine measured physical distribution is not available, so we had to construct artificial distribution (called

KLOE-like distribution) only fulfilling the properties that are available. We have found that the Dalitz plot parameters discrepancy (as described in Section 9.2) cannot be solved by a mere change of the $\pi\pi$ scattering parameters (but since in the other parameters of $\eta \to 3\pi$ there is included also the effect of the $\pi\pi$ scattering this does not tell us much information about the physics) but our KLOE-like distribution indicate that the effects explaining the discrepancy can be included into the $O(p^6)$ LECs C_i. We have also given a few simple criteria, which can falsify this expectation [in terms of the C_i-independent relations between the Dalitz plot parameters (9.41)]. We have also found a region, where the chiral expansion seems to work well (at least at the two-loop order) and performed a matching of the fitted parametrization with the χPT in order to obtain the normalization and thereby the quark mass characteristic R. For the optimistic distribution, we have found

$$R = 37.7 \pm 2.2. \tag{10.1}$$

Moreover, independently on the exact form of the physical distribution, we expect that the correct value of R would lie in the region

$$R = 39.6^{+2.5}_{-5.1}. \tag{10.2}$$

These values constrain the physical m_u and m_d quark masses according to Figure 23. We have discussed that at the current level of knowledge it is important to quote the separately the quark mass characteristics in which the isospin breaking effects are included and the isospin symmetric ones since the most precise methods giving the later cannot include the isospin breaking to the same precision yet. If we use the recent lattice values of $r = m_s/\hat{m}$ and of m_s together with our values of R, we obtain

$$\begin{aligned}
\frac{m_u}{m_d} &= 0.50^{+0.02}_{-0.05}\ \ [0.48(2)]\,, \quad Q = 23.7^{+0.8}_{-1.5}\ \ [23.2(7)]\,,\\
m_u^{\overline{MS},\,\mu=2\,\mathrm{GeV}} &= 2.29^{+0.10}_{-0.17}\,\mathrm{MeV}\ \ [2.21(9)\,\mathrm{MeV}]\,,\\
m_d^{\overline{MS},\,\mu=2\,\mathrm{GeV}} &= 4.57^{+0.19}_{-0.14}\,\mathrm{MeV}\ \ [4.62(12)\,\mathrm{MeV}]\,,
\end{aligned}$$

where the masses are in the $\overline{MS}$ renormalization scheme at the scale $\mu = 2\,\mathrm{GeV}$ and the values in the square brackets are our optimistic estimates.

From the fit of the charged $\eta \to 3\pi$ decay we give our estimate of the neutral Dalitz plot parameter

$$\alpha = -\left(0.038^{+0.005}_{-0.008}\right) \tag{10.3}$$

and of the ratio of the decay rates

$$r_\eta = \frac{\Gamma(\eta \to 3\pi^0)}{\Gamma(\eta \to \pi^+\pi^-\pi^0)} = 1.479(11). \tag{10.4}$$

In the near future there should be at disposal the physical distributions for the charged $\eta \to 3\pi$ decay from the KLOE and WASA-at-COSY collaborations, which should improve these our analyses. Note that these analyses would not be very reliable for the neutral $\eta \to 3\pi$ decay unless the precision of the measurement was so high that we can fit also the isospin breaking effects in this amplitude.

Appendices

Appendix A

General solution of crossing relations

In this appendix, we find the general solution of crossing relations

$$P^S_{J+1}(s,t;u) = P^T_{J+1}(t,s;u) = P^U_{J+1}(u;t,s), \tag{A.1}$$

where P^S_{J+1} and P^T_{J+1} are polynomials in s and t of J-th order with coefficients dependent on u and similarly P^U_{J+1} is a J-th order polynomial in s and u with t-dependent coefficients. At the end we are interested in the special case $J = 3$, in which relation (A.1) corresponds to (2.40) from the proof of the reconstruction theorem.

Thanks to the kinematic condition for the sum of Mandelstam variables (2.6), we can write

$$P^{S,T}_{J+1}(s,t;u) = \sum_{j=0}^{J} a^{S,T}_j(u)(s-t)^j, \tag{A.2}$$

$$P^U_{J+1}(s;t,u) = \sum_{j=0}^{J} a^U_j(t)(s-u)^j. \tag{A.3}$$

The first of relations (A.1) then simply implies

$$a^S_j(u) = (-1)^j a^T_j(u). \tag{A.4}$$

From the second one, it follows [using again (2.6)]

$$\sum_{j=0}^{J} a^T_j(u)(2t+u-s_0)^j = \sum_{j=0}^{J} a^U_j(t)(2u+t-s_0)^j. \tag{A.5}$$

Now, we will use assumption (v) of the theorem ensuring the existence of a point $\bar{u}$ in our kinematic region for some fixed t such that in its neighborhood all the functions $a^T_j(u)$ are analytic and similarly of a point $\bar{t}$ with all the functions $a^U_j(t)$ analytic in its neighborhood. We can then Taylor expand them,

$$a^T_j(u) = \sum_{k=0}^{\infty} a^T_{jk}(u-\bar{u})^k, \tag{A.6}$$

$$a_j^U(t) = \sum_{k=0}^{\infty} a_{jk}^U (t-\bar{t})^k \tag{A.7}$$

and insert these expansions into (A.5) to obtain

$$\sum_{j=0}^{J}\sum_{k=0}^{\infty} a_{jk}^T x^k (2y+x+\zeta)^j = \sum_{j=0}^{J}\sum_{k=0}^{\infty} a_{jk}^U y^k (2x+y+\xi)^j, \tag{A.8}$$

where we have introduced the shorthand notation

$$x = u - \bar{u}, \tag{A.9}$$
$$y = t - \bar{t}, \tag{A.10}$$
$$\xi = 2\bar{u} + \bar{t} - s_0, \tag{A.11}$$
$$\zeta = 2\bar{t} + \bar{u} - s_0. \tag{A.12}$$

This relation should hold for any u from vicinity of $\bar{u}$ and any t from vicinity of $\bar{t}$ and therefore the coefficients in front of $x^\alpha y^\beta$ on its both sides have to coincide. Already from this equation we see that for $\alpha > J$ its right-hand side vanishes and similarly for $\beta > J$ its left-hand side does, i.e. for both $\alpha > J$ and $\beta > J$ we have trivial equalities.

Using binomial expansion, we get

$$\sum_{j=0}^{J}\sum_{k=0}^{\infty}\sum_{l=0}^{j}\sum_{m=0}^{l}\binom{j}{l}\binom{l}{m} a_{jk}^T x^k 2^m y^m x^{l-m}\zeta^{j-l} = \sum_{j=0}^{J}\sum_{k=0}^{\infty}\sum_{l=0}^{j}\sum_{m=0}^{l}\binom{j}{l}\binom{l}{m} a_{jk}^U y^k 2^m x^m y^{l-m}\xi^{j-l}. \tag{A.13}$$

From comparison of the coefficients of $x^\alpha y^\beta$, it follows

$$2^\beta \sum_{j=0}^{J}\sum_{\substack{l=\beta \\ l\le\alpha+\beta}}^{j}\binom{j}{l}\binom{l}{\beta} a_{j,\alpha+\beta-l}^T \zeta^{j-l} = 2^\alpha \sum_{j=0}^{J}\sum_{\substack{l=\alpha \\ l\le\alpha+\beta}}^{j}\binom{j}{l}\binom{l}{\alpha} a_{j,\alpha+\beta-l}^U \xi^{j-l}. \tag{A.14}$$

Finally, since $l \le j$, we can restrict the extent of the sums over j,

$$2^\beta \sum_{j=\beta}^{J}\sum_{\substack{l=\beta \\ l\le\alpha+\beta}}^{j}\binom{j}{l}\binom{l}{\beta} a_{j,\alpha+\beta-l}^T \zeta^{j-l} = 2^\alpha \sum_{j=\alpha}^{J}\sum_{\substack{l=\alpha \\ l\le\alpha+\beta}}^{j}\binom{j}{l}\binom{l}{\alpha} a_{j,\alpha+\beta-l}^U \xi^{j-l}. \tag{A.15}$$

We have obtained the infinite set of linear equations for $a_{j,k}^T$ and $a_{j,l}^U$, which has to be solved. At first, however, let us study its structure. Dealing with its left-hand side it is obvious that for a given $\beta \le J$ and some α there appear only the terms with $a_{j,k}^T$ having $\beta \le j \le J$ and $\alpha + \beta - J \le k \le \alpha$, i.e. for $\beta = J$ on the left-hand side there occurs solely

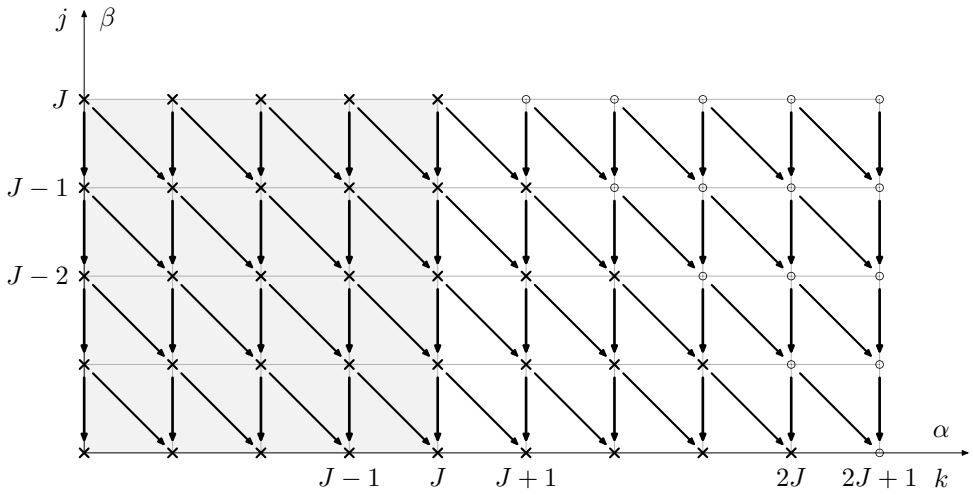

Figure 24: Schematic structure of the left-hand side of the series of equations (A.15). For a given α and β there appear on the left-hand side of the equation the terms $a^T_{j,k}$ with all j and k above and left above it as indicated by the arrows. To the right of the shaded region the right-hand side of the equation vanishes, above that region the left-hand side does. The solution for $a^T_{j,k}$ is indicated by the knots of the lattice — the dot means the coefficient equals to zero whereas the cross indicates that its expression contains some combination of $a^U_{j,k}$.

the coefficient $a^T_{J,\alpha}$ for every given α, for $\beta = J-1$ the coefficients $a^T_{J,\alpha}$, $a^T_{J,\alpha-1}$ and $a^T_{J-1,\alpha}$ appear, and similarly there show up more and more coefficients for lower β. Let us point up again that the left-hand side vanishes for $\beta > J$. The same arguments hold for the right-hand side if we exchange the meaning of α and β. Hence we have a simple triangular structure depicted on Figure 24. In the equation for a coefficient $a^T_{j,k}$ on the left-hand side that is obtained by taking $\beta = j$ and $\alpha = k$ there appear also all the coefficients from the triangle left above it. We use this structure for obtaining a solution of the series.

We begin with $\beta = J$. On the left-hand side there remains only one coefficient $a^T_{J,\alpha}$, the right-hand side depends on α. For $\alpha > J$ it is zero and so the solution for all $a^T_{J,j}$ with $j > J+1$ is trivial, $a^T_{J,j} = 0$. For $\alpha \leq J$ we have some combination of $a^U_{j,k}$ on RHS,

$$2^J a^T_{J,\alpha} = 2^\alpha \sum_{j=\alpha}^{J} \sum_{l=\alpha}^{j} \binom{j}{l} \binom{l}{\alpha} a^U_{j,\alpha+J-l} \xi^{j-l}. \tag{A.16}$$

Next, we take $\beta = J-1$. On the left-hand side there appear the coefficient $a^T_{J-1,\alpha}$ and two already known coefficients $a^T_{J,\alpha}$ and $a^T_{J,\alpha-1}$. So depending on α, we can express the coefficient $a^T_{J-1,\alpha}$ in terms of just these two coefficients for $\alpha > J$, whereas in the expression

for $\alpha \leq J$ there appear these two coefficients together with some combination of $a^U_{j,k}$.

$$2^{J-1}\left(a^T_{J-1,\alpha} + Ja^T_{J,\alpha}\zeta + \chi(\alpha \geq 1)Ja^T_{J,\alpha-1}\right) = 2^\alpha \sum_{j=\alpha}^{J} \sum_{\substack{l=\alpha \\ l\leq \alpha+J-1}}^{j} \binom{j}{l}\binom{l}{\alpha} a^U_{j,\alpha+J-1-l}\xi^{j-l}. \tag{A.17}$$

The function $\chi(\alpha \geq 1)$ is the characteristic function that equals to one when the condition in brackets is complied, otherwise it is zero. Again, note that for $\alpha > J+1$ the right-hand side vanishes and thereby also all the other coefficients. It means then that $a^T_{J-1,k} = 0$ for $k > J+1$.

We can continue further by lowering β and finally get the solution

$$a^T_{jk} = 0 \qquad \text{for } j+k > 2J \tag{A.18}$$

and all the other a^T_{jk} expressed using some combinations of $a^U_{j,k}$.

It remains to use the equations with $\beta > J$ where LHS of (A.15) are zero. We have here the same picture as Figure 24 just with α and β interchanged.

Starting with $\alpha = J$ we obtain all $a_{J,k} = 0$ for $k > J$. The equation for $\alpha = J-1$ gives

$$0 = 2^{J-1}(a^U_{J-1,\beta} + Ja^U_{J,\beta}\xi + Ja^U_{J,\beta-1}), \tag{A.19}$$

i.e. for $\beta > J+1$ all the appearing coefficient a^U_{jk} are zero, whereas for $b = J+1$ we get an expression for $a^U_{J-1,J+1}$ in terms of $a^U_{J,J}$ and vanishing $a^U_{J,J+1}$.

We go on further and find that also

$$a^U_{jk} = 0 \qquad \text{for } j+k > 2J \tag{A.20}$$

and all the other coefficients a^U_{jk} can be expressed in terms of $(J+1)^2$ independent coefficients a^U_{jk} with $0 < j,k < J$.

Summarily, we have found that the general solution of the crossing relations (A.1) are polynomials of maximally $2J$ order with $(J+1)^2$ independent coefficients,

$$P^S_4(s,t;u) = \sum_{j=0}^{J}\sum_{k=0}^{6-j} a^T_{j,k}(t-s)^j(u-\bar{u})^k, \tag{A.21}$$

$$P^T_4(s,t;u) = \sum_{j=0}^{J}\sum_{k=0}^{6-j} a^T_{j,k}(s-t)^j(u-\bar{u})^k, \tag{A.22}$$

$$P^U_4(s;t,u) = \sum_{j=0}^{J}\sum_{k=0}^{6-j} a^U_{j,k}(s-u)^j(t-\bar{t})^k. \tag{A.23}$$

We conclude that in our case, where $J = 3$ the polynomials are maximally of the sixth order with 16 independent coefficients.

Appendix B

Hilbert transform

For a function $\mathcal{K}(s)$ we define n-times subtracted Hilbert transform $\mathcal{H}^n(s)$ by the dispersion integral

$$\mathcal{H}^n(s) = s^n \int_{s_{\text{thr}}}^{\infty} \frac{dx}{x^n} \frac{\mathcal{K}(x)}{x - s}\,. \tag{B.1}$$

For any meromorphic function $\mathcal{K}(s)$ growing at infinity not faster than any polynomial, there always exists an integer $n_{\min}$ such that all $\mathcal{H}^n(s)$ for $n \geq n_{\min}$ exist. Note that from the definition it follows that $\frac{\mathcal{H}^n(s)}{s^n}$ is finite for $s \to 0$, thereby $\lim_{s\to 0} \frac{\mathcal{H}^n(s)}{s^m} = 0$ for all $m < n$.

To find an analytical form of Hilbert transform from its integral definition is a non-trivial task. For some functions it is easier to use the roundabout way trying to find a function analytic in the complex plane except the branch cut on the interval (s_{thr}, ∞) where it has the discontinuity equal to the value of the function $\mathcal{K}(s)$. Different functions satisfying this requirement differ just by a polynomial. It can be restricted by the UV and IR asymptotics of the integral, which depends on the number of subtractions.

In the following, we summarize few formulae that can be of use for computation of the Hilbert transform.

- Formula for raising the number of subtraction

$$\mathcal{H}^{n+1}(s) = s^n \int_{s_{\text{thr}}}^{\infty} \frac{dx}{x^n} \frac{\mathcal{K}(x)}{x - s} - s^n \int_{s_{\text{thr}}}^{\infty} \frac{dx}{x^n} \frac{\mathcal{K}(x)}{x} = \mathcal{H}^n(s) - s^n \left(\frac{\mathcal{H}^n(s)}{s^n} \right)_{s=0}. \tag{B.2}$$

  Denoting the n-th derivation of $\mathcal{H}^n(s)$ with respect to s as $\mathcal{H}^n(s)^{(n)}$ we can write this expression also as

$$\mathcal{H}^{n+1}(s) = \mathcal{H}^n(s) - \frac{s^n}{n!} \mathcal{H}^n(0)^{(n)}. \tag{B.3}$$

- Addition of a new subtraction point $x_1 \neq 0$

$$\begin{aligned}\mathcal{H}^n_{x_1}(s) &= s^n \int_{s_{\rm thr}}^{\infty} \frac{dx}{x^n} \frac{M^2 \mathcal{K}(x)}{(x-s)(x-x_1)} \\ &= \frac{M^2}{s-x_1} s^n \int_{s_{\rm thr}}^{\infty} \frac{dx}{x^n} \frac{\mathcal{K}(x)}{(x-s)} - \frac{M^2}{s-x_1} s^n \int_{s_{\rm thr}}^{\infty} \frac{dx}{x^n} \frac{\mathcal{K}(x)}{x-x_1} \\ &= \frac{M^2}{s-x_1} \left(\mathcal{H}^n(s) - \left(\frac{s}{x_1}\right)^n \mathcal{H}^n(x_1) \right).\end{aligned} \tag{B.4}$$

We have introduced a generic mass M^2 into the functions in order to keep them dimensionless. Note that the limit $x_1 \to 0$ is in correspondence with (B.2). Note also that since the difference between the one subtracted and the Hilbert transformation without subtractions differ by a constant, for $n = 0$ we can write also

$$\mathcal{H}^0_{x_1}(s) = \int_{s_{\rm thr}}^{\infty} \frac{dx}{x-s} \frac{M^2 \mathcal{K}(x)}{(x-x_1)} = \frac{M^2}{s-x_1} \left(\mathcal{H}^1(s) - \mathcal{H}^1(x_1) \right). \tag{B.5}$$

The notation $\mathcal{H}^n_{x_1}(s)$ we are using here is connected with the other possible understanding of the integral on the left-hand side of (B.4) — it corresponds to the Hilbert transform with n subtraction of function

$$\mathcal{K}_{x_1}(s) = \frac{M^2}{s-x_1} \mathcal{K}(s). \tag{B.6}$$

Such functions appear in contributions to amplitudes from P-waves (cf. 7.76) as $\mathcal{K}_\sigma(s) = \frac{M^2}{s\sigma^2(s)} \mathcal{K}(s)$.

- Expression for a change of subtraction point is therefore

$$\begin{aligned}&\frac{s}{M^2} \mathcal{H}^{n-1}_{x_1}(s) = s^n \int_{s_{\rm thr}}^{\infty} \frac{dx}{x^{n-1}} \frac{\mathcal{K}(x)}{(x-s)(x-x_1)} \\ &= \mathcal{H}^n(s) + x_1 s^n \int_{s_{\rm thr}}^{\infty} \frac{dx}{x^n} \frac{\mathcal{K}(x)}{(x-s)(x-x_1)} = \frac{s}{s-x_1} \left(\mathcal{H}^n(s) - \left(\frac{s}{x_1}\right)^{n-1} \mathcal{H}^n(x_1) \right).\end{aligned} \tag{B.7}$$

Again in the other interpretation it is Hilbert transform with $n-1$ subtractions of the function $\mathcal{K}_{x_1}(s)$.

- Using the previous two items we can derive also the Hilbert transforms $\mathcal{H}^n_{(\lambda)}(s)$ of the second type of functions appearing in contributions of P-waves

$$\mathcal{K}_{(\lambda)}(s) = \frac{sM^2}{\lambda(s)} \mathcal{K}(s) = \frac{sM^2}{(s-\mu_+)(s-\mu_-)} \mathcal{K}(s) \tag{B.8}$$

from the knowledge of Hilbert transform $\mathcal{H}^n(s)$ of the function $\mathcal{K}(s)$.

It corresponds to addition of new subtraction point μ_+ to the Hilbert transform $\mathcal{H}^{n-1}_{\mu_-}(s)$. Thus,

$$\mathcal{H}^n_{(\lambda)}(s) = \frac{sM^2}{s-\mu_+}\left(\frac{\mathcal{H}^n(s)-\left(\frac{s}{\mu_-}\right)^{n-1}\mathcal{H}^n(\mu_-)}{s-\mu_-}-\left(\frac{s}{\mu_+}\right)^{n-1}\frac{\mathcal{H}^n(\mu_+)-\left(\frac{\mu_+}{\mu_-}\right)^{n-1}\mathcal{H}^n(\mu_-)}{\mu_+-\mu_-}\right)$$
$$= \frac{sM^2}{\mu_+-\mu_-}\left(\frac{\mathcal{H}^n(s)-\left(\frac{s}{\mu_+}\right)^{n-1}\mathcal{H}^n(\mu_+)}{s-\mu_+}-\frac{\mathcal{H}^n(s)-\left(\frac{s}{\mu_-}\right)^{n-1}\mathcal{H}^n(\mu_-)}{s-\mu_-}\right). \tag{B.9}$$

- Obviously, we can lower the number of subtraction for $\mathcal{K}_{(\lambda)}(s)$,

$$\mathcal{H}^{n-1}_{(\lambda)}(s) = \frac{sM^2}{s-\mu_+}\left(\frac{\mathcal{H}^n(s)-\left(\frac{s}{\mu_-}\right)^{n-1}\mathcal{H}^n(\mu_-)}{s-\mu_-}-\left(\frac{s}{\mu_+}\right)^{n-2}\frac{\mathcal{H}^n(\mu_+)-\left(\frac{\mu_+}{\mu_-}\right)^{n-1}\mathcal{H}^n(\mu_-)}{\mu_+-\mu_-}\right)$$
$$= \frac{sM^2}{\mu_+-\mu_-}\left(\frac{\mathcal{H}^n(s)-\left(\frac{s}{\mu_+}\right)^{n-2}\mathcal{H}^n(\mu_+)}{s-\mu_+}-\frac{\mathcal{H}^n(s)-\left(\frac{s}{\mu_-}\right)^{n-2}\mathcal{H}^n(\mu_-)}{s-\mu_-}\right) \tag{B.10}$$

or raise it

$$\mathcal{H}^{n+1}_{(\lambda)}(s) = \frac{sM^2}{s-\mu_+}\left(\frac{\mathcal{H}^n(s)-\left(\frac{s}{\mu_-}\right)^{n}\mathcal{H}^n(\mu_-)}{s-\mu_-}-\left(\frac{s}{\mu_+}\right)^{n-1}\frac{\mathcal{H}^n(\mu_+)-\left(\frac{\mu_+}{\mu_-}\right)^{n}\mathcal{H}^n(\mu_-)}{\mu_+-\mu_-}\right)$$
$$= \frac{sM^2}{\mu_+-\mu_-}\left(\frac{\mathcal{H}^n(s)-\left(\frac{s}{\mu_+}\right)^{n}\mathcal{H}^n(\mu_+)}{s-\mu_+}-\frac{\mathcal{H}^n(s)-\left(\frac{s}{\mu_-}\right)^{n}\mathcal{H}^n(\mu_-)}{s-\mu_-}\right). \tag{B.11}$$

In all of the previous expressions, we could compute their left-hand side just from the knowledge of the Hilbert transform $\mathcal{H}^n(s)$ and also the existence of the objects appearing there followed from the existence of this transform. This is not the case for the formula for lowering the number of subtractions,

$$\mathcal{H}^{n-1}(s) = s^n\int_{s_{\rm thr}}^{\infty}\frac{dx}{x^n}\frac{\mathcal{K}(x)}{x-s}+s^{n-1}\int_{s_{\rm thr}}^{\infty}dx\,\frac{\mathcal{K}(x)}{x^n} \tag{B.12}$$

where we need to compute the constant $\int_{s_{\rm thr}}^{\infty} dx\, \frac{\mathcal{K}(x)}{x^n}$ and this integral can even diverge (together with the non-existence of the $n-1$ times subtracted transform) — this obviously happens for $n \leq n_{\rm min}$.

General change of the subtraction points

We will not need it in our applications but one could in principle continue with changing of the subtraction points of the Hilbert transform as follows.

An introduction of a new subtraction point (not equal to any previous subtraction points) is easy by the successive application of the formula (B.4) similarly to the procedure that we have done when obtaining (B.9). Consequently, we would like to lower the number of subtraction in 0. For that end we use

$$\frac{x}{x-x_i} = 1 + \frac{x_i}{x-x_i}\,. \tag{B.13}$$

The situation is a little bit different when we want to raise the number of subtractions performed at some point x_i. In this case the simplest method is the use of differentiation of an integral with respect to its parameter. Denoting the integral

$$I(n,m) = s^{n+m} \int_{s_{\rm thr}}^{\infty} \frac{dx}{x^n (x-x_i)^m} \frac{\mathcal{K}(x)}{x-s}\,, \tag{B.14}$$

we obtain by differentiating this integral with respect to x_i the equation ($m > 0$)

$$\frac{\partial}{\partial x_i} I(n,m) = \frac{m}{s} I(n,m+1). \tag{B.15}$$

Further, by using the transposition (B.13) we have

$$I(n-1,m) = I(n,m-1) + \frac{x_i}{s} I(n,m). \tag{B.16}$$

Consequently, for $m > 0$

$$I(n-1,m+1) = I(n,m) + \frac{x_i}{m} \frac{\partial}{\partial x_i} I(n,m). \tag{B.17}$$

As an example of it, from (B.7) we obtain for $I(n-2,2)$

$$\begin{aligned} & s^n \int_{s_{\rm thr}}^{\infty} \frac{dx}{x^{n-2}} \frac{\mathcal{K}(x)}{(x-s)(x-x_1)^2} \\ & \quad = \left(1 + x_1 \frac{\partial}{\partial x_1}\right) s^n \int_{s_{\rm thr}}^{\infty} \frac{dx}{x^{n-1}} \frac{\mathcal{K}(x)}{(x-s)(x-x_1)} \\ & \quad = \frac{s^2}{(s-x_1)^2} \mathcal{H}^n(s) + \frac{s^n}{x_1^{n-1}(s-x_1)} \left(\left(n-1-\frac{s}{s-x} \right) \mathcal{H}^n(x_1) - x_1 \frac{\partial}{\partial x_1} \mathcal{H}^n(x_1) \right). \end{aligned} \tag{B.18}$$

Appendix C

Comments on analyticity of amplitudes, their partial wave expansion and validity of dispersion relations from axiomatic field theory

The important assumptions of the reconstruction theorem are the analyticity of amplitudes, the existence of dispersion relations and also the existence of at least S and P partial waves. Since we are using the amplitudes only perturbatively in the low-energy regions, we do not require the complete physical amplitude possesses these properties, but it is enough for us that the perturbative amplitudes up to the considered order and in the considered region do. However, for the construction of such perturbative amplitudes one can also use the usual Feynman diagram method in the field theoretic framework of χPT and the validity of the assumptions on their analytic structure can be trivially verified by this way.

Nevertheless, for many of the amplitudes we have studied in this work, we can use the results of a long endeavor of studies of analytic properties of the scattering amplitudes in the framework of S-matrix theory, which do not even need the existence of the Lagrangian theory describing these processes as they are older than QCD itself. We do not address them in more detail and summarize just the results important for us instead. For a very good and still topical summary explaining many of the details of such studies we recommend the review article [124] by Sommer.

For the introduction of this appendix let us remind the unfamiliar reader that S-matrix theory has comprised of many rigorous mathematical methods that have tried to tell us as much information about the amplitudes as possible by using just the basic set of principles — axioms (also known as the first principles) such as Lorentz invariance, physical mass spectrum, completeness of physical states and microscopic causality (local commutativity of space-like separated fields). In its original motivations they have taken the axioms of unitarity of the scattering matrix and from it stemming positivity property separately as they bring non-linear properties into the game.

C.1 Analysis without the use of unitarity — Lehmann ellipses

Even without the use of unitarity, Lehmann [105] has shown that for the Mandelstam variable s fixed at some value above the physical threshold the singularities of the amplitude of the process $AB \to CD$ can appear in the $\cos\theta$ plane (cf. (2.8)) only for

$$\cos(\theta - \alpha) > x_0(s), \tag{C.1}$$

where α is arbitrary angle and

$$x_0(s) = \sqrt{1 + \frac{s}{\lambda_{CD}(s)}\,\Xi_{CD}(s)} > 1 \tag{C.2}$$

depends on the lowest masses M_X of two- or more-particle states with the same quantum numbers as particles X for $X = C, D$,

$$\Xi_{XY}(s) = \frac{4(M_X^2 - m_X^2)(M_Y^2 - m_Y^2)}{s - (M_X - M_Y)^2}\,. \tag{C.3}$$

Using the expression for the cosine of sum of two angles, it follows that the scattering amplitude is holomorphic in the interior of ellipse

$$\cos\theta = x_0(s)\cos\alpha + i\sqrt{x_0(s) - 1}\sin\alpha \tag{C.4}$$

with the foci $\cos\theta = \pm 1$ and its major semi-axis equal to $x_0(s)$. This ellipse is called small Lehmann ellipse and by using (2.8) and (2.6) it can be rewritten into interior of the ellipse in the u-plane ($\delta_{XYZW} = (\Delta_{XY} + \Delta_{ZW})^2$)

$$\left|u + \frac{\left(\lambda_{AB}^{1/2}(s) + \lambda_{CD}^{1/2}(s)\right)^2 - \delta_{ABCD}}{4s}\right| + \left|u + \frac{\left(\lambda_{AB}^{1/2}(s) - \lambda_{CD}^{1/2}(s)\right)^2 - \delta_{ABCD}}{4s}\right| < \frac{\lambda_{AB}^{1/2}(s)\lambda_{CD}^{1/2}(s)}{s}\,x_0(s). \tag{C.5}$$

This implies also convergent partial wave expansion of the scattering amplitude inside the small Lehmann ellipse.

Similarly, he has shown that the absorptive parts of the amplitude $\mathrm{Im}\,A(s,t,u)$ for $s \geq s_{\mathrm{thr}}$ and $\mathrm{Im}\,A(s,t,u)$ for $t \geq t_{\mathrm{thr}}$ which turn out to be discontinuities across the cuts in s and t plane are holomorphic inside the (large) Lehmann ellipses

$$\left|u + \frac{\left(\lambda_{AB}^{1/2}(s) + \lambda_{CD}^{1/2}(s)\right)^2 - \delta_{ABCD}}{4s}\right| + \left|u + \frac{\left(\lambda_{AB}^{1/2}(s) - \lambda_{CD}^{1/2}(s)\right)^2 - \delta_{ABCD}}{4s}\right| < Y_0^S(s) \tag{C.6}$$

and

$$\left|u+\frac{\left(\lambda_{AC}^{1/2}(t)+\lambda_{BD}^{1/2}(t)\right)^2-\delta_{ACBD}}{4t}\right|+\left|u+\frac{\left(\lambda_{AC}^{1/2}(t)-\lambda_{BD}^{1/2}(t)\right)^2-\delta_{ACBD}}{4t}\right|<Y_0^T(t), \quad \text{(C.7)}$$

with

$$Y_0^S(s)=\sqrt{\Xi_{AB}(s)}\,\sqrt{\Xi_{CD}(s)}+\sqrt{\Xi_{AB}(s)+\frac{\lambda_{AB}(s)}{s}}\,\sqrt{\Xi_{CD}(s)+\frac{\lambda_{CD}(s)}{s}} \quad \text{(C.8)}$$

and $Y_0^T(s)$ obtained by interchange of $B \leftrightarrow C$. This again implies the convergence of the partial wave expansions of the absorptive parts inside the particular Lehmann ellipse.

Finally, the u-fixed dispersion relations (2.27) can be proved for all real negative values of u which are in the intersection of all these (large) Lehmann ellipses for $s \geq s_{\rm thr}$ and $t \geq t_{\rm thr}$. As their semi-minor axes tends to zero for $s \to \infty$ and $t \to \infty$, if nonempty such intersection is just an interval on the negative real u-axis, $-u_M \leq u \leq -u_m$. In the case $Y_0^S(s)$ and $Y_0^T(t)$ are real for any $s \geq s_{\rm thr}$ and $t \geq t_{\rm thr}$, it is obvious that

$$u_M=\min(u_M^S,u_M^T), \qquad u_m=\max(u_m^S,u_m^T), \quad \text{(C.9)}$$

where

$$u_{\substack{M\\m}}^S=\min_{s>s_{\rm thr}}\left(\frac{\lambda_{AB}(s)+\lambda_{CD}(s)-\delta_{ABCD}}{4s}\pm\frac{1}{2}\,Y_0^S(s)\right) \quad \text{(C.10)}$$

and analogically for $u_{\substack{M\\m}}^T$. In the case some of $Y_0^S(s)$ of $Y_0^T(t)$ is complex on the considered region, the corresponding Lehmann ellipse breaks down and the dispersion relations cannot be proved by this way.

Note that for process $AB \to BA$, $Y_0^S(s)=Y_0^T(s)$ and it reduces to

$$Y_0(s)=2\Xi_{AB}(s)+\frac{\lambda_{AB}(s)}{s}\,. \quad \text{(C.11)}$$

The real limits $u_{M,m}^S$ then simplify into

$$u_M^S=\min\left(\Xi_{AB}(s)+\frac{\lambda_{AB}(s)}{s}\right), \qquad u_m^S=\min\Xi_{AB}(s). \quad \text{(C.12)}$$

The latter is going to zero for $s \to \infty$. Therefore, the interval for which the dispersion relations can be proved is $u \in (-u_M, 0)$, where

$$u_M=\min_{s\geq\min(s_{\rm thr},t_{\rm thr})}\left(\Xi_{AB}(s)+\frac{\lambda_{AB}(s)}{s}\right). \quad \text{(C.13)}$$

C.2 Taking into account unitarity of the S-matrix

By taking into account the unitarity of the S-matrix, one can extent the domains of analyticity and the region where the dispersion relations are valid. For instance, for the elastic amplitude Martin [108], Bros, Epstein and Glaser [41] have shown that the amplitude is analytic in s and u for $|u| < R$ with cuts along the real axis $s \geq s_{\rm thr}$ and $t \geq t_{\rm thr}$ for some R. Its determination from [123] gives

$$R = \min \left[u_M, \max_{s \geq s_{\rm phys}} \left(\frac{\lambda_{AB}(s)}{2s} (x_0(s) - 1) \right) \right]. \tag{C.14}$$

Similarly, it has been shown that $\mathrm{Im}\, A(s,t,u)$ along $s \geq s_{\rm thr}$ is analytic for fixed physical s inside the following ellipse in complex u-plane

$$|u| + \left| u + \frac{\lambda_{AB}(s)}{s} \right| < \frac{\lambda_{AB}(s)}{s} + 2R. \tag{C.15}$$

For the inelastic amplitude similar result are valid, however, they are in more complicated form.

There exist also further methods for enlargement of the analyticity domains. Those methods summarized in [124] lead to the results listed in the following subsections. Let us remind that these regions are only the minimal domains as for instance we did not take into account the further specific crossing (and Bose) symmetries of some of the amplitudes.

C.2.1 Elastic scattering $AB \to BA$

The domains of analyticity and the regions of convergence of partial wave expansion for the absorptive part of the amplitude of elastic scattering are

$$|u| + \left| u + \frac{\lambda_{AB}(s)}{s} \right| < \frac{\lambda_{AB}(s)}{s} + 2\rho(s), \tag{C.16}$$

where $\rho(s)$ is for the absorptive part $\mathrm{Im}\, A(s,t,u)$ for $s > s_{\rm thr}$ given by

$$\rho(s) = \begin{cases} \max\left(R, \Xi_{AB}(s)\right) & \text{for} \quad s_{\rm thr} \leq s < s_{\rm phys}, \\ 4R\left(1 + \frac{sR}{\lambda_{AB}(s)}\right) & \text{for} \quad s_{\rm phys} \leq s < s_{\rm inel}, \\ \Xi_{AB}(s) & \text{for} \quad s_{\rm inel} \leq s < s_{\rm crit}, \\ R & \text{for} \quad s_{\rm crit} \leq s, \end{cases} \tag{C.17}$$

where

$$R = \min \left[u'_M, \max_{s \geq s_{\rm phys}} r_{sL}(s) \right], \tag{C.18}$$

$$r_{sL}(s) = \frac{\lambda_{AB}(s)}{2s} (x_0(s) - 1), \tag{C.19}$$

$$u'_M = -\max_{s\geq s_{\rm inel}} l_{AB}(s), \tag{C.20}$$

$$l_{AB}(s) = -\frac{\lambda_{AB}(s)}{s} - \Xi_{AB}(s) \tag{C.21}$$

and the boundary points of the particular intervals s with different prescriptions for $\rho(s)$ correspond to the threshold, where there starts a two-particle cut in the S-channel of the amplitude; to the physical threshold, for which the amplitude can occur; to the inelasticity threshold, where the intermediate states with more than two particles can appear; and finally to the critical value of s

$$s_{\rm crit} = (M_A - M_B)^2 + \frac{4(M_A^2 - m_A^2)(M_B^2 - m_B^2)}{R}, \tag{C.22}$$

for which the unitarity starts to yield better information than the Lehmann result.

Again the u-fixed dispersion relations can be proved inside the intersection of all these regions for s and t (in T-channel) above their thresholds. In addition to these ellipses, the absorptive parts are for all values of s always analytic inside the small complex neighborhood of the segment $\langle -t'_M, R\rangle$ and this segment is therefore always inside the region, where one can prove the dispersion relations.

The scattering amplitude can be shown to be holomorphic and its partial wave expansion convergent inside the ellipse (C.16) with

$$\rho(s) = \begin{cases} R & \text{for} \quad s_{\rm thr} \leq s < s_1, \\ u'_M - \frac{\lambda_{AB}(s)}{s} & \text{for} \quad s_1 \leq s < s_2 \\ \frac{\lambda_{AB}(s)}{2s}\left(\sqrt{1 + \frac{sR}{\lambda_{AB}(s)}} - 1\right) & \text{for} \quad s_2 \leq s, \end{cases} \tag{C.23}$$

where the boundaries $s_{1,2}$ are defined by conditions

$$\frac{\lambda_{AB}(s_1)}{s_1} = u'_M\left(1 - \frac{R}{u'_M}\right), \tag{C.24}$$

$$\frac{\lambda_{AB}(s_2)}{s_2} = u'_M\left(1 + \frac{R}{4u'_M}\right)^{-1}. \tag{C.25}$$

C.2.2 Inelastic scattering $AB \to CD$

For the inelastic process $AB \to CD$, we use the results for the elastic processes (C.18), R_{AB} corresponding to $AB \to AB$ and R_{CD} corresponding to $CD \to CD$ scattering.

The ellipses of analyticity of the absorptive part and the regions of convergence of its partial wave decomposition are

$$\left|u + \frac{\left(\lambda_{AB}^{1/2}(s) + \lambda_{CD}^{1/2}(s)\right)^2 - \delta_{ABCD}}{4s}\right| + \left|u + \frac{\left(\lambda_{AB}^{1/2}(s) - \lambda_{CD}^{1/2}(s)\right)^2 - \delta_{ABCD}}{4s}\right| < \rho(s) \tag{C.26}$$

with

$$\rho(s) = \max \left\{ \begin{array}{c} \sqrt{\frac{\lambda_{AB}(s)}{s} + \Xi_{AB}(s)}\, \sqrt{\frac{\lambda_{CD}(s)}{s} + \Xi_{CD}(s)} + \sqrt{\Xi_{AB}(s)}\, \sqrt{\Xi_{CD}(s)} \\ \frac{\lambda_{AB}^{1/2}(s)\lambda_{CD}^{1/2}(s)}{2s}\ \frac{1+\eta_{AB}(s)\eta_{CD}(s)}{\sqrt{\eta_{AB}(s)\eta_{CD}(s)}} \end{array} \right\}, \quad \text{(C.27)}$$

where

$$\eta_{XY}(s) = \left(1 + \frac{2sR_{XY}}{\lambda_{AB}(s)}\right) + \sqrt{\left(1 + \frac{2sR_{XY}}{\lambda_{AB}(s)}\right)^2 - 1}\,. \quad \text{(C.28)}$$

The dispersion relations can be proved again inside the intersection of such ellipses for all $s \geq s_{\rm thr}$ and $t \geq t_{\rm thr}$ (in T-channel).

Similarly the scattering amplitude is holomorphic and its partial-wave expansion converges inside (C.26) with

$$\rho(s) = \max \left\{ \begin{array}{c} \frac{\lambda_{CD}^{1/2}(s)}{2\sqrt{s}}\, \sqrt{\frac{\lambda_{AB}(s)}{s} + \Xi_{AB}(s)} \\ \frac{\lambda_{AB}^{1/2}(s)}{2\sqrt{s}}\, \sqrt{\frac{\lambda_{CD}(s)}{s} + \Xi_{CD}(s)} \\ \frac{\lambda_{CD}^{1/2}(s)}{2\sqrt{s}}\, \sqrt{\frac{\lambda_{AB}(s)}{s} + R_{AB}} \\ \frac{\lambda_{AB}^{1/2}(s)}{2\sqrt{s}}\, \sqrt{\frac{\lambda_{CD}(s)}{s} + R_{CD}} \end{array} \right\}. \quad \text{(C.29)}$$

C.3 Results for the particular processes

By employing these results for the processes we are interested in, we obtain the following regions. Note that we ignore again the appearance of resonances and neglect isospin breaking and the existence of weak operators changing the isospin (i.e. all the pseudoscalar mesons are stable).

C.3.1 Processes $AA \to AA$

The most symmetric processes we are interested in are the processes $\pi^+\pi^- \to \pi^0\pi^0$, $K^-K^+ \to \overline{K^0}K^0$ and $\eta\eta \to \eta\eta$. Since we assume isospin conservation we do not need to distinguish the particular isospin states. For simplification of the expressions, we introduce two dimensionless variables

$$r = \frac{m_A}{m_\pi}, \qquad x = \frac{s}{4m_\pi^2}, \quad \text{(C.30)}$$

where m_A is mass of the particle $A = \pi, K, \eta$, i.e. numerically $r_\pi = 1, r_K \approx 3.66, r_\eta \approx 4.06$ [cf. discussion around (4.64)].

The lightest two- or more-particle state with the same quantum numbers as A is $A\pi\pi$, i.e. $M_A = m_\pi(2+r)$ and $\Xi_{AA}(x) = \frac{16m_\pi^2}{x}(1+r)^2$. Similarly, the threshold for production of two-particle states in the considered process is $s_{\rm thr} = 4m_\pi^2$, which corresponds to $x_{\rm thr} = 1$.

The physical threshold is naturally $s_{\rm phys} = 4m_\pi^2 r^2$, which corresponds to $x_{\rm phys} = r^2$ and the inelastic threshold coincide with the threshold of production of four pions, $s_{\rm inel} = 16m_\pi^2 \equiv x_{\rm inel} = 4$.

Further quantities are equal to

$$x_0(x) = \sqrt{1 + \frac{4(1+r)^2}{x\,(x-r^2)}}, \tag{C.31}$$

$$l_{AA}(x) = 4m_\pi^2 \left(r^2 - x - \frac{4(1+r)^2}{x} \right), \tag{C.32}$$

$$r_{sL}(x) = 2m_\pi^2 (x-r^2) \left(\sqrt{1 + \frac{4(1+r)^2}{x\,(x-r^2)}} - 1 \right). \tag{C.33}$$

Thus, for $r \geq 1$

$$u'_M = 4m_\pi^2 \left(4 + 4r - r^2\right), \tag{C.34}$$

which is greater than $4m_\pi^2$ for $r < 2 + \sqrt{7} \approx 4.65$. The maximum of r_{sL} appearing in R is equal to $4m_\pi^2$ and so

$$R = 4m_\pi^2 \quad \Rightarrow s_{\rm crit} = 16m_\pi^2(1+r)^2 \quad \Rightarrow x_{\rm crit} = 4(1+r)^2. \tag{C.35}$$

Therefore, the domains of analyticity for the absorptive part are ellipses

$$|u| + \left| u + 4m_\pi^2 (x-r^2) \right| < 4m_\pi^2 (x-r^2) + 2\rho(x), \tag{C.36}$$

where for $r < 2$

$$\rho(x) = \begin{cases} \frac{16m_\pi^2}{x}(1+r)^2 & \text{for} \quad 1 \leq x < r^2, \\ 16m_\pi^2 \left(1 + \frac{1}{x-r^2}\right) & \text{for} \quad r^2 \leq x < 4, \\ \frac{16m_\pi^2}{x}(1+r)^2 & \text{for} \quad 4 \leq x < 4(1+r)^2, \\ 4m_\pi^2 & \text{for} \quad x \geq 4(1+r)^2, \end{cases} \tag{C.37}$$

while for $r \geq 2$

$$\rho(x) = \begin{cases} \frac{16m_\pi^2}{x}(1+r)^2 & \text{for} \quad 1 \leq x < 4(1+r)^2, \\ 4m_\pi^2 & \text{for} \quad x \geq 4(1+r)^2, \end{cases} \tag{C.38}$$

The fixed u dispersion relation can be thus proved for $u \in \langle -4m_\pi^2 \left(4 + 4r - r^2\right), 4m_\pi^2 \rangle$. Note that without the use of the positivity, the Lehmann theory would give $\rho(x) = \Xi_{AA}(x)$ and the interval of validity of dispersion relations would be only $u \in \langle -4m_\pi^2 \left(4 + 4r - r^2\right), 0 \rangle$.

The regions of validity of dispersion relations for the particular processes, viz $\pi\pi$, KK and $\eta\eta$ elastic scatterings, are depicted on Figure 25. The real intervals contained in them are

$$\pi\pi: \qquad -28m_\pi^2 \leq u \leq 4m_\pi^2, \tag{C.39}$$

$$KK: \qquad -20.98m_\pi^2 \leq u \leq 4m_\pi^2, \tag{C.40}$$

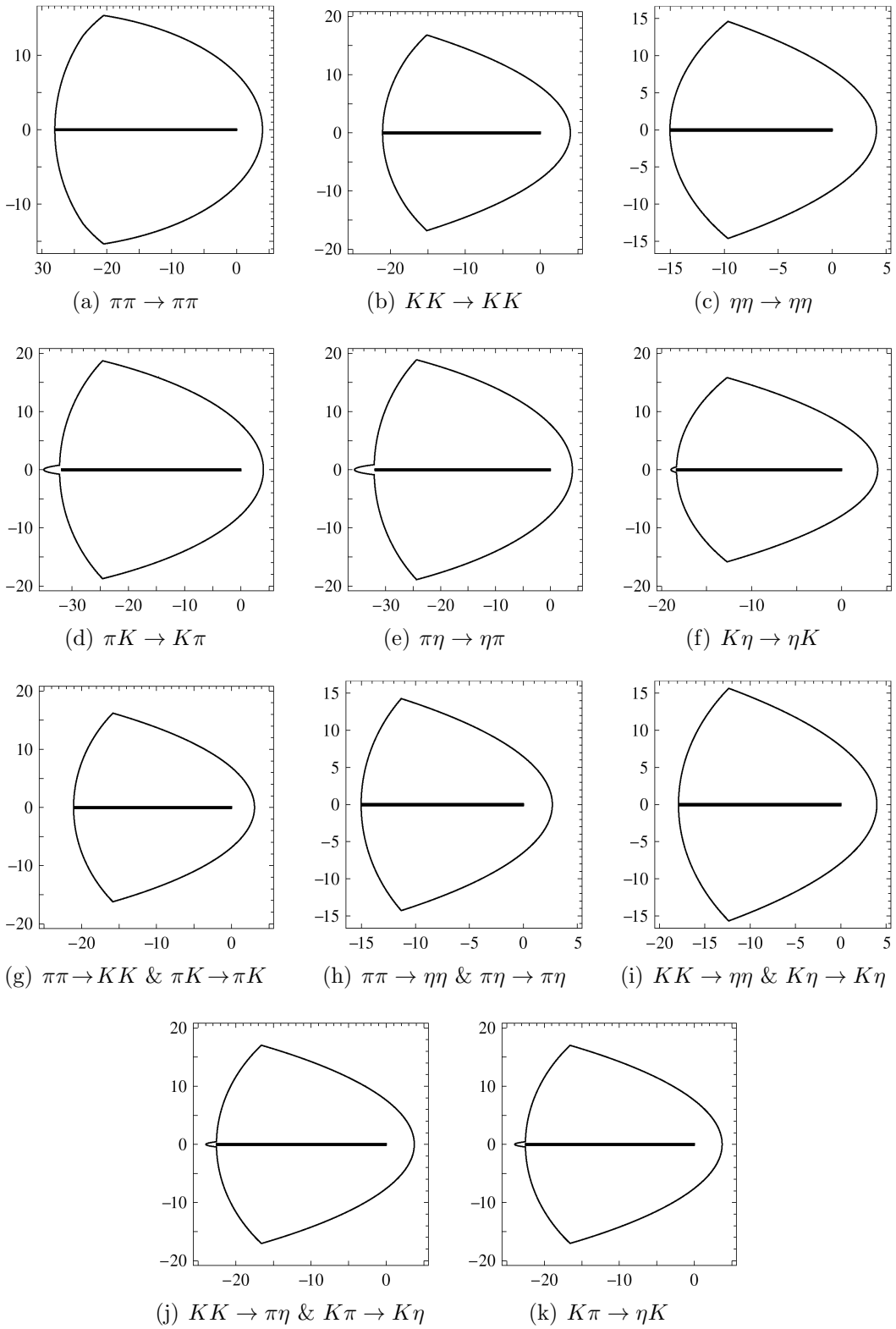

(a) $\pi\pi \to \pi\pi$ (b) $KK \to KK$ (c) $\eta\eta \to \eta\eta$

(d) $\pi K \to K\pi$ (e) $\pi\eta \to \eta\pi$ (f) $K\eta \to \eta K$

(g) $\pi\pi \to KK$ & $\pi K \to \pi K$ (h) $\pi\pi \to \eta\eta$ & $\pi\eta \to \pi\eta$ (i) $KK \to \eta\eta$ & $K\eta \to K\eta$

(j) $KK \to \pi\eta$ & $K\pi \to K\eta$ (k) $K\pi \to \eta K$

Figure 25: Regions of validity of fixed u dispersion relations in complex u-plane (in multiples of m_π^2) for the processes considered in Chapter 4 and therefore also the regions where the assumptions of our theorem for these processes are valid. With the bold lines the intervals of validity coming from the use of just the Lehmann theory (ellipses) depicted.

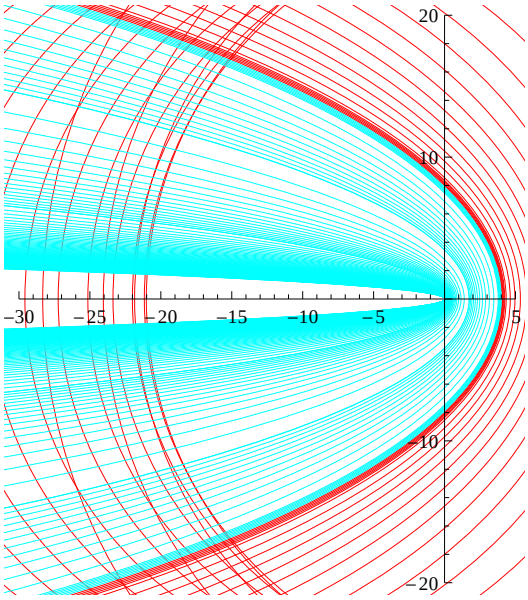

(a) Lehmann ellipses

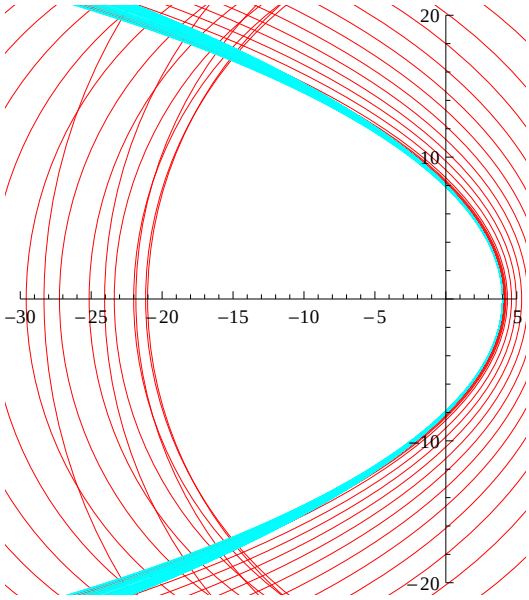

(b) Martin ellipses

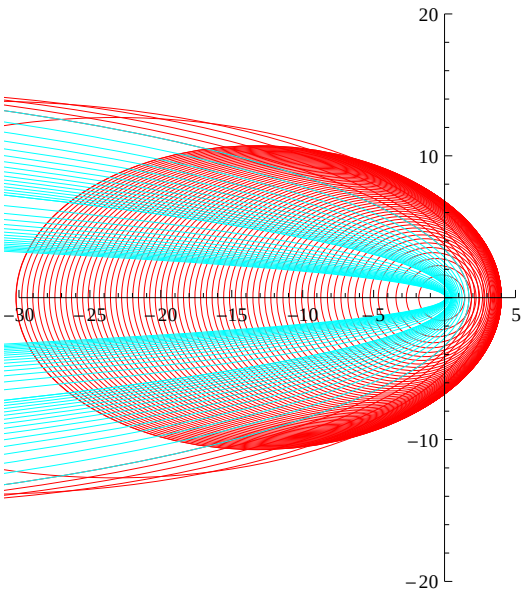

(c) Small Lehmann ellipses

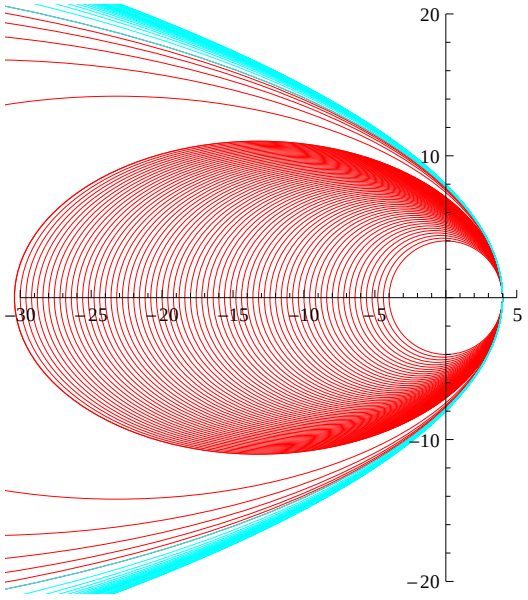

(d) Small Martin ellipses

Figure 26: Analyticity domains for KK scattering in complex u-plane. The upper part depicts the domains where the absorptive parts of KK scattering amplitude are analytic, (a) without the use of the unitarity and (b) by using the prescription given in the main text (taking unitarity into account). The red ellipses are for both cases the same and correspond to $s < s_{\rm crit}$. The cyan ones for $s > s_{\rm crit}$ are different, which leads to the different domains of validity of dispersion relations on the previous figure. On the lower part we have depicted the ellipses, inside which the complete scattering amplitude is analytic, again (c) without the use of unitarity and (d) using it. The red ellipses correspond to $s \in (s_{\rm phys}, 50m_\pi^2)$ whereas the cyan ones to $s \in (50m_\pi^2, 1000m_\pi^2)$. All numbers in labels are in m_π^2 units.

$$\eta\eta: \qquad -15.03m_\pi^2 \leq u \leq 4m_\pi^2. \tag{C.41}$$

For illustration we have also depicted the (large) Lehmann ellipses for various values of s for the process $KK \to KK$ on Figure 26a and the ellipses stemming from the above analysis taking into account the unitarity on Figure 26b. In the case we wanted to find the regions, where the complete amplitude is analytic and its partial wave decomposition is convergent, we would use the small Lehmann ellipses and the ellipses (C.23) — we have depicted them on Figures 26c and 26d. However, for the actual proof of the reconstruction theorem we would need just one value s in whose neighborhood the amplitude is analytic in s and u. Since there always exists the small Lehmann ellipse, which contains also the neighborhood of some u inside the regions of validity of dispersion relations, we fix s at the corresponding value and the amplitude is analytic in small neighborhood in both s and u Mandelstam variables.

Note that in the case we include the isospin violation the possible more-particle state with the same quantum numbers as η would have $M_\eta = 3m_\pi$ and both u_M and u'_M would be negative and one cannot prove the dispersion relations for $\eta\eta$ scattering by this way.

C.3.2 Processes $\pi A \to A\pi$

After the explicit discussion for the previous amplitudes, we can be brief now. Here, we have two types of particles, for them $M_\pi = 3m_\pi$ and $M_A = m_\pi(2+r)$. This leads to $\Xi_{\pi A}(x) = \frac{32m_\pi^2(1+r)}{x-\left(\frac{r-1}{2}\right)^2}$. The particular thresholds are $x_{\rm thr} = x_{\rm phys} = \left(\frac{r+1}{2}\right)^2$ and $x_{\rm inel} = \left(\frac{r+3}{2}\right)^2$.

Then,

$$x_0(x) = \sqrt{1 + \frac{8x(1+r)}{\left(x-\left(\frac{r-1}{2}\right)^2\right)\left(x-\left(\frac{r+1}{2}\right)^2\right)}}\,, \tag{C.42}$$

$$l_{\pi A}(x) = -\frac{4m_\pi^2}{x}\left(x-\left(\frac{r-1}{2}\right)^2\right)\left(x-\left(\frac{r+1}{2}\right)^2\right) - \frac{32m_\pi^2(1+r)}{x-\left(\frac{r-1}{2}\right)^2}, \tag{C.43}$$

$$r_{sL}(x) = \frac{2m_\pi^2}{x}\left(x-\left(\frac{r-1}{2}\right)^2\right)\left(x-\left(\frac{r+1}{2}\right)^2\right)(x_0(x)-1)\,. \tag{C.44}$$

Since $l_{\pi A}(x)$ is for $x > x_{\rm inel}$, $r > 1$ decreasing, its maximum is equal to

$$u'_M = -l_{\pi A}(x_{\rm inel}) = 16m_\pi^2\,\frac{3(r+2)^2+1}{(r+3)^2} \tag{C.45}$$

and greater than $4m_\pi^2$ for any r. The maximum of r_{sL} occurs for $x = \frac{(r+1)(r+3)}{4}$ and is equal to $4m_\pi^2$. The Martin's R is therefore equal to

$$R = 4m_\pi^2 \quad \Rightarrow x_{\rm crit} = \frac{r^2+30r+33}{4}. \tag{C.46}$$

The domains of analyticity for the absorptive parts are ellipses (C.16) with

$$\rho(x) = \begin{cases} 16m_\pi^2 \left(1 + \frac{x}{\left(x-\left(\frac{r-1}{2}\right)^2\right)\left(x-\left(\frac{r+1}{2}\right)^2\right)}\right) & \text{for} \quad \left(\frac{r+1}{2}\right)^2 \le x < \left(\frac{r+3}{2}\right)^2, \\ \frac{32m_\pi^2(1+r)}{x-\left(\frac{r-1}{2}\right)^2} & \text{for} \quad \left(\frac{r+3}{2}\right)^2 \le x < \frac{r^2+30r+33}{4}, \\ 4m_\pi^2 & \text{for} \quad x \ge \frac{r^2+30r+33}{4}. \end{cases} \tag{C.47}$$

The fixed u dispersion relation can be thus proved for $u \in \left\langle -16m_\pi^2 \frac{3(r+2)^2+1}{(r+3)^2}, 4m_\pi^2 \right\rangle$.

The regions of validity of dispersion relations for the πK and $\pi\eta$ elastic scatterings are depicted again on Figure 25. The real intervals contained in them are

$$\pi K: \qquad -35.03m_\pi^2 \le u \le 4m_\pi^2 \qquad \left(-31.87m_\pi^2 \le u \le 0\right), \tag{C.48}$$

$$\pi\eta: \qquad -35.69m_\pi^2 \le u \le 4m_\pi^2 \qquad \left(-31.94m_\pi^2 \le u \le 0\right). \tag{C.49}$$

In brackets, we have added also the intervals following from the Lehmann analysis.

C.3.3 Process $K\eta \to \eta K$

By a simple generalization of the previous processes, we obtain results for the last elastic scattering $K\eta \to \eta K$. We arrive at

$$x_{\text{thr}} = \left(\frac{r_K+1}{2}\right)^2, \tag{C.50}$$

$$x_{\text{phys}} = \left(\frac{r_K+r_\eta}{2}\right)^2, \tag{C.51}$$

$$x_{\text{inel}} = \left(\frac{r_K+3}{2}\right)^2, \tag{C.52}$$

$$\Xi_{K\eta}(x) = \frac{16m_\pi^2(1+r_K)(1+r_\eta)}{x - \frac{1}{4}\left(r_\eta - r_K\right)^2}. \tag{C.53}$$

The maximum of $l_{K\eta}(x)$ for $x > x_{\text{inel}}$ is again equal to $l_{K\eta}(x_{\text{inel}})$, which is larger than $4m_\pi^2$, whereas the maximum of $r_{sL}(x)$ occuring at $x = \frac{1}{4}(2+r_K+r_\eta)(r_K+r_\eta)$ is equal to $4m_\pi^2$. R is thus again equal to $4m_\pi^2$ and $x_{\text{crit}} = (2+r_K+r_\eta)^2 - \frac{3}{4}\left(r_\eta - r_K\right)^2$. In the ellipses of analyticity of the absorptive part of the amplitude

$$\rho(x) = \begin{cases} \frac{16m_\pi^2(1+r_K)(1+r_\eta)}{x-\frac{1}{4}(r_\eta-r_K)^2} & \text{for} \quad \frac{1}{4}\left(r_K+1\right)^2 \le x < (2+r_K+r_\eta)^2 - \frac{3}{4}\left(r_\eta - r_K\right)^2, \\ 4m_\pi^2 & \text{for} \quad x \ge (2+r_K+r_\eta)^2 - \frac{3}{4}\left(r_\eta - r_K\right)^2. \end{cases} \tag{C.54}$$

They are depicted on Figure 25. The real interval of validity of dispersion relations is $u \in \langle -18.96m_\pi^2, 4m_\pi^2 \rangle$. The Lehmann interval would be just $u \in \langle -18.34m_\pi^2, 0 \rangle$.

C.3.4 The inelastic processes

For the remaining processes, which are inelastic, we use the results of Section C.2.2. We illustrate the explicit determinations on the process $\pi\pi \to KK$.

Process $\pi\pi \to KK$

Also for this process $\delta_{ABCD} = 0$ and the ellipses (C.26) simplify into

$$\left|u + \frac{s}{4}\left(\sigma_\pi(s) + \sigma_K(s)\right)^2\right| + \left|u + \frac{s}{4}\left(\sigma_\pi(s) - \sigma_K(s)\right)^2\right| < \rho(s) \tag{C.55}$$

with (we have used the results for $\pi\pi$ and KK elastic scatterings)

$$\rho(s) = \max\left\{ \begin{array}{l} 4m_\pi^2\left(\sqrt{\left(x - 1 + \frac{16}{x}\right)\left(x - r^2 + \frac{4}{x}(1+r)^2\right)} + \frac{8}{x}(1+r)\right) \\ \frac{s}{2}\,\sigma_\pi(s)\sigma_K(s)\,\frac{1+\eta_\pi(s)\eta_K(s)}{\sqrt{\eta_\pi(s)\eta_K(s)}} \end{array} \right\}, \tag{C.56}$$

where

$$\eta_A(s) = 1 + \frac{2}{x - r^2}\left(1 + \sqrt{x - r^2 + 1}\right). \tag{C.57}$$

There is no simple expression for the intervals, where one of the functions appearing in (C.27) prevails the other. We therefore just plot the minimal regions, where the dispersion relations are valid and list here the resulting real intervals belonging to them. However, before we can do this, we need to determine the ellipses also for the t-crossed channel.

Process $\pi\pi \to KK$

In this case the ellipses (C.26) simplify into

$$\left|u + s - 2m_\pi^2 - 2m_K^2\right| + \left|u - \frac{\Delta_{\pi K}^2}{s}\right| < \rho(s) \tag{C.58}$$

with

$$\rho(s) = \max\left\{\frac{\lambda_{\pi K}(s)}{s} + 2\Xi_{\pi K}(s), \frac{\lambda_{\pi K}(s)}{s}\,\frac{1 + \eta_{\pi K}^2(s)}{2\eta_{\pi K}(s)}\right\}, \tag{C.59}$$

where $\Xi_{\pi K}(s)$ corresponds to the value for $\pi K \to K\pi$ process computed above and $\eta_{\pi K}(s)$ follows from (C.28) with $R = 4m_\pi^2$.

The region of validity of dispersion relations depicted on Figure 25 for this process is intersection of the ellipses for both of these crossing channels above their particular thresholds.

Real intervals of validity of fixed u dispersion relations

The real intervals contained in these regions for the remaining processes are the following

$$\pi\pi \to KK: \qquad -21.04m_\pi^2 \leq u \leq 3.05m_\pi^2, \tag{C.60}$$
$$\pi\pi \to \eta\eta: \qquad -14.96m_\pi^2 \leq u \leq 2.68m_\pi^2, \tag{C.61}$$
$$KK \to \eta\eta: \qquad -17.88m_\pi^2 \leq u \leq 3.79m_\pi^2, \tag{C.62}$$
$$KK \to \pi\eta: \qquad -23.96m_\pi^2 \leq u \leq 3.77m_\pi^2, \tag{C.63}$$
$$K\pi \to \eta K: \qquad -23.93m_\pi^2 \leq u \leq 3.75m_\pi^2. \tag{C.64}$$

In the last two cases we have again extended the regions by using the arguments following from elastic unitarity in the $K\pi \to \pi K$ scattering below its inelastic threshold. Without it, the regions would start with $-22.55m_\pi^2$ and $-22.51m_\pi^2$ respectively.

Appendix D

Standard χPT $O(p^4)$ values of the polynomial parameters for meson-meson scattering

We give here the values of polynomial parameters of our parametrization of meson-meson scattering processes in the isospin symmetric case [from Chapter 4] that reproduce the $O(p^4)$ results of the standard chiral perturbation theory. To obtain them we have used the comparison of our results of first iteration of reconstruction procedure with the standard χPT computation of [78], which contains all the considered amplitudes and we have took advantage of the unitary form of their results.

The form of our results is given in terms of physical observables and thus it has to be scale-independent and the same for all the possible regularization schemes. The only thing which can be influenced by using different schemes is the relation between our polynomial parameters and the (renormalised) constants of the Lagrangian theory (LEC). With a change of the renormalization scale, the values of the LEC change but their combinations giving the values of our parameters remain scale-independent — this can be another test of the results obtained from the Lagrangian theory. A further difference between (Lagrangian theory) results of various authors can rise from different choices of the way they parametrize the $O(p^2)$ constants (bare masses and decay constants) using the physical parameters — for instance in [78] they expand F_K and F_η decay constants in terms of F_π, L_4^r and L_5^r.

In [78] they used intensively the Gell-Mann-Okubo relation (GMO) to get their results more simplified. In the standard chiral power counting the GMO formula has a correction of $O(p^4)$ order and thus we could also employ it to simplify our results in the places where it would bring only corrections of $O(p^6)$ order at least. However, to leave the relations from this appendix be closely connected to the results [78], we have not done it. The only place where we refer to the GMO formula (and its correction of $O(p^4)$ order) is in those places where we want to emphasize the validity of the $O(p^2)$ values of the parameters from Section 4.3. Nevertheless, the use of

$$\Delta_{\mathrm{GMO}}(m_\eta^2 - m_\pi^2) = 4m_K^2 - m_\pi^2 - 3m_\eta^2, \tag{D.1}$$

which is in the standard power counting of the $O(p^4)$ order, can be understood also just

as a (though more complicated) notation of the right-hand side of this definition.

In the results there appear chiral logarithms defined in (4.48). Their dependence on the scale μ (in those relations written as Λ) is compensated on the right-hand side of the following relations by the scale-dependence of LEC L_i^r as listed in [74].

- $\eta\eta$

$$\delta_{\eta\eta} = 12(2L_1^r + 2L_2^r + L_3) - \frac{27F_\pi^2\mu_K}{4m_K^2} - \frac{27}{128\pi^2}\,, \tag{D.2}$$

$$\begin{aligned} F_\pi^2(\alpha_{\eta\eta}-1)(m_\pi^2-4m_\eta^2) &= -\frac{4}{3}F_\pi^2\Delta_{\rm GMO}(m_\eta^2-m_\pi^2) + 96m_\eta^4(L_4^r-3L_6^r) \\ &+ 8L_5^r\left(3m_\pi^4-10m_\eta^2m_\pi^2+13m_\eta^4\right) \\ &- 192L_7\left(m_\pi^4-3m_\eta^2m_\pi^2+2m_\eta^4\right) - 48L_8^r\left(2m_\pi^4-6m_\eta^2m_\pi^2+7m_\eta^4\right) \\ &+ \frac{\left(7m_\pi^4-24m_\pi^2m_\eta^2-54m_\eta^4\right)\mu_K F_\pi^2}{3m_K^2} + \frac{\left(48m_\eta^2-7m_\pi^2\right)\mu_\pi F_\pi^2}{3} \\ &+ \frac{\left(m_\pi^4-8m_\eta^2m_\pi^2+24m_\eta^4\right)\mu_\eta F_\pi^2}{m_\eta^2} + \frac{80m_K^4-176m_\eta^2m_K^2+103m_\eta^4}{32\pi^2}\,. \end{aligned} \tag{D.3}$$

- $\eta\pi$

$$\varepsilon_{\eta\pi} = 24L_1^r + 4L_3 - \frac{9F_\pi^2\mu_K}{4m_K^2} - \frac{9}{128\pi^2}\,, \tag{D.4}$$

$$\delta_{\eta\pi} = 12L_2^r + 4L_3 - \frac{9F_\pi^2\mu_K}{4m_K^2} - \frac{9}{128\pi^2}\,, \tag{D.5}$$

$$F_\pi^2\beta_{\eta\pi} = 8L_4^r\left(m_\pi^2+m_\eta^2\right) - \frac{m_\pi^2+m_\eta^2}{32\pi^2} - \frac{\left(m_\pi^2+3m_\eta^2\right)F_\pi^2\mu_K}{3m_K^2} - \frac{2F_\pi^2\mu_\pi}{3}\,, \tag{D.6}$$

$$\begin{aligned} F_\pi^2(\alpha_{\eta\pi}-1)m_\pi^2 &= 16L_4^r\left(m_\pi^4-4m_\eta^2m_\pi^2+m_\eta^4\right) + 16m_\eta^2m_\pi^2(-L_5^r+6L_6^r) \\ &+ 96L_7\left(m_\pi^2-m_\eta^2\right)m_\pi^2 + 48L_8^rm_\pi^4 \\ &- \frac{\left(5m_\pi^4-28m_\eta^2m_\pi^2+6m_\eta^4\right)F_\pi^2\mu_K}{3m_K^2} + \frac{\left(-17m_\pi^4+9m_\eta^2m_\pi^2+4m_\eta^4\right)F_\pi^2\mu_\pi}{3\left(m_\pi^2-m_\eta^2\right)} \\ &+ \frac{\left(m_\pi^4-m_\eta^2m_\pi^2+4m_\eta^4\right)m_\pi^2F_\pi^2\mu_\eta}{3m_\eta^2(m_\pi^2-m_\eta^2)} - \frac{8m_\pi^4-11m_\eta^2m_\pi^2+6m_\eta^4}{96\pi^2}\,. \end{aligned} \tag{D.7}$$

- $\pi\pi$

$$\varepsilon_{\pi\pi} = 4L_2^r + \frac{1}{12}F_\pi^2\left(-\frac{\mu_K}{m_K^2} - \frac{8\mu_\pi}{m_\pi^2}\right) - \frac{7}{384\pi^2}\,, \tag{D.8}$$

$$\delta_{\pi\pi} = 8L_1^r + 4L_3 + \frac{1}{12}F_\pi^2\left(-\frac{\mu_K}{m_K^2} - \frac{8\mu_\pi}{m_\pi^2}\right) - \frac{13}{384\pi^2}\,, \tag{D.9}$$

$$F_\pi^2(\beta_{\pi\pi}-1) = 8\left(2L_4^r + L_5^r\right)m_\pi^2 - \frac{F_\pi^2\mu_K m_\pi^2}{m_K^2} - \frac{5m_\pi^2}{32\pi^2} - 4F_\pi^2\mu_\pi, \tag{D.10}$$

$$\begin{aligned} F_\pi^2(\alpha_{\pi\pi}-1)m_\pi^2 &\\ &= -16\left(2L_4^r + L_5^r - 6L_6^r - 3L_8^r\right)m_\pi^4 - \frac{F_\pi^2\mu_\eta m_\pi^4}{3m_\eta^2} - \frac{F_\pi^2\mu_K m_\pi^4}{m_K^2} \\ &\quad - \frac{7m_\pi^4}{96\pi^2} - F_\pi^2\mu_\pi m_\pi^2. \end{aligned} \tag{D.11}$$

- $K\eta$

$$\varepsilon_{K\eta} = 16L_2^r + \frac{4}{3}L_3 - \frac{F_\pi^2(2\mu_K+\mu_\pi+3\mu_\eta)}{2\left(m_K^2-m_\eta^2\right)} + \frac{1}{64\pi^2}, \tag{D.12}$$

$$\delta_{K\eta} = 32L_1^r + \frac{40}{3}L_3 + \frac{\left(9m_\eta^2-8m_K^2\right)F_\pi^2\mu_K}{2m_K^2\left(m_K^2-m_\eta^2\right)} + \frac{F_\pi^2\left(\mu_\pi-3\mu_\eta\right)}{4(m_K^2-m_\eta^2)} - \frac{11}{64\pi^2}, \tag{D.13}$$

$$\begin{aligned} F_\pi^2(\beta_{K\eta}-1) &= \frac{32}{3}\left(m_K^2+m_\eta^2\right)L_4^r + 8L_5^r m_\pi^2 - \frac{m_\eta^2\left(7m_K^2-9m_\eta^2\right)F_\pi^2\mu_K}{3m_K^2(m_K^2-m_\eta^2)} \\ &\quad + \frac{\left(13m_\eta^2-11m_K^2\right)F_\pi^2\mu_\pi}{3\left(m_K^2-m_\eta^2\right)} + \frac{\left(4m_K^4-15m_\eta^2m_K^2+7m_\eta^4\right)F_\pi^2\mu_\eta}{3m_\eta^2(m_K^2-m_\eta^2)} \\ &\quad - \frac{17m_\eta^2+37m_K^2}{192\pi^2}, \end{aligned} \tag{D.14}$$

$$\begin{aligned} &F_\pi^2(\alpha_{K\eta}-1)\left(3m_\eta^2-m_K^2\right) \\ &\quad = F_\pi^2\Delta_{\mathrm{GMO}}(m_\eta^2-m_\pi^2) + 32L_4^r\left(m_K^4-4m_\eta^2m_K^2+m_\eta^4\right) \\ &\quad + 192L_6^r m_K^2m_\eta^2 + 4L_5^r\left(-3m_\pi^4+6m_K^2m_\pi^2+m_\eta^2m_\pi^2-12m_\eta^4\right) \\ &\quad + 48L_7\left(m_\pi^4-4m_\eta^2m_\pi^2+3m_\eta^4\right) + 24L_8^r\left(m_\pi^4-3m_\eta^2m_\pi^2+6m_\eta^4\right) \\ &\quad - \frac{\left(14m_K^6-84m_\eta^2m_K^4+102m_\eta^4m_K^2-27m_\eta^6\right)F_\pi^2\mu_K}{3(m_K^2-m_\eta^2)} \\ &\quad - \frac{\left(m_K^4+12m_\eta^2m_K^2-14m_\eta^4\right)F_\pi^2\mu_\pi}{2(m_K^2-m_\eta^2)} \\ &\quad + \frac{\left(8m_K^6-41m_\eta^2m_K^4+104m_\eta^4m_K^2-78m_\eta^6\right)F_\pi^2\mu_\eta}{6m_\eta^2(m_K^2-m_\eta^2)} \\ &\quad - \frac{31m_K^4-55m_\eta^2m_K^2+39m_\eta^4}{96\pi^2}. \end{aligned} \tag{D.15}$$

- $\eta\pi K$

$$\varepsilon_{K\eta\pi} = -4L_3 + \frac{6\mu_K F_\pi^2}{m_K^2-m_\pi^2} - \frac{3\mu_\pi F_\pi^2}{2\left(m_K^2-m_\pi^2\right)} + \frac{3\mu_\eta F_\pi^2}{2\left(m_K^2-m_\eta^2\right)} + \frac{1}{64\pi^2}, \tag{D.16}$$

$$\delta_{K\eta\pi} = 8L_3 + \frac{3\left(m_\pi^2 - 2m_K^2\right)\mu_K F_\pi^2}{2m_K^2\left(m_K^2 - m_\pi^2\right)} - \frac{3\mu_\pi F_\pi^2}{4\left(m_K^2 - m_\pi^2\right)} - \frac{3\mu_\eta F_\pi^2}{4\left(m_K^2 - m_\eta^2\right)} - \frac{5}{64\pi^2}\,, \tag{D.17}$$

$$\begin{aligned} F_\pi^2(\beta_{K\eta\pi} - 1) &= \frac{4}{3}L_3\Delta_{\rm GMO}(m_\eta^2 - m_\pi^2) + 8m_\pi^2 L_5^r \\ &+ \frac{\left(-32m_K^4 + 2m_K^2(2m_\pi^2 - 3m_\eta^2) + 3m_\pi^2(m_\pi^2 + m_\eta^2)\right)F_\pi^2\mu_K}{6\left(m_K^2 - m_\pi^2\right)} \\ &+ \frac{\left(-40m_K^2 + 9m_\eta^2 + 33m_\pi^2\right)F_\pi^2\mu_\pi}{12\left(m_K^2 - m_\pi^2\right)} - \frac{\left(m_\pi^2 + 5m_\eta^2\right)F_\pi^2\mu_\eta}{4(m_K^2 - m_\eta^2)} \\ &+ \frac{-57m_K^2 + 4m_\pi^2 + 27m_\eta^2}{192\pi^2}\,, \end{aligned} \tag{D.18}$$

$$\begin{aligned} F_\pi^2\alpha_{K\eta\pi}m_\pi^2 &= -\frac{F_\pi^2}{3}\Delta_{\rm GMO}(m_\eta^2 - m_\pi^2) + \frac{8}{3}L_3\left(8m_K^2 + m_\pi^2 + m_\eta^2\right)\Delta_{\rm GMO}(m_\eta^2 - m_\pi^2) \\ &+ 4\left(m_\pi^4 - 4m_K^2m_\pi^2 + 4m_\eta^2m_\pi^2 - m_\eta^4\right)L_5^r + 24\left(m_\eta^4 - m_\pi^4\right)(2L_7 + L_8^r) \\ &+ \frac{\left(40m_K^6 + 8\left(m_\eta^2 - 10m_\pi^2\right)m_K^4 - 3m_\pi^2(m_\pi^2 + m_\eta^2)^2 + 2m_K^2(17m_\pi^4 + 25m_\pi^2m_\eta^2 - 6m_\eta^4)\right)F_\pi^2\mu_K}{6\left(m_K^2 - m_\pi^2\right)} \\ &+ \frac{\left(-70m_K^4 + 2\left(22m_\pi^2 + 19m_\eta^2\right)m_K^2 - 19m_\pi^4 + 9m_\eta^4 - 12m_\pi^2m_\eta^2\right)F_\pi^2\mu_\pi}{6\left(m_K^2 - m_\pi^2\right)} \\ &+ \frac{\left(14m_K^4 - m_\pi^4 + 21m_\eta^4 + 6m_\pi^2m_\eta^2 - 2m_K^2\left(m_\pi^2 + 18m_\eta^2\right)\right)F_\pi^2\mu_\eta}{2\left(m_K^2 - m_\eta^2\right)} \\ &+ \frac{-408m_K^4 + \left(73m_\pi^2 + 387m_\eta^2\right)m_K^2 + 8m_\pi^4 - 63m_\eta^4 - m_\pi^2m_\eta^2}{192\pi^2}\,. \end{aligned} \tag{D.19}$$

- $K\pi$

$$\varphi_{K\pi} = -4L_3 + \frac{\left(m_\pi^2 - 4m_K^2\right)F_\pi^2\mu_K}{6m_K^2\left(m_K^2 - m_\pi^2\right)} + \frac{\left(m_\pi^2 - 4m_K^2\right)F_\pi^2\mu_\pi}{12m_\pi^2\left(m_K^2 - m_\pi^2\right)} - \frac{F_\pi^2\mu_\eta}{m_\pi^2 - m_\eta^2}\,, \tag{D.20}$$

$$\varepsilon_{K\pi} = 12(4L_2^r + L_3) - \frac{3F_\pi^2\mu_K}{m_K^2 - m_\pi^2} + \frac{15F_\pi^2\mu_\pi}{2(m_K^2 - m_\pi^2)} + \frac{6F_\pi^2\mu_\eta}{m_\pi^2 - m_\eta^2} + \frac{1}{64\pi^2}\,, \tag{D.21}$$

$$\begin{aligned} \delta_{K\pi} &= 24(4L_1^r + L_3) + \frac{3\left(3m_\pi^2 - 4m_K^2\right)F_\pi^2\mu_K}{2m_K^2\left(m_K^2 - m_\pi^2\right)} + \frac{3\left(7m_\pi^2 - 8m_K^2\right)F_\pi^2\mu_\pi}{4m_\pi^2\left(m_K^2 - m_\pi^2\right)} \\ &- \frac{3F_\pi^2\mu_\eta}{m_\pi^2 - m_\eta^2} - \frac{23}{64\pi^2}\,, \end{aligned} \tag{D.22}$$

$$\begin{aligned} F_\pi^2(\gamma_{K\pi} - 1) &= 8m_\pi^2L_5^r - \frac{2m_K^2F_\pi^2\mu_K}{m_K^2 - m_\pi^2} - \frac{\left(m_K^2 - 5m_\pi^2\right)F_\pi^2\mu_\pi}{2(m_K^2 - m_\pi^2)} \\ &+ \frac{\left(2m_K^2 + m_\pi^2 - 3m_\eta^2\right)F_\pi^2\mu_\eta}{m_\pi^2 - m_\eta^2} - \frac{5m_K^2 + m_\pi^2}{192\pi^2}\,, \end{aligned} \tag{D.23}$$

$$
\begin{aligned}
F_\pi^2(\beta_{K\pi}-1) &= 32\left(m_K^2+m_\pi^2\right)L_4^r + 8L_5^r m_\pi^2 - \frac{15m_\pi^2+19m_K^2}{64\pi^2F_\pi^2} \\
&+ \frac{\left(3m_\pi^4+3m_K^2m_\pi^2-8m_K^4\right)F_\pi^2\mu_K}{m_K^2(m_K^2-m_\pi^2)} - \frac{\left(3m_\pi^4-3m_K^2m_\pi^2-4m_K^4\right)F_\pi^2\mu_\pi}{2m_\pi^2(m_K^2-m_\pi^2)} \\
&- \frac{\left(2m_\pi^4+9m_\eta^4+\left(4m_K^2+m_\pi^2\right)m_\eta^2\right)F_\pi^2\mu_\eta}{2m_\eta^2\left(m_\pi^2-m_\eta^2\right)}\,,
\end{aligned}
\tag{D.24}
$$

$$
\begin{aligned}
&F_\pi^2(\alpha_{K\pi}-1)m_\pi m_K \\
&\quad= 16L_4^r\left(m_K^4-4m_\pi^2m_K^2+m_\pi^4\right) + 4L_5^r m_\pi^2\left(m_\pi^2-5m_K^2\right) + 48m_K^2m_\pi^2(2L_6^r+L_8^r) \\
&\quad- \frac{21m_K^4-25m_\pi^2m_K^2+21m_\pi^4}{192\pi^2} + \frac{\left(2m_K^6-4m_K^4m_\pi^2+6m_\pi^4m_K^2-3m_\pi^6\right)F_\pi^2\mu_K}{2m_K^2(m_K^2-m_\pi^2)} \\
&\quad- \frac{\left(8m_K^6-13m_K^4m_\pi^2+12m_\pi^4m_K^2-6m_\pi^6\right)F_\pi^2\mu_\pi}{4m_\pi^2(m_K^2-m_\pi^2)} \\
&- \frac{\left(17m_\pi^6-24m_K^2m_\pi^4+3\left(27m_\eta^2+7m_\pi^2-36m_K^2\right)m_\eta^4+\left(24m_K^4+12m_\pi^2m_K^2+m_\pi^4\right)m_\eta^2\right)F_\pi^2\mu_\eta}{24m_\eta^2\left(m_\pi^2-m_\eta^2\right)}\,.
\end{aligned}
\tag{D.25}
$$

- KK

$$
\varphi_{KK} = 24L_2^r - \frac{17F_\pi^2\mu_K}{4m_K^2} - \frac{F_\pi^2\mu_\pi}{4m_\pi^2} - \frac{7}{64\pi^2}\,,
\tag{D.26}
$$

$$
\varepsilon_{KK} = 12(2L_2^r+L_3) - \frac{F_\pi^2\mu_K}{4m_K^2} - \frac{F_\pi^2}{8}\left(\frac{2}{m_\pi^2}-\frac{27}{m_K^2-m_\pi^2}\right)\mu_\pi + \frac{9F_\pi^2\mu_\eta}{2\left(m_\pi^2-m_\eta^2\right)} - \frac{1}{64\pi^2}\,,
\tag{D.27}
$$

$$
\begin{aligned}
\delta_{KK} &= 12(4L_1^r+L_3) - \frac{11F_\pi^2\mu_K}{4m_K^2} - \frac{F_\pi^2}{16}\left(\frac{10}{m_\pi^2}+\frac{27}{m_K^2-m_\pi^2}\right)\mu_\pi \\
&- \frac{9}{8}F_\pi^2\left(\frac{3}{m_\eta^2}+\frac{2}{m_\pi^2-m_\eta^2}\right)\mu_\eta - \frac{29}{128\pi^2}\,,
\end{aligned}
\tag{D.28}
$$

$$
\begin{aligned}
F_\pi^2\gamma_{KK} &= 16m_K^2L_4^r - \frac{7m_K^2}{64\pi^2} - \frac{3F_\pi^2\mu_K}{2} - \frac{3m_K^2\left(2m_K^2+m_\pi^2\right)F_\pi^2\mu_\pi}{8m_\pi^2(m_K^2-m_\pi^2)} \\
&+ \frac{\left(m_\pi^4-3m_\eta^4+2m_\pi^2m_\eta^2+3\left(m_\eta^2-3m_\pi^2\right)m_K^2\right)F_\pi^2\mu_\eta}{4m_\eta^2\left(m_\pi^2-m_\eta^2\right)}\,,
\end{aligned}
\tag{D.29}
$$

$$
\begin{aligned}
F_\pi^2(\beta_{KK}-1) &= 16m_K^2L_4^r + 8L_5^r m_\pi^2 - \frac{9m_K^2}{64\pi^2} - \frac{3F_\pi^2\mu_K}{2} - \frac{\left(6m_K^4+11m_\pi^2m_K^2-20m_\pi^4\right)F_\pi^2\mu_\pi}{8m_\pi^2(m_K^2-m_\pi^2)} \\
&+ \frac{\left(m_\pi^4-9m_\eta^4+8m_\pi^2m_\eta^2+m_K^2\left(11m_\eta^2-9m_\pi^2\right)\right)F_\pi^2\mu_\eta}{4m_\eta^2\left(m_\pi^2-m_\eta^2\right)}\,,
\end{aligned}
\tag{D.30}
$$

$$
\begin{aligned}
&F_\pi^2(\alpha_{KK}-1)m_K^2 \\
&\qquad = 16m_K^4(-2L_4^r+6L_6^r+3L_8^r)+8L_5^r m_K^2\left(m_\pi^2-3m_K^2\right) \\
&\qquad -\frac{7m_K^4}{192\pi^2}-\frac{3m_K^2F_\pi^2\mu_K}{2}-\frac{m_K^2\left(6m_K^4+17m_\pi^2m_K^2-20m_\pi^4\right)F_\pi^2\mu_\pi}{8m_\pi^2(m_K^2-m_\pi^2)} \\
&-\frac{\left(m_\pi^6+2m_\eta^2m_\pi^4-3m_\eta^4m_\pi^2+3m_K^4(9m_\pi^2-7m_\eta^2)-6m_K^2\left(2m_\pi^4+5m_\eta^2m_\pi^2-7m_\eta^4\right)\right)F_\pi^2\mu_\eta}{12m_\eta^2\left(m_\eta^2-m_\pi^2\right)}.
\end{aligned}
\tag{D.31}
$$

In [78] the authors believe $K^+K^-\to K^+K^-$ to be independent on $K^+K^-\to K^0\overline{K^0}$, but we know that isospin structure (Fierz-like identities) and the crossing symmetry dictate the relation between these two processes given by (4.20) together with (4.19). Therefore, we could use the values of our parameters obtained from their $K^+K^-\to K^0\overline{K^0}$ amplitude to explicitly check their $K^+K^-\to K^+K^-$ result T_{ch}.

Appendix E

Restoring polynomials of $\pi\pi$ scattering

In Section 5.6 we construct the one-loop representation of the $\pi\pi$ scattering amplitudes in terms of the scattering length parameters. Since the unitarity part contributes to the expansion of (the real part of) the amplitude at the threshold and we want to keep the physical meaning of the parameters appearing there, we need to subtract the part of the contribution which was thereby double counted. In this appendix we show the determination of that part.

E.1 Keeping the physical value of the scattering lengths

We begin with the easier case of keeping the physical meaning just of the scattering lengths. The only condition we need to fulfil is

$$\operatorname{Re} A_i(s,t,u)|_{\text{thr}} = 16\pi a_i, \tag{E.1}$$

which can be met just by subtracting the constants

$$w_i = 16\pi \operatorname{Re} U_i(s,t,u)|_{\text{thr}}\,. \tag{E.2}$$

Using relations (5.33)–(5.44) and the threshold values of the one-loop functions (E.37)–(E.45), we get

$$w_0 = \frac{1}{\pi}\left(a_0^2 + \mathcal{Q}_{\pm 0}(q)\left(a_x - 4\frac{b_x}{F_\pi^2}\Delta\right)^2\right), \tag{E.3}$$

$$
\begin{aligned}
w_x = \frac{1}{3\pi\Delta}\Bigg(& 6a_c a_x \Delta - 6a_t\left(a_t - 8\frac{b_t}{F_\pi^2}\right)\left(3m_{\pi^\pm}^2 - m_{\pi^0}^2\right) \\
& - 4\frac{b_t^2}{F_\pi^4}\left(49m_{\pi^\pm}^6 - 17m_{\pi^\pm}^4 m_{\pi^0}^2 - m_{\pi^\pm}^2 m_{\pi^0}^4 + m_{\pi^0}^6\right) \\
& + 4m_{\pi^\pm}^2\left(3a_t^2 - 24a_t\frac{b_t}{F_\pi^2}m_{\pi^\pm}^2 + 8\frac{b_t^2}{F_\pi^4}\left(4m_{\pi^\pm}^4 - m_{\pi^\pm}^2 m_{\pi^0}^2 + m_{\pi^0}^4\right)\right)\log q \\
& + \frac{1}{2}\left(3a_0 a_x \Delta + 12a_t m_{\pi^\pm}^2\left(a_t - 8\frac{b_t}{F_\pi^2}\right) + 128\frac{b_t^2}{F_\pi^4}\right)\mathcal{Q}_{0\pm}(q)\Bigg),
\end{aligned}
\tag{E.4}
$$

$$
w_t = \frac{1}{3\pi}\left(6a_t^2 - 4\frac{b_t^2}{F_\pi^4}\Sigma^2 - 16\frac{b_t^2}{F_\pi^4}m_{\pi^\pm}^2 m_{\pi^0}^2\frac{\Sigma}{\Delta}\log q\right), \tag{E.5}
$$

$$
w_c = \frac{1}{\pi}\left(2a_c^2 + \frac{1}{2}a_x^2\mathcal{Q}_{0\pm}(q)\right), \tag{E.6}
$$

$$
w_d = \frac{1}{\pi}a_d^2\,. \tag{E.7}
$$

The functions $\mathcal{Q}(q)$ depending only on the pion mass ratio $q = m_{\pi^0}/m_{\pi^\pm}$ are given in equations (E.46) and (E.47).

E.2 Keeping the physical value of all the leading order parameters

In the case if we want to keep the physical meaning also of the further parameters, we have to use more complicated polynomials — polynomials of a higher order respecting the s, t, u symmetries of the amplitudes and determine their coefficients by solving sets of linear equations stemming from the definitions of the scattering length parameters. Since they are defined as expansion parameters of the real parts of partial waves, we can use the results for them computed in Section 5.7.4 and expand them at the corresponding thresholds in accordance to the definition (5.11). We have used also this method for a double-check of the results, however, an easier way how to obtain them is the method based on the relation between the scattering length parameters and the values of derivatives of the amplitudes at thresholds, which is described in the following.

E.2.1 Relations between the scattering length parameters and the derivatives of amplitudes

According to the partial wave decomposition (2.14) and the definition of the scattering length parameters (5.11), (the real part of) the amplitude can be expanded at the threshold

as follows

$$\begin{aligned}\frac{1}{16\pi}\,\mathrm{Re}\,A(s,t,u) = a + (s-s_{\rm thr})\frac{r}{F_\pi^2} + \cdots \\ + 3C(s,t)\left(a_1 + (s-s_{\rm thr})\frac{r_1}{F_\pi^2} + \cdots\right) \\ + \frac{5}{2}\left(3C(s,t)^2 - \frac{\lambda_{ab}(s)\lambda_{cd}(s)}{16s^2}\right)\left(a_2 + (s-s_{\rm thr})\frac{r_2}{F_\pi^2} + \cdots\right) \\ + \frac{7}{2}C(s,t)\left(5C(s,t)^2 - 3\frac{\lambda_{ab}(s)\lambda_{cd}(s)}{16s^2}\right)\left(a_3 + (s-s_{\rm thr})\frac{r_3}{F_\pi^2} + \cdots\right) \\ + \cdots .\end{aligned} \tag{E.8}$$

The function $C(s,t)$ is connected with the cosine of the scattering angle (2.8),

$$C(s,t) = \frac{2t+s-3s_0}{4} + \frac{\Delta_{ab}\Delta_{cd}}{4s} = \frac{\lambda_{ab}^{1/2}(s)\lambda_{cd}^{1/2}(s)}{4s}\cos\theta. \tag{E.9}$$

Since the threshold $s_{\rm thr} = (m_x+m_y)^2 = \max\{(m_a+m_b)^2, (m_c+m_d)^2\}$, one of the triangle functions $\lambda_{ab}(s)$ or $\lambda_{cd}(s)$ corresponding to this more massive state is equal to zero. (In general, the second one can be different from zero — in this case we write it as $\lambda_z(s_{\rm thr})$.) Consequently, also the function $C(s,t) = 0$ at the threshold and the following derivatives at the threshold equal

$$\frac{1}{16\pi}\,\mathrm{Re}\,A(s,t,u(s,t))|_{\rm thr} = a, \tag{E.10}$$

$$\frac{\partial}{\partial s}\left(\frac{1}{16\pi}\,\mathrm{Re}\,A(s,t,u(s,t))\right)|_{\rm thr} = \frac{r}{F_\pi^2} + \frac{3}{4}\left(1 - \frac{\Delta_{ab}\Delta_{cd}}{s_{\rm thr}^2}\right)a_1 - \frac{5m_xm_y}{8s_{\rm thr}^2}\lambda_z\left(s_{\rm thr}\right)a_2\,, \tag{E.11}$$

$$\frac{\partial}{\partial t}\left(\frac{1}{16\pi}\,\mathrm{Re}\,A(s,t,u(s,t))\right)|_{\rm thr} = \frac{3}{2}\,a_1\,, \tag{E.12}$$

$$\frac{\partial^2}{\partial t^2}\left(\frac{1}{16\pi}\,\mathrm{Re}\,A(s,t,u(s,t))\right)|_{\rm thr} = \frac{15}{4}\,a_2\,. \tag{E.13}$$

(Note that the dependence of the amplitude on $u(s,t)$ is expanded into the dependence on s and t and the derivatives are also with respect to these contributions.) Therefore, we can obtain the scattering length and the effective range by using the derivatives

$$a = \frac{1}{16\pi}\,\mathrm{Re}\,A(s,t,u(s,t))|_{\rm thr}, \tag{E.14}$$

$$\frac{r}{F_\pi^2} = \left(\frac{\partial}{\partial s} - \frac{1}{2}\left(1 - \frac{\Delta_{ab}\Delta_{cd}}{s_{\rm thr}^2}\right)\frac{\partial}{\partial t} + \frac{m_xm_y}{6s_{\rm thr}^2}\lambda_z\left(s_{\rm thr}\right)\frac{\partial^2}{\partial t^2}\right)\left(\frac{1}{16\pi}\,\mathrm{Re}\,A(s,t,u(s,t))\right)|_{\rm thr}\,. \tag{E.15}$$

For the particular processes (5.13)–(5.17) these relations simplify

$$a_i = \frac{1}{16\pi}\,\mathrm{Re}\,A_i(s,t,u(s,t))|_{\mathrm{thr}}, \tag{E.16}$$

$$\frac{r_0}{F_\pi^2} = \left(\frac{\partial}{\partial s} - \frac{1}{2}\frac{\partial}{\partial t}\right)\left(\frac{1}{16\pi}\,\mathrm{Re}\,A_0(s,t,u(s,t))\right)|_{\mathrm{thr}} = \frac{1}{16\pi}\frac{\partial}{\partial s}\,\mathrm{Re}\,A_0(s,t,u(s,t))|_{\mathrm{thr}}\,, \tag{E.17}$$

$$\begin{aligned}\frac{r_x}{F_\pi^2} &= \left(\frac{\partial}{\partial s} - \frac{1}{2}\frac{\partial}{\partial t} + \frac{\Delta}{6}\frac{\partial^2}{\partial t^2}\right)\left(\frac{1}{16\pi}\,\mathrm{Re}\,A_x(s,t,u(s,t))\right)|_{\mathrm{thr}} \\ &= \frac{1}{16\pi}\left(\frac{\partial}{\partial s} + \frac{\Delta}{6}\frac{\partial^2}{\partial t^2}\right)\mathrm{Re}\,A_x(s,t,u(s,t))|_{\mathrm{thr}}\,,\end{aligned} \tag{E.18}$$

$$\frac{r_t}{F_\pi^2} = \left(\frac{\partial}{\partial s} - \frac{2m_{\pi^\pm}m_{\pi^0}}{\mu_+}\frac{\partial}{\partial t}\right)\left(\frac{1}{16\pi}\,\mathrm{Re}\,A_t(s,t,u(s,t))\right)|_{\mathrm{thr}}\,, \tag{E.19}$$

$$\frac{r_c}{F_\pi^2} = \left(\frac{\partial}{\partial s} - \frac{1}{2}\frac{\partial}{\partial t}\right)\left(\frac{1}{16\pi}\,\mathrm{Re}\,A_c(s,t,u(s,t))\right)|_{\mathrm{thr}}\,, \tag{E.20}$$

$$\frac{r_d}{F_\pi^2} = \left(\frac{\partial}{\partial s} - \frac{1}{2}\frac{\partial}{\partial t}\right)\left(\frac{1}{16\pi}\,\mathrm{Re}\,A_d(s,t,u(s,t))\right)|_{\mathrm{thr}} = \frac{1}{16\pi}\frac{\partial}{\partial s}A_d(s,t,u(s,t))|_{\mathrm{thr}}\,. \tag{E.21}$$

E.2.2 Equations for the restoring polynomials

Thanks to the form of the polynomial parts of the amplitudes (5.56)–(5.60), we obtain for the restoring polynomials the following differential equations

$$w_0(4m_{\pi^0}^2) + 2w_0(0) = 16\pi\,\mathrm{Re}\,U_0(s,t,u(s,t))|_{\mathrm{thr}}\,, \tag{E.22}$$

$$w_x(4m_{\pi^\pm}^2) - 2w_t(-\Delta) = 16\pi\,\mathrm{Re}\,U_x(s,t,u(s,t))|_{\mathrm{thr}}\,, \tag{E.23}$$

$$-w_x(0) + w_t(\mu_+) + w_t(\mu_-) = 16\pi\,\mathrm{Re}\,U_t(s,t,u(s,t))|_{\mathrm{thr}}\,, \tag{E.24}$$

$$w_x'(4m_{\pi^\pm}^2) + w_t'(-\Delta) - \frac{\Delta}{3}w_t''(-\Delta) = 16\pi\left(\frac{\partial}{\partial s} + \frac{\Delta}{6}\frac{\partial^2}{\partial t^2}\right)\mathrm{Re}\,U_x(s,t,u(s,t))|_{\mathrm{thr}}\,, \tag{E.25}$$

$$\frac{2m_{\pi^\pm}m_{\pi^0}}{\mu_+}w_x'(0) + w_t'(\mu_+) - \frac{\Sigma}{\mu_+}w_t'(\mu_-) = 16\pi\left(\frac{\partial}{\partial s} - \frac{2m_{\pi^\pm}m_{\pi^0}}{\mu_+}\frac{\partial}{\partial t}\right)\mathrm{Re}\,U_t(s,t,u(s,t))|_{\mathrm{thr}}\,, \tag{E.26}$$

$$w_c(4m_{\pi^\pm}^2) + w_c(0) + w_d(0) = 16\pi\,\mathrm{Re}\,U_c(s,t,u(s,t))|_{\mathrm{thr}}\,, \tag{E.27}$$

$$2w_c(0) + w_d(4m_{\pi^\pm}^2) = 16\pi\,\mathrm{Re}\,U_d(s,t,u(s,t))|_{\mathrm{thr}}\,, \tag{E.28}$$

$$-\frac{1}{2}w_d'(0) - \frac{1}{2}w_c'(0) + w_c'(4m_{\pi^\pm}^2) = 16\pi\left(\frac{\partial}{\partial s} - \frac{1}{2}\frac{\partial}{\partial t}\right)\mathrm{Re}\,U_c(s,t,u(s,t))|_{\mathrm{thr}}\,, \tag{E.29}$$

$$w_d'(4m_{\pi^\pm}^2) - w_c'(0) = 16\pi\left(\frac{\partial}{\partial s} - \frac{1}{2}\frac{\partial}{\partial t}\right)\mathrm{Re}\,U_d(s,t,u(s,t))|_{\mathrm{thr}}\,. \tag{E.30}$$

In the case we want to keep also the physical meaning of λ_0 as a rescalled effective range parameter $\left(\hat{\lambda}_0 = \frac{F_\pi^2}{24m_{\pi^0}^2} r_0\right)$, we can add the condition

$$w_0'(4m_{\pi^0}^2) - w_0'(0) = 16\pi \frac{\partial}{\partial s} \operatorname{Re} U_0(s,t,u(s,t))|_{\text{thr}}. \tag{E.31}$$

From the structure of these conditions [stemming from our choice of the symmetric form of the restoring polynomials in (5.56)–(5.60) leading to the simple linear crossing relations (5.61)–(5.64)] it is obvious that all the polynomials $w_i(s)$ have to be of (at least) second order. [Naturally, if we abandoned the requirement of this symmetric form, we could find the solutions as some first order polynomials.] We can write them as

$$w_0(x) = w_0^2 x^2 + w_0^0, \tag{E.32}$$
$$w_x(x) = w_x^2 x^2 + w_x^1 x, \tag{E.33}$$
$$w_t(x) = w_t^2 x^2 + w_t^0, \tag{E.34}$$
$$w_c(x) = w_c^2 x^2 + w_c^0, \tag{E.35}$$
$$w_d(x) = w_d^2 x^2 + w_d^1 x. \tag{E.36}$$

On the right-hand side of the equations (E.22)–(E.30) we need the threshold values of the one-loop functions. They are (with the exception of $\bar{J}_0(4m_{\pi^\pm}^2)$ and the derivatives $\bar{J}_x'(4m_x^2)$ and $\bar{J}_0'(4m_{\pi^\pm}^2)$ all of them are real)

$$\bar{J}_x(0) = 0, \qquad \bar{J}_x'(0) = \frac{1}{16\pi^2}\frac{1}{6m_x^2}, \tag{E.37}$$
$$\bar{J}_x(4m_x^2) = \frac{1}{8\pi^2}, \qquad \operatorname{Re}\bar{J}_x'(4m_x^2) = -\frac{1}{32\pi^2}\frac{1}{m_x^2}, \tag{E.38}$$
$$\operatorname{Re}\bar{J}_0(4m_{\pi^\pm}^2) = \frac{1}{16\pi^2}\mathcal{Q}_{0\pm}(q), \qquad \operatorname{Re}\bar{J}_0'(4m_{\pi^\pm}^2) = -\frac{1}{64\pi^2}\frac{1}{\Delta}\left(1 - \frac{m_{\pi^0}^2}{2m_{\pi^\pm}^2}\mathcal{Q}_{0\pm}(q)\right), \tag{E.39}$$
$$\bar{J}_\pm(4m_{\pi^0}^2) = \frac{1}{16\pi^2}\mathcal{Q}_{\pm 0}(q), \qquad \bar{J}_\pm'(4m_{\pi^0}^2) = \frac{1}{64\pi^2}\frac{1}{\Delta}\left(1 - \frac{m_{\pi^\pm}^2}{2m_{\pi^0}^2}\mathcal{Q}_{\pm 0}(q)\right), \tag{E.40}$$

$$\bar{J}_{\pm 0}(\mu_\pm) = \frac{1}{16\pi^2}\left(1 \mp \frac{2m_{\pi^\pm}m_{\pi^0}}{\Delta}\log q\right), \tag{E.41}$$
$$\bar{J}_{\pm 0}'(\mu_\pm) = -\frac{1}{16\pi^2}\frac{1}{\mu_\pm}\left(2 + \frac{\mu_\mp}{\Delta}\log q\right), \tag{E.42}$$
$$\bar{J}_{\pm 0}(-\Delta) = \frac{1}{16\pi^2}\frac{1}{\Delta}\left(-m_{\pi^\pm}^2 - m_{\pi^0}^2 - 2m_{\pi^\pm}^2\log q + m_{\pi^\pm}^2\mathcal{Q}_{0\pm}(q)\right), \tag{E.43}$$
$$\bar{J}_{\pm 0}'(-\Delta) = \frac{1}{16\pi^2}\frac{1}{\Delta^2}\left(-m_{\pi^0}^2 - \Delta\log q + \frac{m_{\pi^\pm}^2}{2}\mathcal{Q}_{0\pm}(q)\right), \tag{E.44}$$
$$\bar{J}_{\pm 0}''(-\Delta) = \frac{1}{16\pi^2}\frac{1}{\Delta^3}\left(-\frac{m_{\pi^\pm}^2 + 2m_{\pi^0}^2}{2} - 2\Delta\log q + \frac{4m_{\pi^\pm}^2 - m_{\pi^0}^2}{4}\mathcal{Q}_{0\pm}(q)\right), \tag{E.45}$$

where we have used the notation

$$\mathcal{Q}_{\pm 0}(q) = 2\left(1 - \frac{\sqrt{1-q^2}}{q}\arctan\frac{q}{\sqrt{1-q^2}}\right), \tag{E.46}$$

$$\mathcal{Q}_{0\pm}(q) = 2\left(1 + \sqrt{1-q^2}\log\frac{1-\sqrt{1-q^2}}{q}\right). \tag{E.47}$$

Substituting the expressions for $w_i(x)$, the unitarity parts from (5.33)–(5.44) and these values into the conditions (E.22)–(E.30), we get few simple sets of linear equations for the coefficients w_i^n. For the sake of extent, we put here only the numerical values of them which were obtained for the physical values

$$m_{\pi^\pm} = 139.6\,\mathrm{MeV}, \qquad m_{\pi^0} = 135.0\,\mathrm{MeV}, \qquad F_\pi = 92.22\,\mathrm{MeV}. \tag{E.48}$$

The coefficients are then

$$w_0^2 = \left(-0.40a_0^2 + 1.11a_x^2 + 8.6a_xb_x - 19b_x^2\right)\cdot 10^{-10}\,\mathrm{MeV}^{-4}, \tag{E.49}$$

$$w_0^0 = 0.18a_0^2 - 0.06a_x^2 - 1.7a_xb_x + 3.5b_x^2, \tag{E.50}$$

$$w_x^2 = \left(-3a_t^2 - 3.5a_ca_x - 1.7a_0a_x + 13a_xb_c + 13a_tb_t + 10b_t^2 + 13a_cb_x + 6a_0b_x + 15b_cb_x\right)\cdot 10^{-10}\,\mathrm{MeV}^{-4}, \tag{E.51}$$

$$w_x^1 = \left(0.5a_t^2 + 0.46a_ca_x + 0.22a_0a_x - 1.2a_xb_c - 2a_tb_t + 0.02b_t^2 - 1.2a_cb_x - 0.6a_0b_x - 2b_cb_x\right)\cdot 10^{-4}\,\mathrm{MeV}^{-2}, \tag{E.52}$$

$$w_t^2 = \left(-2.2a_t^2 - 1.43a_ca_x - 0.67a_0a_x + 3.3a_xb_c + 20a_tb_t - 10b_t^2 + 3.3a_cb_x + 1.4a_0b_x + 15b_cb_x\right)\cdot 10^{-10}\,\mathrm{MeV}^{-4}, \tag{E.53}$$

$$w_t^0 = 0.9a_t^2 + 0.41a_ca_x + 0.19a_0a_x - 0.9a_xb_c - 6a_tb_t + 3b_t^2 - 0.9a_cb_x - 0.4a_0b_x - 4b_cb_x, \tag{E.54}$$

$$w_c^2 = \left(-2.1a_c^2 + 0.7a_d^2 - 1.0a_x^2 + 19a_cb_c + 10b_c^2 - 3a_db_d - 7b_d^2 + 9a_xb_x\right)\cdot 10^{-10}\,\mathrm{MeV}^{-4}, \tag{E.55}$$

$$w_c^0 = 0.95a_c^2 - 0.21a_d^2 + 0.45a_x^2 - 5.8a_cb_c - 3b_c^2 + 1.0a_db_d + 2b_d^2 - 3a_xb_x, \tag{E.56}$$

$$w_d^2 = \left(2.8a_c^2 - 1.7a_d^2 + 1.3a_x^2 - 13a_cb_c - 50b_c^2 + 13a_db_d + 7b_d^2 - 6a_xb_x - 20b_x^2\right)\cdot 10^{-10}\,\mathrm{MeV}^{-4}, \tag{E.57}$$

$$w_d^1 = \left(-0.46a_c^2 + 0.23a_d^2 - 0.22a_x^2 + 2.5a_cb_c + 5b_c^2 - 1.2a_db_d - b_d^2 + a_xb_x + b_x^2\right)\cdot 10^{-4}\,\mathrm{MeV}^{-2}. \tag{E.58}$$

We have rounded off the numerical values of the coefficients taking into account the numerical ordering of the scattering length parameters as follows.

E.2.3 Approximate numerical values of the restoring polynomials

For our further discussion of the numerical order of the corrections, we compute their approximate numerical values as the values for the following specific choice of the scattering

length parameters,

$$a_0 = 0.082, \quad a_x = -0.18, \quad a_t = -0.042, \quad a_c = 0.14, \quad a_d = -0.083, \tag{E.59}$$

$$b_x = b_d = -0.024, \qquad b_c = -b_t = 0.012, \tag{E.60}$$

stemming from the central values $\mathrm{a}_0^0 = 0.22$, $\mathrm{a}_0^2 = -0.044$ from [48, 49] and the expressions (5.25)–(5.31) valid in the lowest order in the isospin breaking.

The coefficients of the polynomials (E.32)–(E.36) read then

$$w_0^2 = 5.9 \cdot 10^{-12}\,\mathrm{MeV}^{-4}, \qquad w_0^0 = -0.0060, \tag{E.61}$$

$$w_x^2 = 2.7 \cdot 10^{-12}\,\mathrm{MeV}^{-4}, \qquad w_x^1 = -6.4 \cdot 10^{-7}\,\mathrm{MeV}^{-2}, \tag{E.62}$$

$$w_t^2 = 2.5 \cdot 10^{-12}\,\mathrm{MeV}^{-4}, \qquad w_t^0 = 0.0064, \tag{E.63}$$

$$w_c^2 = -0.58 \cdot 10^{-12}\,\mathrm{MeV}^{-4}, \quad w_c^0 = 0.013, \tag{E.64}$$

$$w_d^2 = 5.1 \cdot 10^{-12}\,\mathrm{MeV}^{-4}, \qquad w_d^1 = -6.9 \cdot 10^{-7}\,\mathrm{MeV}^{-2}. \tag{E.65}$$

These polynomials bring the corrections to the scattering lengths which are also (from their definition) equal to the constants (E.3)–(E.7),

$$\Delta a_0 = w_0 = 0.013, \quad (16\%), \tag{E.66}$$

$$\Delta a_x = w_x = -0.020, \ (11\%), \tag{E.67}$$

$$\Delta a_t = w_t = 0.0011, \ (2.6\%), \tag{E.68}$$

$$\Delta a_c = w_c = 0.022, \quad (16\%), \tag{E.69}$$

$$\Delta a_d = w_d = 0.0022, \ (2.6\%), \tag{E.70}$$

i.e. in the case we forgot to subtract this double counting (caused by taking the physical values of the scattering lengths and adding the full unitarity contribution), we would get the relative error of the scattering lengths indicated in brackets in these relations.

Similarly, by restoring the physical values of just the scattering lengths and using only the restoring constants (E.3)–(E.7), but taking everywhere the physical values of the effective range parameters, we commit the error[1]

$$\Delta b_0 = 7.3 \cdot 10^{-3}, \tag{E.71}$$

$$\Delta b_x = -1.8 \cdot 10^{-3}, \ (7.7\%), \tag{E.72}$$

$$\Delta b_t = 0.45 \cdot 10^{-3}, \ (3.7\%), \tag{E.73}$$

$$\Delta b_c = 2.2 \cdot 10^{-3}, \quad (18\%), \tag{E.74}$$

$$\Delta b_d = 0.90 \cdot 10^{-3}, \ (3.7\%). \tag{E.75}$$

However, in our further applications we are not aiming to obtain the physical values of b_i with better precision than these maximally 20%.

[1]Note, that from our simple estimate (E.59)– (E.60), we have no guess for the value b_0.

Appendix F

Kinematic functions appearing in results

This appendix summarizes all the kinematic functions appearing in the results of the reconstruction procedure for the $\pi\pi$ scattering and the $P \to 3\pi$ decay amplitudes.

We start with the definitions of shortcuts used in them,

$$\Sigma = m_{\pi^\pm}^2 + m_{\pi^0}^2, \qquad \Delta = m_{\pi^\pm}^2 - m_{\pi^0}^2, \qquad \mu^\pm = (m_{\pi^\pm} \pm m_{\pi^0})^2, \tag{F.1}$$

$$\tilde{\Delta}_+ = m_P^2 - m_{\pi^\pm}^2, \qquad \tilde{\Delta}_0 = m_P^2 - m_{\pi^0}^2, \qquad \tilde{\Delta} = m_P^2 - m_\pi^2, \tag{F.2}$$

$$\tilde{\mu}_c^\pm = (m_P - m_{\pi^\pm})^2, \qquad \tilde{\mu}_0^\pm = (m_P - m_{\pi^0})^2, \qquad \tilde{\mu}^\pm = (m_P - m_\pi)^2, \tag{F.3}$$

$$q = \frac{m_{\pi^0}}{m_{\pi^\pm}}, \qquad \tilde{\xi} = \frac{m_{\pi^\pm}^2}{\Delta}\frac{\tilde{\Delta}_0^2}{\tilde{\Delta}_+}, \qquad \tilde{\varsigma} = m_P^2 m_{\pi^0}^2 - m_{\pi^\pm}^4. \tag{F.4}$$

The kinematic square roots connected with the momenta of particles in the center-of-mass system

$$\sigma_A(s) = \sqrt{1 - \frac{4m_A^2}{s}}, \qquad \lambda_{AB}(s) = s^2 - 2s(m_A^2 + m_B^2) + (m_A^2 - m_B^2)^2 \tag{F.5}$$

with further notation

$$\sigma_+(s) = \sigma_{\pi^\pm}(s), \quad \sigma_0(s) = \sigma_{\pi^0}(s), \quad \lambda(s) = \lambda_{\pi^\pm\pi^0}(s), \tag{F.6}$$

$$\tilde{\lambda}_+(s) = \lambda_{P\pi^\pm}(s), \quad \tilde{\lambda}_0(s) = \lambda_{P\pi^0}(s), \quad \tilde{\lambda}_\pi(s) = \lambda_{P\pi}(s). \tag{F.7}$$

Related functions from mixed processes

$$\sigma_\nabla(s) = \sqrt{\frac{s - 4m_{\pi^0}^2}{s + 4\Delta}}, \qquad \sigma_\Delta(s) = \sqrt{\frac{s - 4m_{\pi^\pm}^2}{s - 4\Delta}}, \tag{F.8}$$

$$\sigma_\odot(s) = \frac{\lambda^{1/2}(s)}{s - \Delta}, \qquad \sigma_\oplus(s) = \frac{\lambda^{1/2}(s)}{s + \Delta}. \tag{F.9}$$

For these functions $\sigma_\varpi(s)$ we define the following corresponding logarithms

$$L_\varpi(s) = \log\frac{1 - \sigma_\varpi(s)}{1 + \sigma_\varpi(s)}, \qquad \mathcal{L}_\varpi(s) = \log\frac{\sigma_\varpi(s) - 1}{1 + \sigma_\varpi(s)}. \tag{F.10}$$

These functions have the same real parts but differ in the imaginary parts. For instance for $s > 4m_{\pi^0}^2$, $\mathrm{Im}\, L_0(s) = 0$ whereas $\mathrm{Im}\, \mathcal{L}_0(s) = \pm\pi$ with the sign depending on the convention.

We also use the logarithms

$$L_\uparrow(s) = \frac{L_\odot(s) + L_\oplus(s)}{2}, \qquad L_\downarrow(s) = \frac{L_\odot(s) - L_\oplus(s)}{2} \tag{F.11}$$

and the corresponding $\mathcal{L}_\uparrow(s)$ and $\mathcal{L}_\downarrow(s)$.

The logarithm connected with the $P\pi \to \pi\pi$ processes is

$$M_0(s) = -2\log\left(1 - \frac{\tilde{\Delta}_0}{s} + \frac{\tilde{\lambda}_0^{1/2}(s)}{s}\right) + \log\frac{4m_{\pi^0}^2}{s}\,. \tag{F.12}$$

We denote with the same symbol also its isospin limit, where we just change $m_{\pi^0} \to m_\pi$.

Finally, in the isospin violating results there appears polylogarithms

$$\mathcal{J}(\tau) = \log q \log\tau + \mathrm{Li}_2(1 - q\tau) - \mathrm{Li}_2\left(1 - \frac{\tau}{q}\right). \tag{F.13}$$

F.1 Kinematic functions appearing in S and P partial waves of NLO amplitudes

F.1.1 $\pi\pi$ scattering amplitudes in isospin limit

In this case only the following functions appear in the relations for the NLO partial waves.

$$\mathcal{M}_0(s) = 1, \qquad \mathcal{M}_1(s) = \frac{L_\pi(s)}{\sigma_\pi(s)}\,, \tag{F.14}$$

$$\mathcal{M}_2(s) = -m_\pi^2\frac{L_\pi^2(s)}{s\sigma_\pi^2(s)}\,, \qquad \mathcal{M}_3(s) = \sigma_\pi(s)\mathcal{L}_\pi(s). \tag{F.15}$$

F.1.2 $\pi\pi$ scattering amplitudes with isospin breaking taken into account

$$\mathcal{M}_0(s) = 1, \qquad \mathcal{M}_{0q}(s) = -\Sigma\frac{\log q}{\Delta}\,, \tag{F.16}$$

$$\mathcal{M}_{1\mathrm{n}}(s) = \frac{L_0(s)}{\sigma_0(s)}\,, \qquad \mathcal{M}_{1+}(s) = \frac{L_+(s)}{\sigma_+(s)}\,, \tag{F.17}$$

$$\mathcal{M}_{1\Delta}(s) = \frac{L_\Delta(s)}{\sigma_\Delta(s)}\,, \qquad \mathcal{M}_{1\nabla}(s) = \frac{L_\nabla(s)}{\sigma_\nabla(s)}\,, \tag{F.18}$$

$$\mathcal{M}_{1\uparrow}(s) = s\frac{L_\uparrow(s)}{\lambda^{1/2}(s)}\,, \qquad \mathcal{M}_{1\downarrow}(s) = \Delta\frac{L_\downarrow(s)}{\lambda^{1/2}(s)}\,, \tag{F.19}$$

$$\mathcal{M}_{2\mathrm{n}}(s) = -m_{\pi^0}^2 \frac{L_0^2(s)}{s\sigma_0^2(s)}\,, \qquad \mathcal{M}_{2+}(s) = -m_{\pi^\pm}^2 \frac{L_+^2(s)}{s\sigma_+^2(s)}\,, \tag{F.20}$$

$$\mathcal{M}_{2\Delta}(s) = -m_{\pi^0}^2 \frac{L_\Delta^2(s)}{s\sigma_+^2(s)}\,, \qquad \mathcal{M}_{2\nabla}(s) = -m_{\pi^\pm}^2 \frac{L_\nabla^2(s)}{s\sigma_0^2(s)}\,, \tag{F.21}$$

$$\mathcal{M}_{2\odot}(s) = -sm_{\pi^0}^2 \frac{L_\odot^2(s)}{\lambda(s)}\,, \qquad \mathcal{M}_{2\oplus}(s) = -sm_{\pi^\pm}^2 \frac{L_\oplus^2(s)}{\lambda(s)}\,, \tag{F.22}$$

$$\mathcal{M}_{2\mathrm{n}+}(s) = -\frac{\Sigma}{2}\frac{L_0(s)L_+(s)}{s\sigma_+(s)\sigma_0(s)}\,, \qquad \mathcal{M}_{2\odot\oplus}(s) = -\frac{\Sigma}{2}\,s\,\frac{L_\odot(s)L_\oplus(s)}{\lambda(s)}\,, \tag{F.23}$$

$$\mathcal{M}_{3\mathrm{n}}(s) = \sigma_0(s)\mathcal{L}_0(s), \qquad \mathcal{M}_{3+}(s) = \sigma_+(s)\mathcal{L}_+(s), \tag{F.24}$$

$$\mathcal{M}_{3\uparrow}(s) = \frac{\lambda^{1/2}(s)}{s}\mathcal{L}_\uparrow(s), \tag{F.25}$$

$$\mathcal{M}_{7x}(s) = \Delta\frac{\mathcal{J}(\tau_+^x) - \mathcal{J}(\tau_-^x)}{s\sigma_0\sigma_+}\,, \tag{F.26}$$

$$\mathcal{M}_{7t}(s) = s\Delta\frac{\mathcal{J}(\tau_+^t) - \mathcal{J}(\tau_-^t)}{\lambda(s)}\,, \tag{F.27}$$

$$\mathcal{M}_{8t}(s) = \Delta\frac{\mathcal{M}_{1\uparrow} + \frac{s}{\Sigma}\mathcal{M}_{0q}(s)}{2\Sigma - s}\,, \tag{F.28}$$

$$\mathcal{M}_{9t}(s) = \frac{1}{2}\mathcal{M}_{8t}(s)\left(\frac{\Delta}{2\Sigma - s} - \frac{\Sigma}{\Delta}\right) + \frac{s\big(1 - \mathcal{M}_{0q}(s)\big)}{2(s - 2\Sigma)}\,. \tag{F.29}$$

In the functions $\mathcal{M}_{7x}(s)$ and $\mathcal{M}_{7t}(s)$ there appear end-points of the particular integrations,

$$\tau_\pm^x = \frac{s}{4m_{\pi^0}m_{\pi^\pm}}\left(1 - \sigma_0(s)\right)\left(1 \pm \sigma_+(s)\right), \tag{F.30}$$

$$\tau_+^t = \frac{s - \Sigma - \lambda^{1/2}(s)}{2m_{\pi^0}m_{\pi^\pm}}\,, \tag{F.31}$$

$$\tau_-^t = \frac{s\Sigma - \Delta^2 - \Delta\lambda^{1/2}(s)}{2s\,m_{\pi^0}m_{\pi^\pm}}\,. \tag{F.32}$$

Note that $L_\uparrow = \log(\tau_+^t)$ and $L_\downarrow = \log(\tau_-^t)$.

F.1.3 $P\pi \to \pi\pi$ partial waves in isospin limit

In addition to the functions appearing in Section F.1.1, in the relations for NLO partial waves of $P\pi \to \pi\pi$ amplitudes in isospin limit there appear the following functions.

$$\mathcal{M}_{1\mathrm{P}}(s) = s\frac{M_0(s)}{\tilde{\lambda}_\pi^{1/2}(s)}\,, \tag{F.33}$$

$$\mathcal{M}_{2\mathrm{P}}(s) = -m_\pi^2\frac{M_0(s)L_0(s)}{\sigma_\pi(s)\tilde{\lambda}_\pi^{1/2}(s)}\,. \tag{F.34}$$

F.1.4 Partial waves of $P^0\pi \to \pi\pi$ processes in the case $m_{\pi^\pm} \neq m_{\pi^0}$

In the expressions for S and P partial waves of $P^0\pi^0 \to \pi\pi$ processes there appear $\pi\pi$ functions from Section F.1.2 together with the following ones

$$\mathcal{M}_{1\mathrm{L}}(s) = s\frac{M_0(s)}{\tilde{\lambda}_0^{1/2}(s)}\,, \tag{F.35}$$

$$\mathcal{M}_{2\mathrm{Ln}}(s) = -m_{\pi^0}^2\frac{M_0(s)L_0(s)}{\sigma_0(s)\tilde{\lambda}_0^{1/2}(s)}\,, \tag{F.36}$$

$$\mathcal{M}_{2\mathrm{L}+}(s) = -\frac{\Sigma}{2}\frac{M_0(s)L_+(s)}{\sigma_+(s)\tilde{\lambda}_0^{1/2}(s)}\,, \tag{F.37}$$

$$\mathcal{M}_{7\mathrm{L}x}(s) = \Delta\frac{\mathcal{J}(\tau_+^{\mathrm{L}x}) - \mathcal{J}(\tau_-^{\mathrm{L}x})}{\sigma_+(s)\tilde{\lambda}_0^{1/2}(s)}\,, \tag{F.38}$$

$$\mathcal{M}_{8\mathrm{L}x}(s) = \frac{2\tilde{\Delta}_0 m_{\pi^\pm}^2 - s\Delta}{2\Delta(s-\tilde{\xi})}\,\mathcal{M}_{1+}(s) - \frac{\tilde{\Delta}_0\Sigma - s\Delta}{2\Delta(s-\tilde{\xi})}\,\mathcal{M}_{1\mathrm{L}}(s) + \frac{s\Delta}{\Sigma(s-\tilde{\xi})}\,\mathcal{M}_{0q}(s), \tag{F.39}$$

$$\begin{aligned}\mathcal{M}_{9\mathrm{L}x}(s) = \frac{s}{s-\tilde{\xi}}\Bigg(&\frac{s-2\Sigma-\tilde{\Delta}_0}{\tilde{\Delta}_+}\,\mathcal{M}_{8\mathrm{L}x}(s) - \frac{1}{2}\,\mathcal{M}_{1+}(s)\\ &- \frac{1}{2}\Big(1-\frac{\tilde{\Delta}_0}{s}\Big)\,\mathcal{M}_{1\mathrm{L}}(s) - \mathcal{M}_{0q}(s) - 1\Bigg)\end{aligned} \tag{F.40}$$

$$\mathcal{M}_{11\mathrm{Ln}}(s) = 2\left(\omega(\tau_+^{\mathrm{L}n}) + \omega(\tau_-^{\mathrm{L}n})\right), \tag{F.41}$$

$$\mathcal{M}_{12\mathrm{Ln}}(s) = 2m_{\pi^\pm}^2\frac{\omega(\tau_+^{\mathrm{L}n}) - \omega(\tau_-^{\mathrm{L}n})}{\sigma_0(s)\tilde{\lambda}_0^{1/2}(s)}\,, \tag{F.42}$$

$$\mathcal{M}_{13\mathrm{Ln}}(s) = m_{\pi^\pm}^2\frac{\log^2\tau_+^{\mathrm{L}n} - \log^2\tau_-^{\mathrm{L}n}}{\sigma_0(s)\tilde{\lambda}_0^{1/2}(s)} \tag{F.43}$$

with

$$\omega(\tau_\pm^{\mathrm{L}n}) = \left(\tau_\pm^{\mathrm{L}n} - \frac{1}{\tau_\pm^{\mathrm{L}n}}\right)\log\tau_\pm^{\mathrm{L}n}. \tag{F.44}$$

The endpoints of integrations appearing in $\mathcal{M}_{7\mathrm{L}x}(s)$ and in the last three functions are

$$\tau_\pm^{\mathrm{L}x} = -\frac{1}{4m_{\pi^\pm}m_{\pi^0}}\left(1\mp\sigma_+(s)\right)\left(\tilde{\Delta}_0 - s - \tilde{\lambda}_0^{1/2}(s)\right), \tag{F.45}$$

$$\tau_\pm^{\mathrm{L}n} = 1 + \frac{t_\pm^{\mathrm{L}n}}{2m_{\pi^\pm}^2}\left(\sigma_+(t_\pm^{\mathrm{L}n}) - 1\right) + i\epsilon\left(\frac{\sigma_+(t_\pm^{\mathrm{L}n}) - 1}{2m_{\pi^\pm}^2} + \frac{1}{\sigma_+(t_\pm^{\mathrm{L}n})t_\pm^{\mathrm{L}n}}\right)\frac{\mathrm{d}t_\pm^{\mathrm{L}n}}{\mathrm{d}m_P^2}, \tag{F.46}$$

$$t_\pm^{\mathrm{L}n} = \frac{1}{2}\left(m_P^2 + 3m_{\pi^0}^2 - s \pm \sigma_0(s)\tilde{\lambda}_0^{1/2}(s)\right). \tag{F.47}$$

F.2 Kinematic functions appearing in NNLO amplitudes

F.2.1 Functions appearing in $P\pi \to \pi\pi$ in isospin limit from S-wave contributions

In the NNLO $P\pi \to \pi\pi$ amplitude in isospin limit there appears five basic functions $\mathcal{G}_i(s), i = 1, \ldots, 5$. They are Hilbert transforms

$$\mathcal{G}_i(s) = s^{n_i} \int_{4m_\pi^2}^{\infty} \frac{\mathrm{d}x}{x^{n_i}} \frac{\mathcal{F}_i(x)}{x - s}, \tag{F.48}$$

which for real s means

$$\mathcal{G}_i(s + i0) = s^{n_i}\,\mathrm{v.p.} \int_{4m_\pi^2}^{\infty} \frac{\mathrm{d}x}{x^{n_i}} \frac{\mathcal{F}_i(x)}{x - s} + i\pi\mathcal{F}_i(s), \tag{F.49}$$

of the following functions

$$\mathcal{F}_1(s) = \sigma_\pi(s), \tag{F.50}$$
$$\mathcal{F}_2(s) = L_\pi(s), \tag{F.51}$$
$$\mathcal{F}_3(s) = -m_\pi^2 \frac{L_\pi^2(s)}{s\sigma_\pi(s)}\,, \tag{F.52}$$
$$\mathcal{F}_4(s) = s\sigma_\pi(s) \frac{M_0(s)}{\tilde{\lambda}_\pi^{1/2}(s)}\,, \tag{F.53}$$
$$\mathcal{F}_5(s) = -m_\pi^2 L_\pi(s) \frac{M_0(s)}{\tilde{\lambda}_\pi^{1/2}(s)} \tag{F.54}$$

with $n_1 = n_2 = 1$, $n_3 = n_5 = 0$ and for $\mathcal{F}_4(s)$ we need two different numbers of subtractions $n_4 = 1, 2$.

The first three Hilbert transforms are easy to determine by using the "roundabout" way described in Appendix B. Since

$$\mathrm{Disc}\,(\sigma_\pi(s)\mathcal{L}_\pi(s)) = \pi\sigma_\pi(s)\theta(s - 4m_\pi^2) = \pi\mathcal{F}_1(s)\theta(s - 4m_\pi^2), \tag{F.55}$$

the Hilbert transform $\mathcal{G}_1(s)$ will be up to a polynomial equal to the function in the brackets. The polynomial is easily to determine from the UV and IR asymptotics of the integral. The considered integral is logarithmically divergent for $s \to \infty$ and equal to zero at $s = 0$. Therefore, we conclude with

$$\mathcal{G}_1^{(1)}(s) = 2 + \sigma_\pi(s)\mathcal{L}_\pi(s) = 16\pi^2 \bar{J}_\pi(s). \tag{F.56}$$

As we have discussed near equation (7.53), $\mathcal{G}_1(s)$ is connected with the $O(p^4)$ unitarity part of the amplitude that corresponds to the single two-pion rescattering in the final state, it is therefore no surprise that this result restores the one-loop function $\bar{J}_\pi(s)$.

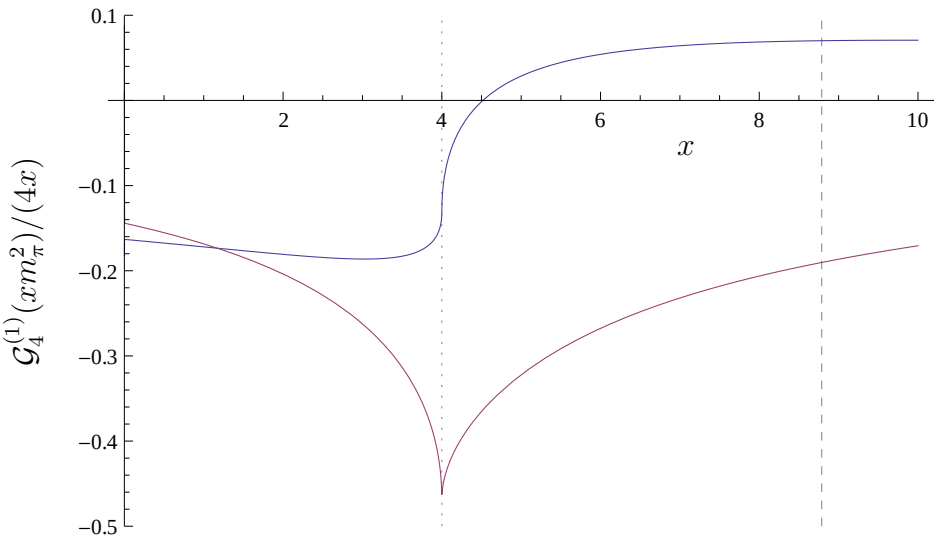

Figure 27: Plot of function $\frac{1}{4x}\mathcal{G}_4^{(1)}(xm_\pi^2)$ used for comparison of the numerical computation of this function used in this work with the analytic approximate determination from [VI].

Similarly, by using the formula

$$\operatorname{Disc} f(x)g(x) = f(x-i0)\operatorname{Disc} g(x) + g(x+i0)\operatorname{Disc} f(x) \tag{F.57}$$

we arrive at

$$\mathcal{G}_2^{(1)}(s) = \frac{1}{2}\mathcal{L}_\pi^2(s)\,, \tag{F.58}$$

$$\mathcal{G}_3^{(0)}(s) = -\frac{m_\pi^2}{3s\sigma_\pi(s)}\mathcal{L}_\pi(s)\left(\mathcal{L}_\pi^2(s)+\pi^2\right). \tag{F.59}$$

Note that these three functions have appeared also in the two-loop pion scattering computation [95].

For functions $\mathcal{G}_4(s)$ and $\mathcal{G}_5(s)$, this roundabout way does not work and we have to employ their integral representations (F.48). We have two possibilities how to compute them: either by integrating these expressions numerically or by means of the construction of analytic approximations which was described[1] in Appendix B of [VI]. The functions $\mathcal{G}_4^{(1)}(s)$ and $\mathcal{G}_4^{(2)}(s)$ are related by (B.2).

One should note that having these two functions only in either of these approximate forms does not mean that they are worse than the others — since they depend only on two masses m_π and m_P and on one variable s, once we fix the masses we can tabulate them for all the needed values of s.

[1]Note however that the definition of these functions in [VI] differs from the one used here by factor of s and $-m_\pi^2$ respectively. It also changes the required number of subtractions for $\mathcal{F}_4(s)$.

We have plotted graphs of all the Hilbert transforms $\mathcal{G}_i^{(n)}(s)$ on Figure 28. For comparison with the analytic approximate determination of $\mathcal{G}_4^{(1)}(s)$ from [VI] we have added also the plot on Figure 27 corresponding to FIG.4 from [VI].

F.2.2 Functions appearing in $P\pi \to \pi\pi$ in isospin limit from P-wave contributions

The contributions of P-waves into the NNLO $P\pi \to \pi\pi$ amplitudes bring in addition to the functions of previous section also functions that are related to the previous one by

$$\mathcal{F}_j^{\sigma}(s) = m_\pi^2 \frac{\mathcal{F}_j(s)}{s\sigma_\pi^2(s)} \qquad \text{or} \qquad \mathcal{F}_j^{\tilde{\lambda}}(s) = m_\pi^2 s\, \frac{\mathcal{F}_j(s)}{\tilde{\lambda}_\pi(s)}\,, \tag{F.60}$$

In Appendix B we have found the expressions for Hilbert transforms of these functions in terms of Hilbert transforms of original functions $\mathcal{F}_j(s)$.

We obtain

$$\mathcal{G}_1^{\sigma;(0)}(s) = \frac{m_\pi^2}{s-4m_\pi^2}\,\left(\mathcal{G}_1^{(1)}(s) - 2\right), \tag{F.61}$$

$$\mathcal{G}_2^{\sigma;(0)}(s) = \frac{m_\pi^2}{s-4m_\pi^2}\,\left(\mathcal{G}_2^{(1)}(s) + \frac{\pi^2}{2}\right), \tag{F.62}$$

$$\mathcal{G}_3^{\sigma;(0)}(s) = \frac{m_\pi^2}{s-4m_\pi^2}\,\left(\mathcal{G}_3^{(0)}(s) + \frac{\pi^2}{3}\right), \tag{F.63}$$

$$\mathcal{G}_i^{\tilde{\lambda};(0)}(s) = \frac{m_\pi}{4m_P}\,\left(\frac{\tilde{\mu}^+}{s-\tilde{\mu}^+}\left(\mathcal{G}_i^{(1)}(s) - \mathcal{G}_i^{(1)}(\tilde{\mu}^+)\right) - \frac{\tilde{\mu}^-}{s-\tilde{\mu}^-}\left(\mathcal{G}_i^{(1)}(s) - \mathcal{G}_i^{(1)}(\tilde{\mu}^-)\right)\right), \tag{F.64}$$

$$\mathcal{G}_i^{\tilde{\lambda};(1)}(s) = \frac{m_\pi}{4m_P}\,\left(\frac{s}{s-\tilde{\mu}^+}\left(\mathcal{G}_i^{(1)}(s) - \mathcal{G}_i^{(1)}(\tilde{\mu}^+)\right) - \frac{s}{s-\tilde{\mu}^-}\left(\mathcal{G}_i^{(1)}(s) - \mathcal{G}_i^{(1)}(\tilde{\mu}^-)\right)\right), \tag{F.65}$$

$$\mathcal{G}_i^{\tilde{\lambda};(2)}(s) = \frac{m_\pi}{4m_P}\,\left(\frac{s}{s-\tilde{\mu}^+}\left(\mathcal{G}_i^{(1)}(s) - \frac{s}{\tilde{\mu}^+}\,\mathcal{G}_i^{(1)}(\tilde{\mu}^+)\right) - \frac{s}{s-\tilde{\mu}^-}\left(\mathcal{G}_i^{(1)}(s) - \frac{s}{\tilde{\mu}^-}\,\mathcal{G}_i^{(1)}(\tilde{\mu}^-)\right)\right), \tag{F.66}$$

$$\mathcal{G}_5^{\tilde{\lambda};(0)}(s) = \frac{m_\pi}{4m_P}\,\left(\frac{s}{s-\tilde{\mu}^+}\left(\mathcal{G}_5^{(0)}(s) - \mathcal{G}_5^{(0)}(\tilde{\mu}^+)\right) - \frac{s}{s-\tilde{\mu}^-}\left(\mathcal{G}_5^{(0)}(s) - \mathcal{G}_5^{(0)}(\tilde{\mu}^-)\right)\right). \tag{F.67}$$

The relations for $\mathcal{G}_i^{\tilde{\lambda};(n)}(s)$ with $i = 1, 2, 4$ look the same since their original functions have the same number of subtractions.

We have plotted the graphs of all these additional functions on Figure 29.

F.2.3 Functions appearing in NNLO $P\pi^0 \to \pi^0\pi^0$ amplitude for $m_{\pi^\pm} \neq m_{\pi^0}$

Just for completeness, we remind the reader that the functions appearing in NNLO $P\pi^0 \to \pi^0\pi^0$ in the case we take isospin breaking into account are listed in Tables 9 and 10. We have a close analytic form of these Hilbert transforms only for the functions $\mathcal{H}_{1n}^{(1)}$, $\mathcal{H}_{1+}^{(1)}$,

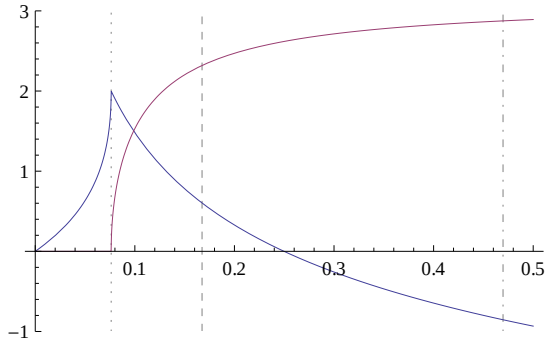

(a) $\mathcal{G}_1^{(1)}(s)$

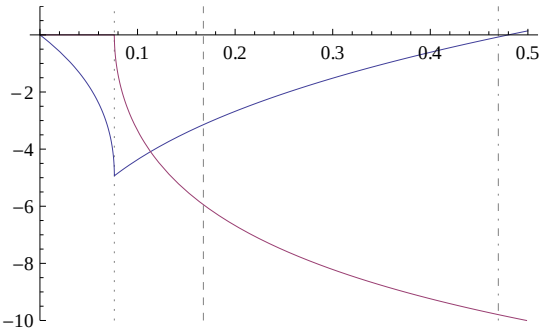

(b) $\mathcal{G}_2^{(1)}(s)$

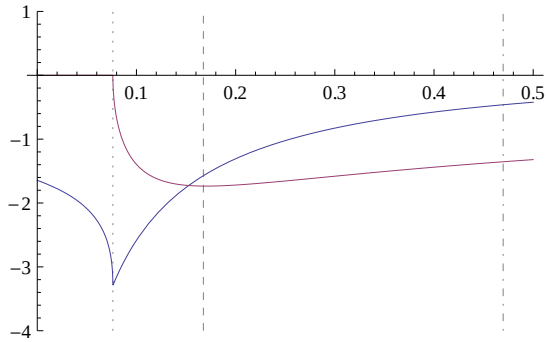

(c) $\mathcal{G}_3^{(0)}(s)$

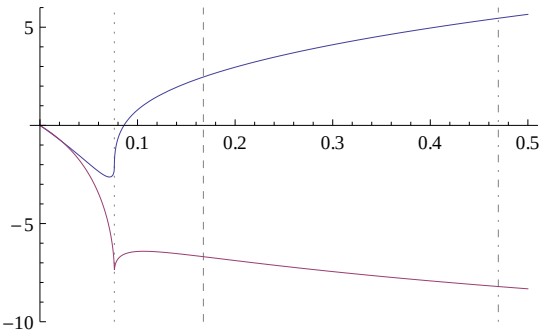

(d) $\mathcal{G}_4^{(1)}(s)$

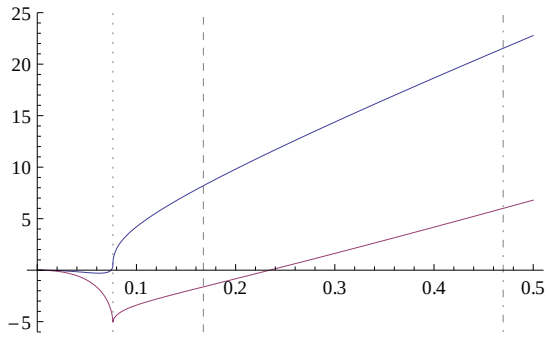

(e) $\mathcal{G}_4^{(2)}(s)$

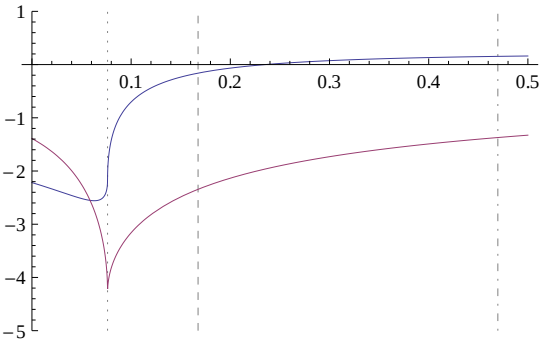

(f) $\mathcal{G}_5^{(0)}(s)$

Figure 28: Plot of Hilbert transforms $\mathcal{G}_j(s)$ appearing in NNLO $P\pi \to \pi\pi$ amplitudes — functions stemming from S wave contribution. Numerical values used for m_π and $m_P = m_\eta$ are taken from (5.197). Abscissea of the plots measure s in GeV units. Vertical lines correspond in turn to $s = 4m_\pi^2, (m_P - m_\pi)^2$, and $(m_P + m_\pi)^2$.

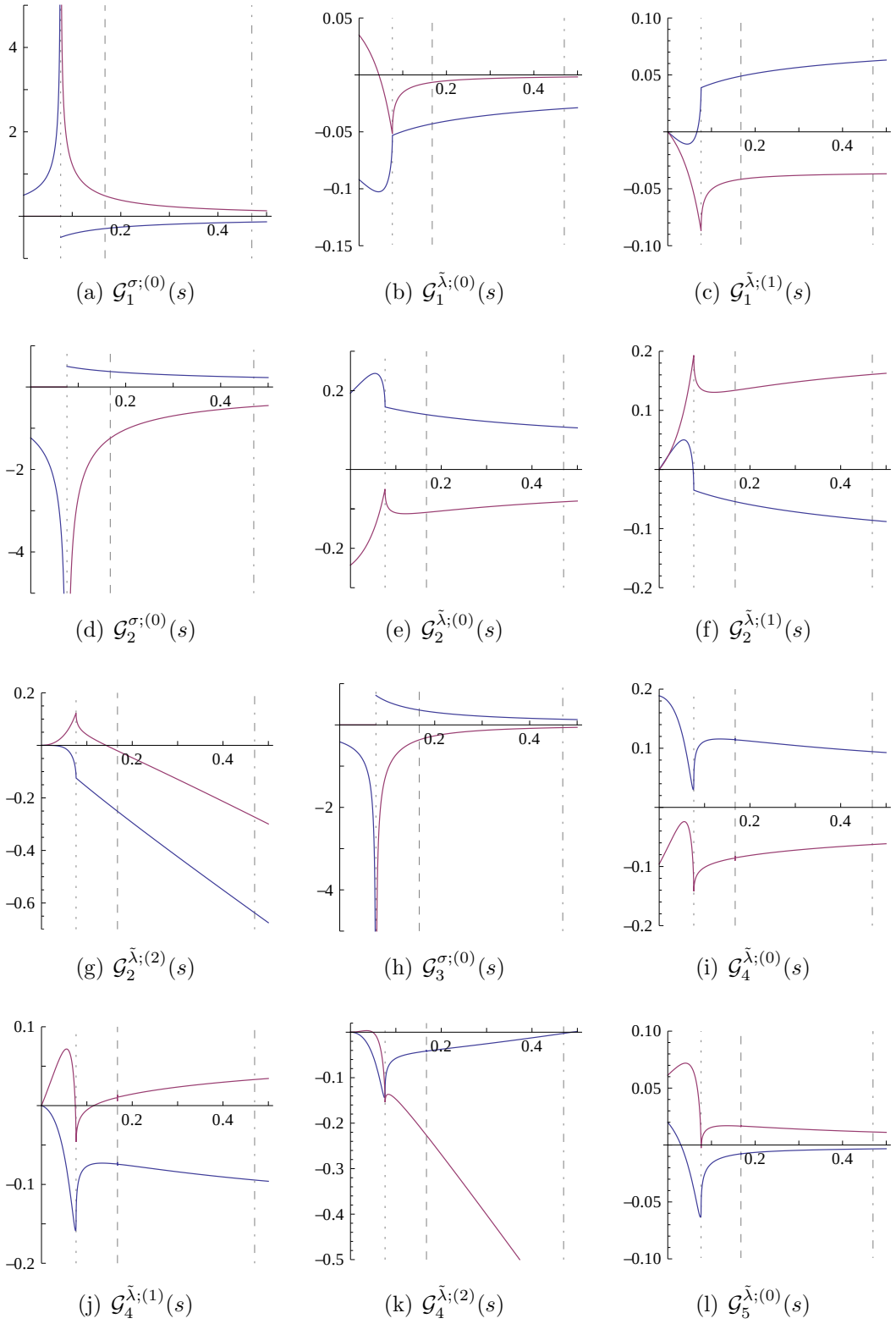

(a) $\mathcal{G}_1^{\sigma;(0)}(s)$ (b) $\mathcal{G}_1^{\tilde{\lambda};(0)}(s)$ (c) $\mathcal{G}_1^{\tilde{\lambda};(1)}(s)$

(d) $\mathcal{G}_2^{\sigma;(0)}(s)$ (e) $\mathcal{G}_2^{\tilde{\lambda};(0)}(s)$ (f) $\mathcal{G}_2^{\tilde{\lambda};(1)}(s)$

(g) $\mathcal{G}_2^{\tilde{\lambda};(2)}(s)$ (h) $\mathcal{G}_3^{\sigma;(0)}(s)$ (i) $\mathcal{G}_4^{\tilde{\lambda};(0)}(s)$

(j) $\mathcal{G}_4^{\tilde{\lambda};(1)}(s)$ (k) $\mathcal{G}_4^{\tilde{\lambda};(2)}(s)$ (l) $\mathcal{G}_5^{\tilde{\lambda};(0)}(s)$

Figure 29: Plot of Hilbert transforms $\mathcal{G}_j(s)$ appearing in NNLO $P\pi \to \pi\pi$ amplitudes — additional functions appearing in P wave contributions. Numerical values used for m_π and $m_P = m_\eta$ are taken from (5.197). Abscissea of the plots measure s in GeV units. Vertical lines denotes the following specific values of s, in turn $4m_\pi^2$, $(m_P - m_\pi)^2$, and $(m_P + m_\pi)^2$.

$\mathcal{H}^{(1)}_{1q}$,$\mathcal{H}^{(1)}_{2n}$, $\mathcal{H}^{(1)}_{1+}$, $\mathcal{H}^{(0)}_{3n}$ as there one just needs to change m_π into the corresponding pion mass and employs the results of the previous section. In addition, function $\mathcal{H}^{(1)}_{6}$ is the product of two one-loop functions (8.42). All the other functions we know at the moment only by numerical computation of their defining integrals.

Appendix G

Polynomials of the NLO partial waves of the $\pi\pi$ scatterings

G.1 The isospin breaking case

In this appendix, we give explicit form of the polynomials appearing in the expressions for partial waves of NLO $\pi\pi$ scattering amplitudes from Section 5.7.4 (in the partial-wave parametrization).

The form of the λ part of the reconstruction polynomial and of the restoring polynomial depends on the specific choice of the restoring procedure as is discussed in Section 5.6.2. We give here the results only for the case we restore just the scattering lengths. In that case the restoring polynomial is simply a constant from (E.3)–(E.7) and so is also its contribution to S partial wave,

$$p_w^{i;0} = -w_i. \tag{G.1}$$

Its contribution to P partial wave is zero

$$p_w^{i;1} = 0. \tag{G.2}$$

The other polynomials are as follows.

- $\pi^0\pi^0 \to \pi^0\pi^0$

$$p_\lambda^{0;0} = \frac{\lambda_0}{F_\pi^4}(5s + 4m_{\pi^0}^2)(s - 4m_{\pi^0}^2), \tag{G.3}$$

$$\begin{aligned} p_0^{0;0} &= 4a_0^2 + 8a_x^2 - a_x\frac{b_x}{F_\pi^2}(s - 20m_{\pi^0}^2 + 68m_{\pi^\pm}^2) \\ &\quad + \frac{b_x^2}{F_\pi^4}\Big(\frac{16}{9}(2s^2 - 7sm_{\pi^0}^2 + 14m_{\pi^0}^4) + \frac{m_{\pi^\pm}^2}{9}(39s - 732m_{\pi^0}^2) + 140m_{\pi^\pm}^4\Big), \end{aligned} \tag{G.4}$$

$$p_{1\mathrm{n}}^{0;0} = a_0^2, \tag{G.5}$$

$$p_{1\nabla}^{0;0} = 2\Big(a_x^2 - a_x\frac{b_x}{F_\pi^2}(s - 4m_{\pi^0}^2 + 10m_{\pi^\pm}^2) + \frac{b_x^2}{3F_\pi^4}\big((s-4m_{\pi^0}^2)^2 + 13m_{\pi^\pm}^2(s-4m_{\pi^0}^2) + 66m_{\pi^\pm}^4\big)\Big), \tag{G.6}$$

$$p_{2\mathrm{n}}^{0;0} = a_0^2, \tag{G.7}$$

$$p_{2\nabla}^{0;0} = 2\left(a_x^2 - 6a_x\frac{b_x}{F_\pi^2}m_{\pi^\pm}^2 + 10\frac{b_x^2}{F_\pi^4}m_{\pi^\pm}^4\right), \tag{G.8}$$

$$p_{3\mathrm{n}}^{0;0} = \frac{1}{2}a_0^2, \tag{G.9}$$

$$p_{3+}^{0;0} = \left(a_x + \frac{b_x}{F_\pi^2}(s - 4m_{\pi^\pm}^2)\right)^2. \tag{G.10}$$

- $\pi^\pm\pi^\mp \to \pi^\pm\pi^\mp$

$$p_\lambda^{c;0} = 2\,\frac{\left(2s + m_{\pi^\pm}^2\right)\lambda_c^{(1)} + 3\left(s + m_{\pi^\pm}^2\right)\lambda_c^{(2)}}{3F_\pi^4}\left(s - 4m_{\pi^\pm}^2\right), \tag{G.11}$$

$$\begin{aligned} p_0^{c;0} = {} & 5a_c^2 + a_c\frac{b_c}{2F_\pi^2}\left(3s - 64m_{\pi^\pm}^2\right) + \frac{7b_c^2}{54F_\pi^4}\left(17s^2 - 124sm_{\pi^\pm}^2 + 512m_{\pi^\pm}^4\right) \\ & + \frac{3}{2}\,a_d^2 - a_d\frac{b_d}{4F_\pi^2}\left(5s + 32m_{\pi^\pm}^2\right) + \frac{b_d^2}{36F_\pi^4}\left(14s^2 + 71sm_{\pi^\pm}^2 + 464m_{\pi^\pm}^4\right) \\ & + \frac{5}{2}\,a_x^2 + a_x\frac{b_x}{4F_\pi^2}\left(3s - 60m_{\pi^\pm}^2 - 4m_{\pi^0}^2\right) \\ & + \frac{b_x^2}{36F_\pi^4}\left(50s^2 - s\left(220m_{\pi^\pm}^2 - 3m_{\pi^0}^2\right) + 4\left(236m_{\pi^\pm}^4 + 33m_{\pi^\pm}^2m_{\pi^0}^2 - 9m_{\pi^0}^4\right)\right), \end{aligned} \tag{G.12}$$

$$\begin{aligned} p_{1+}^{c;0} = {} & a_c^2 + \frac{1}{2}\,a_d^2 - \left(a_c\frac{b_c}{F_\pi^2} + \frac{1}{2}\,a_d\frac{b_d}{F_\pi^2}\right)\left(s + 6m_{\pi^\pm}^2\right) \\ & + \frac{b_c^2}{9F_\pi^4}\left(s^2 + 2sm_{\pi^\pm}^2 + 120m_{\pi^\pm}^4\right) + \frac{b_d^2}{6F_\pi^4}\left(s^2 + 5sm_{\pi^\pm}^2 + 30m_{\pi^\pm}^4\right), \end{aligned} \tag{G.13}$$

$$\begin{aligned} p_{1\Delta}^{c;0} = {} & \frac{1}{2}\,a_x^2 - a_x\frac{b_x}{2F_\pi^2}\left(s + 4m_{\pi^\pm}^2 + 2m_{\pi^0}^2\right) \\ & + \frac{b_x^2}{6F_\pi^4}\left(s^2 + s(4m_{\pi^\pm}^2 + m_{\pi^0}^2) + 2(4m_{\pi^\pm}^2 - m_{\pi^0}^2)(2m_{\pi^\pm}^2 + 3m_{\pi^0}^2)\right), \end{aligned} \tag{G.14}$$

$$p_{2+}^{c;0} = a_c^2 - 6a_c\frac{b_c}{F_\pi^2}m_{\pi^\pm}^2 - \frac{2b_c^2}{3F_\pi^4}m_{\pi^\pm}^2\left(3s - 20m_{\pi^\pm}^2\right) + \frac{1}{2}\,a_d^2 - 3a_d\frac{b_d}{F_\pi^2}m_{\pi^\pm}^2 + 5\frac{b_d^2}{F_\pi^4}m_{\pi^\pm}^4, \tag{G.15}$$

$$p_{2\Delta}^{c;0} = \frac{1}{2}\,a_x^2 + a_x\frac{b_x}{F_\pi^2}\left(m_{\pi^0}^2 - 4m_{\pi^\pm}^2\right) + \frac{b_x^2}{F_\pi^4}\left(8m_{\pi^\pm}^4 - 4m_{\pi^\pm}^2m_{\pi^0}^2 + m_{\pi^0}^4\right), \tag{G.16}$$

$$p_{3\mathrm{n}}^{c;0} = \frac{1}{2}\left(a_x + \frac{b_x}{F_\pi^2}\left(s - 4m_{\pi^\pm}^2\right)\right)^2, \tag{G.17}$$

$$p_{3+}^{c;0} = \left(a_c + \frac{b_c}{F_\pi^2}\left(s - 4m_{\pi^\pm}^2\right)\right)^2. \tag{G.18}$$

The polynomials of P wave:

$$p_\lambda^{c;1} = \frac{\lambda_c^{(2)} - \lambda_c^{(1)}}{6F_\pi^4}\, s, \tag{G.19}$$

$$\begin{aligned}
p_0^{c;1} = {} & \frac{1}{2}a_c^2\Big(\frac{s}{m_{\pi^\pm}^2} - 8\Big) + 2a_c\frac{b_c}{9F_\pi^2}\left(\frac{11s^2}{4m_{\pi^\pm}^2} - 46s + 176m_{\pi^\pm}^2\right) \\
& - \frac{b_c^2}{27F_\pi^4}\left(\frac{s^3}{m_{\pi^\pm}^2} + 100s^2 - 1166sm_{\pi^\pm}^2 + 3072m_{\pi^\pm}^4\right) - \frac{1}{4}\,a_d^2\left(\frac{s}{m_{\pi^\pm}^2} - 8\right) \\
& - a_d\frac{b_d}{9F_\pi^2}\left(\frac{11s^2}{4m_{\pi^\pm}^2} - 46s + 176m_{\pi^\pm}^2\right) \\
& + \frac{b_d^2}{36F_\pi^4}\left(\frac{25s^3}{4m_{\pi^\pm}^2} - 32s^2 - 263sm_{\pi^\pm}^2 + 1344m_{\pi^\pm}^4\right) + \frac{1}{4m_{\pi^\pm}^2}\,a_x^2\,(s - 4\Sigma) \\
& + a_x\frac{b_x}{9F_\pi^2m_{\pi^\pm}^2}\left(\frac{11}{4}s^2 - s(40m_{\pi^\pm}^2 + 6m_{\pi^0}^2) + 4(29m_{\pi^\pm}^4 + 24m_{\pi^\pm}^2m_{\pi^0}^2 - 9m_{\pi^0}^4)\right) \\
& - \frac{b_x^2}{36F_\pi^4m_{\pi^\pm}^2}\Big(\frac{25}{4}s^3 - s^2\left(31m_{\pi^\pm}^2 + m_{\pi^0}^2\right) - s\left(196m_{\pi^\pm}^4 + 88m_{\pi^\pm}^2m_{\pi^0}^2 - 21m_{\pi^0}^4\right) \\
& \qquad + 4\left(220m_{\pi^\pm}^6 + 236m_{\pi^\pm}^4m_{\pi^0}^2 - 165m_{\pi^\pm}^2m_{\pi^0}^4 + 45m_{\pi^0}^6\right)\Big),
\end{aligned} \tag{G.20}$$

$$\begin{aligned}
p_{1+}^{c;1} = {} & a_d^2 - 2a_c^2 + \frac{1}{3}\left(a_c\frac{b_c}{F_\pi^2} - \frac{1}{2}\,a_d\frac{b_d}{F_\pi^2}\right)\left(\frac{s^2}{m_{\pi^\pm}^2} - 10s + 48m_{\pi^\pm}^2\right) \\
& - \frac{b_c^2}{9F_\pi^4}\left(\frac{s}{m_{\pi^\pm}^2} - 6\right)\left(s^2 + 8m_{\pi^\pm}^2s - 60m_{\pi^\pm}^4\right) \\
& + \frac{b_d^2}{12F_\pi^4}\left(\frac{s}{m_{\pi^\pm}^2} + 6\right)\left(s^2 - 10m_{\pi^\pm}^2s + 30m_{\pi^\pm}^4\right),
\end{aligned} \tag{G.21}$$

$$\begin{aligned}
p_{1\Delta}^{c;1} = {} & -a_x^2\frac{m_{\pi^0}^2}{m_{\pi^\pm}^2} + a_x\frac{b_x}{6F_\pi^2m_{\pi^\pm}^2}\left(s^2 - 2s(4m_{\pi^\pm}^2 + m_{\pi^0}^2) + 8(2m_{\pi^\pm}^4 + 7m_{\pi^\pm}^2m_{\pi^0}^2 - 3m_{\pi^0}^4)\right) \\
& - \frac{b_x^2}{12F_\pi^4m_{\pi^\pm}^2}\Big(s^3 - 4s^2m_{\pi^\pm}^2 - 2s(8m_{\pi^\pm}^4 + 8m_{\pi^\pm}^2m_{\pi^0}^2 - m_{\pi^0}^4) \\
& \qquad + 4(16m_{\pi^\pm}^6 + 64m_{\pi^\pm}^4m_{\pi^0}^2 - 50m_{\pi^\pm}^2m_{\pi^0}^4 + 15m_{\pi^0}^6)\Big),
\end{aligned} \tag{G.22}$$

$$\begin{aligned}
p_{2+}^{c;1} = {} & \left(\frac{s}{m_{\pi^\pm}^2} - 2\right)\left(a_c^2 - \frac{1}{2}\,a_d^2\right) + \left(3s - 8m_{\pi^\pm}^2\right)\left(a_d\frac{b_d}{F_\pi^2} - 2a_c\frac{b_c}{F_\pi^2}\right) \\
& - \frac{2b_c^2}{3F_\pi^4}\left(s - 6m_{\pi^\pm}^2\right)\left(3s - 10m_{\pi^\pm}^2\right) - \frac{5b_d^2}{F_\pi^4}m_{\pi^\pm}^2\left(s - 3m_{\pi^\pm}^2\right),
\end{aligned} \tag{G.23}$$

$$
\begin{aligned}
p_{2\Delta}^{c;1} = & \frac{1}{2m_{\pi^\pm}^2}\, a_x^2 \left(s - 4m_{\pi^\pm}^2 + 2m_{\pi^0}^2\right) \\
& + a_x \frac{b_x}{F_\pi^2 m_{\pi^\pm}^2} \left(s(m_{\pi^0}^2 - 4m_{\pi^\pm}^2) + 4(4m_{\pi^\pm}^4 - 3m_{\pi^\pm}^2 m_{\pi^0}^2 + m_{\pi^0}^4)\right) \\
& + \frac{b_x^2}{F_\pi^4 m_{\pi^\pm}^2} \left(s(8m_{\pi^\pm}^4 - 4m_{\pi^\pm}^2 m_{\pi^0}^2 + m_{\pi^0}^4) - 32\Delta m_{\pi^\pm}^4 - 5m_{\pi^0}^4(4m_{\pi^\pm}^2 - m_{\pi^0}^2)\right),
\end{aligned} \tag{G.24}
$$

$$
p_{3+}^{c;1} = \frac{b_c^2}{9F_\pi^4}\left(s - 4m_{\pi^\pm}^2\right). \tag{G.25}
$$

- $\pi^\pm\pi^\pm \to \pi^\pm\pi^\pm$

$$
p_{\lambda}^{d;0} = 2\,\frac{\left(s + 2m_{\pi^\pm}^2\right)\lambda_c^{(1)} + 2\left(2s + m_{\pi^\pm}^2\right)\lambda_c^{(2)}}{3F_\pi^4}\left(s - 4m_{\pi^\pm}^2\right), \tag{G.26}
$$

$$
\begin{aligned}
p_0^{d;0} = & \left(a_d + \frac{b_d}{F_\pi^2}\left(s - 4m_{\pi^\pm}^2\right)\right)^2 + 6a_c^2 - a_c\frac{b_c}{F_\pi^2}\left(5s + 32m_{\pi^\pm}^2\right) \\
& + \frac{b_c^2}{27F_\pi^4}\left(73s^2 + 430sm_{\pi^\pm}^2 + 928m_{\pi^\pm}^4\right) + 3a_x^2 - a_x\frac{b_x}{2F_\pi^2}\left(5s + 28m_{\pi^\pm}^2 + 4m_{\pi^0}^2\right) \\
& + \frac{b_x^2}{18F_\pi^4}\left(14s^2 + s\left(68m_{\pi^\pm}^2 + 3m_{\pi^0}^2\right) + 4\left(92m_{\pi^\pm}^4 + 33m_{\pi^\pm}^2 m_{\pi^0}^2 - 9m_{\pi^0}^4\right)\right),
\end{aligned} \tag{G.27}
$$

$$
p_{1+}^{d;0} = 2a_c^2 - 2a_c\frac{b_c}{F_\pi^2}\left(s + 6m_{\pi^\pm}^2\right) + \frac{2b_c^2}{9F_\pi^4}\left(5s^2 + 28m_{\pi^\pm}^2 s + 60m_{\pi^\pm}^4\right), \tag{G.28}
$$

$$
\begin{aligned}
p_{1\Delta}^{d;0} = & a_x^2 - a_x\frac{b_x}{F_\pi^2}\left(s + 4m_{\pi^\pm}^2 + 2m_{\pi^0}^2\right) \\
& + \frac{b_x^2}{3F_\pi^4}\left(s^2 + s(4m_{\pi^\pm}^2 + m_{\pi^0}^2) + 2(4m_{\pi^\pm}^2 - m_{\pi^0}^2)(2m_{\pi^\pm}^2 + 3m_{\pi^0}^2)\right),
\end{aligned} \tag{G.29}
$$

$$
p_{2+}^{d;0} = 2\left(a_c^2 - 6a_c\frac{b_c}{F_\pi^2}m_{\pi^\pm}^2 + \frac{2b_c^2}{3F_\pi^4}m_{\pi^\pm}^2\left(3s + 10m_{\pi^\pm}^2\right)\right), \tag{G.30}
$$

$$
p_{2\Delta}^{d;0} = a_x^2 + 2a_x\frac{b_x}{F_\pi^2}\left(m_{\pi^0}^2 - 4m_{\pi^\pm}^2\right) + 2\frac{b_x^2}{F_\pi^4}\left(8m_{\pi^\pm}^4 - 4m_{\pi^\pm}^2 m_{\pi^0}^2 + m_{\pi^0}^4\right), \tag{G.31}
$$

$$
p_{3+}^{d;0} = \frac{1}{2}\left(a_d + \frac{b_d}{F_\pi^2}\left(s - 4m_{\pi^\pm}^2\right)\right)^2. \tag{G.32}
$$

- $\pi^\pm\pi^\mp \to \pi^0\pi^0$

$$
p_{\lambda}^{x;0} = -\frac{3\lambda_x^{(1)}s + 2\lambda_x^{(2)}(s + 3m_{\pi^\pm}^2 - m_{\pi^0}^2)}{3F_\pi^4}(s - 4m_{\pi^\pm}^2), \tag{G.33}
$$

$$p_0^{x;0} = \left(a_0 + 2a_c + 2\frac{b_c}{F_\pi^2}(s - 4m_{\pi^\pm}^2)\right)\left(a_x + \frac{b_x}{F_\pi^2}(s - 4m_{\pi^\pm}^2)\right) - 4a_t^2 + 3a_t\frac{b_t}{F_\pi^2}(s + 4\Sigma) - \frac{b_t^2}{27F_\pi^4}\left(5s^2 - 14s\Sigma + 4(171m_{\pi^\pm}^4 + 26m_{\pi^\pm}^2 m_{\pi^0}^2 + 171m_{\pi^0}^4)\right), \tag{G.34}$$

$$p_{0q}^{x;0} = -2\Bigg(a_t^2 + \frac{b_t^2}{9F_\pi^4}\left(s^2 + 2s\Sigma + 8(15m_{\pi^\pm}^4 - 22m_{\pi^\pm}^2 m_{\pi^0}^2 + 15m_{\pi^0}^4)\right) - a_t\frac{b_t}{F_\pi^2}\Big(s + \frac{6m_{\pi^\pm}^4 - 4m_{\pi^\pm}^2 m_{\pi^0}^2 + 6m_{\pi^0}^4}{\Sigma}\Big)\Bigg), \tag{G.35}$$

$$p_{1\mathrm{n}}^{x;0} = -a_t^2 + a_t\frac{b_t}{F_\pi^2}(s + 6m_{\pi^\pm}^2) - \frac{b_t^2}{9F_\pi^4}(s^2 + 2sm_{\pi^\pm}^2 + 120m_{\pi^\pm}^4), \tag{G.36}$$

$$p_{1+}^{x;0} = -a_t^2 + a_t\frac{b_t}{F_\pi^2}(s + 6m_{\pi^0}^2) - \frac{b_t^2}{9F_\pi^4}(s^2 + 2sm_{\pi^0}^2 + 120m_{\pi^0}^4), \tag{G.37}$$

$$p_{2\mathrm{n}+}^{x;0} = -2a_t^2 + 12a_t\frac{b_t}{F_\pi^2}\frac{m_{\pi^\pm}^4 + m_{\pi^0}^4}{\Sigma} + \frac{4b_t^2}{3F_\pi^4}\left(3s\frac{m_{\pi^\pm}^4 + m_{\pi^0}^4}{\Sigma} - 20\frac{m_{\pi^\pm}^6 + m_{\pi^0}^6}{\Sigma}\right), \tag{G.38}$$

$$p_{3\mathrm{n}}^{x;0} = \frac{1}{2}\,a_0\left(a_x + \frac{b_x}{F_\pi^2}(s - 4m_{\pi^\pm}^2)\right), \tag{G.39}$$

$$p_{3+}^{x;0} = \left(a_c + \frac{b_c}{F_\pi^2}(s - 4m_{\pi^\pm}^2)\right)\left(a_x + \frac{b_x}{F_\pi^2}(s - 4m_{\pi^\pm}^2)\right), \tag{G.40}$$

$$p_{7x}^{x;0} = \frac{2}{3}\left(3a_t^2 - 18a_t\frac{b_t}{F_\pi^2}\Sigma - \frac{2b_t^2}{F_\pi^4}\left(3s\Sigma - 20(m_{\pi^\pm}^4 + m_{\pi^\pm}^2 m_{\pi^0}^2 + m_{\pi^0}^4)\right)\right). \tag{G.41}$$

- $\pi^\pm\pi^0 \to \pi^\pm\pi^0$

$$p_\lambda^{t;0} = \frac{\lambda_x^{(1)}\left(s^2 + 2s(2m_{\pi^\pm}^2 - m_{\pi^0}^2) + \Delta^2\right) + \lambda_x^{(2)}\left(4s^2 + s\Sigma + \Delta^2\right)}{3s^2F_\pi^4}\lambda(s), \tag{G.42}$$

$$p_{0q}^{t;0} = a_t^2\Big(2 - \frac{\Delta^2}{s\Sigma}\Big) + a_t\frac{b_t}{F_\pi^2}\left(s - \frac{2}{\Sigma}(5\Delta^2 + 12m_{\pi^\pm}^2 m_{\pi^0}^2) + 7\frac{\Delta^2}{s} - 2\frac{\Delta^4}{s^2\Sigma}\right) + \frac{b_t^2}{9F^4}\Big(-9\frac{\Delta^6}{s^3\Sigma} + 47\frac{\Delta^4}{s^2} - \frac{\Delta^2}{s\Sigma}(101m_{\pi^\pm}^4 + 94m_{\pi^\pm}^2 m_{\pi^0}^2 + 101m_{\pi^0}^4) + 129m_{\pi^\pm}^4 - 82m_{\pi^\pm}^2 m_{\pi^0}^2 + 129m_{\pi^0}^4 - \frac{4}{\Sigma}(5m_{\pi^\pm}^4 + 16m_{\pi^\pm}^2 m_{\pi^0}^2 + 5m_{\pi^0}^4)s + 14s^2\Big), \tag{G.43}$$

$$p_0^{t;0} = 3a_t^2 + a_t\frac{b_t}{2F_\pi^2}\Big(s - 20\Sigma + 7\frac{\Delta^2}{s}\Big) + \frac{b_t^2}{54F_\pi^4}\Big(97s^2 - 61s\Sigma + 693\Delta^2 + 1600m_{\pi^\pm}^2 m_{\pi^0}^2 - 331\Sigma\frac{\Delta^2}{s} + 70\frac{\Delta^4}{s^2}\Big) - a_x\Bigg(3a_c + \frac{3}{2}a_0 - \frac{b_c}{4F_\pi^2}\Big(5s + 2(21m_{\pi^\pm}^2 - 5m_{\pi^0}^2) + 5\frac{\Delta^2}{s}\Big)\Bigg) +$$

$$
\begin{aligned}
&+\frac{b_x}{F_\pi^2}\bigg(\frac{a_0}{8}\left(5s+2(19m_{\pi^\pm}^2-3m_{\pi^0}^2)+5\frac{\Delta^2}{s}\right)\\
&\quad+\frac{a_c}{4}\left(5s+2(21m_{\pi^\pm}^2-5m_{\pi^0}^2)+5\frac{\Delta^2}{s}\right)\\
&\quad-\frac{b_c}{18F_\pi^2}\Big(14s^2+2(345m_{\pi^\pm}^4-155m_{\pi^\pm}^2m_{\pi^0}^2+42m_{\pi^0}^4)\\
&\qquad+s(127m_{\pi^\pm}^2-56m_{\pi^0}^2)+(127m_{\pi^\pm}^2-56m_{\pi^0}^2)\frac{\Delta^2}{s}+14\frac{\Delta^4}{s^2}\Big)\bigg),
\end{aligned}
\tag{G.44}
$$

$$
\begin{aligned}
p_{1\uparrow}^{t;0}&=a_t^2-a_t\frac{b_t}{F_\pi^2}(s+3\Sigma)+\frac{b_t^2}{9F_\pi^4}\left(5s^2+14\Sigma s+5(7\Delta^2+12m_{\pi^\pm}^2m_{\pi^0}^2)\right)\\
&-a_x\bigg(\frac{a_0}{2}\Big(1-\frac{\Delta}{s}\Big)+a_c\Big(1+\frac{\Delta}{s}\Big)-\frac{b_c}{2F_\pi^2}\Big(1+\frac{\Delta}{s}\Big)\left(s+2(4m_{\pi^\pm}^2-m_{\pi^0}^2)+\frac{\Delta^2}{s}\right)\bigg)\\
&+\frac{b_x}{F_\pi^2}\bigg(\frac{a_c}{2}\Big(1+\frac{\Delta}{s}\Big)\Big(s+2(4m_{\pi^\pm}^2-m_{\pi^0}^2)+\frac{\Delta^2}{s}\Big)\\
&\quad+\frac{a_0}{4}\Big(1-\frac{\Delta}{s}\Big)\Big(s+6m_{\pi^\pm}^2+\frac{\Delta^2}{s}\Big)\\
&\quad-\frac{b_c}{3F_\pi^2}\Big(1+\frac{\Delta}{s}\Big)\Big(s^2+(9m_{\pi^\pm}^2-4m_{\pi^0}^2)\Big(s+\frac{\Delta^2}{s}\Big)\\
&\qquad+2(23m_{\pi^\pm}^4-11m_{\pi^\pm}^2m_{\pi^0}^2+3m_{\pi^0}^4)+\frac{\Delta^4}{s^2}\Big)\bigg),
\end{aligned}
\tag{G.45}
$$

$$
\begin{aligned}
p_{1\downarrow}^{t;0}&=-a_t^2+a_t\frac{b_t}{F_\pi^2}\left(2s+5\Sigma-\frac{\Delta^2}{s}\right)\\
&-\frac{b_t^2}{9F_\pi^4}\left(57\Sigma s+2(25\Sigma^2-34m_{\pi^\pm}^2m_{\pi^0}^2)-13\Sigma\frac{\Delta^2}{s}+2\frac{\Delta^4}{s^2}\right)\\
&+a_x\bigg(\frac{1}{2}\,a_0\Big(1-\frac{s}{\Delta}\Big)+a_c\Big(1+\frac{s}{\Delta}\Big)\\
&\quad-\frac{b_c}{2F_\pi^2}\Big(1+\frac{s}{\Delta}\Big)\Big(s+2(4m_{\pi^\pm}^2-m_{\pi^0}^2)+\frac{\Delta^2}{s}\Big)\bigg)\\
&-\frac{b_x}{F_\pi^2}\bigg(\frac{1}{2}\,a_c\Big(1+\frac{s}{\Delta}\Big)\Big(s+2(4m_{\pi^\pm}^2-m_{\pi^0}^2)+\frac{\Delta^2}{s}\Big)\\
&\quad+\frac{1}{4}\,a_0\Big(1-\frac{s}{\Delta}\Big)\left(s+6m_{\pi^\pm}^2+\frac{\Delta^2}{s}\right)\\
&\quad-\frac{b_c}{3F_\pi^2}\Big(1+\frac{s}{\Delta}\Big)\Big(s^2+(9m_{\pi^\pm}^2-4m_{\pi^0}^2)\Big(s+\frac{\Delta^2}{s}\Big)\\
&\qquad+2(23m_{\pi^\pm}^4-11m_{\pi^\pm}^2m_{\pi^0}^2+3m_{\pi^0}^4)+\frac{\Delta^4}{s^2}\Big)\bigg),
\end{aligned}
\tag{G.46}
$$

$$p^{t;0}_{2\odot} = -\frac{1}{2}\,a_0\left(a_x + \frac{b_x}{F_\pi^2}(m^2_{\pi^0} - 4m^2_{\pi^\pm})\right), \tag{G.47}$$

$$p^{t;0}_{2\oplus} = -a_c a_x + 3a_x\frac{b_c}{F_\pi^2}m^2_{\pi^\pm} + 3a_c\frac{b_x}{F_\pi^2}m^2_{\pi^\pm} - 10\frac{b_c b_x}{F_\pi^4}m^4_{\pi^\pm}, \tag{G.48}$$

$$\begin{aligned} p^{t;0}_{2\odot\oplus} &= a_t^2 - 6a_t\frac{b_t}{F_\pi^2}\frac{(m^4_{\pi^\pm} + m^4_{\pi^0})}{\Sigma} \\ &\quad + \frac{2b_t^2}{3F_\pi^4}\frac{1}{\Sigma}\left(13m^6_{\pi^\pm} - 3m^2_{\pi^\pm}m^4_{\pi^0} - 3m^4_{\pi^\pm}m^2_{\pi^0} + 13m^6_{\pi^0} + 3(m^4_{\pi^\pm} + m^4_{\pi^0})s\right), \end{aligned} \tag{G.49}$$

$$p^{t;0}_{3\uparrow} = \left(a_t + \frac{b_t}{sF_\pi^2}(s-\mu_+)(s-\mu_-)\right)^2, \tag{G.50}$$

$$p^{t;0}_{7t} = a_t^2 - 6a_t\frac{b_t}{F_\pi^2}\Sigma + 2\frac{b_t^2}{3F_\pi^4}(13\Sigma^2 - 16m^2_{\pi^\pm}m^2_{\pi^0} + 3\Sigma s), \tag{G.51}$$

$$p^{t;0}_{8t} = 2\frac{b_t}{F_\pi^2}\Delta\left(-a_t + \frac{b_t}{3F_\pi^2}(s+6\Sigma)\right), \tag{G.52}$$

$$p^{t;0}_{9t} = -\frac{4}{3}\frac{b_t^2}{F_\pi^4}\Delta^2. \tag{G.53}$$

Finally, the P wave polynomials are:

$$p^{t;1}_{\lambda} = \frac{-\lambda_x^{(1)}\,(s+\Delta) + \lambda_x^{(2)}\,(s-\Delta)}{6sF_\pi^4}(s+\Delta), \tag{G.54}$$

$$\begin{aligned} p^{t;1}_{0q} &= 4a_t^2\frac{\Delta^2}{\Sigma^2} - 2a_t\frac{b_t}{3F_\pi^2\Sigma}\Big(s^2 + \frac{\Delta^4}{s^2} - 4\Sigma(s+\frac{\Delta^2}{s}) + 2(21\Delta^2 + 8m^2_{\pi^\pm}m^2_{\pi^0})\Big) \\ &\quad + 2\frac{b_t^2}{9F^4\Sigma}\Big(3s^3 - \frac{6}{\Sigma}(3\Delta^2 + 8m^2_{\pi^\pm}m^2_{\pi^0})s^2 + 4(17\Delta^2 + 12m^2_{\pi^\pm}m^2_{\pi^0})s \\ &\qquad + \frac{\Delta^2}{\Sigma}(141\Delta^2 + 352m^2_{\pi^\pm}m^2_{\pi^0}) + \frac{\Delta^2}{s}(19\Delta^2 + 32m^2_{\pi^\pm}m^2_{\pi^0}) \\ &\qquad - 2\frac{\Delta^4}{s^2\Sigma}(7\Delta^2 + 24m^2_{\pi^\pm}m^2_{\pi^0}) + 6\frac{\Delta^6}{s^3} - \frac{\Delta^8}{s^4\Sigma}\Big), \end{aligned} \tag{G.55}$$

$$\begin{aligned} p^{t;1}_{0} &= -\frac{1}{\Sigma}\,a_t^2\Big(s - 4\Sigma - \frac{\Delta^2}{s}\Big) \\ &\quad - a_t\frac{b_t}{9F_\pi^2\Sigma}\left(5s^2 - 68\Sigma s + 38(9\Delta^2 + 16m^2_{\pi^\pm}m^2_{\pi^0}) + 4\Sigma\frac{\Delta^2}{s} + 5\frac{\Delta^4}{s^2}\right) \\ &\quad + \frac{b_t^2}{54F_\pi^4\Sigma}\Big(35s^3 - 248\Sigma s^2 + (545m^4_{\pi^\pm} - 158m^2_{\pi^\pm}m^2_{\pi^0} + 545m^4_{\pi^0})s \\ &\qquad + 20\Sigma(145\Delta^2 + 96m^2_{\pi^\pm}m^2_{\pi^0}) \\ &\qquad + \left(221m^4_{\pi^\pm} - 158m^2_{\pi^\pm}m^2_{\pi^0} + 221m^4_{\pi^0}\right)\frac{\Delta^2}{s} + 4\Sigma\frac{\Delta^4}{s^2} - \frac{\Delta^6}{s^3}\Big) + \end{aligned}$$

$$
\begin{aligned}
&- \frac{a_x}{\Sigma}\Big(a_c\Big(s-2(\Sigma+2m_{\pi^\pm}^2)+\frac{\Delta^2}{s}\Big)+\frac{a_0}{\Sigma}\Big(s-2(\Sigma+2m_{\pi^0}^2)+\frac{\Delta^2}{s}\Big)\Big)\\
&- \frac{1}{18\Sigma}\Big(a_x\frac{b_c}{F_\pi^2}+a_c\frac{b_x}{F_\pi^2}\Big)\Big(11\Big(s^2+\frac{\Delta^4}{s^2}\Big)-4(35m_{\pi^\pm}^2+11m_{\pi^0}^2)\Big(s+\frac{\Delta^2}{s}\Big)\\
&\qquad\qquad +2(201m_{\pi^\pm}^4+118m_{\pi^\pm}^2m_{\pi^0}^2+33m_{\pi^0}^4)\Big)\\
&+ \frac{b_x}{36F_\pi^2\Sigma}\Big(-a_0\Big(11\Big(s^2+\frac{\Delta^4}{s^2}\Big)-4(29m_{\pi^\pm}^2+17m_{\pi^0}^2)\Big(s+\frac{\Delta^2}{s}\Big)\\
&\qquad\qquad +2(105m_{\pi^\pm}^4+262m_{\pi^\pm}^2m_{\pi^0}^2-15m_{\pi^0}^4)\Big)\\
&\qquad + \frac{b_c}{F_\pi^2}\Big(25\Big(s^3+\frac{\Delta^6}{s^3}\Big)+2(11m_{\pi^\pm}^2-75m_{\pi^0}^2)\Big(s^2+\frac{\Delta^4}{s^2}\Big)\\
&\qquad\qquad -(1189m_{\pi^\pm}^4+238m_{\pi^\pm}^2m_{\pi^0}^2-375m_{\pi^0}^4)\Big(s+\frac{\Delta^2}{s}\Big)\\
&\qquad\qquad +4(751m_{\pi^\pm}^6+535m_{\pi^\pm}^4m_{\pi^0}^2+183m_{\pi^\pm}^2m_{\pi^0}^4-125m_{\pi^0}^6)\Big)\Big),
\end{aligned}
\tag{G.56}
$$

$$
\begin{aligned}
p_{1\uparrow}^{t;1} &= 2a_t^2(1+\frac{\Delta^2}{s\Sigma})-2a_t\frac{b_t}{3F_\pi^2\Sigma}\Big(s^2-5\Sigma s+(31\Delta^2+48m_{\pi^\pm}^2m_{\pi^0}^2)+9\Sigma\frac{\Delta^2}{s}\Big)\\
&+2\frac{b_t^2}{9F_\pi^4\Sigma}\Big(2s^3-7s^2\Sigma+s(25\Delta^2+18m_{\pi^\pm}^2m_{\pi^0}^2)+\Sigma(137\Delta^2+90m_{\pi^\pm}^2m_{\pi^0}^2)\\
&\qquad +5(7\Delta^2+12m_{\pi^\pm}^2m_{\pi^0}^2)\frac{\Delta^2}{s}\Big)\\
&+2\frac{a_x}{\Sigma}\Big(a_0m_{\pi^0}^2\Big(1-\frac{\Delta}{s}\Big)+2a_cm_{\pi^\pm}^2\Big(1+\frac{\Delta}{s}\Big)\Big)\\
&-\frac{1}{3\Sigma}\Big(a_x\frac{b_c}{F_\pi^2}+a_c\frac{b_x}{F_\pi^2}\Big)\Big(1+\frac{\Delta}{s}\Big)\Big(s^2+\frac{\Delta^4}{s^2}-2(2\Sigma+m_{\pi^\pm}^2)\Big(s+\frac{\Delta^2}{s}\Big)\\
&\qquad\qquad +2(17m_{\pi^\pm}^4+4m_{\pi^\pm}^2m_{\pi^0}^2+3m_{\pi^0}^4)\Big)\\
&+\frac{b_x}{6F_\pi^2\Sigma}\Big(a_0\Big(\frac{\Delta}{s}-1\Big)\Big(s^2+\frac{\Delta^4}{s^2}-2(2\Sigma+m_{\pi^0}^2)\Big(s+\frac{\Delta^2}{s}\Big)\\
&\qquad\qquad +2(3m_{\pi^\pm}^4+28m_{\pi^\pm}^2m_{\pi^0}^2-7m_{\pi^0}^4)\Big)\\
&\qquad -2\frac{b_c}{F_\pi^2}\Big(1+\frac{\Delta}{s}\Big)\Big(s+2(4m_{\pi^\pm}^2-m_{\pi^0}^2)+\frac{\Delta^2}{s}\Big)\\
&\qquad\qquad \times\Big(s^2+\frac{\Delta^4}{s^2}-2(2\Sigma+m_{\pi^\pm}^2)\Big(s+\frac{\Delta^2}{s}\Big)\\
&\qquad\qquad\qquad +2(8m_{\pi^\pm}^4+4m_{\pi^\pm}^2m_{\pi^0}^2+3m_{\pi^0}^4)\Big)\Big),
\end{aligned}
\tag{G.57}
$$

$$
\begin{aligned}
p_{1\downarrow}^{t;1} &= 2a_t^2\left(\frac{s}{\Sigma}-3\right) - 2a_t\frac{b_t}{3F_\pi^2\Sigma}\Big(6s^2+3s\Sigma-61\Delta^2-144m_{\pi^\pm}^2m_{\pi^0}^2+5\Sigma\frac{\Delta^2}{s}-\frac{\Delta^4}{s^2}\Big)\\
&+2\frac{b_t^2}{9F_\pi^4\Sigma}\Big(57\Sigma s^2-2s(55\Delta^2+174m_{\pi^\pm}^2m_{\pi^0}^2)-\Sigma(263\Delta^2+294m_{\pi^\pm}^2m_{\pi^0}^2)\\
&\qquad+(23\Delta^2+90m_{\pi^\pm}^2m_{\pi^0}^2)\frac{\Delta^2}{s}-8\Sigma\frac{\Delta^4}{s^2}+\frac{\Delta^6}{s^3}\Big)\\
&-2\frac{a_x}{\Sigma}\left(a_0m_{\pi^0}^2\Big(1-\frac{s}{\Delta}\Big)+2a_cm_{\pi^\pm}^2\Big(1+\frac{s}{\Delta}\Big)\right)\\
&+\frac{1}{3\Sigma}\Big(a_x\frac{b_c}{F_\pi^2}+a_c\frac{b_x}{F_\pi^2}\Big)\Big(1+\frac{s}{\Delta}\Big)\Big(s^2+\frac{\Delta^4}{s^2}-2(2\Sigma+m_{\pi^\pm}^2)\Big(s+\frac{\Delta^2}{s}\Big)\\
&\qquad+2(17m_{\pi^\pm}^4+4m_{\pi^\pm}^2m_{\pi^0}^2+3m_{\pi^0}^4)\Big)\\
&+\frac{b_x}{6F_\pi^2\Sigma}\left(a_0\Big(1-\frac{s}{\Delta}\Big)\Big(s^2+\frac{\Delta^4}{s^2}-2(2\Sigma+m_{\pi^0}^2)\Big(s+\frac{\Delta^2}{s}\Big)\right.\\
&\qquad+2(3m_{\pi^\pm}^4+28m_{\pi^\pm}^2m_{\pi^0}^2-7m_{\pi^0}^4)\Big)\\
&\qquad+2\frac{b_c}{F_\pi^2}\Big(1+\frac{s}{\Delta}\Big)\Big(s+2(4m_{\pi^\pm}^2-m_{\pi^0}^2)+\frac{\Delta^2}{s}\Big)\\
&\qquad\times\Big(s^2+\frac{\Delta^4}{s^2}-2(2\Sigma+m_{\pi^\pm}^2)\Big(s+\frac{\Delta^2}{s}\Big)\\
&\qquad\left.+2(8m_{\pi^\pm}^4+4m_{\pi^\pm}^2m_{\pi^0}^2+3m_{\pi^0}^4)\Big)\right)
\end{aligned}
\tag{G.58}
$$

$$
\begin{aligned}
p_{2\odot}^{t;1} &= -\frac{1}{\Sigma}\,a_0\left(a_x\Big(s-2m_{\pi^\pm}^2+\frac{\Delta^2}{s}\Big)\right.\\
&\qquad\left.-\frac{b_x}{F_\pi^2}\Big((4m_{\pi^\pm}^2-m_{\pi^0}^2)\Big(s+\frac{\Delta^2}{s}\Big)-2(4m_{\pi^\pm}^4-m_{\pi^\pm}^2m_{\pi^0}^2+m_{\pi^0}^4)\Big)\right),
\end{aligned}
\tag{G.59}
$$

$$
\begin{aligned}
p_{2\odot\oplus}^{t;1} &= -2\frac{a_t^2}{\Sigma}\left(s-2\frac{(m_{\pi^\pm}^4+m_{\pi^0}^4)}{\Sigma}-\frac{\Delta^2}{s}\right)\\
&+4a_t\frac{b_t}{F_\pi^2\Sigma}\left(3\frac{(m_{\pi^\pm}^4+m_{\pi^0}^4)}{\Sigma}(s-\frac{\Delta^2}{s})-8\frac{(m_{\pi^\pm}^6+m_{\pi^0}^6)}{\Sigma}\right)\\
&-\frac{4b_t^2}{3F_\pi^4\Sigma}\Big(3\frac{(m_{\pi^\pm}^4+m_{\pi^0}^4)}{\Sigma}s^2+(5\Delta^2+2m_{\pi^\pm}^2m_{\pi^0}^2)s-(13\Delta^2+10m_{\pi^\pm}^2m_{\pi^0}^2)\frac{\Delta^2}{s}\\
&\qquad-\frac{3}{\Sigma}(15m_{\pi^\pm}^8-6m_{\pi^\pm}^6m_{\pi^0}^2+2m_{\pi^\pm}^4m_{\pi^0}^4-6m_{\pi^\pm}^2m_{\pi^0}^6+15m_{\pi^0}^8)\Big),
\end{aligned}
\tag{G.60}
$$

$$p_{2\oplus}^{t;0} = -2\frac{a_c a_x}{\Sigma}\Big(s - 2m_{\pi^0}^2 + \frac{\Delta^2}{s}\Big) + 2\Big(a_x\frac{b_c}{F_\pi^2} + a_c\frac{b_x}{F_\pi^2}\Big)\frac{m_{\pi^\pm}^2}{\Sigma}\Big(3s - 2(\Sigma + 2m_{\pi^0}^2) + 3\frac{\Delta^2}{s}\Big) - 20\frac{b_c b_x}{F_\pi^4}\frac{m_{\pi^\pm}^4}{\Sigma}\Big(s - (\Sigma + m_{\pi^0}^2) + \frac{\Delta^2}{s}\Big), \tag{G.61}$$

$$p_{3\uparrow}^{t;1} = \frac{b_t^2}{9sF_\pi^4}\lambda(s), \tag{G.62}$$

$$p_{7t}^{t;1} = -2\frac{a_t^2}{\Sigma}\Big(s - 2\Sigma - \frac{\Delta^2}{s}\Big) + 4a_t\frac{b_t}{F_\pi^2}\Big(3\Big(s - \frac{\Delta^2}{s}\Big) - \frac{8}{\Sigma}(\Delta^2 + 3m_{\pi^\pm}^2 m_{\pi^0}^2)\Big) - \frac{4b_t^2}{3F_\pi^4}\Big(3s^2 + \frac{s}{\Sigma}(5\Delta^2 + 12m_{\pi^\pm}^2 m_{\pi^0}^2) - 9(5\Delta^2 + 8m_{\pi^\pm}^2 m_{\pi^0}^2) - (13\Delta^2 + 36m_{\pi^\pm}^2 m_{\pi^0}^2)\frac{\Delta^2}{s\Sigma}\Big), \tag{G.63}$$

$$p_{8t}^{t;1} = 4\frac{b_t}{F_\pi^2}\frac{\Delta}{\Sigma}\Big(a_t\Big(s - 2\Sigma - \frac{\Delta^2}{s}\Big) - \frac{b_t}{3F_\pi^2}\Big(s^2 + 4s\Sigma - (17\Delta^2 + 48m_{\pi^\pm}^2 m_{\pi^0}^2) - 6\Sigma\frac{\Delta^2}{s}\Big)\Big), \tag{G.64}$$

$$p_{9t}^{t;1} = \frac{8}{3}\frac{b_t^2}{F_\pi^4}\frac{\Delta^2}{\Sigma}\Big(s - 2\Sigma - \frac{\Delta^2}{s}\Big). \tag{G.65}$$

G.2 The case of isospin symmetry conservation

If we take into account the isospin conservation, the partial waves have a simpler form (5.166)–(5.167) with the following polynomials. We give here the results for both choices of the restoring polynomial both the one (5.154) obtained by limiting the isospin violating results (denoted as w_l) and the one (5.165) which has the simplest possible form restoring the physical values for both a and b (denoted as w_s).

- $\pi^0\pi^0 \to \pi^0\pi^0$

$$p_\lambda^{0;0} = \frac{\hat\lambda_1 + 2\hat\lambda_2}{3F_\pi^4}(5s^2 - 16m_\pi^2 s + 32m_\pi^4) + 16m_\pi^4\frac{\hat\lambda_1}{F_\pi^4}, \tag{G.66}$$

$$p_{w_l}^{0;0} = \frac{1}{72m_\pi^4}\Big(11\mathrm{a}^2(5s^2 - 16m_\pi^2 s - 88m_\pi^4) - 64\mathrm{a}\frac{\mathrm{b}}{F_\pi^2}m_\pi^2(5s^2 - 16m_\pi^2 s - 70m_\pi^4) + 72\frac{\mathrm{b}^2}{F_\pi^4}m_\pi^4(5s^2 - 16m_\pi^2 s - 80m_\pi^4)\Big), \tag{G.67}$$

$$p_{w_s}^{0;0} = -\frac{1}{9}\left(327\mathrm{a}^2 - 1344\mathrm{a}\frac{\mathrm{b}}{F_\pi^2}m_\pi^2 + 1184\frac{\mathrm{b}^2}{F_\pi^4}m_\pi^4\right), \tag{G.68}$$

$$p_0^{0;0} = 44\mathrm{a}^2 - \mathrm{a}\frac{\mathrm{b}}{F_\pi^2}(s + 240m_\pi^2) + \frac{\mathrm{b}^2}{9F_\pi^4}(32s^2 - 73sm_\pi^2 + 3056m_\pi^4), \tag{G.69}$$

$$p_1^{0;0} = 11\mathrm{a}^2 - 2\mathrm{a}\frac{\mathrm{b}}{F_\pi^2}(s + 30m_\pi^2) + 2\frac{\mathrm{b}^2}{3F_\pi^4}(s^2 + 5sm_\pi^2 + 126m_\pi^4), \tag{G.70}$$

$$p_2^{0;0} = 11\mathrm{a}^2 - 60\mathrm{a}\frac{\mathrm{b}}{F_\pi^2}m_\pi^2 + 84\frac{\mathrm{b}^2}{F_\pi^4}m_\pi^4, \tag{G.71}$$

$$p_3^{0;0} = \frac{11}{2}\,\mathrm{a}^2 + 2\mathrm{a}\frac{\mathrm{b}}{F_\pi^2}(s - 16m_\pi^2) + \frac{\mathrm{b}^2}{F_\pi^4}(s^2 - 8sm_\pi^2 + 48m_\pi^4). \tag{G.72}$$

- $\pi^\pm\pi^\mp \to \pi^\pm\pi^\mp$

$$p_\lambda^{c;0} = 4\left(s^2 - 5sm_\pi^2 + 16m_\pi^4\right)\frac{\hat{\lambda}_1}{3F_\pi^4} + 2\left(s^2 - 4sm_\pi^2 + 8m_\pi^4\right)\frac{\hat{\lambda}_2}{F_\pi^4}, \tag{G.73}$$

$$p_{w_l}^{c;0} = \frac{1}{24m_\pi^4}\Bigg(\mathrm{a}^2(20s^2 - 93sm_\pi^2 - 164m_\pi^4) - 8\mathrm{a}\frac{\mathrm{b}}{3F_\pi^2}m_\pi^2(35s^2 - 127sm_\pi^2 - 340m_\pi^4) + 16\frac{\mathrm{b}^2}{9F_\pi^4}m_\pi^4(46s^2 - 95sm_\pi^2 - 788m_\pi^4)\Bigg), \tag{G.74}$$

$$p_{w_s}^{c;0} = \frac{1}{24m_\pi^2}\left(\mathrm{a}^2(23s - 612m_\pi^2) - 8\mathrm{a}\frac{\mathrm{b}}{F_\pi^2}m_\pi^2(19s - 324m_\pi^2) + 592\frac{\mathrm{b}^2}{3F_\pi^4}m_\pi^4(s - 12m_\pi^2)\right), \tag{G.75}$$

$$p_0^{c;0} = \frac{1}{4}\left(114\mathrm{a}^2 + \mathrm{a}\frac{\mathrm{b}}{F_\pi^2}(19s - 640m_\pi^2) + \frac{\mathrm{b}^2}{54F_\pi^4}(503s^2 - 4552sm_\pi^2 + 50624m_\pi^4)\right), \tag{G.76}$$

$$p_1^{c;0} = \frac{1}{2}\left(13\mathrm{a}^2 - \mathrm{a}\frac{\mathrm{b}}{F_\pi^2}(s + 70m_\pi^2) + \frac{\mathrm{b}^2}{18F_\pi^4}(13s^2 - 10sm_\pi^2 + 1776m_\pi^4)\right), \tag{G.77}$$

$$p_2^{c;0} = \frac{1}{2}\left(13\mathrm{a}^2 - 70\mathrm{a}\frac{\mathrm{b}}{F_\pi^2}m_\pi^2 - \frac{\mathrm{b}^2}{3F_\pi^4}m_\pi^2(3s - 296m_\pi^2)\right), \tag{G.78}$$

$$p_3^{c;0} = \frac{1}{2}\left(9\mathrm{a}^2 + 2\mathrm{a}\frac{\mathrm{b}}{F_\pi^2}(3s - 28m_\pi^2) + \frac{\mathrm{b}^2}{2F_\pi^4}(3s^2 - 40sm_\pi^2 + 176m_\pi^4)\right). \tag{G.79}$$

The polynomials appearing in the P wave:

$$p_\lambda^{c;1} = \frac{\hat{\lambda}_2(s - 4m_\pi^2) - \hat{\lambda}_1(s + 4m_\pi^2)}{6F_\pi^4}, \tag{G.80}$$

$$p_{w_l}^{c;1} = -\frac{1}{144m_\pi^4}\left(5\mathrm{a}^2(7s + 6m_\pi^2) - 100\mathrm{a}\frac{\mathrm{b}}{F_\pi^2}sm_\pi^2 + 8\frac{\mathrm{b}^2}{F_\pi^4}m_\pi^4(s - 24m_\pi^2)\right), \tag{G.81}$$

$$p_{w_s}^{c;1} = \frac{1}{72m_\pi^2}\left(23\mathrm{a}^2 - 152\mathrm{a}\frac{\mathrm{b}}{F_\pi^2}m_\pi^2 + 592\frac{\mathrm{b}^2}{3F_\pi^4}m_\pi^4\right), \tag{G.82}$$

$$p_0^{c;1} = \frac{1}{36}\Bigg(45\mathrm{a}^2(s-8m_\pi^2) + 5\mathrm{a}\frac{\mathrm{b}}{F_\pi^2}(11s^2-184sm_\pi^2+704m_\pi^4) - \frac{\mathrm{b}^2}{3F_\pi^4}(s^3+496s^2m_\pi^2-6926sm_\pi^4+21504m_\pi^6)\Bigg), \tag{G.83}$$

$$p_1^{c;1} = -\frac{1}{12}\Bigg(60\mathrm{a}^2 - 10\mathrm{a}\frac{\mathrm{b}}{F_\pi^2 m_p i^2}(s^2-10sm_\pi^2+48m_\pi^4) + \frac{\mathrm{b}^2}{3F_\pi^4 m_p i^2}(s^3+74s^2m_\pi^2-828sm_\pi^4+2664m_\pi^6)\Bigg), \tag{G.84}$$

$$p_2^{c;1} = \frac{1}{2m_p i^2}\left(5\mathrm{a}^2(s-2m_\pi^2) - 10\mathrm{a}\frac{\mathrm{b}}{F_\pi^2}m_\pi^2(3s-8m_\pi^2) - \frac{\mathrm{b}^2}{3F_\pi^4}m_\pi^2(3s^2-148sm_\pi^2+444m_\pi^4)\right), \tag{G.85}$$

$$p_3^{c;1} = \frac{\mathrm{b}^2}{36F_\pi^4}\left(s-4m_\pi^2\right). \tag{G.86}$$

- $\pi^\pm\pi^\pm \to \pi^\pm\pi^\pm$

$$p_\lambda^{d;0} = 2\left(s^2+4sm_\pi^2+16m_\pi^4\right)\frac{\hat{\lambda}_1}{3F_\pi^4} + 8\left(s^2-2sm_\pi^2+4m_\pi^4\right)\frac{\hat{\lambda}_2}{3F_\pi^4}, \tag{G.87}$$

$$p_{w_l}^{d;0} = -\frac{1}{36m_\pi^4}\Bigg(\mathrm{a}^2(5s^2-103sm_\pi^2+476m_\pi^4) + 8\mathrm{a}\frac{\mathrm{b}}{F_\pi^2}m_\pi^2(5s^2-sm_\pi^2-220m_\pi^4) - 8\frac{\mathrm{b}^2}{3F_\pi^4}m_\pi^4(43s^2-242sm_\pi^2-584m_\pi^4)\Bigg), \tag{G.88}$$

$$p_{w_s}^{d;0} = -\frac{1}{12m_\pi^2}\left(\mathrm{a}^2(23s+260m_\pi^2) - 8\mathrm{a}\frac{\mathrm{b}}{F_\pi^2}m_\pi^2(19s+124m_\pi^2) + 592\frac{\mathrm{b}^2}{3F_\pi^4}m_\pi^4(s+4m_\pi^2)\right), \tag{G.89}$$

$$p_0^{d;0} = \frac{1}{2}\left(62\mathrm{a}^2 - \mathrm{a}\frac{\mathrm{b}}{F_\pi^2}(23s+320m_\pi^2) + 5\frac{\mathrm{b}^2}{54F_\pi^4}(53s^2+560sm_\pi^2+4544m_\pi^4)\right), \tag{G.90}$$

$$p_1^{d;0} = 9\mathrm{a}^2 - \mathrm{a}\frac{\mathrm{b}}{F_\pi^2}(3s+50m_\pi^2) + \frac{\mathrm{b}^2}{18F_\pi^4}(11s^2+130sm_\pi^2+1248m_\pi^4), \tag{G.91}$$

$$p_2^{d;0} = 9\mathrm{a}^2 - 50\mathrm{a}\frac{\mathrm{b}}{F_\pi^2}m_\pi^2 + \frac{\mathrm{b}^2}{3F_\pi^4}(3s+208m_\pi^2), \tag{G.92}$$

$$p_3^{d;0} = \frac{1}{2}\left(2\mathrm{a} - \frac{\mathrm{b}}{F_\pi^2}(s+4m_\pi^2)\right)^2. \tag{G.93}$$

- $\pi^\pm\pi^\mp \to \pi^0\pi^0$

$$p_\lambda^{x;0} = -\frac{3\hat{\lambda}_1+2\hat{\lambda}_2}{3F_\pi^4}\left(s-4m_\pi^2\right)^2, \tag{G.94}$$

$$p_{w_l}^{x;0} = -\frac{1}{72m_\pi^4}\Bigg(\mathrm{a}^2(65s^2 - 382sm_\pi^2 - 16m_\pi^4) - 48\mathrm{a}\frac{\mathrm{b}}{F_\pi^2}m_\pi^2(5s^2 - 21sm_\pi^2 - 20m_\pi^4) + 8\frac{\mathrm{b}^2}{3F_\pi^4}m_\pi^4(49s^2 + 52sm_\pi^2 - 992m_\pi^4)\Bigg), \tag{G.95}$$

$$p_{w_s}^{x;0} = -\frac{1}{12m_\pi^2}\left(\mathrm{a}^2(23s - 176m_\pi^2) - 8\mathrm{a}\frac{\mathrm{b}}{F_\pi^2}m_\pi^2(19s - 100m_\pi^2) + 592\frac{\mathrm{b}^2}{3F_\pi^4}m_\pi^4(s - 4m_\pi^2)\right), \tag{G.96}$$

$$p_0^{x;0} = -\frac{1}{2}\left(26\mathrm{a}^2 + \mathrm{a}\frac{\mathrm{b}}{F_\pi^2}(21s - 160m_\pi^2) + \frac{\mathrm{b}^2}{54F_\pi^4}(119s^2 - 3676sm_\pi^2 + 13952m_\pi^4)\right), \tag{G.97}$$

$$p_1^{x;0} = -2\mathrm{a}^2 + \mathrm{a}\frac{\mathrm{b}}{F_\pi^2}(s - 10m_\pi^2) + \frac{\mathrm{b}^2}{18F_\pi^4}(s^2 - 70sm_\pi^2 + 264m_\pi^4), \tag{G.98}$$

$$p_2^{x;0} = -2\mathrm{a}^2 + 10\mathrm{a}\frac{\mathrm{b}}{F_\pi^2}m_\pi^2 + \frac{\mathrm{b}^2}{3F_\pi^4}(3s - 44m_\pi^2), \tag{G.99}$$

$$p_3^{x;0} = -\frac{1}{2}\left(7\mathrm{a}^2 + 8\mathrm{a}\frac{\mathrm{b}}{F_\pi^2}(s - 6m_\pi^2) + \frac{\mathrm{b}^2}{F_\pi^4}(s^2 - 24sm_\pi^2 + 80m_\pi^4)\right). \tag{G.100}$$

- $\pi^\pm\pi^0 \to \pi^\pm\pi^0$

$$p_\lambda^{t;0} = \left(s^2 + 4sm_\pi^2 + 16m_\pi^4\right)\frac{\hat{\lambda}_1}{3F_\pi^4} + 4\left(s^2 - 2sm_\pi^2 + 4m_\pi^4\right)\frac{\hat{\lambda}_2}{3F_\pi^4}, \tag{G.101}$$

$$p_{w_l}^{t;0} = -\frac{1}{72m_\pi^4}\Bigg(\mathrm{a}^2(5s^2 - 103sm_\pi^2 + 476m_\pi^4) + 8\mathrm{a}\frac{\mathrm{b}}{F_\pi^2}m_\pi^2(5s^2 - sm_\pi^2 - 220m_\pi^4) - 8\frac{\mathrm{b}^2}{3F_\pi^4}m_\pi^4(43s^2 - 242sm_\pi^2 - 584m_\pi^4)\Bigg), \tag{G.102}$$

$$p_{w_s}^{t;0} = -\frac{1}{24m_\pi^2}\left(\mathrm{a}^2(23s + 260m_\pi^2) - 8\mathrm{a}\frac{\mathrm{b}}{F_\pi^2}m_\pi^2(19s + 124m_\pi^2) + 592\frac{\mathrm{b}^2}{3F_\pi^4}m_\pi^4(s + 4m_\pi^2)\right), \tag{G.103}$$

$$p_0^{t;0} = \frac{1}{4}\left(62\mathrm{a}^2 - \mathrm{a}\frac{\mathrm{b}}{F_\pi^2}(23s + 320m_\pi^2) + \frac{5\mathrm{b}^2}{54F_\pi^4}(53s^2 + 560sm_\pi^2 + 4544m_\pi^4)\right), \tag{G.104}$$

$$p_1^{t;0} = \frac{1}{2}\left(9\mathrm{a}^2 - \mathrm{a}\frac{\mathrm{b}}{F_\pi^2}(3s + 50m_\pi^2) + \frac{\mathrm{b}^2}{18F_\pi^4}(11s^2 + 130sm_\pi^2 + 1248m_\pi^4)\right), \tag{G.105}$$

$$p_2^{t;0} = \frac{1}{6}\left(27\mathrm{a}^2 - 150\mathrm{a}\frac{\mathrm{b}}{F_\pi^2}m_\pi^2 + \frac{\mathrm{b}^2}{F_\pi^4}(3s + 208m_\pi^2)\right), \tag{G.106}$$

$$p_3^{t;0} = \left(\mathrm{a} - \frac{\mathrm{b}}{2F_\pi^2}(s + 4m_\pi^2)\right)^2. \tag{G.107}$$

The P wave polynomials are:

$$p_{\lambda}^{t;1} = \frac{\hat{\lambda}_2(s-4m_\pi^2) - \hat{\lambda}_1(s+4m_\pi^2)}{6F_\pi^4}, \tag{G.108}$$

$$p_{w_l}^{t;1} = -\frac{1}{144m_\pi^4}\left(5\mathrm{a}^2(7s+6m_\pi^2) - 100\mathrm{a}\frac{\mathrm{b}}{F_\pi^2}sm_\pi^2 + 8\frac{\mathrm{b}^2}{F_\pi^4}m_\pi^4(s-24m_\pi^2)\right), \tag{G.109}$$

$$p_{w_s}^{t;1} = \frac{1}{72m_\pi^2}\left(13\mathrm{a}^2 - 152\mathrm{a}\frac{\mathrm{b}}{F_\pi^2}m_\pi^2 + 592\frac{\mathrm{b}^2}{3F_\pi^4}m_\pi^4\right), \tag{G.110}$$

$$\begin{aligned} p_0^{t;1} = \frac{1}{36m_\pi^2}\Bigg(&45\mathrm{a}^2(s-8m_\pi^2) - 5\mathrm{a}\frac{\mathrm{b}}{F_\pi^2}(11s^2 - 184sm_\pi^2 + 704m_\pi^4) \\ &+ \frac{\mathrm{b}^2}{3F_\pi^4}(s^3 + 496s^2m_\pi^2 - 6926sm_\pi^4 + 21504m_\pi^6)\Bigg), \end{aligned} \tag{G.111}$$

$$\begin{aligned} p_1^{t;1} = -\frac{1}{6}\Bigg(&30\mathrm{a}^2 - 5\mathrm{a}\frac{\mathrm{b}}{F_\pi^2m_\pi^2}(s^2 - 10sm_\pi^2 + 48m_\pi^4) \\ &+ \frac{\mathrm{b}^2}{6F_\pi^4m_\pi^2}(s^3 + 74s^2m_\pi^2 - 828sm_\pi^4 + 2664m_\pi^6)\Bigg), \end{aligned} \tag{G.112}$$

$$p_2^{t;1} = \frac{1}{2}\left(5\mathrm{a}^2\left(\frac{s}{m_\pi^2} - 2\right) - 10\mathrm{a}\frac{\mathrm{b}}{F_\pi^2}(3s - 8m_\pi^2) - \frac{\mathrm{b}^2}{6F_\pi^4}(3s^2 - 148sm_\pi^2 + 444m_\pi^4)\right), \tag{G.113}$$

$$p_3^{t;1} = \frac{\mathrm{b}^2}{36F_\pi^4}\left(s - 4m_\pi^2\right). \tag{G.114}$$

Appendix H

Relation between Dalitz parameters of $\eta \to 3\pi$ valid in first order of isospin breaking

In this appendix we derive few relations between the Dalitz plot parameters of $\eta \to 3\pi^0$ and of $\eta \to \pi^+\pi^-\pi^0$ stemming from isospin symmetry. This appendix is inspired by [33].

In the first order isospin breaking, i.e. in the case that all the isospin breaking is included just in normalization of the amplitudes, we can expand the amplitude $\tilde{\mathcal{M}}_x^\eta$ within the decay region into polynomial

$$\tilde{\mathcal{M}}_x^\eta(x,y) = \tilde{\mathcal{M}}_x^\eta(0)\left(1 + \tilde{a}y + \tilde{b}y^2 + \tilde{c}x + \tilde{d}x^2 + \tilde{e}xy + \tilde{f}y^3 + \tilde{g}x^2y + \cdots\right), \tag{H.1}$$

with the parameters $\tilde{a}, \tilde{b}, \ldots$ that are in general complex. x and y are kinematic variables connected with the usual Mandelstam parameters by

$$x = \xi(s_2 - s_1), \qquad y = \sqrt{3}\,\xi(\tilde{s}^\eta - s_3) \tag{H.2}$$

with their normalization $\xi = \sqrt{3}/(2m_\eta Q_\eta)$. Since the variable x change under the charge conjugation its sign and the amplitude has to be symmetric with respect to it, it has to be symmetric also under the change of the sign of x. From that it follows that it has to be even in x, i.e. $\tilde{c} = \tilde{e} = 0$.

By squaring this parametrization and comparing with the standard Dalitz plot parametrization of the amplitude squared (6.37), we obtain the following relations between these two parametric sets

$$a = 2\,\mathrm{Re}\,\tilde{a}, \tag{H.3}$$
$$b = 2\,\mathrm{Re}\,\tilde{b} + |\tilde{a}|^2, \tag{H.4}$$
$$d = 2\,\mathrm{Re}\,\tilde{d}, \tag{H.5}$$
$$f = 2\,\mathrm{Re}\,\tilde{f} + 2\,\mathrm{Re}\,\tilde{a}^\star\tilde{b}, \tag{H.6}$$
$$g = 2\,\mathrm{Re}\,\tilde{g} + 2\,\mathrm{Re}\,\tilde{a}^\star\tilde{d}. \tag{H.7}$$

Similarly, we can expand also the amplitude $\tilde{\mathcal{M}}_n^\eta$ within the decay region into

$$\tilde{\mathcal{M}}_n^\eta(x,y) = \tilde{\mathcal{M}}_n^\eta(0)\left(1 + \tilde{\alpha}z + \tilde{\beta}y(3z - 4y^2) + \tilde{\gamma}z^2 + \cdots\right). \tag{H.8}$$

In the considered limit, the masses of m_{π^0} and $m_{\pi^\pm}$ are taken the same and the parameters appearing in this expansions are the same as in the charged case — the additional crossing symmetry even simplifies the form and there appear the following combination

$$z = x^2 + y^2. \tag{H.9}$$

Again by squaring this parametrization on comparison with (6.40) we obtain the relations

$$\alpha = \operatorname{Re}\tilde{\alpha}, \tag{H.10}$$

$$\beta = \operatorname{Re}\tilde{\beta}, \tag{H.11}$$

$$\gamma = 2\operatorname{Re}\tilde{\gamma} + |\tilde{\alpha}|^2. \tag{H.12}$$

Now, in the first order in isospin breaking there should hold the following relations (cf. 7.3)

$$\tilde{\mathcal{M}}_n^\eta(s_1,s_2,s_3) = -\tilde{\mathcal{M}}_x^\eta(s_1,s_2,s_3) - \tilde{\mathcal{M}}_x^\eta(s_2,s_1,s_3) - \tilde{\mathcal{M}}_x^\eta(s_3,s_2,s_1). \tag{H.13}$$

After introducing the linear parametrizations for both the amplitudes and using the fact that $s_1 + s_2 + s_3 = 3\tilde{s}^\eta$, we obtain relations between linear parameters of both processes

$$\tilde{\mathcal{M}}_n^\eta(0) = -3\tilde{\mathcal{M}}_x^\eta(0), \tag{H.14}$$

$$\tilde{\alpha} = \frac{1}{2}\left(\tilde{b} + \tilde{d}\right), \tag{H.15}$$

$$\tilde{\beta} = \frac{1}{4}\left(\tilde{g} - \tilde{f}\right) \tag{H.16}$$

and similar expression for $\tilde{\gamma}$ containing higher parameters of the charged decay, we did not explicate in the expansion (H.1).

Finally, the relations between the standard Dalitz plot parameters are

$$\alpha = \frac{1}{2}\left(\operatorname{Re}\tilde{b} + \operatorname{Re}\tilde{d}\right) = \frac{1}{4}\left(b + d - |\tilde{a}|^2\right) = \frac{1}{4}\left(b + d - \frac{a^2}{4} - (\operatorname{Im}\tilde{a})^2\right), \tag{H.17}$$

$$\begin{aligned}\beta &= \frac{1}{4}\left(\operatorname{Re}\tilde{g} - \operatorname{Re}\tilde{f}\right) = \frac{1}{4}\left(\frac{1}{2}(g-f) + \operatorname{Re}\tilde{a}^\star(\tilde{b} - \tilde{d})\right) \\ &= \frac{1}{8}(g-f) + \frac{a}{16}(b-d) - \frac{a^3}{64} + \frac{\operatorname{Im}\tilde{a}}{4}\left(\operatorname{Im}\tilde{b} - \operatorname{Im}\tilde{d} - \frac{a}{4}\operatorname{Im}\tilde{a}\right).\end{aligned} \tag{H.18}$$

Since $(\operatorname{Im}\tilde{a})^2$ is always greater than zero, the first relation translate into the famous inequality

$$\alpha \le \frac{1}{4}\left(b + d - \frac{a^2}{4}\right) \tag{H.19}$$

and the equality holds in the case $\operatorname{Im}\tilde{a} = 0$, in which case also the second relation translates into exact equality between the standard Dalitz plot parameters.

Appendix I

Isospin structure of $K \to 3\pi$ processes

Taking the isospin conservation into account, the amplitudes of $K \to 3\pi$ have to be tied together by some isospin relations. We show here their derivation. We can proceed in various ways, the one which is usually done in the literature (i.a. [53, 32]) makes use of the construction of three-pion states of a given isospin by Zemach [134]. Here on the contrary we instead show a different way — we use the crossing symmetry and derive the isospin relations for the $K\pi \to \pi\pi$ scattering processes, which is a simpler task.

These processes, which change the strangeness by 1 ($\Delta S = 1$), are in the standard model governed by the products of currents

$$\sum_{q=u,c,t} \bar{d}\gamma_\mu(1+\gamma_5)q\ \bar{q}\gamma^\mu(1+\gamma_5)s + \text{h.c.}, \tag{I.1}$$

the amplitudes of these processes can be therefore written as

$$\langle\pi\pi|\,\mathcal{O}_{\Delta I=1/2}\,|K\pi\rangle + \langle\pi\pi|\,\mathcal{O}_{\Delta I=3/2}\,|K\pi\rangle\,, \tag{I.2}$$

where $\mathcal{O}_{\Delta I=1/2}$ and $\mathcal{O}_{\Delta I=3/2}$ are some operators changing isospin by $\frac{1}{2}$ and $\frac{3}{2}$ respectively.

We remind the reader that the pions form an isospin triplet, whereas the kaons build two iso-dublets.

$$\begin{pmatrix} |+1\rangle \\ |0\rangle \\ |-1\rangle \end{pmatrix} = \begin{pmatrix} |\pi^+\rangle \\ |\pi^0\rangle \\ |\pi^-\rangle \end{pmatrix}, \quad \begin{pmatrix} |1/2\rangle \\ |-1/2\rangle \end{pmatrix} = \begin{pmatrix} |K^+\rangle \\ |K^0\rangle \end{pmatrix}, \quad \begin{pmatrix} |1/2\rangle \\ |-1/2\rangle \end{pmatrix} = \begin{pmatrix} |\overline{K^0}\rangle \\ |K^-\rangle \end{pmatrix}. \tag{I.3}$$

The charge conjugation connects

$$\mathcal{C}|\pi^\pm\rangle = -|\pi^\mp\rangle, \qquad \mathcal{C}|K^\pm\rangle = -|K^\mp\rangle, \tag{I.4}$$

$$\mathcal{C}|\pi^0\rangle = |\pi^0\rangle, \qquad \mathcal{C}|K^0\rangle = |\overline{K^0}\rangle. \tag{I.5}$$

We start with a construction of the states of given isospin formed out of two pions. We could study it by writing the most general tensor structures and use their symmetries for

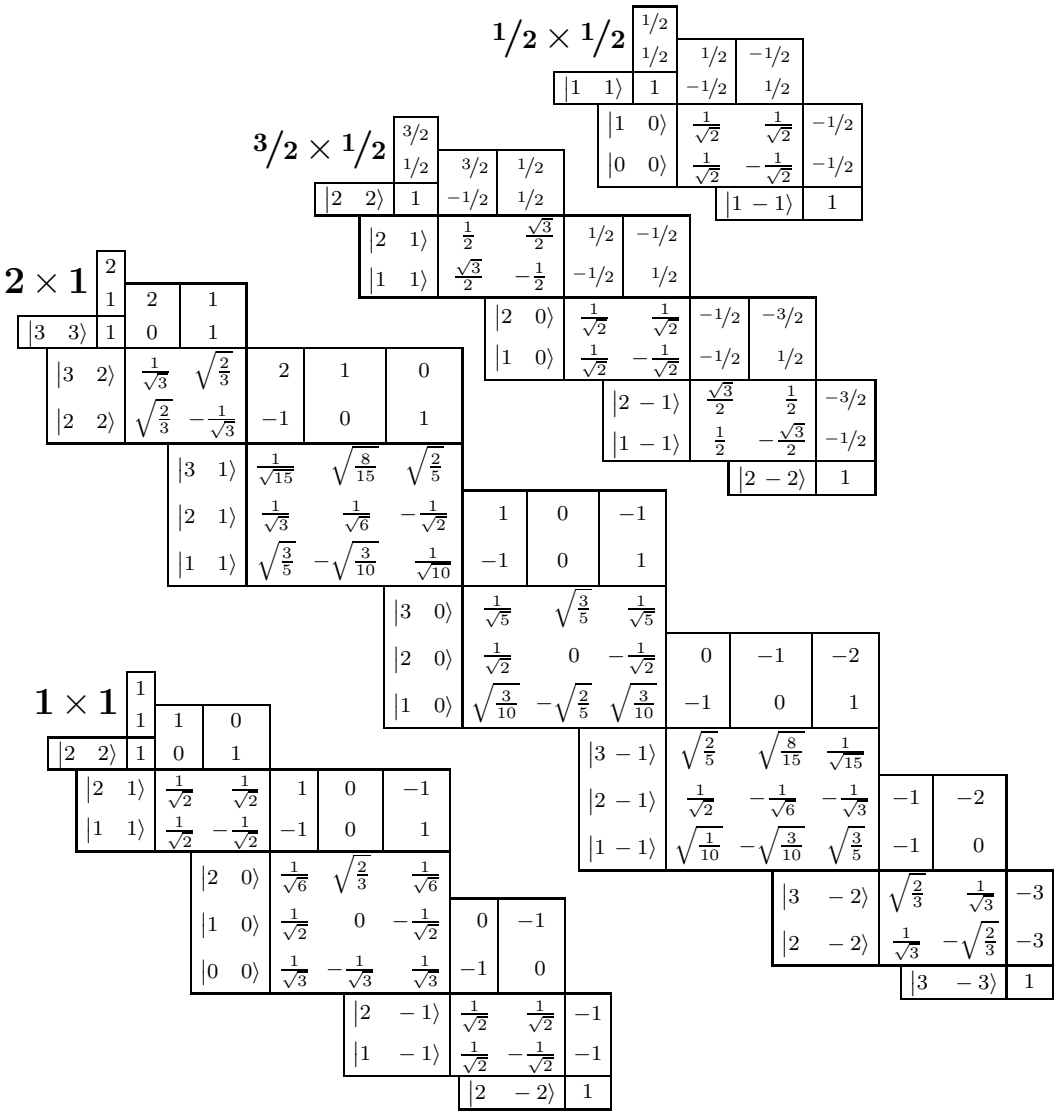

Table 18: Tables of Clebsch-Gordan coefficients.
The tables list the coefficients for an addition of spins $1/2 \times 1/2$, $3/2 \times 3/2$, 2×1 and 1×1, respectively. To a given resulting state $\big|J, m\big\rangle$ there corresponds a line, in which we read the coefficients of a linear combination of states with m_1 and m_2 indicated in the heading of the particular column.

obtaining the wanted relations as in [I] for the isospin $SU(3)$ χPT case (of section 4.2). However, here we follow the straight-forward way of using the Clebsch-Gordan coefficients of Table 18.

The states $\big|I, I_3\rangle$ with a given isospin I and its third component I_3 are composed according to

$$\big|2, \pm 2\rangle = \big|\pi^\pm \pi^\pm\rangle, \tag{I.6}$$

$$\big|2, \pm 1\rangle = \frac{1}{\sqrt{2}} \left(\big|\pi^\pm \pi^0\rangle + \big|\pi^0 \pi^\pm\rangle\right), \tag{I.7}$$

$$\big|2, 0\rangle = \frac{1}{\sqrt{6}} \left(\big|\pi^+ \pi^-\rangle + \big|\pi^- \pi^+\rangle\right) + \sqrt{\frac{2}{3}} \big|\pi^0 \pi^0\rangle, \tag{I.8}$$

$$\big|1, \pm 1\rangle = \pm \frac{1}{\sqrt{2}} \left(\big|\pi^\pm \pi^0\rangle - \big|\pi^0 \pi^\pm\rangle\right), \tag{I.9}$$

$$\big|1, 0\rangle = \frac{1}{\sqrt{2}} \left(\big|\pi^+ \pi^-\rangle - \big|\pi^- \pi^+\rangle\right), \tag{I.10}$$

$$\big|0, 0\rangle = \frac{1}{\sqrt{3}} \left(\big|\pi^+ \pi^-\rangle + \big|\pi^- \pi^+\rangle - \big|\pi^0 \pi^0\rangle\right). \tag{I.11}$$

Note that the third component of the pion states corresponds to their electric charge and that the even-spin states are symmetric with respect to exchange of the first and the second pions, while the odd-spin states are antisymmetric under such exchange. This will be important in the construction of the amplitudes. For the choice of signs of the Clebsch-Gordan coefficients we use the Condon-Shortley convention (the state with the highest possible third component of isospin of the first particle has always a positive coefficient). With that it is connected the sign difference between $\big|\pi^+ \pi^0\rangle$ and $\big|\pi^- \pi^0\rangle$ states.

An isospin analog of the Wigner-Eckart theorem then tells us that the amplitudes with the pions in the final state with isospin $\big|I, I_3\rangle$ can be obtained as products of form-factors dependent only on I and on the total isospin of the coupling of isospin state corresponding to $\frac{1}{2}$ or $\frac{3}{2}$ operator with the isospin state of initial state $\big|K\pi\rangle$ and the Clebsch-Gordan coefficients corresponding to such coupling by which the state $\big|I, I_3\rangle$ is obtained.

Since the reaction conserves the electric charge, we are interested only in such isospin compounds (of $\mathcal{O}_{\Delta I}$ and $\big|K\pi\rangle$) that have their total electric charge equal to the third component of the total isospin (as was the case for $\big|\pi\pi\rangle$). Moreover, because currents (I.1) are electric neutral, the total electric charge of such compound is equal to the sum of electric charges of the kaon and of the pion.

The various possible isospin states obtained by addition of the isospins of operator, kaon and pion are of the following types

(a) $(3/2 \otimes 1/2) \otimes 1 \supset 2 \otimes 1$,

(b) $(3/2 \otimes 1/2) \otimes 1 \supset 1 \otimes 1$,

(c) $(1/2 \otimes 1/2) \otimes 1 \supset 1 \otimes 1$,

(d) $(1/2 \otimes 1/2) \otimes 1 \supset 0 \otimes 1$.

We give them in Table 19. Note that in the case (a) there appear also states with the total isospin equal to 3, which do not contribute to the considered process (actually, generally from the operator $\Delta I = 3/2$ there contribute only the components with $\Delta I_3 = \pm 1/2$).

Putting all the information together, we get the following isospin structure of the individual $K\pi \to \pi\pi$ processes

$$\tilde{A}^{+}_{++} = \frac{1}{2}\left(-\bar{A} - \bar{B} + 2\bar{D}\right), \tag{I.12}$$

$$\tilde{A}^{-}_{--} = \frac{1}{2}\left(\bar{A}_C + \bar{B}_C + 2\bar{D}_C\right), \tag{I.13}$$

$$\tilde{A}^{+}_{+-} = \frac{1}{4}\left(\bar{A} + \frac{3}{\sqrt{5}}\bar{\alpha} - \frac{1}{3}\bar{B} - \bar{\beta} - \frac{2}{3}\bar{C} + \frac{2}{3}\bar{D} + 2\bar{\gamma} + \frac{4}{3}\bar{E}\right), \tag{I.14}$$

$$\tilde{A}^{-}_{-+} = \frac{1}{4}\left(-\bar{A}_C - \frac{3}{\sqrt{5}}\bar{\alpha}_C + \frac{1}{3}\bar{B}_C + \bar{\beta}_C + \frac{2}{3}\bar{C}_C + \frac{2}{3}\bar{D}_C + 2\bar{\gamma}_C + \frac{4}{3}\bar{E}_C\right), \tag{I.15}$$

$$\tilde{A}^{+}_{00} = \frac{1}{2}\left(\bar{A} - \frac{1}{3}\bar{B} + \frac{1}{3}\bar{C} + \frac{2}{3}\bar{D} - \frac{2}{3}\bar{E}\right), \tag{I.16}$$

$$\tilde{A}^{-}_{00} = \frac{1}{2}\left(-\bar{A}_C + \frac{1}{3}\bar{B}_C - \frac{1}{3}\bar{C}_C + \frac{2}{3}\bar{D}_C - \frac{2}{3}\bar{E}_C\right), \tag{I.17}$$

$$\tilde{A}^{+}_{+0} = \frac{1}{4}\left(\bar{A} - \frac{3}{\sqrt{5}}\bar{\alpha} - \bar{B} - \bar{\beta} + 2\bar{D} + 2\bar{\gamma}\right), \tag{I.18}$$

$$\tilde{A}^{-}_{-0} = \frac{1}{4}\left(-\bar{A}_C + \frac{3}{\sqrt{5}}\bar{\alpha}_C + \bar{B}_C + \bar{\beta}_C + 2\bar{D}_C + 2\bar{\gamma}_C\right), \tag{I.19}$$

$$\tilde{A}^{0}_{00} = \frac{1}{3\sqrt{2}}\left(2\bar{B} + \bar{C} + 2\bar{D} + \bar{E}\right), \tag{I.20}$$

$$\tilde{A}^{\bar{0}}_{00} = \frac{1}{3\sqrt{2}}\left(-2\bar{B}_C - \bar{C}_C + 2\bar{D}_C + \bar{E}_C\right), \tag{I.21}$$

$$\tilde{A}^{0}_{+-} = \frac{1}{3\sqrt{2}}\left(-\frac{3}{\sqrt{5}}\bar{\alpha} + \bar{B} - \bar{C} + \bar{D} - \bar{E} + \frac{3}{\sqrt{2}}\bar{\delta}\right), \tag{I.22}$$

$$\tilde{A}^{\bar{0}}_{-+} = \frac{1}{3\sqrt{2}}\left(\frac{3}{\sqrt{5}}\bar{\alpha}_C - \bar{B}_C + \bar{C}_C + \bar{D}_C - \bar{E}_C + \frac{3}{\sqrt{2}}\bar{\delta}_C\right), \tag{I.23}$$

$$\tilde{A}^{0}_{+0} = \frac{1}{2\sqrt{2}}\left(-\bar{A} + \frac{1}{\sqrt{5}}\bar{\alpha} + \bar{B} - \bar{\beta} + \bar{D} - \bar{\gamma} + \sqrt{2}\,\bar{\delta}\right), \tag{I.24}$$

$$\tilde{A}^{\bar{0}}_{-0} = \frac{1}{2\sqrt{2}}\left(\bar{A}_C - \frac{1}{\sqrt{5}}\bar{\alpha}_C - \bar{B}_C + \bar{\beta}_C + \bar{D}_C - \bar{\gamma}_C + \sqrt{2}\,\bar{\delta}_C\right), \tag{I.25}$$

$$\tilde{A}^{0}_{0-} = \frac{1}{2\sqrt{2}}\left(\bar{A} + \frac{1}{\sqrt{5}}\bar{\alpha} + \bar{B} + \bar{\beta} + \bar{D} + \bar{\gamma} + \sqrt{2}\,\bar{\delta}\right), \tag{I.26}$$

$$\tilde{A}^{\bar{0}}_{0+} = \frac{1}{2\sqrt{2}}\left(-\bar{A}_C - \frac{1}{\sqrt{5}}\bar{\alpha}_C - \bar{B}_C - \bar{\beta}_C + \bar{D}_C + \bar{\gamma}_C + \sqrt{2}\,\bar{\delta}_C\right), \tag{I.27}$$

Type	Formf.	I	$I_3 = Q$	$\lvert K^+\pi^+\rangle$	$\lvert K^+\pi^0\rangle$	$\lvert K^0\pi^+\rangle$	$\lvert K^+\pi^-\rangle$	$\lvert K^0\pi^0\rangle$	$\lvert K^0\pi^-\rangle$	$\lvert\overline{K^0}\pi^+\rangle$	$\lvert\overline{K^0}\pi^0\rangle$	$\lvert K^-\pi^+\rangle$	$\lvert\overline{K^0}\pi^-\rangle$	$\lvert K^-\pi^0\rangle$	$\lvert K^-\pi^-\rangle$
(a)	$\bar{A}$	2	2	$-\frac{1}{2}$											
(a)	$\bar{A}$	2	1		$\frac{1}{2\sqrt{2}}$	$-\frac{1}{2}$				$-\frac{1}{2}$					
(a)	$\bar{A}$	2	0				$\frac{\sqrt{3}}{2\sqrt{2}}$					$\frac{-\sqrt{3}}{2\sqrt{2}}$			
(a)	$\bar{A}$	2	-1						$\frac{1}{2}$				$\frac{1}{2}$	$\frac{-1}{2\sqrt{2}}$	
(a)	$\bar{A}$	2	-2												$\frac{1}{2}$
(a)	$\bar{\alpha}$	1	1		$\frac{-3}{2\sqrt{10}}$	$\frac{1}{2\sqrt{5}}$				$\frac{1}{2\sqrt{5}}$					
(a)	$\bar{\alpha}$	1	0				$\frac{3}{2\sqrt{10}}$	$\frac{-1}{\sqrt{5}}$			$\frac{-1}{\sqrt{5}}$	$\frac{3}{2\sqrt{10}}$			
(a)	$\bar{\alpha}$	1	-1						$\frac{1}{2\sqrt{5}}$				$\frac{1}{2\sqrt{5}}$	$\frac{-3}{2\sqrt{10}}$	
(b)	$\bar{B}$	2	2	$-\frac{1}{2}$											
(b)	$\bar{B}$	2	1		$\frac{-1}{2\sqrt{2}}$	$\frac{1}{2}$				$-\frac{1}{2}$					
(b)	$\bar{B}$	2	0				$\frac{-1}{2\sqrt{6}}$	$\frac{1}{\sqrt{3}}$			$\frac{-1}{\sqrt{3}}$	$\frac{1}{2\sqrt{6}}$			
(b)	$\bar{B}$	2	-1						$\frac{1}{2}$				$-\frac{1}{2}$	$\frac{1}{2\sqrt{2}}$	
(b)	$\bar{B}$	2	-2												$\frac{1}{2}$
(b)	$\bar{\beta}$	1	1		$\frac{-1}{2\sqrt{2}}$	$-\frac{1}{2}$				$\frac{1}{2}$					
(b)	$\bar{\beta}$	1	0				$\frac{-1}{2\sqrt{2}}$					$\frac{-1}{2\sqrt{2}}$			
(b)	$\bar{\beta}$	1	-1						$\frac{1}{2}$				$-\frac{1}{2}$	$\frac{-1}{2\sqrt{2}}$	
(b)	$\bar{C}$	0	0				$\frac{-1}{2\sqrt{3}}$	$\frac{-1}{\sqrt{6}}$			$\frac{1}{\sqrt{6}}$	$\frac{1}{2\sqrt{3}}$			
(c)	$\bar{D}$	2	2	1											
(c)	$\bar{D}$	2	1		$\frac{1}{\sqrt{2}}$	$\frac{1}{2}$				$\frac{1}{2}$					
(c)	$\bar{D}$	2	0				$\frac{1}{\sqrt{6}}$	$\frac{1}{\sqrt{3}}$			$\frac{1}{\sqrt{3}}$	$\frac{1}{\sqrt{6}}$			
(c)	$\bar{D}$	2	-1						$\frac{1}{2}$				$\frac{1}{2}$	$\frac{1}{\sqrt{2}}$	
(c)	$\bar{D}$	2	-2												1
(c)	$\bar{\gamma}$	1	1		$\frac{1}{\sqrt{2}}$	$-\frac{1}{2}$				$-\frac{1}{2}$					
(c)	$\bar{\gamma}$	1	0				$\frac{1}{\sqrt{2}}$					$\frac{-1}{\sqrt{2}}$			
(c)	$\bar{\gamma}$	1	-1						$\frac{1}{2}$				$\frac{1}{2}$	$\frac{-1}{\sqrt{2}}$	
(c)	$\bar{E}$	0	0				$\frac{1}{\sqrt{3}}$	$\frac{-1}{\sqrt{2}}$			$\frac{-1}{\sqrt{2}}$	$\frac{1}{\sqrt{3}}$			
(d)	$\bar{\delta}$	1	1			$\frac{1}{\sqrt{2}}$				$\frac{-1}{\sqrt{2}}$					
(d)	$\bar{\delta}$	1	0					$\frac{1}{\sqrt{2}}$			$\frac{-1}{\sqrt{2}}$				
(d)	$\bar{\delta}$	1	-1						$\frac{1}{\sqrt{2}}$				$-\frac{1}{\sqrt{2}}$		
Type	Formf.	I	$I_3 = Q$	$\lvert K^+\pi^+\rangle$	$\lvert K^+\pi^0\rangle$	$\lvert K^0\pi^+\rangle$	$\lvert K^+\pi^-\rangle$	$\lvert K^0\pi^0\rangle$	$\lvert K^0\pi^-\rangle$	$\lvert\overline{K^0}\pi^+\rangle$	$\lvert\overline{K^0}\pi^0\rangle$	$\lvert K^-\pi^+\rangle$	$\lvert\overline{K^0}\pi^-\rangle$	$\lvert K^-\pi^0\rangle$	$\lvert K^-\pi^-\rangle$

Table 19: Isospin states obtained by addition of isospin of an operator $\Delta I = 3/2$ or $\Delta I = 1/2$ with one kaon and one pion. The states with the total isospin equal to 3 are omitted and from the others we select only the contributions whose electric charge is equal to the third component of its total isospin. In the first column the type of the process from the list on page 261 is indicated, in the second we denote the formfactor with which the state appears in the amplitudes, the third and the fourth give the total isospin and its third component of the resulting state and in the subsequent columns we list coefficients of given $K\pi$ states — on the left-hand side there are kaon states from the iso-dublet K^+, K^0; whereas on the right-hand side there are listed the states containing $\overline{K^0}, K^-$.

where $A^c_{ab}(s,t,u)$ is amplitude of the process $K^c\pi^d \to \pi^a\pi^b$. The formfactors $\bar{A}(s,t,u)$, $\bar{B}(s,t,u)$, ..., $\bar{\alpha}(s,t,u)$, ... and $\bar{A}_C(s,t,u)$, $\bar{B}_C(s,t,u)$, ..., $\bar{\alpha}_C(s,t,u)$, ... correspond to the appropriate isospin states according to Table 19. Latin capitals are symmetric with respect to $t \leftrightarrow u$ interchange, whereas the Greek letters are antisymmetric (compare with the symmetries of the two-pion states). The ones with the lower index C, containing $\overline{K^0}$ or K^-, are in general different from the one without such index, which contain K^0 or K^+, however, since we do not violate the CP symmetry, the amplitudes of a process and its CP conjugated one have to be the same. [In this list we have ordered the amplitudes so that there is always an amplitude (without lower indices C) followed by its charged conjugated (with lower indices C).] This gives us eight equations for them and thanks to the given $t \leftrightarrow u$ symmetries of the formfactors, their only solution is

$$\begin{aligned} \bar{A}_C = -\bar{A}, \quad \bar{B}_C = -\bar{B}, \quad \bar{C}_C = -\bar{C}, \quad \bar{D}_C = \bar{D}, \quad \bar{E}_C = \bar{E}, \\ \bar{\alpha}_C = -\bar{\alpha}, \quad \bar{\beta}_C = -\bar{\beta}, \quad \bar{\gamma}_C = \bar{\gamma}, \quad \bar{\delta}_C = \bar{\delta}, \end{aligned} \tag{I.28}$$

i.e. the formfactors of the two kaon doublets connected with the operator $\Delta I = \frac{3}{2}$ differ by the sign, whereas the ones connected with $\Delta I = \frac{1}{2}$ are the same.

Now, we can already make a transition from the eigenstates of isospin K^0 and $\overline{K^0}$ to the eigenstates of the weak interactions (in our case also identical to the CP-even and the CP-odd states) using

$$|K^L\rangle = \frac{1}{\sqrt{2}}\left(|K^0\rangle + |\overline{K^0}\rangle\right), \qquad |K^S\rangle = \frac{1}{\sqrt{2}}\left(|K^0\rangle - |\overline{K^0}\rangle\right). \tag{I.29}$$

Now, using the following combinations of the formfactors

$$\bar{Z} = 2\bar{D} - \bar{B}, \qquad \bar{Y} = \bar{B} + \bar{D}, \tag{I.30}$$

$$\bar{X} = 2\bar{E} - \bar{C}, \qquad \bar{W} = \bar{C} + \bar{E}, \tag{I.31}$$

$$\bar{\omega} = 2\bar{\gamma} - \bar{\beta}, \qquad \bar{\psi} = \bar{\beta} + \bar{\gamma}, \tag{I.32}$$

$$\bar{\chi} = \frac{1}{\sqrt{5}}\,\bar{\alpha}, \qquad \bar{\phi} = \frac{1}{\sqrt{2}}\,\bar{\delta}, \tag{I.33}$$

we get the amplitudes in the form

$$\tilde{A}^+_{++} = \frac{1}{2}\left(-\bar{A} + \bar{Z}\right), \qquad \tilde{A}^+_{+-} = \frac{1}{4}\left(\bar{A} + \frac{1}{3}\bar{Z} + \frac{2}{3}\bar{X} + \bar{\omega} + 3\bar{\chi}\right), \tag{I.34}$$

$$\tilde{A}^+_{00} = \frac{1}{2}\left(\bar{A} + \frac{1}{3}\bar{Z} - \frac{1}{3}\bar{X}\right), \qquad \tilde{A}^+_{+0} = \frac{1}{4}\left(\bar{A} + \bar{Z} + \bar{\omega} - 3\bar{\chi}\right), \tag{I.35}$$

$$\tilde{A}^L_{00} = \frac{1}{3}\left(2\bar{Y} + \bar{W}\right), \qquad \tilde{A}^S_{00} = 0, \tag{I.36}$$

$$\tilde{A}^L_{+-} = \frac{1}{3}\left(\bar{Y} - \bar{W}\right), \qquad \tilde{A}^S_{+-} = -\bar{\chi} + \bar{\phi}, \tag{I.37}$$

$$\tilde{A}^L_{+0} = \frac{1}{2}\left(\bar{Y} - \bar{\psi}\right), \qquad \tilde{A}^S_{+0} = \frac{1}{2}\left(-\bar{A} + \bar{\chi} + 2\bar{\phi}\right), \tag{I.38}$$

$$\tilde{A}^L_{0-} = \frac{1}{2}\left(\bar{Y} + \bar{\psi}\right), \qquad \tilde{A}^S_{0-} = \frac{1}{2}\left(\bar{A} + \bar{\chi} + 2\bar{\phi}\right). \tag{I.39}$$

Note that the relations from the ultimate line are just CP conjugations to the ones from the penultimate line.

We have already used the isospin symmetry, the electric charge conservation and the CP invariance. The last symmetry that restricts the form of the amplitudes is the crossing symmetry. There are lucidly listed in Table 5 on page 108.

We begin with the processes containing K^L. Amplitude $\tilde{A}^L_{00}$ is symmetric with respect to all changes $s \leftrightarrow t \leftrightarrow u$, temporally we use it as a formfactor which we use for expressing formfactor $\bar{W}$ and rewriting

$$\tilde{A}^L_{+-}(s,t,u) = \bar{Y}(s,t,u) - \tilde{A}^L_{00}(s,t,u). \tag{I.40}$$

Since this amplitude is connected by crossing with $\tilde{A}^L_{+0}$, we obtain the relation

$$\bar{\psi}(s,t,u) = \bar{Y}(s,t,u) + 2\bar{Y}(u,t,s) - 2\tilde{A}^L_{00}(s,t,u). \tag{I.41}$$

However, $\bar{\psi}(s,t,u)$ is antisymmetric with respect to the exchange of t and u. This can happen only if

$$\tilde{A}^L_{00}(s,t,u) = \frac{1}{2}\left(\bar{Y}(s,t,u) + \bar{Y}(t,s,u) + \bar{Y}(u,t,s)\right). \tag{I.42}$$

For the sake of simplicity, it is worth to denote the amplitude $\tilde{A}^L_{+-}$ as $\mathcal{A}(s,t,u)$. Then the formfactor $\bar{Y}$ is expressed in its terms as

$$\bar{Y}(s,t,u) = -\left(\mathcal{A}(t,s,u) + \mathcal{A}(u,t,s)\right). \tag{I.43}$$

Now, let us step to K^S processes. We denote amplitude $\tilde{A}^S_{+-}$ as $\mathcal{B}(s,t,u)$. It is antisymmetric in $t \leftrightarrow u$ exchange. The crossing connection to $\tilde{A}^S_{+0}$ then lead to

$$\bar{\phi}(s,t,u) = \mathcal{B}(s,t,u) + \bar{\chi}(s,t,u), \tag{I.44}$$

$$\bar{\chi}(s,t,u) = \frac{1}{3}\left(\bar{A}(s,t,u) - 2\mathcal{B}(s,t,u) - 2\mathcal{B}(u,t,s)\right). \tag{I.45}$$

The symmetry of formfactor $\bar{\chi}(s,t,u)$ then dictates in turn

$$\bar{A}(s,t,u) = \mathcal{B}(u,t,s) - \mathcal{B}(t,s,u), \tag{I.46}$$

$$\bar{\chi}(s,t,u) = -\frac{1}{3}\left(2\mathcal{B}(s,t,u) + \mathcal{B}(t,s,u) + \mathcal{B}(u,t,s)\right), \tag{I.47}$$

$$\bar{\phi}(s,t,u) = \frac{1}{3}\left(\mathcal{B}(s,t,u) - \mathcal{B}(t,s,u) - \mathcal{B}(u,t,s)\right). \tag{I.48}$$

The isospin structure of K^+ is more complicated. We begin with $\tilde{A}^+_{00}$. Using the previous relations for $\bar{A}$ and $\bar{\chi}$, we see that $\mathcal{B}(s,t,u)$ factorizes out of the crossing relations between $\tilde{A}^+_{00}$ and $\tilde{A}^+_{+0}$ and there remains

$$\bar{\omega}(s,t,u) = \frac{1}{3}\left(3\bar{Z}(s,t,u) + 2\bar{Z}(u,t,s) - 2\bar{X}(u,t,s)\right). \tag{I.49}$$

The $t \leftrightarrow u$ antisymmetry of $\bar{\omega}$ then leads to the condition

$$\bar{X}(s,t,u) = \bar{Z}(s,t,u) + 3\bar{Z}(t,s,u) + \bar{Z}(u,t,s) - \bar{X}(u,t,s). \tag{I.50}$$

Similarly, the crossing between $\tilde{A}^+_{++}$ and $\tilde{A}^+_{+-}$ implies the constraint

$$\bar{X}(s,t,u) + 2\bar{Z}(s,t,u) = \bar{X}(u,t,s) + 2\bar{Z}(u,t,s). \tag{I.51}$$

These two relations together give

$$\bar{X}(s,t,u) = \frac{1}{2}\left(-\bar{Z}(s,t,u) + 3\bar{Z}(t,s,u) + 3\bar{Z}(u,t,s)\right). \tag{I.52}$$

Again for the sake of simplicity we take the following combination of the formactors as the basic one,

$$\mathcal{C}(s,t,u) = \frac{1}{2}\left(\bar{Z}(s,t,u) - \bar{Z}(t,s,u) - \bar{Z}(u,t,s)\right) \tag{I.53}$$

and express the formfactor $\bar{Z}$ it terms of it as

$$\bar{Z}(s,t,u) = -\left(\mathcal{C}(t,s,u) + \mathcal{C}(u,t,s)\right). \tag{I.54}$$

In summary, the amplitudes can be written in the form

$$\tilde{A}^+_{++} = -\frac{1}{2}\left(\mathcal{B}(u,t,s) - \mathcal{B}(t,s,u) + \mathcal{C}(t,s,u) + \mathcal{C}(u,t,s)\right), \tag{I.55}$$

$$\tilde{A}^+_{00} = \frac{1}{2}\left(\mathcal{B}(u,t,s) - \mathcal{B}(t,s,u) + \mathcal{C}(s,t,u)\right), \tag{I.56}$$

$$\tilde{A}^L_{00} = -\left(\mathcal{A}(s,t,u) + \mathcal{A}(t,s,u) + \mathcal{A}(u,t,s)\right), \tag{I.57}$$

$$\tilde{A}^S_{00} = 0, \tag{I.58}$$

$$\tilde{A}^L_{+-} = \mathcal{A}(s,t,u), \tag{I.59}$$

$$\tilde{A}^S_{+-} = \mathcal{B}(s,t,u), \tag{I.60}$$

where $\mathcal{A}(s,t,u)$ and $\mathcal{C}(s,t,u)$ are symmetric with respect to $t \leftrightarrow u$ interchange, whereas $\mathcal{B}(s,t,u)$ is antisymmetric.

From this reprezentation we infer the following relations between the amplitudes

$$\tilde{A}^+_{++}(s,t,u) = \tilde{A}^S_{+-}(t,s,u) - \tilde{A}^S_{+-}(u,t,s) - \tilde{A}^+_{00}(t,s,u) - \tilde{A}^+_{00}(u,t,s), \tag{I.61}$$

$$\tilde{A}^L_{00}(s,t,u) = -\left(\tilde{A}^L_{+-}(s,t,u) + \tilde{A}^L_{+-}(t,s,u) + \tilde{A}^L_{+-}(u,t,s)\right) \tag{I.62}$$

and therefore we conclude with the observation that in the isospin limit the only independent amplitudes are $\tilde{A}^L_{00}$, $\tilde{A}^+_{++}$ and $\tilde{A}^S_{+-}$. [Naturally, instead of $\tilde{A}^L_{00}$ we could have chosen $\tilde{A}^L_{++}$ as the amplitude independent on the others.]

For the book-keeping reasons, we list here also a connection of the formfactors from our results with the ones used in [32] (and in [53]). Its straightforward derivation is disturbed

by the fact that in [32] they use different sign conventions. We start therefore with a dictionary between the amplitudes in our convention and in their one (the right-most amplitudes in the following relations are those from [32])

$$\tilde{\mathcal{M}}^L_0(s_1,s_2,s_3) = \quad \tilde{A}^L_{00}(s_3,s_1,s_2) = \quad A^L_{000}(s_1,s_2,s_3), \tag{I.63}$$
$$\tilde{\mathcal{M}}^L_x(s_1,s_2,s_3) = \quad \tilde{A}^L_{+-}(s_3,s_1,s_2) = -A^L_{+-0}(s_1,s_2,s_3), \tag{I.64}$$
$$\tilde{\mathcal{M}}^S_x(s_1,s_2,s_3) = \quad \tilde{A}^S_{+-}(s_3,s_1,s_2) = -A^S_{+-0}(s_1,s_2,s_3), \tag{I.65}$$
$$\tilde{\mathcal{M}}^+_x(s_1,s_2,s_3) = -\tilde{A}^+_{00}(s_3,s_1,s_2) = -A_{00+}(s_1,s_2,s_3), \tag{I.66}$$
$$\tilde{\mathcal{M}}^+_c(s_1,s_2,s_3) = -\tilde{A}^+_{++}(s_3,s_1,s_2) = \quad A_{++-}(s_1,s_2,s_3). \tag{I.67}$$

The formfactors appearing in (24) of [32] are then

$$A_n(s_1,s_2,s_3) = -\frac{1}{3}\left(\mathcal{A}(s_1,s_2,s_3)+\mathcal{A}(s_2,s_3,s_1)+\mathcal{A}(s_3,s_1,s_2)\right), \tag{I.68}$$
$$B_n(s_1,s_2,s_3) = -\frac{1}{3}\left(\mathcal{A}(s_1,s_2,s_3)+\mathcal{A}(s_2,s_3,s_1)-2\mathcal{A}(s_3,s_1,s_2)\right), \tag{I.69}$$
$$A_c(s_1,s_2,s_3) = \frac{1}{6}\left(\mathcal{C}(s_1,s_2,s_3)+\mathcal{C}(s_2,s_3,s_1)+\mathcal{C}(s_3,s_1,s_2)\right), \tag{I.70}$$
$$B_c(s_1,s_2,s_3) = \frac{1}{6}\left(\mathcal{C}(s_1,s_2,s_3)+\mathcal{C}(s_2,s_3,s_1)-2\mathcal{C}(s_3,s_1,s_2)\right), \tag{I.71}$$
$$B_t(s_1,s_2,s_3) = \frac{1}{2}\left(\mathcal{B}(s_1,s_2,s_3)-\mathcal{B}(s_2,s_3,s_1)\right), \tag{I.72}$$
$$C_0(s_1,s_2,s_3) = -\frac{1}{3}\left(\mathcal{B}(s_1,s_2,s_3)+\mathcal{B}(s_2,s_3,s_1)+\mathcal{B}(s_3,s_1,s_2)\right). \tag{I.73}$$

These formfactors are connected to the three-pion states with a given isotopic spin [134], C_0 is associated to the $I=0$ three-pion state, B_t to the $I=2$ one and finally $A_{c,n}$ and $B_{c,n}$ correspond to the $I=1$ final state. It is obvious that they posses the properties discussed in [32].

Appendix J

Analytic properties of $P\pi \to \pi\pi$ amplitudes

Similarly as in Appendix C, we shall discuss here analytic properties of another sort of amplitudes for which we want to use the reconstruction theorem. As was pointed out in that appendix, the methods of S-matrix theory summarized there are not applicable for the processes where K or η can decay into three pions. However, in order to enable the use of the dispersion relations and of the further assumptions that lead to the reconstruction theorem, we do not need to know the complete analytic properties of the complete amplitudes that are considered, but it is enough to verify that the analytic structure of the perturbative amplitudes to the considered order within the considered regions is suitable. Since we deal with the amplitudes only in the kinematic regions, where the usual Feynman diagram methods are applicable, we can proceed in the following way. We determine the analytic structures of all diagrams that would contribute to the perturbative amplitude of the given order and from them we conclude the analytic structure of this amplitude as it cannot be worse than the structure of the individual diagrams. Note also that the presented analysis is independent on the particular form of the Lagrangians that would be used for such a computation as we use only methods dealing with the denominators of the Feynman integrals and they are determined just by the propagator structure. Nevertheless, since we use the chiral expansion for classification of the diagrams, the natural framework within which these diagrams exist is chiral perturbation theory.

J.1 Feynman diagrams contributing to $P\pi \to \pi\pi$ process up to two loops

In correspondence with the beginning of Chapter 3 we assume that the only diagrams that are contributing to our amplitudes are those containing vertices with even number of particles. On Figure 30 we have displayed all different topologies of such diagrams contributing to two-loop-level $P\pi \to \pi\pi$ amplitude. Naturally, at tree level there contributes only the diagram denoted by (a). At one-loop level, in addition to the counter-term diagrams of topology (a), there contribute diagrams of type (b), having, however, the same

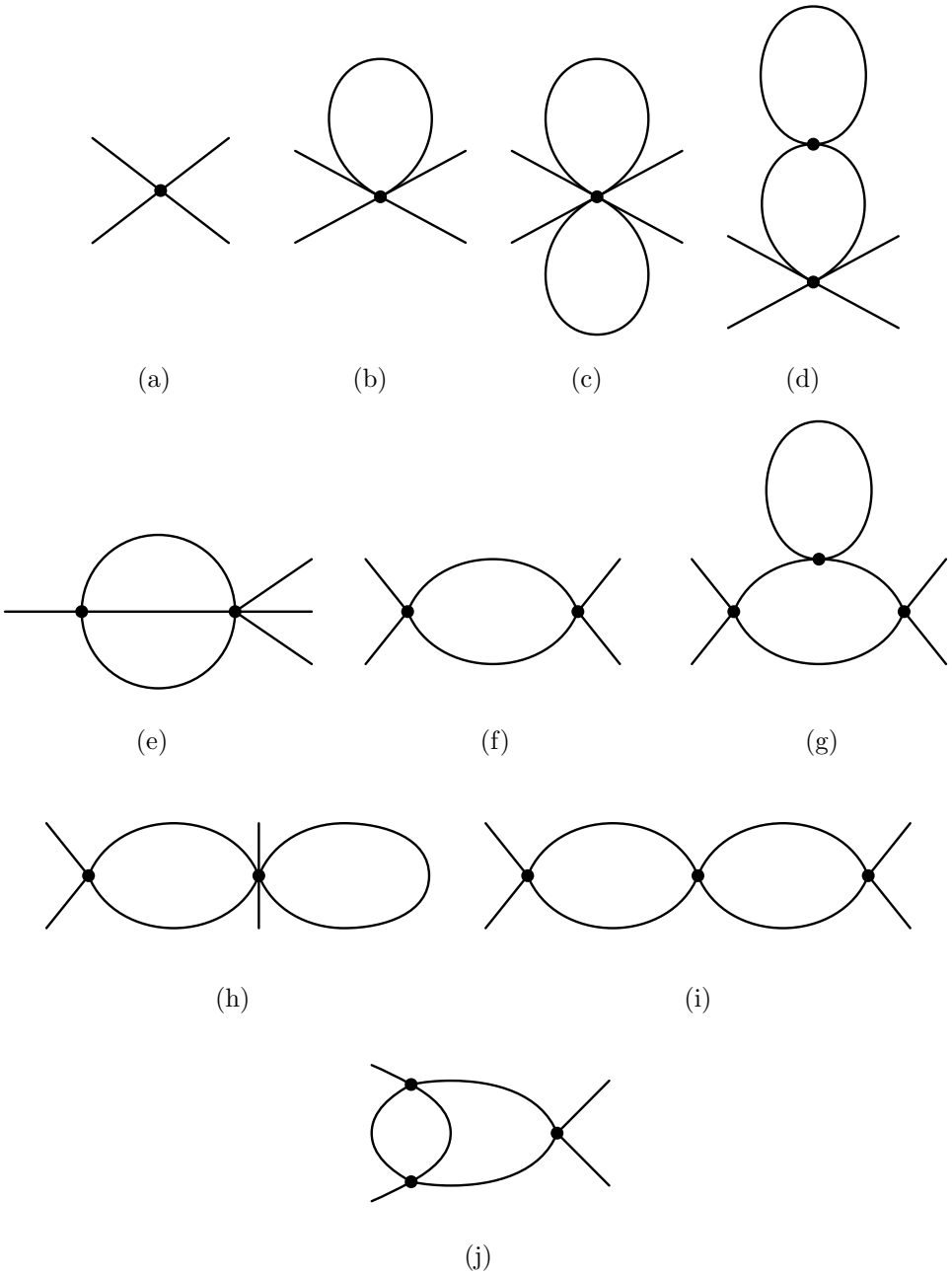

Figure 30: Various topologies of Feynman diagrams contributing to $P \to 3\pi$ processes.

trivial analytic structure, and the bubble diagrams (f). At the two-loop order all diagrams of Figure 30 contribute. Their analytic structures are as follows: diagrams (a)–(e) have the trivial analytic structure of the contact interaction, diagrams (f)-(h) have the structure of the bubble diagram (discussed in Appendix J.3), diagram (i) of the double-bubble diagram and finally diagram (j), which we call fish-diagram, has the most complex analytic structure which is studied in Appendix J.4. Before we start with these discussions for the particular topologies just summarized, let us comment on the sunset-diagram (e). At first sight it could seem that such diagram does contribute to the unitarity cut of the $P\pi \to \pi\pi$ amplitude but it is important to note that in the decay region its contribution is analytic and can be thus expanded into a polynomial. However, this polynomial can be complex for m_P unstable.

J.2 Singularities of Feynman integrals. Landau equations.

We begin with recalling some basic facts about the appearance of singularities for the Feynman integrals. We summarize here only the results important for our applications and refer the interested reader to [65] for more details. These topics are to a certain level also discussed in some general textbooks on quantum field theory such as [84].

If we have a function defined by its integral representation, all its singularities are connected with the singularities of the integrand in this representation. Starting at some point, where this function is analytic (i.e. at some point where the integration contour does not meet the singularities of the integrand), we can move in its variables and the function remains analytic until some of the singularities of the integrand reaches the integration contour. Even then, one can usually continue the function analytically further by deforming the integration contour in such a way that it avoids the singularities (this possibility is a consequence of the Cauchy's theorem). Therefore, the function constructed this way is analytic for all values of its variables for which such deformation can be done. The singularities of the function can then occur only due to one of the following three possible reasons: (i) end-point singularity — if one of the singularities dragging the integration contour reaches an end-point of integrations, which prevents us from a further deformation of the contour that would avoid the singularities; (ii) pinch singularity — if two singularities approach the contour from the opposite sides and then coincide, the contour is trapped between them and has no other possibility than passing through one of the singularities; (iii) infinite deformations — if one singularity dragging the integration contour goes to infinity and such loss of finiteness of the contour can cause the appearance of a singularity.

Any contribution to an amplitude corresponding to some Feynman diagram is represented by the appropriate Feynman integral

$$\int \frac{\mathrm{d}^4 q_1 \dots \mathrm{d}^4 q_L}{(2\pi)^{4l}} \frac{1}{(k_1^2 - m_1^2 + i\varepsilon) \dots (k_N^2 - m_N^2 + i\varepsilon)}, \tag{J.1}$$

where we have leaved out all multiplicative factors in numerator since we assume that the singularities of the integrand are connected just with the propagators (denominators). k_i

and m_i are momenta and masses connected with the i-th internal line and q_j are loop momenta. As each of the integrations is infinite, the contour has no boundaries and there cannot happen the possibility (i). Ignoring for the moment also the possibility (iii), the singularities of the amplitude can occur only if the following equations (Landau equations) are fulfilled,

$$\hat{\alpha}_i(k_i^2 - m_i^2) = 0 \qquad \text{for all internal lines } i, \tag{J.2}$$

$$\sum_i \hat{\alpha}_i k_i \cdot \frac{\partial k_i}{\partial q_l} = 0 \qquad \text{for all loops } l. \tag{J.3}$$

In the case all the numbers $\hat{\alpha}_i$ are non-zero, such singularity is called leading singularity. Having some of the $\hat{\alpha}_i = 0$ is equivalent to a study of singularities of the diagram, which is obtained from the original one by contracting the corresponding ith line to a point.

Similarly, by using Feynman identity we can rewrite the (UV-finite) amplitude into the parametric representation

$$\int_0^1 \mathrm{d}\alpha_1 \dots \mathrm{d}\alpha_N \, \frac{\delta\left(\sum_i \alpha_i - 1\right) C(\alpha)^{N-2L-2}}{D(\alpha)^{N-2L}}, \tag{J.4}$$

where N is the number of internal lines and L the number of loops. Functions $C(\alpha)$ and $D(\alpha)$ can be obtained by the explicit integration using the Feynman trick or by the following set of rules. We perform a set of cuts in internal lines of the diagram such that the diagram (containing all the original vertices) remains connected and any further contraction would disconnect it — we call such diagram as minimal connected diagram. $C(\alpha)$ then involves the sum of products of the α_i's corresponding to the cut lines.

The denominator reads

$$D(\alpha) = Q(\alpha) - C(\alpha) \sum_i \alpha_i m_i^2, \tag{J.5}$$

where $Q(\alpha)$ can be reproduced again by cutting the internal lines — this time in such a way that we obtain two disjoint parts, which are both minimal connected and each of them is connected to at least one of the external lines. Any such set of cuts yields again a product of α_is, which is in addition multiplied by $(\sum P_j)^2$ of all external momenta P_j connected to one of those disjoint parts of the diagram. $Q(\alpha)$ is the sum of such terms corresponding to all distinct sets of such cuts.

Landau equations for the parametric representation read (note that the boundaries of integration correspond to $\alpha_i = 0$)

$$\alpha_i \frac{\partial D}{\partial \alpha_i} = 0 \qquad \text{for each internal line } i, \tag{J.6}$$

$$D = 0. \tag{J.7}$$

Since D is a homogeneous function of α_i's $\left(D \propto \sum \alpha_i \frac{\partial D}{\partial \alpha_i}\right)$, the last constraint is automatically fulfilled when the others are. From the same reason we can ignore the δ-function

in (J.4). Note that there exist also a third representation of the Feynman diagrams (so-called mixed one) with the corresponding set of Landau equations. All of the three sets of equations are equivalent.

A singularity can occur also because of the pinching in infinity [point (iii) from above]. Such singularities would be independent on the internal masses and do not directly follow from Landau equations. There have been therefore called by Cutkosky [52], who first noticed their existence, as non-Landau singularities. Nowadays there is used the more suitable name for them, the second-type singularities. They are connected with the degeneracy of the vector space spanned by the external momenta.

Final note is that the analysis described above leads only to the necessary conditions for the occurrence of the singularities. Thus, the amplitude on the physical sheet does not need to be singular in all of them (it can be singular there just for some other Riemann sheets or it can even happen that it is not singular there on any sheet). In our analysis we are interested in the question whether the amplitude is on the physical sheet singular also in some other points than those coming from unitarity (called normal thresholds) since then the methods of reconstruction theorem could not be used without modifications.

J.3 Bubble diagram singularities

We return back to Figure 30 and discuss the analytic properties of the individual diagrams. The simplest diagram bringing singularities to the amplitude is the bubble diagram from Figure 30f. Denoting the external and the loop momenta by P and q respectively and the masses corresponding to the internal lines by m_1 and m_2, the Landau equations read

$$\hat{\alpha}_1(k_1^2 - m_1^2) = \hat{\alpha}_1(q^2 - m_1^2) = 0, \tag{J.8}$$

$$\hat{\alpha}_2(k_2^2 - m_2^2) = \hat{\alpha}_2((P-q)^2 - m_2^2) = 0, \tag{J.9}$$

$$\hat{\alpha}_1 q + \hat{\alpha}_2(q - P) = 0. \tag{J.10}$$

Their only non-trivial solutions are

$$\hat{\alpha}_1 = \pm\hat{\alpha}_2\frac{m_2}{m_1}, \qquad P^2 = (m_1 \pm m_2)^2. \tag{J.11}$$

After subtracting the ultraviolet divergence of this diagram, we can also work in the parametric space, where the denominator reads

$$D = \alpha_1\alpha_2 P^2 - (\alpha_1 + \alpha_2)(\alpha_1 m_1^2 + \alpha_2 m_2^2). \tag{J.12}$$

The solutions of the corresponding Landau equations are naturally the same — given by (J.11), where we drop the hats above α's.

Note that the suspected points can be identified also by the following heuristic analysis. We search for the situations when the hyperboloids $k_i^2 - m_i^2 = 0$ are tangent. In Euclidean space they correspond to spheres with radii m_1 and m_2 and their centers at 0 and at P respectively. They are tangent only in the case $|P| = m_1 \pm m_2$, which remains valid also

in the Minkowski case. In addition, in the case these hyperboloids (spheres) differ by zero-vector (are concentric), they can be tangent also in infinity. This situation corresponds to the non-Landau singularity $P^2 = 0$. Therefore, we end up with the normal threshold $P^2 = (m_1 + m_2)^2$ and two anomalous thresholds $P^2 = (m_1 - m_2)^2$ and $P^2 = 0$.

We are now interested in the question, in which of these points the amplitude is singular on the physical sheet. The original integration contour in the parametric space is for all $\alpha_i > 0$. We see that for such α's the denominator (J.12) never vanishes for $P^2 < (m_1+m_2)^2$. We therefore do not need to deform the integration contour on this interval and the amplitude has no singularity on the physical sheet. At $P^2 = (m_1+m_2)^2$ a deformation of the integration contour is necessary but because of the pinch, such deformation does not exist and we get the singularity. The analytic continuation above this point then depends on the path. The Feynman prescription chooses the appropriate physical sheet by an addition of a small imaginary part to all internal masses $m_i^2 \to m_i^2 - i\epsilon$, it means that the physical continuation corresponds to $P^2 + i\epsilon$ (for such choice D does not vanish even with Feynman imaginary parts).

In conclusion, the physical amplitude possesses only the normal threshold singularity and one can employ the regular unitarity and dispersion relations.

It is obvious that the double-bubble diagram have independent singularities of the individual bubbles constituting it, i.e. again the reconstruction method can be used also for this diagram.

J.4 Singularities of fish diagrams

The situation is more complicated for the fish diagram (Figure 30j). For the momenta and masses denoted according to Figure 31, the Landau equations read

$$\hat{\alpha}_1 \left(q_1^2 - m_1^2\right) = 0, \tag{J.13}$$
$$\hat{\alpha}_2 \left((q_1 - P_3)^2 - m_2^2\right) = 0, \tag{J.14}$$
$$\hat{\alpha}_3 \left((q_1 - P_2 - q_2)^2 - \hat{m}_3^2\right) = 0, \tag{J.15}$$
$$\hat{\alpha}_4 \left(q_2^2 - \hat{m}_4^2\right) = 0, \tag{J.16}$$
$$\hat{\alpha}_1 q_1 + \hat{\alpha}_2(q_1 - P_3) + \hat{\alpha}_3(q_1 - P_2 - q_2) = 0, \tag{J.17}$$
$$\hat{\alpha}_3(q_1 - P_2 - q_2) - \hat{\alpha}_4 q_2 = 0. \tag{J.18}$$

Note that to the triangle diagram on the right-hand side of Figure 31, there belong the following Landau equations

$$\alpha_1 \left(q_1^2 - m_1^2\right) = 0, \tag{J.19}$$
$$\alpha_2 \left((q_1 - P_3)^2 - m_2^2\right) = 0, \tag{J.20}$$
$$\alpha_3 \left((q_1 - P_2)^2 - \mu^2\right) = 0, \tag{J.21}$$
$$\alpha_1 q_1 + \alpha_2(q_1 - P_3) + \alpha_3(q_1 - P_2) = 0. \tag{J.22}$$

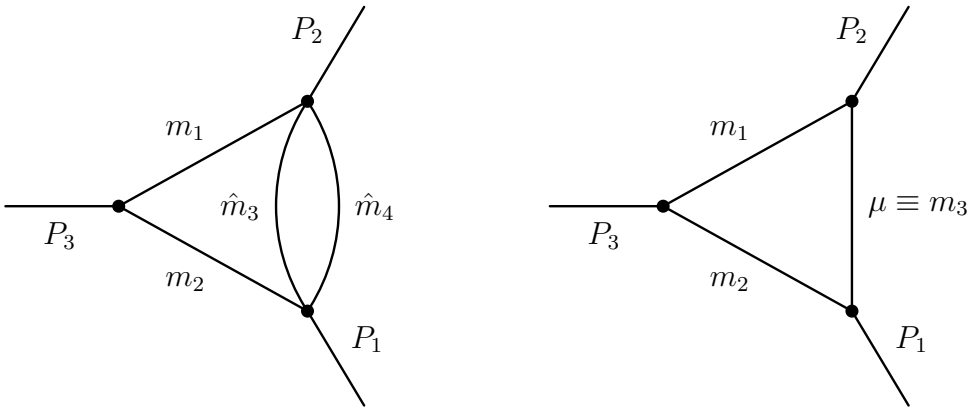

Figure 31: The fish diagram together with the corresponding triangle diagram

By comparison of these two sets, we observe that if some $\hat{\alpha}_i$ and P_i are solution of the first set of equations, the values of parameters

$$\alpha_1 = \hat{\alpha}_1, \quad \alpha_2 = \hat{\alpha}_2, \quad \alpha_3 = \frac{\hat{\alpha}_3\hat{\alpha}_4}{\hat{\alpha}_3 + \hat{\alpha}_4}, \tag{J.23}$$

with the same P_i solve the second set of equations with $\mu^2 = \hat{m}_3^2 + \hat{m}_4^2 + 2\frac{\hat{\alpha}_4}{\hat{\alpha}_3}\hat{m}_4^2$. This correspondence could be used for the study of the fish diagram singularities using the simpler triangle diagram.

However, the connection between the fish and the triangle diagrams goes even further. We can write [18, 40, 76] the additional loop in the fish diagram in the dispersive form, and the integral can be obtained from

$$\int\limits_{(\hat{m}_3+\hat{m}_4)^2}^{\infty} \sigma(\mu^2)\mathrm{d}\mu^2 \int \frac{\mathrm{d}^4 q_1}{(2\pi)^4} \frac{1}{(k_1^2 - m_1^2)(k_2^2 - m_2^2)(k_3^2 - \mu^2)}\,, \tag{J.24}$$

where we have again left out multiplicative factors from the nominator. The important observation is therefore that the analytic structure of the fish diagram can be obtained from the studies of the analytic structure of the simpler triangle diagram with variable μ within the interval $((\hat{m}_3 + \hat{m}_4)^2, \infty)$ as the additional integration can bring only the endpoint singularity at $\mu = (\hat{m}_3 + \hat{m}_4)^2$.

J.4.1 Singularities of triangle diagrams

The Landau equations for the triangle diagram are listed in (J.19)–(J.22). The denominator of the parametric representation can be written in the form

$$D = -\alpha_i z_{ij} \alpha_j + i\epsilon, \tag{J.25}$$

where we have added the Feynman $i\epsilon$ prescription and the symmetric matrix z_{ij} reads (in the following we interchange freely between μ and m_3 in order to simplify the notation)

$$\begin{pmatrix} m_1^2 & \frac{m_1^2+m_2^2-P_3^2}{2} & \frac{m_1^2+m_3^2-P_2^2}{2} \\ \frac{m_1^2+m_2^2-P_3^2}{2} & m_2^2 & \frac{m_2^2+m_3^2-P_1^2}{2} \\ \frac{m_1^2+m_3^2-P_2^2}{2} & \frac{m_2^2+m_3^2-P_1^2}{2} & m_3^2 \end{pmatrix}. \tag{J.26}$$

We can even simplify the following analysis by rescaling the parameters α according to

$$\beta_i = m_i \alpha_i. \tag{J.27}$$

The denominator then becomes (we have dropped the overall minus sign)

$$D = \beta_i y_{ij} \beta_j - i\epsilon, \tag{J.28}$$

where the matrix Y has ones on its diagonal and its off-diagonal elements are given by

$$y_{ij} = \frac{m_i^2 + m_j^2 - P_k^2}{2 m_i m_j}, \tag{J.29}$$

where $k \neq i, j$, i.e. in each y_{ij} there appear just the quantities that meet in one of the vertices of the diagram.

The leading singularities (i.e. all $\alpha_i \neq 0$) lie on the curve

$$\det Y = 1 + 2y_{12}y_{23}y_{31} - y_{12}^2 - y_{23}^2 - y_{31}^2 = 0. \tag{J.30}$$

The subleading singularities correspond to $y_{ij} = \pm 1$, i.e. they are normal and anomalous thresholds. The second-type singularity curve is

$$\lambda(P_1^2, P_2^2, P_3^2) = 0 \tag{J.31}$$

with the triangle function from (2.10).

As was already stated in the general discussion of Section J.2, not all the singularities do occur on the physical sheet. For the more detailed analysis it is useful to identify the domains where D never vanishes in the undistorted region of parametric integration. Since the rescaling (J.27) does not change the sign of the parameters, we can work also with the simplified expressions with β's. Such domains are

(a) imaginary part of two of y_i is less than zero (adding an imaginary part to one of them can be insufficient as one of the β's multiplying it can be zero);

(b) all $y_i \geq 0$; this means (for all $m_i > 0$) that all $P_k^2 \leq m_i^2 + m_j^2$;

(c) for any permutation of $1, 2, 3$ equaling to i, j, k, $y_i \geq 1$, $y_j \geq 0$, $y_k > -1$.

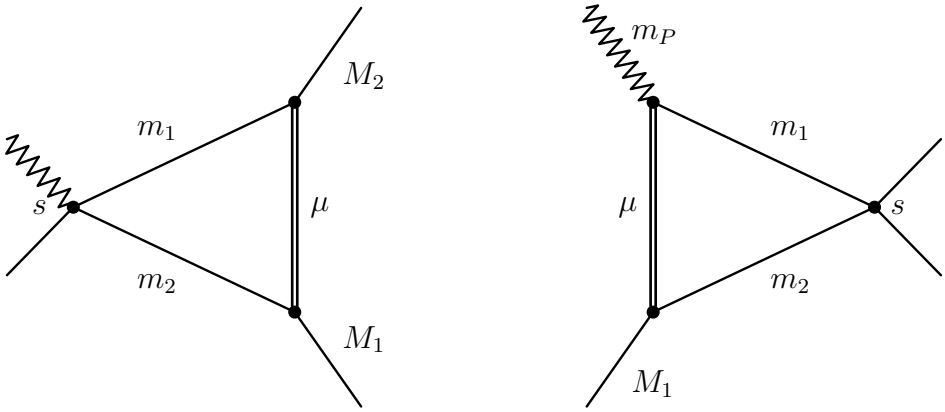

Figure 32: Two basic types of triangle (fish) diagrams contributing to $P\pi \to \pi\pi$ amplitudes. The first diagram with m_P hidden in s we call π-diagram, whereas the second we call P-diagram. The zigzag line denotes the particle P, the double line indicates the dispersive loop and all the other lines correspond to pions.

J.4.2 Triangle diagrams contributing to $P\pi \to \pi\pi$ amplitudes. π-diagrams.

Equipped with all the theoretical knowledge of the previous subsection, we can now study the individual triangle (fish) diagrams contributing to $P\pi \to \pi\pi$. As was discussed in Sections 5.3 and 6.1 we can restrict ourselves just to the studies of singularity structure of the diagrams that contain pions in the internal lines. We therefore start with them and postpone the discussion of the other diagrams to the end of this appendix. To the process $P\pi \to \pi\pi$ there contribute two distinct types of the triangle diagrams depicted on Figure 32. We begin with the first type, whose analysis remains the same also in the case of $\pi\pi$ scattering (m_P is hidden inside s) — we call them therefore π-diagrams and they will turn up to be very simple. As we are interested in the analytic structure of the diagrams in variable s with all the other M_i and m_i fixed at their physical values, we do not release the other quantities unless it is inevitable. We thus do not deform the integration contour in μ, being the line $\mu \geq (\hat{m}_3 + \hat{m}_4)^2$, if not required in order to avoid some singularity.

Conservation of the electric charge guarantees that either both $M_1 = M_2$ and $m_1 = m_2$ or both $M_1 \neq M_2$ and $m_1 \neq m_2$. Before we discuss the individual possibilities for the charges of the pions appearing in the diagram, we recall that in the following domains the original integration contour in parametric space does not need to be deformed and therefore the singularities belonging to these domains do not appear on the physical sheet (here $i \neq j$ are 1 and 2):

(a) $\mathrm{Im}\, s > 0$ and either $\beta_{1,2} \neq 0$ or $\mathrm{Im}\, M_i^2 > 0$ for one of M_i;

(b) since $\mu^2 \geq 4m_{\pi^0}^2 > \Delta \geq (M_i^2 - m_j^2)$, $y_{13} > 0$ and $y_{23} > 0$ are fulfilled automatically and this domain corresponds to $s \leq m_1^2 + m_2^2$;

(c) if in addition $\mu \geq (M_i + m_j)$, the physical singularity does not occur also for $s \leq (m_1 + m_2)^2$.

In any case we thus need to be concerned only with the singularities with $s > m_1^2 + m_2^2$.

The distinct possibilities for the charge states of pions are

- $M_1 = M_2 = m_1 = m_2$: Then we study the amplitudes with fixed $\mu \geq 2m_{\pi^0}$ and the safe domain for physical amplitude is for $s \leq 2m_1^2$. The leading Landau singularities read $s = 0$ and $s = 4m_1^2 - \mu^2$. The subleading singularities are $s = 0$, $s = 4m_1^2$, $\mu^2 = 0$, and $\mu^2 = 4m_1^2$. There appears no new singularity from pinching in infinity. The singularity at $\mu^2 = 0$ does not influence the integration contour of the μ integration and at the anomalous threshold $\mu^2 = 4m_1^2$ there is no singularity on the physical sheet. As expected it means that the only relevant are singularities in s and since only the normal threshold singularity $s = 4m_1^2$ does not belong to the safe region in s, the only relevant singularity for the physical amplitudes is this normal threshold.

- $M_1 = M_2 = m_5$, $m_1 = m_2 \neq m_5$: μ is fixed with $\mu \geq m_{\pi^0} + m_{\pi^\pm}$ and the condition (c) from above is fulfilled automatically and no singularity occurs for $s \leq (m_{\pi^\pm} + m_{\pi^0})^2$ on the physical sheet. The suspected points are: leading Landau singularities at

$$s = 0, \text{ or } s = -\frac{\lambda(\mu^2, m_1^2, m_5^2)}{\mu^2} < 4m_{\pi^0}^2; \tag{J.32}$$

  subleading singularities at $s = 0$, $s = 4m_1^2$, $\mu^2 = (m_1 \pm m_5)^2$; and finally, there appears a non-Landau singularity $s = 4m_5^2$. Therefore, in this case in addition to the normal threshold $s = 4m_1^2$, there occurs a non-Landau singularity at the beginning of the physical region $s = 4m_5^2$, provided $m_5 = m_{\pi^\pm}$ and $m_1 = m_{\pi^0}$.

- $M_1 = m_1 = m_{\pi^\pm}$, $M_2 = m_2 = m_{\pi^0}$: again $\mu \geq m_{\pi^0} + m_{\pi^\pm}$ and no singularity appears on the physical sheet for $s \leq (m_{\pi^\pm} + m_{\pi^0})^2$. All the possible singularities are [Note $\mu^\pm = (m_{\pi^\pm} \pm m_{\pi^0})^2$.]

$$s = \frac{\Delta^2}{\mu^2} < \mu^-, \quad s = 2\Sigma - \mu^2 \leq \mu^-, \quad s = \mu^\pm, \quad \mu^2 = \mu^\pm. \tag{J.33}$$

  Thus, we have again only the normal threshold singularity on the physical sheet, $s = \mu^+$.

- $M_1 = m_2 = m_{\pi^\pm}$, $M_2 = m_1 = m_{\pi^0}$: $\mu \geq 2m_{\pi^0}$ and no singularity occurs on the physical sheet for $s \leq m_{\pi^\pm}^2 + m_{\pi^0}^2$. The singularities in this case read

$$s = \frac{2\Sigma - \mu^2 \pm \sqrt{\left(\mu^2 - 4m_{\pi^\pm}^2\right)\left(\mu^2 - 4m_{\pi^0}^2\right)}}{2}, \quad s = \mu^\pm, \quad \mu^2 = 4m_{\pi^\pm}^2, \quad \mu^2 = 0. \tag{J.34}$$

  Since the first point lies for any $\mu \geq 2m_{\pi^0}$ left from $s = \Delta$, the only remaining singularity on the physical sheet is the normal threshold $s = \mu^+$.

In conclusion the only π-diagram, where there appears an anomalous threshold on the physical sheet is the diagram with $M_1 = M_2 = m_{\pi^\pm}$, $m_1 = m_2 = m_{\pi^0}$ and $m_3 + m_4 = m_{\pi^\pm} + m_{\pi^0}$, which have singularity at the beginning of the physical region $s = 4m_{\pi^\pm}^2$.

J.4.3 Triangle diagrams contributing to $P\pi \to \pi\pi$ amplitudes. P-diagrams.

The second type of diagrams from Figure 32, which we call P-diagrams, needs a more careful analysis. In the following, we denote $m_5 \equiv M_1$. For the leading Landau singularities we obtain from (J.30)

$$\Sigma:\ 2\mu^2 s = -\mu^4 + \mu^2(m_P^2 + m_1^2 + m_2^2 + m_5^2) + \Delta_{25}\Delta_{P1} \pm \lambda^{1/2}(\mu^2, m_P^2, m_1^2)\lambda^{1/2}(\mu^2, m_2^2, m_5^2). \tag{J.35}$$

The subleading singularities read

$$\sigma_{s\pm}:\ s = (m_1 \pm m_2)^2, \quad \sigma_{P\pm}:\ m_P^2 = (\mu \pm m_1)^2, \quad \sigma_{\mu\pm}:\ \mu^2 = (m_2 \pm m_5)^2. \tag{J.36}$$

The second type singularity may occur on the curve

$$\Gamma:\ s = (m_P \pm m_5)^2. \tag{J.37}$$

Note that we have denoted these curves with the Greek letters Σ, $\sigma_{i\pm}$ and Γ.

Again in the end we are interested in the analytic properties in s with m_P and all the other masses fixed at their physical value. However, in the case $m_P > 3m_\pi$ we need to perform an analytic continuation in some other variable from the values, where the diagram is analytic. Inspired by the isospin analysis by Kacser and Bronzan [40, 86], we perform such analytic by starting just with continuation in the external momenta P_i^2 and deform the integration contour in μ from the original line $\mu \geq (\hat{m}_3 + \hat{m}_4)$ [with $\hat{m}_3$ and $\hat{m}_4$ being the appropriate masses of the pions that can appear in the original fish diagram of Figure 31] only when inevitable. The singularity curve $\sigma_{\mu-}$ is therefore again irrelevant and the curve $\sigma_{\mu+}$ corresponding to the anomalous subleading threshold can be in the discussed cases avoided by an addition of a small imaginary part to μ^2 without any change of the analytic structure of s.

For the considered diagrams the domains, where the β integrations do not need to be deformed from the original physical integration contour, are the following

(a) $\operatorname{Im} s > 0$ together with $\operatorname{Im} m_P^2 > 0$;

(b) again $y_{23} > 0$ is fulfilled automatically and the domain $y_i \geq 0$ corresponds to $s \leq m_1^2 + m_2^2$ together with $m_P^2 \leq \mu^2 + m_1^2$;

(c1) for $\mu \geq (M_1 + m_2)$ and $m_P^2 \leq \mu^2 + m_1^2$, we can go with s up to $s \leq (m_1 + m_2)^2$;

(c2) similarly for $\mu \geq (M_1 + m_2)$ and $s \leq m_1^2 + m_2^2$, $m_P^2 \leq (\mu + m_1)^2$;

(c3) the other possibility for the extension in s is when $m_P^2 \leq (\mu - m_1)^2$, $s \leq (m_1 + m_2)^2$;

(c4) similarly for $s \leq (m_1 - m_2)^2$, $m_P^2 \leq (\mu + m_1)^2$.

We therefore see that the anomalous thresholds σ_{s-} and σ_{P-} bring no singularity to the physical sheet, but for $m_P > 3m_\pi$ there are always some parts of Σ and Γ which do not belong to the regions (b) or (c) and we therefore need to perform the analysis very carefully,

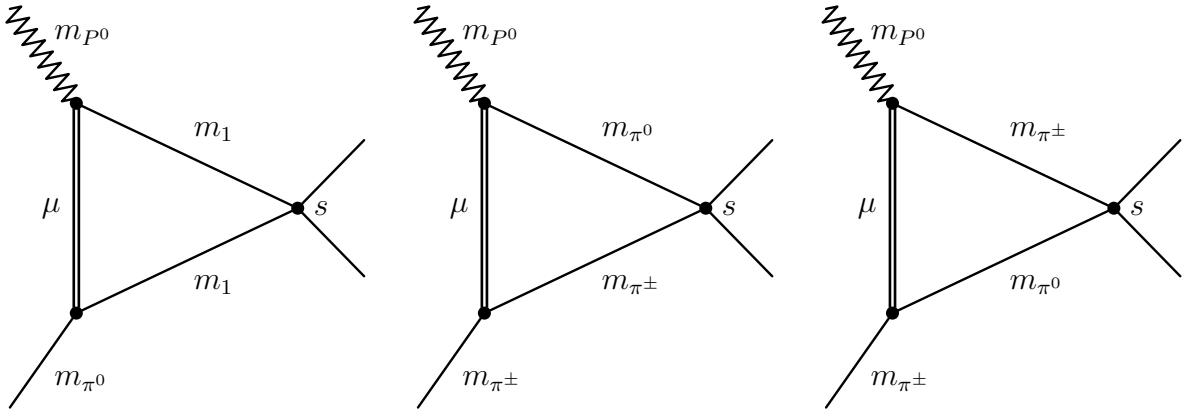

Figure 33: P-diagrams contributing to $P^0\pi \to \pi\pi$ scattering. The zigzag line denotes the particle P, the double line indicates the dispersive loop and all the other lines correspond to pions.

in order to see whether it is possible to continue the amplitude there without the appearance of singularities. It depends on the relative positions of the individual singularity curves. An important observation is that the remaining curves of potential singularities meet only in the following points

$$A_{1,2} = \Sigma \cap \Gamma: \qquad m_P^2 = \mu^2 + m_1^2 + \frac{\lambda(\mu^2, m_2^2, m_5^2)}{2m_5^2} \pm \frac{(\mu^2 + m_5^2 - m_2^2)\sqrt{\lambda(\mu^2, m_2^2, m_5^2) + 4m_1^2 m_5^2}}{2m_5^2}, \quad s = s(A_{1,2}), \tag{J.38}$$

$$B = \Sigma \cap \sigma_{P+}: \qquad m_P^2 = (\mu + m_1)^2, \qquad s = m_1^2 + m_2^2 + \frac{m_1}{\mu}(\mu^2 + m_2^2 - m_5^2), \tag{J.39}$$

$$C = \Sigma \cap \sigma_{s+}: \qquad m_P^2 = \mu^2 + m_1^2 + \frac{m_1}{m_2}(\mu^2 + m_2^2 - m_5^2), \qquad s = (m_1 + m_2)^2, \tag{J.40}$$

$$D_{1,2} = \Gamma \cap \sigma_{P+}: \quad m_P^2 = (\mu + m_1)^2, \qquad s = (\mu + m_1 \pm m_5)^2, \tag{J.41}$$

$$E_{1,2} = \Gamma \cap \sigma_{s+}: \quad m_P^2 = (m_1 + m_2 \pm m_5)^2, \qquad s = (m_1 + m_2)^2. \tag{J.42}$$

Now, we proceed to the individual diagrams. The distinct types of diagrams with the neutral P^0 are displayed on Figure 33.

Analytic properties of the first diagram from Figure 33

For the first of these diagrams ($m_2 = m_1$, $m_5 = m_{\pi^0}$), the singularity curves are:

- leading Landau curve Σ:

$$2\mu^2 s = -\mu^4 + \mu^2(m_P^2 + m_{\pi^0}^2 + 2m_1^2) + \Delta_{10}\Delta_{P1} \pm \lambda^{1/2}(\mu^2, m_P^2, m_1^2)\lambda^{1/2}(\mu^2, m_{\pi^0}^2, m_1^2). \tag{J.43}$$

- subleading singularities

$$\sigma_{s-}: \ s = 0, \qquad \sigma_{s+}: \ s = 4m_1^2, \qquad \sigma_{P\pm}: \ m_P^2 = (\mu \pm m_1)^2. \tag{J.44}$$

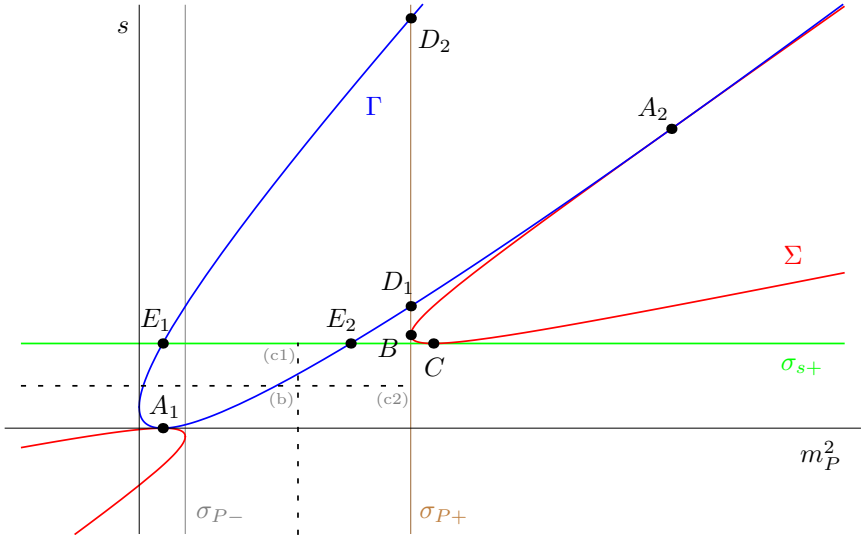

Figure 34: The real section of the singularity curves for the diagrams without the occurrence of the anomalous threshold on the physical Riemann sheet. The labels of the various curves as well as of the points of intersections are introduced in main text.

- second-type singularities

$$\Gamma: \ s = (m_P \pm m_{\pi^0})^2. \tag{J.45}$$

The integration contour for the dispersive loop is the line $\mu \geq (m_{\pi^0} + m_1)$. For $m_1 = m_{\pi^0}$, the situation simplifies into the one studied by Kacser and Bronzan in [86, 40]. However, the relative position of the curves is the same also for $m_1 = m_{\pi^\pm}$ as is depicted on Figure 34, and one therefore expects that also the singularity structure will remain the same.

Since $\mu \geq (M_1 + m_2)$, the denominator of the parametric integrand does not vanish for $\alpha_i \geq 0$ also in the regions (c1) and (c2) and the contribution of this diagram is without singularities on the physical sheet for all s and m_P left or below from the dashed lines on Figure 34. Since the normal-threshold lines σ_{s+} and σ_{P+} correspond to the singularity curves with one of the α's equal to zero and the other two positive, the only part of the real section of the singularity curve Σ where D vanishes for all $\alpha_i > 0$ is the arc between the points B and C and this remains true for the appropriate complex hypercontours connected to this real arc. All the other parts of Σ are non-singular since we can continue the integral analytically in the following way. We start in the domain (c1), where the integration contour in α's is the original one, we add a small imaginary part to s and m_P (coming so to the domain (a)), which is non-singular for any values of s and m_P without the need of deformation of the contour. This way we can come to any point, where the singularity does not occur for positive α's, by limiting the added imaginary parts to zero (without deformation of the integration curve).

However, the arc CB is connected to the non-singular lower-left part of Σ by a continuous complex parts of Σ. Since all intersections of Σ with the other curves are just the real points from above, by performing the analytic continuation from the lower-left

part by the path along Σ, we do not pass through any branch cut until we come to the real arc CB, where either σ_{P+} or σ_{s+} have to be crossed. Similarly in all the points of Γ the function can be made analytic by continuation along this complex curve. Therefore, there are no complex singularities in this case and the only singularities occurring for the diagram considered on the physical sheet are the normal thresholds σ_{s+} and σ_{P+} and the anomalous threshold on the real arc BC (cf. [65]). [Note that the CB section can be made analytic without the appearance of singularities by deforming the integration contour of the parametric integration to $\alpha_1\alpha_2 < 0$.]

The singularity at this anomalous threshold occurs only for m_P^2 within the interval $m_P^2 \in \big((\mu + m_1)^2, 2\mu^2 + 2m_1^2 - m_{\pi^0}^2\big)$. By addition to μ^2 a small negative imaginary part, we can avoid this singularity. The only point where this is not possible is the endpoint of the integration $\mu = m_{\pi^0} + m_1$. In conclusion, for the fish diagram connected with the first diagram of Figure 33 there appears the anomalous threshold singularity in s-plane only for $m_P^2 \in \big((m_{\pi^0} + 2m_1)^2, 4m_1^2 + 4m_1 m_{\pi^0} + m_{\pi^0}^2\big)$. For the physical $m_{\pi^\pm}$ and m_{π^0} masses this corresponds[1] to $m_P < 415\,\mathrm{MeV}$, which is not the case of kaons or eta. For the physical masses the only singularities appearing for this diagram are therefore just the regular normal thresholds. The important observation is that we obtain the correct physical analytic continuation of the amplitude also on the leading singularity curve by taking $m_P^2 \to m_P^2 + i\varepsilon$.

Analytic properties of the second diagram from Figure 33

The singularity curves for the second of these diagrams ($m_1 = m_{\pi^0}$, $m_2 = m_5 = m_{\pi^\pm}$) read

- leading Landau curve Σ

$$2s = m_P^2 + m_{\pi^0}^2 + 2m_{\pi^\pm}^2 - \mu^2 \pm \lambda^{1/2}(\mu^2, m_P^2, m_{\pi^\pm}^2)\sigma_+(\mu^2). \tag{J.46}$$

- subleading singularities

$$\sigma_{s\pm}:\ s = \mu^\pm, \qquad \sigma_{P\pm}:\ m_P^2 = (\mu \pm m_{\pi^0})^2. \tag{J.47}$$

- second-type singularities

$$\Gamma:\ s = (m_P \pm m_{\pi^\pm})^2. \tag{J.48}$$

For $\mu \geq 2m_{\pi^\pm}$ the relative position of these curves is again the one depicted on Figure 34 and thus by the same procedure as in the previous case we obtain the contributions, whose singularities on the physical sheet are just the normal thresholds. However, the integration in the dispersive loop start at $\mu = 2m_{\pi^0} < 2m_{\pi^\pm}$. For these values of μ the real section of the curves moves into the situation depicted on Figure 35 and the analytic continuation proceeds as follows.

[1] Note that for the physical masses and μ corresponding to end-point even the extremal value of the position of C, $m_P^2 = 5m_{\pi^\pm}^2 + \frac{m_{\pi^\pm}}{m_{\pi^0}}\big(5m_{\pi^\pm}^2 - m_{\pi^0}^2\big)$ corresponds to $m_P \approx 423\,\mathrm{MeV}$. For kaons and eta we can therefore this complication with the BC section ignore.

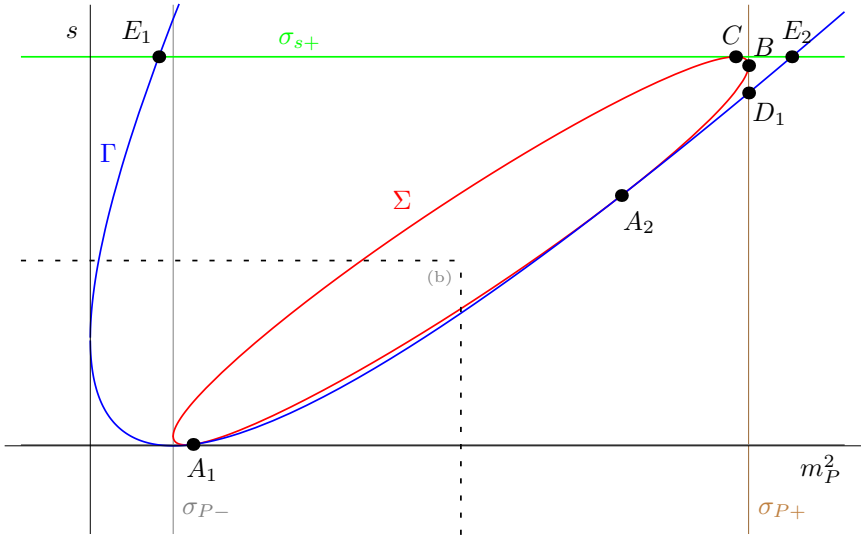

Figure 35: The real section of the singularity curves for the diagrams with the anomalous threshold on the physical Riemann sheet. The labels of the various curves as well as of the points of intersections are introduced in main text.

The original integration contour in parametric space is free of singularities in the domain (b), i.e. left and below from the dashed lines of Figure 35. We can continue the contribution of this diagram along the ellipsis Σ further up to B and C without the appearance of the singularities on the physical sheet even without deforming the original integration contour similarly as in the previous case since the only part of the real section of Σ which corresponds to $\alpha_i > 0$ is the arc BC. In order to avoid singularities also on this arc we would need to deform the integration contour there. However, all paths from the parts we have identified to be non-singular to the arc BC along Σ pass through a singularity curve, either σ_{P+} or σ_{s+}. Since the curve Σ is here real for real m_P, for any complex singularity curve in the α space there exists a complex conjugated one and therefore if we want to evade the complex singularities in one side, we encounter the complex conjugated one (cf. [65]). We have therefore no way how to avoid singularities on the BC arc. This diagram thus possesses on the physical sheet in addition to the normal threshold also the anomalous threshold (J.46) on the arc BC and on all the corresponding complex hypercontours.

We can try to avoid these singularities by an addition of small imaginary part also to μ^2. However, this does not work again for the endpoint of μ^2 integrations, in this case for $\mu = 2m_{\pi^0}$ and even though the real arc BC is again to the left of the physical m_P^2 for both the kaons and eta, the singular complex hypercontour connected with this arc extends to the region, where $m_P > 3m_{\pi^0}$. We are therefore left with two complex conjugated anomalous thresholds in s for the physical $m_P > 3m_{\pi^0}$,

$$2s = m_P^2 + 2m_{\pi^\pm}^2 - 3m_{\pi^0}^2 \pm \lambda^{1/2}(m_P^2, m_{\pi^\pm}^2, 4m_{\pi^0}^2)\sigma_+(4m_{\pi^0}^2). \tag{J.49}$$

Thus, for the amplitudes to which this diagram contributes we cannot use the reconstruction theorem without serious modifications.

Analytic properties of further diagrams

We have seen that the appearance of the anomalous thresholds on the physical sheet is connected with the position of the real section of the curve Σ between the $\sigma_{s\pm}$ and the $\sigma_{P\pm}$ subleading curves, in which case we cannot evade the corresponding normal threshold branch cuts when trying to avoid the singularities Σ on the complex hypercontours connected with the arc BC. We can therefore observe a simple condition for this appearance of the anomalous threshold. It occurs on the physical sheet only in the case (J.35) is real in the interval $m_P^2 \in ((\mu - m_1)^2, (\mu + m_1)^2)$. Since the first triangle function appearing there is on this interval imaginary, the condition means that the second triangle function $\lambda(\mu^2, m_2^2, m_5^2)$ has to be imaginary as well. It occurs in the interval $\mu^2 \in ((m_2 - m_5)^2, (m_2 + m_5)^2)$.

From this condition is we can make the following simple rule of thumb telling that the $\pi\pi$ fish diagram has the anomalous threshold singularity on the physical sheet in the variable s only in the case when in the corresponding triangle diagram one of the other vertices (than the one adjacent to s) is stable and the second one is unstable, where for μ we take its endpoint value $(\hat{m}_3 + \hat{m}_4)$. The vertex is called unstable if the masses on the adjoined lines are such that for at least one of them the following inequality holds

$$m_i \geq m_j + m_k, \tag{J.50}$$

i.e. at least one of them is greater than the sum of the other two. Note that this rule does not take into account the singularity on the real arc BC of Figure 34 (we have found that for the pion lines this singularity never occurs) and the non-Landau singularities as is obvious from its application to the π-diagrams (the only unstable mass there can be μ which appears in both vertices, i.e. this rule tells there is no anomalous threshold for all π-diagrams). However, in our previous analysis we have taken also its existence into the account and there is no other change with respect to it.

Since the vertex with m_P in P-diagrams is for $\mu = (\hat{m}_3 + \hat{m}_4)$ always unstable, the anomalous threshold appears only in the case $(\hat{m}_3 + \hat{m}_4) < (m_2 + m_5)$. Furthermore, since all $\hat{m}_3, \hat{m}_4, m_2$ and m_5 are pion masses and we do not want to violate the electric charge conservation, the only possibility is $\hat{m}_3 = \hat{m}_4 = m_{\pi^0}$ and $m_2 = m_5 = m_{\pi^\pm}$.

In conclusion the only P-diagrams possessing the anomalous threshold singularity on the physical sheet for the physical masses of m_P and of the pions are those depicted on Figure 36. These diagrams contribute to the processes $P^0 \to \pi^0\pi^+\pi^-$, $P^+ \to \pi^-\pi^+\pi^+$ and $P^+ \to \pi^+\pi^0\pi^0$. Therefore, the only $P \to 3\pi$ decay processes, where such singularity does not occur is the process $P^0 \to 3\pi^0$.

J.4.4 Fish diagrams containing also other than pion internal lines

We can perform the same analysis also for the diagrams containing also kaons and η in internal lines. Naturally, then it can happen that there will occur anomalous threshold singularity for some value of m_P. However, thanks to the hierarchy of the masses prohibiting decays of the type $P \to P'\pi$, where P and P' are kaons or η, the physical mass m_P will be each time smaller than the mass, where such anomalous threshold singularity can occur.

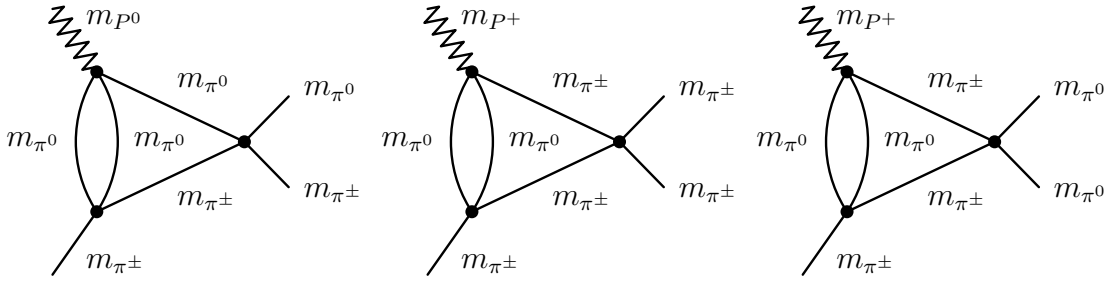

Figure 36: P-diagrams possessing anomalous threshold singularity on the physical sheet for the physical masses of m_P and of the pions

In other words in all the cases the physical mass m_P is left to the points B and C in one of the situation from Figures 34 and 35, i.e. in the region, where the anomalous threshold singularity does not appear.

The inclusion of these other internal lines, therefore, does not change the conclusions of our analysis from the previous sections.

Appendix K

Analytic continuation of NLO partial waves of $P\pi \to \pi\pi$ amplitudes

In this appendix we derive relations, which will be used for computation of S and P partial waves of NLO $P\pi \to \pi\pi$ amplitudes. In Section 6.6 we have discussed that in order to obtain the correct physical result for (some of) the NNLO $P\pi \to \pi\pi$ amplitudes from the reconstruction process of Chapter 3, we start by performing the computation for an unphysical mass m_P such that the decay into three pions becomes kinematically impossible and eventually continue the result analytically in m_P^2 according to (6.46). In the previous appendix we have shown that such simple procedure is possible only for process $P\pi^0 \to \pi^0\pi^0$ in IB and for all the other $P\pi \to \pi\pi$ processes just in the case we take $m_{\pi^\pm} = m_{\pi^0}$. Thus, in the following we will deal with these two situations.

For finding the continuation in m_P of the results, we will use its integral form. As is obvious from its computation, to that end we need to know analytic structure of the continuation of partial waves of the intermediate processes. Since the continuation is written in terms of m_P and in the reconstruction process we take into account just the $\pi\pi$ intermediate states, the only non-trivial continuation is connected with the one of NLO $P\pi \to \pi\pi$ partial waves, what is discussed here.

For the construction of $P\pi^0 \to \pi^0\pi^0$, we need S and P waves of the $P\pi^0 \to \pi^a\pi^b$ amplitudes, where $\pi^a\pi^b$ are mutually charge conjugated pion states, i.e. either $\pi^0\pi^0$ or $\pi^+\pi^-$. Subsequently, the kinematic functions appearing in the case of the same-mass amplitudes $P\pi \to \pi\pi$ can be obtained from those with $P\pi^0 \to \pi^a\pi^b$ by limiting

$$q = \frac{m_{\pi^0}}{m_{\pi^\pm}} \to 1 \tag{K.1}$$

as is shown in Section K.4.

The computation of partial waves employs again the general results of Section 3.4.

K.1 Endpoints of integration

We start with the analysis of endpoints of integration (3.30) and (3.31) for $P\pi^0 \to \pi^a\pi^b$. In accordance to the papers [40, 86] we write (3.28) and (3.29) as

$$t_\pm(s) = \frac{1}{2}\left(3\tilde{s}_0 - s \pm \tilde{K}^{1/2}(s)\right) = u_\mp(s), \tag{K.2}$$

where $\tilde{s}_0$ denotes generically the center of Dalitz plot of this process and

$$\tilde{K}(s) = \frac{s-4m_a^2}{s}\left(s-\tilde{\mu}_0^-\right)\left(s-\tilde{\mu}_0^+\right) \tag{K.3}$$

with $\tilde{\mu}_0^\pm$ from (6.20) is called Kacser function. They take its square root to be positive within the physical decay limits $4m_a^2 < s < \tilde{\mu}_0^-$ and continue it analytically into the complex plane according to

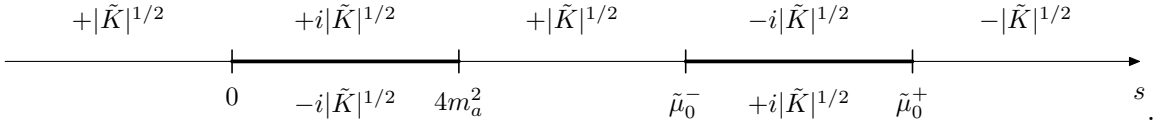

(K.4)

The perturbative analysis [40, 86] tells us that the right physical continuation leading to the correct values of (K.2) is given by prescription $m_P^2 \to m_P^2 + i\varepsilon$ with s keeping real. Nevertheless, for $\tilde{K}^{1/2}(s)$ this is equivalent to taking $s \to s - i\varepsilon$ and keeping a real m_P^2 (but this equivalence is valid only for $\tilde{K}^{1/2}(s)$ and not as a general feature).

To enable some further simplifications of the results we split the square root into

$$\tilde{K}^{1/2}(s) = \sigma_a(s)\tilde{\lambda}_0^{1/2}(s), \tag{K.5}$$

where $\sigma_a(s)$ is the kinematic square root for pion of mass m_a and $\tilde{\lambda}_0(s)$ is Källen function (2.10) for m_P and m_{π^0}. In order to keep the definition of the cut and of the branches of $\sigma_a(s)$ as they were in the pion case (Section 3.2) while preserving (K.4), the analytic structure of $\tilde{\lambda}_0^{1/2}(s)$ has to be chosen in the way

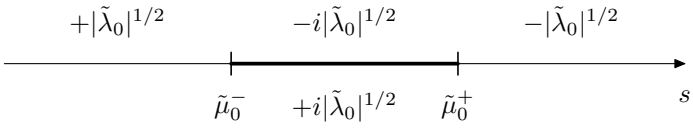

(K.6)

and the physical branch of $\sigma_a(s)$ has to be taken as the one stemming from $s \to s - i\varepsilon$. However, since we need these partial waves only for $s > 4m_a^2$, the choice for $\sigma_a(s)$ is not so important and we obtain the same physical results even if we take the opposite choice. Nevertheless, one should pay attention to the fact that the [40, 86] choice (K.4) leads to the square root of $\tilde{\lambda}_0(s)$ that is defined exactly opposite to the general definition we made in (3.16). This has the consequence that for $K\pi$ partial waves the $t_\pm(s)$ endpoints

of integrations (3.30)–(3.31) are formally interchanged with respect to other processes. Naturally, this change of sign of integrals (3.30)–(3.31) is compensated by the change of sign of $\lambda_{AB}^{1/2}(s)$ appearing in (3.28)–(3.31) and so the final forms of the partial waves are not affected by this sign. The only thing we should keep in mind is using this definition of $\tilde{\lambda}_0(s)$ consistently in all expressions. (This should be reminded to us by the tilde.)

Since in the reconstruction procedure for these processes we take into account only the intermediate states containing two pions (we neglect the non-analytic structure of the amplitudes connected with particle P), all the kinematic functions appearing in integrals (3.30) and (3.31) remain the same as they were in the case of $\pi\pi$ scattering. (Naturally, the polynomials occurring here are different and depend now also on m_P.) Therefore, after factoring the polynomials out of the integrals, the only source of change of them with respect to the $\pi\pi$ case will be the endpoints and with them connected choice of the right physical branches of the resulting functions, which is given by Kacser prescription for the analytic continuation in m_P^2. In fact we anticipate thus also that it will be possible to use the (analytically continued) results of integrations based on the primitive functions from Section 3.4.1 evaluated in these endpoints.

After this general consideration let us proceed to the particular processes.

K.2 Computation of S and P partial waves of process $P\pi^0 \to \pi^+\pi^-$

Since the only intermediate state appearing in T- and U- channels of process $P\pi^0 \to \pi^+\pi^-$ is $\pi^+\pi^0$, there appear in U_{T} and U_{U}, which have to be integrated, solely the functions $\bar{J}_{\pm 0}(t)$ and $\bar{\bar{J}}_{\pm 0}(t)$. Their branch cuts begin in common at $t = (m_{\pi^\pm} + m_{\pi^0})^2 = \mu^+$ and the contours of these integrations have to avoid them.

The traveling of endpoints (K.2) in dependence on s in this case is outlined on Figure 37. We present there something like a blueprint for the construction of these trajectories, which consists of three parts. First three plots describe the course of dependencies of t_+ and t_- on s. They are deformed in order to have the important points equidistant, to make the sign of these functions together with the one of their first derivative evident on the whole range of s, and finally they are compactified by making ∞ and ϵ finite. We will need the partial waves only for $s > 4m_{\pi^\pm}^2$, which is denoted by the bold vertical line and the situation for lower values is depicted just for the sake of completeness. The trajectories of these endpoints in the complex t-plane for $s > 4m_{\pi^\pm}^2$ are then depicted on the next plot. The significant points of these dependencies are labeled by roman capital letters according to the table displayed next to it, where also the values of $t_\pm$ for these points are presented. For sake of brevity we have used there the shortcuts defined in (5.2)–(5.4), (6.19)–(6.20), (K.8) together with

$$Q = \frac{m_P}{m_{\pi^\pm}}, \qquad \tilde{\varsigma} = m_P^2 m_{\pi^0}^2 - m_{\pi^\pm}^4. \tag{K.7}$$

From the t-plane plot it is obvious that the routes of $t_\pm$ avoid the branch cut of the amplitude starting at $t = \mu^+$ (this branch cut is indicated there by the bold line starting near the gray point C), i.e. indeed we can obtain the results for the physical value of m_P^2

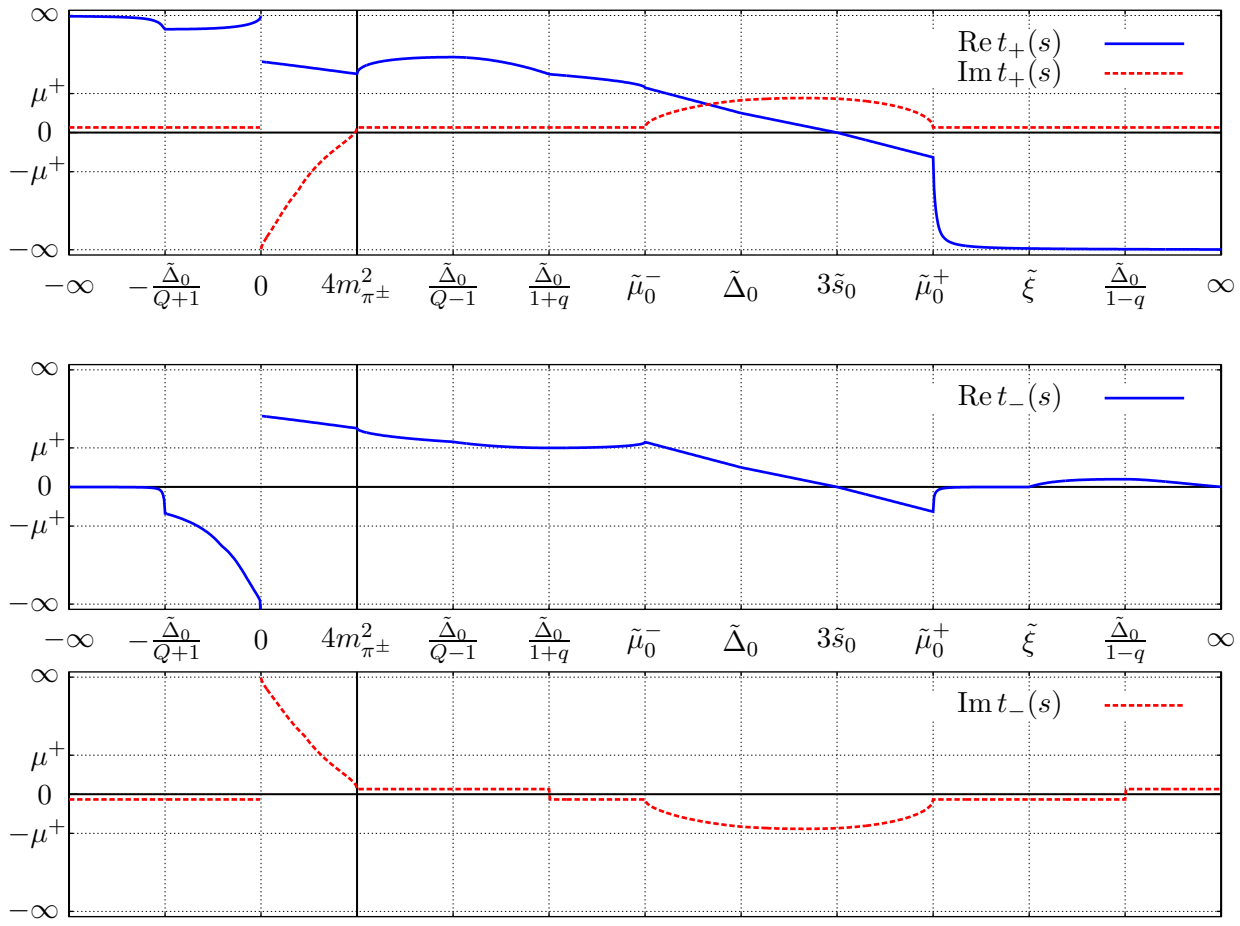

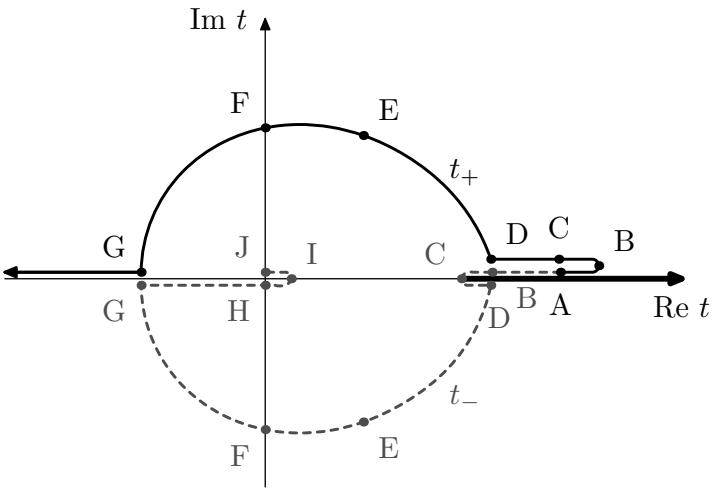

	s	$t_+(s)$	$t_-(s)$
	$-\infty$	∞	0
	$-\frac{\tilde\Delta_0}{Q+1}$	$\tilde\mu_c^+$	$-\frac{\tilde\Delta_+ + Q\Delta}{Q+1}$
	0	$\frac{3}{2}\tilde s_0 \mp i\infty$	
A	$4m_{\pi^\pm}^2$	$\frac{1}{2}\big(\tilde\Delta_+ - \Delta\big)$	
B	$\frac{\tilde\Delta_0}{Q-1}$	$\tilde\mu_c^-$	$\frac{\tilde\Delta_+ - Q\Delta}{Q-1}$
C	$\frac{\tilde\Delta_0}{1+q}$	$\frac{q\tilde\Delta_+ + \Delta}{1+q}$	μ^+
D	$\tilde\mu_0^-$	$m_{\pi^\pm}^2 + m_P m_{\pi^0}$	
E	$\tilde\Delta_0$	$\Sigma \pm i m_{\pi^0}\sqrt{\tilde\Delta_0 - 4m_{\pi^\pm}^2}$	
F	$3\tilde s_0$	$0 \pm i\sqrt{\frac{\tilde\Delta_+ - \Delta}{3\tilde s_0}}\sqrt{\tilde\zeta}$	
G	$\tilde\mu_0^+$	$m_{\pi^\pm}^2 - m_P m_{\pi^0}$	
H	$\tilde\xi$	$\frac{\Delta - \tilde\Delta_+}{\Delta\tilde\Delta_+}\,\tilde\zeta$	0
I	$\frac{\tilde\Delta_0}{1-q}$	$\frac{\Delta - q\tilde\Delta_+}{1-q}$	μ^-
J	∞	$-\infty$	0

Figure 37: Blueprints for construction of the trajectories of endpoints of integration $t_\pm(s)$ that occur in the computation of partial waves of $P\pi^0 \to \pi^+\pi^-$ amplitude. Details are presented in the text around relation (K.7).

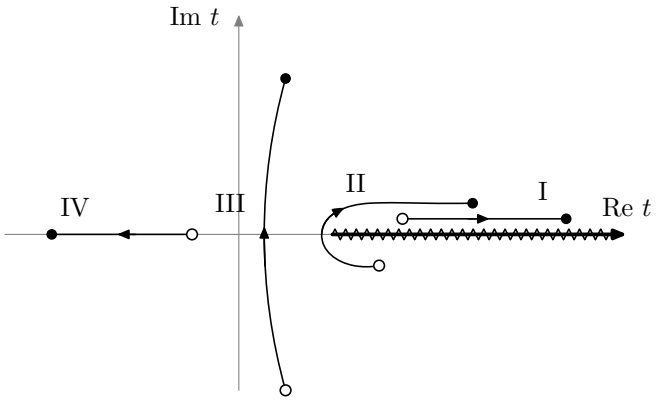

Figure 38: Four types of integration contours for computation of partial waves of $P\pi^0 \to \pi^+\pi^-$. Contour I corresponds to $s \in \left(4m_{\pi^\pm}^2, \frac{\tilde{\Delta}_0}{1+q}\right)$, contour II then to $s \in \left(\frac{\tilde{\Delta}_0}{1+q}, \tilde{\mu}_0^-\right)$, contour III to $s \in (\tilde{\mu}_0^-, \tilde{\mu}_0^+)$, and finally contour IV corresponds to $s > \tilde{\mu}_0^+$. With the open dot there is denoted the position of t_-, whereas the full dot identifies the position of t_+. The wiggled line represents the branch-cut of the amplitude.

by employing a simple analytic continuation in m_P^2 without any distortion of dispersion relations.

Note that the only principal difference with respect to the isospin case discussed in Section K.4 and [40, 86] is the existence of the interval $s > \tilde{\xi}$ with

$$\tilde{\xi} = \frac{m_{\pi^\pm}^2}{\Delta} \frac{\tilde{\Delta}_0^2}{\tilde{\Delta}_+}, \qquad t_-(\tilde{\xi}) = 0, \tag{K.8}$$

where $t_-(s)$ rises above zero, then reaches the value μ_- for $s = \frac{\tilde{\Delta}_0}{1-q}$ and after that descends back to zero. (In the isospin limit whole this interval falls into infinity and $t_-(s)$ is then for $s > \tilde{\mu}_0^+$ monotonously ascending function of s.) Since this change happens below the branch cut of $U_{\rm T}$ $[t_-(I) = \mu^- < t_-(C) = \mu^+]$, it brings no principal difference to the analysis with respect to [40, 86].

Contours of integrations $\mathcal{C}(t_-, t_+)$ from (3.30) and (3.31) avoiding the branch cut $t > \mu^+$ are of the four types depicted on Figure 38. Since all the discontinuities of the integrands and of the primitive functions from Section 3.4.1 lie solely on that branch cut, there always exists an open neighborhood of every point of the contour, where the integrand and its primitive functions are continuous, and the results of these integrations are thus equal to the differences of values of these primitive functions evaluated in the endpoints. (The only complication occurs for the point $s = \frac{\tilde{\Delta}_0}{1+q}$, for which we need to employ an infinitesimal displacement to fulfill these requirements.)

Therefore, we focus our interest to primitive functions (3.51)–(3.56) and find here their values in these endpoints, or better to say we find here just some simplifications of these expressions without writing here the results explicitly. To that end we use conformal

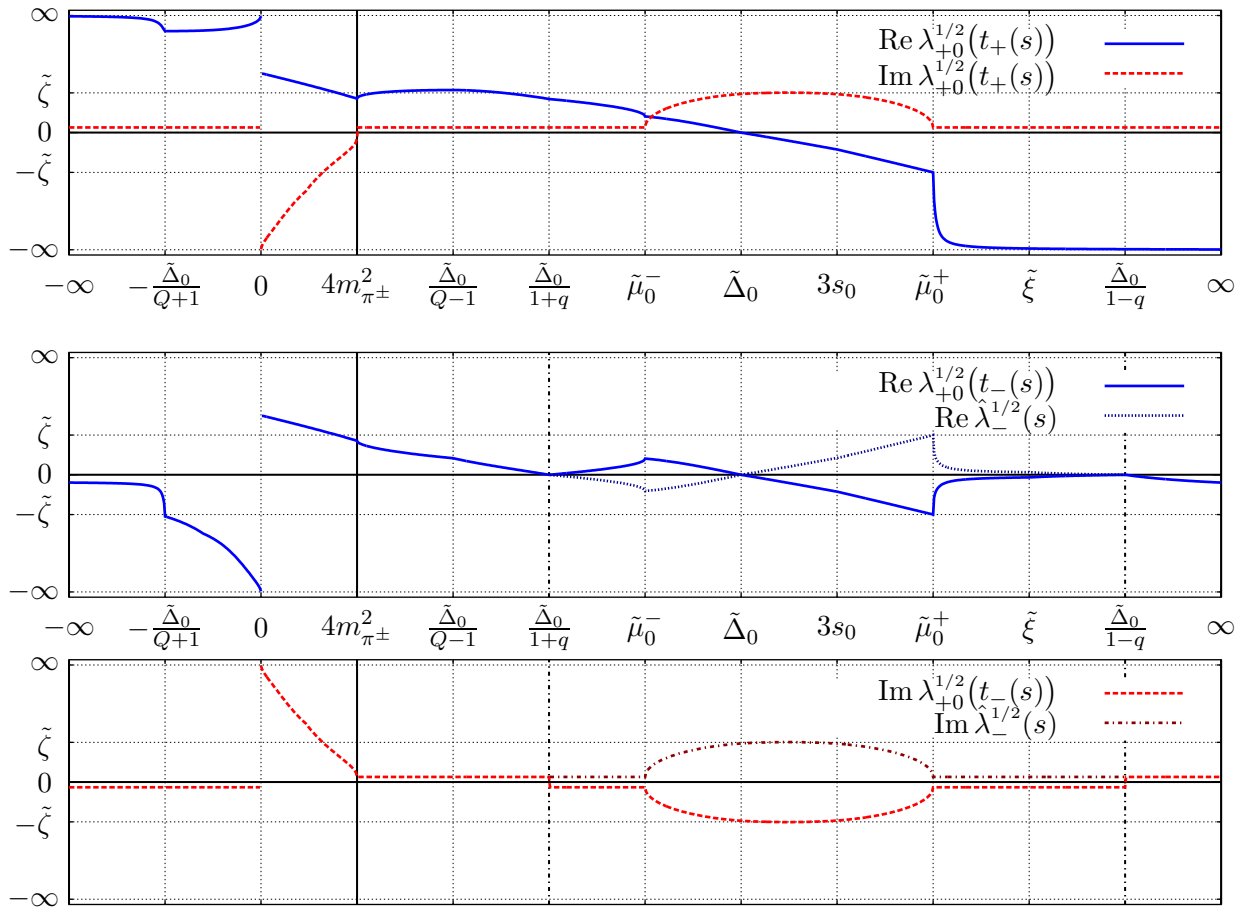

Figure 39: The correct square root of the triangle function, $\lambda_{\pm 0}^{1/2}(t)$, evaluated in the endpoints of integration $t_\pm(s)$ from Figure 37, together with its naive counterpart, $\hat{\lambda}_\pm^{1/2}(s)$ from (K.10). In these plots $\tilde{\zeta} = m_{\pi^0}\sqrt{\tilde{\mu}_0^+ - 4m_{\pi^\pm}^2}$.

transformation (3.36) [cf. also Figure 2]. After some straightforward algebra we find

$$\lambda_{\pm 0}(t_\pm(s)) = \frac{1}{4}\left(\tilde{\lambda}_0^{1/2}(s) \pm \sigma_\pm(s)(\tilde{\Delta}_0 - s)\right)^2 . \tag{K.9}$$

From that one would naively expect the square root of this function merely equal to

$$\hat{\lambda}_\pm^{1/2}(s) = \frac{1}{2}\left(\tilde{\lambda}_0^{1/2}(s) \pm \sigma_\pm(s)(\tilde{\Delta}_0 - s)\right). \tag{K.10}$$

However, the correct sign of this square root has to correspond to our choice from Section 3.2, i.e. for instance for $t < \mu^-$ there should hold $\lambda_{\pm 0}^{1/2}(t) = -|\lambda_{\pm 0}(t)|^{1/2}$.

The course of the correct function $\lambda_{\pm 0}(t_\pm(s))$ together with the one of the naive square root $\hat{\lambda}_\pm^{1/2}(s)$ are sketched on Figure 39 (it is deformed in the same way as the plots from Figure 37). We observe that the naive square root reproduces the correct result $\lambda_{\pm 0}^{1/2}(t_\pm(s)) = \hat{\lambda}_\pm^{1/2}(s)$ for every s with the exception of interval $s \in \left(\frac{\tilde{\Delta}_0}{1+q}, \frac{\tilde{\Delta}_0}{1-q}\right)$, where

$\lambda_{\pm 0}^{1/2}(t_-(s)) = -\hat{\lambda}_-^{1/2}(s)$. In both cases the sign of the infinitesimal imaginary displacement is determined by Kacser prescription $\frac{\partial \lambda_{\pm 0}^{1/2}(t_\pm(s))}{\partial m_P^2}$.

Using this naive square root, conformal transformation (3.36) simplifies into

$$\hat{\tau}_\pm(s) = -\frac{1}{4m_{\pi^\pm}m_{\pi^0}}\left(1 \mp \sigma_+(s)\right)\left(\tilde{\Delta}_0 - s - \tilde{\lambda}_0^{1/2}(s)\right) \tag{K.11}$$

with a small imaginary part

$$-\frac{\hat{\tau}_\pm(s)}{\lambda_{L0}^{1/2}(s)}\, i\epsilon. \tag{K.12}$$

According to the discussion of $\lambda_{\pm 0}^{1/2}(t_\pm(s))$, the correct conformal transformation $\tau(t_\pm(s))$ coincides with the naive one

$$\tau_\pm(s) \equiv \tau(t_\pm(s)) = \hat{\tau}_\pm(s) - \frac{\hat{\tau}_\pm(s)}{\lambda_{L0}^{1/2}(s)}\, i\epsilon \tag{K.13}$$

with the exception of

$$\tau_-(s) \equiv \tau(t_-(s)) = \frac{1}{\hat{\tau}_-(s)} + \frac{1}{\hat{\tau}_-(s)\lambda_{L0}^{1/2}(s)}\, i\epsilon, \quad \text{for } s \in \Big(\frac{\tilde{\Delta}_0}{1+q}, \frac{\tilde{\Delta}_0}{1-q}\Big). \tag{K.14}$$

The small displacement is needed only for negative real τ (where the cut of $\bar{J}_{\pm 0}$ is mapped into). On Figure 40 we present the trajectories of the endpoints in this transformed plane. We plot there the absolute values of $\tau_\pm(s)$ and the values of their complex arguments, which are chosen in correspondence with the mapping of the branch cut so that they fall into interval $\langle -\pi, \pi\rangle$. The only deformation we have done in these plots is making the significant points to be equidistant.

Note that the correct $\tau_\pm(s)$ indeed lies inside the unit circle and we see also in this transformed plane that there is no problem to find the contours of integration avoiding the branch cut [=segment $(-1, 0)$] and fulfilling the conditions for the computation of integral using the primitive functions.

When computing values of primitive functions (3.51)–(3.56) at the endpoint $t_-(s)$, we can use the fact that these functions are invariant with respect to the change $\tau \leftrightarrow 1/\tau$ and so working everywhere with the naive functions $\hat{\lambda}_\pm(s)$ and $\hat{\tau}_\pm(s)$ yields also the correct values of the primitive functions. In addition, the use of these naive quantities has the advantage that then all the imaginary displacements for $s > 4m_{\pi^\pm}^2$ are positive, i.e. for instance that arguments of $\hat{\tau}_\pm(s)$ fall into $(-\pi, \pi\rangle$, what is the standardly used choice for the definition of branches of logarithms and dilogarithms, which appear in (3.51)–(3.56). (Therefore, among other simplifications we can use then symbolic manipulation programs for their computation without much concerns.)

The form of (K.11) implies validity of the following formulae

$$\log\hat{\tau}_+ - \log\hat{\tau}_- = L_+(s), \tag{K.15}$$

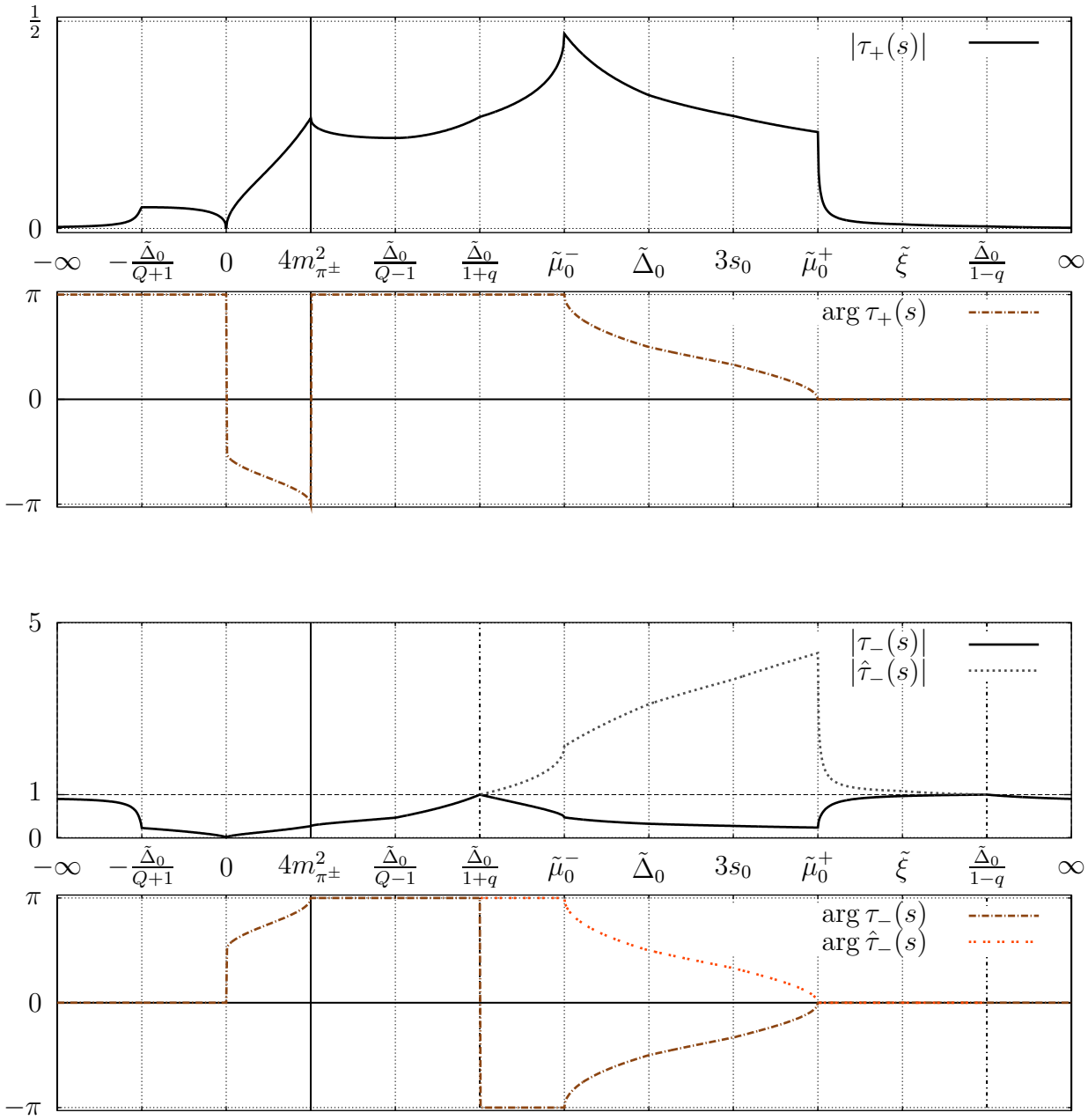

Figure 40: Trajectories of endpoints of integration from the computation of partial waves of $P\pi^0 \to \pi^+\pi^-$ amplitude transformed using (3.36), $\tau_\pm(s)$, together with their naive values $\hat{\tau}_\pm(s)$ stemming from (K.11).

$$\log\hat{\tau}_+ + \log\hat{\tau}_- = -M_0(s), \tag{K.16}$$

$$\log^2\hat{\tau}_+ - \log^2\hat{\tau}_- = -L_+(s)M_0(s), \tag{K.17}$$

which can be used for simplification of the results. For $s > 4m_{\pi^\pm}^2$ the function $L_+(s)$ coincides[1] with (5.74) from Chapter 5 and

$$-M_0(s) = 2\log\left(1 - \frac{\tilde{\Delta}_0}{s} + \frac{\tilde{\lambda}_0^{1/2}(s)}{s}\right) - \log\frac{4m_{\pi^0}^2}{s}\,. \tag{K.19}$$

The results of integrations (3.32)–(3.33)

$$I_n = I_n(t_+) - I_n(t_-) \tag{K.20}$$

are then given by

$$\begin{aligned}
\frac{I_2}{\tilde{\lambda}_0^{1/2}\sigma_+} &= 2m_{\pi^\pm}^2 m_{\pi^0}^2\,\mathcal{M}_{2\mathrm{L}+}(s) + \frac{1}{12}\Big(\big(s-\tilde{\Delta}_0\big)\Big(2s - (2m_P^2 + 9m_{\pi^\pm}^2 + 3m_{\pi^0}^2) + 2m_{\pi^0}^2\frac{\tilde{\Delta}_0}{s} \\
&\qquad - 6m_{\pi^\pm}^2\frac{\tilde{\Delta}_+}{s}\Big) - 2m_{\pi^0}^2\frac{\tilde{\Delta}_0^2}{s}\Big)\mathcal{M}_{1+}(s) \\
&\quad + \frac{1}{12}\Big(\Big(1-\frac{\tilde{\Delta}_0}{s}\Big)\Big(2s^2 - s(4m_P^2+5\Sigma) + 2\tilde{\Delta}_0^2 + \tilde{\Delta}_0(7m_{\pi^\pm}^2 + 3m_{\pi^0}^2) + 6m_{\pi^0}^2\Sigma \\
&\qquad + 2(3m_{\pi^0}^2\Sigma - m_{\pi^\pm}^2\tilde{\Delta}_0)\frac{\tilde{\Delta}_0}{s}\Big) + 6m_{\pi^0}^2\Sigma\frac{\tilde{\Delta}_0^2}{s^2}\Big)\mathcal{M}_{1\mathrm{L}}(s) \\
&\quad + \frac{1}{36}\Big(16s^2 - s(32\tilde{\Delta}_0 + 61\Sigma) + 16\tilde{\Delta}_0^2 + \tilde{\Delta}_0(77m_{\pi^\pm}^2 + 45m_{\pi^0}^2) \\
&\qquad + 4(9\Sigma^2 + 4m_{\pi^\pm}^2 m_{\pi^0}^2) - 16m_{\pi^\pm}^2\frac{\tilde{\Delta}_0^2}{s}\Big) \\
&\quad + \frac{1}{6}\Big(2s^2 - s\Big(4\tilde{\Delta}_0 + 5\Sigma + \frac{12m_{\pi^\pm}^2 m_{\pi^0}^2}{\Sigma}\Big) + 2\tilde{\Delta}_0^2 + \tilde{\Delta}_0\Big(3\Sigma + 4\frac{m_{\pi^\pm}^2 + 4m_{\pi^0}^2}{\Sigma}\Big) \\
&\quad + 32m_{\pi^\pm}^2 m_{\pi^0}^2 - 2m_{\pi^\pm}^2\frac{\tilde{\Delta}_0^2}{s}\Big)\mathcal{M}_{0q}(s),
\end{aligned} \tag{K.21}$$

$$\frac{I_0}{\tilde{\lambda}_0^{1/2}\sigma_+} = -\mathcal{M}_{7\mathrm{L}x}(s) - \mathcal{M}_{2\mathrm{L}+}(s) + \frac{1}{2}\,\mathcal{M}_{1+}(s) + \frac{1}{2}\Big(1-\frac{\tilde{\Delta}_0}{s}\Big)\mathcal{M}_{1\mathrm{L}}(s) + \mathcal{M}_{0q}(s) + 2, \tag{K.22}$$

[1] The validity of (K.15)–(K.17) can be extended to any value of s by changing on their right-hand sides

$$L_+(s) \to L_+(s) - 2\pi i\,\chi_{\left(0,4m_{\pi^\pm}^2\right)}(s), \qquad -M_0(s) \to -M_0(s) - 2\pi i\,\chi_{\left(0,4m_{\pi^\pm}^2\right)}(s), \tag{K.18}$$

where $\chi_{(a,b)}(s)$ is the characteristic function of interval (a,b) (equal to 1 within this interval and 0 elsewhere), and taking the $s \to s - i\epsilon$ branch of $\sigma_+(s)$ on the interval $s \in (0, 4m_{\pi^\pm}^2)$ [cf. the note below (K.6)].

$$\begin{aligned}\frac{I_1}{\tilde{\lambda}_0^{1/2}\sigma_+} &= \frac{2m_{\pi^\pm}^2 m_{\pi^0}^2}{\Sigma}\,\mathcal{M}_{2\mathrm{L}+}(s) + \frac{(s-\tilde{\Delta}_0)(2m_{\pi^\pm}^2 - s)}{4s}\,\mathcal{M}_{1+}(s) \\ &\quad - \frac{1}{4}\Big(2m_{\pi^0}^2 + \frac{\tilde{\lambda}_0(s)}{s}\Big)\mathcal{M}_{1\mathrm{L}}(s) + \frac{1}{4}\big(3(m_P^2 - s) + 4m_{\pi^\pm}^2 + m_{\pi^0}^2\big) \\ &\quad + \frac{1}{2}\Big(\frac{8m_{\pi^\pm}^2 m_{\pi^0}^2}{\Sigma} - s + \tilde{\Delta}_0\Big)\mathcal{M}_{0q}(s),\end{aligned} \tag{K.23}$$

$$\frac{I_{-1}}{\tilde{\lambda}_0^{1/2}\sigma_+} = \frac{\Sigma}{\Delta^2}\,\mathcal{M}_{7\mathrm{L}x}(s) - \frac{1}{\Sigma}\,\mathcal{M}_{2\mathrm{L}+}(s) + \frac{1}{\tilde{\Delta}_+}S_1(s), \tag{K.24}$$

$$\frac{I_{-2}}{\tilde{\lambda}_0^{1/2}\sigma_+} = \frac{2m_{\pi^\pm}^2 m_{\pi^0}^2}{\Delta^4}\mathcal{M}_{7\mathrm{L}x}(s) - \frac{\Sigma}{2\Delta^2\tilde{\Delta}_+}S_1(s) + \frac{1}{2\tilde{\Delta}_+\Delta}S_2(s). \tag{K.25}$$

In these relations, we have introduced functions $S_1(s)$ and $S_2(s)$ which comprise terms containing single pole and double pole in $s = \tilde{\xi}$ respectively,

$$S_1(s) = \frac{2\tilde{\Delta}_0 m_{\pi^\pm}^2 - s\Delta}{2\Delta(s-\tilde{\xi})}\,\mathcal{M}_{1+}(s) - \frac{\tilde{\Delta}_0\Sigma - s\Delta}{2\Delta(s-\tilde{\xi})}\,\mathcal{M}_{1\mathrm{L}}(s) + \frac{s\Delta}{\Sigma(s-\tilde{\xi})}\,\mathcal{M}_{0q}(s), \tag{K.26}$$

$$S_2(s) = \frac{s}{s-\tilde{\xi}}\bigg(\frac{s - 2\Sigma - \tilde{\Delta}_0}{\tilde{\Delta}_+}\,S_1 - \frac{1}{2}\,\mathcal{M}_{1+}(s) - \frac{1}{2}\Big(1 - \frac{\tilde{\Delta}_0}{s}\Big)\,\mathcal{M}_{1\mathrm{L}}(s) - \mathcal{M}_{0q}(s) - 1\bigg) \tag{K.27}$$

However, in these functions these poles are canceled and their values at the point $s = \tilde{\xi}$ are

$$S_1(\tilde{\xi}) = \frac{\tilde{\Delta}_+^2\Delta}{(\tilde{\Delta}_+ - \Delta)\,\tilde{\varsigma}} + \frac{\Delta\tilde{\Delta}_+^2\big(\Delta^2 m_{\pi^\pm}^2 - \tilde{\Delta}_+^2 m_{\pi^0}^2\big)}{(\tilde{\Delta}_+ - \Delta)^2\,\tilde{\varsigma}^2}\,\log\frac{\tilde{\Delta}_+}{\Delta} - \frac{2m_{\pi^\pm}^2 m_{\pi^0}^2\tilde{\Delta}_+^2}{\tilde{\varsigma}^2}\,\log q, \tag{K.28}$$

$$\begin{aligned}S_2(\tilde{\xi}) &= -\frac{\tilde{\Delta}_+\Delta(\Delta^2 - 4m_{\pi^\pm}^2 m_{\pi^0}^2) + \Sigma\big(\tilde{\Delta}_+^2 m_{\pi^0}^2 + \Delta^2 m_{\pi^\pm}^2\big)}{2(\tilde{\Delta}_+ - \Delta)^2\,\tilde{\varsigma}^2}\,\tilde{\Delta}_+^2 \\ &\quad - \frac{\tilde{\Delta}_+^3\Delta^3(\Delta^2 m_{\pi^\pm}^2 - \tilde{\Delta}_+^2 m_{\pi^0}^2)}{(\tilde{\Delta}_+ - \Delta)^3\,\tilde{\varsigma}^3}\,\log\frac{\tilde{\Delta}_+}{\Delta} + \frac{2m_{\pi^\pm}^2 m_{\pi^0}^2\tilde{\Delta}_+^2(\Delta m_{\pi^\pm}^4 - \tilde{\Delta}_+ m_{\pi^0}^4)}{\Delta\,\tilde{\varsigma}^3}\,\log q.\end{aligned} \tag{K.29}$$

The shortcut variable $\tilde{\varsigma}$ was introduced in (K.7).

K.3 Computation of S and P waves of process $P\pi^0 \to \pi^0\pi^0$

Endpoints of integration (K.2) for $P\pi^0 \to \pi^0\pi^0$ can be obtained from the ones computed in the previous case by limiting $m_{\pi^\pm} \to m_{\pi^0}$. We can therefore employ the blueprints from Figure 37 with these changes. Besides the natural change of all appearances of $m_{\pi^\pm}$ into m_{π^0}, what implies among others $\Delta \to 0$, the main difference is that the points H, I, and J

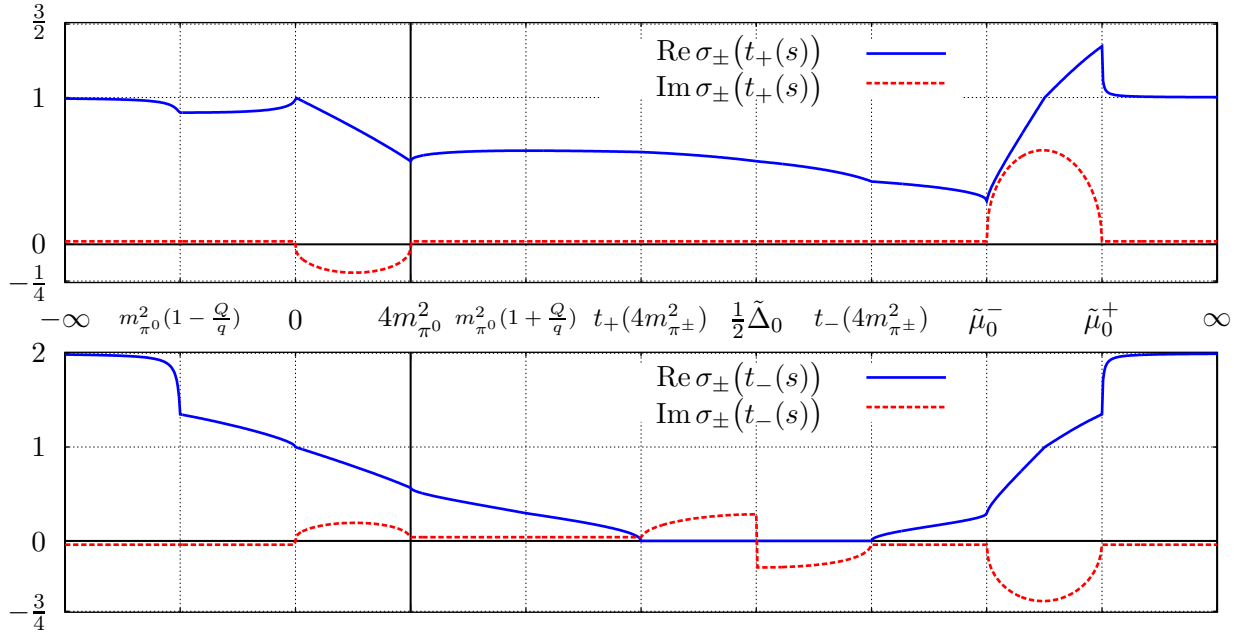

Figure 41: Course of the kinematic square root, $\sigma_\pm(t)$, evaluated in the endpoints of integration $t_\pm(s)$ from Figure 43.

melt into one point. Note the following relation valid for all s

$$t_+(s)t_-(s) = m^2_{\pi^0}\frac{\tilde{\Delta}_0^2}{s}\,. \tag{K.30}$$

Since in the equations for these endpoints only one mass of pion m_{π^0} occurs, they reproduce the isolimit case of Section K.4. This implies that the trajectories of these endpoints are the same as the one plotted on Figure 43 with the change $m_\pi \to m_{\pi^0}$. Similarly, when computing integrals of $t^n\bar{J}_0(t)$, the whole computation including the results of the primitive functions is the same as the one in the isospin limit.

In T- and U-channels of this process there appear two possible intermediate states, either $\pi^0\pi^0$ or $\pi^+\pi^-$. This corresponds to the appearance of $\bar{J}_0(t)$ and $\bar{J}_\pm(t)$ in U_T and U_U. Since their branch cuts begin at $4m^2_{\pi^0}$ and $4m^2_{\pi^\pm}$ respectively, while the turning point $t_-(C)$ moved into $4m^2_{\pi^0}$, the trajectories of the endpoints avoid the branch points of the integrands and we are again safe to use the simple analytic continuation in m_P^2 with no distortion of the dispersion relations.

From the reasons we have stated above, we postpone the discussion of the integrations with $\bar{J}_0(t)$ to the next section and for now we fully concentrate on the integrations of the functions $t^n\bar{J}_\pm(t)$. Since the turning point is now far below the branch point of these functions, $4m^2_{\pi^\pm} > t_-(C) = 4m^2_{\pi^0}$, the arguments leading to the possibility of using the primitive functions are even more obvious than in the previous section.

We discuss again carefully the behavior of the results of conformal transformation

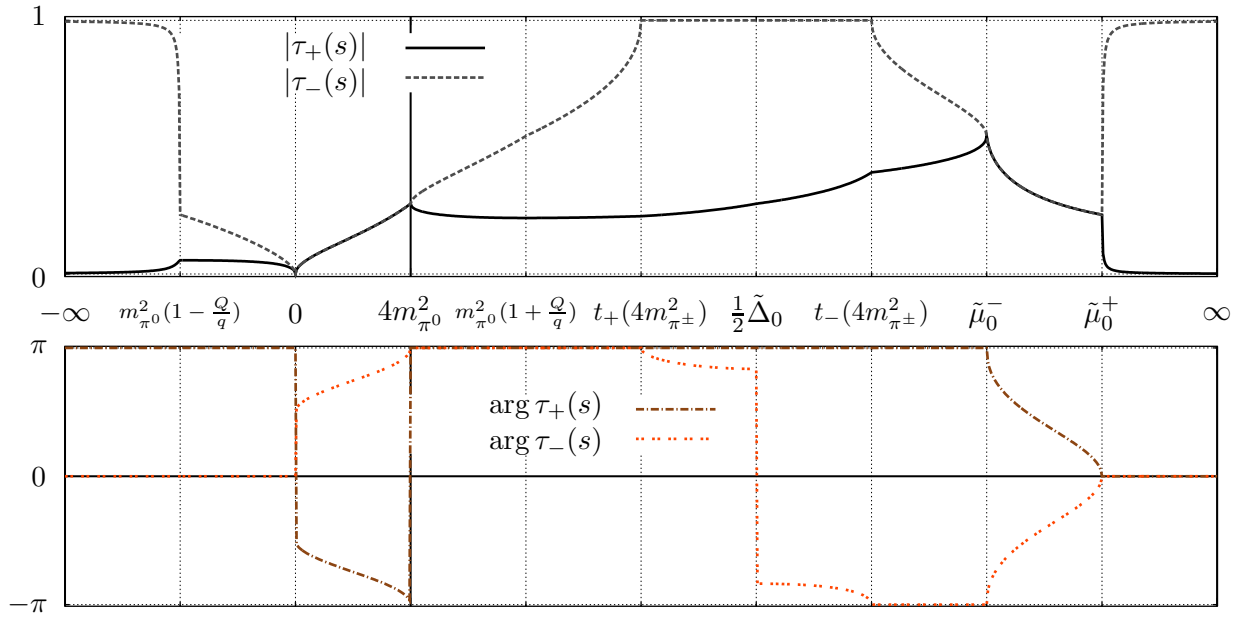

Figure 42: Conformal transformation (K.33) of the endpoints of integration $t_\pm(s)$ from Figure 43.

(3.37). In this case the kinematic square root simplifies into

$$\sigma_+^2(t_\pm(s)) = 1 - \frac{4m_{\pi^\pm}^2}{t_\pm(s)} = \frac{1}{m_{\pi^0}^2\tilde{\Delta}_0^2}\left(m_{\pi^\pm}^2\left(\tilde{\lambda}_0^{1/2}(s) \pm s\sigma_0(s)\right)^2 - \Delta\tilde{\Delta}_0^2\right) \tag{K.31}$$

but, unfortunately, we do not see any simpler algebraic form of the square root (even the naive one).

The choices of the branches of $\sigma_\pm(t)$ from Section 3.2, and of $\sigma_0(s)$ and $\tilde{\lambda}_0^{1/2}(s)$ from Section K.1 together with the Kacser prescription

$$\frac{\mathrm{d}\sigma_+^2(t_\pm(s))}{\mathrm{d}m_P^2} = \frac{4m_{\pi^\pm}^2}{t_\pm^2(s)}\frac{\mathrm{d}t_\pm(s)}{\mathrm{d}m_P^2} \tag{K.32}$$

lead to the courses of the square roots $\sigma_+(t_\pm(s))$ depicted on Figure 41. To the set of significant points there we have added the points $s = t_\pm(4m_{\pi^\pm}^2)$, where $t_-(s) = 4m_{\pi^\pm}^2$ and so the value of $\sigma_+(t)$ at these points is zero. Note that $\sigma_+(t_\pm)$ are complex in intervals $s \in (0, 4m_{\pi^0}^2)$ and $s \in (\tilde{\mu}_0^-, \tilde{\mu}_0^+)$, where the values of these two functions are mutually complex conjugated, $\sigma_+(t_+(s)) = (\sigma_+(t_+(s)))^\star$. Further on, the value of $\sigma_+(t_-(s))$ is for $s \in (t_-(4m_{\pi^\pm}^2), t_+(4m_{\pi^\pm}^2))$ purely imaginary. Everywhere else they are real.

From this, we compute the conformal transformation of the endpoints

$$\tau_\pm(s) \equiv \tau(t_\pm(s)) = 1 + \frac{t_\pm}{2m_{\pi^\pm}^2}(\sigma_+(t_\pm) - 1) + i\epsilon\left(\frac{\sigma_+(t_\pm) - 1}{2m_{\pi^\pm}^2} + \frac{1}{\sigma_+(t_\pm)t_\pm}\right)\frac{\mathrm{d}t_\pm}{\mathrm{d}m_P^2} \tag{K.33}$$

which are plotted on Figure 42.

In analogy to relations (K.15)–(K.17), we introduce a couple of functional combinations

$$\log\tau_+ - \log\tau_- = N_\nabla(s), \tag{K.34}$$
$$\log\tau_+ + \log\tau_- = -M_\nabla(s), \tag{K.35}$$
$$\log^2\tau_+ - \log^2\tau_- = -N_\nabla(s)M_\nabla(s), \tag{K.36}$$
$$t_+\sigma_+(t_+) \pm t_-\sigma_+(t_-) = \Lambda^\pm_\nabla(s). \tag{K.37}$$

This functions, however, have no simple algebraic representation other the the direct form stemming from these relations. Fortunately, in the results of integrations using primitive functions (3.73)–(3.73) there appear only the following combinations[2]

$$K^0_\nabla(s) = (t_+ - t_-) = \sigma_0(s)\tilde\lambda_0^{1/2}(s), \tag{K.38}$$
$$K^1_\nabla(s) = (N_\nabla\Lambda^-_\nabla - M_\nabla\Lambda^+_\nabla)(t_+ - t_-) = 2\left(t_+\sigma_+(t_+)\log\tau_+ + t_-\sigma_+(t_-)\log\tau_-\right)\sigma_0(s)\tilde\lambda_0^{1/2}(s), \tag{K.39}$$
$$K^2_\nabla(s) = N_\nabla\Lambda^+_\nabla - M_\nabla\Lambda^-_\nabla = 2\left(t_+\sigma_+(t_+)\log\tau_+ - t_-\sigma_+(t_-)\log\tau_-\right), \tag{K.40}$$
$$K^3_\nabla(s) = -N_\nabla M_\nabla = \log^2\tau_+ - \log^2\tau_-. \tag{K.41}$$

These functions are discussed in Appendix F.1.4. In terms of them the results of integrations

$$I_n = I_n(t_+) - I_n(t_-) \tag{K.42}$$

read

$$I_0 = 3K^0_\nabla(s) + \frac{1}{2}K^2_\nabla(s) + m^2_{\pi^\pm}K^3_\nabla(s), \tag{K.43}$$
$$I_1 = \left(\frac{5}{4}(3\tilde s_0 - s) - m^2_{\pi^\pm}\right)K^0_\nabla(s) + \frac{1}{8}\left(K^1_\nabla(s) + (\tilde\Delta_0 - 4\Delta - s)K^2_\nabla(s)\right) + m^4_{\pi^\pm}K^3_\nabla(s), \tag{K.44}$$
$$I_2 = \left(\frac{7}{9}\left((3\tilde s_0 - s)^2 - m^2_{\pi^0}\frac{\tilde\Delta_0^2}{s}\right) - \frac{m^2_{\pi^\pm}}{6}(3\tilde s_0 - s) - 2m^4_{\pi^\pm}\right)K^0_\nabla(s) + 2m^6_{\pi^\pm}K^3_\nabla(s) + \frac{1}{12}\Bigg((\tilde\Delta_c + 3m^2_{\pi^0} - s)K^1_\nabla(s) + \left((3\tilde s_0 - s)^2 - m^2_{\pi^\pm}(3\tilde s_0 - s + 12m^2_{\pi^\pm}) - 2m^2_{\pi^0}\frac{\tilde\Delta_0^2}{s}\right)K^2_\nabla(s)\Bigg), \tag{K.45}$$

[2]For $s > \frac{1}{2}\tilde\Delta_0$ we could again use the $\tau \leftrightarrow \frac{1}{\tau}$ symmetry of the primitive functions and use $\hat\sigma_-(s) = -\sigma_+(t_-(s))$ and $\hat\tau_-(s) = \frac{1}{\tau_-(s)}$, whose complex argument belongs to the interval $(-\pi, \pi\rangle$. This would then simplify again the computation of functions $K^i_\nabla(s)$ using some computer algebra system.

$$
\begin{aligned}
I_3 = {} & 5m_{\pi^\pm}^8 K_\nabla^3(s) + \frac{1}{48}\left(3(3\tilde{s}_0 - s)^2 - 2m_{\pi^\pm}^2(3\tilde{s}_0 - s) - 10m_{\pi^\pm}^4 - 3m_{\pi^0}^2\frac{\tilde{\Delta}_0^2}{s}\right) K_\nabla^1(s) \\
& + \frac{1}{16}\Bigg(9(3\tilde{s}_0 - s)\left((3\tilde{s}_0 - s)^2 - 2m_{\pi^0}^2\frac{\tilde{\Delta}_0^2}{s}\right) - \frac{8}{9}m_{\pi^\pm}^2\Big((3\tilde{s}_0 - s)^2 - m_{\pi^0}^2\frac{\tilde{\Delta}_0^2}{s}\Big) \\
& \qquad - \frac{20}{3}m_{\pi^\pm}^4(3\tilde{s}_0 - s) - 80m_{\pi^\pm}^6\Bigg) K_\nabla^0(s) \\
& + \frac{1}{48}\Bigg(3(3\tilde{s}_0 - s)\Big((3\tilde{s}_0 - s)^2 - 3m_{\pi^0}^2\frac{\tilde{\Delta}_0^2}{s}\Big) - 2m_{\pi^\pm}^2\Big((3\tilde{s}_0 - s)^2 - 2m_{\pi^0}^2\frac{\tilde{\Delta}_0^2}{s}\Big) \\
& \qquad - 10m_{\pi^\pm}^4(3\tilde{s}_0 - s) - 120m_{\pi^\pm}^6\Bigg) K_\nabla^2(s),
\end{aligned}
\tag{K.46}
$$

$$
I_{-1} = \frac{s}{2m_{\pi^0}^2\tilde{\Delta}_0^2}\left(K_\nabla^1(s) - (3\tilde{s}_0 - s)K_\nabla^2(s)\right) - \frac{1}{2}K_\nabla^3(s), \tag{K.47}
$$

$$
I_{-2} = \frac{s^2}{24m_{\pi^\pm}^2 m_{\pi^0}^4\tilde{\Delta}_0^4}\Bigg(\Big(-4m_{\pi^\pm}^2(3\tilde{s}_0 - s)^2 + m_{\pi^0}^2\frac{\tilde{\Delta}_0^2}{s}(3\tilde{s}_0 - s + 8m_{\pi^\pm}^2)\Big)K_\nabla^2(s) \tag{K.48}
$$

$$
+ \Big(4m_{\pi^\pm}^2(3\tilde{s}_0 - s) - m_{\pi^0}^2\frac{\tilde{\Delta}_0^2}{s}\Big)K_\nabla^1(s)\Bigg) + \frac{4s}{3m_{\pi^0}^2\tilde{\Delta}_0^2}K_\nabla^0(s). \tag{K.49}
$$

K.4 Computation of S and P waves of $P\pi \to \pi\pi$ processes in the isospin limit

As was already stated, we can obtain the results of integrations (3.30) and (3.31) for $P\pi \to \pi\pi$ in the isospin case simply by limiting $m_{\pi^\pm} \to m_{\pi^0}$ in the results of either the previous section or of Section K.2. This fact can be used as a partial check of the computations of those two sections.

We proceed here very briefly. Trajectories of endpoints of integration (K.2) simplify with respect to the situation on Figure 37 into the ones depicted on Figure 43. Note that here the points H, I, and J melt into $s = \infty$. Similarly, the points where $t_-(s) = 4m_\pi^2$, i.e. where $\sigma_\pi(t_-) = 0$, coincide now with the point C.

Relations (K.9) and (K.31) for the square of the kinematic square root simplify into

$$
\sigma_\pi^2(t_\pm(s)) = \frac{1}{4t_\pm^2(s)}\left(\tilde{\lambda}^{1/2}(s) \pm \sigma_\pi(s)(\tilde{\Delta} - s)\right)^2 = \left(\frac{\tilde{\lambda}^{1/2}(s) \pm s\sigma_\pi(s)}{\tilde{\Delta}}\right)^2. \tag{K.50}
$$

It implies the possibility to define a naive square root equal

$$
\hat{\sigma}_\pm(s) = \frac{\tilde{\lambda}^{1/2}(s) \pm s\sigma_\pi(s)}{\tilde{\Delta}}. \tag{K.51}
$$

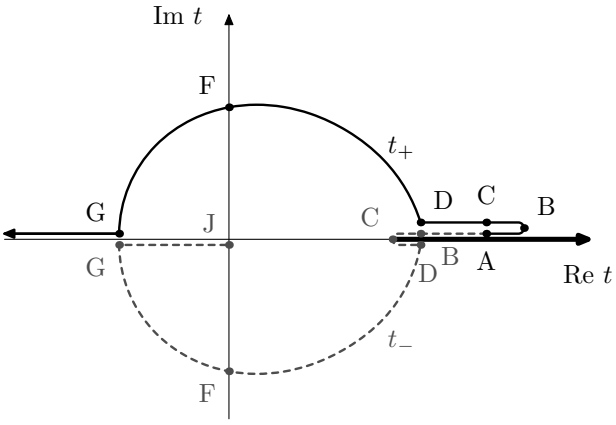

	s	$t_+(s)$	$t_-(s)$
	$-\infty$	∞	0
	$m_\pi^2(1-Q)$	$\tilde{\mu}^+$	$m_\pi^2(1-Q)$
	0	$\frac{3}{2}\tilde{s}_0 \mp i\infty$	
A	$4m_\pi^2$	$\frac{1}{2}\tilde{\Delta}$	
B	$m_\pi^2(1+Q)$	$\tilde{\mu}^-$	$m_\pi^2(1+Q)$
C	$\frac{1}{2}\tilde{\Delta}$	$\frac{1}{2}\tilde{\Delta}$	$4m_\pi^2$
D	$\tilde{\mu}^-$	$m_\pi^2(1+Q)$	
F	$3\tilde{s}_0$	$0 \pm i\frac{m_\pi\tilde{\Delta}}{\sqrt{3\tilde{s}_0}}$	
G	$\tilde{\mu}^+$	$m_\pi^2(1-Q)$	
J	∞	$-\infty$	0

Figure 43: Trajectories of the endpoints of integration $t_\pm(s)$ that occur in the computation of partial waves of $P\pi \to \pi\pi$ amplitude in the isospin limit.

The correct square root has the course similar to Figure 41, where we have to shrink the interval $s \in (t_-(4m_{\pi^\pm}^2), t_+(4m_{\pi^\pm}^2))$ into one point $s = \frac{1}{2}\tilde{\Delta}$. The naive square root $\hat{\sigma}_\pm(s)$ differs only for $s > \frac{1}{2}\tilde{\Delta}$, where $\hat{\sigma}_-(s) = -\sigma_-(s)$. The real part of the naive square root $\hat{\sigma}_-(s)$ is therefore monotonously decreasing function of s.

From that there follows the naive value of the transformed endpoints

$$\hat{\tau}_\pm(s) = -\frac{1}{4m_\pi^2}\left(1 \mp \sigma_\pi(s)\right)\left(\tilde{\Delta} - s - \tilde{\lambda}^{1/2}(s)\right), \tag{K.52}$$

which is in correspondence with relation (K.11).

The behavior of the correct values of $\tau_\pm(s)$ is displayed on Figure 44, the only difference between these and the naive values are in $\tau_-(s)$ for $s > \frac{1}{2}\tilde{\Delta}$, where they are reciprocal values to each other, i.e.

$$\operatorname{Re}\hat{\tau}_-(s) = \frac{1}{\operatorname{Re}\tau_-(s)}, \quad \operatorname{Im}\hat{\tau}_-(s) = -\operatorname{Im}\tau_-(s) \qquad \text{for } s > \frac{1}{2}\tilde{\Delta}. \tag{K.53}$$

However, thanks to the symmetries of the primitive functions we can also use instead of $\sigma(t_-)$ and $\tau_-(s)$ the naive values (K.51) and (K.52) with all the advantages we have discussed in the previous two situations.

For the sum and for the difference of logarithms we have again the simple relations (K.15)–(K.17). This means that the functions appearing in (K.34)–(K.37) have simple

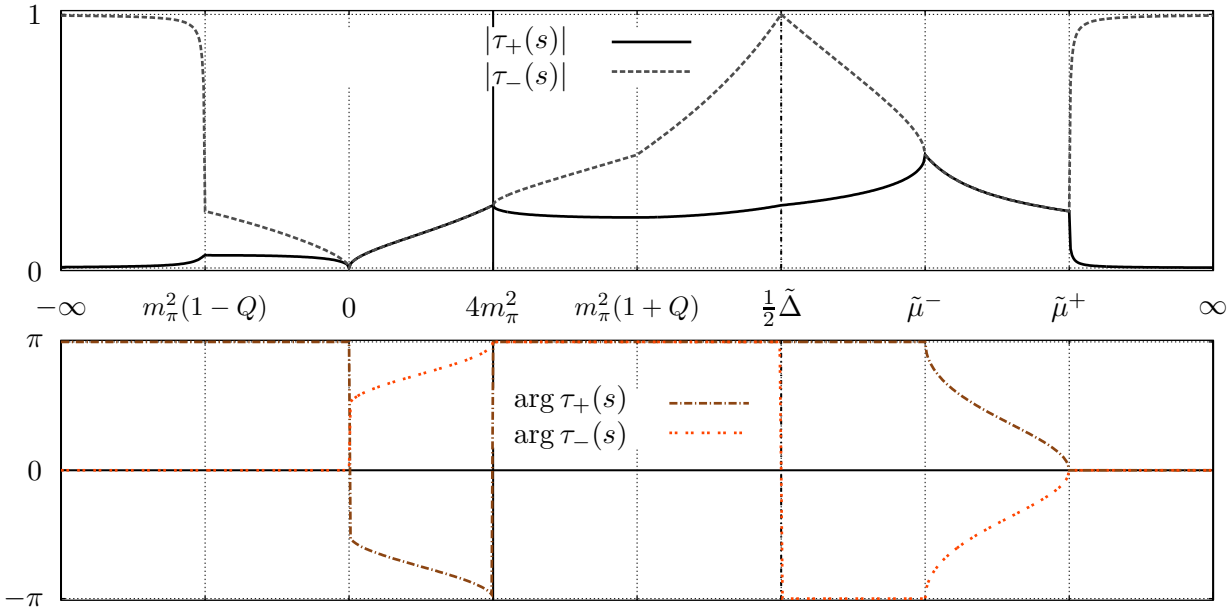

Figure 44: Transformed trajectories of endpoints of integrations from the computation of partial waves of $P\pi \to \pi\pi$ amplitude in the isospin limit.

limits[3]

$$N_\nabla(s) \to L_0(s), \qquad \Lambda_\nabla^+(s) \to \tilde{\lambda}^{1/2}(s), \tag{K.55}$$

$$M_\nabla(s) \to M_0(s), \qquad \Lambda_\nabla^-(s) \to \sigma_\pi(s)(\tilde{\Delta} - s). \tag{K.56}$$

Thus, we know that in the primitive functions there will appear only the functions

$$K_\nabla^0(s) \to \sigma_\pi(s)\tilde{\lambda}^{1/2}(s), \tag{K.57}$$

$$K_\nabla^1(s) \to \left(3\tilde{s}_0 - s - 4m_\pi^2\frac{\tilde{\Delta}}{s}\right) L_0(s)\tilde{\lambda}^{1/2}(s) - \tilde{\lambda}(s)M_0(s)\sigma_\pi(s) \tag{K.58}$$

$$K_\nabla^2(s) \to L_0(s)\tilde{\lambda}^{1/2}(s) - (\tilde{\Delta} - s)M_0(s)\sigma_\pi(s) \tag{K.59}$$

$$K_\nabla^3(s) \to -M_0(s)L_0(s). \tag{K.60}$$

Finally, limiting (K.43)–(K.49), we obtain the following results for differences of primitive functions evaluated in the endpoints

$$I_0 = 3\sigma_\pi(s)\tilde{\lambda}^{1/2}(s) + \frac{1}{2}\left(L_0(s)\tilde{\lambda}^{1/2}(s) - (\tilde{\Delta} - s)M_0(s)\sigma_\pi(s)\right) - m_\pi^2 M_0(s)L_0(s), \tag{K.61}$$

[3]This relations hold in this form only if we take there instead of $\tau_-(s)$ the naive value $\hat{\tau}_-(s)$, otherwise for $s > \frac{1}{2}\tilde{\Delta}$ there are interchanged

$$N_\nabla(s) \leftrightarrow -M_\nabla(s), \qquad \Lambda_\nabla^+(s) \leftrightarrow \Lambda_\nabla^-(s) \tag{K.54}$$

in these relations for limits.

$$
\begin{aligned}
I_1 &= \frac{1}{4}\left(-5s + 5m_P^2 + 11m_\pi^2\right)\sigma_\pi(s)\tilde{\lambda}^{1/2}(s) - m_\pi^4 M_0(s)L_0(s) \\
&\quad + \frac{1}{4}\left(\frac{1}{s}(s-2m_\pi^2)(\tilde{\Delta}-s)L_0(s)\tilde{\lambda}^{1/2}(s) - (s^2 - 2sm_P^2 + \tilde{\Delta}^2)M_0(s)\sigma_0(s)\right),
\end{aligned}
\tag{K.62}
$$

$$
\begin{aligned}
I_2 &= \frac{1}{6}\left((s-m_P^2)^2 - m_\pi^2\left(5s + 2m_\pi^2 - 7m_P^2 + 3\tilde{\Sigma}\frac{\tilde{\Delta}}{s}\right)\right)L_0(s)\tilde{\lambda}^{1/2}(s) \\
&\quad + \frac{1}{6}\left((s-m_P^2)^3 - m_\pi^2\left(4s^2 + 3s(m_\pi^2 - 2m_P^2) + 5m_\pi^4 - 9m_\pi^2 m_P^2 + 3m_P^4 - \frac{\tilde{\Delta}^3}{s}\right)\right)M_0(s)\sigma_\pi(s) \\
&\quad + \left(\frac{7}{9}(s-m_P^2)^2 + \frac{9}{2}m_\pi^2(\tilde{\Sigma}-s) - \frac{7}{9}m_\pi^2\frac{\tilde{\Delta}^2}{s}\right)\sigma_\pi(s)\tilde{\lambda}^{1/2}(s) - 2m_\pi^6 M_0(s)L_0(s),
\end{aligned}
\tag{K.63}
$$

$$
\begin{aligned}
I_3 &= -5m_\pi^8 M_0(s)L_0(s) \\
&\quad + \frac{1}{144}\Bigg(m_\pi^2\Big(721s^2 - 7s(206m_P^2 + 297m_\pi^2) + (883m_P^4 + 1755m_P^2 m_\pi^2 + 1377m_\pi^4) \\
&\qquad\qquad - 2\frac{\tilde{\Delta}^2}{s}(81m_P^2 + 239m_\pi^2)\Big) + 81(m_P^2 - s)^3\Bigg)\sigma_\pi(s)\tilde{\lambda}^{1/2}(s) \\
&\quad + \frac{1}{24}\Bigg(m_\pi^2\Big(25s^2 - s(56m_P^2 + 53m_\pi^2) + 43m_P^4 + 67m_P^2 m_\pi^2 - 53m_\pi^4 \\
&\qquad\qquad - 6\frac{\tilde{\Delta}}{s}(2m_P^4 + 7m_P^2 m_\pi^2 + m_\pi^4) + 6m_\pi^2\frac{\tilde{\Delta}^3}{s^2}\Big) + 3(m_P^2 - s)^3\Bigg)L_0(s)\tilde{\lambda}^{1/2}(s) \\
&\quad + \frac{1}{12}\Bigg(m_\pi^2\Big(11s^3 - 10s^2(3m_P^2 + 2m_\pi^2) + 6s(5m_P^4 + 3m_P^2 m_\pi^2 - 4m_\pi^4) - 14m_P^6 + 3m_P^4 m_\pi^2 \\
&\qquad\qquad + 42m_P^2 m_\pi^4 - \frac{59}{2}m_\pi^6 + (3m_P^2 + 5m_\pi^2)\frac{\tilde{\Delta}^3}{s}\Big) - \frac{3}{2}(m_P^2 - s)^4\Bigg)M_0(s)\sigma_\pi(s),
\end{aligned}
\tag{K.64}
$$

$$
I_{-1} = \frac{2}{\tilde{\Delta}}\left(sM_0(s)\sigma_\pi(s) - L_0(s)\tilde{\lambda}^{1/2}(s)\right) + \frac{1}{2}M_0(s)L_0(s), \tag{K.65}
$$

$$
\begin{aligned}
I_{-2} &= \frac{4s}{3m_\pi^2\tilde{\Delta}^2}\sigma_0(s)\tilde{\lambda}^{1/2}(s) + \frac{1}{6m_\pi^2\tilde{\Delta}^3}\left(4s^2 - 2s(m_P^2 + 7m_\pi^2) + \tilde{\Delta}^2\right)L_0(s)\tilde{\lambda}^{1/2}(s) \\
&\quad - \frac{1}{6m_\pi^2\tilde{\Delta}^3}\left(4s^2 - 2s(3m_P^2 + 5m_\pi^2) + 3\tilde{\Delta}^2\right)M_0(s)\sigma_\pi(s).
\end{aligned}
\tag{K.66}
$$

K.5 Construction of partial waves of $P\pi \to \pi\pi$ for $m_P < 3m_\pi$

We want to add a short comment on computation of the partial waves in the case that the mass of particle P kinematically forbids its decay into those three pions, i.e. the case when there should be no problem with the definition of the partial waves and with the validity of the dispersion relations. For the sake of concreteness, we will speak here about process

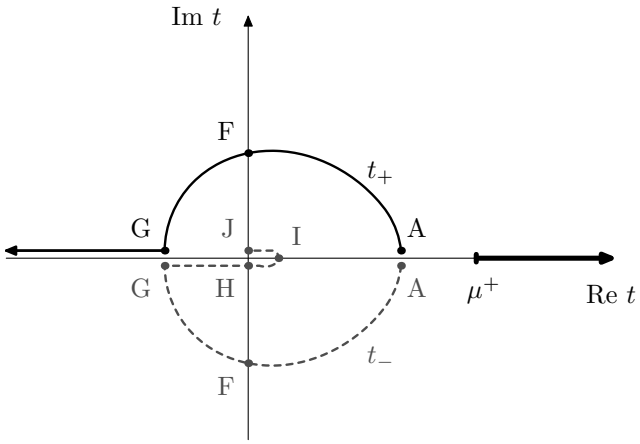

Figure 45: Trajectories of the endpoints of integration $t_\pm(s)$ that occur in computation of partial waves of $P\pi \to \pi\pi$ amplitude for an unphysical mass of m_P.

$P\pi^0 \to \pi^+\pi^-$ from Section K.2 and take some unphysical mass $m_P < 2m_{\pi^\pm} + m_{\pi^0}$, but it should be obvious that the similar situation arises for any such process.

In this case the threshold $s = 4m_{\pi^\pm}^2$ from which we need to integrate the partial waves is larger than $\tilde{\mu}_0^-$ (point D on Figure 37), so here we are interested only in the part of the trajectory that begins at point D. In addition, this point is in this case moved left from the branching point $t = \mu^+$, i.e. $\mathrm{Re}\, t_\pm(s) < \mu^+$, for $s > 4m_{\pi^\pm}^2$.

Therefore, these trajectories (cf. Figure 45) never meet the branch cut of the integrands, where the contour of the dispersion integrals is located, and we have no problem in their computation. Moreover, any infinitesimal displacement of all contours $\mathcal{C}(t_-, t_+)$ leaves the results of integrations (3.30) and (3.31) the same and so in principle there exists only one analytic continuation of the partial waves of $P\pi \to \pi\pi$ below their physical threshold $\tilde{\mu}_0^+$. With that we have verified the statement of Appendix J that the complications appear not until we want to continue the partial waves below the point D (i.e. when we compute them for $m_P > 2m_{\pi^\pm} + m_{\pi^0}$, when $4m_{\pi^\pm}^2$ goes below $\tilde{\mu}_0^-$), where $t_\pm(s)$ approach the branch cut and we need to find the right infinitesimal displacement that avoids this branch cut [= contour of dispersion integration].

Computation of partial waves of $\pi^0\pi^0 \to \pi^+\pi^-$ process

As a specific example of this type we can take the process $\pi^0\pi^0 \to \pi^+\pi^-$ that was discussed in Section 5.7.2. Repeating the discussions of Section K.2 in the limit $m_P \to m_{\pi^0}$, we should reproduce the results of Section 5.7.2. Note, however, that the particular choice of signs of $\tilde{K}^{1/2}(s)$ in (K.4) in this limit is the opposite to the choice used in Section 5.7.2 for the computations with $t_\pm(s)$, or more specifically

$$\lim_{m_P \to m_{\pi^0}} \tilde{\lambda}_0^{1/2}(s) = -s\sigma_0(s). \tag{K.67}$$

Thus, as is discussed below relation (K.6), by performing this limit we obtain the expressions for $t_+(s)$ and $t_-(s)$ interchanged — this change of sign in integrals (3.30)–(3.31) should be afterwards compensated by the limit (K.67) of all the further appearances of $\tilde{\lambda}_0^{1/2}(s)$ in the expressions (3.30)–(3.31). Since now the threshold for the dispersion relations $s = 4m_{\pi^\pm}^2$ is even larger than $\tilde{\mu}_0^+ \to 4m_{\pi^0}^2$, the endpoints $t_\pm(s)$ move with the values of s that are needed just on the real part of the axis — on Figure 45 this corresponds to the part of GHIJ trajectories, far below the branch point μ^+.

The triangle function in these endpoints simplifies into [by taking the limit of (K.9)]

$$\lambda(t_\pm(s)) = \frac{1}{4}\big(-s\sigma_0(s) \pm (-s)\sigma_\pm(s)\big)^2 = \frac{1}{4}\big(s(\sigma_0(s) \pm \sigma_+(s))\big)^2. \tag{K.68}$$

The choice of sign from (3.16) leads to [cf. with (5.85)]

$$\lambda^{1/2}(t_\pm(s)) = -\frac{s}{2}\left(\sigma_0(s) \pm \sigma_+(s)\right). \tag{K.69}$$

The conformal transformation (3.36) then reads

$$\tau(t_\pm(s)) = \frac{s}{4m_{\pi^0}m_{\pi^\pm}}\big(1 \mp \sigma_+(s)\big)\big(1 - \sigma_0(s)\big) \tag{K.70}$$

and since function $M_0(s)$ from (K.19) goes in the limit

$$\lim_{m_P \to m_{\pi^0}} M_0(s) = -L_0(s), \tag{K.71}$$

to function $L_0(s)$ from (5.68), relations (K.15)–(K.17) simplify in this case into

$$\log\hat{\tau}_+ - \log\hat{\tau}_- = L_+(s), \tag{K.72}$$

$$\log\hat{\tau}_+ + \log\hat{\tau}_- = L_0(s), \tag{K.73}$$

$$\log^2\hat{\tau}_+ - \log^2\hat{\tau}_- = L_+(s)L_0(s), \tag{K.74}$$

which is in correspondence with (5.89)–(5.91) taking into account the interchange of t_+ and t_- here.

Appendix L

Polynomials of the NLO partial waves of the $P\pi \to \pi\pi$ scatterings

We list here the polynomials multiplying the dimensionless functions from Appendix F in our expressions for the NLO partial waves of $P\pi \to \pi\pi$ amplitudes and also in our NNLO results for these amplitudes.

L.1 Isospin limit

- $K^\pm\pi^\pm \to \pi^\pm\pi^\pm$

$$\tilde{p}_\lambda^{Cd;0} = \frac{C_c}{F_\pi^4}(s-\tilde{s}_0)^2 + \frac{2D_c}{3F_\pi^4}\left(s^2 - 3s\tilde{s}_0 + 3\tilde{s}_0^2 - m_\pi^2\frac{\tilde{\Delta}^2}{s}\right), \tag{L.1}$$

$$\begin{aligned}\tilde{p}_0^{Cd;0} = {} & A_x\left(31a - \frac{b}{4F_\pi^2}\left(23s - 15m_P^2 + 335m_\pi^2\right)\right) \\ & + \frac{B_x}{4F_\pi^2}\left(\frac{b}{9F_\pi^2}\left(28s^2 - s(41m_P^2 - 63m_\pi^2) + 13m_P^4 + 48m_P^2m_\pi^2 + 99m_\pi^4 - 28m_\pi^2\frac{\tilde{\Delta}^2}{s}\right)\right. \\ & \qquad \left. - a\left(5s - \tilde{\Delta}\right)\right) \\ & + \frac{B_c}{6F_\pi^2}\left(\frac{b}{18F_\pi^2}\left(181s^2 - s(137m_P^2 - 1215m_\pi^2) + 2(14m_P^4 - 135m_P^2m_\pi^2 - 279m_\pi^4)\right.\right. \\ & \qquad \left.\left. - 28m_\pi^2\frac{\tilde{\Delta}^2}{s}\right) - a\left(27s - 7m_P^2 - 9m_\pi^2\right)\right),\end{aligned} \tag{L.2}$$

$$\tilde{p}_1^{Cd;0} = \frac{A_x}{2}\left(9a - \frac{b}{2F_\pi^2}\left(3s - 3m_P^2 + 53m_\pi^2 + 6m_\pi^2\frac{\tilde{\Delta}}{s}\right)\right) +$$

$$
\begin{aligned}
&+\frac{B_x}{12F_\pi^2}\bigg(\frac{b}{F_\pi^2}\Big(2s^2-s(3m_P^2-5m_\pi^2)+(m_P^2+5m_\pi^2)\tilde{\Sigma}-4m_\pi^2(m_P^2-6m_\pi^2)\frac{\tilde{\Delta}}{s}\Big)\\
&\qquad\qquad -a\Big(3s-m_P^2+3m_\pi^2+6m_\pi^2\frac{\tilde{\Delta}}{s}\Big)\bigg)\\
&+\frac{B_c}{6F_\pi^2}\bigg(\frac{b}{6F_\pi^2}\Big(5s^2-s(7m_P^2-59m_\pi^2)+2(\tilde{\Delta}^2+6m_\pi^4)-6m_\pi^2(m_P^2-15m_\pi^2)\frac{\tilde{\Delta}}{s}\Big)\\
&\qquad\qquad -a\Big(3s-m_P^2+3m_\pi^2+6m_\pi^2\frac{\tilde{\Delta}}{s}\Big)\bigg),
\end{aligned}
\tag{L.3}
$$

$$
\begin{aligned}
\tilde{p}_{1\mathrm{P}}^{Cd;0} &= \frac{A_x}{2}\bigg(9a\Big(1-\frac{\tilde{\Delta}}{s}\Big)-\frac{b}{2F_\pi^2}\Big(3s-6m_P^2+56m_\pi^2+(3m_P^2-59m_\pi^2)\frac{\tilde{\Delta}}{s}\Big)\bigg)\\
&+\frac{B_x}{12F_\pi^2}\bigg(\frac{b}{F_\pi^2}\Big(2s^2-s(5m_P^2-7m_\pi^2)+2(2m_P^4-5m_P^2m_\pi^2+9m_\pi^4)\\
&\qquad -(m_P^4+2m_P^2m_\pi^2+29m_\pi^4)\frac{\tilde{\Delta}}{s}+2m_\pi^2\frac{\tilde{\Delta}^3}{s^2}\Big)\\
&\qquad -a\Big(3s-4m_P^2+6m_\pi^2+(m_P^2-9m_\pi^2)\frac{\tilde{\Delta}}{s}\Big)\bigg)\\
&+\frac{B_c}{6F_\pi^2}\bigg(\frac{b}{6F_\pi^2}\Big(5s^2-4s(3m_P^2-16m_\pi^2)+3(3m_P^4-30m_P^2m_\pi^2+31m_\pi^4)\\
&\qquad -2(m_P^4-8m_P^2m_\pi^2+55m_\pi^4)\frac{\tilde{\Delta}}{s}+2m_\pi^2\frac{\tilde{\Delta}^3}{s^2}\Big)\\
&\qquad -a\Big(3s-4m_P^2+6m_\pi^2+(m_P^2-9m_\pi^2)\frac{\tilde{\Delta}}{s}\Big)\bigg),
\end{aligned}
\tag{L.4}
$$

$$
\begin{aligned}
\tilde{p}_{2\mathrm{P}}^{Cd;0} &= A_x\left(9a-\frac{25b}{F_\pi^2}m_\pi^2\right)-\frac{B_x}{3F_\pi^2}\left(am_P^2-\frac{3b}{F_\pi^2}m_\pi^2\tilde{\Sigma}\right)\\
&-\frac{B_c}{3F_\pi^2}\left(2am_P^2-\frac{b}{F_\pi^2}m_\pi^2(3s+4m_P^2-2m_\pi^2)\right),
\end{aligned}
\tag{L.5}
$$

$$
\tilde{p}_3^{Cd;0} = \left(A_x-\frac{B_c}{2F_\pi^2}(s-\tilde{s}_0)\right)\left(2a-\frac{b}{F_\pi^2}(s+4m_\pi^2)\right). \tag{L.6}
$$

- $K^\pm\pi^\mp \to \pi^\pm\pi^\mp$

$$
\tilde{p}_\lambda^{Cc;0} = \frac{C_c}{3F_\pi^4}\left(s^2-3s\tilde{s}_0+3\tilde{s}_0^2-m_\pi^2\frac{\tilde{\Delta}^2}{s}\right)+\frac{D_c}{3F_\pi^4}\left(4s^2-9s\tilde{s}_0+6\tilde{s}_0^2-m_\pi^2\frac{\tilde{\Delta}^2}{s}\right), \tag{L.7}
$$

$$
\tilde{p}_0^{Cc;0} = \frac{A_x}{2}\left(57a+\frac{b}{4F_\pi^2}\left(19s+5m_P^2-645m_\pi^2\right)\right)+
$$

$$+\frac{B_x}{24F_\pi^2}\Big(\frac{b}{3F_\pi^2}\Big(100s^2-s(65m_P^2+297m_\pi^2)+13m_P^4+144m_P^2m_\pi^2+387m_\pi^4 \\ -28m_\pi^2\frac{\tilde\Delta^2}{s}\Big)+a\left(9s-5m_P^2-27m_\pi^2\right)\Big) \\ +\frac{B_c}{F_\pi^2}\Big(\frac{b}{216F_\pi^2}\Big(203s^2-s(181m_P^2+1917m_\pi^2)+2(25m_P^4+423m_P^2m_\pi^2+1008m_\pi^4) \\ -140m_\pi^2\frac{\tilde\Delta^2}{s}\Big)+2a\left(s-\tilde s_0\right)\Big),$$

(L.8)

$$\tilde p_1^{Cc;0}=\frac{A_x}{4}\Big(13a-\frac{b}{2F_\pi^2}\Big(s-m_P^2+71m_\pi^2+2m_\pi^2\frac{\tilde\Delta}{s}\Big)\Big) \\ +\frac{B_x}{24F_\pi^2}\Big(\frac{b}{F_\pi^2}\Big(2s^2-s(3m_P^2-5m_\pi^2)+(m_P^2+5m_\pi^2)\tilde\Sigma-4m_\pi^2(m_P^2-6m_\pi^2)\frac{\tilde\Delta}{s}\Big) \\ -a\Big(3s-m_P^2+3m_\pi^2+6m_\pi^2\frac{\tilde\Delta}{s}\Big)\Big) \\ +\frac{B_cb}{72F_\pi^4}\Big(7s^2-s(11m_P^2+29m_\pi^2)+4(m_P^4+10m_P^2m_\pi^2+4m_\pi^4)-18m_\pi^2(m_P^2-3m_\pi^2)\frac{\tilde\Delta}{s}\Big),$$

(L.9)

$$\tilde p_{1\mathrm{P}}^{Cc;0}=\frac{A_x}{4}\Big(13a\Big(1-\frac{\tilde\Delta}{s}\Big)-\frac{b}{2F_\pi^2}\Big(s-2m_P^2+72m_\pi^2+(m_P^2-73m_\pi^2)\frac{\tilde\Delta}{s}\Big)\Big) \\ +\frac{B_x}{24F_\pi^2}\Big(\frac{b}{F_\pi^2}\Big(2s^2-s(5m_P^2-7m_\pi^2)+2(2m_P^4-5m_P^2m_\pi^2+9m_\pi^4) \\ -(m_P^4+2m_P^2m_\pi^2+29m_\pi^4)\frac{\tilde\Delta}{s}+2m_\pi^2\frac{\tilde\Delta^3}{s^2}\Big) \\ -a\Big(3s-4m_P^2+6m_\pi^2+(m_P^2-9m_\pi^2)\frac{\tilde\Delta}{s}\Big)\Big) \\ +\frac{B_cb}{72F_\pi^4}\Big(7s^2-2s(9m_P^2+11m_\pi^2)+15\tilde\Sigma^2-4(m_P^4+7m_P^2m_\pi^2+16m_\pi^4)\frac{\tilde\Delta}{s}+10m_\pi^2\frac{\tilde\Delta^3}{s^2}\Big),$$

(L.10)

$$\tilde p_{2\mathrm{P}}^{Cc;0}=\frac{A_x}{2}\left(13a-\frac{35b}{F_\pi^2}m_\pi^2\right)-\frac{B_x}{6F_\pi^2}\left(am_P^2-\frac{3b}{F_\pi^2}m_\pi^2\tilde\Sigma\right)-\frac{B_cb}{6F_\pi^4}m_\pi^2(3s-2m_P^2-8m_\pi^2),$$

(L.11)

$$\tilde p_3^{Cc;0}=\frac{A_x}{2}\left(9a+\frac{b}{F_\pi^2}(3s-28m_\pi^2)\right)+\frac{B_x}{F_\pi^2}\Big(a+\frac{b}{2F_\pi^2}(s-4m_\pi^2)\Big)(s-\tilde s_0) \qquad \text{(L.12)}$$

$$+\frac{B_c}{F_\pi^2}\Big(a+\frac{b}{4F_\pi^2}(s-12m_\pi^2)\Big)(s-\tilde s_0). \qquad \text{(L.13)}$$

$$\tilde{p}_{\lambda}^{Cc;1} = \frac{C_c - D_c}{6F_\pi^4}\,(s - \tilde{s}_0)\,, \tag{L.14}$$

$$\begin{aligned}
\tilde{p}_{0}^{Cc;1} = \frac{5A_x}{4m_\pi^2}\Bigg(&\frac{b}{18F_\pi^2}\Big(11s^2 - 2s(11m_P^2 + 81m_\pi^2) + 11m_P^4 + 162m_P^2m_\pi^2 + 531m_\pi^4 \\
&\qquad - 56m_\pi^2\frac{\tilde{\Delta}^2}{s}\Big) + a(s - m_P^2 - 7m_\pi^2)\Bigg) \\
- \frac{B_x}{72F_\pi^2m_\pi^2}\Bigg(&\frac{b}{6F_\pi^2}\Big(75s^3 - 7s^2(29m_P^2 + 51m_\pi^2) + s(181m_P^4 + 390m_P^2m_\pi^2 - 783m_\pi^4) \\
&\qquad - 53m_P^6 - 351m_P^4m_\pi^2 + 2481m_P^2m_\pi^4 + 2787m_\pi^6 \\
&\qquad + 2m_\pi^2(103m_P^2 - 375m_\pi^2)\frac{\tilde{\Delta}^2}{s}\Big) \\
&- a\Big(11s^2 - 4s(7m_P^2 + 27m_\pi^2) + 17m_P^4 + 150m_P^2m_\pi^2 + 153m_\pi^4 - 56m_\pi^2\frac{\tilde{\Delta}^2}{s}\Big)\Bigg) \\
+ \frac{B_c}{18F_\pi^2m_\pi^2}\Bigg(&\frac{b}{24F_\pi^2}\Big(71s^3 - s^2(167m_P^2 + 1497m_\pi^2) + s(121m_P^4 + 2958m_P^2m_\pi^2 + 9693m_\pi^4) \\
&\qquad - 25m_P^6 - 1775m_P^4m_\pi^2 - 10811m_P^2m_\pi^4 - 12221m_\pi^6 + 2m_\pi^2(53m_P^2 + 2139m_\pi^2)\frac{\tilde{\Delta}^2}{s}\Big) \\
&+ a\Big(11s^2 - 4s(7m_P^2 + 27m_\pi^2) + 17m_P^4 + 150m_P^2m_\pi^2 + 153m_\pi^4 - 56m_\pi^2\frac{\tilde{\Delta}^2}{s}\Big)\Bigg),
\end{aligned} \tag{L.15}$$

$$\begin{aligned}
\tilde{p}_{1}^{Cc;1} = \frac{5A_x}{2m_\pi^2}\Bigg(&\frac{b}{12F_\pi^2}\Big(s^2 - 2s(m_P^2 + 4m_\pi^2) + m_P^4 + 10m_P^2m_\pi^2 + 37m_\pi^4 \\
&\qquad - 6m_\pi^2(m_P^2 - 9m_\pi^2)\frac{\tilde{\Delta}}{s}\Big) - am_\pi^2\Big(1 + \frac{\tilde{\Delta}}{s}\Big)\Bigg) \\
- \frac{B_x}{24F_\pi^2m_\pi^2}\Bigg(&\frac{b}{3F_\pi^2}\Big(3s^3 - 4s^2(2m_P^2 + 3m_\pi^2) + s(7m_P^4 + 22m_P^2m_\pi^2 - 39m_\pi^4) \\
&\qquad - 2(m_P^6 + 13m_P^4m_\pi^2 - 50m_P^2m_\pi^4 - 42m_\pi^6) \\
&\qquad + 6m_\pi^2(2m_P^4 + 3m_P^2m_\pi^2 + 33m_\pi^4)\frac{\tilde{\Delta}}{s} - 18m_\pi^4\frac{\tilde{\Delta}^3}{s^2}\Big) \\
&- a\Big(s^2 - 2s(m_P^2 + 4m_\pi^2) + \tilde{\Sigma}^2 + 12m_P^2m_\pi^2 - 2m_\pi^2(m_P^2 - 9m_\pi^2)\frac{\tilde{\Delta}}{s}\Big)\Bigg) \\
+ \frac{B_c}{6F_\pi^2m_\pi^2}\Bigg(&\frac{b}{12F_\pi^2}\Big(2s^3 - s^2(5m_P^2 + 49m_\pi^2) + 2s(2m_P^4 + 47m_P^2m_\pi^2 + 160m_\pi^4) \\
&\qquad - (m_P^6 + 55m_P^4m_\pi^2 + 433m_P^2m_\pi^4 + 99m_\pi^6) \\
&\qquad + 6m_\pi^2(m_P^4 + 11m_P^2m_\pi^2 - 106m_\pi^4)\frac{\tilde{\Delta}}{s} - 6m_\pi^4\frac{\tilde{\Delta}^3}{s^2}\Big) \\
&+ a\Big(s^2 - 2s(m_P^2 + 4m_\pi^2) + \tilde{\Sigma}^2 + 12m_P^2m_\pi^2 - 2m_\pi^2(m_P^2 - 9m_\pi^2)\frac{\tilde{\Delta}}{s}\Big)\Bigg),
\end{aligned} \tag{L.16}$$

$$\begin{aligned}
\tilde{p}_{1\mathrm{P}}^{Cc;1} = \frac{5A_x}{2m_\pi^2}\Bigg(&\frac{b}{12F_\pi^2}\Big(s^2 - s(3m_P^2+7m_\pi^2) + 3(m_P^4+4m_P^2m_\pi^2+11m_\pi^4) \\
&\quad - (m_P^4+10m_P^2m_\pi^2+85m_\pi^4)\frac{\tilde{\Delta}}{s} + 4m_\pi^2\frac{\tilde{\Delta}^3}{s^2}\Big) - am_\pi^2(1-2\frac{\tilde{\Delta}}{s})\Bigg) \\
-\frac{B_x}{24F_\pi^2m_\pi^2}\Bigg(&\frac{b}{3F_\pi^2}\Big(3s^3 - s^2(11m_P^2+9m_\pi^2) + s(15m_P^4+14m_P^2m_\pi^2-39m_\pi^4) \\
&\quad - 3(3m_P^6+5m_P^4m_\pi^2-47m_P^2m_\pi^4-13m_\pi^6) \\
&\quad + 2(m_P^6+10m_P^4m_\pi^2-95m_P^2m_\pi^4-108m_\pi^6)\frac{\tilde{\Delta}}{s} - 8m_\pi^2(m_P^2-6m_\pi^2)\frac{\tilde{\Delta}^3}{s^2}\Big) \\
&- a\Big(s^2 - s(3m_P^2+7m_\pi^2) + 3m_P^4 + 16m_P^2m_\pi^2 - 3m_\pi^4 \\
&\quad - (m_P^4+18m_P^2m_\pi^2+13m_\pi^4)\frac{\tilde{\Delta}}{s} + 4m_\pi^2\frac{\tilde{\Delta}^3}{s^2}\Big)\Bigg) \\
+\frac{B_c}{6F_\pi^2m_\pi^2}\Bigg(&\frac{b}{12F_\pi^2}\Big(2s^3 - s^2(7m_P^2+47m_\pi^2) + s(9m_P^4+130m_P^2m_\pi^2+279m_\pi^4) \\
&\quad - (5m_P^6+129m_P^4m_\pi^2+627m_P^2m_\pi^4-173m_\pi^6) \\
&\quad + (m_P^6+51m_P^4m_\pi^2+615m_P^2m_\pi^4+485m_\pi^6)\frac{\tilde{\Delta}}{s} - 4m_\pi^2(m_P^2+33m_\pi^2)\frac{\tilde{\Delta}^3}{s^2}\Big) \\
&+ a\Big(s^2 - s(3m_P^2+7m_\pi^2) + 3m_P^4 + 16m_P^2m_\pi^2 - 3m_\pi^4 \\
&\quad - (m_P^4+18m_P^2m_\pi^2+13m_\pi^4)\frac{\tilde{\Delta}}{s} + 4m_\pi^2\frac{\tilde{\Delta}^3}{s^2}\Big)\Bigg),
\end{aligned} \tag{L.17}$$

$$\begin{aligned}
\tilde{p}_{2\mathrm{P}}^{Cc;1} = \frac{5A_x}{2m_\pi^2}&\left(a(s-\tilde{\Sigma}) - \frac{b}{F_\pi^2}m_\pi^2(3s-3m_P^2-5m_\pi^2)\right) \\
-\frac{B_x}{6F_\pi^2m_\pi^2}&\left(a\big(m_P^2(s-\tilde{\Sigma}) - 6m_\pi^4\big) - \frac{b}{F_\pi^2}m_\pi^2(3s\tilde{\Sigma} - 3m_P^4 - 8m_P^2m_\pi^2 - 15m_\pi^4)\right) + \\
-\frac{B_c}{6F_\pi^2m_\pi^2}&\Bigg(4a\big(m_P^2(s-\tilde{\Sigma}) - 6m_\pi^4\big) + \frac{b}{F_\pi^2}m_\pi^2\big(3s^2 - s(15m_P^2+7m_\pi^2) \\
&\quad + 2(6m_P^4+7m_P^2m_\pi^2+36m_\pi^4)\big)\Bigg),
\end{aligned} \tag{L.18}$$

$$\tilde{p}_3^{Cc;1} = \frac{B_c b}{36F_\pi^4}(s-4m_\pi^2). \tag{L.19}$$

- $K^\pm\pi^\mp \to \pi^0\pi^0$

$$\tilde{p}_\lambda^{Cx;0} = \frac{C_x}{F_\pi^4}(s-\tilde{s}_0)^2 + \frac{2D_x}{3F_\pi^4}\left(s^2 - 3s\tilde{s}_0 + 3\tilde{s}_0^2 - m_\pi^2\frac{\tilde{\Delta}^2}{s}\right), \tag{L.20}$$

$$\tilde{p}_0^{Cx;0} = -A_x\left(13a + \frac{b}{4F_\pi^2}\left(21s - 5m_P^2 - 155m_\pi^2\right)\right) - \frac{B_c}{F_\pi^2}(s-\tilde{s}_0)\left(a + \frac{b}{F_\pi^2}(s-4m_\pi^2)\right)$$
$$- \frac{B_x}{4F_\pi^2}\Bigg(\frac{b}{27F_\pi^2}\Big(11s^2 - s(22m_P^2 + 1566m_\pi^2) + 11m_P^4 + 558m_P^2m_\pi^2 + 1287m_\pi^4$$
$$- 56m_\pi^2\frac{\tilde{\Delta}^2}{s}\Big) + a\left(17s - 5m_P^2 - 11m_\pi^2\right)\Bigg), \tag{L.21}$$

$$\tilde{p}_1^{Cx;0} = -A_x\Big(a + \frac{b}{4F_\pi^2}\Big(s - m_P^2 - 9m_\pi^2 + 2m_\pi^2\frac{\tilde{\Delta}}{s}\Big)\Big)$$
$$- \frac{B_x}{12F_\pi^2}\Big(\frac{b}{3F_\pi^2}\Big(s^2 - 2s(m_P^2 + 22m_\pi^2) + \tilde{\Sigma}^2 + 20m_P^2m_\pi^2 - 18m_\pi^2\tilde{s}_0\frac{\tilde{\Delta}}{s}\Big) \tag{L.22}$$
$$+ a\Big(3s - m_P^2 + 3m_\pi^2 + 6m_\pi^2\frac{\tilde{\Delta}}{s}\Big)\Big),$$

$$\tilde{p}_{1\mathrm{P}}^{Cx;0} = -A_x\Big(a\Big(1 - \frac{\tilde{\Delta}}{s}\Big) + \frac{b}{4F_\pi^2}\Big(s - 2m_P^2 - 8m_\pi^2 + (m_P^2 + 7m_\pi^2)\frac{\tilde{\Delta}}{s}\Big)\Big)$$
$$- \frac{B_x}{12F_\pi^2}\Big(\frac{b}{3F_\pi^2}\Big(s^2 - s(3m_P^2 + 43m_\pi^2) + 3m_P^4 + 60m_P^2m_\pi^2 - 39m_\pi^4 - (m_P^2 + 23m_\pi^2)\frac{\tilde{\Delta}^2}{s}$$
$$+ 4m_\pi^2\frac{\tilde{\Delta}^3}{s^2}\Big) + a\Big(3s - 4m_P^2 + 6m_\pi^2 + (m_P^2 - 9m_\pi^2)\frac{\tilde{\Delta}}{s}\Big)\Big), \tag{L.23}$$

$$\tilde{p}_{2\mathrm{P}}^{Cx;0} = -A_x\Big(2a - \frac{5b}{F_\pi^2}m_\pi^2\Big) - \frac{B_x}{3F_\pi^2}\Big(am_P^2 - \frac{b}{F_\pi^2}m_\pi^2(3s + m_P^2 - 5m_\pi^2)\Big), \tag{L.24}$$

$$\tilde{p}_3^{Cx;0} = -A_x\Big(\frac{7a}{2} + \frac{2b}{F_\pi^2}(s - 6m_\pi^2)\Big) - \frac{B_x}{2F_\pi^2}\Big(3a - \frac{8b}{F_\pi^2}m_\pi^2\Big)(s-\tilde{s}_0)$$
$$- \frac{B_c}{2F_\pi^2}\Big(a + \frac{b}{F_\pi^2}(s-4m_\pi^2)\Big)(s-\tilde{s}_0). \tag{L.25}$$

- $K^\pm\pi^0 \to \pi^\pm\pi^0$

$$\tilde{p}_\lambda^{Ct;0} = -\frac{C_x}{3F_\pi^4}\left(s^2 - 3s\tilde{s}_0 + 3\tilde{s}_0^2 - m_\pi^2\frac{\tilde{\Delta}^2}{s}\right) - \frac{D_x}{3F_\pi^4}\left(4s^2 - 9s\tilde{s}_0 + 6\tilde{s}_0^2 - m_\pi^2\frac{\tilde{\Delta}^2}{s}\right), \tag{L.26}$$

$$\tilde{p}_0^{Ct;0} = \frac{A_x}{2}\left(31a - \frac{b}{4F_\pi^2}(23s - 15m_P^2 + 335m_\pi^2)\right)$$
$$+ \frac{B_x}{12F_\pi^2}\Bigg(\frac{b}{18F_\pi^2}\Big(181s^2 - s(137m_P^2 - 1215m_\pi^2) + 2(14m_P^4 - 135m_P^2m_\pi^2 - 279m_\pi^4)$$
$$- 28m_\pi^2\frac{\tilde{\Delta}^2}{s}\Big) - a\left(27s - 7m_P^2 - 9m_\pi^2\right)\Bigg) +$$

$$+\frac{B_c}{8F_\pi^2}\Big(\frac{b}{9F_\pi^2}\Big(28s^2-s(41m_P^2-63m_\pi^2)+13m_P^4+48m_P^2m_\pi^2+99m_\pi^4 \\ -28m_\pi^2\frac{\tilde\Delta^2}{s}\Big)-a\Big(5s-\tilde\Delta\Big)\Big), \tag{L.27}$$

$$\tilde p_1^{Ct;0}=\frac{A_x}{4}\Big(9a-\frac{b}{2F_\pi^2}\Big(3s-3m_P^2+53m_\pi^2+6m_\pi^2\frac{\tilde\Delta}{s}\Big)\Big) \\ +\frac{B_x}{12F_\pi^2}\Big(\frac{b}{6F_\pi^2}\Big(5s^2-s(7m_P^2-59m_\pi^2)+2(\tilde\Delta^2+6m_\pi^4)-6m_\pi^2(m_P^2-15m_\pi^2)\frac{\tilde\Delta}{s}\Big) \\ -a\Big(3s-m_P^2+3m_\pi^2+6m_\pi^2\frac{\tilde\Delta}{s}\Big)\Big) \\ +\frac{B_c}{24F_\pi^2}\Big(\frac{b}{F_\pi^2}\Big(2s^2-s(3m_P^2-5m_\pi^2)+(m_P^2+5m_\pi^2)\tilde\Sigma-4m_\pi^2(m_P^2-6m_\pi^2)\frac{\tilde\Delta}{s}\Big) \\ -a\Big(3s-m_P^2+3m_\pi^2+6m_\pi^2\frac{\tilde\Delta}{s}\Big)\Big), \tag{L.28}$$

$$\tilde p_{1\mathrm{P}}^{Ct;0}=\frac{A_x}{4}\Big(9a\Big(1-\frac{\tilde\Delta}{s}\Big)-\frac{b}{2F_\pi^2}\Big(3s-6m_P^2+56m_\pi^2+(3m_P^2-59m_\pi^2)\frac{\tilde\Delta}{s}\Big)\Big) \\ +\frac{B_x}{12F_\pi^2}\Big(\frac{b}{6F_\pi^2}\Big(5s^2-4s(3m_P^2-16m_\pi^2)+3(3m_P^4-30m_P^2m_\pi^2+31m_\pi^4) \\ -2(m_P^4-8m_P^2m_\pi^2+55m_\pi^4)\frac{\tilde\Delta}{s}+2m_\pi^2\frac{\tilde\Delta^3}{s^2}\Big) \\ -a\Big(3s-4m_P^2+6m_\pi^2+(m_P^2-9m_\pi^2)\frac{\tilde\Delta}{s}\Big)\Big)+ \\ +\frac{B_c}{24F_\pi^2}\Big(\frac{b}{F_\pi^2}\Big(2s^2-s(5m_P^2-7m_\pi^2)+2(2m_P^4-5m_P^2m_\pi^2+9m_\pi^4) \\ -(\tilde\Sigma^2+28m_\pi^4)\frac{\tilde\Delta}{s}+2m_\pi^2\frac{\tilde\Delta^3}{s^2}\Big) \\ -a\Big(3s-4m_P^2+6m_\pi^2+(m_P^2-9m_\pi^2)\frac{\tilde\Delta}{s}\Big)\Big), \tag{L.29}$$

$$\tilde p_{2\mathrm{P}}^{Ct;0}=\frac{A_x}{2}\left(9a-\frac{25b}{F_\pi^2}m_\pi^2\right)-\frac{B_x}{6F_\pi^2}\left(2am_P^2-\frac{b}{F_\pi^2}m_\pi^2(3s+4m_P^2-2m_\pi^2)\right) \\ -\frac{B_c}{6F_\pi^2}\left(am_P^2-3\frac{b}{F_\pi^2}m_\pi^2\tilde\Sigma\right), \tag{L.30}$$

$$\tilde p_3^{Ct;0}=\left(A_x-\frac{B_x}{2F_\pi^2}(s-\tilde s_0)\right)\left(a-\frac{b}{2F_\pi^2}(s+4m_\pi^2)\right). \tag{L.31}$$

$$\tilde{p}_{\lambda}^{Ct;1} = \frac{C_x - D_x}{6F_\pi^4}\,(s - \tilde{s}_0)\,, \tag{L.32}$$

$$\begin{aligned}
\tilde{p}_{0}^{Ct;1} = {}& \frac{5A_x}{4m_\pi^2}\bigg(\frac{b}{18F_\pi^2}\Big(11s^2 - 2s(11m_P^2 + 81m_\pi^2) + 11m_P^4 + 162m_P^2m_\pi^2 + 531m_\pi^4 \\
& - 56m_\pi^2\frac{\tilde{\Delta}^2}{s}\Big) + a(s - m_P^2 - 7m_\pi^2)\bigg) \\
& + \frac{B_x}{18F_\pi^2m_\pi^2}\bigg(\frac{b}{24F_\pi^2}\Big(71s^3 - s^2(167m_P^2 + 1497m_\pi^2) + s(121m_P^4 + 2958m_P^2m_\pi^2 + 9693m_\pi^4) \\
& - 25m_P^6 - 1775m_P^4m_\pi^2 - 10811m_P^2m_\pi^4 - 12221m_\pi^6 \\
& + 2m_\pi^2(53m_P^2 + 2139m_\pi^2)\frac{\tilde{\Delta}^2}{s}\Big) \\
& + a\Big(11s^2 - 4s(7m_P^2 + 27m_\pi^2) + 17m_P^4 + 150m_P^2m_\pi^2 + 153m_\pi^4 - 56m_\pi^2\frac{\tilde{\Delta}^2}{s}\Big)\bigg) \\
& - \frac{B_c}{72F_\pi^2m_\pi^2}\bigg(\frac{b}{6F_\pi^2}\Big(75s^3 - 7s^2(29m_P^2 + 51m_\pi^2) + s(181m_P^4 + 390m_P^2m_\pi^2 - 783m_\pi^4) - 53m_P^6 \\
& - 351m_P^4m_\pi^2 + 2481m_P^2m_\pi^4 + 2787m_\pi^6 + 2m_\pi^2(103m_P^2 - 375m_\pi^2)\frac{\tilde{\Delta}^2}{s}\Big) \\
& - a\Big(11s^2 - 4s(7m_P^2 + 27m_\pi^2) + 17m_P^4 + 150m_P^2m_\pi^2 + 153m_\pi^4 - 56m_\pi^2\frac{\tilde{\Delta}^2}{s}\Big)\bigg),
\end{aligned} \tag{L.33}$$

$$\begin{aligned}
\tilde{p}_{1}^{Ct;1} = {}& \frac{5A_x}{2m_\pi^2}\bigg(\frac{b}{12F_\pi^2}\Big(s^2 - 2s(m_P^2 + 4m_\pi^2) + m_P^4 + 10m_P^2m_\pi^2 + 37m_\pi^4 \\
& - 6m_\pi^2(m_P^2 - 9m_\pi^2)\frac{\tilde{\Delta}}{s}\Big) - am_\pi^2\Big(1 + \frac{\tilde{\Delta}}{s}\Big)\bigg) \\
& + \frac{B_x}{6F_\pi^2m_\pi^2}\bigg(\frac{b}{12F_\pi^2}\Big(2s^3 - s^2(5m_P^2 + 49m_\pi^2) + 2s(2m_P^4 + 47m_P^2m_\pi^2 + 160m_\pi^4) \\
& - (m_P^6 + 55m_P^4m_\pi^2 + 433m_P^2m_\pi^4 + 99m_\pi^6) \\
& + 6m_\pi^2(m_P^4 + 11m_P^2m_\pi^2 - 106m_\pi^4)\frac{\tilde{\Delta}}{s} - 6m_\pi^4\frac{\tilde{\Delta}^3}{s^2}\Big) \\
& + a\Big(s^2 - 2s(m_P^2 + 4m_\pi^2) + m_P^4 + 14m_P^2m_\pi^2 + m_\pi^4 - 2m_\pi^2(m_P^2 - 9m_\pi^2)\frac{\tilde{\Delta}}{s}\Big)\bigg) \\
& - \frac{B_c}{24F_\pi^2m_\pi^2}\bigg(\frac{b}{3F_\pi^2}\Big(3s^3 - 4s^2(2m_P^2 + 3m_\pi^2) + s(7m_P^4 + 22m_P^2m_\pi^2 - 39m_\pi^4) \\
& - 2(m_P^6 + 13m_P^4m_\pi^2 - 50m_P^2m_\pi^4 - 42m_\pi^6) \\
& + 6m_\pi^2(2m_P^4 + 3m_P^2m_\pi^2 + 33m_\pi^4)\frac{\tilde{\Delta}}{s} - 18m_\pi^4\frac{\tilde{\Delta}^3}{s^2}\Big) \\
& - a\Big(s^2 - 2s(m_P^2 + 4m_\pi^2) + \tilde{\Sigma}^2 + 12m_P^2m_\pi^2 - 2m_\pi^2(m_P^2 - 9m_\pi^2)\frac{\tilde{\Delta}}{s}\Big)\bigg),
\end{aligned} \tag{L.34}$$

$$\begin{aligned}
\tilde{p}_{1\mathrm{P}}^{Ct;1} = \frac{5A_x}{2m_\pi^2}\Bigg(&\frac{b}{12F_\pi^2}\Big(s^2 - s(3m_P^2+7m_\pi^2) + 3(m_P^4+4m_P^2m_\pi^2+11m_\pi^4) \\
&\qquad - (m_P^4+10m_P^2m_\pi^2+85m_\pi^4)\frac{\tilde{\Delta}}{s} + 4m_\pi^2\frac{\tilde{\Delta}^3}{s^2}\Big) - am_\pi^2\Big(1-2\frac{\tilde{\Delta}}{s}\Big)\Bigg) \\
+\frac{B_x}{6F_\pi^2m_\pi^2}\Bigg(&\frac{b}{12F_\pi^2}\Big(2s^3 - s^2(7m_P^2+47m_\pi^2) + s(9m_P^4+130m_P^2m_\pi^2+279m_\pi^4) \\
&\qquad - (5m_P^6+129m_P^4m_\pi^2+627m_P^2m_\pi^4-173m_\pi^6) \\
&\qquad + (m_P^6+51m_P^4m_\pi^2+615m_P^2m_\pi^4+485m_\pi^6)\frac{\tilde{\Delta}}{s} - 4m_\pi^2(m_P^2+33m_\pi^2)\frac{\tilde{\Delta}^3}{s^2}\Big) \\
&+ a\Big(s^2 - s(3m_P^2+7m_\pi^2) + 3m_P^4 + 16m_P^2m_\pi^2 - 3m_\pi^4 \\
&\qquad - (m_P^4+18m_P^2m_\pi^2+13m_\pi^4)\frac{\tilde{\Delta}}{s} + 4m_\pi^2\frac{\tilde{\Delta}^3}{s^2}\Big)\Bigg) \\
-\frac{B_c}{24F_\pi^2m_\pi^2}\Bigg(&\frac{b}{3F_\pi^2}\Big(3s^3 - s^2(11m_P^2+9m_\pi^2) + s(15m_P^4+14m_P^2m_\pi^2-39m_\pi^4) \\
&\qquad - 3(3m_P^6+5m_P^4m_\pi^2-47m_P^2m_\pi^4-13m_\pi^6) \\
&\qquad + 2(m_P^6+10m_P^4m_\pi^2-95m_P^2m_\pi^4-108m_\pi^6)\frac{\tilde{\Delta}}{s} - 8m_\pi^2(m_P^2-6m_\pi^2)\frac{\tilde{\Delta}^3}{s^2}\Big) \\
&- a\Big(s^2 - s(3m_P^2+7m_\pi^2) + 3m_P^4 + 16m_P^2m_\pi^2 - 3m_\pi^4 \\
&\qquad - (m_P^4+18m_P^2m_\pi^2+13m_\pi^4)\frac{\tilde{\Delta}}{s} + 4m_\pi^2\frac{\tilde{\Delta}^3}{s^2}\Big)\Bigg),
\end{aligned} \tag{L.35}$$

$$\begin{aligned}
\tilde{p}_{2\mathrm{P}}^{Ct;1} = \frac{5A_x}{2m_\pi^2}&\left(a(s-\tilde{\Sigma}) - \frac{b}{F_\pi^2}m_\pi^2(3s-3m_P^2-5m_\pi^2)\right) \\
-\frac{B_x}{6F_\pi^2m_\pi^2}&\Big(\frac{b}{F_\pi^2}m_\pi^2(3s^2 - s(15m_P^2+7m_\pi^2) + 2(6m_P^4+7m_P^2m_\pi^2+36m_\pi^4)) \\
&\qquad + 4a(sm_P^2 - m_P^4 - m_P^2m_\pi^2 - 6m_\pi^4)\Big) \\
-\frac{B_c}{6F_\pi^2m_\pi^2}&\left(a(sm_P^2 - m_P^4 - m_P^2m_\pi^2 - 6m_\pi^4) - \frac{b}{F_\pi^2}m_\pi^2(3s\tilde{\Sigma} - 3m_P^4 - 8m_P^2m_\pi^2 - 15m_\pi^4)\right),
\end{aligned} \tag{L.36}$$

$$\tilde{p}_3^{Ct;1} = \frac{B_xb}{36F_\pi^4}(s-4m_\pi^2). \tag{L.37}$$

- $K^L\pi^0 \to \pi^\pm\pi^\mp$

$$\tilde{p}_\lambda^{Lx;0} = \frac{C_x}{F_\pi^4}(s-\tilde{s}_0)^2 + \frac{2D_x}{3F_\pi^4}\left(s^2 - 3s\tilde{s}_0 + 3\tilde{s}_0^2 - m_\pi^2\frac{\tilde{\Delta}^2}{s}\right), \tag{L.38}$$

$$\tilde{p}_0^{Lx;0} = -A_x\left(13a + \frac{b}{4F_\pi^2}\left(21s - 5m_P^2 - 155m_\pi^2\right)\right) - \frac{B_x}{12F_\pi^2}\left(\frac{b}{9F_\pi^2}\Big(119s^2 - s(58m_P^2 + 2106m_\pi^2) + 11m_P^4 + 702m_P^2m_\pi^2 + 1719m_\pi^4 - 56m_\pi^2\frac{\tilde{\Delta}^2}{s}\Big) + a\left(63s - 19m_P^2 - 45m_\pi^2\right)\right) \tag{L.39}$$

$$\tilde{p}_1^{Lx;0} = -A_x\Big(a + \frac{b}{4F_\pi^2}\Big(s - m_P^2 - 9m_\pi^2 + 2m_\pi^2\frac{\tilde{\Delta}}{s}\Big)\Big) - \frac{B_x}{12F_\pi^2}\Big(\frac{b}{3F_\pi^2}\Big(s^2 - 2s(m_P^2 + 22m_\pi^2) + \tilde{\Sigma}^2 + 20m_P^2m_\pi^2 - 18m_\pi^2\tilde{s}_0\frac{\tilde{\Delta}}{s}\Big) + a\Big(3s - m_P^2 + 3m_\pi^2 + 6m_\pi^2\frac{\tilde{\Delta}}{s}\Big)\Big), \tag{L.40}$$

$$\tilde{p}_{1\mathrm{P}}^{Lx;0} = -A_x\Big(a\Big(1 - \frac{\tilde{\Delta}}{s}\Big) + \frac{b}{4F_\pi^2}\Big(s - 2m_P^2 - 8m_\pi^2 + (m_P^2 + 7m_\pi^2)\frac{\tilde{\Delta}}{s}\Big)\Big) - \frac{B_x}{12F_\pi^2}\Big(\frac{b}{3F_\pi^2}\Big(s^2 - s(3m_P^2 + 43m_\pi^2) + 3m_P^4 + 60m_P^2m_\pi^2 - 39m_\pi^4 - (m_P^2 + 23m_\pi^2)\frac{\tilde{\Delta}^2}{s} + 4m_\pi^2\frac{\tilde{\Delta}^3}{s^2}\Big) + a\Big(3s - 4m_P^2 + 6m_\pi^2 + (m_P^2 - 9m_\pi^2)\frac{\tilde{\Delta}}{s}\Big)\Big), \tag{L.41}$$

$$\tilde{p}_{2\mathrm{P}}^{Lx;0} = -A_x\Big(2a - \frac{5b}{F_\pi^2}m_\pi^2\Big) - \frac{B_x}{3F_\pi^2}\Big(am_P^2 - \frac{b}{F_\pi^2}m_\pi^2(3s + m_P^2 - 5m_\pi^2)\Big), \tag{L.42}$$

$$\tilde{p}_3^{Lx;0} = -A_x\Big(\frac{7a}{2} + \frac{2b}{F_\pi^2}(s - 6m_\pi^2)\Big) - \frac{B_x}{2F_\pi^2}\Big(4a + \frac{b}{F_\pi^2}(s - 12m_\pi^2)\Big)(s - \tilde{s}_0). \tag{L.43}$$

- $K^L\pi^\pm \to \pi^0\pi^\pm$

$$\tilde{p}_\lambda^{Lt;0} = -\frac{C_x}{3F_\pi^4}\left(s^2 - 3s\tilde{s}_0 + 3\tilde{s}_0^2 - m_\pi^2\frac{\tilde{\Delta}^2}{s}\right) - \frac{D_x}{3F_\pi^4}\left(4s^2 - 9s\tilde{s}_0 + 6\tilde{s}_0^2 - m_\pi^2\frac{\tilde{\Delta}^2}{s}\right), \tag{L.44}$$

$$\tilde{p}_0^{Lt;0} = \frac{A_x}{2}\left(31a - \frac{b}{4F_\pi^2}(23s - 15m_P^2 + 335m_\pi^2)\right) + \frac{B_x}{24F_\pi^2}\Big(\frac{b}{9F_\pi^2}\Big(265s^2 - 52s(5m_P^2 - 27m_\pi^2) + 67m_P^4 - 126m_P^2m_\pi^2 - 261m_\pi^4 - 112m_\pi^2\frac{\tilde{\Delta}^2}{s}\Big) - a\left(69s - 17m_P^2 - 15m_\pi^2\right)\Big), \tag{L.45}$$

$$\tilde{p}_1^{Lt;0} = \frac{A_x}{4}\Big(9a - \frac{b}{2F_\pi^2}\Big(3s - 3m_P^2 + 53m_\pi^2 + 6m_\pi^2\frac{\tilde{\Delta}}{s}\Big)\Big) + \frac{B_x}{8F_\pi^2}\Big(\frac{b}{9F_\pi^2}\Big(11s^2 - s(16m_P^2 - 74m_\pi^2) + 5m_P^4 + 14m_P^2m_\pi^2 + 29m_\pi^4 - 18m_\pi^2(m_P^2 - 9m_\pi^2)\frac{\tilde{\Delta}}{s}\Big) - a\Big(3s - m_P^2 + 3m_\pi^2 + 6m_\pi^2\frac{\tilde{\Delta}}{s}\Big)\Big), \tag{L.46}$$

$$\tilde{p}_{1\mathrm{P}}^{Lt;0} = \frac{A_x}{4}\Big(9a\Big(1 - \frac{\tilde{\Delta}}{s}\Big) - \frac{b}{2F_\pi^2}\Big(3s - 6m_P^2 + 56m_\pi^2 + (3m_P^2 - 59m_\pi^2)\frac{\tilde{\Delta}}{s}\Big)\Big) + \frac{B_x}{8F_\pi^2}\Big(\frac{b}{9F_\pi^2}\Big(11s^2 - s(27m_P^2 - 85m_\pi^2) + 3(7m_P^4 - 40m_P^2m_\pi^2 + 49m_\pi^4) - (5\tilde{\Delta}^2 + 192m_\pi^4)\frac{\tilde{\Delta}}{s} + 8m_\pi^2\frac{\tilde{\Delta}^3}{s^2}\Big) - a\Big(3s - 4m_P^2 + 6m_\pi^2 + (m_P^2 - 9m_\pi^2)\frac{\tilde{\Delta}}{s}\Big)\Big), \tag{L.47}$$

$$\tilde{p}_{2\mathrm{P}}^{Lt;0} = \frac{A_x}{2}\left(9a - \frac{25b}{F_\pi^2}m_\pi^2\right) - \frac{B_x}{6F_\pi^2}\left(3am_P^2 - \frac{b}{F_\pi^2}m_\pi^2(3s + 7m_P^2 + m_\pi^2)\right), \tag{L.48}$$

$$\tilde{p}_3^{Lt;0} = \left(A_x - \frac{B_x}{2F_\pi^2}(s - \tilde{s}_0)\right)\left(a - \frac{b}{2F_\pi^2}(s + 4m_\pi^2)\right). \tag{L.49}$$

$$\tilde{p}_\lambda^{Lt;1} = \frac{C_x - D_x}{6F_\pi^4}(s - \tilde{s}_0), \tag{L.50}$$

$$\tilde{p}_0^{Lt;1} = \frac{5A_x}{4m_\pi^2}\Big(\frac{b}{18F_\pi^2}\Big(11s^2 - 2s(11m_P^2 + 81m_\pi^2) + 11m_P^4 + 162m_P^2m_\pi^2 + 531m_\pi^4 - 56m_\pi^2\frac{\tilde{\Delta}^2}{s}\Big) + a(s - m_P^2 - 7m_\pi^2)\Big) - \frac{B_x}{36F_\pi^2m_\pi^2}\Big(\frac{b}{3F_\pi^2}\Big(s^3 - 3s^2(3m_P^2 - 95m_\pi^2) + 3s(5m_P^4 - 214m_P^2m_\pi^2 - 873m_\pi^4) - 7m_P^6 + 356m_P^4m_\pi^2 + 3323m_P^2m_\pi^4 + 3752m_\pi^6 + m_\pi^2(25m_P^2 - 1257m_\pi^2)\frac{\tilde{\Delta}^2}{s}\Big) - \frac{5a}{2}\Big(11s^2 - 4s(7m_P^2 + 27m_\pi^2) + 17m_P^4 + 150m_P^2m_\pi^2 + 153m_\pi^4 - 56m_\pi^2\frac{\tilde{\Delta}^2}{s}\Big)\Big), \tag{L.51}$$

$$\tilde{p}_1^{Lt;1} = \frac{5A_x}{2m_\pi^2}\Big(\frac{b}{12F_\pi^2}\Big(s^2 - 2s(m_P^2 + 4m_\pi^2) + m_P^4 + 10m_P^2m_\pi^2 + 37m_\pi^4 - 6m_\pi^2(m_P^2 - 9m_\pi^2)\frac{\tilde{\Delta}}{s}\Big) - am_\pi^2\Big(1 + \frac{\tilde{\Delta}}{s}\Big)\Big) +$$

$$
\begin{aligned}
&- \frac{B_x}{24F_\pi^2 m_\pi^2}\Bigg(\frac{b}{3F_\pi^2}\Big(s^3 - s^2(3m_P^2 - 37m_\pi^2) + s(3m_P^4 - 72m_P^2m_\pi^2 - 359m_\pi^4) \\
&\qquad - (m_P^6 - 29m_P^4m_\pi^2 - 533m_P^2m_\pi^4 - 183m_\pi^6) \\
&\qquad + 6m_\pi^2(m_P^4 - 8m_P^2m_\pi^2 + 139m_\pi^4)\frac{\tilde{\Delta}}{s} - 12m_\pi^4\frac{\tilde{\Delta}^3}{s^2}\Big) \\
&\quad - 5a\Big(s^2 - 2s(m_P^2 + 4m_\pi^2) + m_P^4 + 14m_P^2m_\pi^2 + m_\pi^4 - 2m_\pi^2(m_P^2 - 9m_\pi^2)\frac{\tilde{\Delta}}{s}\Big)\Bigg),
\end{aligned}
\tag{L.52}
$$

$$
\begin{aligned}
\tilde{p}_{1\mathrm{P}}^{Lt;1} = &\frac{5A_x}{2m_\pi^2}\Bigg(\frac{b}{12F_\pi^2}\Big(s^2 - s(3m_P^2 + 7m_\pi^2) + 3(m_P^4 + 4m_P^2m_\pi^2 + 11m_\pi^4) \\
&\qquad - (m_P^4 + 10m_P^2m_\pi^2 + 85m_\pi^4)\frac{\tilde{\Delta}}{s} + 4m_\pi^2\frac{\tilde{\Delta}^3}{s^2}\Big) - am_\pi^2\Big(1 - 2\frac{\tilde{\Delta}}{s}\Big)\Bigg) \\
&- \frac{B_x}{24F_\pi^2 m_\pi^2}\Bigg(\frac{b}{3F_\pi^2}\Big(s^3 - 2s^2(2m_P^2 - 19m_\pi^2) + 2s(3m_P^4 - 58m_P^2m_\pi^2 - 159m_\pi^4) \\
&\qquad - 2(2m_P^6 - 57m_P^4m_\pi^2 - 384m_P^2m_\pi^4 + 67m_\pi^6) \\
&\qquad + (m_P^6 - 31m_P^4m_\pi^2 - 805m_P^2m_\pi^4 - 701m_\pi^6)\frac{\tilde{\Delta}}{s} - 4m_\pi^2(m_P^2 - 45m_\pi^2)\frac{\tilde{\Delta}^3}{s^2}\Big) \\
&\quad - 5a\Big(s^2 - s(3m_P^2 + 7m_\pi^2) + 3m_P^4 + 16m_P^2m_\pi^2 - 3m_\pi^4 \\
&\qquad - (m_P^4 + 18m_P^2m_\pi^2 + 13m_\pi^4)\frac{\tilde{\Delta}}{s} + 4m_\pi^2\frac{\tilde{\Delta}^3}{s^2}\Big)\Bigg),
\end{aligned}
\tag{L.53}
$$

$$
\begin{aligned}
\tilde{p}_{2\mathrm{P}}^{Lt;1} = &\frac{5A_x}{2m_\pi^2}\left(a(s - \tilde{\Sigma}) - \frac{b}{F_\pi^2}m_\pi^2(3s - 3m_P^2 - 5m_\pi^2)\right) \\
&- \frac{B_x}{6F_\pi^2 m_\pi^2}\Big(\frac{b}{F_\pi^2}m_\pi^2(3s^2 - 2s(9m_P^2 + 5m_\pi^2) + 15m_P^4 + 22m_P^2m_\pi^2 + 87m_\pi^4) \\
&\qquad + 5a(sm_P^2 - m_P^4 - m_P^2m_\pi^2 - 6m_\pi^4)\Big),
\end{aligned}
\tag{L.54}
$$

$$
\tilde{p}_3^{Lt;1} = \frac{B_x b}{36F_\pi^4}(s - 4m_\pi^2). \tag{L.55}
$$

- $K^L\pi^0 \to \pi^0\pi^0$

$$
\begin{aligned}
\tilde{p}_0^{Ln;0} = &A_x\left(44a - \frac{b}{2F_\pi^2}\left(s - 5m_P^2 + 245m_\pi^2\right)\right) \\
&+ \frac{B_x}{6F_\pi^2}\Bigg(\frac{b}{3F_\pi^2}\Big(64s^2 - s(53m_P^2 + 117m_\pi^2) + 13m_P^4 + 96m_P^2m_\pi^2 + 243m_\pi^4 \\
&\qquad - 28m_\pi^2\frac{\tilde{\Delta}^2}{s}\Big) - a\left(3s + m_P^2 + 15m_\pi^2\right)\Bigg),
\end{aligned}
\tag{L.56}
$$

$$\tilde{p}_\lambda^{Ln;0} = -\frac{C_x + 2D_x}{3F_\pi^4}\Big(5s^2 - 12s\tilde{s}_0 + 9\tilde{s}_0^2 - 2m_\pi^2\frac{\tilde{\Delta}^2}{s}\Big), \tag{L.57}$$

$$\begin{aligned}\tilde{p}_1^{Ln;0} = {}& \frac{A_x}{2}\bigg(11a - \frac{b}{F_\pi^2}\Big(s - m_P^2 + 31m_\pi^2 + 2m_\pi^2\frac{\tilde{\Delta}}{s}\Big)\bigg) \\ & + \frac{B_x}{6F_\pi^2}\bigg(\frac{b}{F_\pi^2}\Big(2s^2 - s(3m_P^2 - 5m_\pi^2) + (m_P^2 + 5m_\pi^2)\tilde{\Sigma} - 4m_\pi^2(m_P^2 - 6m_\pi^2)\frac{\tilde{\Delta}}{s}\Big) \\ & \qquad - a\Big(3s - m_P^2 + 3m_\pi^2 + 6m_\pi^2\frac{\tilde{\Delta}}{s}\Big)\bigg),\end{aligned} \tag{L.58}$$

$$\begin{aligned}\tilde{p}_{1\mathrm{P}}^{Ln;0} = {}& \frac{A_x}{2}\bigg(11a\Big(1 - \frac{\tilde{\Delta}}{s}\Big) - \frac{b}{F_\pi^2}\Big(s - 2m_P^2 + 32m_\pi^2 + (m_P^2 - 33m_\pi^2)\frac{\tilde{\Delta}}{s}\Big)\bigg) \\ & + \frac{B_x}{6F_\pi^2}\bigg(\frac{b}{F_\pi^2}\Big(2s^2 - s(5m_P^2 - 7m_\pi^2) + 4m_P^4 - 10m_P^2m_\pi^2 + 18m_\pi^4 - (\tilde{\Sigma}^2 + 28m_\pi^4)\frac{\tilde{\Delta}}{s} \\ & \qquad + 2m_\pi^2\frac{\tilde{\Delta}^3}{s^2}\Big) - a\Big(3s - 4m_P^2 + 6m_\pi^2 + (m_P^2 - 9m_\pi^2)\frac{\tilde{\Delta}}{s}\Big)\bigg),\end{aligned} \tag{L.59}$$

$$\tilde{p}_{2\mathrm{P}}^{Ln;0} = A_x\Big(11a - \frac{30b}{F_\pi^2}m_\pi^2\Big) - \frac{2B_x}{3F_\pi^2}\Big(am_P^2 - \frac{3b}{F_\pi^2}m_\pi^2\tilde{\Sigma}\Big), \tag{L.60}$$

$$\tilde{p}_3^{Ln;0} = A_x\Big(\frac{11a}{2} + \frac{b}{F_\pi^2}(s - 16m_\pi^2)\Big) + \frac{B_x}{F_\pi^2}\Big(a + \frac{b}{F_\pi^2}(s - 4m_\pi^2)\Big)(s - \tilde{s}_0). \tag{L.61}$$

- $K^S\pi^0 \to \pi^+\pi^-$

$$\tilde{p}_\lambda^{Sx;1} = \frac{C_x}{3F_\pi^4}\left(s - \tilde{s}_0\right), \tag{L.62}$$

$$\begin{aligned}\tilde{p}_0^{Sx;1} = {}& -\frac{B_x}{12F_\pi^2m_\pi^2}\bigg(\frac{b}{9F_\pi^2}\Big(73s^3 - s^2(185m_P^2 + 927m_\pi^2) + s(151m_P^4 + 1674m_P^2m_\pi^2 + 4455m_\pi^4) \\ & \qquad - 39m_P^6 - 1063m_P^4m_\pi^2 - 4165m_P^2m_\pi^4 - 4717m_\pi^6 \\ & \qquad + 12m_\pi^2(13m_P^2 + 147m_\pi^2)\frac{\tilde{\Delta}^2}{s}\Big) \\ & \quad + a\Big(11s^2 - 4s(7m_P^2 + 27m_\pi^2) + 17m_P^4 + 150m_P^2m_\pi^2 + 153m_\pi^4 - 56m_\pi^2\frac{\tilde{\Delta}^2}{s}\Big)\bigg),\end{aligned} \tag{L.63}$$

$$\begin{aligned}\tilde{p}_1^{Sx;1} = {}& -\frac{B_x}{4F_\pi^2m_\pi^2}\bigg(\frac{b}{9F_\pi^2}\Big(5s^3 - s^2(13m_P^2 + 61m_\pi^2) + s(11m_P^4 + 116m_P^2m_\pi^2 + 281m_\pi^4) \\ & \qquad - 3(m_P^2 + 5m_\pi^2)(\tilde{\Sigma}^2 + 20m_P^2m_\pi^2) \\ & \qquad + 6m_\pi^2(3m_P^4 + 14m_P^2m_\pi^2 - 73m_\pi^4)\frac{\tilde{\Delta}}{s} - 24m_\pi^4\frac{\tilde{\Delta}^3}{s^2}\Big) +\end{aligned}$$

$$+ a\Big(s^2 - 2s(m_P^2 + 4m_\pi^2) + m_P^4 + 14m_P^2 m_\pi^2 + m_\pi^4 - 2m_\pi^2(m_P^2 - 9m_\pi^2)\frac{\tilde{\Delta}}{s}\Big)\Big), \tag{L.64}$$

$$\begin{aligned}\tilde{p}_{1\mathrm{P}}^{Sx;1} = -\frac{B_x}{4F_\pi^2 m_\pi^2}\Big(&\frac{b}{9F_\pi^2}\Big(5s^3 - 2s^2(9m_P^2 + 28m_\pi^2) + 24s(m_P^4 + 6m_P^2 m_\pi^2 + 10m_\pi^4)\\ &- 2(7m_P^6 + 72m_P^4 m_\pi^2 + 243m_P^2 m_\pi^4 - 106m_\pi^6)\\ &+ (3m_P^6 + 71m_P^4 m_\pi^2 + 425m_P^2 m_\pi^4 + 269m_\pi^6)\frac{\tilde{\Delta}}{s} - 12m_\pi^2(m_P^2 + 7m_\pi^2)\frac{\tilde{\Delta}^3}{s^2}\Big)\\ &+ a\Big(s^2 - s(3m_P^2 + 7m_\pi^2) + 3m_P^4 + 16m_P^2 m_\pi^2 - 3m_\pi^4\\ &- (m_P^4 + 18m_P^2 m_\pi^2 + 13m_\pi^4)\frac{\tilde{\Delta}}{s} + 4m_\pi^2\frac{\tilde{\Delta}^3}{s^2}\Big)\Big),\end{aligned} \tag{L.65}$$

$$\begin{aligned}\tilde{p}_{2\mathrm{P}}^{Sx;1} = \frac{B_x}{3F_\pi^2 m_\pi^2}\Big(&\frac{b}{F_\pi^2}m_\pi^2(3s^2 - 4s(3m_P^2 + m_\pi^2) + 9m_P^4 + 6m_P^2 m_\pi^2 + 57m_\pi^4)\\ &+ 3a(sm_P^2 - m_P^4 - m_P^2 m_\pi^2 - 6m_\pi^4)\Big),\end{aligned} \tag{L.66}$$

$$\tilde{p}_3^{Sx;1} = -\frac{B_x b}{18F_\pi^4}(s - 4m_\pi^2). \tag{L.67}$$

- $K^S\pi^+ \to \pi^0\pi^+$

$$\tilde{p}_\lambda^{St;0} = -\frac{C_x}{3F_\pi^4}(2s - \tilde{\Delta})\left(s - 2m_\pi^2 - m_\pi^2\frac{\tilde{\Delta}}{s}\right), \tag{L.68}$$

$$\begin{aligned}\tilde{p}_0^{St;0} = \frac{B_x}{8F_\pi^2}\Big(&\frac{b}{9F_\pi^2}\Big(97s^2 - 2s(7m_P^2 - 513m_\pi^2) - 11m_P^4 - 414m_P^2 m_\pi^2 - 855m_\pi^4\\ &+ 56m_\pi^2\frac{\tilde{\Delta}^2}{s}\Big) - a\Big(39s - 11m_P^2 - 21m_\pi^2\Big)\Big),\end{aligned} \tag{L.69}$$

$$\begin{aligned}\tilde{p}_1^{St;0} = -\frac{B_x}{8F_\pi^2}\Big(&\frac{b}{3F_\pi^2}\Big(s^2 - 2s(m_P^2 + 22m_\pi^2) + (m_P^4 + 22m_P^2 m_\pi^2 + m_\pi^4)\\ &- 6m_\pi^2(m_P^2 + 3m_\pi^2)\frac{\tilde{\Delta}}{s}\Big)\\ &+ a\Big(3s - (m_P^2 - 3m_\pi^2) + 6m_\pi^2\frac{\tilde{\Delta}}{s}\Big)\Big),\end{aligned} \tag{L.70}$$

$$\begin{aligned}\tilde{p}_{1\mathrm{P}}^{St;0} = -\frac{B_x}{8F_\pi^2}\Big(&\frac{b}{3F_\pi^2}\Big(s^2 - s(3m_P^2 + 43m_\pi^2) + 3(m_P^4 + 20m_P^2 m_\pi^2 - 13m_\pi^4)\\ &- (m_P^2 + 23m_\pi^2)\frac{\tilde{\Delta}^2}{s} + 4m_\pi^2\frac{\tilde{\Delta}^3}{s^2}\Big)\\ &+ a\Big(3s - 2(2m_P^2 - 3m_\pi^2) + (m_P^2 - 9m_\pi^2)\frac{\tilde{\Delta}}{s}\Big)\Big),\end{aligned} \tag{L.71}$$

$$\tilde{p}_{2\mathrm{P}}^{St;0} = -\frac{B_x}{2F_\pi^2}\Big(am_P^2 - \frac{b}{F_\pi^2}m_\pi^2(3s + m_P^2 - 5m_\pi^2)\Big), \tag{L.72}$$

$$\tilde{p}_3^{St;0} = -\frac{3B_x}{2F_\pi^2}(s - \tilde{s}_0)\Big(a - \frac{b}{2F_\pi^2}(s + 4m_\pi^2)\Big). \tag{L.73}$$

$$\tilde{p}_\lambda^{St;1} = \frac{C_x}{6F_\pi^4}\,(s - \tilde{s}_0)\,, \tag{L.74}$$

$$\begin{aligned}\tilde{p}_0^{St;1} = -\frac{B_x}{24F_\pi^2 m_\pi^2}\Bigg(&\frac{b}{9F_\pi^2}\Big(73s^3 - s^2(185m_P^2 + 927m_\pi^2) + s(151m_P^4 + 1674m_P^2m_\pi^2 + 4455m_\pi^4)\\ &- 39m_P^6 - 1063m_P^4m_\pi^2 - 4165m_P^2m_\pi^4 - 4717m_\pi^6\\ &+ 12m_\pi^2(13m_P^2 + 147m_\pi^2)\frac{\tilde{\Delta}^2}{s}\Big)\\ &+ a\Big(11s^2 - 4s(7m_P^2 + 27m_\pi^2) + 17m_P^4 + 150m_P^2m_\pi^2 + 153m_\pi^4 - 56m_\pi^2\frac{\tilde{\Delta}^2}{s}\Big)\Bigg),\end{aligned} \tag{L.75}$$

$$\begin{aligned}\tilde{p}_1^{St;1} = -\frac{B_x}{8F_\pi^2 m_\pi^2}\Bigg(&\frac{b}{9F_\pi^2}\Big(5s^3 - s^2(13m_P^2 + 61m_\pi^2) + s(11m_P^4 + 116m_P^2m_\pi^2 + 281m_\pi^4)\\ &- 3(m_P^2 + 5m_\pi^2)(m_P^4 + 22m_P^2m_\pi^2 + m_\pi^4)\\ &+ 6m_\pi^2(3m_P^4 + 14m_P^2m_\pi^2 - 73m_\pi^4)\frac{\tilde{\Delta}}{s} + 24m_\pi^4\frac{\tilde{\Delta}^3}{s^2}\Big) +\\ &+ a\Big(s^2 - 2s(m_P^2 + 4m_\pi^2) + m_P^4 + 14m_P^2m_\pi^2 + m_\pi^4 - 2m_\pi^2(m_P^2 - 9m_\pi^2)\frac{\tilde{\Delta}}{s}\Big)\Bigg),\end{aligned} \tag{L.76}$$

$$\begin{aligned}\tilde{p}_{1\mathrm{P}}^{St;1} = -\frac{B_x}{8F_\pi^2 m_\pi^2}\Bigg(&\frac{b}{9F_\pi^2}\Big(5s^3 - 2s^2(9m_P^2 + 28m_\pi^2) + 24s(m_P^4 + 6m_P^2m_\pi^2 + 10m_\pi^4)\\ &- 2(7m_P^6 + 72m_P^4m_\pi^2 + 243m_P^2m_\pi^4 - 106m_\pi^6)\\ &+ (3m_P^6 + 71m_P^4m_\pi^2 + 425m_P^2m_\pi^4 + 269m_\pi^6)\frac{\tilde{\Delta}}{s} + 12m_\pi^2(m_P^2 + 7m_\pi^2)\frac{\tilde{\Delta}^3}{s^2}\Big)\\ &+ a\Big(s^2 - s(3m_P^2 + 7m_\pi^2) + 3m_P^4 + 16m_P^2m_\pi^2 - 3m_\pi^4\\ &- (m_P^4 + 18m_P^2m_\pi^2 + 13m_\pi^4)\frac{\tilde{\Delta}}{s} + 4m_\pi^2\frac{\tilde{\Delta}^3}{s^2}\Big)\Big),\end{aligned} \tag{L.77}$$

$$\begin{aligned}\tilde{p}_{2\mathrm{P}}^{St;1} = \frac{B_x}{2F_\pi^2 m_\pi^2}\Big(&\frac{b}{3F_\pi^2}m_\pi^2(3s^2 - 4s(3m_P^2 + m_\pi^2) + 3(3m_P^4 + 2m_P^2m_\pi^2 + 19m_\pi^4))\\ &+ a(sm_P^2 - m_P^4 - m_P^2m_\pi^2 - 6m_\pi^4)\Big),\end{aligned} \tag{L.78}$$

$$\tilde{p}_3^{St;1} = -\frac{B_x b}{36F_\pi^4}(s - 4m_\pi^2). \tag{L.79}$$

L.2 The case with $m_{\pi^\pm} \neq m_{\pi^0}$

- $K_L\pi^0 \to \pi^0\pi^0$

$$\tilde{p}_\lambda^{Ln;0} = \frac{C_n}{3F_\pi^4}\Big(5s^2 - 12s\tilde{s}_0 + 9\tilde{s}_0^2 - 2m_{\pi^0}^2\frac{(3\tilde{s}_0 - 4m_{\pi^0}^2)^2}{s}\Big), \tag{L.80}$$

$$\begin{aligned}\tilde{p}_0^{\mathrm{L}n;0} = \frac{B_x}{2F_\pi^2}\Big(\frac{b_x}{9F_\pi^2}\Big(&64s^2 + 3s(16m_{\pi^\pm}^2 - 2m_{\pi^0}^2 - 53\tilde{s}_0) - 28m_{\pi^0}^2\frac{(3\tilde{s}_0 - 4m_{\pi^0}^2)^2}{s}\\ &+ 3\big(39\tilde{s}_0^2 - 6\tilde{s}_0(2m_{\pi^\pm}^2 - 5m_{\pi^0}^2) + 8m_{\pi^\pm}^2(20m_{\pi^\pm}^2 - 17m_{\pi^0}^2)\big)\Big)\\ &- a_x(s + \tilde{s}_x + 14m_{\pi^\pm}^2 - 10m_{\pi^0}^2)\Big)\\ + A_x\Big(8a_x - \frac{b_x}{2F_\pi^2}&(s - 15\tilde{s}_0 + 68m_{\pi^\pm}^2)\Big) + 4A_0a_0,\end{aligned} \tag{L.81}$$

$$\tilde{p}_{1n}^{Ln;0} = \frac{1}{2}A_0a_0, \tag{L.82}$$

$$\tilde{p}_{1\mathrm{L}}^{Ln;0} = \frac{1}{2}A_0a_0\Big(1 - \frac{\tilde{\Delta}_0}{s}\Big), \tag{L.83}$$

$$\tilde{p}_{2\mathrm{L}n}^{Ln;0} = A_0a_0, \tag{L.84}$$

$$\tilde{p}_{3n}^{Ln;0} = \frac{1}{2}A_0a_0, \tag{L.85}$$

$$\tilde{p}_{3c}^{Ln;0} = \Big(A_x + \frac{B_x}{F_\pi^2}(s - \tilde{s}_x)\Big)\Big(a_x + \frac{b_x}{F_\pi^2}(s - 4m_{\pi^\pm}^2)\Big), \tag{L.86}$$

$$\tilde{p}_{11\mathrm{L}}^{Ln;0} = A_x\frac{b_x}{4F_\pi^2}m_{\pi^\pm}^2 + \frac{B_x}{4F_\pi^2}\Big(a_x - \frac{b_x}{3F_\pi^2}\big(2s - 3\tilde{s}_0 - 2m_{\pi^0}^2 + 16m_{\pi^\pm}^2\big)\Big)m_{\pi^\pm}^2, \tag{L.87}$$

$$\begin{aligned}\tilde{p}_{12\mathrm{L}}^{Ln;0} = \frac{B_x}{12F_\pi^2}\Big(\frac{b_x}{F_\pi^2}\Big(&2s^2 + s(16m_{\pi^\pm}^2 - 2m_{\pi^0}^2 - 9\tilde{s}_0) - 4m_{\pi^0}^2\frac{(3\tilde{s}_0 - 4m_{\pi^0}^2)^2}{s}\\ &+ 9\tilde{s}_0^2 + 6\tilde{s}_0(2m_{\pi^\pm}^2 + m_{\pi^0}^2) + 8m_{\pi^\pm}^2(8m_{\pi^\pm}^2 - 5m_{\pi^0}^2)\Big)\\ &- 3a_x(s + \tilde{s}_x + 6m_{\pi^\pm}^2 - 2m_{\pi^0}^2)\Big)\\ + A_x\Big(a_x - \frac{b_x}{4F_\pi^2}&(s - 3\tilde{s}_0 + 20m_{\pi^\pm}^2)\Big),\end{aligned} \tag{L.88}$$

$$\tilde{p}_{13\mathrm{L}}^{Ln;0} = 2\Big(A_x - \frac{B_x}{3F_\pi^2}\tilde{\Sigma}_0\Big)\Big(a_x - 3\frac{b_x}{F_\pi^2}m_{\pi^\pm}^2\Big) + 2a_x\frac{B_x}{3F_\pi^2}m_{\pi^\pm}^2. \tag{L.89}$$

- $K_L\pi^0 \to \pi^+\pi^-$

$$\tilde{p}_\lambda^{Lx;0} = \frac{C_x}{F_\pi^4}(s - \tilde{s}_x)^2 + \frac{2D_x}{3F_\pi^4}\Big(s^2 - 3s\tilde{s}_x + 3\tilde{s}_x^2 + \Delta\tilde{\Delta}_+ - m_{\pi^\pm}^2\frac{\tilde{\Delta}_0^2}{s}\Big), \tag{L.90}$$

$$\begin{aligned}
\tilde{p}_0^{Lx;0} &= A_0\Big(a_x + \frac{b_x}{F_\pi^2}\big(s - 4m_{\pi^\pm}^2\big)\Big) \\
&\quad + 2A_x\bigg(a_c + 2a_t + \frac{b_c}{F_\pi^2}\big(s - 4m_{\pi^\pm}^2\big) - \frac{3b_t}{4F_\pi^2}\big(s - 3\tilde{s}_x + 6\Sigma\big)\bigg) \\
&\quad + \frac{B_x}{4F_\pi^2}\bigg(8\big(s - \tilde{s}_x\big)\Big(a_c + \frac{b_c}{F_\pi^2}\big(s - 4m_{\pi^\pm}^2\big)\Big) + a_t\big(3s - \tilde{s}_x + 2\Sigma\big) \\
&\qquad - \frac{2b_t}{27F_\pi^2}\bigg(5s^2 - 6s\big(5\tilde{s}_x + 8\Sigma\big) + 45\tilde{s}_x^2 - 96\tilde{s}_x\big(2m_{\pi^\pm}^2 - 5m_{\pi^0}^2\big) \\
&\qquad\qquad + 4\big(135m_{\pi^\pm}^4 - 122m_{\pi^\pm}^2 m_{\pi^0}^2 + 23m_{\pi^0}^4\big) - 32m_{\pi^\pm}^2\frac{\tilde{\Delta}_0^2}{s}\bigg)\bigg),
\end{aligned} \tag{L.91}$$

$$\begin{aligned}
\tilde{p}_{0q}^{Lx;0} &= A_x\bigg(2a_t - \frac{b_t}{F_\pi^2}\Big(s - \tilde{\Delta}_0 + 4\frac{m_{\pi^\pm}^4 + m_{\pi^0}^4}{\Sigma}\Big)\bigg) \\
&\quad - \frac{B_x}{F_\pi^2}\bigg(\frac{b_t}{9F_\pi^2}\Big(\big(s - 3\tilde{s}_x\big)^2 - 8\Delta\tilde{\Delta}_0 + 44\Delta^2 - 4m_{\pi^\pm}^2\frac{\tilde{\Delta}_0^2}{s}\Big) - \frac{a_t}{2}\Big(s - \tilde{s}_x + \frac{2\Delta^2}{\Sigma}\Big)\bigg),
\end{aligned} \tag{L.92}$$

$$\begin{aligned}
\tilde{p}_{1c}^{Lx;0} &= A_x\Big(a_t - \frac{b_t}{2F_\pi^2}\Big(s - \tilde{\Delta}_0 + 2m_{\pi^\pm}^2 + 4m_{\pi^0}^2 + 2m_{\pi^\pm}^2\frac{\tilde{\Delta}_0}{s}\Big)\Big) \\
&\quad - \frac{B_x}{2F_\pi^2}\bigg(\frac{b_t}{9F_\pi^2}\bigg(s^2 - 2s\big(3\tilde{s}_x + m_{\pi^\pm}^2\big) + \tilde{\Delta}_0^2 + 12\tilde{\Delta}_0 m_{\pi^0}^2 + 24m_{\pi^\pm}^2\Delta \\
&\qquad\qquad + 48m_{\pi^0}^4 - 6m_{\pi^\pm}^2(\tilde{\Delta}_0 - 4\Sigma)\frac{\tilde{\Delta}_0}{s}\bigg) \\
&\qquad - \frac{1}{2}a_t\Big(s - \tilde{s}_x + 2m_{\pi^0}^2 + 2m_{\pi^\pm}^2\frac{\tilde{\Delta}_0}{s}\Big)\bigg),
\end{aligned} \tag{L.93}$$

$$\begin{aligned}
\tilde{p}_{1\mathrm{L}}^{Lx;0} &= A_x\bigg(a_t\Big(1 - \frac{\tilde{\Delta}_0}{s}\Big) - \frac{b_t}{2F_\pi^2}\Big(s - \tilde{\Delta}_+ - \tilde{\Delta}_0 + 3\Sigma + (\tilde{\Delta}_0 - 4\Sigma)\frac{\tilde{\Delta}_0}{s}\Big)\bigg) \\
&\quad - \frac{B_x}{2F_\pi^2}\bigg(\frac{b_t}{9F_\pi^2}\bigg(s^2 - s\big(9\tilde{s}_x - 2m_{\pi^\pm}^2\big) + 3\tilde{\Delta}_0^2 + 18\tilde{\Delta}_0 m_{\pi^0}^2 - 24m_{\pi^0}^2\Delta + 48m_{\pi^\pm}^4 \\
&\qquad\qquad - (\tilde{\Delta}_0^2 + 12m_{\pi^0}^2\tilde{\Delta}_0 + 48(m_{\pi^\pm}^4 + m_{\pi^0}^4))\frac{\tilde{\Delta}_0}{s} + 4m_{\pi^\pm}^2\frac{\tilde{\Delta}_0^3}{s^2}\bigg) \\
&\qquad - \frac{1}{2}a_t\Big(s - 4\tilde{s}_x + 4m_{\pi^\pm}^2 + 2m_{\pi^0}^2 + (\tilde{\Delta}_0 - 4\Sigma)\frac{\tilde{\Delta}_0}{3s}\Big)\bigg),
\end{aligned} \tag{L.94}$$

$$\begin{aligned}
\tilde{p}_{2\mathrm{L}+}^{Lx;0} &= \frac{B_x}{F_\pi^2}\bigg(\frac{2b_t}{F_\pi^2}\Big(\frac{s(m_{\pi^\pm}^4 + m_{\pi^0}^4) + 3\tilde{s}_x(m_{\pi^\pm}^4 - 3m_{\pi^0}^4)}{\Sigma} - \frac{4}{3}(5m_{\pi^\pm}^2\Delta - m_{\pi^0}^4)\Big) \\
&\qquad + a_t\Big(\tilde{s}_x - \frac{2m_{\pi^\pm}^2 m_{\pi^0}^2 + \tilde{\Delta}_+\Delta}{\Sigma}\Big)\bigg) + 2A_x\Big(a_t - \frac{3b_t}{F_\pi^2}\frac{m_{\pi^\pm}^4 + m_{\pi^0}^4}{\Sigma}\Big),
\end{aligned} \tag{L.95}$$

$$\tilde{p}^{Lx;0}_{3n} = \frac{1}{2}\,A_0\Big(a_x + \frac{b_x}{F_\pi^2}(s - 4m^2_{\pi^\pm})\Big), \tag{L.96}$$

$$\tilde{p}^{Lx;0}_{3c} = \Big(A_x + \frac{B_x}{F_\pi^2}(s - \tilde{s}_x)\Big)\Big(a_c + \frac{b_c}{F_\pi^2}(s - 4m^2_{\pi^\pm})\Big), \tag{L.97}$$

$$\begin{aligned}\tilde{p}^{Lx;0}_{7\mathrm{L}x} = -\frac{B_x}{F_\pi^2}\Bigg(&\frac{2b_t}{3F_\pi^2}\Big(3s\Sigma - 2(7\Delta^2 + 18m^2_{\pi^\pm}m^2_{\pi^0}) + 3\frac{\tilde{\Delta}_0}{\Delta}(m^4_{\pi^\pm} + 3m^4_{\pi^0})\Big)\\ &+ a_t\Big(\tilde{s}_x - \Sigma\frac{\tilde{\Delta}_+}{\Delta}\Big)\Bigg) - 2A_x\Big(a_t - \frac{3b_t}{F_\pi^2}\Sigma\Big),\end{aligned} \tag{L.98}$$

$$\tilde{p}^{Lx;0}_{8\mathrm{L}x} = \Delta\left(2A_x\frac{b_t}{F_\pi^2}\frac{\Delta}{\tilde{\Delta}_+} + \frac{B_x}{F_\pi^2}\left(a_t - \frac{2b_t}{3F_\pi^2}\left(5\Sigma + \frac{\Delta}{\tilde{\Delta}_+}(s - 3\tilde{s}_x)\right)\right)\right), \tag{L.99}$$

$$\tilde{p}^{Lx;0}_{9\mathrm{L}x} = \frac{2b_t}{3F_\pi^2}\frac{B_x}{F_\pi^2}\Delta^2. \tag{L.100}$$

List of publications

[I] M. Zdráhal, *Dispersive approach to chiral perturbation theory*, Diploma Thesis, Faculty of Mathematics and Physics, Charles University, Prague (2004).

[II] M. Zdráhal and J. Novotný, *"Dispersive Approach to Chiral Perturbation Theory"*, Phys. Rev. D **78** (2008) 116016 [arXiv:0806.4529[hep-ph]].

[III] K. Kampf, M. Knecht, J. Novotný and M. Zdráhal, *"Dispersive representation of $K \to 3\pi$ amplitudes and cusps"*, Nucl. Phys. Proc. Suppl. **186** (2009) 334 [arXiv:0810.1906[hep-ph]].

[IV] M. Zdráhal, K. Kampf, M. Knecht and J. Novotný, *"Dispersive construction of two-loop $P \to 3\pi$ ($P = K, \eta$) amplitudes"*, PoS **EFT09** (2009) 063 [arXiv:0905.4868[hep-ph]].

[V] M. Zdráhal, K. Kampf, M. Knecht and J. Novotný, *"Construction of the $\eta \to 3\pi$ (and $K \to 3\pi$) amplitudes using dispersive approach"*, PoS **CD09** (2009) 122 [arXiv:0910.1721[hep-ph]].

[VI] K. Kampf, M. Knecht, J. Novotný and M. Zdráhal, *"Analytical dispersive construction of $\eta \to 3\pi$ amplitude: First order in isospin breaking"*, Phys. Rev. D **84** (2011) 114015 [arXiv:1103.0982[hep-ph]].

[VII] M. Zdráhal, *"Determination of the m_u and m_d quark masses from $\eta \to 3\pi$ decay"*, Nucl. Phys. Proc. Suppl. **219-220C** (2011) 68 [arXiv:1109.1835[hep-ph]].

[VIII] M. Zdráhal, *"Prague-Lund-Marseille (analytical) dispersive approach to $\eta \to 3\pi$"*, in *Primenet Proceedings* (2011) , to appear at arXiv.

[IX] M. Zdráhal, *"Determination of the m_u and m_d quark masses from $\eta \to 3\pi$ decay"*, PoS **EPS-HEP2011** (2011) 411, to appear in PoS.

[X] K. Kampf, M. Knecht, J. Novotný and M. Zdráhal, *"Dispersive construction of two-loop $P \to 3\pi$ ($P = K, \eta$) amplitudes I."*, in preparation.

References

[1] A. Abele *et al.* (Crystal Barrel), Decay dynamics of the process $\eta \to 3\pi^0$, Phys. Lett. B **417** (1998) 193.

[2] A. Abele *et al.* (Crystal Barrel), Momentum dependence of the decay $\eta \to \pi^+\pi^-\pi^0$, Phys. Lett. B **417** (1998) 197.

[3] E. Abouzaid *et al.* (KTeV), Detailed Study of the $K_L \to \pi^0\pi^0\pi^0$ Dalitz Plot, Phys. Rev. D **78** (2008) 032009 [arXiv:0806.3535[hep-ex]].

[4] M. Achasov, V. Aulchenko, K. Beloborodov, A. Berdyugin, A. Bogdanchikov *et al.*, Study of the $e^+e^- \to \eta\gamma$ process with SND detector at the VEPP-2M e^+e^- collider, Phys. Rev. D **74** (2006) 014016 [arXiv:hep-ex/0605109].

[5] C. Adolph *et al.* (WASA-at-COSY), Measurement of the $\eta \to 3\pi^0$ Dalitz Plot Distribution with the WASA Detector at COSY, Phys. Lett. B **677** (2009) 24 [arXiv:0811.2763[nucl-ex]].

[6] F. Ambrosino, T. Capussela and F. Perfetto, Dynamics of $\eta \to \pi^+\pi^-\pi^0$, KLOE note n. 215, KLOE collaboration (2007), http://www.lnf.infn.it/kloe/pub/knote/kn215.pdf.

[7] F. Ambrosino *et al.* (KLOE), Precise measurements of the eta and the neutral kaon meson masses with the KLOE detector, JHEP **0712** (2007) 073 [arXiv:0710.5892[hep-ex]].

[8] F. Ambrosino *et al.* (KLOE), Determination of $\eta \to \pi^+\pi^-\pi^0$ Dalitz plot slopes and asymmetries with the KLOE detector, JHEP **0805** (2008) 006 [arXiv:0801.2642[hep-ex]].

[9] F. Ambrosino *et al.* (KLOE), Measurement of the $\eta \to 3\pi^0$ slope parameter α with the KLOE detector, Phys. Lett. B **694** (2010) 16 [arXiv:1004.1319[hep-ex]].

[10] G. Amoros, J. Bijnens and P. Talavera, QCD isospin breaking in meson masses, decay constants and quark mass ratios, Nucl. Phys. B **602** (2001) 87 [arXiv:hep-ph/0101127].

[11] B. Ananthanarayan and P. Buettiker, Comparison of πK scattering in SU(3) chiral perturbation theory and dispersion relations, Eur. Phys. J. C **19** (2001) 517 [arXiv:hep-ph/0012023].

[12] B. Ananthanarayan, P. Buettiker and B. Moussallam, πK sum rules and the SU(3) chiral expansion, Eur. Phys. J. C **22** (2001) 133 [arXiv:hep-ph/0106230].

[13] B. Ananthanarayan, G. Colangelo, J. Gasser and H. Leutwyler, Roy equation analysis of $\pi\pi$ scattering, Phys. Rept. **353** (2001) 207 [arXiv:hep-ph/0005297].

[14] B. Ananthanarayan and B. Moussallam, Four-point correlator constraints on electromagnetic chiral parameters and resonance effective Lagrangians, JHEP **0406** (2004) 047 [arXiv:hep-ph/0405206].

[15] A. Angelopoulos *et al.* (CPLEAR), The neutral kaon decays to $\pi^+\pi^-\pi^0$: A detailed analysis of the CPLEAR data, Eur. Phys. J. C **5** (1998) 389.

[16] A. Angelopoulos *et al.* (CPLEAR), Physics at CPLEAR, Phys. Rept. **374** (2003) 165.

[17] A. Anisovich and H. Leutwyler, Dispersive analysis of the decay $\eta \to 3\pi$, Phys. Lett. B **375** (1996) 335 [arXiv:hep-ph/9601237].

[18] G. Barton and C. Kacser, Some analytic properties of a decay amplitude with final state interactions. 1. The Vertex diagrams in $K \to 3\pi$ decay, Nuovo Cim. **21** (1961) 593.

[19] M. Bashkanov *et al.*, Measurement of the Slope Parameter for the $\eta \to 3\pi^0$ Decay in the $pp \to pp\eta$ Reaction, Phys. Rev. C **76** (2007) 048201 [arXiv:0708.2014[nucl-ex]].

[20] J. Batley *et al.* (NA48/2), Observation of a cusp-like structure in the $\pi^0\pi^0$ invariant mass distribution from $K^\pm \to \pi^\pm\pi^0\pi^0$ decay and determination of the $\pi\pi$ scattering lengths, Phys. Lett. B **633** (2006) 173 [arXiv:hep-ex/0511056].

[21] J. R. Batley *et al.* (NA48), A measurement of the CP-conserving component of the decay $K_S \to \pi^+\pi^-\pi^0$, Phys. Lett. B **630** (2005) 31 [arXiv:hep-ex/0510008].

[22] J. R. Batley *et al.* (NA48/2), Empirical parameterization of the $K^\pm \to \pi^\pm\pi^0\pi^0$ decay Dalitz plot, Phys. Lett. B **686** (2010) 101 [arXiv:1004.1005[hep-ex]].

[23] R. Baur, J. Kambor and D. Wyler, Electromagnetic corrections to the decays $\eta \to 3\pi$, Nucl. Phys. B **460** (1996) 127 [arXiv:hep-ph/9510396].

[24] J. S. Bell and D. G. Sutherland, Current algebra and $\eta \to 3\pi$, Nucl. Phys. B **4** (1968) 315.

[25] V. Bernard, M. Oertel, E. Passemar and J. Stern, Dispersive representation and shape of the K(l3) form factors: Robustness, Phys. Rev. D **80** (2009) 034034 [arXiv:0903.1654[hep-ph]].

[26] J. Bijnens, Chiral perturbation theory beyond one loop, Prog. Part. Nucl. Phys. **58** (2007) 521 [arXiv:hep-ph/0604043].

[27] J. Bijnens and F. Borg, Isospin breaking in $K \to 3\pi$ decays. 1. Strong isospin breaking, Nucl. Phys. B **697** (2004) 319 [arXiv:hep-ph/0405025].

[28] J. Bijnens and F. Borg, Isospin breaking in $K \to 3\pi$ decays. II. Radiative corrections, Eur. Phys. J. C **39** (2005) 347 [arXiv:hep-ph/0410333].

[29] J. Bijnens and F. Borg, Isospin breaking in $K \to 3\pi$ decays III: Bremsstrahlung and fit to experiment, Eur. Phys. J. C **40** (2005) 383 [arXiv:hep-ph/0501163].

[30] J. Bijnens, G. Colangelo, G. Ecker, J. Gasser and M. Sainio, Elastic $\pi\pi$ scattering to two loops, Phys. Lett. B **374** (1996) 210 [arXiv:hep-ph/9511397].

[31] J. Bijnens, G. Colangelo, G. Ecker, J. Gasser and M. Sainio, Pion pion scattering at low-energy, Nucl. Phys. B **508** (1997) 263 [arXiv:hep-ph/9707291].

[32] J. Bijnens, P. Dhonte and F. Borg, $K \to 3\pi$ decays in chiral perturbation theory, Nucl. Phys. B **648** (2003) 317 [arXiv:hep-ph/0205341].

[33] J. Bijnens and K. Ghorbani, $\eta \to 3\pi$ at Two Loops In Chiral Perturbation Theory, JHEP **11** (2007) 030 [arXiv:0709.0230[hep-ph]].

[34] J. Bijnens and I. Jemos, A new global fit of the L_i^r at next-to-next-to-leading order in Chiral Perturbation Theory, Nucl.Phys. B **854** (2012) 631 [arXiv:1103.5945[hep-ph]].

[35] J. Bijnens and J. Prades, Electromagnetic corrections for pions and kaons: Masses and polarizabilities, Nucl. Phys. B **490** (1997) 239 [arXiv:hep-ph/9610360].

[36] M. Bissegger, A. Fuhrer, J. Gasser, B. Kubis and A. Rusetsky, Cusps in $K_L \to 3\pi$ decays, Phys. Lett. B **659** (2008) 576 [arXiv:0710.4456[hep-ph]].

[37] M. Bissegger, A. Fuhrer, J. Gasser, B. Kubis and A. Rusetsky, Radiative corrections in $K \to 3\pi$ decays, Nucl. Phys. B **806** (2009) 178 [arXiv:0807.0515[hep-ph]].

[38] T. Blum, R. Zhou, T. Doi, M. Hayakawa, T. Izubuchi *et al.*, Electromagnetic mass splittings of the low lying hadrons and quark masses from $2+1$ flavor lattice QCD+QED, Phys.Rev. D **82** (2010) 094508 [arXiv:1006.1311[hep-lat]].

[39] B. Borasoy and R. Nissler, Hadronic η and η' decays, Eur. Phys. J. A **26** (2005) 383 [arXiv:hep-ph/0510384].

[40] J. B. Bronzan and C. Kacser, The Khuri-Treiman representation and perturbation theory, Phys. Rev. **132** (1963) 2703.

[41] J. Bros, H. Epstein and V. Glaser, Some rigorous analyticity properties of 4-point function in momentum space, Nuovo Cimento **31** (1964) 1265.

[42] J. Bros, H. Epstein and V. Glaser, A proof of the crossing property for two-particle amplitudes in general quantum field theory, Comm. Math. Phys. **1** (1965) 240.

[43] N. Cabibbo, Determination of the $a_0 - a_2$ pion scattering length from $K^+ \to \pi^+\pi^0\pi^0$ decay, Phys. Rev. Lett. **93** (2004) 121801 [arXiv:hep-ph/0405001].

[44] N. Cabibbo and G. Isidori, Pion pion scattering and the $K \to 3\pi$ decay amplitudes, JHEP **0503** (2005) 021 [arXiv:hep-ph/0502130].

[45] J. M. Cline, Can $\theta(\mathrm{QCD}) = \pi$?, Phys. Rev. Lett. **63** (1989) 1338.

[46] G. Colangelo, S. Durr, A. Juttner, L. Lellouch, H. Leutwyler *et al.*, Review of lattice results concerning low energy particle physics, Eur. Phys. J. C **71** (2011) 1695 [arXiv:1011.4408[hep-lat]].

[47] G. Colangelo, J. Gasser, B. Kubis and A. Rusetsky, Cusps in $K \to 3\pi$ decays, Phys. Lett. B **638** (2006) 187 [arXiv:hep-ph/0604084].

[48] G. Colangelo, J. Gasser and H. Leutwyler, The $\pi\pi$ S wave scattering lengths, Phys. Lett. B **488** (2000) 261 [arXiv:hep-ph/0007112].

[49] G. Colangelo, J. Gasser and H. Leutwyler, $\pi\pi$ scattering, Nucl. Phys. B **603** (2001) 125 [arXiv:hep-ph/0103088].

[50] G. Colangelo, S. Lanz and E. Passemar, A New Dispersive Analysis of $\eta \to 3\pi$, PoS **CD09** (2009) 047 [arXiv:0910.0765[hep-ph]].

[51] J. A. Cronin, Phenomenological model of strong and weak interactions in chiral U(3)×U(3), Phys. Rev. **161** (1967) 1483.

[52] R. Cutkosky, Singularities and Discontinuities of Feynman Amplitudes, J. Math. Phys. **1** (1960) 429.

[53] G. D'Ambrosio, G. Isidori, A. Pugliese and N. Paver, Strong rescattering in $K \to 3\pi$ decays and low-energy meson dynamics, Phys.Rev. D **50** (1994) 5767 [arXiv:hep-ph/9403235].

[54] R. F. Dashen, Chiral SU(3)×SU(3) as a symmetry of the strong interactions, Phys. Rev. **183** (1969) 1245.

[55] S. Descotes-Genon, Low-energy pi-pi and pi-K scatterings revisited in three-flavour resummed chiral perturbation theory, Eur. Phys. J. C **52** (2007) 141 [arXiv:hep-ph/0703154].

[56] S. Descotes-Genon, N. Fuchs, L. Girlanda and J. Stern, Analysis and interpretation of new low-energy $\pi\pi$ scattering data, Eur. Phys. J. C **24** (2002) 469 [arXiv:hep-ph/0112088].

[57] S. Descotes-Genon, N. Fuchs, L. Girlanda and J. Stern, Resumming QCD vacuum fluctuations in three flavor chiral perturbation theory, Eur. Phys. J. C **34** (2004) 201 [arXiv:hep-ph/0311120].

[58] L. Di Lella, *Review of $\pi\pi$ scattering measurements in K decays*, Talk given at Kaon2007, Frascati (2007), http://www.cern.ch/NA48/Welcome/images/talks/KAON07/luigi.dilella.pdf.

[59] C. Ditsche, B. Kubis and U.-G. Meissner, Electromagnetic corrections in $\eta \to 3\pi$ decays, Eur. Phys. J. C **60** (2009) 83 [arXiv:0812.0344[hep-ph]].

[60] C. Dominguez, Quark masses in QCD: a progress report, Mod.Phys.Lett. A **26** (2011) 691 [arXiv:1103.5864[hep-ph]].

[61] S. Durr, Z. Fodor, C. Hoelbling, S. Katz, S. Krieg *et al.*, Lattice QCD at the physical point: Simulation and analysis details, JHEP **1108** (2011) 148 [arXiv:1011.2711[hep-lat]].

[62] G. Ecker, Strong interactions of light flavours, arXiv:hep-ph/0011026.

[63] G. Ecker, J. Gasser, H. Leutwyler, A. Pich and E. de Rafael, Chiral Lagrangians for Massive Spin 1 Fields, Phys. Lett. B **223** (1989) 425.

[64] G. Ecker, J. Gasser, A. Pich and E. de Rafael, The Role of Resonances in Chiral Perturbation Theory, Nucl. Phys. B **321** (1989) 311.

[65] R. Eden, P. Landshoff, D. Olive and J. Polkinghorne, *The analytic S-matrix*, Cambridge University Press, (1966).

[66] M. Froissart, Asymptotic behavior and subtractions in the Mandelstam representation, Phys. Rev. **123** (1961) 1053.

[67] N. H. Fuchs, H. Sazdjian and J. Stern, How to probe the scale of $(\bar{q}q)$ in chiral perturbation theory, Phys. Lett. B **269** (1991) 183.

[68] E. Gamiz, J. Prades and I. Scimemi, $K \to 3\pi$ final state interactions at NLO in CHPT and Cabibbo's proposal to measure $a_0 - a_2$, Eur. Phys. J. C **50** (2007) 405 [arXiv:hep-ph/0602023].

[69] R. García-Martín, R. Kamiński, J. Peláez, J. Ruiz de Elvira and F. Ynduráin, The Pion-pion scattering amplitude. IV: Improved analysis with once subtracted Roy-like equations up to 1100 MeV, Phys. Rev. D **83** (2011) 074004 [arXiv:1102.2183[hep-ph]].

[70] J. Gasser, Light-quark dynamics, Lect. Notes Phys. **629** (2004) 1 [arXiv:hep-ph/0312367].

[71] J. Gasser, On the history of pion-pion scattering, PoS **EFT09** (2009) 029.

[72] J. Gasser, B. Kubis and A. Rusetsky, Cusps in $K \to 3\pi$ decays: a theoretical framework, Nucl. Phys. B **850** (2011) 96 [arXiv:1103.4273[hep-ph]].

[73] J. Gasser and H. Leutwyler, Chiral Perturbation Theory To One Loop, Annals Phys. **158** (1984) 142.

[74] J. Gasser and H. Leutwyler, Chiral Perturbation Theory: Expansions in the Mass of the Strange Quark, Nucl. Phys. B **250** (1985) 465.

[75] J. Gasser and H. Leutwyler, $\eta \to 3\pi$ to One Loop, Nucl. Phys. B **250** (1985) 539.

[76] J. Gasser and M. Sainio, Two loop integrals in chiral perturbation theory, Eur. Phys. J. C **6** (1999) 297 [arXiv:hep-ph/9803251].

[77] S. Giudici (NA48 Collaboration), pion pion scattering lengths measurement at NA48-CERN, PoS **CD09** (2009) 002.

[78] A. Gomez Nicola and J. R. Pelaez, Meson meson scattering within one loop chiral perturbation theory and its unitarization, Phys. Rev. D **65** (2002) 054009 [arXiv:hep-ph/0109056].

[79] M. Gormley *et al.*, Experimental determination of the dalitz-plot distribution of the decays $\eta \to \pi^+\pi^-\pi^0$ and $\eta \to \pi^+\pi^-\gamma$, and the branching ratio $\eta \to \pi^+\pi^-\gamma/\eta \to \pi^+$, Phys. Rev. D **2** (1970) 501.

[80] P. Goslawski, *High precision η meson mass determination at ANKE-COSY*, Talk given at PrimeNet Workshop, Jülich (2011), http://www2.fz-juelich.de/ikp//primenet/2011_Workshop_Juelich/talks/PGoslawskiPrimeNet2011.pdf.

[81] C.-O. Gullstrom, A. Kupsc and A. Rusetsky, *Fits of the Dalitz plot distributions for the $\eta \to 3\pi$ decays using non-relativistic effective field theory*, presented at Chiral Dynamics 09.

[82] C.-O. Gullstrom, A. Kupsc and A. Rusetsky, Predictions for the cusp in $\eta \to 3\pi^0$ decay, Phys. Rev. C **79** (2009) 028201 [arXiv:0812.2371[hep-ph]].

[83] F.-K. Guo, C. Hanhart and U.-G. Meissner, Extracting the light quark mass ratio m_u/m_d from bottomonia transitions, Phys. Rev. Lett. **105** (2010) 162001 [arXiv: 1007.4682[hep-ph]].

[84] C. Itzykson and J.-B. Zuber, *Quantum field theory*, Mc Graw Hill, (1980).

[85] Y. S. Jin and A. Martin, Jin and Martin, Phys. Rev. **123** (1961) 1053.

[86] C. Kacser, Analytic structure of partial-wave amplitudes for production and decay processes, Phys. Rev. **132** (1963) 2712.

[87] R. Kaiser and H. Leutwyler, Pseudoscalar decay constants at large N_c, arXiv: hep-ph/9806336.

[88] J. Kambor, J. H. Missimer and D. Wyler, The Chiral Loop Expansion of the Nonleptonic Weak Interactions of Mesons, Nucl. Phys. B **346** (1990) 17.

[89] J. Kambor, J. H. Missimer and D. Wyler, $K \to 2\pi$ and $K \to 3\pi$ decays in next-to-leading order chiral perturbation theory, Phys. Lett. B **261** (1991) 496.

[90] J. Kambor, C. Wiesendanger and D. Wyler, Final State Interactions and Khuri-Treiman Equations in $\eta \to 3\pi$ decays, Nucl. Phys. B **465** (1996) 215 [arXiv: hep-ph/9509374].

[91] K. Kampf and B. Moussallam, Chiral expansions of the π^0 lifetime, Phys. Rev. D **79** (2009) 076005 [arXiv:0901.4688[hep-ph]].

[92] D. B. Kaplan and A. V. Manohar, Current Mass Ratios of the Light Quarks, Phys. Rev. Lett. **56** (1986) 2004.

[93] A. Kastner and H. Neufeld, The $K_{\ell 3}$ scalar form factors in the standard model, Eur. Phys. J. C **57** (2008) 541 [arXiv:0805.2222[hep-ph]].

[94] M. Knecht, B. Moussallam, J. Stern and N. Fuchs, Determination of two loop $\pi\pi$ scattering amplitude parameters, Nucl. Phys. B **471** (1996) 445 [arXiv: hep-ph/9512404[hep-ph]].

[95] M. Knecht, B. Moussallam, J. Stern and N. H. Fuchs, The Low-energy $\pi\pi$ amplitude to one and two loops, Nucl. Phys. B **457** (1995) 513 [arXiv:hep-ph/ 9507319].

[96] M. Knecht and A. Nyffeler, Resonance estimates of $O(p^6)$ low-energy constants and QCD short distance constraints, Eur. Phys. J. C **21** (2001) 659 [arXiv:hep-ph/ 0106034].

[97] M. Knecht and J. Stern, Generalized chiral perturbation theory, arXiv:hep-ph/ 9411253.

[98] M. Knecht and R. Urech, Virtual Photons in Low Energy $\pi\pi$ Scattering, Nucl. Phys. B **519** (1998) 329 [arXiv:hep-ph/9709348].

[99] M. Kolesár, Analysis of discrepancies in Dalitz plot parameters in eta to 3 pion decay, arXiv:1109.0851[hep-ph].

[100] B. Kubis, *Rescattering effects in $\eta \to 3\pi$ decays*, Talk given at EuroFlavour2010, Munich (2010), http://intern.universe-cluster.de/indico/getFile.py/access?contribId=22&sessionId=4&resId=0&materialId=slides&confId=1486.

[101] A. Lai *et al.* (NA48 Collaboration), Measurement of the quadratic slope parameter in the $K_L \to 3\pi^0$ decay Dalitz plot, Phys.Lett. B **515** (2001) 261 [arXiv:hep-ex/0106075].

[102] J. Laiho, E. Lunghi and R. S. Van de Water, Lattice QCD inputs to the CKM unitarity triangle analysis, Phys.Rev. D **81** (2010) 034503, updates at www.latticeaverages.org [arXiv:0910.2928[hep-ph]].

[103] S. Lanz, *Determination of the quark mass ratio Q from $\eta \to 3\pi$*, Ph.D. thesis, Universität Bern (2011).

[104] J. G. Layter *et al.*, Study of dalitz-plot distributions of the decays $\eta \to \pi^+\pi^-\pi^0$ and $\eta \to \pi^+\pi^-\gamma$, Phys. Rev. D **7** (1973) 2565.

[105] H. Lehmann, Analytic properties of scattering amplitude as functions of momentum transfer, Nuovo Cimento **10** (1958) 579.

[106] H. Leutwyler, in M. Shifman, ed., *At the frontier of particle physics*, volume 1, 271–316 World Scientific, Singapore, (2000), contribution to the Festschrift in honor of B. L. Ioffe, arXiv:hep-ph/0008124.

[107] H. Leutwyler, Light quark masses, PoS **CD09** (2009) 005 [arXiv:0911.1416[hep-ph]].

[108] A. Martin, Extension of axiomatic analyticity domain of scattering amplitudes by unitarity I., Nuovo Cimento A **42** (1966) 930.

[109] B. Moussallam and J. Stern, Chiral symmetry aspects of the scalars, arXiv:hep-ph/9404353.

[110] K. Nakamura *et al.* (Particle Data Group), Review of particle physics, J. Phys. G **37** (2010) 075021.

[111] A. Nehme, The Eta decay into three neutral pions is mainly electromagnetic, arXiv:1106.3491[hep-ph].

[112] A. Nehme and S. Zein, Electromagnetic Corrections to the $\eta \to 3\pi$ Neutral Decay, arXiv:1106.0915[hep-ph].

[113] J. A. Oller and L. Roca, Non-Perturbative Study of the Light Pseudoscalar Masses in Chiral Dynamics, Eur. Phys. J. A **34** (2007) 371 [arXiv:hep-ph/0608290].

[114] H. Osborn, Chiral su(3)×su(3) theorems for pseudoscalar- pseudoscalar scattering amplitudes, Nucl. Phys. B **15** (1970) 501.

[115] H. Osborn and D. J. Wallace, Eta - x mixing, $\eta \to 3\pi$ and chiral lagrangians, Nucl. Phys. B **20** (1970) 23.

[116] S. Pislak *et al.* (BNL-E865), A new measurement of K^+_{e4} decay and the s-wave $\pi\pi$ scattering length a(0)(0), Phys. Rev. Lett. **87** (2001) 221801 [arXiv:hep-ex/0106071].

[117] S. Prakhov *et al.* (Crystal Ball at MAMI), Measurement of the Slope Parameter α for the $\eta \to 3\pi^0$ decay with the Crystal Ball at MAMI-C, Phys. Rev. C **79** (2009) 035204 [arXiv:0812.1999[hep-ex]].

[118] S. Roy, Exact integral equation for pion pion scattering involving only physical region partial waves, Phys. Lett. B **36** (1971) 353.

[119] S. Saks and A. Zygmund, *Analytic functions*, volume 28 of *Monografie Matematyczne*, Nakladem Polskiego Towarzystwa Matematycznego, Warsaw, (1952), trans. by E. J. Scott.

[120] A. Schenk, Absorption and dispersion of pions at finite temperature, Nucl. Phys. B **363** (1991) 97.

[121] S. Scherer, Introduction to chiral perturbation theory, Adv. Nucl. Phys. **27** (2003) 277 [arXiv:hep-ph/0210398].

[122] S. P. Schneider, B. Kubis and C. Ditsche, Rescattering effects in $\eta \to 3\pi$ decays, JHEP **1102** (2011) 028 [arXiv:1010.3946[hep-ph]].

[123] G. Sommer, Dispersion relations for complex values of t from axiomatic field theory, Nuovo Cimento A **48** (1967) 92.

[124] G. Sommer, Present state of rigorous analytic properties of scattering amplitudes, Fortsch. Phys. **18** (1970) 577.

[125] J. Stern, H. Sazdjian and N. H. Fuchs, What $\pi - \pi$ scattering tells us about chiral perturbation theory, Phys. Rev. D **47** (1993) 3814 [arXiv:hep-ph/9301244].

[126] D. G. Sutherland, Current algebra and the decay $\eta \to 3\pi$, Phys. Lett. **23** (1966) 384.

[127] W. B. Tippens *et al.* (Crystal Ball), Determination of the quadratic slope parameter in $\eta \to 3\pi^0$ decay, Phys. Rev. Lett. **87** (2001) 192001.

[128] M. Unverzagt *et al.* (Crystal Ball at MAMI), Determination of the Dalitz plot parameter alpha for the decay $\eta \to 3\pi^0$ with the Crystal Ball at MAMI-B, Eur. Phys. J. A **39** (2009) 169 [arXiv:0812.3324[hep-ex]].

[129] S. Weinberg, Pion scattering lengths, Phys. Rev. Lett. **17** (1966) 616.

[130] S. Weinberg, Phenomenological Lagrangians, Physica A **96** (1979) 327.

[131] S. Weinberg, Effective Field Theory, Past and Future, PoS **CD09** (2009) 001 [arXiv:0908.1964[hep-th]].

[132] J. Wess and B. Zumino, Consequences of anomalous Ward identities, Phys. Lett. B **37** (1971) 95.

[133] E. Witten, Global Aspects of Current Algebra, Nucl. Phys. B **223** (1983) 422.

[134] C. Zemach, Three pion decays of unstable particles, Phys.Rev. **133** (1964) B1201.